IAEA TECDOC SERIES

IAEA-TECDOC-1766

IAEA-TECDOC-1766

# Status of Accelerator Driven Systems Research and Technology Development

IAEA
International Atomic Energy Agency

# STATUS OF ACCELERATOR DRIVEN SYSTEMS RESEARCH AND TECHNOLOGY DEVELOPMENT

The following States are Members of the International Atomic Energy Agency:

AFGHANISTAN
ALBANIA
ALGERIA
ANGOLA
ARGENTINA
ARMENIA
AUSTRALIA
AUSTRIA
AZERBAIJAN
BAHAMAS
BAHRAIN
BANGLADESH
BELARUS
BELGIUM
BELIZE
BENIN
BOLIVIA, PLURINATIONAL STATE OF
BOSNIA AND HERZEGOVINA
BOTSWANA
BRAZIL
BRUNEI DARUSSALAM
BULGARIA
BURKINA FASO
BURUNDI
CAMBODIA
CAMEROON
CANADA
CENTRAL AFRICAN REPUBLIC
CHAD
CHILE
CHINA
COLOMBIA
CONGO
COSTA RICA
CÔTE D'IVOIRE
CROATIA
CUBA
CYPRUS
CZECH REPUBLIC
DEMOCRATIC REPUBLIC OF THE CONGO
DENMARK
DJIBOUTI
DOMINICA
DOMINICAN REPUBLIC
ECUADOR
EGYPT
EL SALVADOR
ERITREA
ESTONIA
ETHIOPIA
FIJI
FINLAND
FRANCE
GABON
GEORGIA
GERMANY
GHANA
GREECE
GUATEMALA
GUYANA
HAITI
HOLY SEE
HONDURAS
HUNGARY
ICELAND
INDIA
INDONESIA
IRAN, ISLAMIC REPUBLIC OF
IRAQ
IRELAND
ISRAEL
ITALY
JAMAICA
JAPAN
JORDAN
KAZAKHSTAN
KENYA
KOREA, REPUBLIC OF
KUWAIT
KYRGYZSTAN
LAO PEOPLE'S DEMOCRATIC REPUBLIC
LATVIA
LEBANON
LESOTHO
LIBERIA
LIBYA
LIECHTENSTEIN
LITHUANIA
LUXEMBOURG
MADAGASCAR
MALAWI
MALAYSIA
MALI
MALTA
MARSHALL ISLANDS
MAURITANIA
MAURITIUS
MEXICO
MONACO
MONGOLIA
MONTENEGRO
MOROCCO
MOZAMBIQUE
MYANMAR
NAMIBIA
NEPAL
NETHERLANDS
NEW ZEALAND
NICARAGUA
NIGER
NIGERIA
NORWAY
OMAN
PAKISTAN
PALAU
PANAMA
PAPUA NEW GUINEA
PARAGUAY
PERU
PHILIPPINES
POLAND
PORTUGAL
QATAR
REPUBLIC OF MOLDOVA
ROMANIA
RUSSIAN FEDERATION
RWANDA
SAN MARINO
SAUDI ARABIA
SENEGAL
SERBIA
SEYCHELLES
SIERRA LEONE
SINGAPORE
SLOVAKIA
SLOVENIA
SOUTH AFRICA
SPAIN
SRI LANKA
SUDAN
SWAZILAND
SWEDEN
SWITZERLAND
SYRIAN ARAB REPUBLIC
TAJIKISTAN
THAILAND
THE FORMER YUGOSLAV REPUBLIC OF MACEDONIA
TOGO
TRINIDAD AND TOBAGO
TUNISIA
TURKEY
UGANDA
UKRAINE
UNITED ARAB EMIRATES
UNITED KINGDOM OF GREAT BRITAIN AND NORTHERN IRELAND
UNITED REPUBLIC OF TANZANIA
UNITED STATES OF AMERICA
URUGUAY
UZBEKISTAN
VENEZUELA, BOLIVARIAN REPUBLIC OF
VIET NAM
YEMEN
ZAMBIA
ZIMBABWE

The Agency's Statute was approved on 23 October 1956 by the Conference on the Statute of the IAEA held at United Nations Headquarters, New York; it entered into force on 29 July 1957. The Headquarters of the Agency are situated in Vienna. Its principal objective is "to accelerate and enlarge the contribution of atomic energy to peace, health and prosperity throughout the world".

IAEA-TECDOC-1766

# STATUS OF ACCELERATOR DRIVEN SYSTEMS RESEARCH AND TECHNOLOGY DEVELOPMENT

INTERNATIONAL ATOMIC ENERGY AGENCY
VIENNA, 2015

## COPYRIGHT NOTICE



For further information on this publication, please contact:

Nuclear Power Technology Development Section
International Atomic Energy Agency
Vienna International Centre
PO Box 100
1400 Vienna, Austria
Email: Official.Mail@iaea.org


Printed by the IAEA in Austria
June 2015

IAEA Library Cataloguing in Publication Data

Status of accelerator driven systems research and technology development. — Vienna : International Atomic Energy Agency, 2015.
p. ; 30 cm. — (IAEA-TECDOC series, ISSN 1011–4289 ; no. 1766)
ISBN 978–92–0–105315–2
Includes bibliographical references.

1. Radioactive wastes — Transmutation. 2. Reactor fuel reprocessing. 3. Accelerator-driven systems. I. International Atomic Energy Agency. II. Series.

IAEAL 15–00977

## FOREWORD

One of the greatest challenges for nuclear energy is how to properly manage the highly radioactive waste generated during irradiation in nuclear reactors. In order for nuclear power to exploit its full potential as a major sustainable energy source, there needs to be a safe and effective way to deal with this waste. Since 1995, several scenario studies have been conducted on different advanced nuclear fuel cycle and waste management options in various countries. Examples include the collaborative projects under "Global sustainable nuclear energy scenarios for long term development and deployment of nuclear energy" of the IAEA International Project on Innovative Nuclear Reactors and Fuel Cycles (INPRO) initiative, and the scenario studies conducted under the auspices of the OECD Nuclear Energy Agency and the Euratom research project PATEROS — Partitioning and Transmutation European Roadmap for Sustainable Nuclear Energy.

Some of the proposed long term nuclear fuel cycles include an innovative concept of a hybrid system for the transmutation of long lived radioisotopes. This is usually the called accelerator driven system (ADS) — or accelerator driven transmutation of waste (ATW) — and consists of a high power proton accelerator, a heavy metal spallation target that produces neutrons when bombarded by the high power beam, and a subcritical core that is neutronically coupled to the spallation target. The ADS, which has been developed in different countries for more than 40 years, is claimed to offer new prospects and advantages for the transmutation of high level radioactive waste. The ADS would convert highly radioactive material to non-radioactive material or material with a much shorter half-life. In addition, these hybrid systems can generate electricity during the conversion of transuranic waste.

In 1997, under the guidance of its Technical Working Group on Fast Reactors (TWG-FR), the IAEA published IAEA-TECDOC-985, Accelerator Driven Systems: Energy Generation and Transmutation of Nuclear Waste — Status Report. The objective was to present the state of the art of ADS technology by reviewing the status and progress of national and international programmes in this field, as well as the most interesting projects which were conducted at that time in the Member States. Following the recommendation of the TWG-FR, the IAEA decided in 2006 to launch an initiative for updating the ADS status report, considering the relevant progress and advances recently made in many countries. In 2009, the IAEA published IAEA-TECDOC-1626, Advanced Reactor Technology Options for Utilization and Transmutation of Actinides in Spent Nuclear Fuel, which includes several studies concerning the use of ADS for long lived radioactive waste utilization and transmutation.

The objective of this status report is threefold. Firstly, it aims to review the state of the art of this technology by presenting the different ADS concepts proposed worldwide since 2000, as well as the related R&D activities and demonstration initiatives carried out at national and international levels. Secondly, it contributes to establishing an international roadmap up to the full deployment of ADS, in the context of advanced nuclear fuel cycles. Thirdly, it helps to identify and possibly to stimulate important directions of national and international efforts in this area.

The IAEA would like to express its appreciation to D. De Bruyn, who chaired this study. The IAEA is grateful to all those who helped in the preparation of this report, which benefited from contributions from Belarus, Belgium, China, the Czech Republic, France, Germany, India, Italy, Japan, the Republic of Korea, the Netherlands, the Russian Federation, Spain, Sweden, Switzerland and the United States of America. The IAEA officer responsible for this publication was S. Monti of the Division of Nuclear Power.

*EDITORIAL NOTE*

*This publication has been prepared from the original material as submitted by the contributors and has not been edited by the editorial staff of the IAEA. The views expressed remain the responsibility of the contributors and do not necessarily represent the views of the IAEA or its Member States.*

*Neither the IAEA nor its Member States assume any responsibility for consequences which may arise from the use of this publication. This publication does not address questions of responsibility, legal or otherwise, for acts or omissions on the part of any person.*

*The use of particular designations of countries or territories does not imply any judgement by the publisher, the IAEA, as to the legal status of such countries or territories, of their authorities and institutions or of the delimitation of their boundaries.*

*The mention of names of specific companies or products (whether or not indicated as registered) does not imply any intention to infringe proprietary rights, nor should it be construed as an endorsement or recommendation on the part of the IAEA.*

*The IAEA has no responsibility for the persistence or accuracy of URLs for external or third party Internet web sites referred to in this publication and does not guarantee that any content on such web sites is, or will remain, accurate or appropriate.*

## CONTENTS

# CHAPTER 1

# BACKGROUND AND OVERVIEW OF NUCLEAR FUEL CYCLES SCENARIOS AND THE ROLE OF ADS

## 1.1. PATHS FOR FUTURE DEVELOPMENT OF NUCLEAR POWER

In the current context of growing energy needs and concerns for the environment, the development of abundant, affordable, and environmentally responsible energy technologies is considered as one of the main objectives for the coming decades. Nuclear power has the potential to meet future generations' energy needs in sustainable way and in long term scenarios; however, acceptance of nuclear energy as a large scale contributor to the world's energy mix depends on satisfaction of strict requirements in the areas of economy, safety, adequacy of natural resources, waste reduction, non-proliferation and public acceptance.

One of the main public concerns related to the use of nuclear energy for electricity generation is the long term hazard of radioactive wastes arising from the nuclear fuel cycle. Light water reactor power plants, representing currently almost the totality of the fleet of nuclear power plants under operation worldwide, have been developed for fifty years and a high industrial maturity has been reached. However, LWR technology presents several disadvantages related to its fuel cycle characteristics. In particular, it allows only a poor exploitation of the energy potential of resources (natural uranium), generating problems and concerns related to their preservation and to the management of the radioactive waste.

The world nuclear community is devoting efforts in the development of innovative technologies to make utilization of nuclear energy safer and more sustainable in terms of resource utilization and waste management. In order to achieve these objectives, innovative systems and advanced nuclear fuel cycle options are being studied and developed in various countries and at international level.

Different paths and strategies for future utilization of nuclear energy can be envisaged and are currently being investigated and their development and deployment will be depending on the energy policies and priorities of the different countries. In this framework, the development of innovative nuclear systems like critical and subcritical fast neutron systems and their associated advanced fuel cycles will play an important role, due to their potentialities and flexibility in different sustainable nuclear energy scenarios.

## 1.2. FUEL CYCLE OPTIONS AND FUTURE SCENARIOS

Nowadays, in the nuclear industry, two different fuel cycle options have reached the industrial maturity. The first one is the once through nuclear fuel cycle (the open fuel cycle), in which the spent fuel discharged from the reactor is not further reprocessed but is directly sent to the geological disposal. This fuel cycle, currently adopted in several countries such as USA, Finland, Sweden, generates problem and concern regarding the inefficient utilization of natural uranium and the waste management. However, such a strategy presents also advantages, especially in terms of costs and proliferation resistance.

A second option, which has been adopted in some countries (e.g. Russian Federation, Japan and several European countries), is the reprocessing strategy. This option foresees that uranium and plutonium generated from fertile nuclides are extracted from the spent fuel and used to fabricate fresh MOX fuel. Actinides and fission products arising from the reprocessing plant are vitrified and disposed in geological repositories. This fuel cycle option allows a better utilization of the resources and a reduction of the volume, as well as heat load and radiotoxicity, of final waste to be sent to the geological disposal. However, reprocessing option doesn't solve the characteristic problems related to the open fuel cycle, namely the minor actinides and fission products long life radiotoxicity.

Advanced fuel cycles options are currently being developed in many countries in order to solve the main problems related to the current strategies. With proper combinations of innovative reactor systems and advanced reprocessing technologies, these innovative fuel cycles would allow a complete utilization of natural resources and guarantee a suitable waste management.

An important role in these future scenarios will be played by the deployment of technologies for the partitioning and transmutation (P&T) of the actinides and of the long lived fission products, which allows the radiotoxicity and the volume of the high level waste (HLW) to be strongly reduced compared with the current fuel cycles. Recognizing these potentialities, several countries with nuclear power programmes are currently developing innovative reactors and fuel cycle technologies to implement radioactive waste transmutation in the scope of their radioactive waste management strategies. The main development options and advantages related to the use of partitioning and transmutation, with particular emphasis on the role that accelerator driven systems (ADS) would play in transmutation strategies, are presented in the following paragraphs of this chapter.

## 1.3. PARTITIONING AND TRANSMUTATION (P&T) STRATEGIES

### 1.3.1. P&T objectives and benefits

Most of the radioactive hazard from irradiated nuclear fuel originates from only a few chemical elements: plutonium, neptunium, americium, curium and some long lived fission products such as iodine and technetium. These radioactive by-products, although present at very low concentrations in the irradiated fuel, are a hazard to life forms when released into the environment. As such, their disposal requires isolation from the biosphere in stable deep geological formations for long periods of time.

Partitioning and transmutation (P&T) is considered as a means of reducing the burden on a geological disposal [1.7]–[1.12]. As plutonium and the minor actinides (MA) are mainly responsible for the long term radiotoxicity, when these nuclides are first removed from the irradiated fuel (partitioning) and then fragmented by fission (transmutation), the remaining waste loses most of its long term radiotoxicity. Moreover, the P&T strategy allows in principle a combined reduction of the radionuclide masses to be stored, their associated residual heat, and, as a potential consequence, the volume and the cost of the repository.

Different P&T scenarios have been envisaged (IAEA, PATEROS, OECD/NEA, GIF). All of them imply fuel reprocessing and recycling of actinides and possibly fission products in a fission reactor.

The P&T approach has been developed within radioactive waste management strategy studies in terms of reduction of potential source of radiotoxicity, a potential mitigation to the consequences of accidental scenarios (e.g. human intrusion) in the repository evolution with time, and reduction of heat load in the repository. However, despite this common generic interest for P&T, different objectives are pursued that can be gathered into three categories:

#### *1.3.1.1. Sustainable development of nuclear energy and waste minimization*

For this objective, multi recycling is needed in fast reactors (FRs) of the TRU as unloaded from LWRs and, successively, from FRs, if a transition from a LWR fleet to a FR fleet is foreseen. This objective could also be compatible with an increased proliferation resistance of the fuel cycle, as we will see below.

#### *1.3.1.2. Reduction of TRU inventory as unloaded from LWRs*

This objective is related to the management of spent fuel inventories, as legacy of previous operation of nuclear power plants.

*1.3.1.3. Reduction of MA inventory*

This objective is compatible both with a use of Pu as a resource in LWRs for a limited period of time, in the hypothesis of a delayed deployment of fast reactors, and with a sustainable development of nuclear energy, based on the deployment of fast reactors.

P&T offers significant potential benefit, in particular:

— Reduction of the potential source of radiotoxicity in a deep geological storage (of relevance e.g. in the so-called 'intrusion' scenarios);
— Reduction of the heat load: larger amount of wastes can be stored in the same repository (depending on the host formations);
— If transuranic (TRU) are not separated (e.g. in the homogeneous recycling in a fast neutron reactor), improved proliferation resistance is expected.

As far as the first point (i.e. radiotoxicity reduction), while P&T will not replace the need for appropriate geological disposal of high level waste, studies confirmed that different transmutation strategies could significantly reduce the long term radiotoxicity, as shown in Fig. 1.1.

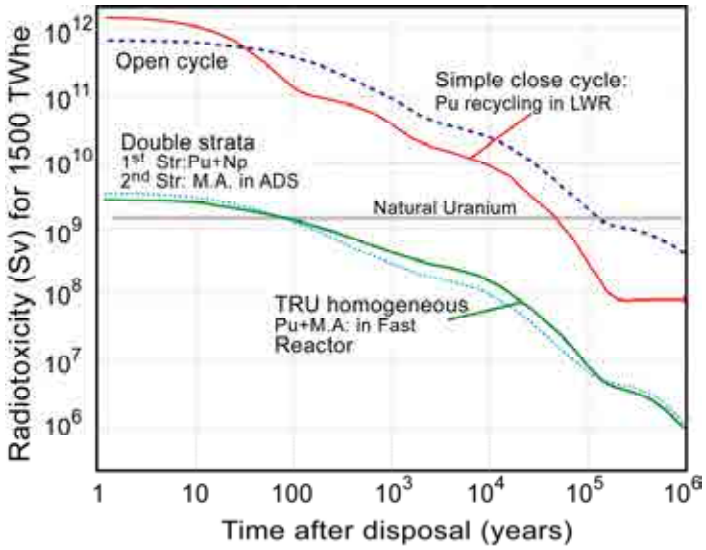


*FIG. 1.1. Radiotoxicity reduction for different transmutation strategies.*

As for the second point (i.e. heat load reduction), generally, the high level radioactive waste arising from the advanced fuel cycle scenarios associated to P&T, generate less heat than the LWR spent fuel. In case of disposal in hard rock, clay and tuff formations the maximum allowable disposal density is determined by thermal limitations.

The reduction of decay heat of the stored material is illustrated in Fig. 1.2.

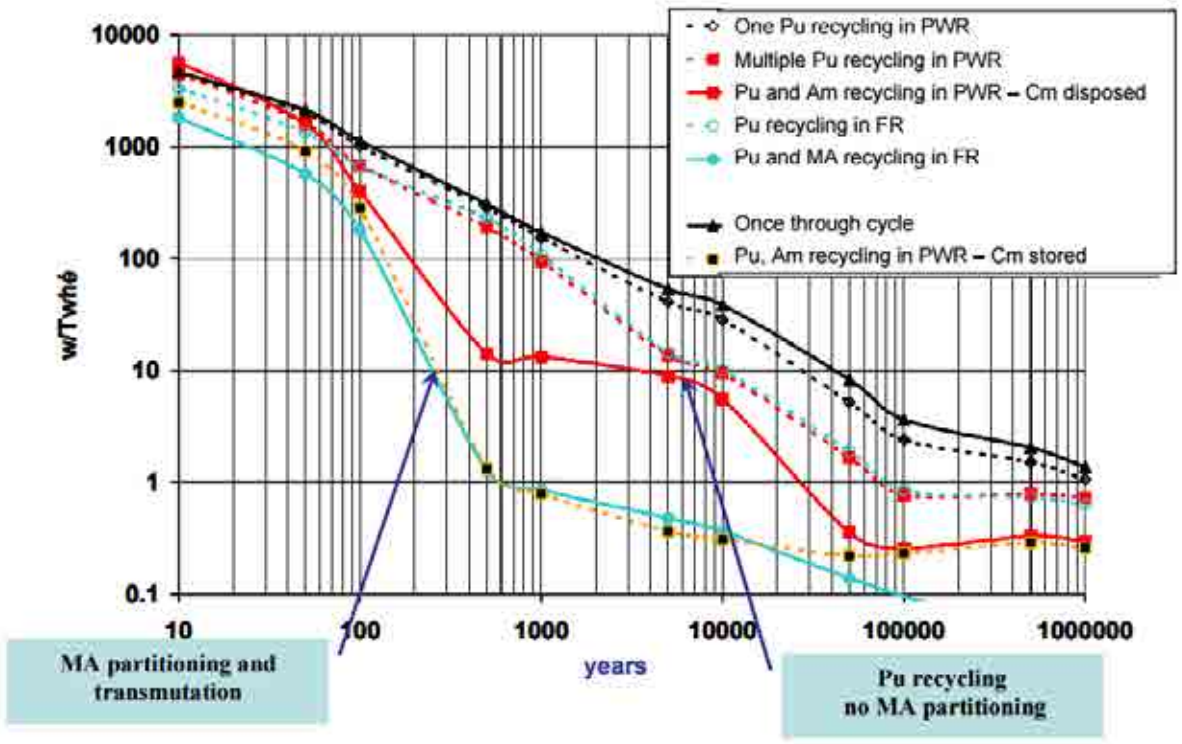


*FIG. 1.2. Reduction of decay heat for different transmutation strategies.*

As an example, it was shown in a European project sponsored by the EU [1.1] that in the case of a fully closed fuel cycle, the considerably smaller thermal output of the high level waste at the considered cooling time of 50 years allows a significant reduction in the total length of disposal galleries required.

Separation of Cs and Sr allows further reduction in the HLW repository size. In the case of disposal in a clay formation the required length of the HLW disposal galleries is reduced by a factor of 3.5 when comparing the waste from the fully closed fuel cycle to once through fuel cycle, and by a factor of 9 when Cs and Sr are separated. Extending the cooling time from 50 to 200 years will result in a reduction of the thermal output of the high level waste and, consequently, of the required size of the repository. In the case of advanced fuel cycles this reduction is a factor of about 30.

Thermal power is a critical characteristic of HLW as it strongly affects the required repository volume (gallery length). In scenarios where Pu or MA are largely included in the HLW, after the 50 years cooling time the contributions from actinides dominate the thermal load of the HLW and consequently the evolution of HLW thermal power is rather slow and takes about 1000 years to reduce by a factor 10 and about 10000 years for a factor 100. On the other hand, for scenarios with full Pu and MA recycling, fission fragments (mainly $^{90}$Sr and $^{137}$Cs) dominate the thermal power for 300 years in the waste streams and so, the total thermal power for these scenarios is reduced by about a factor 10 in only 100 years and by more than a factor 100 at year 300 after unloading.

These reductions show the possibility, for scenarios with full Pu and MA recycling, of large gains in the reduction of the thermal load to the repository and on its associated capacity by delaying the disposal time 100–200 years more. Similar reduction on the HLW thermal power can be gained at shorter times by separating the Sr and Cs from the HLW. In fact, when Pu and MA are recycled, the heat from the actinides plus 1% of these fission fragments, at the reference disposal time of 50 years, is only 2% of the total. This effect combined with the minimization of fissile materials, might help reducing the volume of the repository for granite and clay formations.

Similar results have been obtained as outcome of studies performed in the US at the Argonne National Laboratory .The following Fig. 1.3 is taken from the study performed at ANL [1.2], which gives the

potential volume reduction factor associated to the separation of different fractions of Cs and Sr and of TRU:

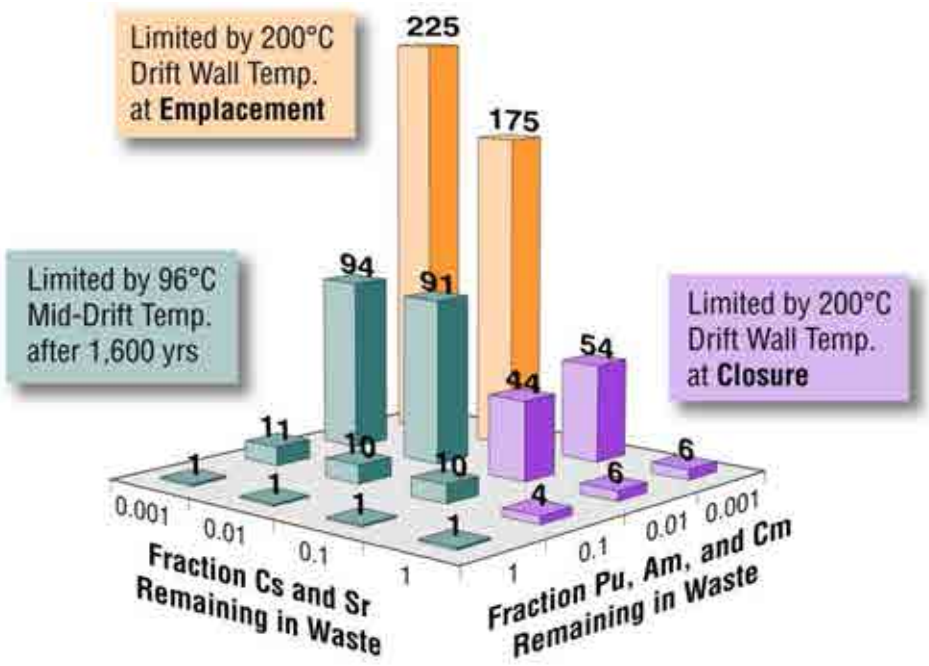


*FIG. 1.3. Potential volume reduction factor associated to the separation of different fractions of Cs and Sr and of TRU.*

This result makes once more clear that, since plutonium, americium, cesium, strontium, and curium are primarily responsible for the decay heat that can cause repository temperature limits to be reached, large gains in repository space are possible by processing spent nuclear fuel to remove those elements.

Of course the recovered elements must be treated:

— Cesium and strontium can be stored separately for 200–300 years;
— Plutonium, americium and curium can be recycled for transmutation and/or fission by irradiation in fast reactors, according to the strategies and scenarios indicated previously.

## 1.4. THE ROLE OF ADS IN DIFFERENT FUEL CYCLE STRATEGIES

Accelerator driven systems (ADS) are advanced nuclear systems which are particularly suitable for transmutation objectives [1.13]. An ADS consists of a high power proton accelerator, a heavy metal spallation target that produces neutrons when bombarded by the high power beam, and a subcritical core that is neutronically coupled to the spallation target. Such a nuclear reactor may be employed to address several missions, including:

— Transmutation of selected isotopes present in radioactive waste (e.g. minor actinides, fission products), the reduce the burden these isotopes place on geological repositories;
— Generate electricity and/or process heat;
— Produce fissile materials for subsequent use in critical or subcritical systems by irradiating fertile elements.

A schematic view of an accelerator driven transmutation system is reported in Fig. 1.4.

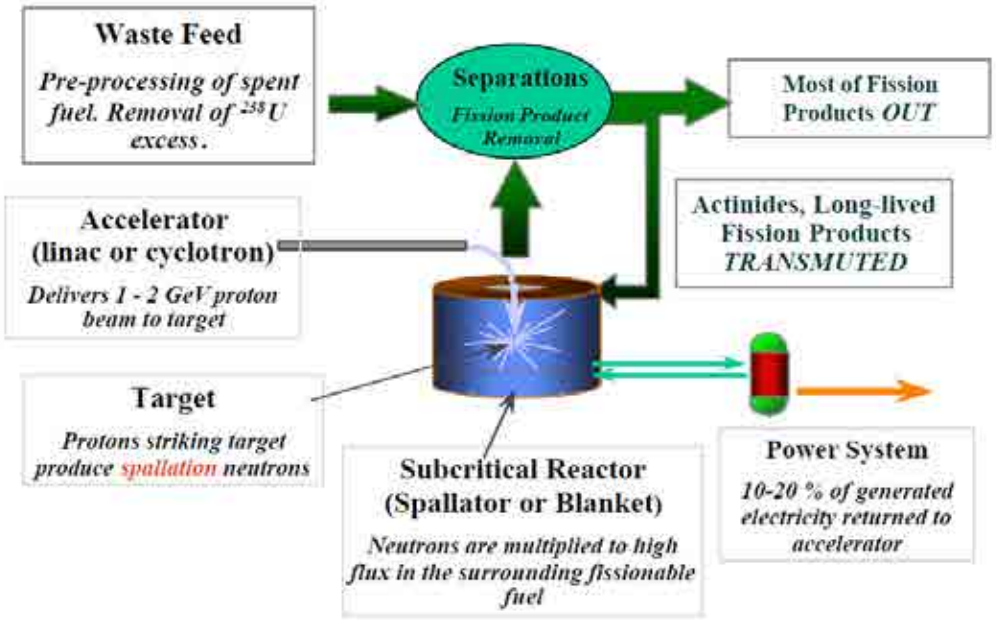


*FIG. 1.4. Scheme of ADS systems.*

The use of ADS presents several advantages; in particular, they offer greater flexibility with respect to fuel composition, and potentially enhanced safety. With regard to the first aspect, the most important feature of ADS system is related to the possibility of using non-fissile fuels (e.g. Th), therefore without the incorporation of U or Pu, which is required in critical fast reactors. The enhanced safety of ADS is due to the fact that once the accelerator is turned off, the system shuts down. If the margin to critical is sufficiently large, reactivity induced transients can never result in a super critical accident with potentially severe consequences. Power control in accelerator driven systems is achieved through the control of the beam current, a feature which can be utilized for fuel burnup compensation.

The advantages of ADSs have to be balanced with several critical issues related to this technology.

As design and operation desadvantages, we can quote, among others:

— The beam window and targets are subjected to stress, irradiation and corrosion;

— It increases the complexity of the final installation;

— Reduction of the electrical efficiency of the plant due to the consumption of the accelerator.

The exploitation of the potentialities of ADS technology require further technology advances to be reached through a technology roadmap that will include the following key steps:

— Transmutation demonstration, the demonstration of ADS and transmutation technologies in a flexible research facility in which a subcritical core is coupled to a MW-scale proton accelerator;

— Industrial scale transmutation, a facility for transmutation of radioactive waste on an industrial scale;

— Industrial scale power generation with energy storage, a power generation facility that utilizes energy storage technology to mitigate lengthy beam interruptions;

— Industrial scale power generation, a power generation facility that burns either transuranic or thorium based fuel and is an integral part of the electric grid.

As far as the first step, a representative example of a transmutation demonstration facility will be the MYRRHA Project, in Belgium. Further details about this project as well as other national and international ADS projects and R&D activities will be discussed in the next chapters of this report.

## 1.5. HISTORY OF ADS

The basic process of accelerator driven systems is nuclear transmutation. This process was first demonstrated by Rutherford in 1919, who transmuted $^{14}N$ to $^{17}O$ using energetic α particles. I. Curie and F. Joliot produced the first artificial radioactivity in 1933 using α particle from naturally radioactive isotopes to transmute boron and aluminium into radioactive nitrogen and oxygen. It was not possible to extend this type of transmutation to heavier elements as long as the only available charged particles were the α particles from natural radioactivity, since the Coulomb barriers surrounding heavy nuclei are too great to permit the entry of such particles into atomic nuclei. The invention of the cyclotron by E.O. Lawrence [1.3] removed this barrier and opened quite new possibilities. When coupled with the spallation process, high power accelerators can be used to produce large numbers of neutrons, thus providing an alternative method to the use of nuclear reactors for this purpose. Spallation offers exciting new possibilities for generating intense neutron fluxes for a variety of purposes.

The first practical attempts to promote accelerators to generate potential neutron sources were made by Lawrence in the late 1940's in the United States, and by W.N. Semenov in the USSR. The first such application for the production of fissile material was the MTA [1.4] project at the Lawrence Livermore Radiation Laboratory. This project was abandoned in 1952 when high grade Uranium ores were discovered in the United States. The Canadian team at Chalk River [1.5] has always been a strong proponent of such a producer of fissile material which could be used in conjunction with a conversion efficient CANDU reactor.

When the United States administration decided to slowdown the development the fast breeder to promote non-proliferation goals, Brookhaven National Laboratory presented several proposals for accelerator breeders such as the Na cooled fast reactor target, the molten salt target, the He gas cooled target, as well as the LWR fuel regenerator.

This concept of the accelerator breeder has also been studied by Russian scientists. Under the guidance of V.I. Goldanski, R.G. Vassylkov [1.6] made a neutron yield experiment in depleted Uranium blocks using the accelerator at Dubna.

The original idea of exploiting the spallation process to transmute actinide and fission products directly was soon abandoned. The proton beam currents required were much larger than the most optimistic theoretical designs that an accelerator could achieve, which are around 300 mA. Indeed, it was shown that the yearly transmutation rate of a 300 mA proton accelerator would correspond only to a fraction of the waste generated annually by a LWR of 1 GW(e).

To use only the spallation neutrons generated in a proton target, the fission products would be placed around the target. For the highest efficiency, depending on the material to be transmuted, either the fast neutrons would be used as they are emitted from the target or they would be slowed down by moderators to energy bands with higher transmutation cross-sections, for example, the resonance or the thermal region.

In the last few years hybrid systems were proposed for different purposes. ADS on fast neutrons for the incineration of higher actinides was proposed at Brookhaven National Laboratory (PHOENIX project) and is now carried out in Japan as a part of OMEGA programme. Los Alamos National Laboratory has developed several ideas to use the hybrid system on thermal neutrons with a linear accelerator for incineration of plutonium and higher actinides, for transmutation of some fission products in order to effectively reduce long term radioactivity of radioactive waste as well as for producing energy based on the thorium fuel cycle, hi 1993 Carlo Rubbia and his European group at CERN proposed a cyclotron based on an hybrid system to produce nuclear energy with thorium based fuel. This is an attractive option reducing the concerns about higher actinides in the spent fuel and giving the possibility of utilizing cheap and quite abundant thorium. First experiments have already been performed by the CERN-group.

Many countries are considering to permanently store long lived highly radioactive material in stable geological formations. There is concern that the waste remains dangerous for thousands of years. Therefore, it is worthwhile studying an alternative approach that would separate the long lived nuclei from the high level waste by transmuting such nuclei into short lived or non-radioactive wastes.

ADS operates in non self-sustained chain reaction mode and therefore minimizes the power excursion concern. ADS is operated in a subcritical mode and stays subcritical, regardless of the accelerator being on or off. The accelerator provides a more convenient control mechanism for subcritical systems than that provided by control rods in critical reactors, and subcriticality itself adds an extra level of operational safety concerning critical accidents. As described later, a subcritical system driven with an accelerator decouples the neutron source (spallation neutrons) from the fissile fuel (fission neutrons). Accelerator driven systems can in principle work without safe shutdown mechanisms (like control rods) and can accept fuels that would not be acceptable in critical systems.

The technology of accelerating a charged particle to high energy has been well demonstrated in recent years, as has the technology of the target. However, extension of this capability to high current beam acceleration is required.

## 1.6. CONTENTS OF THE REPORT

This report is divided into several chapters.

Chapter 2 describes the ADS concept in terms of basic physics and general layout.

Chapter 3 presents the state of development of different ADS concepts developed or under development at national, regional or international level.

Chapter 4 represents the core of this report, providing a detailed description of the main systems, components and technologies involved in an accelerator driven system: from the existing R&D and experimental facilities to the accelerator and the spallation source, from the advanced transmutation fuel to structural materials and components for ADS, from nuclear data to core neutronics and safety issues.

Chapters 5, 6 are devoted to a review of ongoing national and international programmes in the field.

Finally chapter 7 presents the conclusion of report.

## 1.7. REFERENCES TO CHAPTER 1


[1.1] RED-I M PACT Impact of Partitioning, Transmutation and Waste Reduction Technologies on the Final Nuclear Waste Disposal, systhesis report, vol. 15, (July 2008).

[1.2] Advanced Spent Fuel Processing Technologies for the Global Nuclear Energy Partnership, Argonne National Laboratory, 9th IEM on Actinide and Fission Product Partitioning and Transmutation Nîmes, France, (September 2006).

[1.3] KADI, Y., REVOL, J.P., Design of an Accelerator Driven System for the Destruction of Nuclear Waste, Lectures given at the Workshop on Hybrid Nuclear Systems for Energy Production, Utilisation of Actinides & Transmutation of Long lived Radioactive Waste Trieste, Italy, 3–7 September 2001.

[1.4] VAN ATTA, C.M., Abrief History of the MTA Project, ERDA Information, Meeting on Accelerator Breeding, January 19–29 (1977).

[1.5] BARTHOLOMEW, G.A., TUNNICLIFFE, P.R., (EDS), The AECL Study for an Intense Neutron Generator, Atomic Energy of Canada Limited, Report No. AECL-2600 (1966).

[1.6] VASSYLKOV, R.G., GOLDANSKII, V.L., et al., Atomnaya Energiya 48, 329 (1978).

[1.7] STEINBERG, M., et al., Neutron Burning of Long lived Fission Products for Waste Disposal, NL 8558 (1964).

[1.8] CROFF, A.G., et al., A Preliminary Assessment of Partitioning and Transmutation as a Radioactive Waste Management Concept, ORNL-TM-5808 (1977).

[1.9] CROFF, A.G., et al., Actinide Partitioning Transmutation Programme Final Report, Vol. 1, overall Assessment, ORNL-TM-5566 (1980).

[1.10] Evaluation of Actinide Partitioning and Transmutation. IAEA Technical Report, Series

[1.11] MUKAIYAMA, T., et al., Importance of the double strata fuel cycle for minor actinide transmutation, paper presented in the 3rd OECD NEA Int. Inf. Exchange Mtg. on Partitioning and transmutation, Aix-en-Provence, France, Dec. 1994.

[1.12] SALVATORES, M., Transmutation: a decade of revival. Issues, relevant experiments and perspectives, paper presented in the 6th Inf. Exch. Meeting of OECD/NEA on Partitioning and transmutation, Madrid, Spain, December 2000.

[1.13] A Roadmap for developing Accelerator Transmutation of Waster (ATW) Technology, Report to Congress, DOE-RW-0519, (October 1999).

# CHAPTER 2
# PHYSICAL BASIS OF ACCLERATOR DRIVEN SYSTEMS

## 2.1. INTRODUCTION

An ADS is a subcritical nuclear reactor in which the chain fission reaction and therefore the power level is sustained by a spallation neutrons source by means of a proton accelerator (either linear or circular) coupled with the subcritical core. In such a system, the accelerator bombards a target with high energy protons that produce neutrons by means of particular nuclear reactions called spallation reactions. The neutrons produced in the target are subsequently multiplied in the subcritical cores which surrounds the target. A simplified scheme of ADS is depicted in Fig. 2.1.

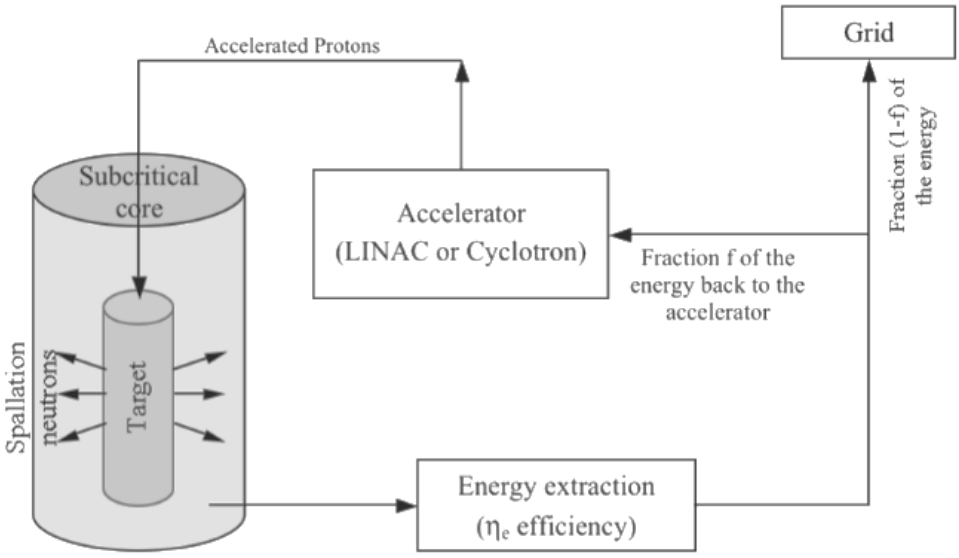


*FIG. 2.1. Scheme of ADS concept.*

## 2.2. THE SPALLATION PROCESS

There are several nuclear reactions characterized by the production of neutrons. However, it was recognized over the years that spallation reactions are the most suitable for a subcritical reactor as they minimize the energetic cost of the neutron production [2.1].

Table 2.1 gives an overview of the main reactions characterized by production of neutrons.

TABLE 2.1. REACTIONS CHARACTERIZED BY PRODUCTION OF NEUTRONS

| Nuclear Reactions | Incident particle & typical energies | Beam currents (part./s) | Neutron yelds (n/inc.part.) | Target power | Deposited energy per neutron (MeV) | Neutron emitted (n/s) |
|---|---|---|---|---|---|---|
| (e,γ) & (γ,n) | $e^-$ (60 MeV) | 5 x E15 | 0.04 | 0.045 | 1500 | 2 x E14 |
| $H^2(tn)He^4$ | $H^3$ (0.3 MeV) | 6 x E19 | 1xE-4–1xE-5 | 0.3 | 1 x E4 | 1 x E15 |
| Fission | ---- | ---- | ~1 | 57 | 200 | 2 x E18 |
| Spallation (non-fissile target) | p (800 MeV) | 1 x E15 | 14 | 0.09 | 30 | 2 x E16 |
| Spallation (fissionable target) | p (800 MeV) | 1 x E15 | 30 | 0.4 | 55 | 4 x E16 |

The idea of producing neutrons by spallation reactions was proposed in the early inception of nuclear energy, with the first tentative to produce fissile materials from fertile species. Renewed interest in this area was observed in the 1980's with transmutation purposes.

The term spallation refers to the interaction of high energy protons (or more generally hadrons or light nuclei) with a target nucleus. This process proceeds in multiple stages: when the projectile collides with the target, due to its high energy (from hundred MeV to several GeV) it leads to a series of fast direct reactions called *intranuclear cascade*, which end with the ejection of nucleons or small groups of nucleons from the target nucleus. At the end of this process, the nucleus is left in an excited stated, and therefore it decreases its energy level either through multi fragmentation, fission or evaporation. In Fig. 2.2 are schematically shown the main physical processes which occur in spallation reactions.

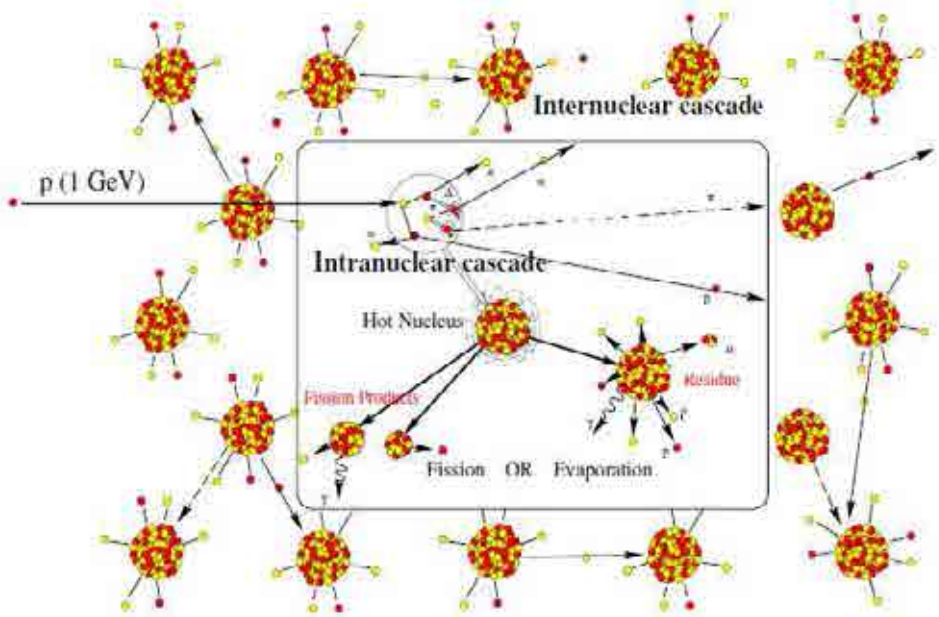


*FIG. 2.2. Scheme of spallation reactions.*

The major aspects characterizing spallation processes can be summarized as follow:

— Spallation neutron yield, which is directly related to accelerator power. The number of emitted neutrons varies as a function of the target nuclei and the energy of the incident particle, reaching saturation around *2 GeV*, as shown in Fig. 2.3. The neutron yield for deuterons and tritons injected into a uranium target is shown in Fig. 2.4.

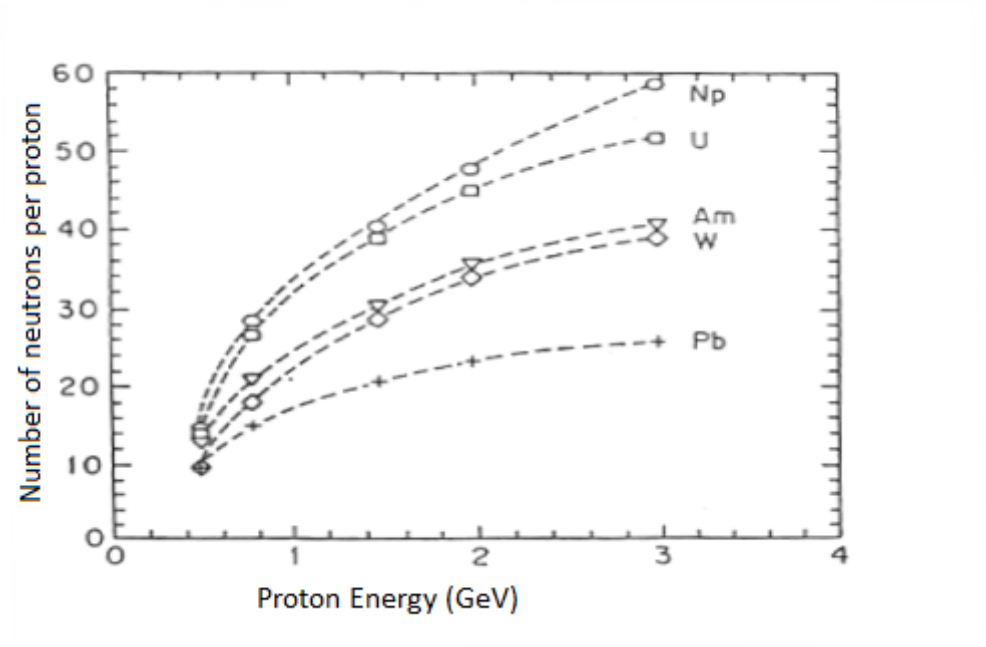


*FIG. 2.3. Number of emitted neutrons as a function of incident proton energy.*

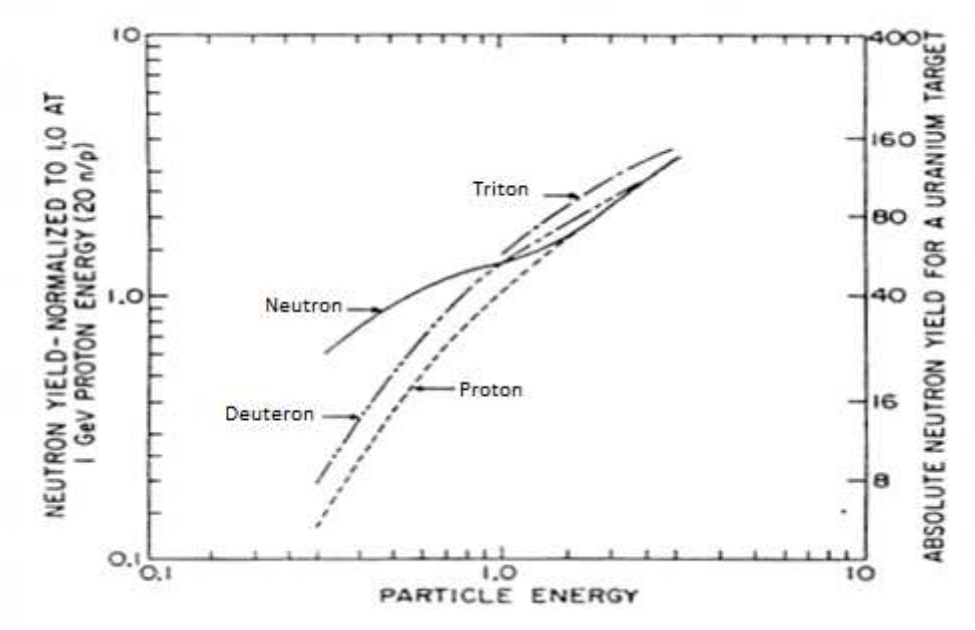


*FIG. 2.4. Neutron yield vs. energy for proton, deuteron, triton and neutron particles.*

— Spallation neutron spectrum, related to the damage and activation of structural materials. Generally the energy distribution of spallation neutrons evaporated from an excited heavy nucleus bombarded by high energy particles is similar to that of fission neutrons, as it is shown in Fig. 2.5.

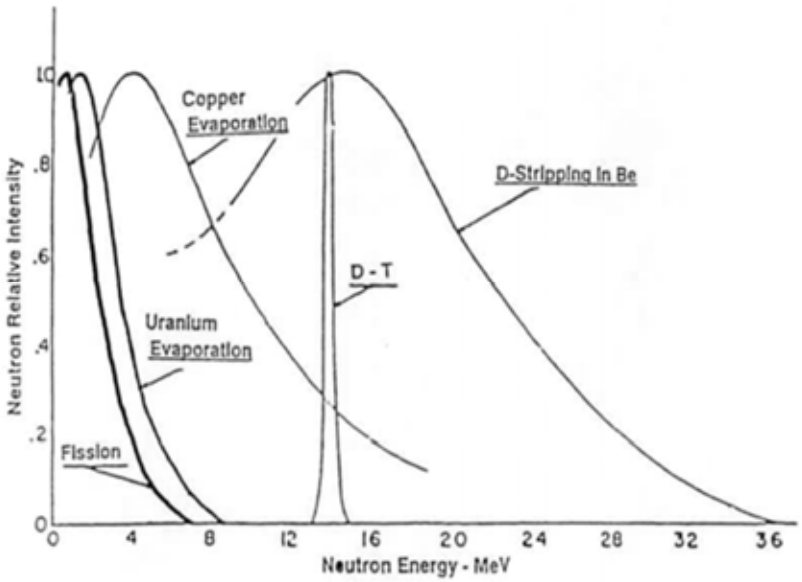


*FIG. 2.5. Energy distribution of emitted neutrons for different nuclear reactions.*

— Energy deposition in the beam window determines the requirements for the thermal hydraulics design of the target. The heat deposition in a beam window and a lead target for various incident proton energies is shown in Fig. 2.6

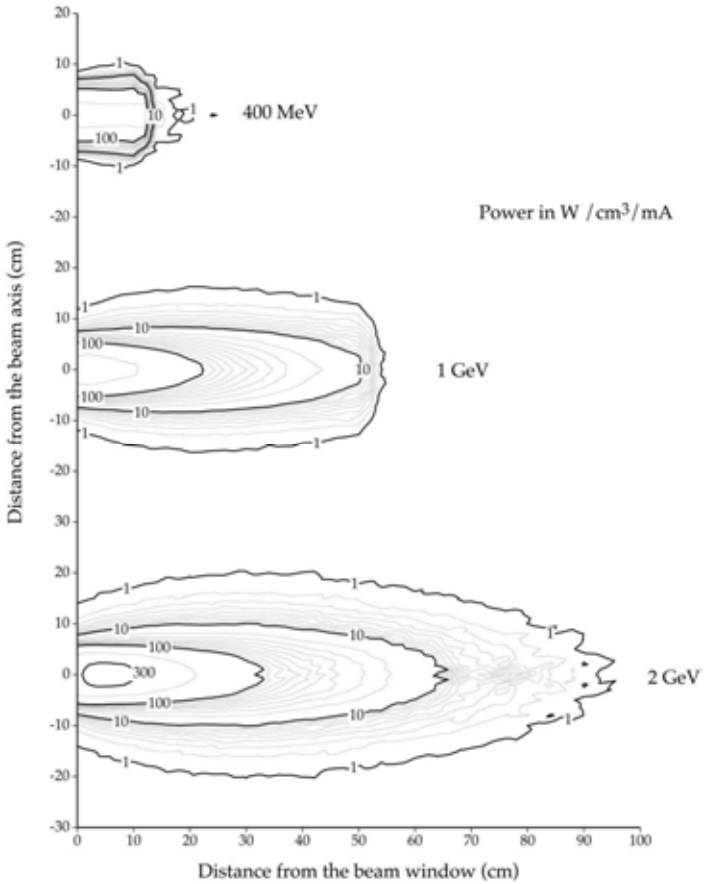


*FIG. 2.6. Energy distribution of emitted neutrons for different nuclear reactions.*

— Spallation products distribution is related to the contribution of the spallation products to the waste stream. The distribution, shown in Fig. 2.7, varies as a function of the target material and the energy of the incident protons.

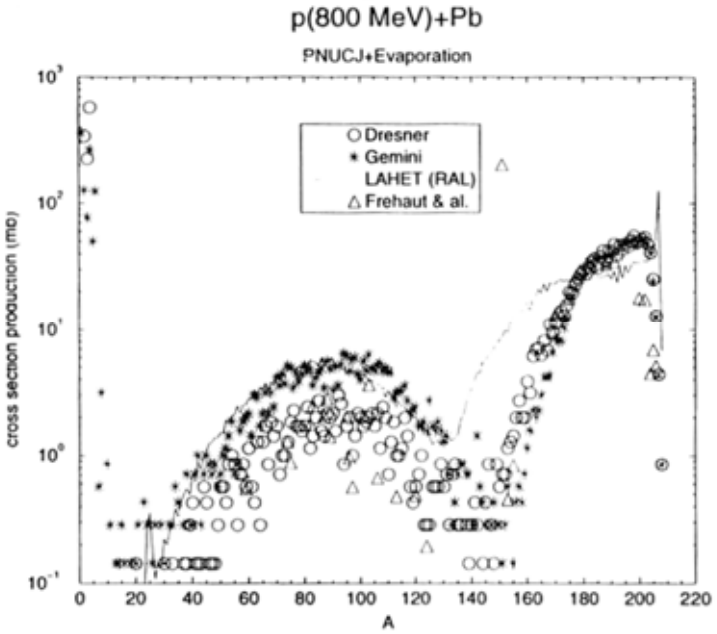


*FIG. 2.7. Spallation product distribution from 800 MeV protons impinging on a thick lead target.*

## 2.3. MAJOR PHYSICAL FEATURES OF SUBCRITICAL CORES

### 2.3.1. Neutron spatial distribution

The main difference between the neutronics characteristics of critical reactors and ADS is that in the first ones the neutron spatial distribution is mainly related to the boundary conditions, while in ADS cores the high energy cascade is dominant.The two spatial distributions are expected to differ substantially as shown in Fig. 2.8.

The neutron spatial distribution in an ADS core can be described starting from the basic equation for monoenergetic or thermal neutron diffusion at equilibrium:

$$D\nabla^2\Phi - \Sigma_a\Phi + S = 0 \qquad \text{(Eq. 2.1)}$$

in which $\Phi$ is neutron flux, $\nabla^2$ laplacian operator is dependent on the coordinate system, $D$ is the diffusion coefficient, $S$ is the neutron source and $\Sigma_a$ is the macroscopic adsorption cross-section. Introducing the parameter $k_\infty$, defined as the number of neutrons produced at each adsorption in the fuel (for an infinite homogenous system), and considering the neutron source $S$ as decomposed in the term due to fissions ($k_\infty\Sigma_a\Phi$) and in a term $C$ related to the high energy cascade, the previous equation can be rearranged in the following form:

$$\nabla^2\Phi - \frac{1-k_\infty}{L_c^2}\Phi + \frac{C}{D} = 0 \qquad \text{(Eq. 2.2)}$$

where

$L_c = \sqrt{\frac{D}{\Sigma a}}$ is known as neutron diffusion length. The quantity $B_M^2 = \frac{k_\infty - 1}{L_c^2}$ is called the 'material buckling' . A positive value of this parameter means that the solution of the previous equation is of oscillatory nature. In a finite system, with vanishing flux at the extrapolated boundaries and neutrons source also vanishing at and outside the boundaries, it is possible to write the solution of the equation of neutron diffusion in terms of the eigenvectors of the characteristic 'wave equation':

$$\nabla^2 \psi + B^2 \psi = 0 \qquad \text{(Eq. 2.3)}$$

The neutron flux can be thus expressed in terms of an infinite series of the eigenfunctions $\psi_n(\vec{x})$:

$$\Phi(\vec{x}) = \sum_{n=1}^{\infty} \Phi_n \psi_n(\vec{x}) \qquad \text{(Eq. 2.4)}$$

where the coefficients $\Phi_n$ are

$$\Phi_n = \int_V \psi_n(\vec{x})\ \Phi(\vec{x}) dV \qquad \text{(Eq. 2.5)}$$

In similar way, even the neutron source can be expressed as follow:

$$\mathrm{C}(\vec{x}) = D \sum_{n=1}^{\infty} \mathrm{c}_n \psi_n(\vec{x}) \qquad \text{(Eq. 2.6)}$$

with

$$\mathrm{c}_n = \frac{1}{D} \int_V \psi_n(\vec{x})\, \mathrm{C}(\vec{x}) dV \qquad \text{(Eq. 2.7)}$$

Using the last expressions it is possible to determine the coefficients $\Phi_n$:

$$\Phi_n = \frac{c_n}{B_n^2 - B_M^2} \qquad \text{(Eq. 2.8)}$$

If we consider for instance parallelepiped geometry with dimensions a, b and c and origin at one edge, such as $\psi(x) = 0$ for the planes $x = a$, $x = 0$, $y = b$, $y = 0$ and $z = c$, $z = 0$, the eigenvectors of the characteristic wave equation have the following form:

$$\psi_{l,m,n}(\vec{x}) = \sqrt{\frac{8}{abc}} \sin\left(l\frac{\pi x}{a}\right) \sin(m\frac{\pi y}{b}) \sin(n\frac{\pi z}{c}) \qquad \text{(Eq. 2.9)}$$

with the following eigenvalues:

$$B_{l,m,n}^2 = \pi^2 \left(\frac{l^2}{a^2} + \frac{m^2}{b^2} + \frac{n^2}{c^2}\right) \qquad \text{(Eq. 2.10)}$$

Analogue expressions can be obviously given for different geometries. Analysing the last expression, it is possible to see the value of the $B_i$ increases with the mode. Therefore, starting from the expression for the $k_i$ related to the mode $i$:

$$k_i = \frac{k_\infty}{1 + L_c^2 B_i^2} \qquad \text{(Eq. 2.11)}$$

it is possible to see that if the first mode is subcritical, all the others modes will be more subcritical. From the expressions for the $k_i$ it is also possible to see that there are two ways for the system to be subcritical; if $k_\infty > 1$ the subcritical status is related to the neutron leakage, while if $k_\infty < 1$, the system is intrinsically subcritical.

Starting from the expression for $\Phi_{l,m,n}$ it is possible to write:

$$\Phi_{l,m,n} = \frac{c_{l,m,n}}{B_{l,m,n}^2 - B_M^2} = \frac{c_{l,m,n}}{B_{l,m,n}^2 - \frac{k_\infty - 1}{L_c^2}} = \frac{L_c^2 c_{l,m,n}}{1 + B_{l,m,n}^2 L_c^2} \times \frac{1}{1 - k_{l,m,n}} \qquad \text{(Eq. 2.12)}$$

Therefore, the general solution can be written as follow:

$$\Phi(\vec{x}) = \sum_{l,m,n} \Phi_{l,m,n}\, \psi_{l,m,n}(\vec{x}) = L_c^2 \sum_{l,m,n} \frac{c_{l,m,n}}{1 + B_{l,m,n}^2 L_c^2} \times \frac{\psi_{l,m,n}(\vec{x})}{1 - k_{l,m,n}} \qquad \text{(Eq. 2.13)}$$

As mentioned before, $k_1$ is higher than $k_n$ with $n > 1$. It means that when the $k_1$ approaches unity, the first term of the series diverges, while the other term remains finite. If there is not any external source, it possible to write $k_1 = k_{eff}$.

## 2.4. NEUTRON MULTIPLICATION IN ADS

In an accelerator driven, subcritical fission device, the 'primary' (or 'source') neutrons produced via spallation by the interaction of the protons beam with a suitable target, initiate a cascade process. The source neutrons are multiplied by fissions and $(n, xn)$ reactions through a factor $M$ defined as follow:

$$M = 1 + k + k^2 + k^3 + \ldots k^n = \tfrac{1}{1-k} \text{ per n} \to \infty \text{ and } k < 1$$

If we assume that all generations in the cascade are equivalent, we can define an average criticality factor k (ratio between the neutron population in two subsequent generations), such that:

$$k = \frac{M-1}{M} = 1 - \frac{1}{M} < 1$$

or

$$k_{src} = \frac{M-1}{M}$$

It has to be underlined that in an ADS, due to the presence of a neutron source, $k_{eff} \neq k$. It is indicated with $k_{src}$ the value of $k$ calculated from the factor $M$ in the presence of an external source. $k_{src}$ is in general conceptually and numerically different from the effective criticality factor $k_{eff}$, commonly used in reactor theory, which is in fact only relevant to the fundamental mode of the neutron flux distribution, and is independent on the source.

Therefore, if $N_0$ is the number of primary neutrons following, for example, interaction of a proton with a target surrounded by a multiplying medium and characterized by a factor $k_{src}$ the total number of generated neutrons after multiplication is:

$$N = N_0 \frac{1}{1 - k_{src}} = N_0 M$$

## 2.5. NEUTRON SOURCE IMPORTANCE

By definition, a constant power operation requires $\upsilon / k_{eff}$ neutrons per fission, which means that an external source has to provide a number of neutrons per fission which is:

$$\mu_{eff} = \upsilon\left(\frac{1}{k_{eff}} - 1\right) = \frac{\upsilon}{M_{eff} - 1}$$

In the case of an arbitrary external source, this number becomes:

$$\mu_{src} = \upsilon\left(\frac{1}{k_{src}} - 1\right) = \frac{\upsilon}{M_{src} - 1}$$

The ratio is known as the importance of source neutrons:

$$\frac{\mu_{eff}}{\mu_{src}} = \frac{(1 - k_{eff})/(k_{eff}/\upsilon)}{(1 - k_{src})/(k_{src}/\upsilon)} = \frac{k_{src}}{k_{eff}}\frac{M_{src}}{M_{eff}} = \varphi^*$$

Where

$\upsilon$ is average numbers of neutron emitted per fission

In general, $\varphi^*$ grows with $k_{src}$ . At a given $k$, $\varphi^*$ increases with:

— 'Containment' of the neutron source;
— Ratio of the neutron diffusion length to the size of fissile core;
— Presence of an absorbing medium, enclosing the fissionable core, which, in a sense, limits the 'widening' of the neutron flux distribution as $k$ is increased.

As $\varphi^*$ is a ratio, it is necessary to have a discussion about it:

— If $\varphi^* < 1$: the neutrons from the external source are multiplying less than those coming from the fission;
— If $\varphi^* = 1$: the external source is equal to the fission one (same energetics and spatial distribution);
— If $\varphi^* > 1$: it is the researched case in order to optimize the system: the external source brings neutrons from which multiplication is, in average, better than the one obtained by neutrons from fission.

## 2.6. NEUTRONIC CHARACTERISTICS OF INTRINSICALLY SUBCRITICAL SYSTEMS

In order to explain the neutronics characteristics of intrinsically subcritical systems ($k_\infty < 1$), it is possible to consider a simplified system made of a point neutrons source at the centre of an infinite diffusion medium. Expressing the Laplace operator in spherical coordinates, the diffusion equation can be written as follow:

$$\frac{d^2\Phi(r)}{dr^2} + \frac{2}{r}\frac{d\Phi(r)}{dr} - \frac{1 - k_\infty}{L_c^2}\,\Phi(r) = 0$$

In this particular case, the solution of this equation is of exponential type:

$$\Phi(r) = A\frac{e^{-\kappa r}}{r} + C\frac{e^{\kappa r}}{r}$$

where

$$\kappa = \sqrt{\frac{1 - k_\infty}{L_c^2}}$$

with $1 - k_\infty > 0$

The coefficient $C$ must obviously be equal to zero; otherwise the flux would become infinite as $r \to \infty$ .

Using the Fick's law, we can write that:

$$J = -D\frac{d\phi(r)}{dr} = DAe^{-\kappa r}\frac{1+\kappa r}{r^2}$$

and so, as

$$Q = \lim_{r\to 0} 4\pi r^2 J$$

we have

$$Q = \lim_{r\to 0} 4\pi r^2 \; DAe^{-\kappa r}\frac{1+\kappa r}{r^2}$$

$$A = \frac{Q}{4\pi D}$$

The final solution will be thus of the following type:

$$\Phi(r) = \frac{Q}{4\pi D r}e^{-\kappa r}$$

Where $Q$ is the source strength in neutron/s. As it is possible to see analysing this expression, the most important characteristic of an intrinsic subcritical system is the exponential decrease of the flux as a function of the distance from the source. In case of a non-point type source, this behaviour will be valid at enough distance from the source.

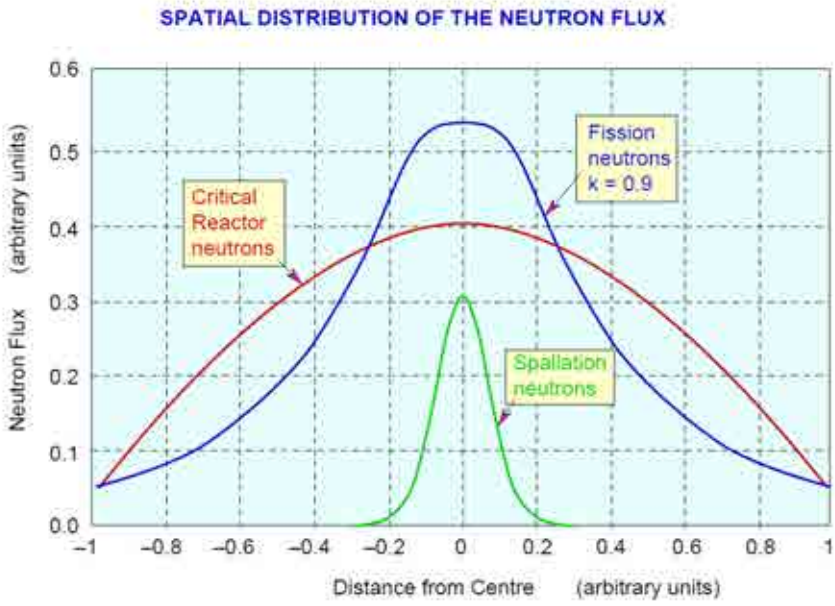


*FIG. 2.8. Typical spatial distribution of the neutron flux of critical reactors and ADS.*

## 2.7. ENERGETIC CONSIDERATIONS

Unlike critical reactors, which can be operated at any power that can be safely removed, the power level in ADS is related to the proton current $i$. In the subcritical core, the number of secondary fission reactions can be easily expressed as follow:

$$N_f = N_0\frac{k}{1-k}\frac{1}{v}$$

Hence, expressing the number of neutrons generated by the neutron source as function of the proton current $i$ and spallation neutrons yield $v_{sp}$, the power generated can be written as follow:

$$P_{el} = \frac{i\upsilon_{sp}\varphi^* k_{eff}}{1 - k_{eff}} \frac{1}{\upsilon} E_f$$

Where $E_f$ is the energy generated per fission, $i$ the proton current, $\upsilon$ the number of neutrons produced in fission and $\upsilon_{sp}$ the number of neutrons produced in spallation.

It is interesting to give an expression of the energetic cost of the accelerator, which power is defined as follow:

$$P_{acc} = \frac{E_p i}{\eta_{acc}}$$

Where $E_p$, is the energy of the incident proton. Hence, the ratio between the electric power output of the ADS and the power needed by the accelerator is:

$$\frac{P_{acc}}{P_{el}} = \frac{\frac{E_p i}{\eta_{acc}}}{\eta_{el} P_{tot}} = \frac{1}{\eta_{acc}\eta_{el}} \frac{E_p i}{P_{tot}} = \frac{1}{\eta_{acc}\eta_{el}} \frac{E_p}{P_{tot}} \frac{P_{tot}(1 - k_{eff})\upsilon}{\upsilon_{sp}\varphi^* E_f k_{eff}} = \frac{1}{\eta_{acc}\eta_{el}} \frac{E_p(1 - k_{eff})\upsilon}{\upsilon_{sp}\varphi^* E_f k_{eff}}$$

and

$$\frac{P_{acc}}{P_{el}} = \frac{1}{\eta_{acc}\eta_{el}} \frac{E_p}{\upsilon_{sp}\varphi^* E_f} \mu_{eff}$$

or

$$\frac{P_{acc}}{P_{el}} = \frac{1}{\eta_{acc}\eta_{el}} \frac{E_p}{E_f} \frac{\mu_{src}}{\upsilon_{sp}}$$

If we call $f = \frac{P_{acc}}{P_{el}}$, it is interesting to have a discussion about the factor $f$.

— If $f < 1$: the system produces more energy than the accelerator consumption. It is the favourable case;
— If $f = 1$: the all energy freed by the core of the reactor returned to the accelerator;
— If $f > 1$: the accelerator consumes more energy than what the reactor can provide.

## 2.8. REFERENCES TO CHAPTER 2

[2.1] KADI, Y., REVOL, J.P., Design of an Accelerator Driven System for the Destruction of Nuclear Waste, Lectures given at the Workshop on Hybrid Nuclear Systems for Energy Production, Utilisation of Actinides & Transmutation of Long lived Radioactive Waste Trieste, Italy, 3–7 September 2001.

# CHAPTER 3
# ADS CONCEPTS

Since the early 1990s the international scientific community has begun to consider the ADS as a concept suitable to be developed to properly demonstrate its potential to address the HLW issue. Several basic research programmes have been launched, leading to the definition of possible conceptual alternatives and to the related investigation of technological issues.

R&D programmes addressing conceptual and more detailed ADS designs have been carrying out in Europe, Japan, Republic of Korea and USA. The section 3.1 presents the ADS concepts conceived worldwide as demonstration plants, whilst section 3.2 provides a summary of the design of proposed industrial scale ADS.

The situation pictured in this chapter represents the status at the end of 2009. Progress has been obtained since then and new projects and/or developments have been made. When appropriate, a short description of this evolution will be made.

## 3.1. DEMONSTRATION ADS

### 3.1.1. EAP80-Italian XADS

One of the first ADS concept presented in 1993 to the international attention was the EA [3.33], an innovative and in principle inherently safe ADS plant, conceived by Prof. C. Rubbia and his staff at CERN (Geneva, Switzerland), also providing evidence of the key features through FEAT and TARC experiments.

Starting from 1996, a growing interest on the EA has taken place in Italy and has given origin to several basic R&D activities and to an industrial programme involving ENEA (the Italian national research body for New Technologies, Energy and the Environment), INFN (the Italian national research institute for nuclear physics), CIRTEN (Inter University Consortium for Technological Nuclear Research) and industrial partners as Ansaldo Nucleare, CRS4 and SIET. The final outcome of this CERN–Italian effort is commonly referred as the Reference Configuration of the ADS Experimental Facility (namely, XADS or EAP80) which evolution was the European PDS-XADS project described in section 3.1.2. In this section a summary of the XADS reference configuration which is based on the Energy Amplifier concept developed at CERN, is illustrated.

As further described below, a hybrid reactor consists of a subcritical core reactor coupled to an ion beam accelerator. A subcritical core cannot sustain by itself the neutron chain reaction, but needs an external neutron source. The ion beam from the accelerator, injected into a heavy metal target located inside the subcritical core, produces the required neutron source, via spallation reactions. These reactions occur when accelerated (very energetic) light ions interact with heavy nuclei (lead, lead-bismuth, mercury, tungsten, or even uranium), leading to the emission of a large number of neutrons. In the case of the EA, the hybrid reactor concept proposed by CERN [3.1] and at the base of the XADS, accelerated protons interact with molten lead, which, besides being the target, is also used as the primary coolant. Subcritical systems do not rely on delayed neutrons for control or power change; they are only driven by the ion beam coming from the accelerator. Control rods and reactivity feedback have very little or no importance: subcritical systems are decoupled from the external neutron source.

The features and associated working principles of the reference configuration of the XADS are listed as follows:

— Simple primary system layout. The reactor assembly presents a simple flow path of the primary coolant with a riser and a downcomer. The heat source (the core), located below the riser, and the

heat sink (IHX) at the top of the downcomer, allow an efficient natural circulation of the coolant. The additional means provided to enhance the primary coolant flowrate is not a mechanical pump, but bases on the principle of gas lifting: Argon of the cover gas plenum is injected into the bottom of the riser and generates the gas-coolant mixture that, being lighter than coolant alone in the downcomer, keeps the coolant circulating at a higher flowrate, the level of which can be controlled by the amount of gas injected [3.2].

— Consequent to the elimination of the mechanical pump and to the natural circulation configuration of the primary circuit, there is assurance of no high speed of the coolant, not even across the smallest cross-sectional areas of the flow path. This technological option helps to reduce the erosion–corrosion of the structural material brought about by flowing LBE, and creates a large gas bubbles to primary coolant interface area for faster reaching the equilibrium dissolution of atomic oxygen in the LBE.

— All primary coolant remains inside the reactor vessel, including the coolant that circulates through the LBE purification unit, which is immersed in the reactor pool;

— Use of LBE as the primary coolant, to exploit its low melting point, and to allow a relatively low operating temperature, in order to eliminate risks of creep damage of the reactor structures and to reduce their corrosion rate;

— Use of an organic diathermic fluid as the secondary coolant with low vapour pressure and chemically inert against the primary coolant;

— Components and construction materials of proven technology;

— Removable main components (intermediate heat exchangers, fuel handling machines, target unit);

— Accelerator design compatible with the XADS construction timetable.

Fig. 3.1 and Fig. 3.2 show, respectively, the general arrangement and the reactor assembly of the reference configuration of the XADS.

The mission of the XADS can be summarized as follows:

— To demonstrate the operability of an accelerator-spallation target-fission reactor complex at a significant power level;

— To confirm the capability to reduce the inventory of Pu and the remaining transuranic actinides;

— To assess the ability to transmute selected long lived fission fragments;

— To test the operation and performance and to provide the qualification of innovative fuels and fuel cycles.

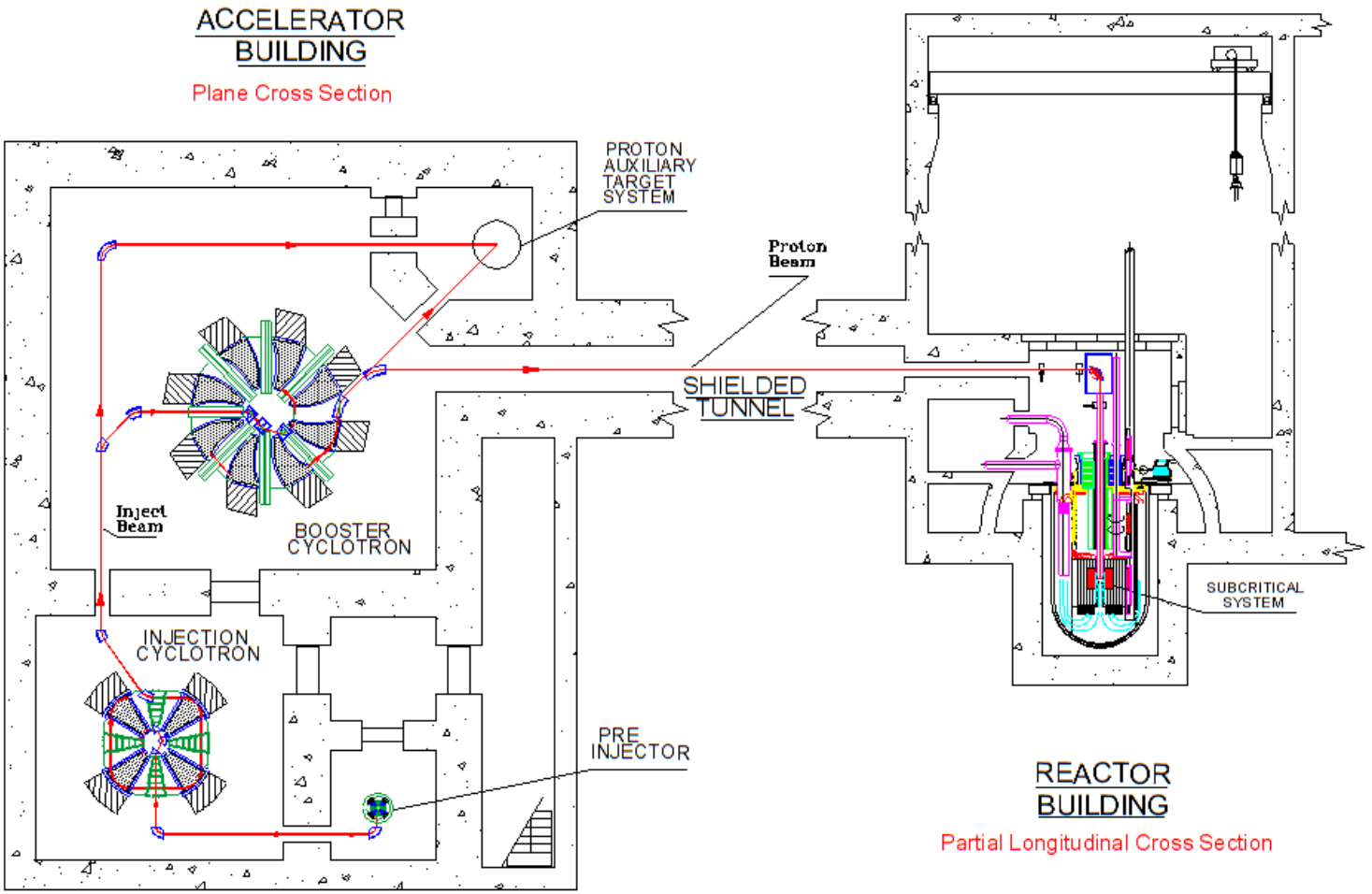


*FIG. 3.1. XADS Reference configuration (general arrangement).*

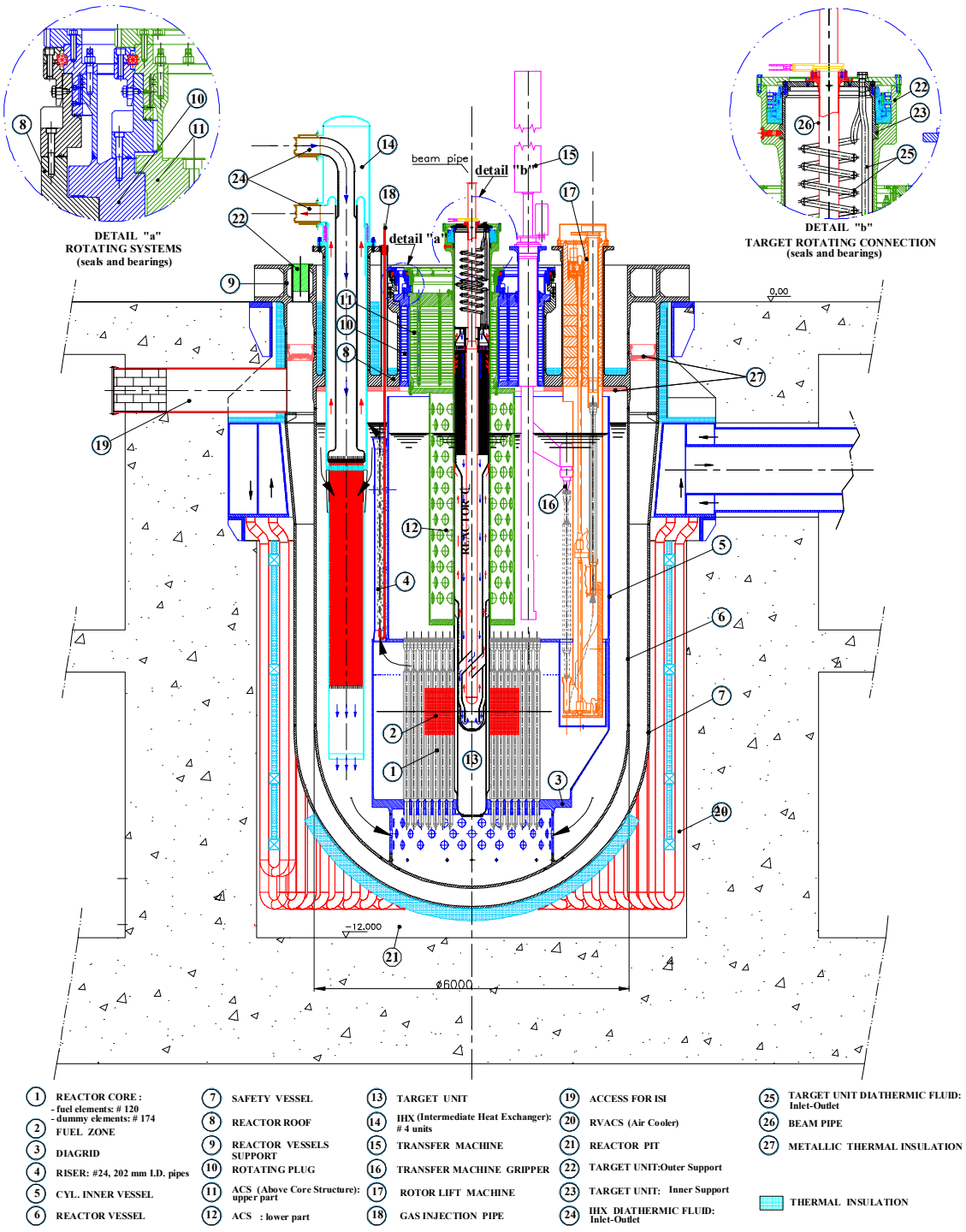


*FIG. 3.2. XADS Reference configuration (reactor assembly).*

The use of a cyclotron Accelerator System allows producing the medium to high energy proton beam required to obtain the specified yield of neutrons, while keeping its dimensions reduced to fit into the compact XADS plant layout. This, however, implies the possibility of upgrading existing accelerators, such as that at the PSI of Zurich.

To the purpose, the INFN-LNS of Catania has carried out an exploratory study of an accelerator system based on a fairly compact cyclotron. This work has screened a two machines system, operating

in series, capable to supply a proton beam of around 3 MW power, sufficient to sustain the XADS (Fig. 3.1). This system has been focused on extrapolation of the present uprating project of the PSI proton accelerator facility. Based on a three stages system (pre injector, injection cyclotron, booster cyclotron), it will be capable to supply a proton beam output with maximum energy of around 600 MeV and up to 5–6 mA maximum nominal current. Such proton energy and proton beam currents allow to operate an 80 MW(th) subcritical reactor within a range of multiplication coefficient consistent with maintaining subcriticality, with adequate margin, both during operation at power and following foreseeable transient and accident conditions.

The first stage, made of a proton source (100 KeV) coupled to a small cyclotron, supplies a low energy pre-injection beam (5.5 MeV) to an intermediate separated sectors cyclotron (second stage) which accelerates the protons to an energy of around 100 MeV and gives them over to a ring cyclotron (third stage) which boosts the beam up to the final energy of 600 MeV (Table 3.1).

TABLE 3.1. PARAMETERS OF THE CYCLOTRON

| | | | |
|---|---|---|---|
| Compact injection cyclotron (first stage) | | | |
| Injection energy | 100 keV | Extraction energy | 5.5 MeV |
| First orbit radius | 5.5 cm | Extraction radius | 41 cm |
| Number of sectors | 4 | Harmonic mode | h=4 |
| Sector width | 40° | $B_{hill}$ | 1.5 T |
| Sector gap | 45 mm | Ampere turns | 130000 |
| Energy gain /turn | 400 keV | Turns separation | 15 mm |
| $\Delta\varphi_{ext}$ | 20°÷10° | Momentum spread δP/P | ± 0.2÷0.1% |
| Yoke radius | 75 cm | Weight | 20 Tons |
| Intermediate separated sector cyclotron (second stage) | | | |
| Injection energy | 5.5 MeV | Extraction radius | 3.3 m |
| Injection radius | 0.82 m | Harmonic mode | h=8 |
| Number of sectors | 4 | Spiral angle | 0° |
| Sector width | 30° | $B_{hill}$ | 1.2 T |
| Sector gap | 35 mm | Turns separation | 20 mm |
| Energy gain /turn | 1.4 MeV | Energy spread | ± 0.15% |
| $\Delta\varphi_{ext}$ | 10° | Total weight | 700 Tons |
| Extraction energy | 100 MeV | | |
| Ring cyclotron (third stage) | | | |
| Injection energy | 100 MeV | Beam power | 2950 kW |
| Beam current | 5 mA | Extraction radius | 4.45 m |
| Injection radius | 2.45 m | Harmonic mode | h=6 |
| Number of sectors | 8 | RF frequency | 50.6 MHz |
| Number of cavities | 6 | Spiral angle | 35° |
| Sector width | 18° | $B_{hill}$ | 2.09 T |
| Sector gap | 50–90 mm | Turns separation | 11÷15 mm |
| Energy gain /turn | 4÷5.3 MeV | Energy spread | 0.2% |
| $\Delta\varphi_{ext}$ | 10°–15° | Total weight | 2000 Tons |
| Extraction energy | 590 MeV | | |

Whereas the final energy level is quite similar to the current PSI and other facilities design, the proton beam current, which is requested for adequately feeding the spallation source in the XADS core, requires substantial changes to the architecture of the ring cyclotron. The main changes proposed

require the augmentation of the number of the RF acceleration cavities and the increase of their maximum operating voltage.

The high beam current required constitutes the principal upgrading problem for an accelerator system, due to the substantial expansion of the space charge effects. In the case of a cyclotron, this requires a wider separation of the proton revolution orbits (also necessary for extracting the beam at the outer orbit with minimum loss and damage-activation) with a consequent reduction of the turns number and the need of higher acceleration voltages in the cavities.

Because of the practical limit of the voltage of around one million volts, it is necessary to increase the number of the cavities. For the XADS case, it has been deemed sufficient to add two more cavities, thus employing six cavities in comparison with the four of the PSI reference. The six cavities, operating at 50 MHz (harmonic mode six, as the PSI ones), are accommodated between the eight magnetic sector poles which shape and spatially tune the isochronous cyclotron magnetic field, in order to maintain the revolution orbits of the proton beam bunches in phase with the RF applied at the cavities.

The final beam energy and the magnetization saturation limits of the material utilized for the normal conductive magnetic pole sectors concur to define a booster ring of about 15 m diameter.

The beam transport lines, both from the intermediate and the booster machines, can be bypassed to a secondary line which heads to a beam dumping device. This is necessary in order to allow decoupling of the accelerator system from the reactor during the tuning tests of the proton beam at startup.

The spallation neutrons are generated in the liquid LBE target, which constitutes the connection of the accelerator system to the subcritical core. There are four main constraints to be complied with, while engineering this connection:

- The proton beam must travel in vacuo;
- The proton beam must impinge on the target at or near the centre of the core;
- The power generated by the spallation reactions must be removed, without overheating LBE or interposed structures;
- The radioactive elements produced in the LBE by the spallation reactions must be kept confined.

The LBE melt containing the spallation products is kept confined within a structure called target unit (or spallation module), in order to prevent the contamination of the primary LBE coolant. The target Unit has been designed as a removable Unit, because its service life is anticipated to be shorter than the reactor lifetime, owing to the intense irradiation and local high thermal stresses. The target unit is a slim component of cylindrical form, positioned coaxially with the reactor vessel and hung from the above core structure. Because it serves also as inner radial restraint of the core, the outline of its shell fits the inner outline of the core. Its component parts are the proton beam pipe, the heat exchanger and the LBE circulation system, which can be designed in forced or natural circulation, depending on the design option.

Two target unit options have been designed for the XADS. Both options present the target at the centre of the core, but they differ in the target to the proton beam pipe interface principle.

The hot window target unit features a thin metallic sheet, called hereinafter the hot window (i.e. proton beam entrance) or more simply the Window, as a barrier between the liquid target and the proton beam vacuum pipe (Fig. 3.3). The window (and by extension also most of the target unit) is made of ferritic martensitic 9Cr1Mo, a steel chosen to withstand the severe duty cycle, that encompasses thermal and pressure loads, ageing by the intense proton–neutron irradiation and erosion–corrosion by the flowing LBE melt. In particular this material is a good choice among the available steels, according to the following list of favourable properties:

- Low density;
- High thermal conductivity;
- Low thermal expansion coefficient;

— High tensile strength;

— Good fracture toughness;

— Low DBTT (ductile to brittle transition temperature);

— Corrosion resistance to LBE exposure;

— Low susceptibility to proton–neutron radiation damage.

These properties are temperature dependent. For instance, tensile strength and corrosion resistance decrease with temperature, while fracture toughness improves with temperature.

The heat generated by the spallation reactions is removed by natural convection. The LBE recirculates from the heat source to the heat exchanger located at a higher level, an arrangement typical of natural circulation cooling circuits.

A stable, properly directed natural circulation of the target LBE is possible also when the accelerator is off, owing to the crosswise arranged flow path from inner to outer annulus and *viceversa*, provided at the bottom of the target unit and illustrated by the arrows in Fig. 3.3. With the reactor in hot shutdown and the target unit cooling circuit in operation, the primary coolant at 300°C, as a distributed heat source, heats up the LBE in the outer annulus. The cold flow in the downcomer is diverted by baffles from the inner annulus to the outer annulus The LBE of the Target, in turn, by mean of intermediate heat exchanger, placed in the upper part of the Target, transfer the heat to a cooling circuit filled with organic diathermic fluid which is back cooled by water. The cold flow in the downcomer is diverted by baffles from the inner annulus to the outer annulus in the bottom part of the target unit. With the onset of natural circulation, effective cooling of the window takes place from the very beginning of the spallation reactions.

The use of a diathermic fluid gives higher flexibility in the choice of the thermal cycle of the target LBE and allows remaining below 500°C at the hottest spot of the window.

In the ***windowless target unit*** option the proton beam impinges directly on the free surface of the liquid LBE target. In this case a natural circulation pattern in the cooling circuit is no longer possible, because the heat source near the free surface of the LBE is at a higher level due to the vacuum in the proton beam pipe. Thus the hotter LBE must be driven downwards to the heat exchanger by some means, in this case a dedicated gas lifting system. A stream of primary LBE is diverted from the cold plenum to the heat exchanger to serve as a cooling medium.

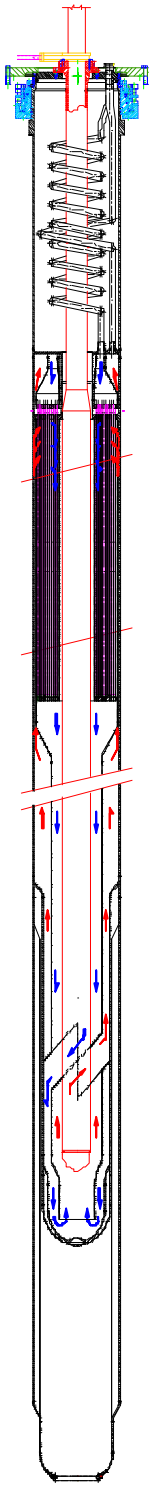

*FIG. 3.3. The hot window target unit.*

In the windowless target unit no structural material is exposed to the direct proton irradiation. This option has the advantage of overcoming issues related to material structural resistance, but presents issues related to the proton beam impact area, flow stability and evaporation of LBE.

The earlier axisymmetrical design of the free surface has been disregarded because tests in water have substantiated the risk of stagnation about the coalescence zone.

The alternative design currently being developed (Fig. 3.4) features an asymmetric free surface and offset downcomer.

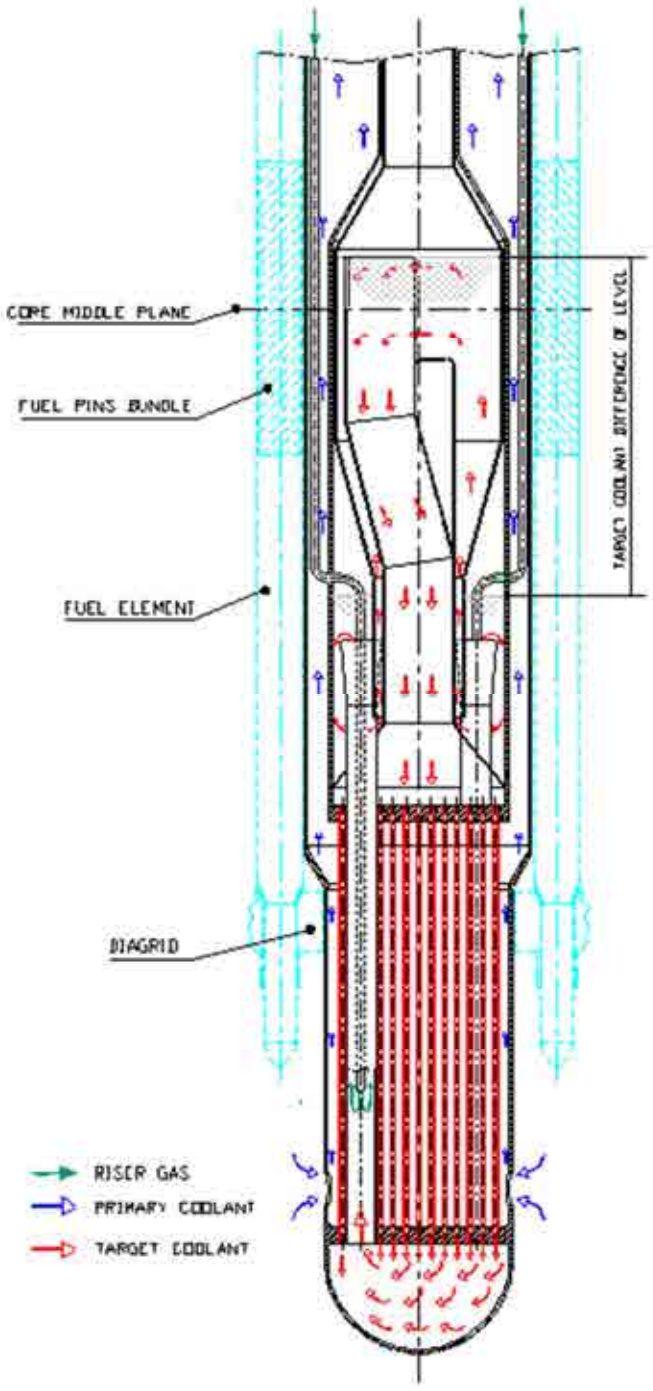


*FIG. 3.4. The windowless target unit.*

The core layout is shown in Fig. 3.5 and Fig. 3.6. The fuel subassemblies are arranged in an annular array of five rounds, the circumscribed and inscribed circles of which have diameters 183 cm and 58 cm respectively. The outermost round is only partially filled by six peripheral couples that have been added to reach the specified core reactivity and to provide smoothening of the radial power peaking. The total number of fuel subassemblies amounts to 120. The active core height is 870 mm with 23.25% uniform Pu enrichment.

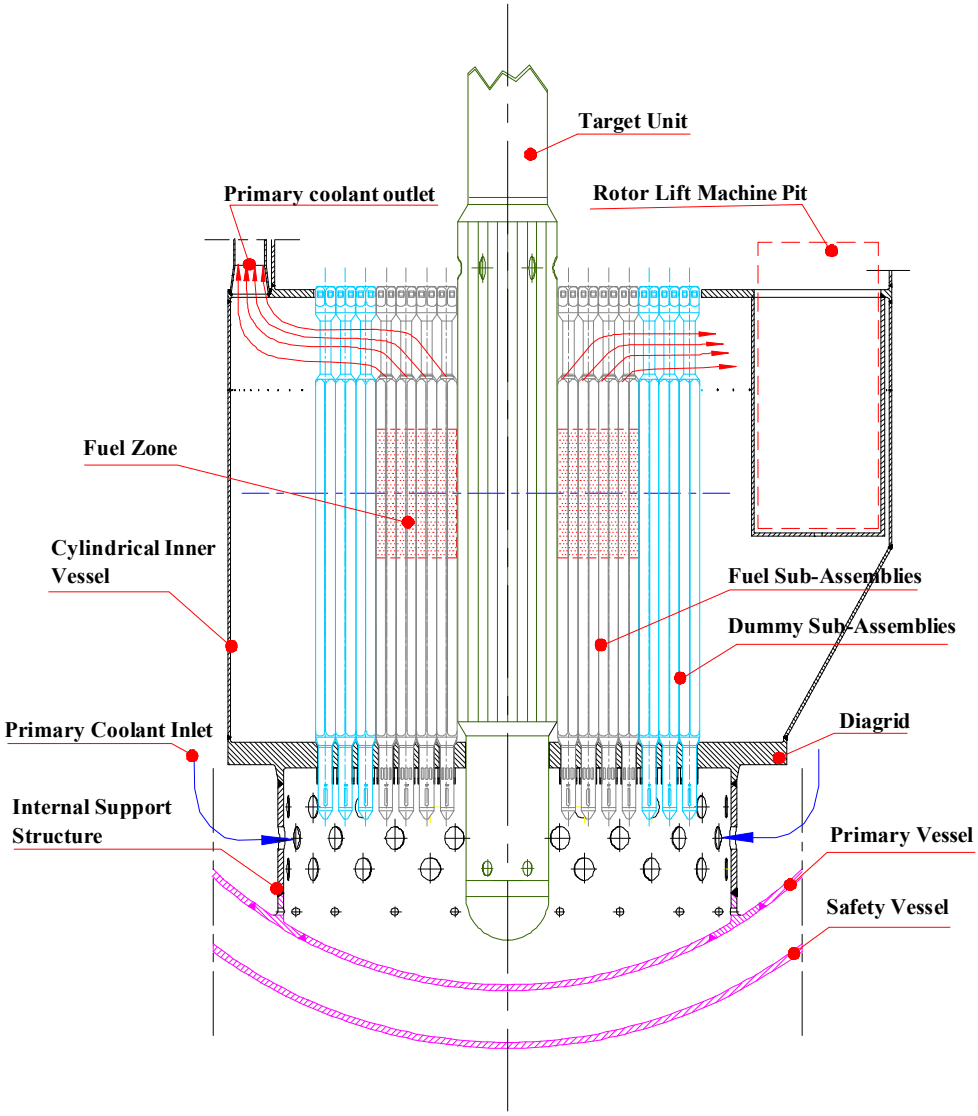


*FIG. 3.5. Core region vertical section.*

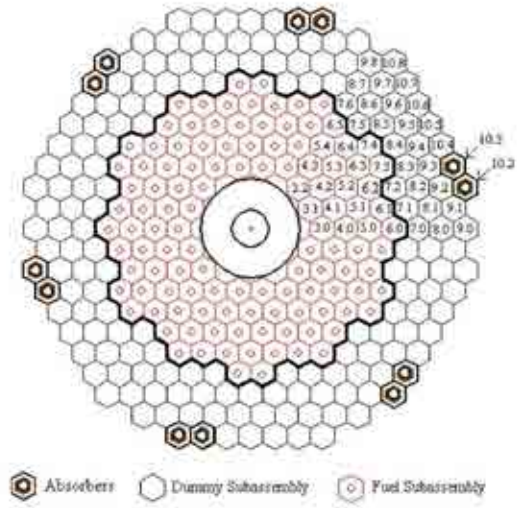


*FIG. 3.6. XADS Core cross-section.*

The core is surrounded by a region of three filled in rows of dummy subassemblies, the circumscribed circle of which has 267 cm diameter, plus one partially filled inner round (the complementary subassemblies of this round are the peripheral fuel subassemblies of the outermost round of the core). The dummies have the same hexagonal cross-section as the fuel, but are empty duct structures.

This design choice allows to:

— Create a buffer region, which keeps the fixed internal structures away from the high, fast neutron flux, in order to protect them from suffering excessive radiation damage;

— Mechanically couple the core, through the subassemblies handling heads, with the core radial, outer restraint plate.

It offers:

— Continuous fast to thermal neutron flux region, useable to fission minor actinides and transmute selected long lived fission fragments, particularly where the neutron energy corresponds to the resonance absorption of the waste, thus maximizing the incineration yield;

— Adequate mass of LBE surrounding the core, to exploit the reflecting capability of LBE for improving neutron economy and flattening the flux profile;

— Flexibility of initially operating the XADS with a proven core and later converting to a core tailored for burning Pu and radioactive waste, after irradiation test results provide sufficient confidence.

The core radial inner restraint is ensured by the target unit, the cylindrical shell of which has been designed to fit its inner outline.

There are no absorbers subassemblies dispersed in the core during normal operation. There is, however, a set of 12 absorbers, which are kept parked, during operation, at the periphery of the buffer region. At scheduled outages, these absorbers will be moved close to the core by means of the in vessel handling machine, before extraction of the Target Unit. This allows to compensate for any reactivity insertion brought about by the extraction and to maintain the core at safe shutdown with the subcriticality required during refuelling ( $k_{eff} \leq 0.95$ ). A suitable absorbers management strategy would also allow the possibility to control the excess reactivity at BOL of prospective core designs.

The main design objective for the XADS core is the twofold demonstration that, when coupled to the accelerator, it can generate the rated power of 80 MW(th) while remaining subcritical with adequate margin, and it is designed consistently with a natural circulation primary coolant circuit, so that decay heat can be removed by natural convection.

The former objective has been achieved with the maximum effective $k_{eff} = 0.97$ at BOL and full power, that ensures safety over core lifetime in any occurrence, including accident conditions, without control and shutdown rods and taking into account the positive reactivity feedback accompanying core cooling from full power to zero power at 20°C (corresponding to $k_{eff} = 0.984$).

The second objective has been achieved by the combination of low power density and less than 25 kPa pressure loss at full power, a figure that is made possible because the LBE coolant does not require a close packed pin lattice (for comparison, it is less than one tenth the pressure loss of sodium cooled cores).

The main core parameters are listed in Table 3.2–Table 3.6.

TABLE 3.2. XADS MAIN CORE PARAMETERS

| Parameter | Unit | Design value |
|---|---|---|
| Nominal thermal power | MW(th) | 80 |
| Target cavity rows equivalent [1] | No. | 2 |
| Core annulus, inscribed circle diameter | mm | 577 |
| Core annulus, circumscribed circle diameter | mm | 1828 |
| Fuel subassembly rows | No. | 5 |
| FSA's in the partially filled 5$^{th}$ row, by couples | No. | 6 |
| Total fuel subassemblies | No. | 120 |
| Total number of fuel pins | No. | 10.800 |
| FSA's pitch | mm | 137.6 |
| FSA–FSA gap | mm | 4 |
| TRU (Pu plus MA) enrichment | at% | 23.25 |
| Loaded fuel mass | tonnes | 3.24 |
| Core equivalent outer diameter | mm | 1703 |

TABLE 3.3. XADS MAIN CORE PARAMETERS

| Parameter | Unit | Design value |
|---|---|---|
| *Fuel assembly* | | |
| Wrapper thickness | mm | 2.0 |
| Wrapper across flats | mm | 133.6 |
| Wrapper to pin cluster gap | mm | 2.5 |
| Fastening bar diameter | mm | 11 |
| Outline length of the assembly | mm | 3600 |
| Number of fuel pin rows | | 5 |
| Fuel pin pitch | mm | 13.4 |
| Fuel pin per assembly | | 90 |
| MOX fuel mass | kg | 30.4 kg |
| *Fuel Pin* | | |
| Outer cladding diameter | mm | 8.50 |
| Cladding thickness | mm | 0.565 |
| Fuel pellet outer diameter | mm | 7.14 |
| Fuel pellet inner diameter | mm | 1.8 |
| Fuel pellet density | g/cm$^3$ | 10.35 |
| Fuel clad diam. gap | mm | 0.23 |
| Active length | mm | 870 |
| Fill gas | | He |
| Fill gas pressure | Pa | 101,325 |
| Upper plenum height | mm | 162 |
| Lower plenum height | mm | 150 |
| Fuel weight, av. | g | 337.8 |
| Outline pin length | mm | 1272 |

Each fuel subassembly contains a 90 pin gridded bundle partially evolved from the SPX 2$^{nd}$ reload fuel.

[1] Does not include the central position

The fuel cladding is 8.5 mm nominal outer diameter and the material 9Cr-1Mo ferritic–martensitic, high chromium alloy steel.

Starting at the bottom end closure, the first section of 150 mm length forms the fission gas lower storage plenum. Inside the plenum a stainless tube provides the support for the fuel stack.

The fuel comprises an 870 mm long stack of annular pelleted mixed oxide ($UO_2$-$PuO_2$) fuel at a nominal smear density of 95% theoretical density. On both ends of the fuel stack a 15 mm thick layer of depleted uranium oxide serves as thermal shielding.

The last section of cladding of 162 mm length forms the upper gas storage plenum. A fuel stack retaining spring is inserted in the plenum to prevent axial movement of the fuel during pre-irradiation handling. The pins are evacuated and filled with helium at nearly the atmospheric pressure. A complete pin has an overall nominal length of 1272 mm.

The final length of the gas plena, and hence of the pin, may be revised to a shorter length, if sizing is based on the amount of gas released at the design burnup, that is set substantially lower than usual for fast reactors.

The fuel pin bundle is contained within a hexagonal wrapper tube. The top of the wrapper tube is welded to the handling head assembly and the bottom to the spike assembly. The overall length of the subassembly is 3600 mm, and the external across flats size is 134 mm. The pitch between adjacent subassemblies is 138 mm.

The fuel subassembly is anchored to the diagrid by means of a locking device, because of the net upward force acting upon it.

TABLE 3.4. CORE MAIN THERMALHYDRAULIC PARAMETERS — NOMINAL CONDITIONS

| Parameter | Unit | Design value | |
|---|---|---|---|
| Subassembly power, av. | MW | 0.667 | |
| LBE core mass flowrate | kg/s | 5460 | |
| LBE temperature at core inlet | °C | 300 | |
| LBE temperature at core outlet | °C | 400 | |
| Average fuel power density | $W/cm^3$ | 227 | |
| Average pin surface heat flux | $W/cm^2$ | 31.9 | |
| Average linear power | W/cm | 85.2 | |
| Hottest fuel subassembly | | BOL | EOL |
| Mass flow rate | Kg/s | 44.2 | 44.2 |
| Power | MW | 0.841 | 0.888 |
| Av. coolant outlet temperature | °C | 429.8 | 437.3 |
| Power in the hottest pin | W | 10246 | 11082 |
| Max. temperature of the hottest subchannel | °C | 489 | 504 |
| Coldest sub-channel outlet temperature | °C | 416 | 423 |
| Max. ΔT between the two subchannels | °C | 73 | 81 |
| Max. clad temp. of the hottest pin | °C | 514 | 530 |

The configuration of the primary system is pool-type, similar to the design solution adopted for most sodium cooled reactors (Fig. 3.1, Fig. 3.2 and Fig. 3.7). This concept permits to contain all the primary coolant within the reactor vessel, thus eliminating all problems related to the out-of-vessel transport of the primary coolant.

TABLE 3.5. MAIN NUCLEAR FUNCTIONAL PARAMETERS

| FUNCTIONAL PARAMETERS | BOL | EOL |
|---|---|---|
| Proton energy (MeV) | 600 | 600 |
| Neutrons < 20 MeV, per proton | 13.85 | 13.93 |
| Spallation neutron multiplication (M) | 34.13 | 14.76 |
| Multiplication factor with external source (k) | 0.971 | 0.936 |
| I (mA) | 2.48 | 5.67 |
| $k_{eff}$ | 0.972 | 0.937 |
| Burnup (MWd/kgHM) | - | 22.30 |
| Total peaking factor, $F_Q$ | 1.80 | 1.97 |
| Enthalpy rise hot channel factor, $F_{\Delta H}$ | 1.15 | 1.17 |
| Core radial hot channel factor, $F^n_r$ | 1.30 | 1.37 |
| Fuel Subassembly hot channel factor, $F_a$ | 1.10 | 1.12 |

The primary coolant is molten LBE, which is characterized by good nuclear properties, operating temperatures lower than molten lead alone and compatibility with the organic secondary coolant.

The pool design has important beneficial features, verified by the experience of design and operation of sodium cooled fast reactors. These include a simple low temperature boundary containing all primary coolant, the large thermal capacity of the coolant in the primary vessel, a minimum of components and structures operating at the core outlet temperature. Whenever the sodium experience did not appear applicable to the specific tasks of the LBE cooled XADS, however, solutions have been worked out, that, though being innovative in the nuclear field, are not new to the industrial practice. It is the case of the primary coolant circulation as illustrated here below.

The primary coolant of XADS circulates in enhanced natural circulation, and precisely 5/6th the driving head required to maintain the nominal flowrate at the full power is provided by gas injection into the riser and 1/6th by the thermal density difference between Riser and cold leg inside the IHX. This solution combines the high level of reliability required by the Core cooling safety related function with the advantages of reactor compactness, operational flexibility, and the lower thermal loading on the structures typical of the forced circulation. Pumping of fluids by gas lifting is a standard practice in the industry, whenever the installation of a mechanical pump is not practical.

The natural drought shall not be underestimated, however, because it ensures the flowrate required to keep the core cooled at shutdown with no gas injection. This natural circulation capability has been made possible by the low pressure loss design of core and IHX. While the natural circulation alone can provide decay heat removal for unlimited time with the reactor at shutdown, with reactor at power, the associated increase of hot collector temperatures can be accepted for a limited time.

The LBE coolant leaving the core discharges into the hot plenum above and enters the 24 vertical pipes which make up the riser. Reactor cover gas is fed by a compressor via submerged spargers into the bottom part of each riser pipe and generates a LBE gas mixture two phase flow that, being lighter than LBE alone in the downcomer by the amount corresponding to the mean void fraction in the riser, creates the additional driving force for the nominal coolant flow rate.

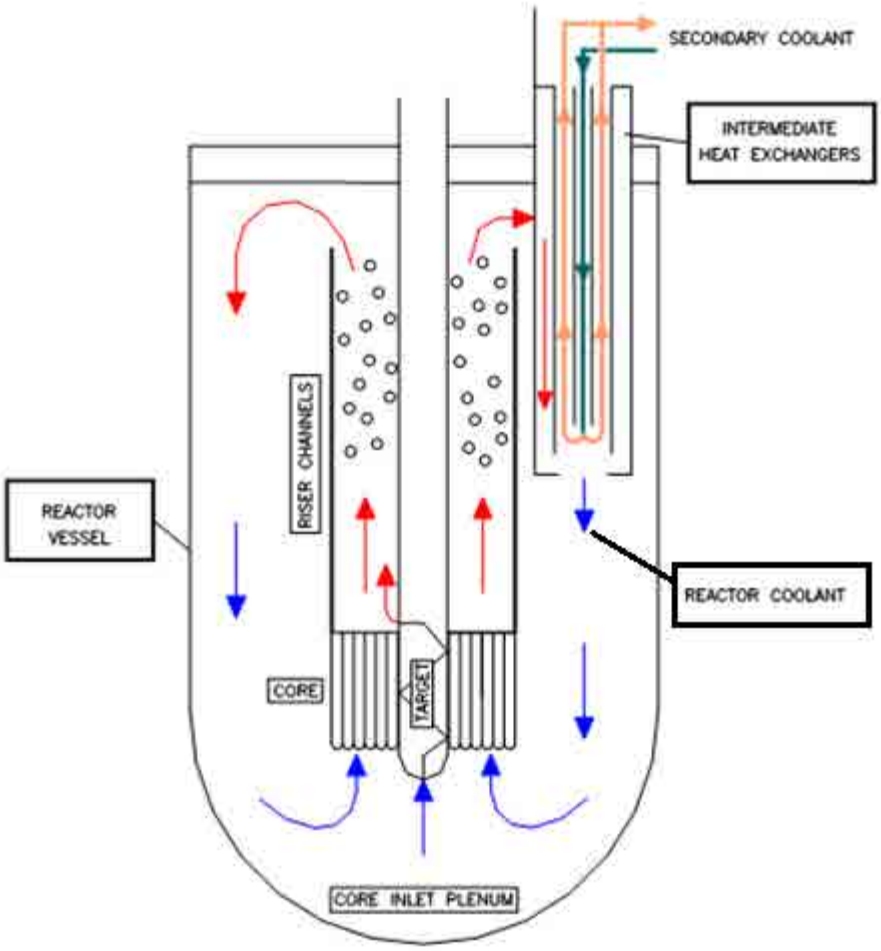


*FIG. 3.7. Primary system process scheme.*

At the top of the riser, but still underneath the LBE free level, the mixture slows down until LBE reverses its velocity and flows downwards along the annular downcomer where it is cooled by the IHXs. The gas cannot follow the path of the LBE, because buoyancy prevails over entrainment, and separates at the interface with the cover gas plenum, thereby closing the gas loop.

The IHXs are freely immersed in the Downcomer, without membrane spanning the vessel to separate hot and cold plena (no Redan). The percentage coolant flowrate that flows through the IHXs depends on the relative weight of the cold leg inside the IHXs with respect to the corresponding hot leg outside, and precisely it is determined by the equilibrium between the weight difference of the two legs (driving force) and the pressure loss through the IHXs (the friction in the downcomer outside the IHXs is negligible). At steady state and full power, a thermal stratification establishes in the downcomer, with an upper temperature of slightly less than 400°C (hot pool mixed mean temperature) and an axial gradient to 320°C at the lower edge of the IHXs shell.

The stratification is brought about by the heat exchange across the IHX shell, the hot inner vessel and by IHXs and inner vessel bypass flows. In particular, the properly designed bypass flow recirculating across the inner vessel fulfils the twofold purpose of stabilisation of the thermal stratification and determination of its profile shaped as a gentle transition to the cold plenum temperature, thereby avoiding excessive thermal stresses in the adjacent structures (reactor vessel and inner vessel including the upper core restraint plate).

All structures and components of the primary circuit are fabricated from type AISI 316L stainless steel with the exception of the reactor roof, the guard vessel and the upper part of the ACS which are AISI 304. Developments in size of the target unit, rotating plug, IHXs and other auxiliary equipment

have resulted in a design having a vessel of 6.0 m diameter and 11.1 m depth with a LBE inventory of about 1900 tonnes.

The lift gas is kept circulating by the primary cover gas system in a loop, that is laid out outside the reactor vessel and is subdivided into an atmospheric pressure section and a pressure section.

More precisely, the atmospheric pressure argon of the cover gas plenum is fed through a two stage condenser, where it is cooled down to compressor gas intake temperature and purified of any volatile polonium compounds or trace contaminants evaporated from the melt. Before reaching the suction nozzle of the reciprocating compressor, the gas is passed through a filter for removing any remaining dust. Hydrogen and water steam sampling and injection lines are branched off the 50 mm pressure piping and connected to the control unit of the oxygen activity, where hydrogen in argon can be measured at concentration levels down to tenths of ppm.

The 4-bar pressure argon is fed to each riser pipe via ½" injection lines branched off a manifold. The gas loop is normally disconnected from any supply of make-up gas so that the cumulated amount of gas in the reactor gas plenum and in the loop is constant and any accidental overpressurization of the reactor vessel is prevented by design. Provisions are also available for first argon filling up and for massive hydrogen gas injection into the bottom of the reactor vessel, for the occasional cleaning by reduction, at reactor shutdown, of any thick oxide layer on the heat transfer surfaces. Table 3.6 provides the main reactor operating parameters.

TABLE 3.6. XADS REACTOR COOLANT SYSTEM OPERATING PARAMETERS

| Operating Parameter | Unit | Value |
|---|---|---|
| Nominal core inlet temperature | °C | 300 |
| Nominal core outlet temperature | °C | 400 |
| IHX secondary coolant inlet temperature | °C | 280 |
| IHX secondary coolant outlet temperature | °C | 320 |
| Primary coolant flow rate | kg/s | 5961 |
| Core flow (enhanced circulation) | kg/s | 5471 |
| Coolant velocity through core (enhanced circulation) | m/s | ~ 0.42 |
| Argon injection flow rate | N-liters/s | 120 |
| Argon injection pressure (enhanced circulation) | Pa | ~ 5E5 |
| Core pressure loss | Pa | 25.000 |
| Total primary system pressure loss | Pa | 29.000 |
| Primary coolant mass inventory | tons | ~ 1936 |
| Rated core power | MW | 80 |
| Maximum power from spallation | MW | 3.0 |

### 3.1.2. European XADS the PDS-XADS project

The PDS-XADS Project (Preliminary Design Study of an eXperimental Accelerator Driven System [3.3] was a major step of a consistent European effort toward the detailed design of an integral installation for the ADS technology demonstration. Its main objective was to demonstrate the feasibility for ADS of possible technical solutions for coupling accelerator technology with nuclear reactor technology and envisage with a limited scope their potential for waste transmutation. The XADS features have hence been designed to demonstrate first the safe coupling of an accelerator with a subcritical reactor.

Another goal of the project was to optimize the XADS plant in order to demonstrate transuranics (plutonium and minor actinides, according to different countries strategies) and long lived fission

fragments elimination (use of the XADS as an eXperimental Accelerator Driven Transmuter (XADT)).

In agreement with the recommendations established by the ETWG on ADS published earlier in 2001[3.4], two main phases were identified as necessary steps to progress forward an ADS industrial application:

— *Phase 1* which uses available fuel technology and is devoted to the demonstration of the ADS concept (coupling of different innovative features) and possibly for irradiation purposes (in particular fuels dedicated to transmutation);

— *Phase 2* which is devoted to the transmutation demonstration with a large number of minor actinides based fuel assemblies; during this phase the XADS will be used more and more as demonstration of a transmuter. This second phase requires the successful development of the fuel and fuel cycle facilities.

In order to achieve the phase 2 goals in a reasonable time scale, the key requirements of the XADS were clearly identified as a fast neutron spectrum and a high fast flux level. However, studies on Phase 2 during the course of the PDS-XADS project were very limited and were only indicative of what directions it would be necessary to go in the follow on programme (i.e. the XT-ADS described in section 3.1.3 and the EFIT presented in section 3.2.1, both developed within the EUROTRANS project of the 6$^{th}$ European Framework Programme [3.5]).

As far as Phase 1, three different concepts were developed within the PDS-XADS Project, respectively:

— The MYRRHA concept (50 MW(th), LBE cooled), developed by SCK•CEN;

— The 80 MW(th) LBE cooled concept, designed by Ansaldo Nucleare;

— The 80 MW(th) gas cooled concept, designed by FRAMATOME;

The following sections provide a general description and some technical details of these three concepts.

#### *3.1.2.1. MYRRHA*

SCK•CEN in partnership with Ion Beam Applications s.a. (IBA) and many European research laboratories, since 1998 is designing a multipurpose ADS for R&D applications — MYRRHA [3.6], [3.7]. In parallel, SCK•CEN is conducting an associated R&D support programme addressing the key issues of the design options and the associated heavy liquid metal technology chosen in the project.

MYRRHA aims to serve as a basis for the European experimental ADS providing protons and neutrons for various R&D applications. It consists in its '2005' design version of a high power proton accelerator of 350 MeV*5 mA proton beam bombarding a liquid Pb-Bi spallation target that in turn couples to a 50 MW thermal power, Pb-Bi cooled, subcritical fast core.

In a first stage, the MYRRHA project was intended to fit into the European strategy towards an ADS Demo facility for radioactive waste transmutation as described in the PDS-XADS FP5 project and EUROTRANS FP6 Project (see section 3.1.3). For a later stage, the MYRRHA/XT-ADS project is developed as a multipurpose irradiation facility for R&D applications based on ADS technology. As such, it should serve the following task catalogue:

— ADS concept demonstration;

— Safety studies for ADS;

— Minor Actinides transmutation studies;

— Long Lived Fission Products transmutation studies;

— Medical radioisotopes production;

— Material research;

— Fuel research.

The MYRRHA machine should be a multi purpose research facility of reasonable dimensions, but with high level requirements in terms of irradiation performances, among others high flux levels ($\Phi_{tot} > 5.10^{15}$ n/cm²s and $\Phi_{>0.75\ MeV} = \sim 10^{15}$ n/cm²s) and high availability rate.

As a direct consequence, the central hole in the core (which houses the spallation target) should be of limited dimensions (~10 cm) in order to keep many locations available in the core (to install experiments) where the neutron fluxes are sufficiently high. Because of the desired high fast flux and the high power density, a liquid metal as coolant has been adopted. Sodium has not been retained due to the fire safety reasons and to its incompatibility with the Pb-Bithat is already decided as a first choice for the spallation target material. The alternative liquid metal as a coolant were Pb or Pb-Bi; the latest has been chosen due to its low melting temperature (123°C), allowing the primary systems to function at rather low temperature levels. The low working temperatures are evident mitigating approach to limit the corrosion problems due to HLM.

Furthermore, from the very beginning of the project a windowless target design has been selected because of the high beam load on a hypothetic window that would sustain a proton current density of c.a. 140 μA/cm². No existing material can withstand these conditions. Even if such a design is quite challenging, the experimental and theoretical design work of the windowless target and associated R&D programme conducted since 1998, is giving more and more evidence that the windowless spallation target based on HLM would be feasible.

The subcriticality level ($k_s$) of 0.95 has been considered as an appropriate level for a first of kind medium scale ADS. Indeed, this is the criticality level accepted by the safety authorities for fuel storage and would allow for the MYRRHA concept to remain subcritical in all circumstances even when account for the possible positive reactivity injections.

To take profit of the thermal inertia provided by a large coolant volume, a pool type system in which the components of the primary loop (pumps, heat exchangers, fuel handling tools, experimental rigs, etc) are inserted from the top in penetrations in the cover has been chosen (see Fig. 3.8). The fuel assemblies loaded is foreseen to be from underneath, which is not the classical approach of the sodium fast reactors, but the used technology is the same and the reasons behind the approach is to hold a large flexibility for the experimental devices loading and from the safety point of view as all structures including the spallation module are in place before starting the core loading.

The configuration selected is a standing vessel with flat bottom that is fully supported by a lattice made of steel frames. A standing vessel might present a better seismic resistance than a hanging vessel due to the very high mass of coolant. A flat bottom configuration was chosen for several reasons, despite the fact that it is not optimum on a mechanical point of view:

— It allows ultrasonic testing of the bottom plate from the side, so there is no need to have access under the bottom,

— It allows minimising the volume of Pb-Biin the bottom, compared to a hemispherical bottom.

The main parameters of MYRRHA are listed in Table 3.7.

TABLE 3.7. GENERAL CHARACTERISTICS OF MYRRHA (2005)

| Parameter | Unit | Value |
|---|---|---|
| Core diameter | mm | 1000 |
| Core height | mm | 1800 |
| Fuel length | mm | 600 |
| Vessel inner diameter | mm | 4400 |
| Vessel total height (cover not included) | mm | 7000 |
| Vessel internal volume | $m^3$ | abt. 100 |
| LBE volume | $m^3$ | abt. 65 |
| Vessel cover thickness | m | abt. 2 |
| Nominal core power | $MW_{(th)}$ | 50 |
| Primary coolant | --- | LBE |
| Core inlet temperature | °C | 200 |
| Core average outlet temperature | °C | 337 |
| Coolant maximum velocity in the core | m/s | 2.0 |
| Primary coolant flow rate (nominal) | kg/s | 2500 |
| Secondary coolant | --- | Water |

The pool vessel, which contains the core of the MYRRHA machine and the whole series of internals, is located in an air controlled containment environment. Furthermore, several factors lead to the decision to design both operation and maintenance and In Service Inspection & Repair (ISI&R) of the MYRRHA machine with fully remote handling systems:

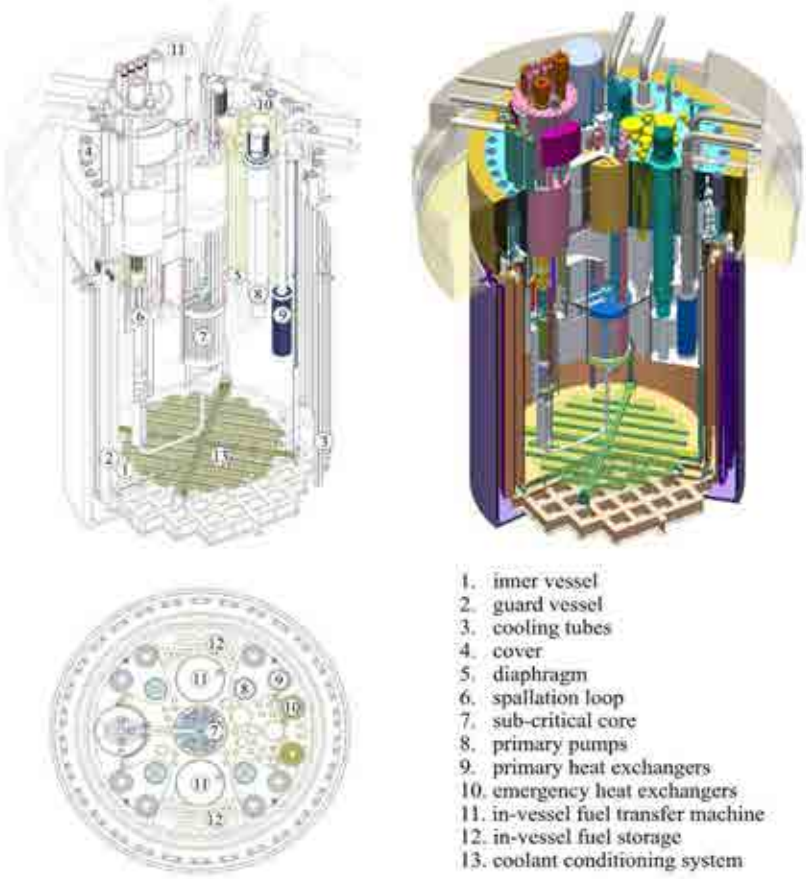


*FIG. 3.8. Overall views of MYRRHA 2005, showing its main internal components.*

— High availability rate desired for the machine (70–75%);

— High activation on the top of the reactor (due to the neutron leakage through the beam line);

— Po contamination when extracting components;

— Non-visibility under Pb-Bi; and

— Oxygen free atmosphere in the MYRRHA hall.

The main properties for the MYRRHA proton beam are presented in Table 3.8. The time structure of the beam is continuous wave operation with the implementation of well defined beam interruptions of 200 μs that occur every second. In these beam holes the neutron source is effectively shut down and accurate on-line measurements and monitoring of the reactor subcriticality can take place. As indicated above, accelerator reliability is a crucial issue for the operation of an ADS. In order to reach the reliability goal three main strategies are used: over design (avoid operating components close to their maximal capabilities), redundancy (include several components to provide a particular function) and fault tolerance (the capability of the system to use the redundancy to cover failure of a single component). The extent to which these strategies can be implemented in the design of the different accelerator types (Linac or cyclotron) will play a crucial role in the eventual type selection.

TABLE 3.8. MYRRHA PROTON BEAM SPECIFICATIONS

| Parameter | Value |
|---|---|
| Proton energy | 350 MeV (possible upgrade to 800 MeV) |
| Max. beam intensity | 5 mA continuous wave on target |
| Beam entry | Vertically from above |
| Beam trip number | Less than 5–10 per year (exceeding 1 second) |
| Beam stability | Energy: ± 1%, Intensity: ± 2%, Size: ± 10% |
| Beam footprint on target | Circular, 'doughnut' $Ø_{out}$=72 mm, $Ø_{out}$≈30 mm |

At present, megawatt beam power proton accelerators have been produced in only two basic concepts: sector focused cyclotrons and linear accelerators. The fundamental difference between the two types is that cyclotrons are essentially monolithic circular devices whereas Linacs that are built from many repetitive accelerating sections are highly modular. Clearly, the cyclotron option is attractive with respect to construction costs and the required beam parameters are within the feasibility of the cyclotron concept. However, because of the compact nature of cyclotrons, they are not modular so a given cyclotron is not upgradeable in energy nor is it well suited for the reliability strategy mentioned above. An equivalent superconducting linear accelerator on the other hand has higher construction costs. Yet, they are highly modular and upgradeable without fundamental limitations in energy and intensity. These properties give an excellent potential for optimized operation costs because of beam efficiency and for high reliability based on the fault tolerance concept. Because of these arguments, the Linac has been chosen in the MYRRHA project as reference solution for the accelerator whereas the cyclotron option is retained as backup solution.

The design of the MYRRHA spallation target must fulfil a number of requirements determined by the general concept of the MYRRHA ADS. In order to reach the required neutronic performance of the ADS, the target should produce about $10^{17}$ neutrons to feed the subcritical core at its $k_{eff}$ value of 0.95. To do this, it must accept the 350 MeV, 5 mA proton beam delivered by the accelerator. Consequently the target has to be able to evacuate the 1.43 MW heat (81.7% of 1.75 MW) deposited by the beam. This fact calls for a liquid metal target to allow forced convective heat removal. LBE has been chosen as target material. LBE is also the subcritical core main coolant although both two liquids are separated. The target evidently must fit into the central hole in the subcritical core that is created by removing three fuel assemblies. Finally the spallation target must reach an appropriate lifetime and it must comply with the role of MYRRHA as a flexible high intensity experimental irradiation device.

Inside the compact core geometry only a Ø 72 mm effective target surface is possible. Together with the beam properties, this leads to a beam current density of 125–175 μA/cm$^2$, which effectively prohibits the use of a target window close to the spallation zone since it would not realistically survive the harsh conditions for a sufficient period of time. A windowless design means that vacuum conditions of $10^{-5}$–$10^{-6}$ Pa above the target surface must be reached to avoid plasma formation and to guarantee compatibility with the vacuum of the accelerator beamline. The vacuum condition implies that sufficient pumping capacity must be foreseen while at the same time, outgassing of the LBE, liquid metal evaporation and emanation of volatile spallation products must be kept under control. In addition, confinement of the (radioactive) spallation products that leave the target material inside the target loop vacuum system must be ensured. The lack of a target window also means that the flow of the liquid LBE must be carefully controlled in the target zone so that a stable free target surface can be created.

Space constraints dictate the choice for a vertical confluent LBE flow in a funnel type configuration as free target surface formation mechanism. Upon this free surface the proton beam impinges from the top. The LBE subsequently flows away from the beam impact zone, removing the deposited heat by forced convection. The LBE flow rate will be 10 l/s leading to an average temperature increase of less than 100°C over the nominal 240°C operational temperature. Free surface temperatures are kept low to prevent excessive evaporation into the beamline which needs to be under vacuum.

Because of the space limitations, the spallation loop is closed around the subcritical core so that the LBE flow only crosses the core once. All active components are put in the return leg in an off centre spallation unit including:

— Heat exchanger that uses the main vessel coolant LBE on its secondary side;

— Mechanical pump for the delivery of the bulk of the pumping power. It lifts the LBE to a second free surface in the spallation unit;

— Magneto hydrodynamic (MHD) pump that takes the liquid from the spallation unit free surface for fast flow regulation to govern the position of the target free surface. The latter is sensed by a LIDAR (LIght Detection And Ranging) in line with the proton beam. Its signal is fed back to the MHD pump controller;

— LBE conditioning and filtering unit that ensures that the LBE contains sufficient oxygen to prevent corrosion attacks on the structural material of the loop and removes insoluble impurities that may block the flow in e.g. the heat exchanger.

The interlinking design makes a split in base plate of the subcritical core necessary to be able to remove the spallation loop. A sector of subcritical core's mechanical structure, base plate and barrel is part of the spallation loop, complementing the core structure when the loop is mounted. The spallation unit penetrates the reactor lid. All services are provided from the top.

The entire spallation target system was designed to be compatible with the MYRRHA remote handling scheme. The loop can be removed from the main vessel after core unloading. This avoids criticality issues, improves safety and allows in situ commissioning of the spallation loop. In addition, a separate subunit containing all active components is foreseen allowing servicing without removal of the complete spallation loop. Finally, the closed outer housing allows yearly replacement of the spallation zone (required because of embrittlement) and replacement of the heat exchanger when needed. The spallation loop and all its components are designed in accordance with the remote handling requirements that are needed because of the high radioactivity levels that are expected.

The spallation loop with the subunit removed from the main shell is shown in Fig. 3.9. Different components of the spallation loop are indicated

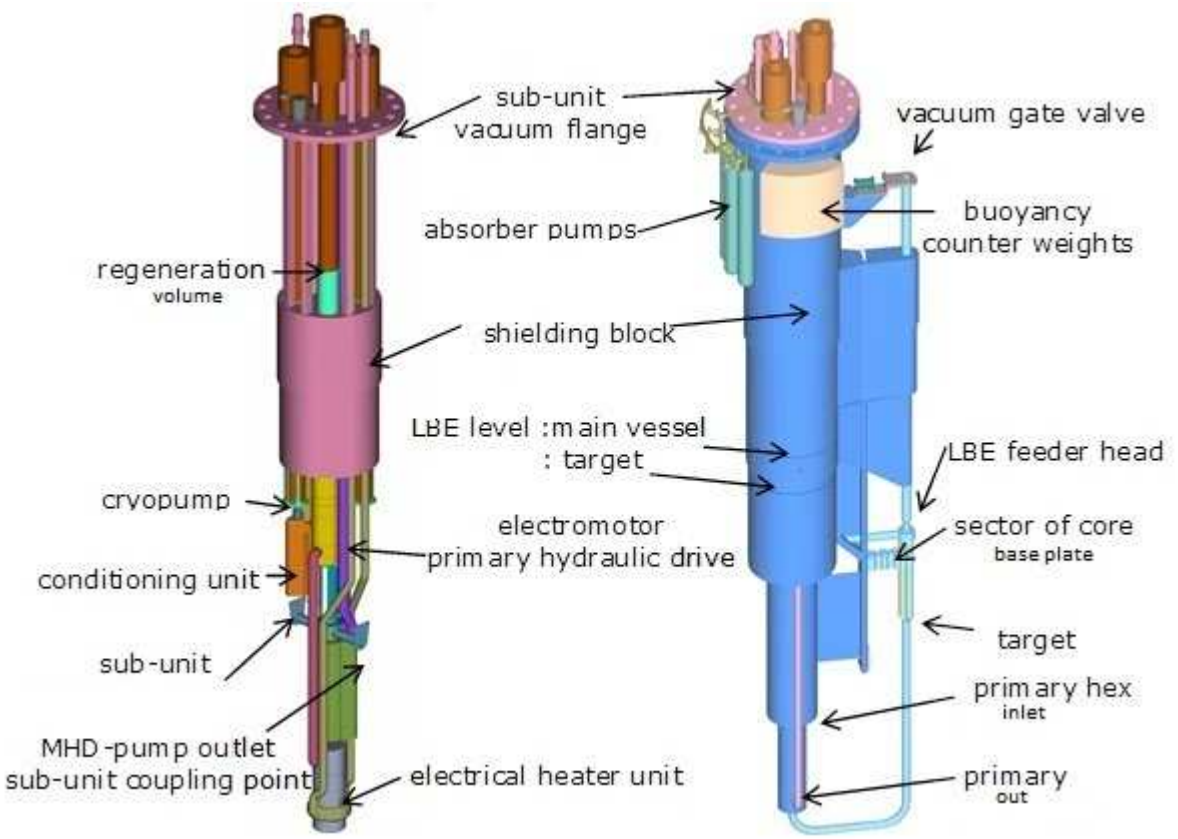


*FIG. 3.9. The MYRRHA spallation target loop and the subunit lifted from the main vessel.*

One of the main objectives of the MYRRHA ADS is to yield very high neutron fluxes within a small size subcritical core. The adopted reference subcritical core used to derive the basic neutronics parameters is displayed in Fig. 3.10.

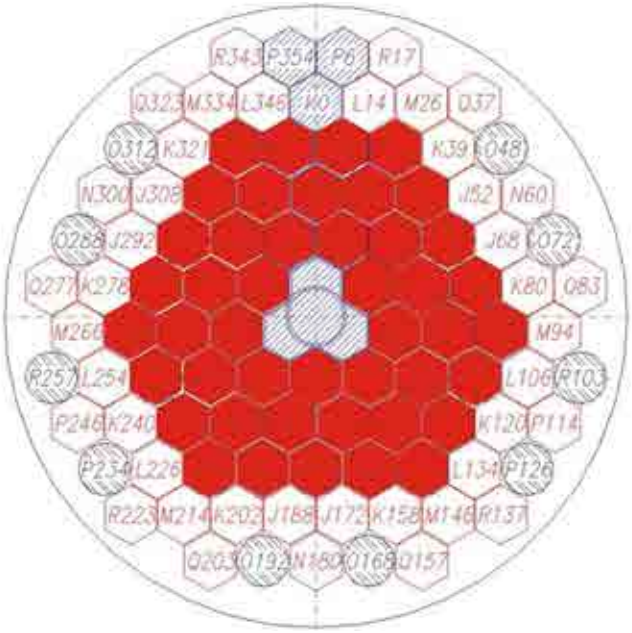

*FIG. 3.10. MYRRHA fresh core configuration.*

The core consists of a lattice of 99 hexagonal channels of which 45 are loaded with fuel assemblies housing 30wt% Pu enriched (Pu-HM; HM=Heavy Metal) MOX fuel pins arranged in a triangular pitch of 8.55 mm. The fuel rods have an active length of 60 cm. The $(U\text{-}Pu)O_2$ fuel pellets have a density of 10.55 g/cm$^3$ (95%TD) and each assembly contains 91 fuel pins yielding a 514 kg heavy metal load for the fresh core.

A space of three hexagons is cleared at the centre of the subcritical core to house the spallation target module. The spallation target consists of a windowless column of eutectic Pb-Biinside a 4 mm thick 9% Cr martensitic steel pipe having an inner diameter of 72 mm. The liquid metal target free surface lies 75 mm above the core midplane to have an optimum neutron yield and to achieve an axial symmetrical power and flux distribution in the core.

In the framework of the FP6-IP-EUROTRANS project (see section 3.1.3), calculations were done to compare the MYRRHA neutronics characteristics obtained with a 350 MeV proton beam to those of a 600 MeV one. For the calculation with a 600 MeV proton beam, the free surface has been set at z=+15 cm above the core midplane.

An overview of neutronics static design parameters calculated for a proton beam of 350 MeV and of 600 MeV are summarised in Table 3.9.

The neutron yield per incident proton is about 2.5 times higher for a 600 MeV incident proton compared to a 350 MeV proton. As a result, the required beam intensity to achieve the targeted subcritical core thermal power is a factor 2.5 lower in the case of a 600 MeV beam than for the 350 MeV case (2 mA for 600 MeV protons compared to 5 mA for 350 MeV protons).

For a 350MeV - 5 mA proton beam, the incident beam power is 1.75 MW and the volume integrated heating rate over the spallation target amounts to 1.43 MW, which is about 82% of the beam power. In case of a 600 MeV - 2 mA, calculations yield a heating rate of 0.74 MW, which is 61% of the beam power. This agrees with the expectation: the higher the beam energy, the lower the fraction of the deposited energy and the deeper the penetration in the spallation target liquid.

Using either the 350 MeV - 5 mA beam or the 600 MeV - 2 mA beam, the core power amounts to just above the targeted value of 50 MW(th). The core specific power density is 101 kW per kg of heavy metal, which is almost equal to the specific density in a LMFBR. The core radial power form factor is 1.05 and the axial one is equal to 1.3.

The adopted subcriticality level, ~4700 pcm ( $k_{eff}$ ~ 0.955) assures a comfortable margin for safe operation taking into account foreseeable positive reactivity insertions due to temperature effects, loading errors etc.

The burnup reactivity swing amounts to about -20 pcm/EFPD starting from a fresh core, which means a $k_{eff}$ drop of about 1800 pcm after 3 months (90 days) of operation. This results in 30% a drop of the core thermal power.

The Doppler constant, Tdk/dT, is -370 pcm, which is lower but of same order of magnitude as in Na-cooled fast reactor. On the other hand, the LBE coolant temperature coefficient, dk/dT, is small but negative, -1.5 pcm, over the temperature range from 130 to 600°C. In Na cooled systems this reactivity coefficient can be positive.

The hottest segment of the hottest fuel assembly undergoes a burnup of about 11 MWd/kg. Assuming a fuel irradiation limitation of 100 MWd/kg, one foresees overall residence time up to 810 EFPDs, which corresponds to a 3 years campaign.

TABLE 3.9. OVERVIEW OF THE MYRRHA CHARACTERISTICS (BOL)

| Neutronics Parameters | | Units | Values | |
|---|---|---|---|---|
| Proton beam energy | | MeV | 350 | 600 |
| Accelerator current | | mA | 5 | 2 |
| Proton beam energy | | MW | 1.75 | 1.20 |
| Proton beam heating | | MW | 1.43 | 0.74 |
| Deposited fraction of beam energy | | % | 81.5 | 61.4 |
| In depth proton beam penetration (~Bragg peak) | | mm | 126 | 290 |
| Free surface position (above mid plane) | | mm | +75 | +150 |
| Source neutron yield per incident proton | | n/p | 6.0 | 15.6 |
| Neutron source intensity | | n/s | 1.9 x E17 | 1.9 x E17 |
| Initial fuel mixture | | --- | (U-Pu) $O_2$ | (U-Pu) $O_2$ |
| Initial (HM) fuel mass | | Kg | 514 | 514 |
| Initial Pu-enrichment (Pu-HM) | | % (wt) | 30 | 30 |
| $k_{eff}$ | | --- | 0.995 | 0.995 |
| $K_s$ | | --- | 0.960 | 0.958 |
| Source Importance φ* | | --- | 1.13 | 1.08 |
| Thermal Power | | MW | 51.75 | 51.27 |
| Specific power | | kW/KgHM | 101 | 100 |
| Peak linear power | | W/cm | 352 | 324 |
| Hottest pin to core mean pin | | --- | 1.290 | 1.284 |
| Hottest pin to hottest S/A mean pin | | --- | 1.053 | 1.048 |
| Hottest S/A to core S/A | | --- | 1.225 | 1.225 |
| (-5 cm ≤ Z ≤ 5 cm) averaged Neutron Fluxes | | | | |
| $\phi_{total}$ | fast core-averaged | n/ $cm^2$.s | 3.31 x E15 | 3.27 x E15 |
| | Within hexagons around spal.target | n/ $cm^2$.s | 4.11 x E15 | 3.86 x E15 |
| $\phi_{> 1\ Mev}$ | fast core-averaged | n/ $cm^2$.s | 0.50 x E15 | 0.50 x E15 |
| | Within hexagons around spal.target | n/ $cm^2$.s | 0.79 x E15 | 0.65 x E15 |
| $\phi_{> 0.75\ Mev}$ | fast core-averaged | n/ $cm^2$.s | 0.69 x E15 | 0.67 x E15 |
| | Within hexagons around spal.target | n/ $cm^2$.s | 1.02 x E15 | 0.86 x E15 |

In Fig. 3.11 and Fig. 3.12 the radial profiles of the fast flux ($\Phi_{> 0.75\ MeV}$) and of the total flux are shown at the midplane core, over a fine (x, $\bar{y}$=0) mesh grid (the x-axis and the y-axis being, respectively, the cartesian coordinate axis in Fig. 3.11).

High levels of neutron flux are achieved throughout the facility. One has fast fluxes ($\Phi_{> 0.75\ MeV}$) close to $1.0\times10^{15}$ n/cm².s and total fluxes close to $4.0\times10^{15}$ n/cm².s inside the target clearance hexagonal boxes within the neighbourhood of the spallation target. In the subcritical core (5 cm ≤ radius ≤ 25 cm) beyond the target the averaged flux over a 10 cm height segment are close to $7.0\times10^{14}$ n/cm².s and total fluxes close to $3.3\times10^{15}$ n/cm².s.

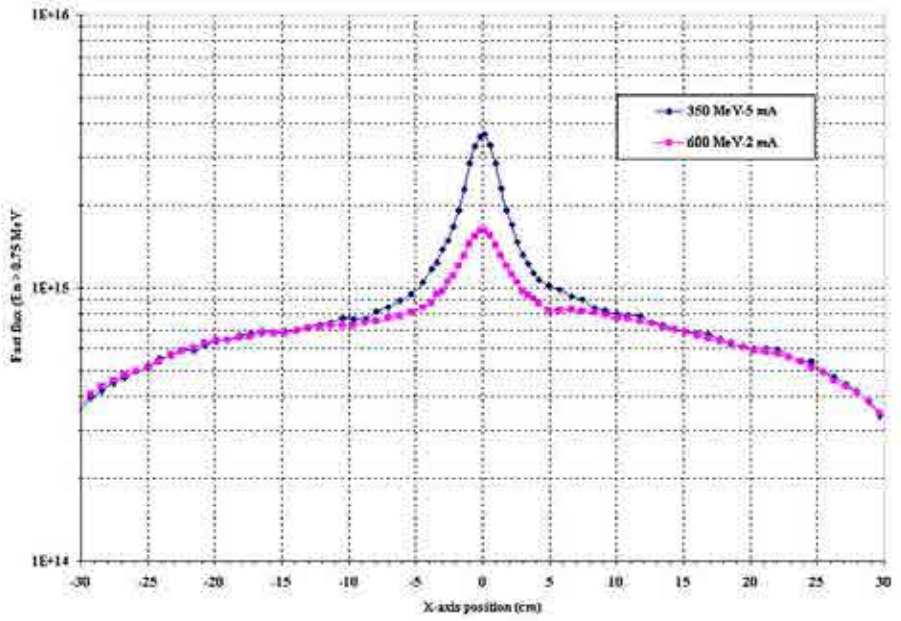


*FIG. 3.11. Fast flux (> 0.750 MeV) through the x-axis at the core midplane.*

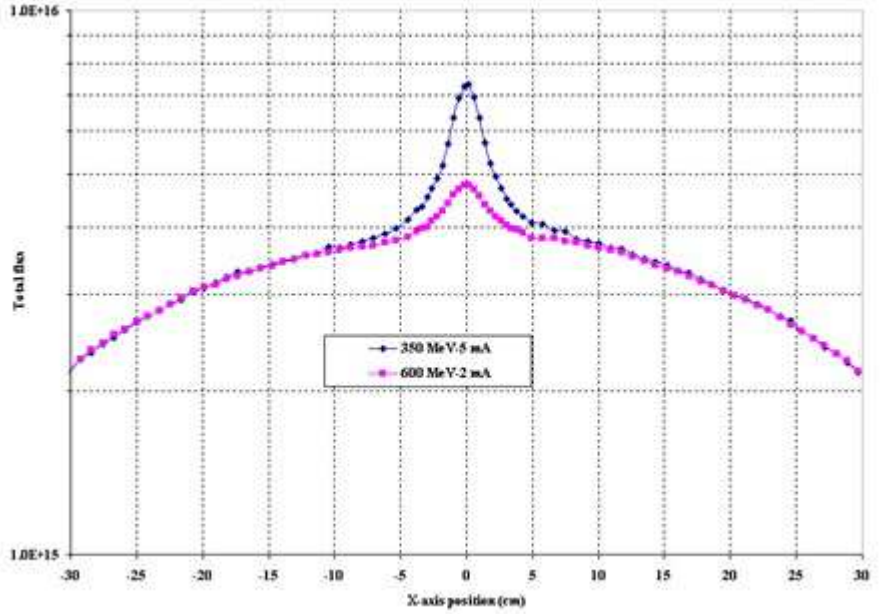


*FIG. 3.12. Total flux through the x-axis at the core midplane.*

A typical core loading pattern adopted to carry out a preliminary assessment of the potential MYRRHA design concept to the MA transmutations and LLFP incineration in a fast spectrum is displayed in Fig. 3.13. The minor actinide load consists of six assemblies similar in geometry to the driver ones, but housing the fuel rods with pellets containing IMF (inert matrix fuel): 40 vol.% $(Pu_{0.4}Am_{0.5}Cm_{0.1})\ O_{1.88}$ fuel and 60 vol.% MgO matrix.

Besides a shorter active length (400 mm), the dimensions of these rods are the same as those of the driver ones. The density of the IMF pellet is 6.077g/cm$^3$ (~90 % TD) yielding a total amount of 7.24 kg low quality Pu (from PWR spent fuel), 9.04 kg of americium and 1.81 kg of curium irradiated in fast spectrum channels during a 3-years campaign (810 EFPDs).

The calculations yield a net decrease of 2.48 kg in the actinide mass, mainly due to the removal of americium (-2.46 kg). There is a net increase of 0.46 kg in the curium mass due to the buildup of $^{242}$Cm and $^{244}$Cm from the decay or neutron capture of americium. The burnedout mass of plutonium is 0.51 kg.

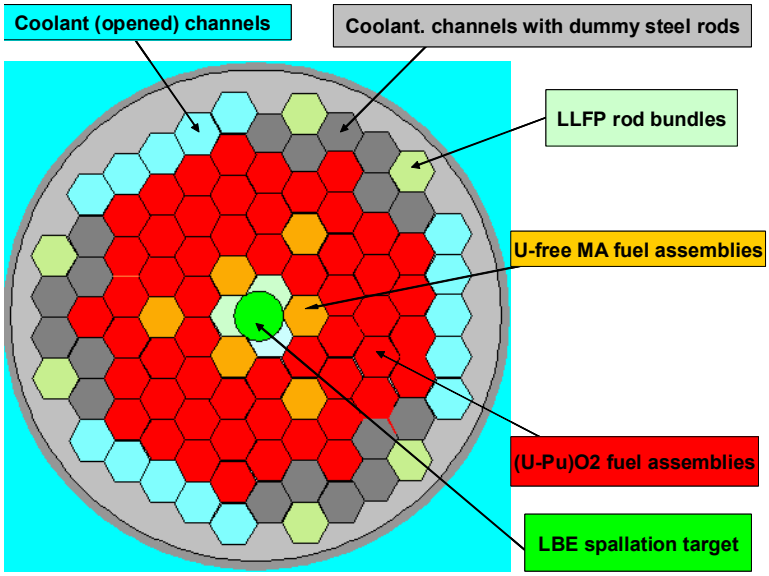


*FIG. 3.13. A dedicated MYRRHA core configuration for MA & LLFP transmutation studies.*

Mixed plutonium-uranium oxide fuel (MOX) was selected as the main candidate, taking into account a large experience in the MOX production in Europe and its better neutronic properties in a fast neutron spectrum than uranium dioxide. Aiming at a compact core with high neutron flux, an enrichment of 30–35 wt. % of reactor grade Pu has been preliminary chosen.

Ferritic martensitic steel (FMS) T91 has been chosen as the main candidate for the fuel cladding in MYRRHA. This choice was based on the fact that T91 shows a lower swelling rate and embrittlement under irradiation at T > 350°C, and higher resistance to dissolution in the oxygen free LBE, compared to austenitic steels. However, taking into account that all FMS suffer strongly from irradiation embrittlement below 350°C and show higher corrosion rate in present of oxygen, the well known austenitic steels 15–15 Ti, AISI 316 L and few Russian steels were kept as a backup solution.

The available experimental data on LBE technology and corrosion resistance of different steels in contact with LBE indicate that their long term operation (> 10000 h) is possible only at temperatures lower than 560°C. Therefore, the allowable maximum local temperature of 450°C has been chosen for the LBE coolant normal operation. The minimum coolant temperature has a natural limit of ~ 125°C due to the LBE melting temperature. In order to have a technological margin, the minimum LBE operation temperature of 200°C has been chosen at this stage of the predesign. However, one should keep in mind that embrittlement problems related to joint effects of LBE and neutron damage on the cladding materials can force to increase this temperature up to 250–300°C. The LBE velocity limit of 2 m/s has been fixed because of possible erosion of structures during a long term operation.

The selected above fuel and clad features are collected in Table 3.10.

TABLE 3.10. THE PREDESIGN INPUT PARAMETERS FOR FUEL, CLADDING AND COOLANT OF ADS MYRRHA

| Fuel: $(U,Pu)O_2$ MOX | |
|---|---|
| Enrichment | 30 wt. % of RG-Pu |
| Density | 95% TD |
| Max. burnup | 100 MWd/kg-iHM |
| Max. normal temperature | 0.9 $T_{melt}$ |
| Cladding: FMS T91 (backup - 316Ti or 316L) | |
| Normal temperature | 200–500°C |
| Short term excursions | < 600°C |
| Allowed damage | 100 dpa |
| Allowed swelling | 5% |
| Allowed limit for corrosion | 10% of thickness |
| Coolant: LBE | |
| Operation temperature | 200–450°C |
| Max. velocity | 2 m/s |

A schematic view of the MYRRHA fuel rod is illustrated by Fig. 3.14.

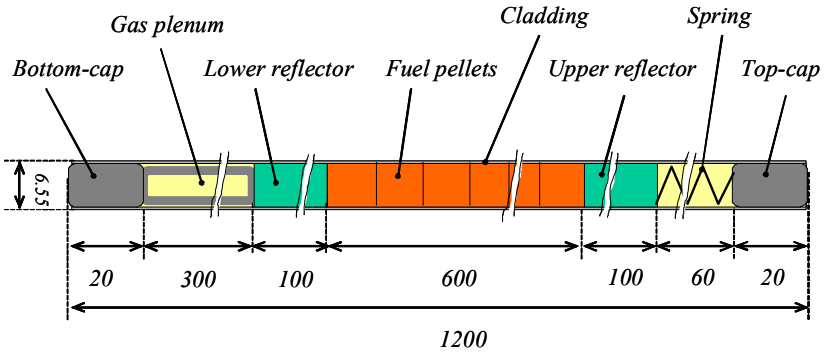


*FIG. 3.14. Schematic view of the MYRRHA fuel rod.*

On the basis of the design of the fuel element described here above, the reference basic configuration of the MYRRHA core has been proposed and thermal power distribution over the core has been calculated at BOL with the MCNPX code. The total thermal power of the hottest FA is 1466 kW. The power of the hottest rod is 16.93 kW. The maximum (peak pellet) linear heat generation rate (LHGR) is 352 W/cm with the axial form factor of 1.30. Based on these results the preliminary thermo mechanical modelling of the hottest fuel rod was performed with the modified version (LBEmod SCK) of the code FEMAXI-V.1.

Some parameters of the hottest rod thermal state at the nominal BOL conditions are summarised in Table 3.11.

TABLE 3.11. STEADY STATE THERMAL PARAMETERS OF THE HOTTEST ROD AT BOL

| Parameter | Units | Values |
|---|---|---|
| Peak linear heating rate (LHGR) | W/cm | 352 |
| Axial power form factor | --- | 1.3 |
| Peak fast neutron flux (En > 1 MeV) | n/cm²s | 8×E14 |
| Fuel peak temperature | °C | 1830 |
| Cladding peak temperature | °C | 450 |
| Minimum radial pellet-clad gap | micron | 19.3 |

Fig. 3.15 presents the axial temperature distribution on the fuel centre line, on the pellet surface, on the outside surface of the cladding and in the fuel cell coolant. The maximum fuel temperature of 1830°C is reached at midplane of the rod. This temperature is for about 830°C lower than the melting temperature of the fresh 30% MOX fuel.

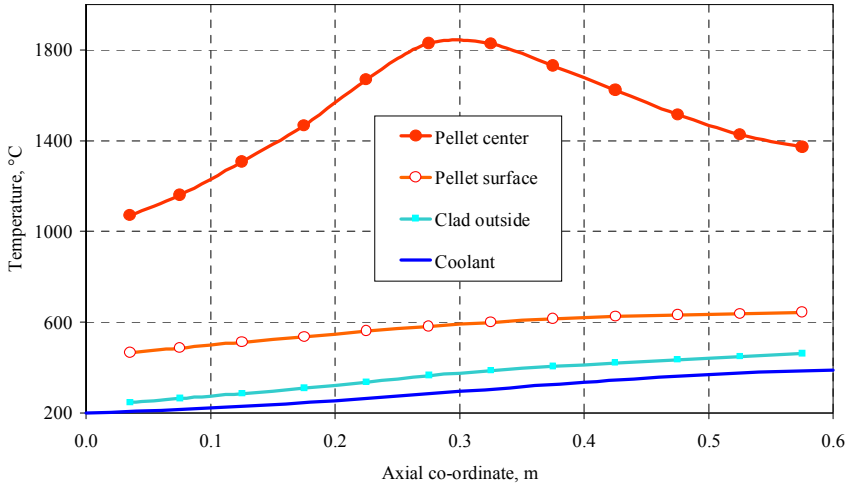


*FIG. 3.15. Axial temperature distribution in the fuel column, in the cladding and in the coolant of the hottest sub-channel at BOL.*

MYRRHA is being proposed to be erected at the SCK•CEN Centre of Mol (Belgium). Fig. 3.16 shows a (rather old) rendering view of the MYRRHA facility inside this Centre.

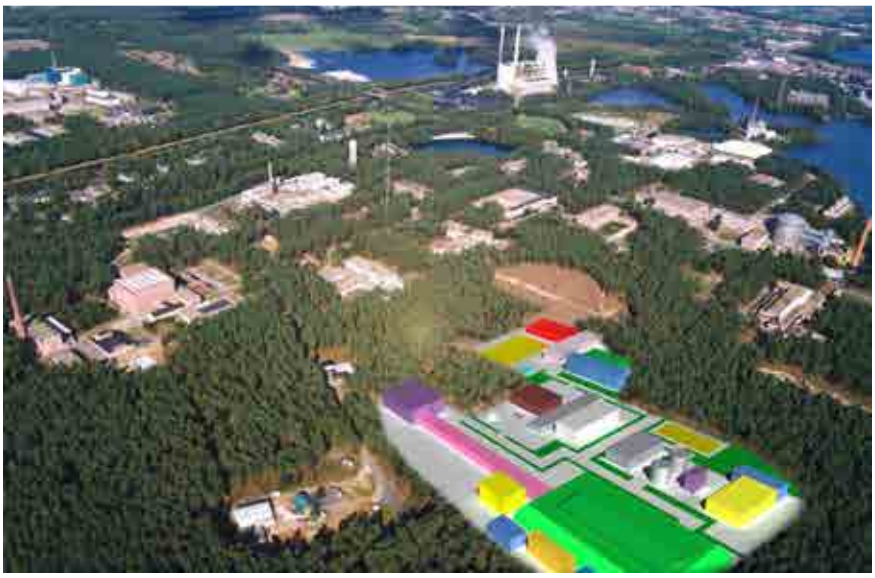

*FIG. 3.16. MYRRHA Facility at the SCK•CEN Centre of Mol.*

### *3.1.2.2. XADS: common design objectives, requirements and features of the Pb-Bi and gas cooled XADS.*

From a general point of view, the following missions have been assigned to both the Pb-Bi and gas cooled XADS:

— To be representative of a future ADS system, used to burn the minor actinides and the fission products. This implies that the XADS has a fast spectrum core with a spallation source allowing

a possible range of subcritical level between 0.95 and 0.995, depending on the control strategy and safety approach;

— To get the validation of a system having a minimum power level, in order to demonstrate the feasibility of an ADS based on the main three components: the high energy proton accelerator, the spallation target, the subcritical core. The demonstration must focus on the control, on the behaviour of the system with power, taking into account the feedback effects, on the burner capability demonstration and on the technology reliability of the system;

— To be a final step after the physical validation based on MUSE and the target technological demonstration with MEGAPIE.

In order to fulfil those missions, the following technical objectives were assigned to the XADS plant ([3.3], [3.8]):

— Power in the range 60–100 MW(th);

— Irradiation volume: a few hundred litres;

— High fast flux level with a goal for the average neutron flux in the order of $1\times10^{15}$ n/cm².s and a peak flux of about 2.5 to $3\times10^{15}$ n/cm².s;

— Keeping into account the basic objective of moving from technology demonstration (XADS) to transmutation demonstration (XADT), the XADS must have a large flexibility in terms of subcriticality level and fuel technology (with and without minor actinides), be robust and based on a sound and safe technology for the first step, have the potential to attain neutron flux and damage levels close to those of the ADS burner, in order to allow to get information from irradiated materials in a relatively short term.

To summarise, taking into account the main goals assigned to the XADS, the status of current technologies and timescales for the development of enhanced ones, the recommendations and requirements given in Table 3.12 were proposed for the characteristics of the reference XADS main components (accelerator, spallation module and subcritical reactor).

Moreover, it was recommended that the design of the XADS makes use of proven technologies as far as possible, for materials, systems etc. Any innovative feature of the XADS should undergo a series of experimental and validation tests which should be identified and specified. In this view, MEGAPIE (see section 4.4 in chapter 4) and MUSE (see section 4.9 in chapter 4) experimental programmes in the first place and MYRRHA (see above) in a more advanced place will offer intermediate validation of possible technical solutions for coupling accelerator technology with nuclear reactor technology.

TABLE 3.12. STEADY STATE THERMAL PARAMETERS OF THE HOTTEST ROD AT BOL

| Accelerator requirements | |
|---|---|
| Max. beam intensity | 6 mA |
| Proton energy | 600 MeV |
| Beam entry | To be defined |
| Beam trip number | Less than 5 per year for the accelerator design<br>Less than 50 per year for the reactor design |
| Beam type | CW, best solution<br>Pulsed, backup solution |
| Beam power stability | ± 2% |
| Beam energy stability | ± 1% |
| Beam intensity stability | ± 2% |
| Beam footprint dimensions | ± 10% |
| Target requirements | |
| Target life time | Not higher than one fuel cycle |
| Target material | LBE |
| Target power | 2–5 MW |
| Proton current intensity | Lower than 50 μA/cm² for the window concept |
| Subcritical core requirements | |
| Operational subcriticality | To be determined according to coolant technology, design choice and required margins (transient and safety analysis) |
| Power | 60–100 MW(th) |
| Min. core volume | 500 litres |
| Vol. power | 80–200 W/cm$^3$ |
| Fuel technology | MOX |
| Pu | Less than 35%+ |
| Max flux | 1xE15 n.cm$^{-2}$s$^{-1}$ |
| Load factor | 0.5 |

The two large size XADS also share the same accelerator options. In particular, both the Pb-Biand gas cooled XADS require a proton energy of 600 MeV. This value constitutes a good compromise between the spallation efficiency, the accelerator length and the target beam load. In fact, neutron production per unit energy through spallation rises sharply with the incident proton energy and starts levelling off at energies around 1 GeV, but higher proton energy also implies higher irradiation damage in the subcritical system components and a production of high energy neutrons that require heavy and expensive shielding. Of course an extrapolation up to 800 MeV or 1 GeV, necessary for XADT needs, must be easily implementable.

The accelerator average current is the main parameter that determines the overall thermal power. Therefore it is fully adjustable from zero to maximum full beam. The range of the proton beam current is sufficient to sustain constant the XADS power in excess of 80 MW(th) along the fuel core cycle. For a final core subcriticality of $k_{eff} = 0.95$ and for the above mentioned core power level, the beam intensity reaches a maximum of 6 mA for 600 MeV proton acceleration energy.

In order to limit the variation of the XADS power (± 2% total power), a beam intensity stability of ± 2% is required. This is a rather stringent requirement considering the actual fluctuations of nowadays ion sources, which asks for some specific development on diagnostics to properly achieve

that requirement. Considering that the energy stability will be almost perfectly under control (by means of implementation of a suitable achromatic optical system), the final beam power stability on target will be fully determined by the actual beam intensity stability that can be achieved.

Regarding the time structure of the proton beam, a CW operation mode has been chosen for the XADS accelerator with the RF power continuously applied on the RF structures and the beam intensity shaped as in Fig. 3.17 to allow for on-line subcriticality measurements.

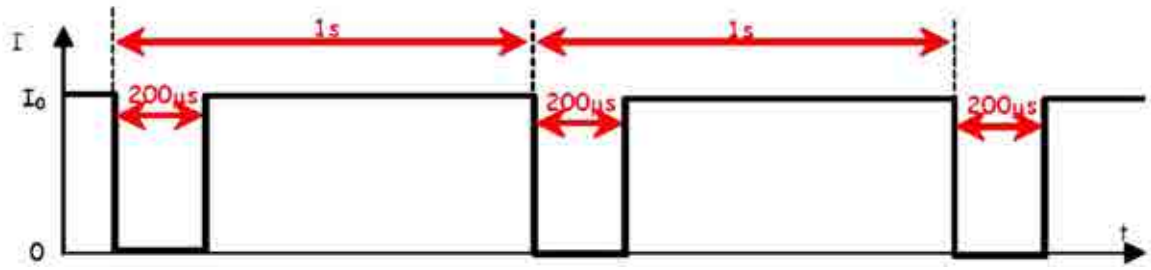


*FIG. 3.17. Accelerator current with periodic square shape signals.*

The number of beam interruptions with duration > 1 s, which leads to the plant shutdown, should not exceed 5 per year. This requirement for the accelerator availability and reliability of the accelerator is very stringent. Since the availability and reliability of a system also strongly depends on the maintenance strategy of its components, the accelerator scheduled maintenance plan will be compatible with the existing maintenance policy of nuclear power plants. It is therefore clear that the accelerator, in the absence of short and frequent (weekly) maintenance stops (as in most accelerator facilities), should be capable of operating with some faulty components, and its design needs to take into account criteria for derating of components (avoiding stresses on components close to their maximal operational capabilities), redundancy and fault tolerance (the capability of the system to use the redundancy in order not to fail after the failure of one of its components). Thus the 'long' maintenance period will be scheduled after an operational period ranging from three months to a full year.

Two accelerator options have been proposed for the XADS: the cyclotron and the linear accelerator (LINAC). Although the cyclotron allows to fulfil the actual demonstrator needs, more attention has been dedicated to the LINAC design, as a high power cyclotron would be currently approaching its technological limits (limited focusing capability and high activation of the structures, for instance, for a demo sized cyclotron, energy level and maximum beam current for an industrial sized ADS prototype).

Likewise high power proton LINACs, XADS Linear Accelerator System constitutes of three main sections ([3.9], [3.10]):

— Low energy section (injector) that includes the source, usually delivering a continuous current, followed by an accelerating structure that bunches the beam at the operating frequency. The beam usually comes out from the injector at energies between 2 and 10 MeV.

— Intermediate section, which brings up the beam to energies in the vicinity of 100 MeV.

— High energy section that brings up from 100 MeV up to any desired final energy. At 100 MeV, although the proton is not yet fully relativistic ($\beta = v/c = 0.428$), its speed is already high enough to use 'low beta' elliptical cavities.

Fig. 3.18 shows a possible reference layout for the XADS accelerator optimized for reliability, where all selected components have the capability to accelerate higher beam currents (~ 40 mA) without major changes. It uses a 'classical' proton injector (Electron Cyclotron Resonance (ECR) source + normal conducting Radio Frequency Quadrupole (RFQ)), followed by additional warm IH-DTL or/and superconducting CH-DTL structures up to a transition energy still to be defined between 5 and 50 MeV. At this point, a fully modular superconducting LINAC accelerates the beam up to the final energy.

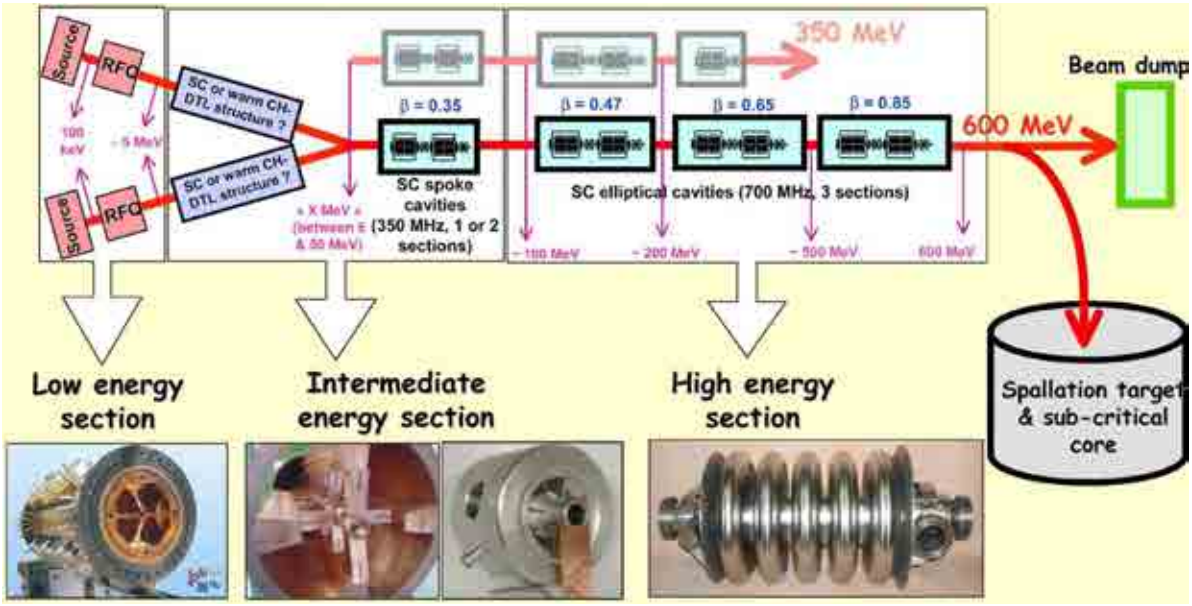


*FIG. 3.18. XADS linear accelerator reference scheme.*

Up to transition energy, fault tolerance is guaranteed by means of a 'hot standby' spare, keeping the possibility to switch the second injector on if the first one fails or has any long beam trip. Above this energy, 'spoke' and, from 100 MeV on, 'elliptical' cavities are used. An individual cavity failure in this part can be handled at all stages without loss of the beam. Besides this fault tolerance, another remarkable feature of the concept is its validity for a very different output energy range: 350 MeV for the smaller scale XADS (i.e. MYRHHA, see above) requires for example nine β=0.65 elliptical cavities cryomodules; in order to obtain 600 MeV, simply ten more cryomodules have to be added (7 with β=0.65 and 3 with β=0.85) and 12 additional (β=0.85) boost the energy to 1 GeV. Therefore, already the small scale XADS accelerator is fully demonstrative not only of the 600 MeV XADS (and could be converted to it), but even for an industrial machine.

The low energy section consists of: ECR ion source, Low Energy Beam Transport (LEBT) and RFQ section.

The source is an ECR ion source, based on the experience accumulated in many laboratories around the world ([3.11],[3.12]). ECR sources have demonstrated delivering reliable proton beams exceeding 100 mA, an order of magnitude higher than the requirements needed for the XADS. This type of source does not need any filament or antenna inside the plasma chamber. Also other types of ion sources would fulfil the ADS requirements (as microwave sources or volume sources), but may suffer from its lifetime. The ion source should deliver up to 10 mA at 95 keV to the RFQ operating at 2.45 or 3 GHz with an axial magnetic field providing two ECR resonance zones at both plasma chamber ends simultaneously. The source and its ancillaries are installed on a 100 kV insulated platform to fit in with the RFQ entrance energy. The RF power is produced either by a 1.2 kW magnetron source or a klystron and fed to the source via standard rectangular waveguides. An automatic tuning system helps to accommodate and adapt the RF load. The magnetic field is provided either by coils or permanent magnets. The small copper plasma chamber (0.5 litre) located at the centre of the magnetic structure has to be watercooled. A single aperture extraction system has been designed. An intermediate electrode located in the accelerating gap can be tuned to minimize the distortions in the phasespace distribution. An electrode at ~ -2 or -3 kV is inserted between two water cooled grounded electrodes to avoid the acceleration of electrons produced by ionization of the residual gas in the beam line. The electrode construction takes into account possible beam losses leading to damage. Fig. 3.19 shows a scheme of the French source SILHI [3.13], which has already produced a 130 mA, 95 keV proton beam with an emittance better than 0.15 π.mm.mrad (r–r', rms normalized), and with a very promising reliability, and accelerator column developed in the framework of the IPHI project.

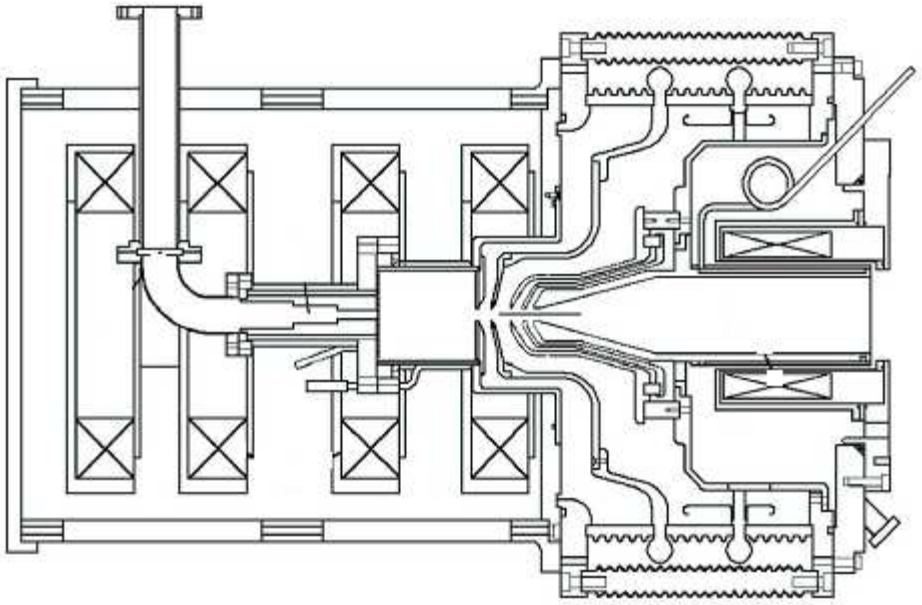

*FIG. 3.19. Source and 95 kV extraction column.*

The LEBT line is designed to guide the beam into the RFQ acceptance, taking into account the variable space charge compensation. It consists of 2 solenoids which match the proton beam into the acceptance of the following RFQ, whereas the unwanted ions from the source (H2+ , H3 +,etc.) will be separated from the main beam. The SCC depends on the amount of free electrons due to beam losses on the walls or beam interaction with the residual gas. A small amount of heavy gas (Ar or Kr) in the LEBT allows better space charge compensation. Interceptive diagnostics also lead to secondary electron production and locally modify the beam compensation. To allow an accurate beam matching to the RFQ, a precise knowledge of the beam characteristics is required at the cavity entrance. Presently the beam position and size could be obtained from CCD cameras. Faraday cup, beam stopper and toroids (DC and AC current toroids) allow the measurement of the beam current and of its high frequency fluctuations. Insulated screens give information on beam losses and beam axis.

Emittance at the RFQ entrance also has to be well known to minimize RFQ transmission limitation.

The RFQ section has two main functions: it prepares the particles in bunches separated by the RF period (the beam is now microscopically pulsed in bursts of particles flowing at the rate of the RFQ frequency) and it accelerates the beam to an energy of a few MeV while maintaining a strong confinement. This section shall be a four vane type RFQ [3.14] to overcome the difficult problem of the cooling of a 4-rod RFQ. The structure is made up of 8 one meter long sections accurately machined, brazed, and then assembled with resonant coupling every 2 meters, like for the LEDA and the IPHI designs (Fig. 3.20). The coupling plates allow a damping of the RF longitudinal parasitic modes and the introduction of fingers to push away the dipolar modes.

*FIG. 3.20. Sketch of a 5MeV, 8 meters RFQ for the XADS LINAC.*

The RFQ will be fed by 1.3 MW of RF power that might be provided by two 352.2 MHz, 1.3 MW klystrons (LEP type) through highly reliable windows and RF couplers (> 250 kW). RF windows, similar to those needed, have been already successfully tested up to 700 kW at LANL for LEDA. The cooling system of the RFQ must fulfil two essential functions: first to evacuate the 1.2 MW of dissipated power in the copper (independently of the current beam value) and then to maintain, by adjustment of the temperature, the resonance frequency of the cavity at the right value. The slow frequency tuning will be done using the cooling system of the cavity based on the LEDA design. The inlet water temperature is 10°C with a tuneable water flow up to 6 m/s. The input energy of 95 keV is the result of a compromise between RFQ length, source reliability and space charge control. The 5 MeV output energy results of a compromise between cavity length, feasibility of the next accelerating structure (DTL using EM or PM quadrupoles, superconducting CH-DTL or spoke type cavities), and high beam transmission. The design current of 100 mA is selected to reach a high reliability at the lower currents needed by the application. The expected normalized rms emittance from the source is 0.2 π.mm.mrad. Nevertheless, a safety margin is taken using 0.25 π.mm.mrad in beam dynamics calculations. The maximum field inside the RFQ, commonly measured in Kilpatrick units, is a parameter that strongly influences the length of the structure, its transmission and its robustness with regards to RF breakdowns. The maximum electric field has been limited to 1.7 Kp (31.34 MV/m) due to the CW mode and taking into account experience with the CRITS Experiment at Los Alamos, the LEDA test stand in Los Alamos and RFQs operated at Saclay in the past.

Two basic concepts have been elaborated for a final solution of the intermediate section (E ranging from 5 MeV to 100 MeV) to be developed in the future. The first concept consists in extending the low energy accelerating philosophy towards high energies by using DTL (Drift Tube Linac) type structures. These structures are classically room temperature normal conducting devices, and are generally considered as the base solution in most of the existing (and under design) proton LINACs developed in the last years. Superconducting versions of such devices also have been recently developed, like the superconducting CH-DTL structure that can be a very good candidate (Fig. 3.21). The second concept is to extend the high energy superconducting LINAC philosophy towards low energies by using independently phased superconducting ‘low beta’ resonators like spoke cavities (Fig. 3.22), and benefiting from all the advantages of SCRF cavities towards ‘warm’ devices (large beam apertures, negligible RF losses, modularity).

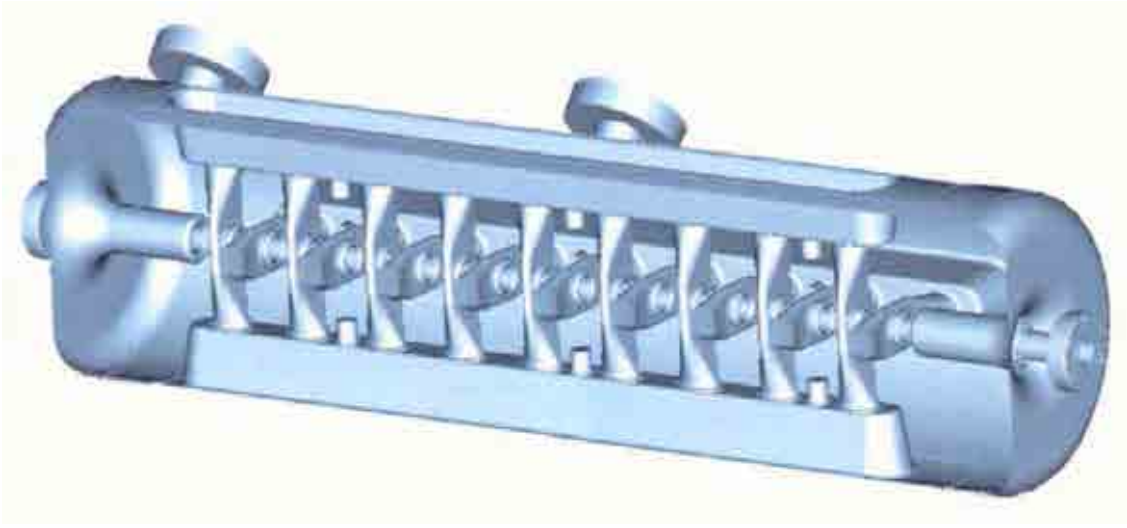

*FIG. 3.21. Sectional view of 352.2 MHz Multigap SC CH-DTL cavity prototype for XADS.*

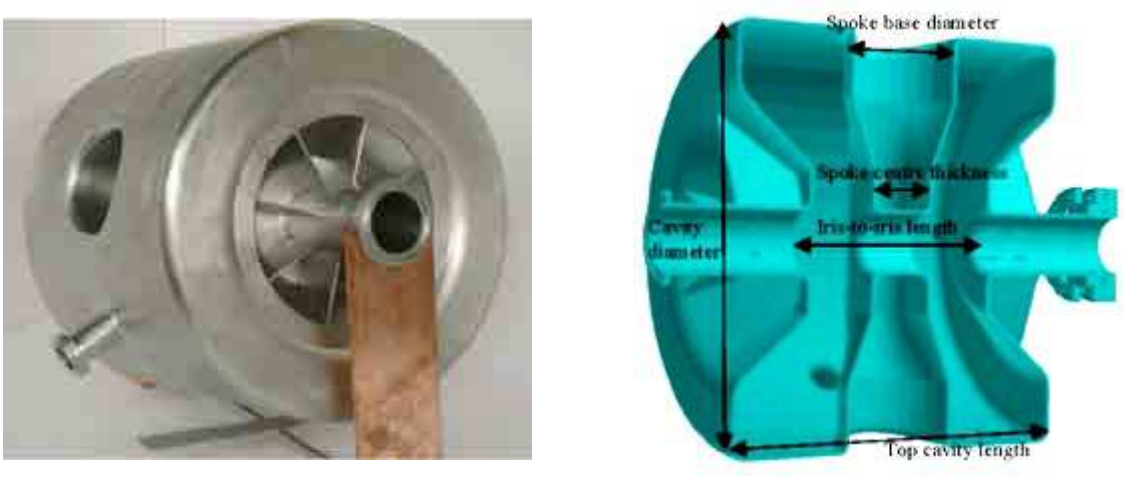


*FIG. 3.22. View and cross-section of the 350 MHz, β= 0.35, 2-gaps spoke cavity prototype.*

A superconducting solution is very promising, especially because it leads to a strongly reduced AC power consumption which makes big savings in the operating cost. Moreover, the spoke cavities solution, with its independently phased modular structures, has the capability to guarantee stable and reliable operation, even in the case of the failure of one cavity (fault tolerance concept). This is a crucial advantage in order to achieve the XADS reliability requirement. Nevertheless, in the very low energy region (~ <0.2), the beam dynamics in such a spoke LINAC becomes quite inefficient, leading to very low real estate accelerating gradients. In this low velocity region, DTL like structures are far more efficient in terms of accelerating gradients. But on the other hand, they have the disadvantage of not exhibiting any fault tolerance capability, which means that a fault in such a structure would lead to a complete beam shutdown. The proton beam is transported from the RFQ exit to the entrance of the following accelerating structure (here a DTL like structure or a spoke LINAC) by a Medium Energy Beam Transport (MEBT). At this energy (5 MeV), such a MEBT is usually composed of at least 4 quadrupoles for the transverse focusing, of 2 bunching cavities for longitudinal focusing, and of adequate diagnostics. A second MEBT will also have to be used at the transition between the DTL section and the spoke LINAC if the DTL option is chosen. A fast switching bending magnet will have to be included before the spoke section.

The superconducting elliptical cavities are the most efficient and cost effective solution for the XADS. Due to the varying velocity of the moderately relativistic protons, the superconducting section is divided in three parts, each covering an energy range with a single type of structure. The geometrical β values of these structures are 0.47, 0.65 and 0.85, respectively. A 700.4 MHz SC elliptical cavity with a β=0.47 tested at INFN laboratories in Milano is shown in Fig. 3.23

*FIG. 3.23. 700 MHz, β= 0.47 SC elliptical cavity prototype.*

Concerning the operating conditions of these elliptical cavities, a good compromise is an operation at a temperature of 2 K and at a frequency of 704.4 MHz, twice the frequency of the RFQ. These superconducting cavities are subject to important R&D programmes. The performance of the prototypes has been measured to exceed the operational characteristics for the XADS by a very comfortable safety margin that ensures the 'overdesign' criteria imposed by the reliability strategy.

### *3.1.2.3. PDS-XADS Pb-Bi OPTION*

The eXperimental Accelerator Driven System (XADS) ([3.15],[3.16]) is a facility designed for demonstrating basic aspects of the ADS power prototype such as the viability of the system made of a subcritical Reactor driven by an Accelerator via a Target Unit.

Some of the main features of the XADS are typical of the design of large pool type LMFBRs, whereas a few are peculiar to the ADS (e.g. proton accelerator feeding a target unit placed inside an hollow core) or to the heavy coolant (gas injection instead of mechanical pumps) or to the experimental mission of the facility (power dissipated by air coolers via an intermediate low pressure organic fluid loop).

The whole Nuclear Island lies on a single foundation consisting of an upper and a lower basement separated by seismic support pads (Fig. 3.24), installed to decouple the civil structure from soil vibrations in horizontal direction. In fact, owing to the large dead weight of the LBE coolant and its large free surface, seismic loading and sloshing may become very important. The isolators are of the high damping rubber bearing type, made of alternate layers of vulcanized rubber and reinforcing steel plates.

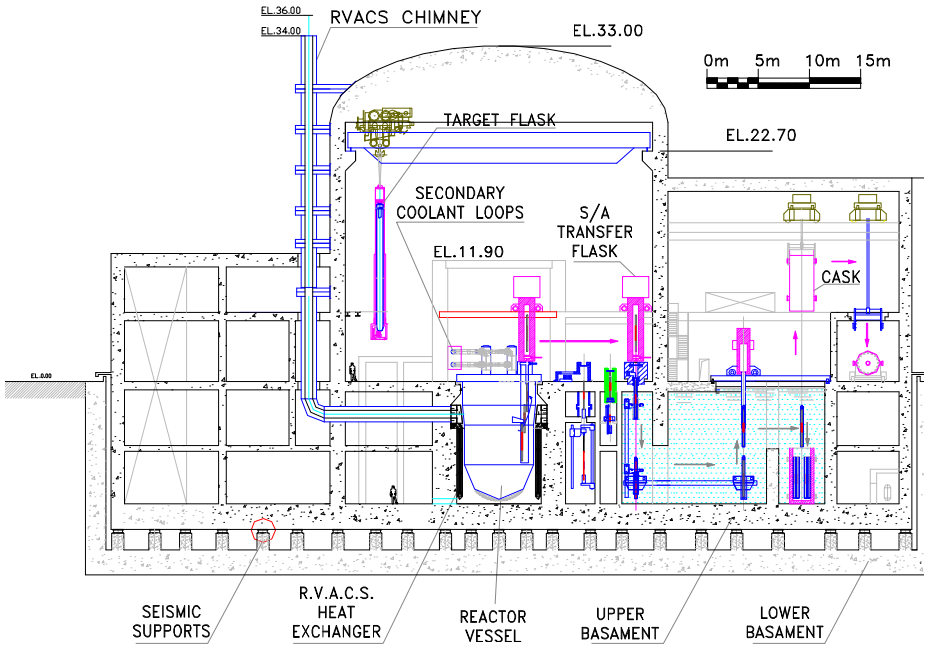


*FIG. 3.24. Nuclear island of LBE cooled XADS.*

The primary coolant is molten lead-bismuth eutectic, which is characterized by good nuclear properties, operating temperatures lower than pure molten lead and compatibility with the low pressure diathermic organic fluid used in the secondary system.

The configuration of the primary system [3.17] is pool type (Fig. 3.25), similar to the design solution adopted for most sodium cooled reactors, which has important beneficial features. These include a simple boundary (the reactor vessel) containing all the LBE, thus eliminating all problems related to out of vessel primary coolant. Table 3.13 provides the main parameters of the XADS primary system.

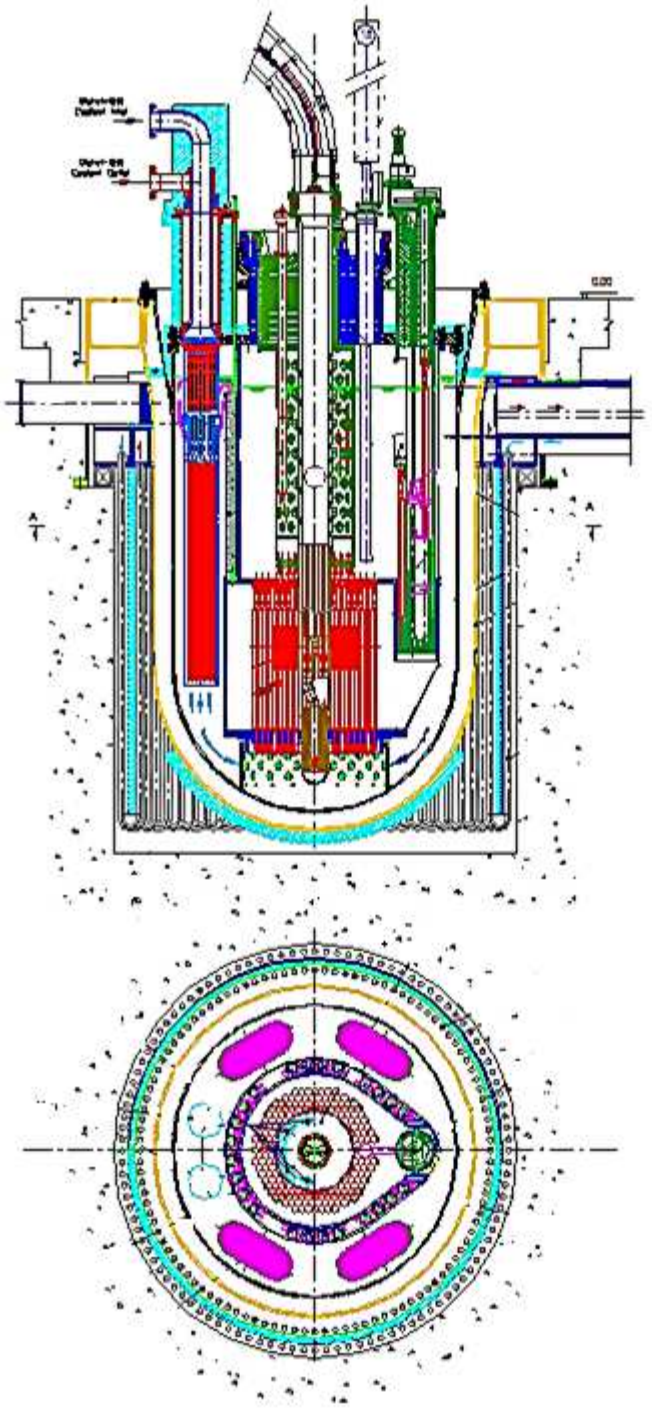

*FIG. 3.25. Reactor vessel & primary system of the LBE cooled XADS.*

TABLE 3.13. STEADY STATE THERMAL PARAMETERS OF THE HOTTEST ROD AT BOL

| Parameter | Units | Value |
|---|---|---|
| Core power | MW | 80 |
| Maximum power from spallation | MW | 3 |
| Core inlet temperature | °C | 300 |
| Core outlet temperature | °C | 400 |
| IHX diphyl THT sec. coolant inlet temperature | °C | 270 |
| IHX Diphyl THT sec. coolant outlet temperature | °C | 312 |
| Coolant flow rate in the core | Kg/s | 5471 |
| Coolant velocity in the core | m/s | ~0.42 |
| Argon flow rate | Nl/s | 120 |
| Core pressure loss | Pa | 25000 |
| Primary circuit pressure loss | Pa | 29000 |
| LBE Inventory | tons | ~ 1700 |

The reactor vessel is surrounded by the safety vessel to ensure containment of the primary coolant and its circulation through the core also in case of reactor vessel leakage. The reactor vessel rests on the same boxed annular beam, anchored to the civil structure to which the safety vessel is suspended, and supports the reactor roof and the internals.

The gap between the two vessels is sufficient to allow the access of a remote controlled device, of the free rolling vehicle type, for ISI of the welds of the reactor vessel.

Both Reactor and Safety Vessel are made of a nozzle free cylindrical shell with hemispherical bottom head. The upper side of the cylindrical shells ends with a Y-piece, the inner branch of which supports the Reactor Roof.

The internal structure, of asymmetrical cross-section, hangs from the reactor roof. Its shape is determined by the need of including the in vessel handling equipment and limiting the reactor vessel diameter, while leaving a large outer space to install the heat exchangers.

The reactor roof ensures the reactor cover gas containment, the biological protection of the above roof area and the support for rotating plug, intermediate heat exchangers, purification units, rotor lift machine and gas injection pipes.

The rotating plug supports the above core structure, eccentric installed inside a penetration, and the transfer machine with double gas tight seals to insure the integrity of the reactor boundary even in case of rotation for refuelling.

The above core structure is a crank shaped structure that supports the target unit and the core monitoring equipment and can rotate to allow refuelling.

The in vessel fuel handling system allows handling without opening the primary containment. it consists of a transfer machine that can reach all diagrid positions, and of a rotor lift machine that transfers the assemblies to/from a flask positioned on the reactor roof.

To avoid rotating parts immersed in Pb-Bi, no mechanical pumps are used for primary coolant circulation which is obtained by an argon gas lift system.

The primary coolant leaves the core in radial direction about half a meter below the top of the fuel assemblies and enters the riser channels arranged at the periphery of the internal structure. Argon is injected at the bottom of riser channels to increase the density difference between the lead-bismuth in the downcomer and the lead-bismuth gas mixture in the riser. The argon gas leaves the coolant at the free surface and escapes into the cover gas plenum. This solution combines the high level of reliability of the natural circulation required by a safe core cooling function, with reactor compactness, operational flexibility, and lower thermal loading on the structures typical of the forced circulation.

Four bayonet tube IHXs are freely immersed in the downcomer, without membrane spanning the vessel to separate hot and cold plena (no Redan), to ensure coolant flow even in case of solidification of the LBE inside the IHXs. The IHXs transfer heat from the LBE coolant to the secondary diathermic fluid during normal and Decay Heat Removal (DHR) conditions. The LBE coolant enters radially the IHXs through a window provided in the upper part of the tube bundle, leaves axially the IHXs and reaches the core to start a new thermal cycle.

In the case of the windowless target unit option, a small fraction of primary coolant (~ 5%) is bypassed through the target unit to remove the spallation power.

All primary system components are made of stainless steel (Z2 CND 17.12 Az.Co RCC-MR for Main Vessel and Internals, and Z2 CN 18.10 RCC-MR for Safety Vessel) compatible with LBE at the XADS low operating temperature.

The mechanical analyses confirm the feasibility of the primary system components, thanks to the horizontal antiseismic supports that drastically reduce the most important load which is induced by the seismic excitation.

Inside the reactor vessel cavity, the large U-tube type heat exchanger of the Reactor Vessel Air Cooling System (RVACS) keeps cooled the concrete walls of the vessel cavity and is always available to removes decay heat through two concentric headers and four stacks that constitute redundant inlet and outlet air paths.

The target unit provides the physical and functional coupling between the proton beam accelerator and the subcritical core. The LBE target, containing the spallation products, is kept confined within the target unit in order to prevent the contamination of the primary LBE coolant. The target unit is a removable component of slim cylindrical form, positioned coaxially with the reactor vessel which serves also as inner radial restraint of the core. Its component parts are the proton beam pipe, the heat exchanger and the LBE circulation system, that can be designed in forced or natural circulation, depending on the two design options currently under study: windowless or window). The hot window target unit features a thin metallic sheet as a barrier between the LBE target and the proton beam vacuum pipe. The window and most of the target unit are made of ferritic martensitic 9Cr1Mo. The heat generated by the spallation reactions is removed by LBE in natural circulation. The LBE is cooled by the heat exchanger located at a higher level, an arrangement typical of natural circulation cooling circuits. The use of a diathermic fluid as secondary coolant gives high flexibility in the choice of the thermal cycle and in particular it allows limiting the temperature of the hottest spot of the window.

In the windowless target (see Fig. 3.26) unit the proton beam impinges directly on the free surface of the liquid LBE target. Natural circulation of the LBE is no longer possible, because the heat source is at the top of the circuit. Thus the heated LBE must be driven downwards to the heat exchanger by some means, in this case two mechanical pumps in series. A stream of primary LBE is bypassed from the cold plenum to the heat exchanger to serve as a cooling medium. In the windowless target unit no structural material is exposed to the direct proton irradiation. This option has the advantage of overcoming the material damage due to proton irradiation and hence allows lifetime and handling intervals similar to that of the fuel assemblies.

A drawback of the ADS concept is neutron streaming from the beam tube which makes difficult refuelling and ISI&R owing to the activation of structures and components above the vessel roof. An estimate of the activation with 200 mm ID beam pipe has given an unacceptable level. In the case of the windowless target Unit this problem seems of straightforward solution because it is sufficient to scan the proton beam perpendicularly to the horizontally flowing LBE (1-D scanning).

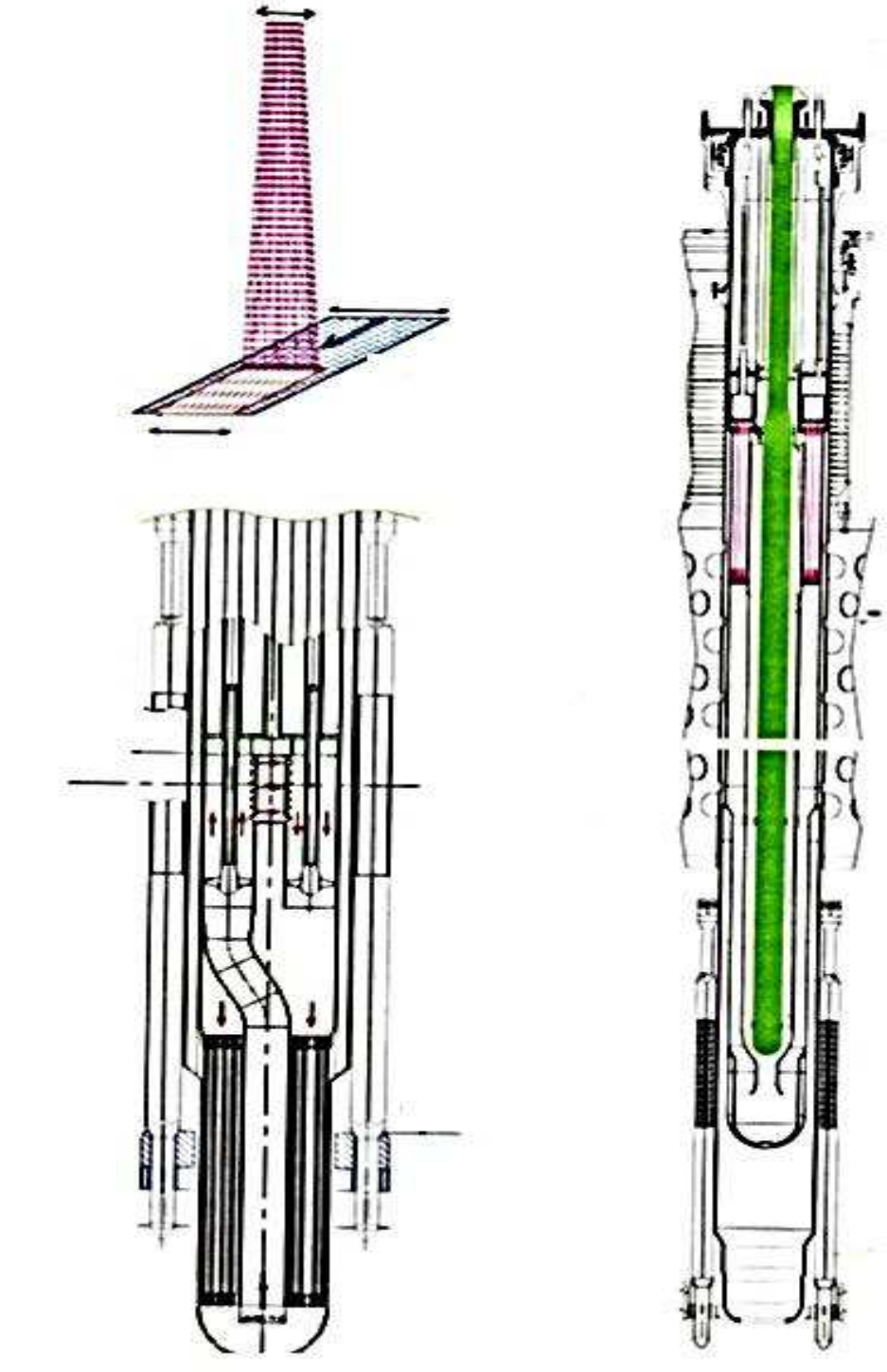

*FIG. 3.26. Windowless and window target unit of the XADS.*

The smaller beam pipe of rectangular cross-section of the new windowless target design is expected to reduce material activation, extending manned activities in the area (a few days after proton beam shutoff) to several hundred hours without exceeding the yearly averaged dose limit for professionals.

The core (see Fig. 3.27) consists of 120 fuel assemblies arranged in an annular array of five rows. The inner row surrounds the target unit. The assemblies are all alike, each loaded with 90 fuel pins which have the same cross-section and fuel MOX composition with two different enrichments.

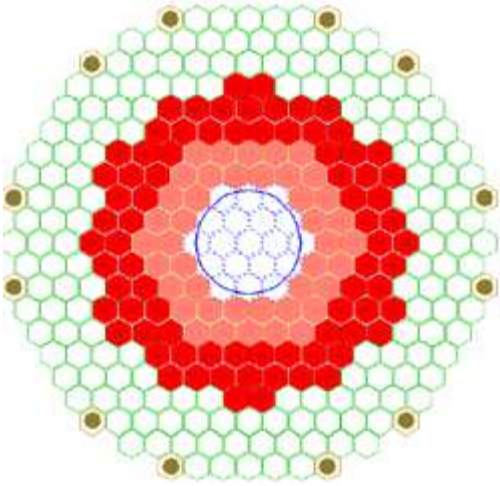

*FIG. 3.27. Core cross-section of the LBE cooled XADS.*

The 42 fuel assemblies of the two innermost rows are enriched as the standard Superphénix reload fuel, the remaining 78 fuel assemblies are higher enriched at 28.25% Pu, to set an operational $k_{eff} = 0.97$ at nominal power and BOL [3.18].

The fuel pin cluster is enclosed by a hexagonal wrapper; the lattice is about 40% larger than for SPX, while the active fuel length is slightly shorter (87 vs 100 cm). The fuel assemblies are surrounded by a buffer region of 174 dummy elements, the purpose of which is to keep the fixed structures away from the hard neutron region. LBE in the buffer region and adjacent downcomer provides a substantial neutron reflector for improving the overall neutron economy. Moreover, the core buffer allows a flexible management for irradiation testing of prototypical fuel assemblies containing different kinds of fuel or LLFP's and for positioning neutron absorbers to lower $k_{eff}$ below 0.95 before refueling.

Because LBE is a highly diffusive and fairly transparent medium for neutrons, it has been possible to adopt a wide fuel pin lattice with associated reduced friction losses. This allows core cooling by natural convection even in the case of loss of the argon lift system.

The BOL and EOL subcriticality range, associated with the cycle length and core management, is a crucial parameter for defining the proton beam current.

The operational subcriticality range (Fig. 3.28) is established in order to stay away from criticality ( $k_{eff} = 1$ ) with adequate margin under normal operational conditions so that postulated accidents which may lead to large temperature changes and positive reactivity insertions may also be taken into account without achieving criticality. For Design Basis Conditions (DBC), a safety margin of $\Delta k$=1% and 0.6% allowance for measurement error are subtracted from the criticality state, so that the resulting upper limit for the multiplication factor becomes ( $k = 0.984$ ). Furthermore, consideration of core cooling from operating down to assumed ambient temperature, beam pipe flooding by LBE or geometrical variations associated to earthquake or temperature variation and Doppler effect cumulate to a predictable reactivity insertion of about 1.4%. The core multiplication factor for normal operation at full power and BOL is thus set at $k = 0.984 - 0.014 = 0.970$, i.e. a subcriticality margin of 3%.

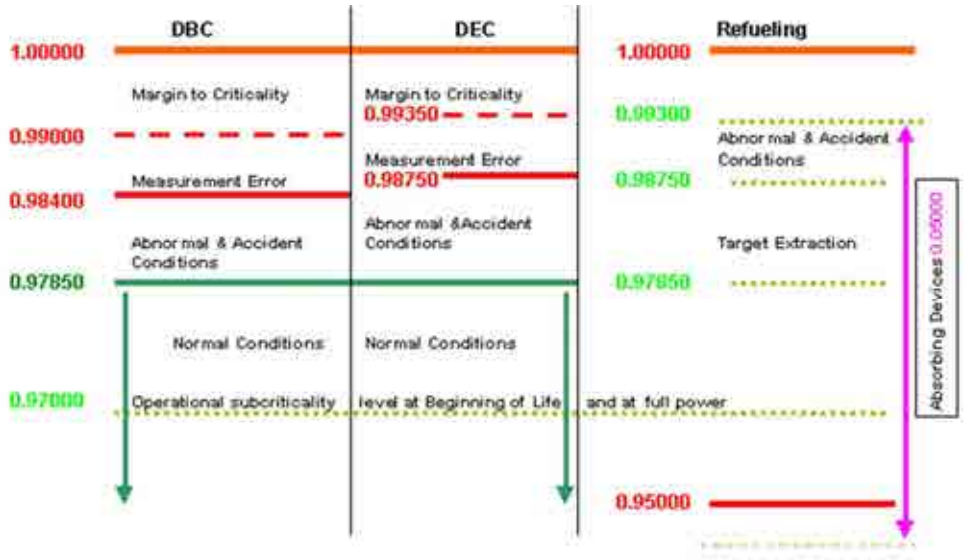


*FIG. 3.28. Subcriticality limit vs. operating and accident conditions.*

Accidents like those involving large core compaction which may be worth about 0.5–0.6%, may be allocated to Design Extended Conditions (DEC). Also for these accidents the core remains subcritical, though with a reduced safety margin. As a conclusion the 0.97 core multiplication factor is sufficiently low to ensure the safe operation of the core without need of shutoff rods.

During operation, the core reactivity decreases at a rate of about 0.004%/day. Thus for the targeted 1000 days full power operation, the reactivity depletion would not exceed 4%, i.e. the operating multiplication factor reduces from 0.97 at BOL to 0.93 at EOL. The Core can be operated in these EOL conditions with a proton current of about 6 mA.

In order to assess the safety characteristic of the system, extensive dynamic transient analyses have been performed, using different codes (RELAP5-PARCS, TRAC-M-PARCS, SIMADS, SIMMER, SAS4ADS, EAC2, and STAR-CD), thereby allowing not only an independent comparison of the codes, but also providing a certain confidence in the methods used for the verifications of these new innovative reactors.

The purpose of these transient investigations is to:

— Study the dynamic characteristics of the subcritical cores; and

— Study the transient response of the entire system design to different plant transient initiators.

A total of 26 transient initiators (e.g., spurious beam trip, protected-unprotected loss of flow, loss of heat sink, subassembly blockage) have been chosen for detailed analysis and classified into operational transients, protected transients, and unprotected transients.

Fig. 3.29 and Fig. 3.30 show that in case of unprotected loss of argon gas lift system (ULOF), natural circulation ensures about 50% of the nominal flow rate and a core outlet temperature increase of only 100 K over the nominal value of 400°C. Thus the results of all these analyses indicate that this design exhibits a large safety margin on account of a combination of very favorable safety characteristics, namely 1) good heat transfer properties of the coolant, 2) high boiling point of the coolant preventing voiding within the core, 3) favorable natural convection behaviour of the coolant in a primary circuit purposely designed for natural circulation, 4) large thermal inertia of the coolant inside the core region, 5) very large thermal inertia of the coolant because of the pool type primary system and 6) peculiar design choices, i.e. decay heat removal by the RVACS with air cooler in natural circulation.

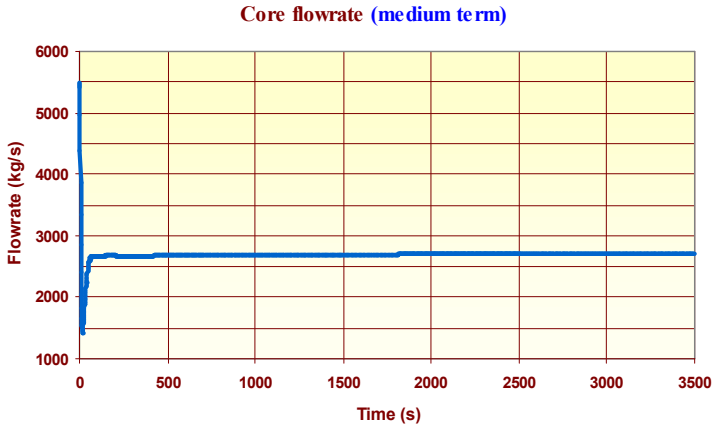


*FIG. 3.29. Unprotected loss of flow, core flowrate.*

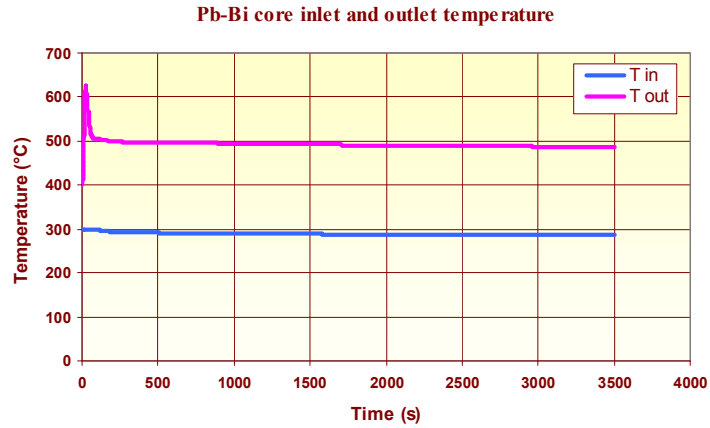


*FIG. 3.30. Unprotected loss of flow, LBE Core inlet and outlet temperature.*

The combination of these features make it very unlikely any overheating of the fuel clad and risk of release of fission products into the primary system even under the most severe transient conditions.

### *3.1.2.4. PDS-XADS GAS OPTION*

The gas cooled reactor has been selected with a view to use, as far as possible, existing and proven technologies or at least to take benefit of the technologies under development for other helium cooled reactor projects [3.19]. The overall architecture of the plant is derived and extrapolated from modular thermal HTR projects such as the GT-MHR. The primary coolant is helium at about 6 MPa, by similitude with the GT-MHR and compatible with adequate core cooling. An overall arrangement of the primary system is shown on Fig. 3.31.

The reactor primary system comprises a reactor vessel housing the core, a separate vessel that houses the PCS and a cross vessel linking the two vessels. The primary vessel accommodates the Target Unit TU, the subcritical core and associated systems for fuel handling and the Shutdown Cooling System (SCS) for decay heat removal. The PCS vessel provides the coolant circulation, by a motor driven blower, and the heat exchanger transferring heat to an external cooling water circuit.

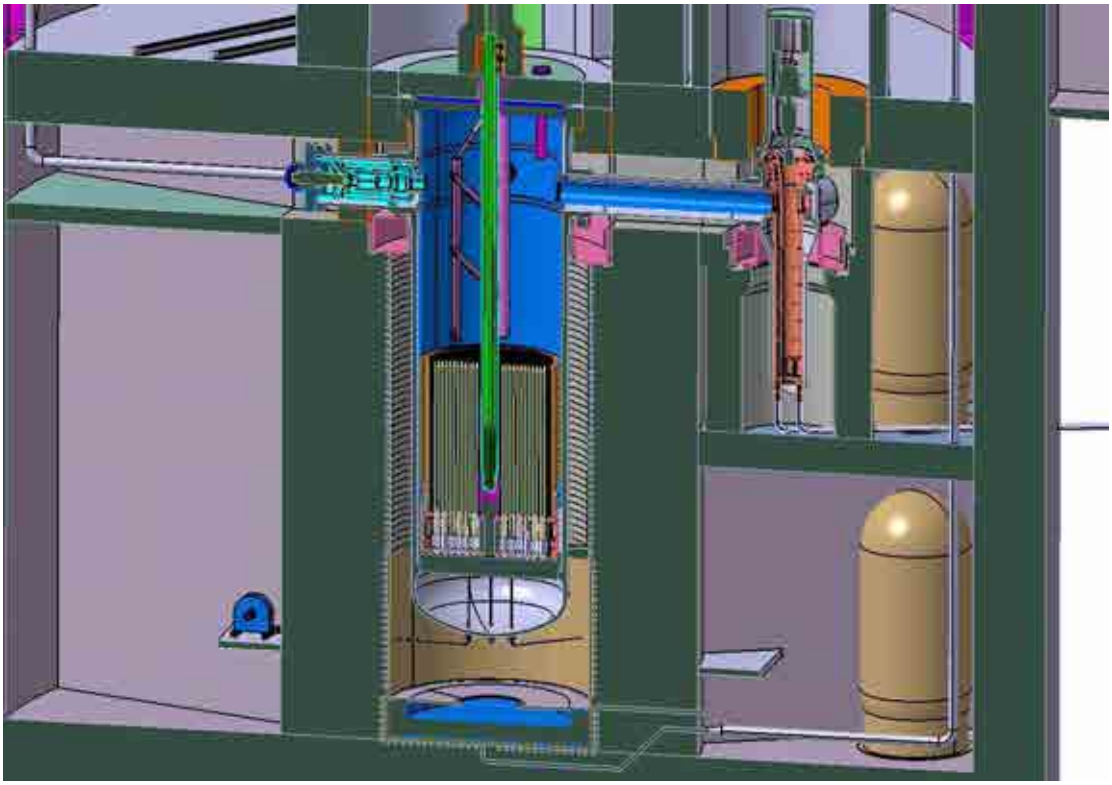

*FIG. 3.31. Primary system architecture of the gas cooled XADS.*

Metallic vessels have been preferred to prestressed concrete pressure vessels for consistency with current HTR projects justified mainly by the extensive fabrication in existing NPP factory facilities which brings significant cost and schedule gains.

The reactor vessel is located within a concrete reactor vault and the whole system within the reactor building. The reactor vault is cooled by a specific circuit. The direction of entry of the proton beam and the target to the reactor has a large influence on the overall layout of the reactor building and, in case of the reference inlet from the top, on the above roof area where the proton beam transfer line has to be accommodated.

For the mitigation of severe accidents, provision is made for an external core catcher located under the reactor vessel in the pit and cooled by a specific passive water cooling circuit.

The gas coolant medium is helium with forced circulation during power operation. In case of accidental loss of the forced circulation of helium, the decay heat can be removed in natural circulation using the helium-water heat exchangers and natural circulation on the water side of the shutdown cooling system. A circulator is provided as part of the SCS for decay heat removal for both normal operation and in accidental depressurised state.

As well as the interface with the core, there are important interfaces with the accelerator and the target unit. The primary system also has a role in each of the main safety functions for shutdown, decay heat removal and containment. The main parameters of the primary circuit are listed in Table 3.14.

TABLE 3.14. MAIN DESIGN PARAMETERS OF THE PRIMARY SYSTEM OF THE GAS COOLED XADS

| Parameter | Units | Value |
|---|---|---|
| Core power | MW | 80 |
| Primary coolant (helium) | MPa | ~6 |
| Core inlet temperature | °C | 200 |
| Core outlet temperature | °C | 450 |
| Coolant flow rate in the core | kg/s | 61.6 |
| Coolant velocity in the core | m/s | ~30 |
| Primary system target pressure drop | MPa | 0.1 |
| Primary helium containment | --- | Metallic vessels |
| Power conversion system | --- | Heat exchanger and circulator |
| Secondary coolant | --- | Water |
| IHX sec. coolant inlet temperature | °C | 25°C |
| IHX sec. coolant outlet temperature | °C | 65°C |

The core layout is rather compact. The nineteen positions at the centre of the core are left empty to accommodate the spallation target assembly. Outside this, there are ninety fuelled subassemblies, all of the same fresh fuel composition. The core will be fuelled with conventional mixed oxide (MOX) fuel, with maximum plutonium enrichment not exceeding 35% by mass and an isotopic composition specified in Table 3.15, which is similar to that of SuperPhenix.

TABLE 3.15. ISOTOPIC COMPOSITION OF PLUTONIUM AND URANIUM IN THE FUEL BY MASS

| Isotope | Fraction by mass |
|---|---|
| Np237 | 0.00021 |
| Pu238 | 0.00271 |
| Pu239 | 0.69088 |
| Pu240 | 0.24412 |
| Pu241 | 0.02545 |
| Pu242 | 0.01285 |
| Am241 | 0.02377 |
| *Total Pu-MA* | *1.00000* |
| U234 | 0.00005 |
| U235 | 0.00518 |
| U236 | 0.00005 |
| U238 | 0.99472 |
| *Total U* | *1.00000* |

Surrounding the fuel are approximately three rows of steel reflector subassemblies and outside this there are approximately five rows of shield subassemblies. Absorber rods are used only during refuelling. It was assumed that during normal operation at power, the absorber rod locations will be occupied by reflectors (with the control rods placed in ‘storage’ positions in the outer shield). The principal subassembly dimensions and those of the fuel and shield pin and bundle are summarized in Table 3.16.

TABLE 3.16. PRINCIPAL SUBASSEMBLY AND PIN BUNDLE DIMENSIONS OF THE GAS COOLED XADS

| Subassembly | |
|---|---|
| Overall length | 4.800 m |
| Subassembly pitch | 120 mm |
| Inter subassembly gap | 5 mm |
| Wrapper | |
| External across flats | 115 mm |
| Wall thickness | 4.5 mm |
| Fuel pin bundle | |
| Overall length | 2620 mm |
| Number of pins | 37, triangular pitch |
| Pin pitch | 16.78 mm |
| Pitch/diameter ratio | 1.291 |
| Length of the fuel column | 1500 mm |
| Length of the cold plenum | 750 mm |
| Length of upper plenum | 100 mm |
| Fuel pin and pellet | |
| External diameter of clad | 13.0 mm |
| Clad thickness | 0.5 mm |
| pellet external diameter | 11.5 mm |
| pellet internal diameter | 3.2 mm |
| Neutron shield pin bundle | |
| Overall length | 1000 mm |
| Length of steel reflector | 380 mm |
| Length of boron carbide shield | 500 mm |
| Length of plenum | 50 mm |
| Number of pins | 7, triangular pitch |
| Shield pin clad diameter | 30 mm |
| Clad thickness | 1.0 mm |
| Boron carbide pellet diamater | 27.0 mm |
| Steel reflector rod diameter | 27.8 mm |

### 3.1.3. XT-ADS: European eXperimental Transmutation in Accelerator Driven System

Already in the beginning of the European EUROTRANS project [3.5], SCK•CEN offered to use the MYRRHA 2005 design file [3.7] described in section 3.1.2 as a starting basis for the XT-ADS design [3.19]. This allowed optimizing an existing design towards the needs of XT-ADS and within the limits of the safety requirements instead of starting from a blank page. MYRRHA and XT-ADS differ however on several topics that are listed below for each field of the design and are detailed for the core design and for the general configuration of the primary system.

The reference accelerator for XT-ADS has a 600 MeV beam while it was limited to 350 MeV for MYRRHA, the latter value being however kept as backup option (see section 3.1.2 for a full description of this accelerator). The core inlet and outlet temperature have been significantly increased and reach now 300°C (inlet) and 400°C (outlet). On the other hand the fuel power density has been limited to 700 W/cm³, while it reached 1000 W/cm³ for MYRRHA. The thermal power of the installation should range between 50 and 70 MW(th).

As in MYRRHA, the XT-ADS is designed to use MOX as fuel material. Both designs start with a 30wt% of plutonium MOX. While MYRRHA was designed using a reactor grade plutonium vector,

for XT-ADS a plutonium vector coming from the reprocessing of PWR fuel (initial enrichment of 4.5% in $^{235}$U, burnup of 45 GWd/t, cooling period of fifteen years) has been chosen.

The pin itself (Fig. 3.32) consists of a fuel pellet column of 60 cm with on both ends a neutron reflector to increase the neutron economy, a fission gas plenum and a closing cap.

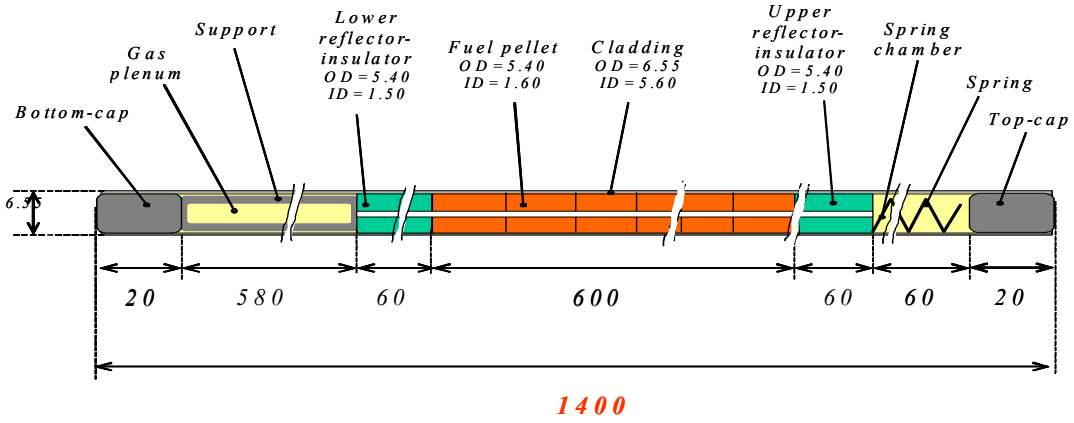


*FIG. 3.32. XT-ADS fuel pin.*

The fuel pellets are of the hollow type (diameter = 1.6 mm). This reduces the center line temperature and hence gives larger margins to fuel melting limits. The fuel assembly contains 90 of these fuel pins in a hexagonal lattice together with one 'instrumentation pin' in the centre of the assembly.

Another major difference with the MYRRHA design is the larger fuel pin pitch. This increase was needed to reduce the pressure drop over the core. It was very clear from the beginning that the T91 cladding material would be the weakest link and hence defining the operational limits of the XT-ADS core. The present design is the result of several iterations between neutronic and thermohydraulic calculations. The most important feedback parameters were the pressure drop over the core and the needed coolant speed to keep the inlet and outlet temperatures fixed to the ones fixed in the characteristics (300–400°C). Mechanical calculations showed that a wall thickness of 2 mm was sufficient for the wrapper. The clearance between the assemblies was fixed to 3 mm, which is the double of that of MYRRHA. The final result (Fig. 3.33) is an assembly total width (flat–flat) of 93.2 mm and an assembly pitch (center–center) of 96.2 mm.

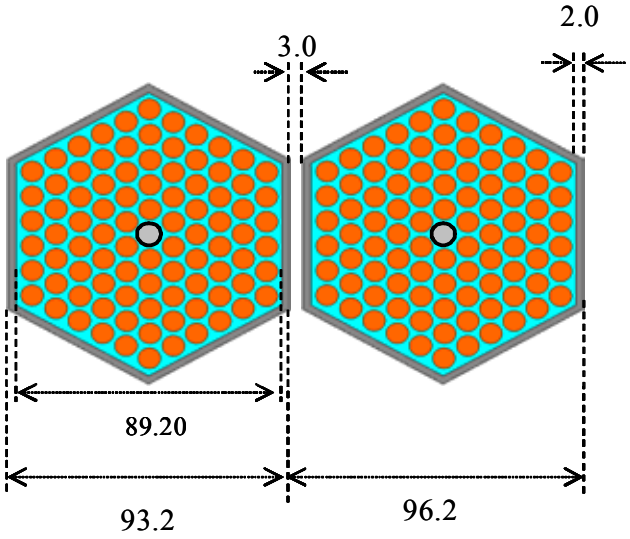


*FIG. 3.33. XT-ADS fuel assembly.*

As a result of both the degrading of the MOX fuel and the enlargement of the fuel assemblies and assembly pitch (the fuel density has been reduced significantly) the $k_{eff}$ of the core dropped. Three

options were open to get back to the reference value of $k_{eff}$ = 0.95: either increase the active length, or use more fuel assemblies, or allow for a higher Pu ratio (more than 30wt %). Taking into account pros and cons of each option, it was decided to increase the Pu wt% at 31.5wt; in such a way $k_{eff}$ reaches the value of 0.953.

The core layout (Fig. 3.34) was fixed to 72 fuel assemblies encircling a 'gap' of three emptied positions to allow for the placement of the spallation target module. The proton beam current of the 600 MeV beam was fixed in order to have a fuel power density of 700 W/cm$^3$. This results in a beam current of 2.33 mA, a core power of about 57 MW(th) and a fast peak flux $\Phi_{>0.75MeV}$ of $0.72\times10^{15}$ n/(cm².s).

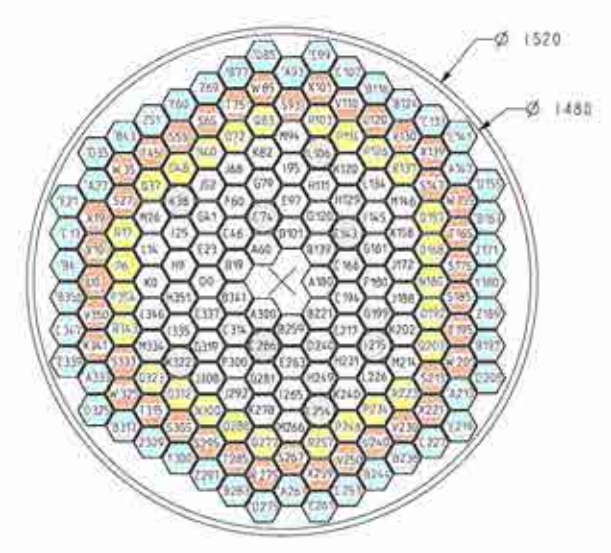


*FIG. 3.34. XT-ADS core configuration.*

The design of the XT-ADS spallation target [3.21] also started from the MYRRHA design with three central emptied positions in the core and the modifications described above. Some topics should in principle facilitate the design: the larger fuel assemblies — 93.2 mm instead of 85.5 mm flat–flat imply more room for the target, the heat load deposited by the 600 MeV proton beam is lower — 0.98 MW instead of 1.75 MW in the 2005 design, but such a design requires quite a lot of R&D effort already ongoing.

Also the vessel and the primary system configuration were developed starting from the MYRRHA design and include some enhancements.

A large part of the work has been devoted to investigate the possibility of fuel handling from the top. Although fuel loading from the bottom, like in the MYRRHA design, is far from the classical options in reactor technology, fuel loading from beneath the core was still preferred. The main advantage of such a solution is a minimized interference with the experimental rigs (inpile sections) that are loaded/unloaded from the top and must be kept in position during fuel loading operations. Interference with the spallation loop, with the instrumentation above the core and with the beam line tube is also minimized. The classical option of fuel handling from the top would therefore penalize the plant availability. A final advantage of the loading by the bottom is the possibility to avoid a fuel assembly locking system for buoyancy reasons.

Seismic events were considered in the fuel assembly as well as in the vessel design; there is no need to install seismic dumpers since the very smooth seismic activity at the Mol site where XT-ADS is supposed to be erected.

The present (2008) XT-ADS design is illustrated by Fig. 3.35 (cross-section) and Fig. 3.36 (vertical section) and differs significantly from the MYRRHA design presented in section 3.1.2.1.

1. Core
2. Heat exchangers (2 x 2)
3. Pumps (2 x 1)
4. Spallation loop
5. Fuel manipulators (2 units)
6. Vessel

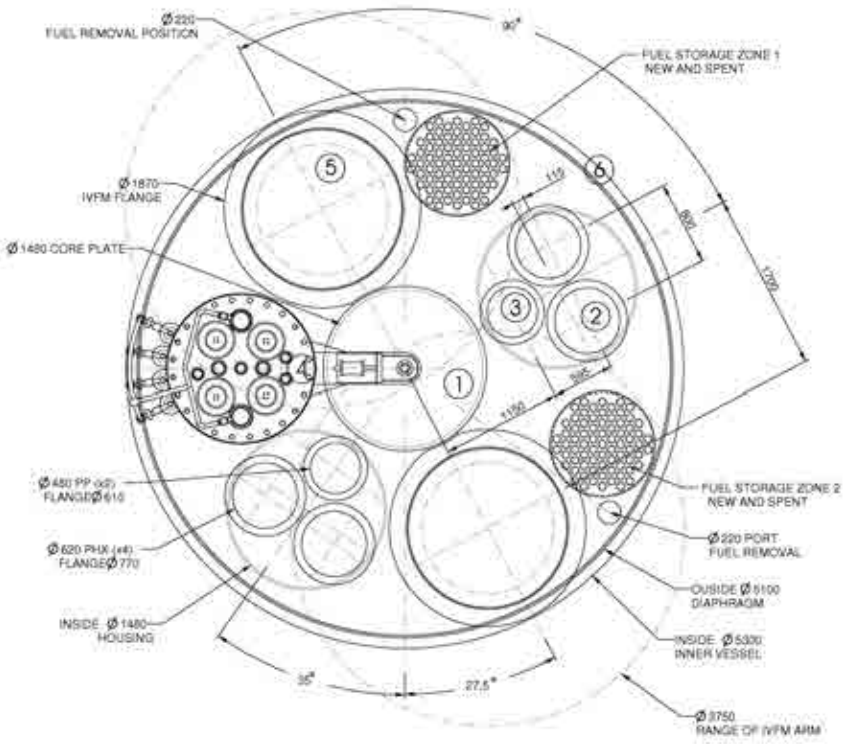


*FIG. 3.35. XT-ADS cross-section in the vessel.*

1. Core
2. Heat exchangers (2 x 2)
3. Pumps (2 x 1)
4. Spallation loop
5. Vessels
6. LBE hot level
7. LBE cold level

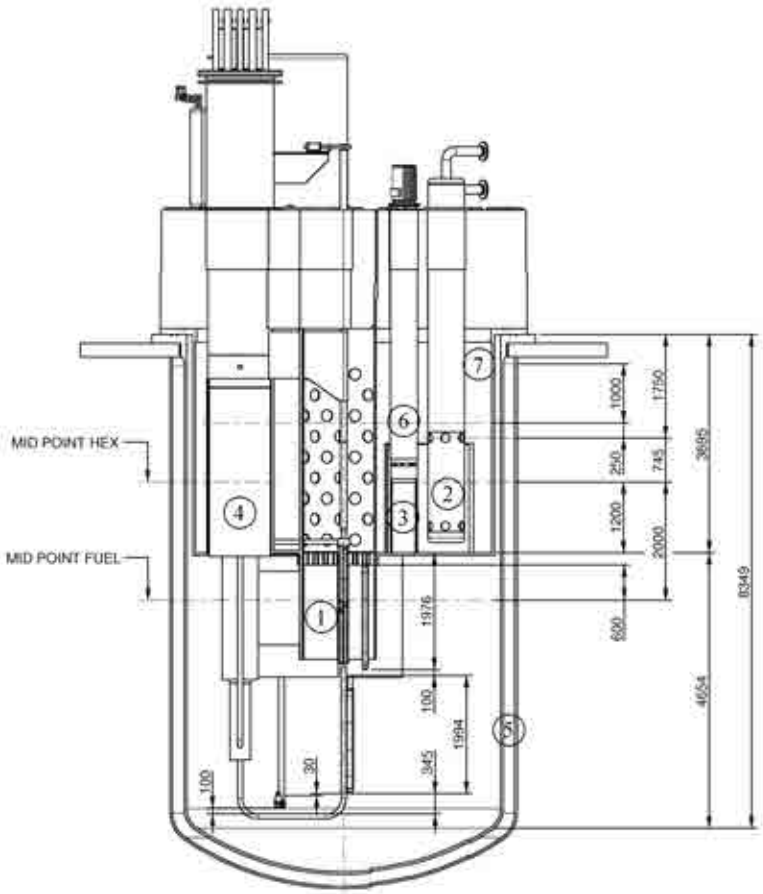


*FIG. 3.36. XT-ADS vertical section through the vessel.*

The main evolutions from MYRRHA to XT-ADS, which are also summarized in Table 3.17, are the following:

— Reactor and safety vessels have now an elliptical bottom and are hanging (while MYRRHA was standing); a special shape has been adopted for reducing the thermal loads on the vessel support;

— Shape of the diaphragm has been changed from conical to cylindrical to minimize the core bypass flow rate, to reduce the mechanical loads and to improve its constructability; the number of the penetrations in the diaphragm has also been reduced from 17 to 8 for the same reasons;

— Number of primary components was kept as low as possible to reduce the plant cost and maintenance without jeopardizing safety functions and availability; a comparison exercise was performed and the final chosen configuration contains two groups (MYRRHA had four groups) of each one primary pump and two boiling water heat exchangers;

— Primary system has been designed to evacuate a total of 70 MW(th) (this value takes into account not only the core, but also the spallation target, the decay heat from the fuel storage and other minor heat sources) by two independent secondary loops using water that boils in the primary heat exchangers and condensing the produced steam in the air coolers cooled by forced air;

— Elevation of the HX with regard to the core has been increased to improve natural circulation capabilities;

— Secondary system is designed as a safety grade system and is able to evacuate the decay heat also in emergency conditions in natural circulation with 200% of redundancy.

— Reactor vault cooling system has been adopted as ultimate decay heat removal in case of loss of heat sink.

TABLE 3.17. SUMMARY OF THE EVOLUTION FROM THE MYRRHA 2005 DESIGN TO THE XT-ADS DESIGN

| Parameter | MYRRHA 2005 design | XT-ADS |
|---|---|---|
| Design level | Conceptual design | Advanced design |
| Power | ~50 MW(th) | ~70 MW(th) |
| Core inlet temperature | 200°C | 300°C |
| Core outlet temperature | 340°C | 400°C |
| Fuel | MOX (accept for a few MA Fuel samples) | MOX (accept for a few MA Fuel assemblies) |
| Fuel power density | ~1000 W/cm³ | 700 W/cm³ |
| Fuel pin spacer | Wire | Grid |
| Secondary coolant | High pressure water or low pressure boiling water | Low pressure boiling water |
| Accelerator | LINAC (350 MeV*5 mA) | LINAC (600 MeV*2.5 mA or 350 MeV*5 mA) |
| MOX Fuel type | reactor grade | from reprocessing |
| Fuel pin hole | no | yes (Ø=1.6 mm) |
| Pu content | 20 & 30% | >31% |
| Fuel assembly centre–centre | 87.0 mm | 96.2 mm |
| Fuel assemblies in core | 45 | 72 |
| Number of possible IPS | 17 | 8 |
| Vessel type | standing | hanging |
| Vessel bottom | flat | elliptical |
| Number of groups HX + PP | 4 | 2 |
| Ultimate decay heat removal | emergency cooling loops | vault cooling system |

The EUROTRANS FP6 project has ended in March 2010. The design achievements have been reported, among others in [3.22] and [3.22]. The conceptual design of the XT-ADS machine was then

ready for a new evolution, the FASTEF version, which design is the purpose of the FP7 project called CDT for Central Design Team (2009–2012). The major modification from XT-ADS to FASTEF [3.23] is its operation mode. While XT-ADS, and its predecessors, was solely designed for running in ADS mode, FASTEF is from the beginning designed to be capable to run in both critical and subcritical modes.

On March 3rd, 2010 the Belgian federal government decides to support the realisation of the project. It has allocated 60 M€, as a first step, to conduct R&D, to finalize the engineering design, to secure licensing and finally to implement a structure at international level. The present schedule is foreseen for arriving to the construction and operation of the FASTEF facility:

- 2010–2014: Front End Engineering Design, drafting the technical specifications and preparing the call for tenders; development and testing of components for both accelerator & reactor; starting, on a more formal basis, iterations with the Belgian safety authorities;
- 2015: Tendering and procurement;
- 2016–2018: Construction of components and civil engineering works on the Mol site;
- 2019: Assembling together the different components;
- 2020–2022: Commissioning of the facility at progressive levels of power;
- 2023: Progressive startup;
- 2024: Fully operational.

### 3.1.4. JAEA Experimental ADS

Objectives of the JAEA Experimental ADS [3.25] are:

- Examination of the MA irradiation and transmutation performance;
- Validation of simulation accuracy;
- Demonstration of system safety;
- Development of devices for measurement and operation; and
- Determination of design criteria of commercial scale ADS through several tens MW operation.

There are two options for the Experimental ADS in JAEA: the primary candidate is a subcritical system cooled by lead-bismuth eutectic and the other one is cooled by liquid sodium. Here after, only the liquid sodium cooled ADS is briefly described because the lead-bismuth cooled option is still under designing.

The system is composed of a proton accelerator with several MW (J-PARC class) beam power, a solid spallation target made by tungsten and a sodium cooled subcritical core. At the first stage, subcritical core is loaded with conventional uranium oxide fuel (20% $^{235}$U enrichment) to omit the uncertainty caused by MAs. At the second stage, oxide fuel is changed to uranium nitride fuel. The MA nitride fuel is partially loaded to get the data of irradiation effect and transmutation performance.

In this Experimental ADS, $k_{eff}$ is set to 0.93 to ensure enough safety margins. The rated power is 30 MW by injection of 2.3 MW proton beam. The average neutron flux is in the order of $10^{14}$ n/cm$^2$.sec. At the second stage, accelerator power and thermal output is increased to 4.5 MW and 60 MW respectively, with uranium nitride fuel.

The subcritical core is composed of 7 target subassemblies (ducted), 228 fuel subassemblies (ductless) and 570 reflector subassemblies (ducted). Overall core diameter is about 1m. About 3200 kg of uranium is loaded at the first stage.

Table 3.18 and Table 3.19 provide the main core and system parameters respectively, while Fig. 3.37 shows a schematic view of the JAEA Experimental ADS.

TABLE 3.18. MAIN CORE PARAMETERS OF THE JAEA EXPERIMENTAL ADS

| Parameter | First stage | Second stage |
|---|---|---|
| Thermal output | 30 MW | 60 MW |
| Core $k_{eff}$ | 0.93 | |
| Core height/diameter | 1000 / 960 (mm) | |
| Fuel pin diameter/ pin pitch | 5.4 / 7.14 (mm) | |
| Fuel material | Oxide | Nitride |
| Cladding thickness | 0.3 mm (316 SS) | |
| Width of fuel assembly | 68 mm (85 fuel pins 7 assembly) | |
| Initial uranium inventory | 3200 kg | |

TABLE 3.19. MAIN SYSTEM PARAMETERS OF THE JAEA EXPERIMENTAL ADS

| Parameter | Value |
|---|---|
| Thermal output | 60 MW |
| Beam injection direction | Downward vertical injection |
| Proton beam | 1.5 GeV-1.5 mA (2.3 MW) |
| Plant type | Loop |
| Cooling system | 1 loop |
| Primary and secondary coolant | Sodium |
| Final coolant | Air |
| Operation cycle | 1 year |
| Core vessel structure | Coolant side entry type with guard vessel |

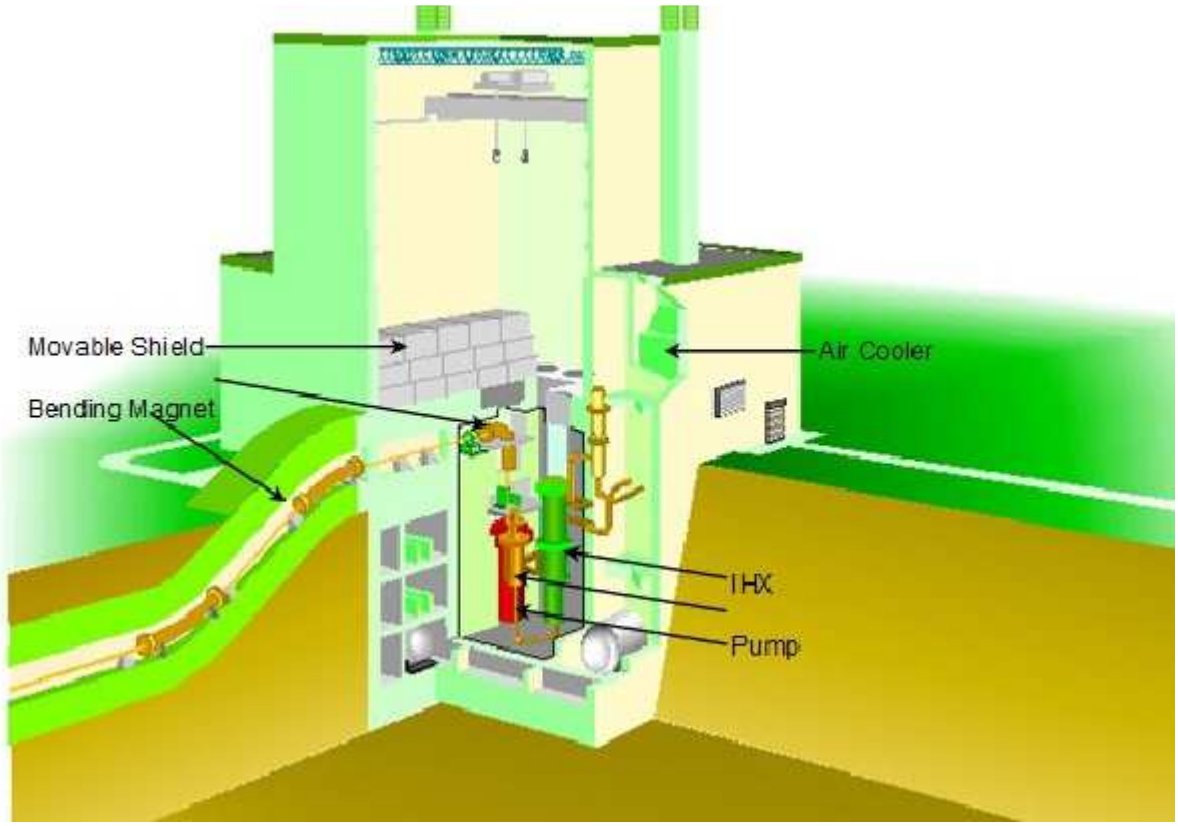


*FIG. 3.37. Schematic view of the JAEA Experimental ADS.*

### 3.1.5. KAERI Demonstration ADS

KAERI (Korea Atomic Energy Research Institute) has been developing an accelerator driven system (ADS) since 1997. The accelerator driven transmutation system developed by KAERI is called HYPER (HYbrid Power Extraction Reactor) [3.26]. It is designed to transmute the TRU and LLFP such as Tc-99 and I-129 coming from PWRs.

HYPER is a 1000 MW(th) fast spectrum ADS with $k_{eff} = 0.98$ [3.27]. U-TRU-Zr metal fuels are considered for HYPER since they fit with the pyroprocess separation system which is adequate for non-proliferation. Fuels are located into 3 different batch zones, and the batch is shifted every 6 months.

Pb-Biis used as the material for the coolant and the target which are not separated. The pool type cooling system is adopted. The bottom inlet and upper outlet temperatures are 340C° and 490°C, respectively. The maximum temperature of the outer part of the cladding does not exceed 570°C.

KAERI used a simulation code called MC-CARD. REBUS-3 and DIF3D are deterministic codes used for the core analysis. LAHET code system was used for the calculation related to the external source. KAERI also developed a kinetics code called DESINUR (Design Evaluation and Simulation of Nuclear Reactor) to study safety analysis and transient cases. The steady state performance computer codes were developed for the fuel analysis. MACSIS-H is the code for the analysis of metal alloy fuel and DIMAC is for the dispersion fuel. Both codes were developed to calculate temperature distribution, gas production, strain etc. Existing U-TRU-Zr thermal conductivity model was modified for high TRU and Zr fraction fuels. MATRA and SLTHEN were used for the core thermalhydraulic calculations. CFX and FLUENT were used for the thermalhydraulic calculations of the target. ANSYS was used for the stress calculation of the beam window.

Fig. 3.38 shows a schematic configuration of the HYPER core with 186 ductless hexagonal fuel assemblies. Fig. 3.39 shows a vertical view of the same HYPER Core.

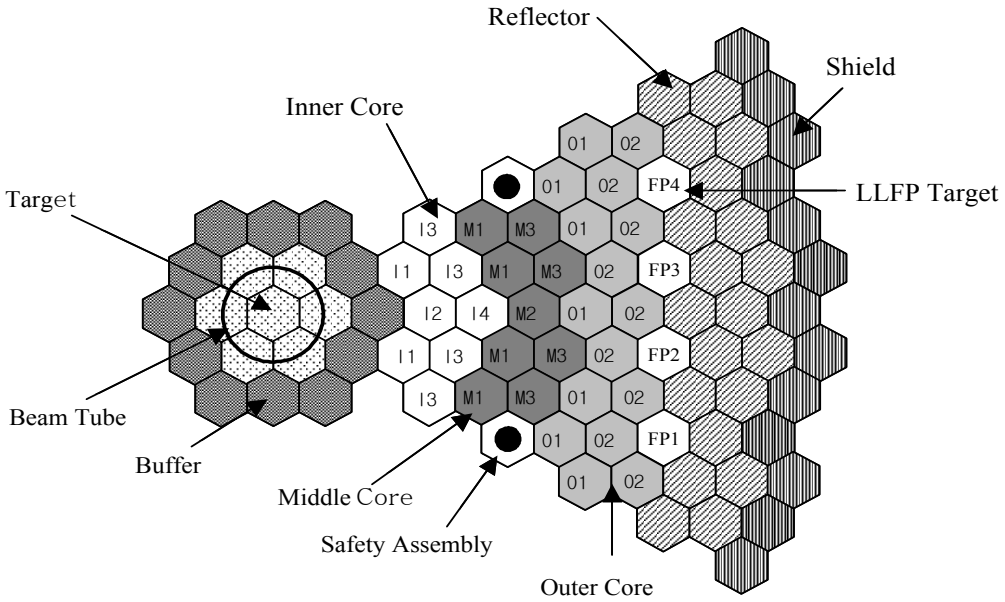


*FIG. 3.38. HYPER Core configuration.*

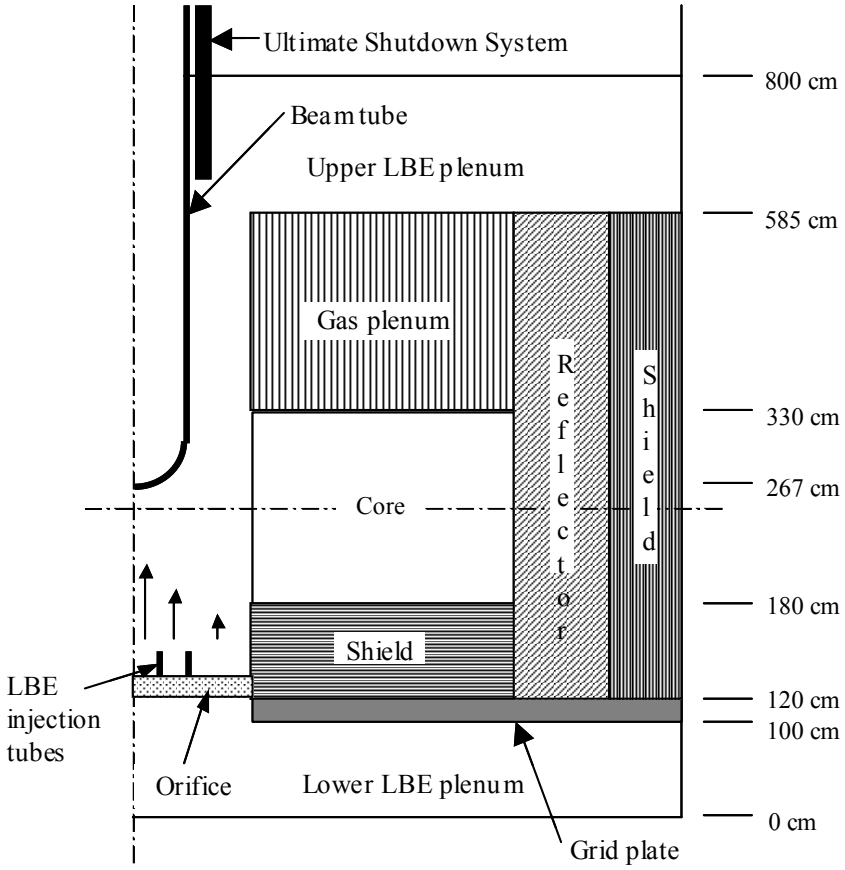


*FIG. 3.39. Vertical view of HYPER core.*

As shown in Fig. 3.38, the fuel blanket is divided into 3 TRU enrichment zones to flatten the radial power distribution.

In HYPER, a beam of 1 GeV protons is delivered to the central region of the core to generate the spallation neutrons.

In addition to the ultimate shutdown system, six safety assemblies are placed in the HYPER core for an emergency situation. The safety rods are also used to control the reactivity of the core.

For a balanced transmutation of both TRU and LLFP (Tc-99 and I-129), Tc-99 and I-129 are incinerated in moderated LLFP assemblies loaded into the reflector zone.

The net TRU transmutation rate is 282 kg/yr. When it comes to the LLFP transmutation in a TRU burner, it is desirable that the supporting ratios of the LLFPs are equal to that of the TRU, thus assuring that neither the long lived TRUs nor LLFPs are accumulated. For a typical PWR with an 85% capacity factor, the TRU support ratio of HYPER is about 3.2. Consequently, in order to achieve the same support ratios for the LLFPs while accounting for a LLFP production in the HYPER core, 28.0 kg of Tc-99 and 7.0 kg of I-129 need to be incinerated per year (14.0 kg/cycle for Tc-99 and 3.5 kg/cycle for I-129) in the target assemblies.Table 3.20 lists the main parameters of HYPER.

TABLE 3.20. MAIN DESIGN PARAMETERS OF HYPER

| Parameter | Value |
|---|---|
| Capacity | 1000 MW(th) |
| $k_{eff}$ | 0.98 |
| Proton beam | 1 GeV |
| Fuel type | U-TRU-Zr metal alloy |
| Coolant | Pb-Bi |
| Transmutation | TRU, FP (Tc-99, I-129) |
| TRU Transmutation rate | 282 kg/yr |
| FP Transmutation rate | 28 kg/yr (Tc-99), 7 kg/yr (I-129) |
| Support ratio | 3.2 |

## 3.2. INDUSTRIAL SCALE ADS

### 3.2.1. EFIT: European Facility for Industrial Transmutation of Minor Actinides

In the frame of the project IP EUROTRANS [3.6] of the 6th Framework Programme (FP) of the European Union (EU), 51 European Organizations have the strategic R&D objective to pursue an European Transmutation Demonstration (ETD). The aim of the 4-years lasting programme, funded by the European Community, is twofold:

— Develop the conceptual design of an European Facility for Industrial Transmutation (EFIT) with a pure lead cooled reactor of several hundreds MW with considerable Minor Actinides burning capability and electricity generation at reasonable cost. The design will be worked out to a level of detail which allows a study cost estimate.

— Carry out the detailed design of the smaller XT-ADS (eXperimental Transmutation in an Accelerator Driven System), as irradiation facility to be constructed in the short term. The XT-ADS is also intended to be as much as possible a test facility for the main components and for operation of EFIT, at the lower working temperatures allowed by the use of the lead-bismuth Eutectic as the primary coolant and spallation target material.

The XT-ADS has been already described in section 3.1.3.

EFIT is being designed as a transmutation demonstrator, loaded with MA fuel. It is intended to become operational many years after the XT-ADS (around 2040) and therefore to profit of the experience gained from the running European Research and Development (R&D) programmes on fuel and materials and of the operation of the XT-ADS, which is to be built and operational in the near future.

EFIT is an industrial scale transmutation facility, the characteristics of which are efficiency of transmutation, simple operation and maintenance, and high availability in order to achieve effective MA transmutation and electric energy generation at reasonable cost ([3.27],[3.28]).

The EFIT description is given below by main design areas.

The core design approach is as follows. Starting from the Pu and MA vectors, which are the nuclides deriving from reprocessing the spent fuel of Light Water Reactor (LWR) used for the U free fuel of EFIT, a preliminary ratio of MA nuclides to all nuclides is determined that brings about a burnup reactivity swing of a few hundreds pcm/cycle or less ($\Delta K \approx 100$ pcm/cycle) without burning or breeding Pu. The selected fuel is a U free oxide fuel in a MgO matrix (50–65 vol%; a metallic $^{92}Mo$ matrix is retained as backup option), with Pu and MA vectors deriving from reprocessing the spent fuel of LWRs.

The ratio of MA nuclides to all nuclides is determined to bring about a MA burning rate of 42 kg/TWh (mass of fissioned MA per TWh generated energy), no Pu burning or breeding and a

burnup reactivity swing of a few hundreds pcm/cycle (ΔK≈200 pcm/cycle). As a matter of fact, under the neutronic flux a part of MA is fissioned and other MA are transmuted into different isotopes (Pu). Since the fission energy is about 200 MeV/fission, it can be calculated that the actual *overall* fissioned balance must be in any case ~42 kg/$TWh_{th}$ (independently of the design of the reactor). Of course this is the algebraic sum of the MA and Pu net balances. When the MA net balance is lower than this value, it means that other fuel (Pu) has been fissioned too. While, when it is higher than this value, it means that a part of MA has been transmuted into new Pu instead of being burnt. In the first case the reactor acts as a Pu burner, in the second one as a Pu breeder.

The choice in EFIT has been to fix the fuel enrichment (45.7% in Pu) in such a way to dedicate all the fissions (directly or indirectly) to MA. In terms of balance it means that the MA balance has to be ~ 42 kg/TWh(th) (corresponding in EFIT to about 120 kg/year), while the Pu balance will correspond to ~0 kg/TWh(th). This is called the '42–0' approach ([3.28],[3.29]). With this enrichment, the reactivity swing along the fuel cycle is as low as few hundreds pcm (200 pcm/year).

For the case of ΔK≈0 and Pu breeding ratio ≈ 1, this means that reactor operation, intended as combined operation of subcritical core and spallation neutron source, takes place at constant proton beam current over each cycle and that, at the end of each fuel cycle, the new fuel can be fabricated by adding fresh MA only to the reprocessed fuel of the previous cycle. The requirement of nearly zero burnup reactivity swing is dictated by the wish not to have to heavily rely on the proton beam for the generation of extra spallation neutrons for burnup reactivity swing compensation and this gives the designer the freedom to tailor the accelerator for a narrower range of proton beam current and to avoid oversizing. The choice of Pu breeding ratio ≈ 1 implies that Pu is required for the first fuel only, a feature that limits to a minimum Pu handling and does not contribute to pile stocking in times of surplus of Pu, considering also that Pu can be advantageously fissioned in (possibly new generation) fast reactors, all facilities that are predictably less expensive than EFIT.

The EFIT core is being designed for a thermal power of about 400 MW, aiming at performance and radial power flattening. The latter permits to work with a high average power density (70.7 W/$cm^3$) and, as a consequence, high burnup (about 78.3 MWd/kg). This result can be obtained while respecting present technological limits such as the maximum allowable temperature for pellet (about 1380°C) and clad (550°C) integrity. The specific burning rate (mass of fissioned MA per TWh generated energy) is around 42 kg MA/TWh. The fuel enrichment in Pu has been chosen at about 45.7% to keep the reactivity swing, along the fuel cycle, as low as few hundreds pcm (200 pcm).The selected fuel is a U-free oxide fuel in a MgO matrix (50–65 vol%; a metallic $^{92}$Mo matrix is retained as backup option).

The EFIT core is made of 180 hexagonal Fuel Assemblies, with 168 fuel rods each; the active length is 90 cm, the equivalent inner and outer radius are 43.7 cm and 151.5 cm respectively.

Because EFIT is a hybrid reactor controlled by the spallation neutrons, it must be ensured that the core remains always subcritical, without having to rely on shutoff or control rods. The margin to criticality is an important requirement for the core definition that leads, eventually, to define core size and reactor power.

The operating subcriticality level has been chosen in accordance to the following requirement: the reactor core shall be designed so that it remains subcritical under all plant conditions, namely DBC and DEC.

Subcriticality is a safety requirement of paramount importance, since the ADS has to be designed without shutoff or control rods. Analyses of the 80 MW LBE cooled XADS described in section 3.1.2, have determined the range of the effective multiplication factor ($k_{eff}$) for normal operation, transient and accident conditions. The maximum $k_{eff}$ for the XADS core at full power and BOL has been determined as 0.97, a value that strictly holds for the XADS only. For EFIT, the determination of the $k_{eff}$ range that ensures the compliance with the subcriticality requirement is still outstanding. This determination will not be a *da-capo* design activity, however, since the same core design approach can be adopted and the results of XADS, adjusted occasionally in consideration of the EFIT peculiarities, can be reasonably assumed as starting data for the iteration process.

It is assumed that a margin of 0.016 $\Delta K$ to criticality, a figure that includes allowance for measurement errors, be required at DBC, akin to standard practice for light water reactors. $k_{eff}$ shall hence not exceed 0.984 at any time during DBC. It is further assumed that a thinner margin is acceptable for DEC, owing to their postulated very low frequency, and that $k_{eff}$ shall not be greater than 0.95 during refueling or target unit removal for replacement. Fig. 3.40 illustrates these safety criteria showing that at no time $k_{eff}$ shall move into the red regions, which represent the margins to criticality allocated to the three mentioned conditions.

The green region covers the range of $k_{eff}$ allowed for normal operation. The yellow regions cover the excursion ranges of $k_{eff}$ predicted by the transient analyses for DBC and DEC respectively. Because completion of design is outstanding and the transient analyses will follow, both regions are depicted, but not figured out. As starting point for the design $k_{eff} = 0.97$ has been preliminary assumed for EFIT as the maximum value for the nominal full power conditions (upper limit of the green region).

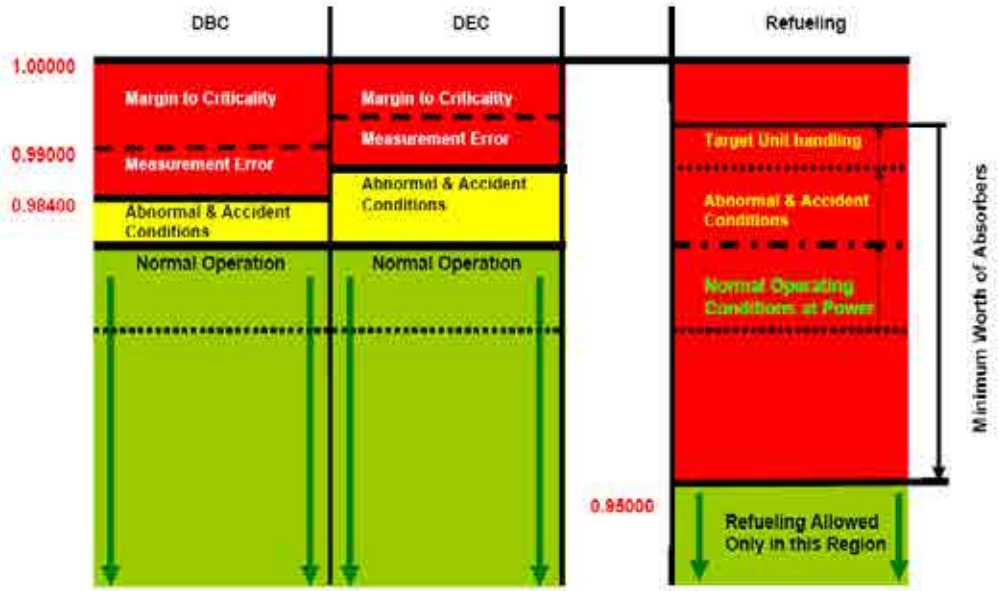


*FIG. 3.40. Safety criteria (required subcriticality margins) for DBC, DEC, refueling and target unit handling.*

The target unit constitutes the physical and functional interface between the accelerator complex (LINAC type accelerator has been chosen for EFIT, see section 3.1.2) and the core of EFIT. The spallation neutrons are generated in the target unit by interaction of the high energy proton beam with lead as the liquid target, which is kept in forced circulation inside the target unit. The target unit is a slim mechanical component of cylindrical shape, positioned coaxially with the reactor vessel and the core and hung to the reactor roof. Because it serves also as inner radial restraint of the core, the outline of its outer shell fits the inner outline of the core.

Its main component parts are the proton beam pipe, the heat exchanger and the two axial flow pumps arranged in series in the vertical legs of the loop, upstream and downstream the target region, respectively (Fig. 3.41). The proton beam travels *in vacuo* and the midpoint of its penetration depth (estimated 43 cm for a proton beam energy of 800 MeV) in the target lead matches the mid plane of the core. The target lead transfers the deposited energy to the primary lead via the heat exchanger of the target unit. The spallation products are kept confined in the target unit. Neutron back streaming through the beam pipe is minimized by the small cross-section and shape of the vacuum pipe and the narrow clearances of the mechanical structure, in order to limit the associated dose rate and the activation of the structures above the reactor roof.

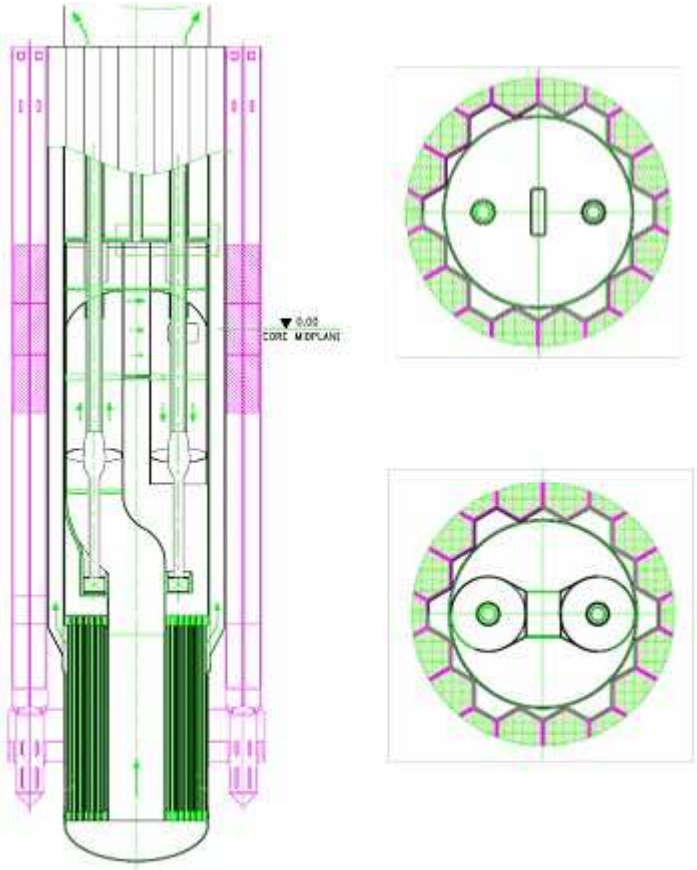

*FIG. 3.41. EFIT Target unit.*

Because the heat source is at the top of the loop and hence a natural circulation is not possible, lead circulation is forced by means of two axial flow pumps in series, fed by independent power supplies, in order to ensure circulation by at least one pump in case of failure of the companion pump. Limitation of erosion is ensured by a speed of lead of less than 2 m/s, except for the blades of the propellers for which the higher relative speed requires erosion resistant construction materials. Promising candidate materials are programmed for testing in the frame of R&D activities. This material issue is common to the propeller blades of the primary pumps.

The configuration of the primary system is pool type, similar to the design adopted for most sodium cooled reactors and for the previous XADS design (Fig. 3.42 and Fig. 3.43). All the primary coolant is contained within the reactor vessel, a cylindrical shell with hemispherical bottom head and top Y-piece, both branches of which terminate with a flange. The conical, outer branch is flanged to, and hangs from, the Annular Structure anchored to the civil structure of the reactor cavity, whereas the inner branch supports the reactor upper closures. Temperature and temperature gradient of the outer branch of the Y-piece can be kept low by adequate thermal insulation.

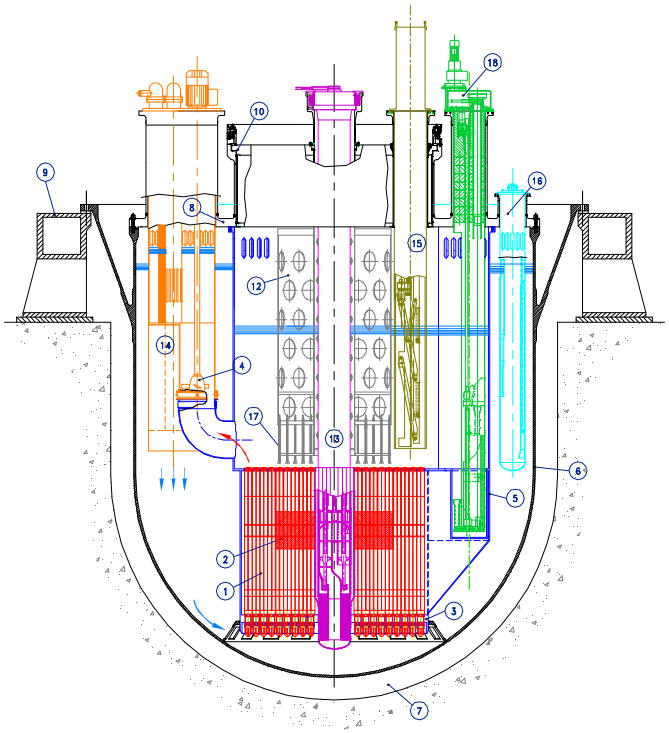

.

*FIG. 3.42. EFIT Primary system assembly: vertical section.*

(1 Reactorc, 2 Active zone, 3 Diagrid, 4 Primary pump, 5 Cylindrical inner vessel, 6 reactor vessel, 7 Reactor cavity, 8 Reactor roof, 9 Reactor vessel support, 10 Rotating plug, 12 Above core structure, 13 Target unit, 14 Steam generator, 15 Fuel handling machine, 16 Filter, 17 Core instrumentation, 18 Rotor lift machine, 19 DRC Dip cooler)

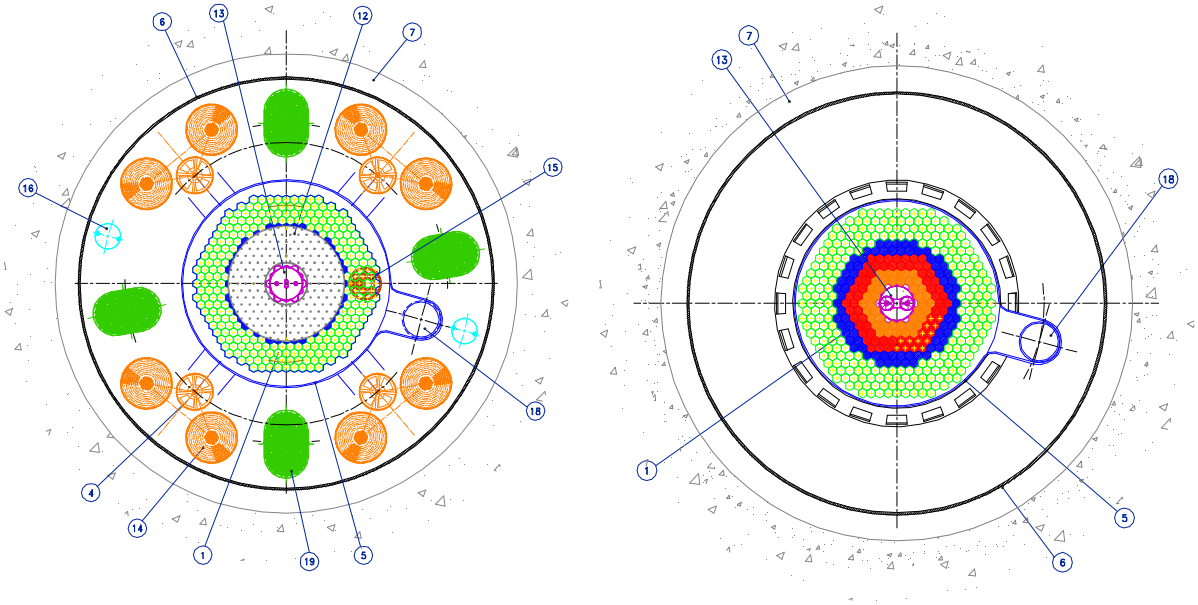

*FIG. 3.43. EFIT Primary system assembly: horizontal section over the core and at core elevation.*

Key components for reactor operation at power are the primary pumps (PP) and the steam generators (SG). Four identical groups of these components are provided, each comprising two SGs, one PP in between, piping for hot coolant circulation and a casing at the SGs top that encloses the coolant and direct it to the SGs. Thus the hot coolant region within the Reactor Vessel is rather small, being delimited by the inner vessel, the four PPs, suction and discharging piping and of the four regions enclosed by the four casings. The cross-section of the casings is kidney shaped, because the component groups are located in the annular region between inner vessel and reactor vessel. The free level of the hot pools inside the casings is higher than the free level inside the inner vessel, whereas the free level of the cold pool is in between the two hot pool levels, the different heads depending on the pressure losses across primary circuit component.

DHR is provided by four independent loops filled with organic, diathermic fluid that dissipate the decay heat to the atmosphere by natural convection.

The safety vessel, surrounding the reactor vessel, is essentially a liner anchored to the reactor vault, with back cooling; in case of reactor vessel leak, the resulting primary coolant free level stabilizes above the top of the core as well as of the SGs and DHR heat exchangers to preserve the core cooling function.

Unlike previous designs, the primary system features pure lead as the coolant, which is characterized by good nuclear properties and no fast chemical reaction with water and the organic diathermic fluid of the safety grade DHR system. There is a significant experience on metal cooled fast reactors that is the result of past and current work on sodium cooled fast reactors (e.g. Superphenix) and, in addition, a substantial effort is also being carried out in the use of the LBE technology in subcritical reactors. It is a natural development to select pure lead as a coolant for EFIT since it is much cheaper, more abundant, and presents a substantially lower radiological concern than LBE. Lead tends to retain hazardous radionuclides, even in the event of a severe accident involving extensive fuel damage. Moreover the rate of polonium production is 3 to 4 orders of magnitude lower than in case of LBE. Further, heavy metals have the advantage that, in the hypothetical case of a core disruption accident, core compaction scenarios, which might cause the insertion of large amounts of reactivity in a short time, are unlikely.

The pool design has important beneficial features, verified by the experience of design and operation of sodium cooled fast reactors. These include a simple low temperature boundary containing all primary coolant, the large thermal capacity of the coolant in the primary vessel, a minimum of components and structures operating at the core outlet temperature. Whenever the sodium experience does not appear applicable to the specific tasks of EFIT, however, solutions are being worked out that, though being innovative in the nuclear field, are not new to the industrial practice.

The operating temperatures are: 400°C at core inlet (to have sufficient margin from the risk of lead freezing) and 480°C at core outlet. The core outlet temperature is chosen taking into account, on the one hand, the corrosion risk of structures in molten lead environment that increases with temperature (the current limit for candidate structural materials protected from corrosion by oxygen dissolved in the melt is about 500°C) and, on the other hand, considering that the outlet temperature cannot be too low because the associated increase of coolant flow rate would bring about unacceptable erosion of the structures. The proposed operating temperatures are, hence, a compromise between corrosion-erosion protection and performance.

The reactor vessel is designed to operate at the colder temperature of 400°C, and therefore corrosion protected even assuming that the oxygen activity control within the melt would be temporarily lost. All other reactor internals will have to rely, with margin, on dissolved oxygen control, whereas fuel cladding shall be aluminized for improved corrosion protection. With a core mean outlet temperature of 480°C it is possible to limit the cladding temperature to 550°C. Increasing the cladding temperature largely over 550°C would mean taking an unjustified risk, even crediting the research results of the promising technology of Fe-Al alloy surface coating.

The primary circuit is designed for effective natural circulation, i.e. relatively low pressure losses and driving force brought about by the core mid plane elevation arranged wide below the mid plane of the steam generators or, in case of emergency decay heat removal, the mid plane of the DHR dip coolers.

The speed of the primary coolant is kept low by design (less than 2 m/s), in order to limit the erosion. Wherever this cannot be complied with, e.g. at the tip of the propellers blades, the relative speed is kept lower than 10 m/s and appropriate construction materials are selected for qualification (among them, the machinable $Ti_3SiC_2$).

Protection of structural steel against corrosion is ensured, in general, by controlled activity of oxygen dissolved in the melt and additional coating for the hotter structures. Wherever stagnation of the primary coolant is predicted, e.g. within dummies, provisions ensure a minimum coolant flow.

Other components within the reactor vessel and design choices worth to be mentioned (Fig. 3.42 and Fig. 3.43) are as follows:

— Cylindrical inner vessel, hung to the reactor roof, welded directly on the diagrid; 4 welded elbows as fittings of the suction pipework of the PP, with mechanical piston seal at the vertical upper ends.

— Diagrid, shaped as a thick disc welded to the bottom end of the cylindrical inner vessel.

— Core lateral restraints: a) outer restraints are the cylindrical shell, welded to the bottom head of the reactor vessel, that prevents the diagrid from excessive lateral swinging, and the upper disc plate, that is welded to the cylindrical inner vessel. b) inner restraint is the outer shell of the target unit, which fits the inner outline periphery of the core.

— Above core structure: integral with rotating plug.

— Rotating plug: thick metal plate on ball bearings with inflatable seals, coaxial to the core.

— Reactor roof: thick metal plate bolted to inner branch of the Y-piece forming the upper part of the reactor vessel.

— Component for in vessel fuel handling: one machine with extendible arm, on the rotating plug.

— DHR Direct Reactor Cooling (DRC) dip coolers: 4 independent and redundant in vessel, bayonet tube heat exchanger; organic diathermic fluid as the coolant; natural convection circulation.

— Lead purification: two in vessel gravitational filter units.

— Corrosion protection: dissolved oxygen activity control for formation and self-healing of a compact oxide layer, and Fe-Al alloy coating of the hotter structures.

— Ruptured fuel cladding detection system.

The lead coolant flow path is as follows. Within the SG/PP Assembly, hot lead is pumped into the enclosed pool above the PP and SG and driven shell-side downwards across the SG helical tube bundles into the cold pool. At normal steady state operation, the free level of the hot pool inside the casing is higher than the free level of the cold pool outside, which is higher, in turn, than the free level of the hot pool above the core enclosed by the inner vessel. In case of loss of service power to the level keeping PP, there would be no need of large mechanical inertia to slowly coast down the pumps and continue for a while the forced circulation, because the available head would ensure the prompt onset of the natural circulation, and hence preserve the safety function of core cooling since the very beginning of the transient. The loss of a PP would bring about reverse flow in the affected subassembly and merely create a temporary core bypass flow without seriously affecting the function of core cooling. Holes are provided on the upper part of the casing for creating a common, large reactor cover gas plenum and ensure overflow of surging coolant in case of SG tube rupture accident.

Removal of heat from the primary coolant of EFIT takes place by means of heat exchange between the primary lead coolant and water in eight identical SGs installed inside the reactor vessel. The steam generator is a vertical unit with an inner and an outer shell. The primary coolant flows downwards

shell-side through the inner shell and the annulus between inner and outer shell. The tube bundle is made of U-tubes, the inlet legs of which are straight inside the inner shell. After the U-turn, the outlet tube legs are helical inside the annulus and become straight again at the exit. Lead and water flow cocurrently in the inner shell and counter currently in the annulus. Both tube plates are located above the free level of lead. Table 3.21 provides the main primary and secondary systems parameters of EFIT.

TABLE 3.21. EFIT PRIMARY AND SECONDARY SYSTEMS PARAMETERS

| Parameter | Units | Value |
|---|---|---|
| Primary system design power | MW | 416 |
| Present core power | MW | 395 |
| Maximum power from spallation | MW | 11.2 |
| Primary system flow rate | kg/s | 36000 |
| Primary coolant target flow rate | kg/s | 1500 |
| Core flow rate | kg/s | 34500 |
| Fuel assembly flow rate | kg/s | 33300 |
| Dummy assemblies flow rate | kg/s | 400 |
| Absorber elements flow rate | kg/s | 150 |
| Core bypass flow rate | kg/s | 650 |
| Nominal core inlet temperature | °C | 400 |
| Nominal core mean outlet temperature | °C | 480 |
| Reactor pressure (cover gas plenum) | MPa | 0.11 |
| Secondary system steam pressure | MPa | 14 |
| Secondary system water/steam flow rate | kg/s | 257 |
| Feed water temperature | °C | 335 |
| Steam temperature | °C | 450 |
| Steam superheating | K | 116 |

Two systems contribute to the DHR function in EFIT: the non-safety grade water-steam system and the safety related DRC system. Following reactor shutdown, the non-safety grade water-steam system is used for the normal decay heat removal. In case of unavailability of the water-steam system, the DRC system is called upon.

The DRC System is composed of four identical loops (3 loops out of 4 are sufficient to perform the DHR intended functions), one of which is shown schematically in Fig. 3.44. The main components of the loop are: a molten lead diathermic oil heat exchanger (dip cooler, DHX) and an air diathermic oil vapour condenser (AVC) with stack chimney.

The DHX is a bayonet tube bundle cooler immersed in the cold pool of the reactor with both tube plates located above the primary coolant free level. The AVC is an air cooler condenser with vertical finned tubes cooled by cross flow atmospheric air driven by the natural draft provided by a stack chimney. Extra tubes are placed in front of the tube bundle that connects the lower header with the inert gas storage tank. The vapour is separated in the oil vapour separator from the oil vapour mixture rising from the DHX and fed to the upper header where it is distributed to the AVC tubes. The condensate runs by gravity into the lower header and eventually into the condensate drum where it mixes up with the hot oil and returns to DHX closing the oil loop. The inert gas that fills the AVC tube bundle and headers, during reactor normal operation, is pushed and confined by oil vapour into the inert gas storage tank, during accident conditions when the DRC is called to operate.

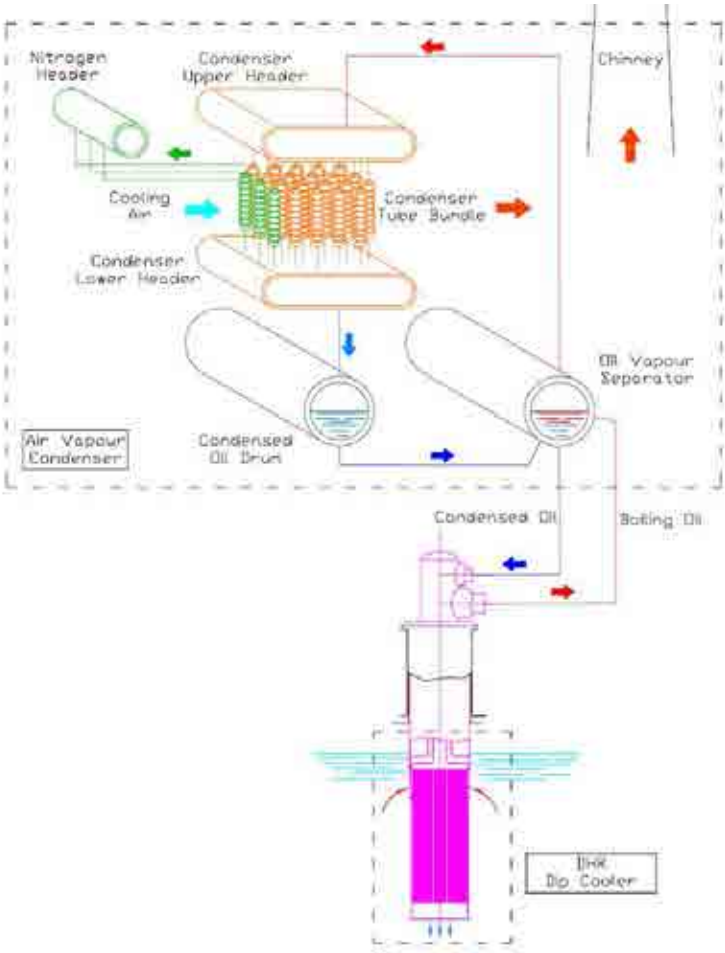


*FIG. 3.44. Direct reactor cooling system of EFIT.*

Decay heat is removed by means of partial vaporization of the oil in the DHX and oil vapour condensation in the AVC. Oil vaporization and condensation take place at about 400°C, in order to maintain the primary coolant at a temperature of about 440–450°C.

The higher boiling point of the oil with respect to the boiling point at atmospheric pressure is the consequence of superimposed pressure of inert gas (nitrogen, about 10 bars). The pressure is manually controlled by the operator in order to compensate for any significant system pressure variation due to the seasonal evolution of the ambient temperature.

### 3.2.2. JAEA Industrial scale ADS

#### *3.2.2.1. 800 MW(th) Industrial scale lead-bismuth target/cooled ADS*

The JAEA industrial scale ADS aims at actual transmutation of long lived nuclides discharged from spent nuclear fuel. One ADS unit of 800 MW(th) is designed to support about ten units of typical light water power reactors of 1GWe.

The ADS is mainly composed of a superconducting proton LINAC and a fast subcritical core with lead-bismuth eutectic which acts as both a spallation target and a core coolant simultaneously [3.31]. A superconducting LINAC is adopted to supply several tens mA of proton beam with appropriate efficiency. The subcritical core is designed to have a hard neutron energy spectrum to transmute MAs effectively by threshold fission reactions. The fission reaction of MA is also useful to supply the own operation electricity.

Fig. 3.45 shows a schematic view of the JAEA industrial scale LBE cooled ADS.

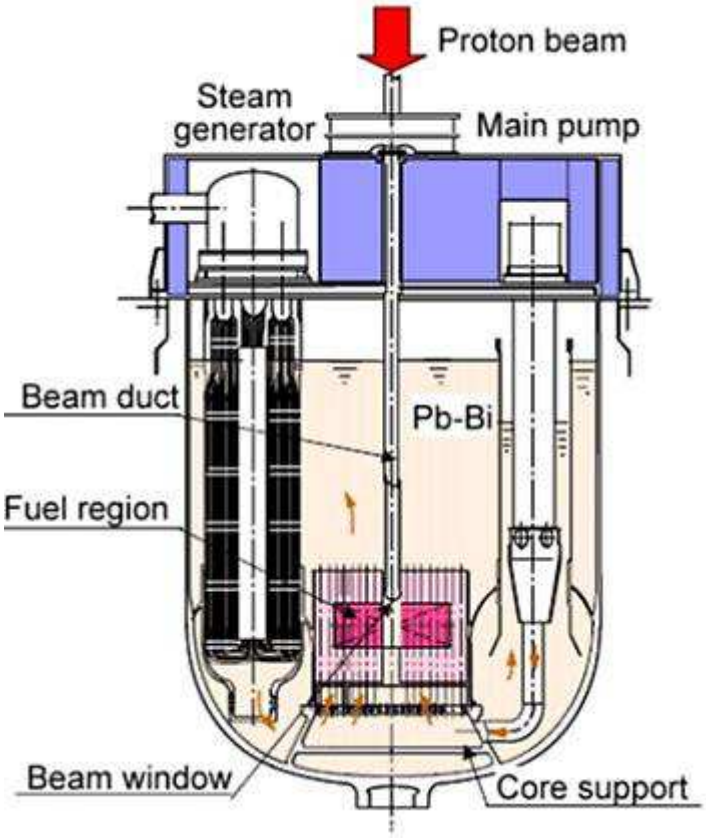


*FIG. 3.45. Schematic view of the JAEA Pb-Bitarget/cooled ADS.*

A nitride fuel mainly composed of MA which can be reprocessed by pyrochemical process is used to achieve the large loading amount of MA into subcritical core and improve chemical stability of MA during the burnup. To prevent the generation of $^{14}C$, a long lived nuclide, $^{15}N$ enriched nitrogen is used. The composition of MA is delivered from the spent fuel of commercial PWR at burnup of 33 GWd/tHM with 8 years cooling including reprocessing process period. Inert matrix is mixed to adjust the reactivity and linear power density. For the effective cooling of standby and spent fuel and suppression of the radioactive waste, ductless type fuel assembly is adopted.

The thermal power of the system is set to 800 MW to transmute MA from 10 units of 1000 MWe commercial power reactors. 600 days operation per one cycle is assumed with consideration of the lifetime of proton beam window and fuel cladding. Coolant inlet and outlet temperatures are 300 and 410ºC, respectively. The nominal velocity of coolant was set to 2 m/s.

To avoid the piping of lead-bismuth, tank type vessel is selected. Two primary coolant circuits are installed in the vessel. The secondary coolant is pressurized water.

Several merits of lead-bismuth coolant such as negative void reactivity and common use of spallation target and coolant can be observed but there exists several engineering difficulties for compatibility with structural materials and soundness of beam window.Table 3.22 provides the main system parameters of the JAEA industrial scale LBE cooled ADS.

TABLE 3.22. MAIN SYSTEM PARAMETERS OF THE JAEA INDUSTRIAL SCALE LBE COOLED ADS

| Parameter | Value |
|---|---|
| Proton beam | 1.5 GeV~20MW |
| Spallation target | Pb-Bi |
| Coolant | Pb-Bi |
| Coolant inlet/outlet temp. | 300/407°C |
| Initial $k_{eff}$ | 0.97 |
| Thermal output | 800 MW(th) |
| Core height | 1000 mm |
| MA initial inventory | 2.5 t |
| Fuel composition | (60%MA + 40%Pu) mononitride |
| Transmutation rate | 10%MA / Year |
| Burnup reactivity swing | 1.8% Δk/k |

### *3.2.2.2. 800 MW(th) Industrial scale sodium cooled ADS*

In this version, the industrial scale JAEA ADS is mainly composed of a superconducting proton LINAC and a sodium cooled fast subcritical core with a spallation target made by solid tungsten [3.32]. Similar to the case of the lead-bismuth cooled ADS, a superconducting LINAC and nitride fuel are used in the sodium cooled ADS. The solid spallation target made by tungsten is located at the center of the subcritical core. The axial structure (layout and thickness) of each target disc is optimized to suppress the hot spot caused by the peaking of emitted spallation neutron distribution from the target. The target assemblies are commonly cooled by sodium. Because of the high heat deposition, target assembly has a wrapper tube to manage coolant flow through the target. The thermal power of the system is set to 800 MW to transmute MA from 10 units of 1000 MWe commercial power reactors. 600 days operation per one cycle is assumed with consideration of the lifetime of beam window and fuel cladding. Coolant inlet and outlet temperatures are 330 and 430°C, respectively. Maximum velocity of coolant is fixed at 8 m/s during the all burnup stages.

Table 3.23 gives the main system parameters of the JAEA industrial scale sodium cooled ADS, while Fig. 3.46 provides the time evolution of the $k_{eff}$ and MA inventory along the cycle.

TABLE 3.23. MAIN SYSTEM PARAMETERS OF THE JAEA INDUSTRIAL SCALE SODIUM COOLED ADS

| Parameter | Value |
|---|---|
| Fuel | TRU-mononitride |
| Inert matrix | Yttrium-Nitride |
| Fuel pin radius / pin pitch | 0.2 cm / 0.48 cm |
| Initial fuel composition | 60% MA–40% Pu |
| Target | Solid Tungsten Disc |
| Coolant | Liquid Sodium |
| Inlet/outlet temperature | 330 / 430 ˚C |
| Initial MA inventory | 1925 kg |
| Initial proton beam intensity | 1.5 GeV–15 mA |
| Initial $k_{eff}$ | 0.95 |
| Coolant void reactivity | + 4.5 % Δk/k |
| Doppler coefficient | -2.2 x $10^{-4}$ T•dk/dT |
| Thermal output | 820 MW |
| MA transmutation ratio | 7.4 %/year |
| Average neutron energy | 670 keV |
| Average neutron flux | 4.1 x $10^{15}$ (n/cm$^2$/s) |

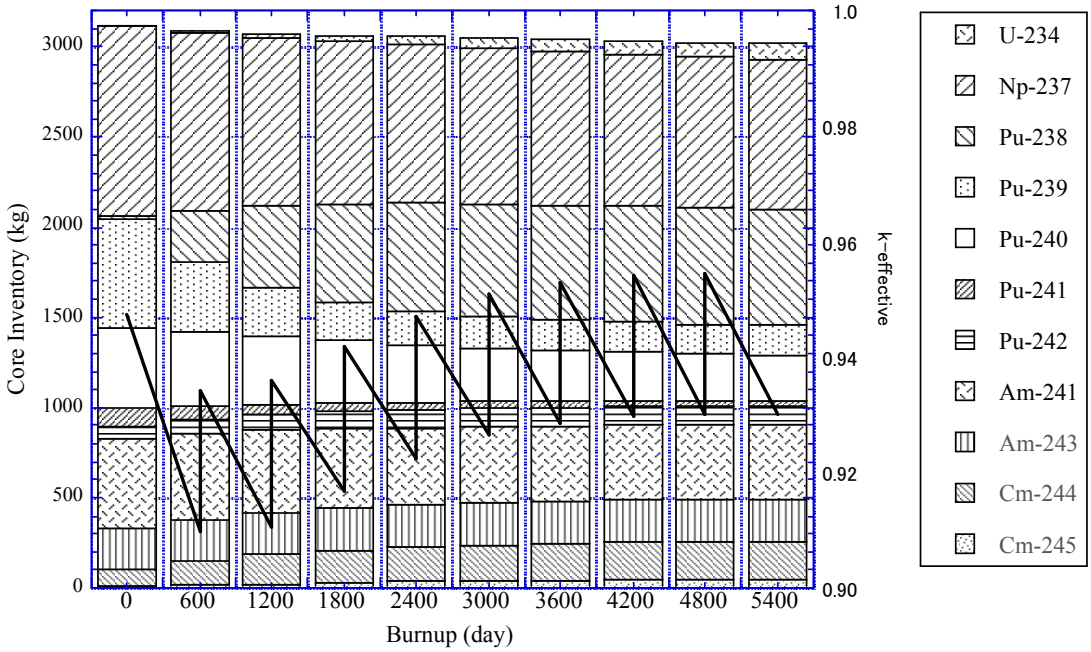


*FIG. 3.46. Time evolution of $k_{eff}$ (solid line) and MA Inventory (histogram).*

## 3.3. REFERENCES TO CHAPTER 3


[3.1] RUBBIA, C., et al., Conceptual Design of a Fast Neutron Operated High Power Energy Amplifier; CERN/AT/95-44(ET) (1995).

[3.2] CINOTTI, L., CORSINI, G., A Proposal for Enhancing the Primary Coolant Circulation in the EA, paper presented in Int. Workshop on Physics of Accelerator Driven Systems for Nuclear Transmutation and Clean Energy Production, Trento, Italy, 1997.

[3.3] RICHARD, P., DELPECH, M., RIMPAULT, G., PDS-XADS: Technical Specifications, Missions of XADS, Recommendations for the Main Characteristics, Deliverable of the PDS-XADS WP1, DEL02/001 rev1 (2002).

[3.4] THE EUROPEAN TECHNICAL WORKING GROUP ON ADS, A European Roadmap for Developing ADS for Nuclear Waste Incineration, ENEA, Italy, April 2001.

[3.5] KNEBEL, J., AÏT ABDERRAHIM, H., CINOTTI, L., MANSANI, L., DELAGE, F., FAZIO, C., GIOT, M., GIRAUD, B., GONZALEZ, E., GRANGET, G., MONTI, S., MUELLER, A., EUROTRANS*:* European Research Programme for the Transmutation of High level Nuclear Waste in an Accelerator driven System, paper presented in Ninth Information Exchange Meeting, Nimes, France, 25–29 September 2006.

[3.6] AIT ABDERRAHIM, H., et al., MYRRHA: A Multipurpose Accelerator Driven System for Research & Development, Nuclear Instrumentation & Methods in Physics Research, 463, Issue 3 (11 May 2001) pp 487–494.

[3.7] AIT ABDERRAHIM, H., et al., MYRRHA Predesign File Draft 2*,* R-4234, SCK•CEN (2005).

[3.8] LOCATELLI, G., XADS Requirements Constraints and Key Data, Deliverable of the PDS-XADS WP1, DEL03/005 (2003).

[3.9] SAFA, H., Requirements for the XADS Accelerator & the Technical Answers, Deliverable of the PDS-XADS WP3, DEL02/009 (2002).

[3.10] BIAROTTE, J.-L., et al., Definition of the XADS-class Reference accelerator Concept & Needed R&D, Deliverable of the PDS-XADS WP3, DEL04/063 (2004)

[3.11] SHERMAN, J., et al., A 75 keV, 140 mA Proton Injector, Rev. Sci. Instrum, 73, Issue 2, (2002).

[3.12] GOBIN, R., et al., High Intensity ECR ion source (H+, D+, H-) Developments at CEA/Saclay, Rev. Sci. Instrum., 73, Issue 2 (2002).

[3.13] BEAUVAIS, P-Y., Status Report on the Construction of the French High Intensity Proton Injector (IPHI), paper presented in EPAC 2002, Paris, France (2002).

[3.14] FERDINAND, R., et al., Optimization of RFQ design, paper presented in EPAC 1998, Stockholm, Sweden (1998).

[3.15] CINOTTI, L., et al., XADS Pb-BiCooled Experimental Accelerator Driven System Reference Configuration summary Report, ANSALDO ADS1SIFX0500, Rev 0 (June 2001).

[3.16] CINOTTI, L., BUZZONE, M., CARDINI, S., CORSINI, G., SACCARDI, G., Conception and development of a Pb-BiCooled Experimental ADS., paper presented in ANS Winter Meeting (Acc App. ADTTA'01), Reno Nevada, 2001.

[3.17] CINOTTI, L., et al, Primary System Summary Report for LBE cooled XADS, Deliverable of the PDS-XADS WP5.1, DEL04/075 (2004).

[3.18] BURN, K.W., GLINATSIS, G., MANSANI, L., NAVA, E., PETROVICH, C., SAROTTO, M., Preliminary nuclear design calculations for the PDS-XADS LBE cooled core, Proceedings of the International Workshop on P&T and ADS Development, Mol, Belgium, 6-8 October 2003.

[3.19] RICHARD, P., et al., Technical Option Report on the Gas cooled XADS, Deliverable of the PDS-XADS WP1, DEL04/062 (2004).

[3.20] DE BRUYN, D., GIRAUD, B., MAES, D., MANSANI, L., From MYRRHA to XT-ADS: the design evolution of an experimental ADS system, Proc. AccApp'07, Pocatello, Idaho, 29 July–2 August 2007, ANS, ISBN: 0-89448-054-5, CD-ROM.

[3.21] SCHUURMANS, P., et al., Design and supporting R&D of the XT-ADS spallation target, presented at the OECD NEA Information Exchange Meeting (IEM), Nîmes, France, 25–29 September 2006.

[3.22] MANSANI, L., REALE, M., ARTIOLI, C., DE BRUYN, D., The designs of an experimental ADS facility (XT-ADS) and of an European industrial transmutation demonstrator (EFIT), paper presented in OECD Nuclear Energy Agency International Workshop on Technology & Components of Accelerator Driven Systems (TCADS), Karlsruhe, Germany, 15–17 March 2010.
[3.23] DE BRUYN, D., LARMIGNAT, S., HUNE, W., A., MANSANI, L., RIMPAULT, G., ARTIOLI, C., Accelerator driven systems for transmutation: main design achievements of the XT-ADS and EFIT systems within the FP6 IP-EUROTRANS integrated project, Proc. ICAPP'10, San Diego, California, 13–17 June 2010, ANS, ISBN: 978-89448-081-2, CD-ROM.
[3.24] DE BRUYN, D., BAETEN, P., LARMIGNAT, S., HUNE, W., A., MANSANI, L., The FP7 Central Design Team project: towards a fast-spectrum transmutation experimental facility, Proc. ICAPP'10, San Diego, California, 13–17 June 2010, ANS, ISBN: 978-89448-081-2, CD-ROM
[3.25] CENTER FOR NEUTRON SCIENCE (Ed.), Status of R&D for Neutron Science Project, JAERI-Tech 99-031 (1999) pp. 348–370 (in Japanese).
[3.26] PARK, W. S., et al., Development of Nuclear Transmutation Technology, Technical Report KAERI/RR-1702/96, Korea Atomic Energy Research Institute (1996).
[3.27] SONG, T.Y., et al., Design and Analysis of HYPER, Annals of Nuclear Energy, 34 (2007) pp. 902-909.
[3.28] MANSANI, L., et al., EFIT: The European facility for industrial transmutation of minor actinides, Proc. AccApp'07, Pocatello, Idaho, 29 July–2 August 2007, ANS, ISBN: 0-89448-054-5, CD-ROM.
[3.29] ARTIOLI, C., et al., Optimization of the Minor Actinides transmutation in ADS: the European facility for industrial transmutation EFIT-Pb concept, Proc. AccApp'07, Pocatello, Idaho, 29 July–2 August 2007, ANS, ISBN: 0-89448-054-5, CD-ROM.
[3.30] ARTIOLI, C., CHEN, X., GABRIELLI, F., GLINATSIS, G., LIU, P., MASCHEK, W., PETROVICH, C., RINEISKI, A., SAROTTO, M., SCHIKORR, M., Minor Actinide transmutation in ADS: the EFIT core design, Proc. PHYSOR 2008, Interlaken, Switzerland, 14–19 September 2008, Publisher: Paul Scherrer Institute (2008).
[3.31] TSUJIMOTO, K., SASA, T., NISHIHARA, K., et al., Neutronics Design for lead-bismuth Cooled Accelerator Driven System for Transmutation of Minor Actinide, J. Nucl. Sci. and Technol., 41, Issue 1 (2004) pp. 21–36.
[3.32] SASA, T., TSUJIMOTO, K., TAKIZUKA, T., TAKANO, H., Code Development for the Design Study of OMEGA Programme Accelerator driven Transmutation Systems, Nuclear Instruments and Methods in Physics Research, 463 (2001) pp. 495–504.
[3.33] RUBBIA, C., RUBIO, J.A., BUONO, S., et al., Conceptual Design of a Fast Neutron Operated High Power energy Amplifier. CERN/AT/95-44(ET) (1995).

# CHAPTER 4
# R&D AND TECHNOLOGICAL DEVELOPMENT STATE OF THE ART

## 4.1. EXISTING OR PLANNED ADS R&D FACILITIES

The section provides a general overview of the main existing or planned R&D facilities to support the development of ADS systems.

### 4.1.1. The Subcritical assembly at Dubna (SAD)

#### *4.1.1.1. Introduction*

To construct accelerator driven systems (ADS) of industrial scale, with power of hundreds megawatts, it is necessary to solve a series of technological problems, and also to carry out a series of R&D for studying properties of such installations, safety substantiation, nuclear data for the isotopes, which have to be incinerated (measurements of rates of transmutation reactions, integral cross-sections etc). The decision of these tasks is expedient to carry out at the experimental installations of the minimal non-zero power (up to 100 kW). Such facilities should demonstrate the feasibility of joining subcritical reactor and proton accelerator, the maintenance of their stable joint operation, providing subcriticality monitoring. Implementation of these requirements is one of the important conditions for safety substantiation and licensing of the ADS facilities.

For the decision of these tasks it has been proposed to create an experimental facility in JINR. This facility was called 'The Subcritical Assembly at Dubna (SAD)'. Development of the SAD design has been carried out in close collaboration with European research centers: KTH (Stockholm, Sweden), FZK (Karlsruhe, Germany), CIEMAT (Madrid, Spain), CEA Cadarache (St. Paul les Durance, France) and JIENR (Minsk Sosny, Byelorussia). From the Russian side the following organizations participated in the Project besides JINR: GSPI, VNIINM, NIKIET, IA 'Mayak'. The basic design of the SAD facility has been completed.

#### *4.1.1.2. SAD basic design*

The SAD project basic features are determined by the characteristics of the 'PHASOTRON' proton accelerator at JINR —driving accelerator for the SAD facility [4.1] and by the choice of the regular Russian MOX fuel elements of the BN-600 reactor type [4.2]. The proton current (maximum value is 3.2 μA) and the corresponding power dumped in the spallation target determine, together with the value of the multiplicity $k_{eff}$ of the core, the total thermal power of the facility. The basic data of the SAD facility are listed in the Table 4.1.

TABLE 4.1. MAIN BASIC DATA OF THE SAD

| Parameter | Value |
|---|---|
| Thermal power | up to 30 kW |
| Proton energy | 660 MeV |
| Beam power | up to 1 kW |
| Proton beam / target orientation | Vertical |
| Fuel elements orientation | Vertical |
| Criticality coefficient | $k_{eff} \approx 0.95$ |
| Fuel | MOX, $UO_2 + PuO_2$ |
| Cladding tubes maximum temperature | 300°C |
| Spallation target | Replaceable: Pb, W |
| Reflector | Pb |
| Coolant | Air |

Installation consists of subcritical blanket, proton beam transport channel and replaceable target. The spallation target irradiated by accelerated protons is an external neutron source for subcritical blanket.

(a) Subcritical assembly

— Subcritical blanket

Subcritical blanket of the SAD facility (active core (AC) with reflector) is located inside a biological shielding that is made of heavy concrete and disposed in a lateral and upper direction from the fissile region (Fig. 4.1). Inside shielding blocks there are located the fittings for cooling systems pipes, experimental channels (vertical and horizontal), proton beam line, power control channels etc.The upper part of the biological shielding, consisting of removable and stationary blocks, provides access to a fissile region and the experimental channels during the loading–unloading operations with fuel and experiments with detectors and irradiated samples.

— SAD fuel assembly and fuel element

SAD core consists of 141 fuel assemblies (FA). Each FA combines 18 fuel elements (FE). In SAD facility rod like fuel elements physically representing stainless steel cladding tube with fuel column inside are used, composed of U-Pu MOX fuel pellets. FE inner volume is filled with high purity helium. The elliptic spacing wire spiral is wound around the outer surface of the cladding tube. FE features are listed in Table 4.2.

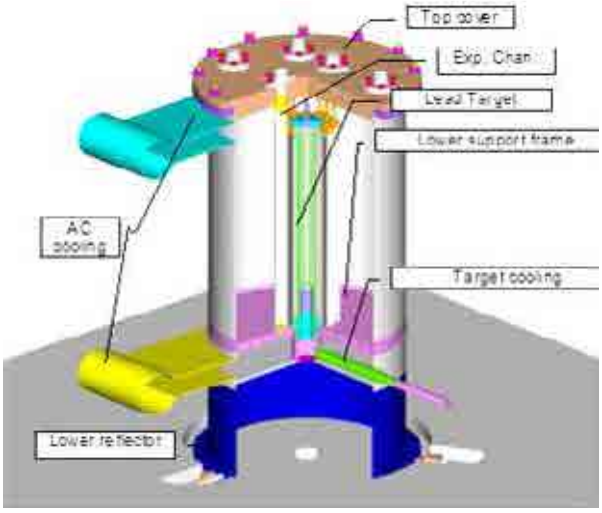


*FIG. 4.1. General view of the SAD core (fuel assemblies and lead reflectors are not shown).*

FA doesn't have side walls, but only lower and upper grids, where FE are fixed. Central rod made of stainless steel is a bearing element that provides stiffness of the FA construction. The number of the

FA in the core is specified at a stage of physical startup to provide a subcriticality level set in the SAD design (it is approximately equal to 5%). Few cells which do not contain FA are used for location of three vertical experimental channels (VEC) and lead hexagonal blocks arranging spallation target. The outer contour of the core is made of segments replicating FA dimensions and pitch to provide reliable spacing of the peripheral FA. The low level of the specific energy release allows one to use air for cooling both the core and the target.

— Fuel pellets

During works in the frame of the project the technology of manufacturing plutonium powders of ceramic quality has been fulfilled. Physical and chemical characteristics of depleted uranium dioxide have been investigated, laboratory researches of sintering ability of the received plutonium and uranium dioxide powders have been carried out, production line has been prepared and the experimental batch of MOX fuel pellets has been made.

TABLE 4.2. SAD FUEL ELEMENT SPECIFICATIONS

| Parameter | Value |
|---|---|
| Fuel composition, % (mass) | 70% $UO_2$ + 30% $PuO_2$ |
| $^{239}Pu$ content in Pu %(mass), not less than | 95 |
| $^{235}U$ content in U %(mass), not more than | 0,7 |
| Cladding material | Steel ChS-68 cw |
| End caps material | Steel EI-847 |
| Spacing wire material | Steel ChS-68cw |
| Spring plunger material | Steel 12X18H10T |
| Fuel pellet dimensions, mm: | |
| diameter | $5,95^{-0,15}$ |
| height | 9,0 ± 1 |
| Cladding tube dimensions, mm: | |
| Outer diameter | 6,9 ± 0,03 |
| Inner diameter | 6,1 ± 0,03 |
| He content in gas inside cladding tube, % (vol.), not less | 95 |
| Spacing wire dimensions, mm | 0,6 × 1,3 |
| Spacing wire pitch, mm | 100 ±5 |
| Fuel pellet density, g/cm$^3$ | 10,4 ±0,2 |
| Fuel column weight, g | 160 ±3 |
| Height of active part of fuel column, mm | 580 ±10 |

— Replaceable target

Two types of replaceable targets (lead and tungsten) are used in the SAD. The lead target (Fig. 4.2) consists of the corrosion proof housing hermetically welded with bottom and top caps, also executed of stainless steel. Shape of the housing looks like a construction which consists of seven hexagonal prisms with the width across flats equal to 34 mm that are installed with a pitch equal to 36 mm. Six U-shape corrosion proof tubes ∅6x0.5 are installed inside the target, then the volume is filled with lead. U-shape tubes provide cooling of the lead target during facility operation. In the bottom part of the target the cylindrical cavity (58 mm in diameter and 179 mm in depth) is made to provide optimum conditions for spallation neutrons generation.The tungsten target is made of two types of hexagonal plates of TNI-95 alloy (tungsten–nickel–iron) with the central hole of 58 mm in diameter and without it. Target represents the assembly made of hexagonal plates with the width across flats equal to 33 mm that are installed with the pitch 36 mm. There is a layer of lead (0.2–0.1 mm) between plates which serves as a heat conductor. In the bottom part of the target there is a cylindrical cavity of 58 mm in diameter and 179 mm in depth (within five lover plates).

— Reflector

The SAD core is surrounded with lead reflector of 600 mm thickness in lateral direction and 300 mm thickness in top and bottom directions. Reflector is assembled of lead blocks and inserts enveloped with steel sheets. Lead block arranging outer side perimeter of the reflector have two outer concentric shells forming 30 mm thick cylindrical layer filled with B4C. Reflector housing has embedded fittings for core case, cooling system pipes, three VEC and two horizontal experimental channels (HEC).

*SAD technical data* are presented in Table 4.3.

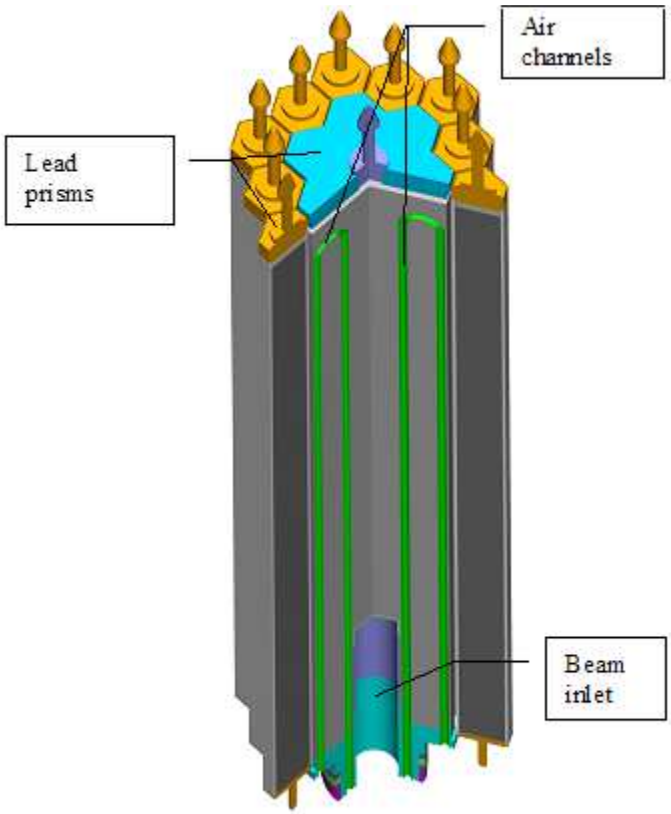


*FIG. 4.2. General view of the SAD lead target.*

TABLE 4.3. SAD TECHNICAL DATA

| Parameter | Value |
|---|---|
| Service life, h | 10000 |
| Fuel element cladding diameter, mm | 6,9 |
| FE pitch in triangle lattice, mm | 7,6 |
| Number of FE in FA | 18 |
| FA pitch in triangle lattice, mm | 36 |
| Maximum number of FA in core | 141 |
| Maximum burnup of fuel, % h.a. | 0,1 |
| SAD neutronics (with lead target) | |
| Number of FA in core with lead target | 134 |
| Neutron source intensity, 1/s | 1,21 x E14 |
| Neutron yield to core, 1/s | 1,14· x E14 |
| Energy release in target, kW | 0,94 |
| Fuel ($UO_2$-$PuO_2$) mass, kg | 396,8 |
| $k_{eff}$ | 0,951 |
| Prompt neutron lifetime, s | $2{,}4 \cdot 10^{-5}$ |
| Delayed neutrons effective fraction, % | 0,373 |
| Energy release in fuel, kW | 26,1 |

| Parameter | Value |
|---|---|
| Total energy release, kW | 28,5 |
| Neutron multiplication coefficient | 22,6 |
| Neutron generation in core, 1/s | 2,57·x E15 |
| Maximum neutron flux density in the core at 28.5 kW power, 1/($cm^2$·s): | |
| energy from 20 down to 1,0 MeV | 5,83 x E11 |
| energy from 1.0 down to 0.1 MeV | 1,62·x E12 |
| energy from 100 keV down to 1.0 keV | 7,13·x E11 |
| energy from 0 to 20 MeV | 2,92·x E12 |
| Average neutron flux density in the core at 28.5 kW power, 1/($cm^2$·s): | |
| energy from 0 to 20 MeV | $1,7 \cdot 10^{12}$ |
| SAD neutronics (with tungsten target) | |
| Number of FA | 132 |
| Neutron source intensity, 1/s | 1,14·x E14 |
| Neutron yield to core, 1/s | 1,04·x E14 |
| Energy release in target, kW | 1,01 |
| Fuel ($UO_2$-$PuO_2$) mass, kg | 390,9 |
| $k_{eff}$ | 0,9526 |
| Energy release in fuel, kW | 23,8 |
| Total energy release, kW | 26,1 |
| Neutron multiplication coefficient | 23,1 |
| Neutron generation in core, 1/s | 2,4·x E15 |
| Prompt neutron lifetime, s | 2,24·x E-5 |
| Thermalhydraulic features of the core and targets | |
| Coolant | Dry air |
| Coolant flow direction | From top to bottom |
| Target material: | |
| lead | lead C1 |
| tungsten | TNI-95 alloy |
| Reflector material | lead C1 |
| Core coolant inlet pressure, MPa | 0,135 |
| Core coolant inlet temperature, °C | Up to 50 |
| Total coolant rate, kg/s: | |
| - with lead target | 0,60662 |
| - with tungsten target | 0,65 |
| Core coolant average outlet temperature, °C | |
| - with lead target | 93 |
| - with tungsten target | 88 |
| Pressure drop in core, kPa: | |
| - with lead target | 9,72 |
| - with tungsten target | 12,66 |
| Coolant rate in lead target, kg/s | 0,00662 |
| Pressure drop in lead target, kPa | 13,65 |
| Maximum calculated FE temperature, °C: | |
| - with lead target | 131 |
| - with tungsten target | 159 |
| Maximum calculated FE temperature with deviations, °C: | |
| - with lead target | 185 |
| - with tungsten target | 232 |

| Parameter | Value |
|---|---|
| Maximum calculated temperature of the lead in target, °C: | |
| - without deviations | 176 |
| - with deviations | 214 |
| Maximum calculated temperature of the tungsten in target, °C: | |
| - without deviations | 242 |
| - with deviations | 286 |

(b) Proton beam transport channel

It is supposed to use in SAD project existing at JINR proton accelerator 'Phasotron'. Its main parameters are listed in Table 4.4. Beam transport channel is intended to the safe and reliable beam transportation from the phasotron to the SAD spallation target with designed parameters.

TABLE 4.4. PHASOTRON BEAM FEATURES

| Parameter | Value |
|---|---|
| Proton energy, MeV | 659 |
| Proton energy dispersion, MeV | 6 |
| Maximum power of the proton beam, kW | 1,0 |
| Maximum current of the extracted beam, mkA | 1.52 |
| Pulse frequency, Hz | 250 |
| Pulse duration FWHM, mks | 20 |
| Number of the protons in pulse | 4.0 x E10 |
| Pulse microstructure: | |
| - bunch duration FWHM, ns | 10 |
| - bunch period, ns | 70 |
| - number of the bunches in pulse | 385 |

Beam transport line includes bending magnets and doublets of quadruple focusing lenses, proton guide, beam diagnostics elements, beam stoppers, Faraday cylinder for beam intensity sensors calibration, support frames etc. The scheme of the SAD beam transportation line is presented in Fig. 4.3 Magnetic elements of the channel should provide:

— Beam transport to the SAD spallation target;

— Shaping on the target beam spot with required dimensions;

— Regulation of the beam spot position on the target with accuracy ±1 mm;

— Intensity of beam losses during its transportation not exceeding 5%;

Total electric power of the beam line is equal to approximately 700 kW, total beam line length amounts to 37.6 m.

#### *4.1.1.3. Conclusion*

The SAD project implementation is planned to permit the international community working in the field of transmutation of long lived components of nuclear spent fuel at ADS facilities, to gain unique experimental research. The research programme for the SAD facility is well coordinated with the Integrated Project EUROTRANS of the Sixth Framework Programme of EU.

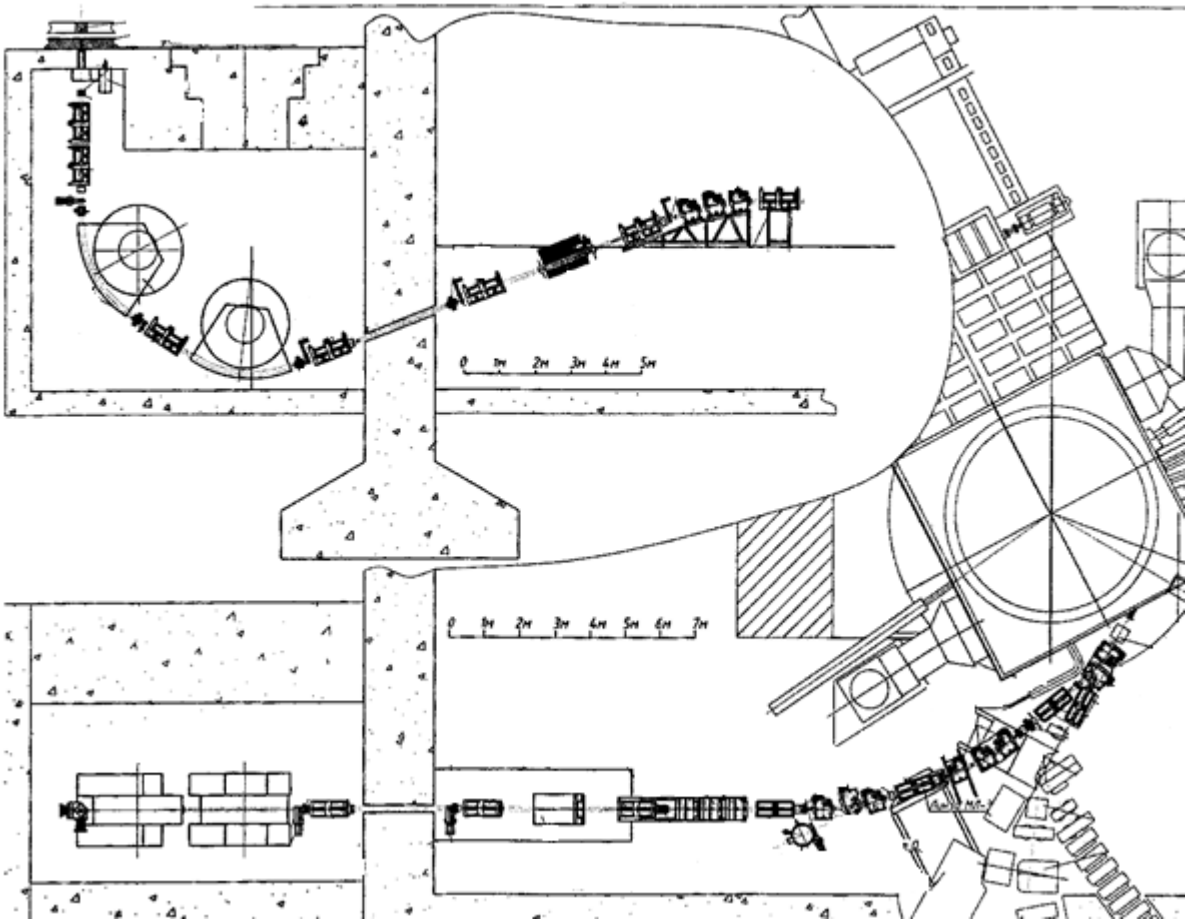

*FIG. 4.3. Beam line general scheme in SAD facility.*

### 4.1.2. Electro Nuclear Neutron Generator (ENNG) at ITEP

#### *4.1.2.1. Introduction*

Electro Nuclear Neutron Generator (ENNG) is under construction presently at the Institute of Theoretical and Experimental Physics, Moscow (ITEP) on the basis of a heavy water subcritical reactor and a proton linac and will be used mainly as an experimental accelerator driven system (XADS). Construction of the facility implies achieving the following purposes:

- Acting as experimental base for investigating many engineering, technological, and nuclear physical problems peculiar to the joint operation of such the different installations as proton accelerator and nuclear reactor;
- Being a technical base for the wide range of applied usage of proton beams and neutron fluxes;
- Create an educational center for training of specialists in some branches of nuclear technology and science;
- Practically demonstrate the possibility to converse a decommissioned experimental heavy water reactor to a new high level safety experimental facility;
- Represent an experimental mock-up prototype for the future high power ADS.

*4.1.2.2. Structure and main specifications of the ENNG*

ENNG, which scheme is presented in Fig. 4.4, is in the process of construction with application of the basic elements and equipment of the ITEP's decommissioned experimental heavy water reactor and the developed in ITEP pulse proton linear accelerator ISTRA-36.

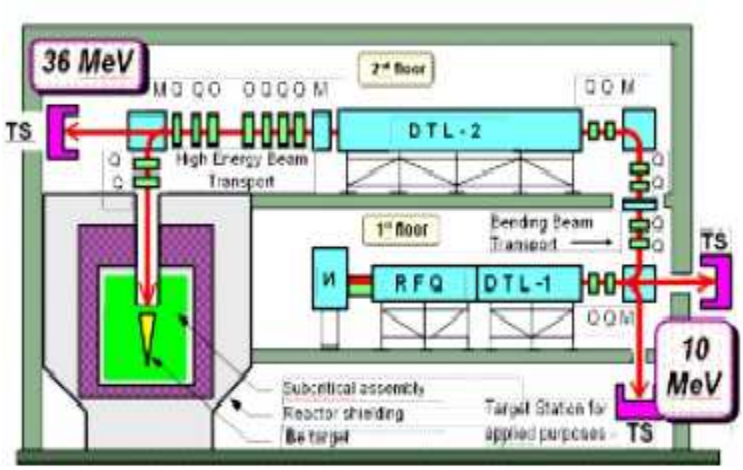


*FIG. 4.4. Scheme of the ENNG.*

The linac driver ISTRA-36 will be placed on the two floors of a special hall in the immediate vicinity to the subcritical blanket, both in a common building. Parameters of the ENNG are given in the Table 4.5 .

TABLE 4.5. BASIC PARAMETERS OF THE ENNG FACILITY

| Parameter | Units | Value |
|---|---|---|
| Output proton beam energy, | MeV | 36 |
| Average beam current, | mA | 0.5 |
| Target | --- | Be |
| Intensity of fast neutrons, | n/s | 3xE 14 |
| $k_{eff}$ | --- | 0.95 |
| Thermal neutron flux in experimental channels, | n/cm$^2$·s | 2xE12 |
| Thermal power at $k_{eff}$ = 0.95, | kW | 100 |

The accelerator driver consists of an injector with unheated cathode duoplasmatron ion source, section RFQ and two DTL cavities in which drift tubes are used. Linac will work in a pulse mode. Its key parameters are given in Table 4.6.

The RF cavities are made from three types of metal (stainless steel, steel 20, copper), which provides easy removal of the heat released. The cross-section of the RFQ cavity is shown in Fig. 4.5. The focusing channel in the DTL cavities is constructed on the base of quadrupoles with original permanent magnets (PMQ with $SmCo_5$, see Fig. 4.6), that makes it suitable, reliable and economical.

The proposed in ITEP and realized at the accelerator ISTRA-36 junction of internal volumes of the drift tubes and the vacuum volume of the DTL cavities, simplified fabrication and increased reliability of the tubes had been checked by now in the real conditions for the long time (several years) operation. Absence of gas emission materials in design of PMQ in internal volumes of the tubes allows avoiding the hermetic sealing of these volumes and gas pumping out through the holes which may be seen (on Fig. 4.6) at the external cylindrical surface of the tubes.

TABLE 4.6. PARAMETERS OF THE ACCELERATOR

| Parameter | Units | Value |
|---|---|---|
| Pulse beam current | mA | 100 |
| Duration of pulses | μs | 220 |
| Repetition rate | Hz | 25 |
| Beam power (pulse) | MW | 3.6 |
| Beam power (average) | kW | 18 |
| Intensity of protons (average) | $s^{-1}$ | 3.1× E15 |
| Frequency of RFQ RF field | MHz | 150 |
| Frequency of DTL RF field | MHz | 300 |

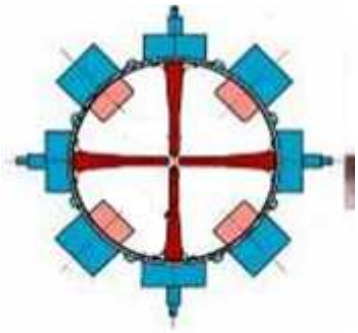

*FIG. 4.5.Cross-section of the RFQ cavity.*

*FIG. 4.6.Quadrupole with permanent magnet in drift tube.*

*Target blanket*. The horizontal section of the target blanket part of the ENNG is shown in Fig. 4.7 and its main physical parameters are presented in Table 4.7. The conic shaped beryllium target has a thickness of 6 mm. The proton beam with energy 36 MeV is virtually completely absorbed in the first 2 mm. Additional thickness serves to increasing the fast neutrons yield due to Be(n,2n) reaction.

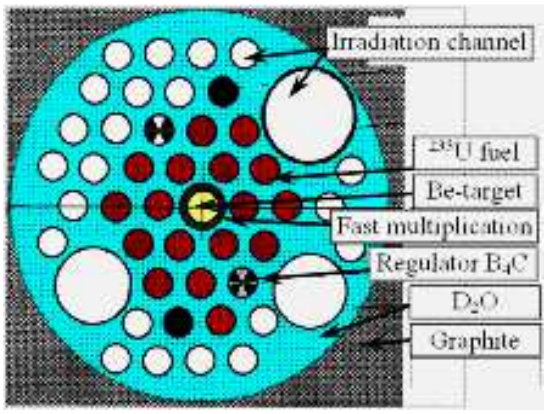


*FIG. 4.7. Horizontal section of the subcritical assembly.*

As a result, source neutrons emission from the target is increased by 25 %. The thermal blanket has a triangular lattice of 110 mm pitch. In lattice nodes the heat generating channels with highly enriched uranium (90 % of $^{235}$U) are placed, the height of an active part of assembly is 110 cm. Vertical experimental channels are located in the blanket reflector. According to calculations, on the internal surface of a conic target (diameter of the cone's base of 96 mm, the corner at top 24°) falls 98–99 % particles from the total number of those in the output beam of the accelerator. Thus, density of a proton beam in the middle part of the beam section is uniform. Such distribution is quite acceptable to

implementation of satisfactory thermal conditions of the target. The use of three types of experimental channels 250, 100, and 42 mm in diameter is being examined; the vertical channels are placed in the lattice nodes.

TABLE 4.7.BLANKET MAIN PARAMETERS

| Parameters | Units | Value |
|---|---|---|
| Heavy water vessel diameter/height | m | 1.71/3.44 |
| $k_{eff}$ in operation | --- | 0.95–0.97 |
| Fuel channels number | --- | 16 |
| U-235 load | kg | 1.30 |
| U-235 enrichment | % | 90 |
| Fuel lattice step | mm | 110 |
| Fuel assembly height | mm | 1110 |
| Moderator | --- | $D_2O$ |
| Primary coolant | --- | $D_2O$ |
| Reflector | --- | $D_2O$ followed by graphite |

#### *4.1.2.3. Present status*

The main part of R&D has been completed and the basic design has been issued. The considerable number of technological systems such as subcritical target blanket assembly and linac driver has been designed. The physical startup of a final branch of the linac in a temporary building has been carried out. Unused parts and systems of the decommissioned reactor are being dismounted and the preparation of the halls for re-equipment is being carried out. The new reactor vessel has been manufactured and delivered to the site for final mounting.

#### *4.1.2.4. The programme of the research and applied activities at the ENNG facility*

There are scheduled the following researches at the ENNG facility.

— Development and experimental validation of principles for control and monitoring of accelerator driven systems (ADS), including investigation of interconnections and inter-influences between such the distinguishing facilities that are the accelerator and the target blanket unity.

— Development and testing methods for the high intensity proton beam distribution over the target surface and control of this distribution.

— Experimental modeling abnormal situations in ADS and development of methods for their prevention (obtained results are planned to be used in developing the future high power ADS for energy production).

— Development of methods for certification of ADS control and monitoring system.

#### *4.1.2.5. Conclusion*

The ENNG facility will be an effective and safe experimental system integrating all classic components of ADS system: the proton linac, the neutron productive target and the subcritical blanket. This complex will allow carrying out researches of ADS characteristics and substantiating appropriate technologies.

Proton beams and neutron fluxes applied using will serve to the medical diagnostic and therapeutic purposes, to solve some problems of an industry and radiation materials technology and will have commercial significance.

### 4.1.3. J-PARC Transmutation experimental facility

#### *4.1.3.1. Introduction*

To study the basic characteristics of the ADS and to demonstrate the feasibility from the viewpoints of the reactor physics and the spallation target engineering, JAEA plans to build the Transmutation Experimental Facility (TEF) under a framework of the J-PARC Project. TEF consists of two buildings named Transmutation Physics Experimental Facility (TEF-P) and ADS Target Test Facility (TEF-T) respectively (Fig. 4.8). TEF-P is a zero power critical facility where a low power proton beam is available to research the reactor physics and the controllability of the ADS. In TEF-P, it is also possible to measure the reaction cross-sections of minor actinides, structural materials and so on. TEF-T is planned as a material irradiation facility which can accept a maximum 600 MeV–200 kW proton beam into the Pb-Bieutectic alloy spallation target [4.3].

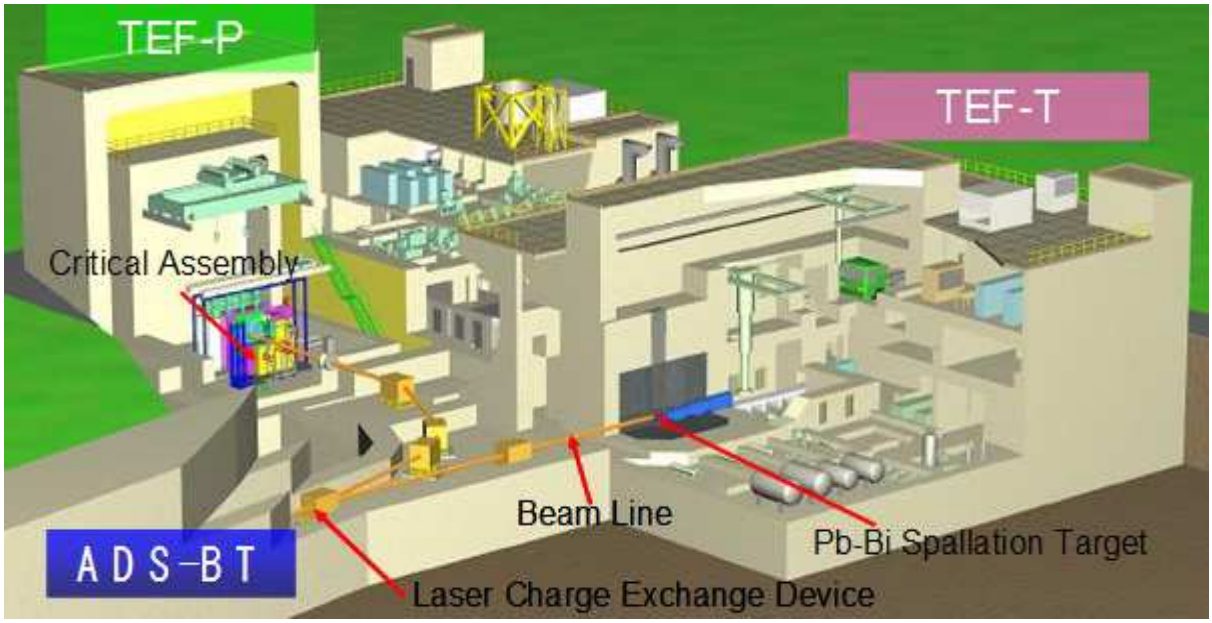


*FIG. 4.8. Transmutation experimental facility.*

#### *4.1.3.2. Description of theory and/or instruments*

(a) TEF-P

The purpose of the TEF-P is divided roughly into three subjects:

— Reactor physics aspects of the subcritical core driven by a spallation source;

— Demonstration of the controllability of the subcritical core including a power control by the proton beam power adjustment;

— Investigation of the transmutation performance of the subcritical core using certain amount of MA and LLFP.

The following section describes the detail of these experimental items.

In the experiment with the proton beam, $k_{eff}$ of the assembly will be kept less than 0.98. The 600 MeV–10 W proton beam supplies $1.5\times10^{12}$ neutrons/s from Pb target, which is strong enough to measure the power distribution at the deep subcritical state. In the viewpoint of the neutronics of the subcritical system, power distribution, $k_{eff}$ effective neutron source strength, and neutron energy spectrum will be measured by changing subcriticality and spallation neutron source position,

parametrically. The target material will be altered with Pb, Pb-Bi, W, and so on. The reactivity worth is also measured for the case of the coolant void and the intrusion of the coolant into the beam duct. It is desirable to make the core critical in order to ensure the quality of experimental data of the subcriticality and the reactivity worth. For the demonstration of hybrid system, feedback control of the thermal power is examined by adjusting the beam intensity. Operating procedures at the startup–shutdown, beam trip and restart are also examined. As for the transmutation characteristics of MA and LLFP, fission chambers and activation foils are used to measure the transmutation rates. The cross-section data of MA and LLFP for high energy region (up to several hundreds MeV) can be measured by the Time of Flight (TOF) technique with the proton beam of about 1ns pulse width. Several kinds of MA and LLFP samples are also prepared to measure their reactivity worth, which is important for the integral validation of cross-section data. Installation of a partial mock-up region of MA nitride fuel with air cooling is considered to measure the physics parameters of the transmutation system. The central rectangular region (28cm × 28cm) will be replaced with a hexagonal subassembly which can partially load the pin type MA fuel around the spallation target as shown in Fig. 4.9. The mock up of MA loading FBR cores is also possible without installing a spallation target in critical state operation.

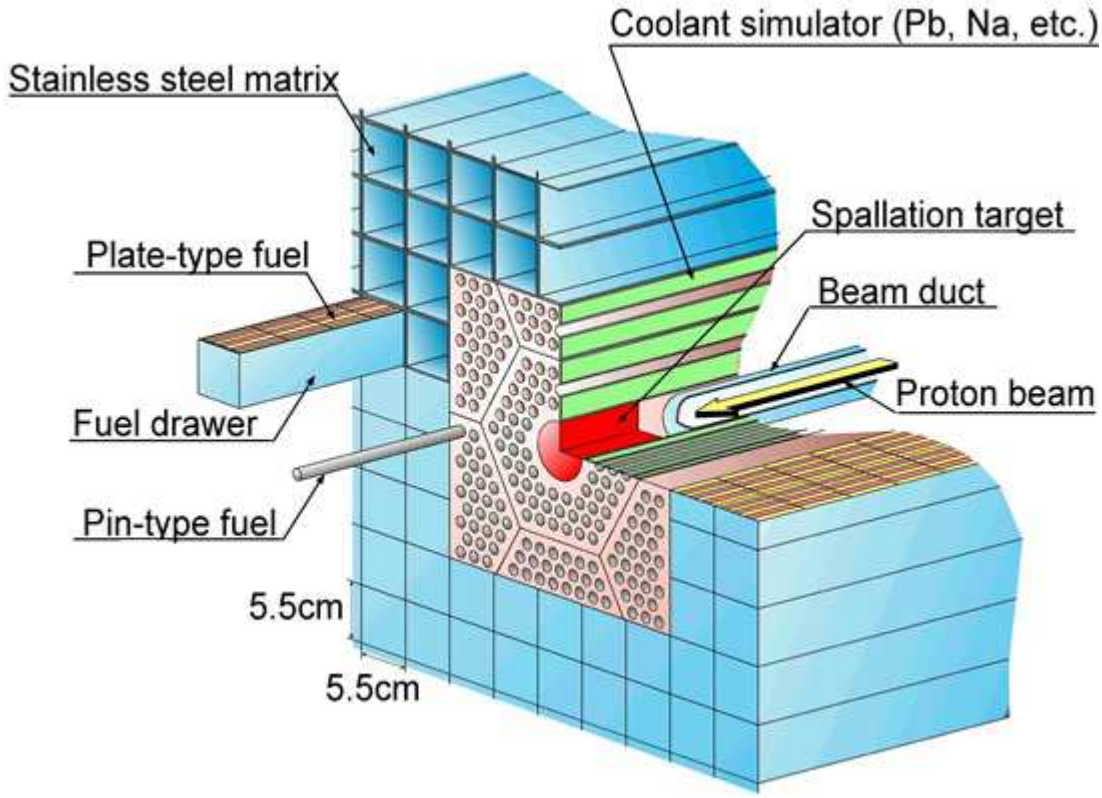


*FIG. 4.9. TEF-P assembly with partial loading of pin type fuel.*

(b) TEF-T

JAEA proposes the Pb-Bitarget/cooled ADS. Pb-Biis one of the alternative options of the coolant of the fast system and it also has a function of liquid spallation target simultaneously in the ADS. There are, however, many technical issues to use Pb-Bisafely. TEF-T aims at preparation of the engineering design database required for ADS. Another important component for ADS is a beam window which forms a boundary between an accelerator and a subcritical core. It is subjected to heavy irradiation by proton and spallation neutron, mechanical stress caused by the pressure difference between the accelerator and flowing Pb-Bitarget, thermal stress arising from heat deposition of high energy particles and beam transients (startup/shutdown and beam trip) and chemical interaction with Pb-Bi. It is important to prepare the database to estimate a lifetime of the window. So that, the experiments to obtain the design database for beam window are also the important mission of TEF-T.

TEF-T mainly consists of a Pb-Bi spallation target, a secondary cooling circuit, and an access cell to handle the spent target vessel and irradiation test pieces. The primary Pb-Bi loop is designed to allow Pb-Bi flow with 2 meter per second of a maximum velocity and 450 degree centigrade of maximum temperature. Target vessel is a sealed double annular cylindrical tube with a 90 degree bend section. An effective size of the tube is about 15 cm in diameter and 3 to 4 meter long. Several kinds of target head are planned and designed according to the objective of the experiment. Pb-Bi is circulated by electromagnetic pump that is completely separated from the target tube. This newly designed target can be replaced quickly and easily by withdrawing the target tube in upward direction from heat exchanger electromagnetic flowmeter, and electromagnetic pump without cutting or disconnecting the circuit pipes. The access cell has functions to deal with the spent or new target, to clean up residual Pb-Bi to reduce exposure dose by the spallation products, and to pick up irradiated material test pieces by using remote handling devices.

### 4.1.4. Indian experimental ADS subcritical facility

#### *4.1.4.1. Introduction*

A programme for conducting reactor physics studies on subcritical neutron multiplying assembly with the neutron generator has been initiated in BARC. Measurement of flux distribution, flux spectra, total fission power, source multiplication, and degree of subcriticality will be carried out during experiments planned.

#### *4.1.4.2. Subcritical assembly*

A subcritical assembly of natural-U fuel elements and light water has been chosen for the purpose of basic reactor physics experiments. It consists of natural Uranium metal rods of 3.45 cm diameter clad in 1 mm thick aluminum tube. These fuel rods are placed horizontally inside aluminum tubes arranged in a hexagonal lattice of pitch 5.5 cm within a tank. The central axial aluminum tube houses the tritium target. The core length is 100 cm and a loading of 300 rods gives a $k_{eff}$ that is about 0.87. Design of this subcritical assembly is completed, and procurement–fabrication of various hardware and mechanical components are in progress.

#### *4.1.4.3. Driver neutron source*

A 14 MeV neutron generator (Fig. 4.10) has been in existence in PURNIMA laboratory in BARC for several years for conducting fusion blanket neutronics studies. It consists of a DC high voltage accelerator, which produces about 200 micro ampere current of deuteron beam, accelerated to an energy of ~300 keV. The deuteron beam falls on a Ti target loaded with Tritium. The 14 MeV neutrons are produced by the D-T fusion reaction resulting in a continuous neutron source of about $3x10^9$ n/s with a 5-curie tritium target on titanium substrate at 260 kV. Neutron yield can be further improved by an order and also made pulsed at about 100–1000 Hz. for specific experiments.

The deuteron source is currently being modified for, pulsing at 10 sec width and rep. rate up to 500 Hz, higher ion current up to 2 mA, operating voltage with improved stability up to 350 KV and later by using a 400 keV deuteron RFQ accelerator. This facility is under refurbishment with a subcritical core in which natural uranium metallic fuel rods arrayed in light water filled calandria and tube assembly. The planned subcritical assembly (Fig. 4.11) will be an aluminium shell & tube type calandria vessel of about 1.4 m.

#### *4.1.4.4. Experimental programme*

As mentioned above, measurement of flux distribution, flux spectra, total fission power, source multiplication, and degree of subcriticality are part of the experimental programme at BARC.

Measurement of the degree of reactor subcriticality is an important experiment being planned, as monitoring this parameter for ADS will be a mandatory safety requirement. This will be done by pulsing the accelerator beam and by reactor noise analysis. The new theory of Reactor Noise in ADS, described previously can be tested in this facility.

*FIG. 4.10. 400 kV DC deuteron accelerator (right) for 14 MeV neutron source (on the left side).*

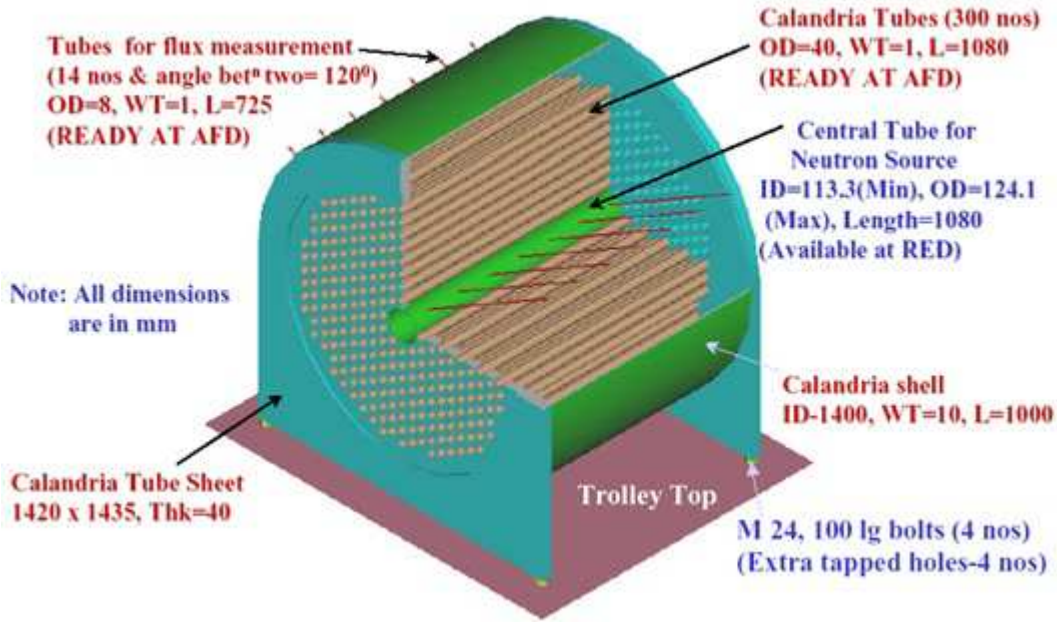


*FIG. 4.11. Calandria for ADS subcritical core experiments.*

The kind of experiments planned will help in validation of calculation tools and neutron cross-section data, neutron flux profiling and real time measuring of the $k_{eff}$. First experiments planned with this system include benchmarking the calculations of $k_{eff}$ values under various fuel moderator combinations and distribution of neutron flux through the core. More details are still being worked out.

The effective neutron multiplication factor ( $k_{eff}$) of a subcritical system is an important parameter, which is required for the safe operation of an accelerator driven systems. The measurement of $k_{eff}$ is not very simple for a system, which is deeply subcritical. Two types of methods are normally used to measure $k_{eff}$. The stationery methods like neutron source measurement where total numbers of neutrons are measured with and without the presence of nuclear fuel, and modified source multiplication method. These stationery methods are not very accurate, as many corrections are needed to obtain the correct values.

The other is the dynamic method that is based on the measurement of neutron multiplication as a function of time at a location deep inside the subcritical assembly. This method is more accurate and it also has the advantage that it can be used to measure the $k_{eff}$ value at any time during the operation of the actual ADS. It requires the neutron generator working in the pulsed mode. The width of the neutron pulse should be ~10 μsec with a frequency of around 500 Hz and each burst should contain about $10^4$–$10^5$ neutrons for thermal systems. The measurement can be performed with various neutron monitors like He-3, BF3 or U-235 fission detectors. The counting rate evolution of neutrons is recorded in an analyzer operating in time mode (10 μs/channel) after each burst of 14 MeV source neutrons up to 1 millisecond for several thousands sweeps till one gets good statistics.

Monte Carlo calculations were performed in time mode to study the dynamic behaviour of the Purnima subcritical assembly driven by a central pulsed neutron source of 14 MeV energy. Tallies are obtained for the reaction rates for various types of detectors like $^3$He(n,p), BF-3(n,alpha) and $^{235}$U (n,f) fission detectors located inside different fuel rods and also inside the water reflector as a function of time.

## 4.2. EXISTING EXPERIMENTAL FACILITIES

A wide use of pure lead, as well as its alloys (such as lead-bismuth, lead-lithium), thanks to its favourable properties, is foreseen in several nuclear related fields, i.e. it is studied as coolant for critical nuclear reactors, for tritium generation in fusion systems and as both coolant and spallation target in accelerator driven systems (ADS). Given this possible future extensive use of lead in nuclear systems, a deep understanding of its physical properties and engineering applications is mandatory. As a consequence, given the quite limited nowadays experience, large efforts both at national and international level are dedicated to the development and understanding of heavy liquid metal technologies. In this frame a large effort has been dedicated to build and operate an unique patrimony of infrastructures operating heavy liquid metals (HLM), now available worldwide, comprising both large facilities and small loops that constitute an important technological platform in the field of materials studies, thermalhydraulics and liquid metal chemistry. In this section several HLM facilities are presented, outlining their objectives and describing in detail their operational parameters and geometrical characteristics.

### 4.2.1. Existing HLM Facilities for experimental applications in NRI ŘEŽ PLC (Czech Republic)

#### *4.2.1.1. Purpose and goal*

Scientific and technological activities on materials compatibility and technology issues have been launched during the last years in relation to the use of heavy liquid metal (HLM) lead bismuth eutectic (LBE) and pure lead Pb as cooling medium and spallation materials in the field of accelerator driven system (ADS) which are devoted to transmute and reduce the radiotoxicity on radioactive waste.

Main aim of the use our experimental HLM facilities is the material testing. The facilities used to characterise the materials behaviour in the liquid metal are principally of two types in NRI Řež plc. One are the convectional loops COLONRI I (LBE) and COLONRI II (pure Pb) for the evaluation of the long term corrosion resistance of materials under the normal conditions and for short term tests

under the abnormal conditions (higher temperature, extreme oxygen content etc.). The second one is the static cell CALLISTO for mechanical testing in high temperature in the HLM environment. Secondary aim is the development of oxygen control system (OCS).

The main goal of the facilities here described is the reference materials characterisation in HLM and the development of HLM technologies.

The objectives of the convectional loops COLONRI I and II are:

- Long term corrosion investigations of structural materials and coatings in lead alloys (LBE and Pb) at different oxygen content;
- Effect of oxygen content on corrosion processes;
- Investigation of corrosion mechanisms;
- Influence assessment of protection layer and coatings on corrosion;
- Possibility of the shortterm tests under the abnormal conditions (higher temperature, extreme oxygen content, etc.);
- Development of oxygen control system (OCS);
- Optimization of oxygen sensor performance as for reference system, reproducibility and long term stability;
- Measurement of oxygen mass exchange rates.

The objective of the cell for mechanical tests CALLISTO is the effect assessment of HLM on the mechanical properties of the structural materials. Tests that can be carried out are:

- Slow strain rate tests;
- Constant load;
- Rising load;
- Cyclic fatigue.

#### *4.2.1.2. Description of the facilities*

Since 2001 experimental tests on the first convectional loop COLONRI I in NRI Řež plc with liquid LBE were started. During the several years the HLM technology development was innovated and the experiences were generalized [4.5]–[4.12]. In 2006 the second convectional loop COLONRI II with pure Pb was opened and a new cell CALLISTO for mechanical testing under the high temperature in HLM environment was designed and built. The experiments in LBE were carried out in the frame of the project IP EUROTRANS, domain DEMETRA, while for the pure lead experiments are on progress in the frame of the project VELLA, Joint Research Activity 1.

(a) Convectional loops COLONRI I and II

The thermal COnvection LOops in the NRI (Fig. 4.13,Fig. 4.14) were developed following an extensive experience in the use of convection loops for monitoring the corrosion of structural materials in heavy and alkaline liquid metals [4.10]. The first natural convection loop COLONRI I, in the NRI, was designed and developed over the years. The experimental structure was designed as a vertical convectional loop. The latest development of the natural convectional loop (named type VII), was constructed in the NRI. The small structure of the loop offers the possibility to run short and long term experiments with flowing heavy liquid metals and to control several variables, such as temperature and oxygen content.

The vertical experimental structures were assembled in a square shaped loop, with the equalising tank at the top and the filling tank at the bottom part. The loops were manufactured from the austenitic

stainless steel Ti stabilized AISI 321. The inner surfaces of the tubes working at the highest temperatures were covered with a molybdenum plate.

The COLONRI I contains liquid Pb-Bieutectic, LBE, and the COLONRI II contains pure liquid Pb. The loops have high (H) and low (L) temperature experimental sections and heating (h) and cooling (c) legs (Fig. 4.13), each about 100cm long. Main parameters of the loop are listed in Table 4.8.

Along the test sections, the temperature is maintained constant. Thermocouples monitor the temperature along the structure with an accuracy of ±1°C. The two loops can work in a range of temperatures that allow a maximum ΔT of 150°C. The specimen holders (4 for each experimental chamber) can contain up to three rows of specimens, for a total length of about 140 cm. The loops contain about 1.7 litres of liquid metal.

These type of loops allows dosing of the inlet $H_2O$ + $H_2$ mixture, in any ratio, both above and below (bubbling through) the level of the liquid metal in the upper, equalising tank. The equalising tank is also used as a cold trap, since impurities can precipitate and float on the colder surface of the liquid metal. The medium can be monitored and purified during the experiments by varying the content of oxygen and removing the solid corrosion products at the free surface of the liquid in the equalising tank.

The level of impurities in the loops is maintained very low due to the fact that the material dissolved at the highest temperature can precipitate and deposit in the colder areas, till a steady state condition is reached. In this way the purity of the liquid metal at the entrance of the hot legs is high and, thus, the media cannot reach the saturation and the dissolution of the specimens exposed continues during the whole exposure time.

The content of oxygen in the LBE was adjusted by dosing a mixture of Ar and $H_2$ bubbled through the water tank and then into the expansion tank. The expected oxygen content was calculated through the solubility of $O_2$ in LBE, given by the formula

$$log\ C_o^* = 1.2 - \frac{3400}{T\ [K]}$$

where $C_o^*$ is the concentration of the oxygen dissolved, in weight percent.

The gas mixture introduced in the system with pure Pb in COLONRI II by using the formula for the solubility of oxygen in pure lead:

$$log\ C_o^* = 3.2 - \frac{5000}{T\ [K]}$$

where $C_o^*$ is the concentration of the oxygen dissolved, in weight percent.

One oxygen sensors (based on the Bi-$Bi_2O_3$ electrode) were placed in the as much as four positions of the loops and on-line monitored an oxygen content.

(b) Cell for mechanical testing CALLISTO

The cell was designed to contain the HLM and carry out tests with specimens immersed in the HLM (Fig. 4.15). The cell was mounted on a hydraulic loading machine with a max loading capacity of 50kN. The maximum volume of the cell is about 900 $cm^3$ (internal diameter about 100mm) and its height was designed for a maximum specimen size of about 65 mm (corresponding to the SENT specimens). The cell was built with austenitic AISI 316 steel. The main parameters of the cell are listed in Table 4.9 (see also Fig. 4.12. )Inside the cell, specimens and grips are totally immersed into the HLM. A thermocouple measures the inner temperature at a distance of about 10mm from the specimen surface. A maximum operating temperature of about 550°C can be reached. The oxygen content into the cell can be controlled through gas bubbling. Moreover, an aperture for the future use of an oxygen sensor is present.

TABLE 4.8. MAIN PARAMETERS OF THE CONVECTIONAL LOOPS COLONRI I AND COLONRI II

| Parameter | COLONRI I | COLONRI II |
|---|---|---|
| Medium | LBE | Pb |
| Operational temperature | 550°C | 600°C |
| Max. temperature | 650°C | 700°C |
| Max. temperature gradient between the two test section | 150°C | 150°C |
| Flow rate | Max. 2cm/s | Max.2cm/s |
| Number of test section | 2 | 2 |
| Test section diameter | 2,5 cm | 2,5 cm |
| Total electric power | 4 kW | 5 kW |
| Medium purity | 99,5% | 99,5% |
| OCS (oxygen control system) | hydrogen dissolved water<br>OCS sensor $Bi/Bi_2O_3$ | hydrogen dissolved water<br>OCS sensor $Bi/Bi_2O_3$ |
| Loop material | AISI 321 | AISI 321 |

TABLE 4.9. MAIN PARAMETRS OF THE CELL FOR MECHANICAL TESTING CALLISTO

| Parameter | CALLISTO |
|---|---|
| Max. temperature | 550°C |
| Medium | Air, LBE, Pb |
| Max. electricity power | 3 kW |
| Test section | 1 (autoclave) |
| Volume of medium | 900 $cm^3$ |
| OCS | yes |
| Max. load | 50 kN |
| Conditioning gasses | Ar, $H_2$, $N_2$ |
| Autoclave materials | AISI 316 |

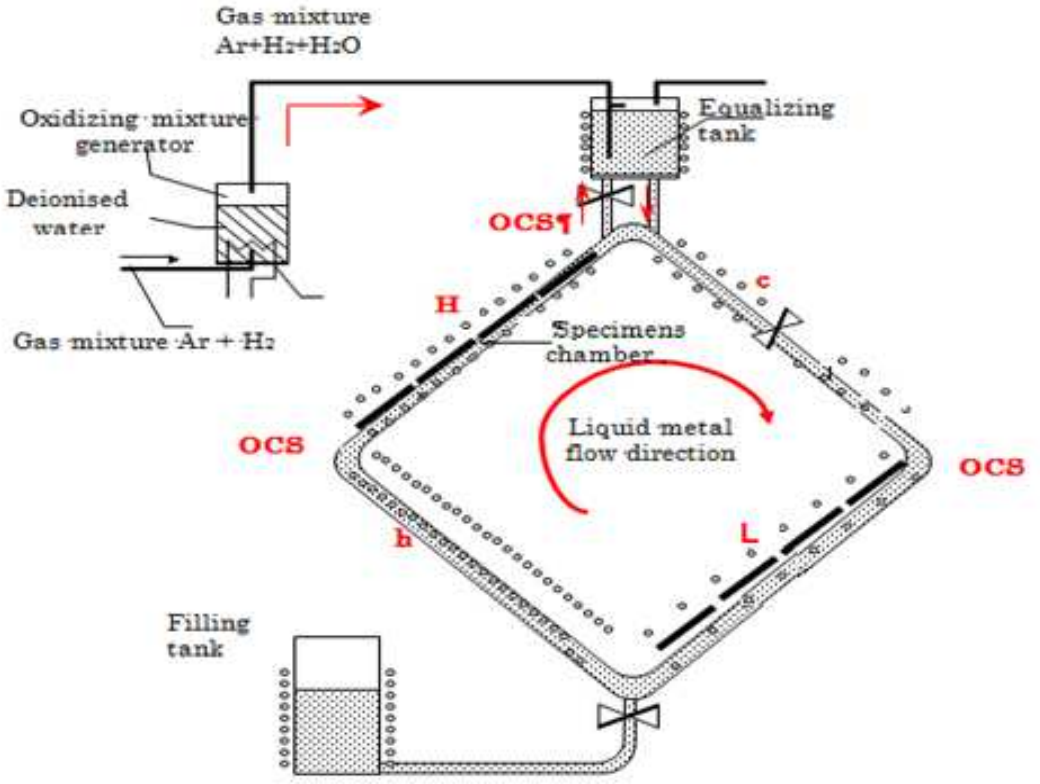


*FIG. 4.12. Cell for mechanical tests CALLISTO.*

*FIG. 4.13. Convectional loop for corrosion tests in LBE COLONRI I.*

*FIG. 4.14. Hall with the convectional loops COLONRI I and COLONRI II.*

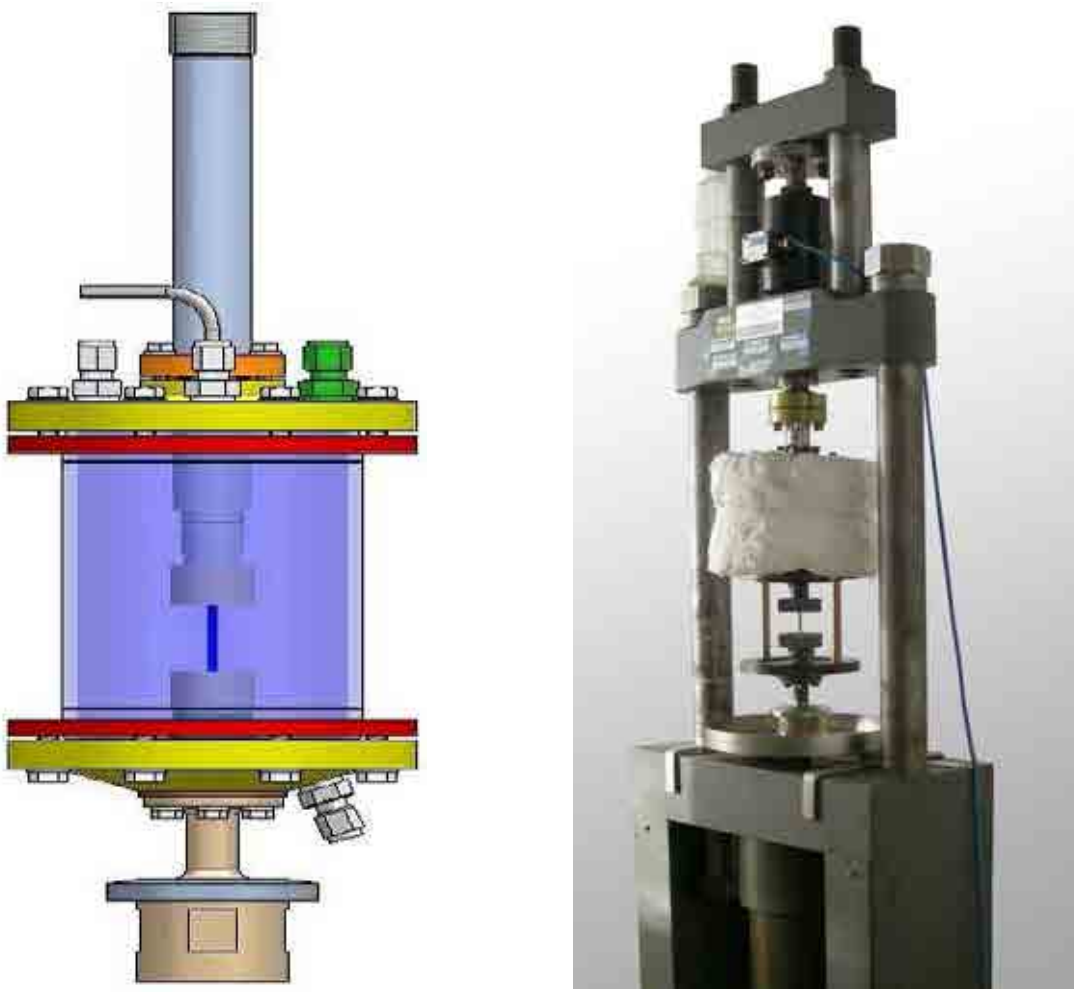

*FIG. 4.15. Cell CALLISTO (schematic view, photo) mounted on the hydraulic machine.*

### 4.2.2. The Karlsruhe Liquid Metal Laboratory (KALLA, Germany)

#### *4.2.2.1. Purpose and goal*

The KALLA (KArlsruhe Liquid Metal LAboratory) programme has been defined with the objective of demonstrating the practical use of LM, which consists of several stagnant and loop experiments. Currently, KALLA represents one of the most relevant infrastructures in Europe dedicated to liquid metal technologies. The KALLA facility enables to study flow in complex geometries, to develop measurement techniques for local and global quantities, to assess the materials compatibility in different conditions and to generate basic physic chemical data as for instance the wetting capability of the liquid metals, oxygen solubility and others. This article gives a short glance of the available experimental facilities installed in KALLA and it outlines the main focus of each of the test stands. KALLA is operating since several years and a broad data base has been gained for the individual components typically appearing in reactor systems like pumps, valves, and oxygen monitoring and control systems.

#### *4.2.2.2. Description of the facility:*

The name KALLA summarizes the experimental and numerical activities in liquid metal technology, thermalhydraulics and material research with different loop experiments and different liquids as lead

or lead-bismuth, sodium, indium-gallium tin and in the near future lithium [4.13],[4.14]. The individual facilities, which are described below, can be divided in two subgroups; the first one involves stagnant liquids (mainly Pb or $Pb^{45}Bi^{55}$) while the second concerns flowing liquid metals. Each KALLA test facility is equipped with the Karlsruhe OCS. The facilities using stagnant fluids are:

— COSTA 1 to 6 (Corrosion test stand for Stagnant liquid lead Alloys)

— KOSIMA 1 to 6 (Karlsruhe Oxygen Sensor In Molten Alloys)

— KOCOS (Kinetics of Oxygen Control Systems)

— OCEAN (Oxygen Controlled Experimental container, shown in Fig. 4.16a.

In the COSTA experiments, crucibles filled with liquid metal are placed in glass tubes located in a furnace at a given temperature. The COSTA experiments are dedicated to investigate.

— Corrosion mechanisms;

— Influence of protection layers and coatings on the corrosion behaviour;

— Corrosion resistance and degradation rates of GESA treated surfaces;

— Impact of surface alloying on corrosion.

KOSIMA operating since 1998 consists of liquid metal filled ceramic crucibles kept at a prescribed temperature equipped with an OCS with up to 3 oxygen meters. The KOSIMA experiments focus on the

— Development and calibration of oxygen sensors;

— Optimization of oxygen sensor performance with different reference systems;

— Reproducibility of the sensor reading;

— Study of the long term stability of each sensor type.

Also KOCOS consists of a heated crucible filled with liquid metal and operates since 1999. It is concentrating on the:

— Development of the Karlsruhe OCS;

— Measurement of diffusion coefficients of oxygen in Pb-Bi; and

— Determination of oxygen mass exchange rates.

The OCEAN experiment is an actively oxygen controlled experimental container in which different experiments can be conducted on a small scale, such as:

— Measurements of the oxygen solubility in PbBi;

— Development of free surface distance sensors for the reflecting liquid metals;

— Contact angle measurements of liquids on steel probes at different temperatures;

— Measurement of thermophysical properties of metals at different $O_2$ levels;

— Insertion of small scale horse track like loops for screening experiments.

In addition, four KALLA loop experiments are operating, and a fifth (TELEMAT) is almost operational, all controlled with an active OCS. These loops are available also to external users, which is supported by the integrated infrastructure initiative VELLA of the $6^{th}$ European Framework Programme. The liquid metal inventory and the most relevant technical data of each loop are summarised in TABLE 4.10.

— THESYS

— THEADES

— CORRIDA

— ALINA

— TELEMAT

The THEADES loop, shown in Fig. 4.16b, concentrates on thermalhydraulic investigations of reactor components in prototypical dimensions. The main objectives are:

— Cooling of targets in both in window–windowless configurations;

— Flow temperature distribution and surface shape measurements in components;

— Cooling of single fuel elements and fuel rod bundles;

— Heat transfer characteristics of different heat exchanger types.

The THESYS loop experiments, depicted in Fig. 4.16c concentrates on the development of fundamental liquid metal technologies and generic experiments like:

— Qualification of monitoring and conditioning systems for loop applications such as OCS, flowmeters, heat flux simulators, and pressure transducers;

— Development of thermalhydraulic measurement techniques for mean and local thermo-physical quantities like temperatures, local pressures and local velocities;

— Thermalhydraulic benchmark experiments for code validation as heat transfer benchmark experiments and turbulent flow measurements in complex geometries.

The Corrosion Loop CORRIDA is designed as an 8-shaped loop. It consists of an electromagnetic pump, a recuperator, an OCS, two preheaters, and two test sections containing up to 32 cylindrically shaped test specimen. CORRIDA is dedicated to generic corrosion investigations of structural materials with low activation and beam window materials considered for future reactor design. Thus CORRIDA is focussed on:

— Fundamental corrosion mechanisms and kinetics;

— Formation and stability of protection layers;

— Performance of mechanical tests;

— Development of structural and beam window materials.

The oil cooled ALINA loop operated with sodium is related to windowless targets with free surfaces as well as to small scale generic heat transfer experiments. It is shown in Fig. 4.16d.

More advanced reactor studies attempt to reach higher operation temperatures and thus to increase the net efficiency. Therefore, temperatures beyond 550°C are under consideration involving a dedicated material qualification programme. In this context the high temperature loop TELEMAT (design temp. 750°C) operated with liquid lead is projected and already partly fabricated. In a first stage, the corrosion/erosion effects of flowing liquid lead will be investigated for potential cladding materials.

Starting from target investigations, future thermalhydraulic studies will also concentrate on core components like fuel bundles and spacer problems. They will be extended to study the performance of reactor components like heat exchangers and new advanced pump concepts. In the field of material research and qualification, the focus of the studies will be broadened to investigate more pure liquid lead systems and to intensify the material investigation to higher temperatures. Another issue will be the test of material protection systems for fuel claddings using the GESA facility. Regarding the liquid metal adapted instrumentation techniques, more reliable oxygen sensors are being developed. Moreover, an optical technique determining both the free surface shape and distance with a high time and space resolution is developed to investigate the stability of windowless targets appearing in several nuclear applications.

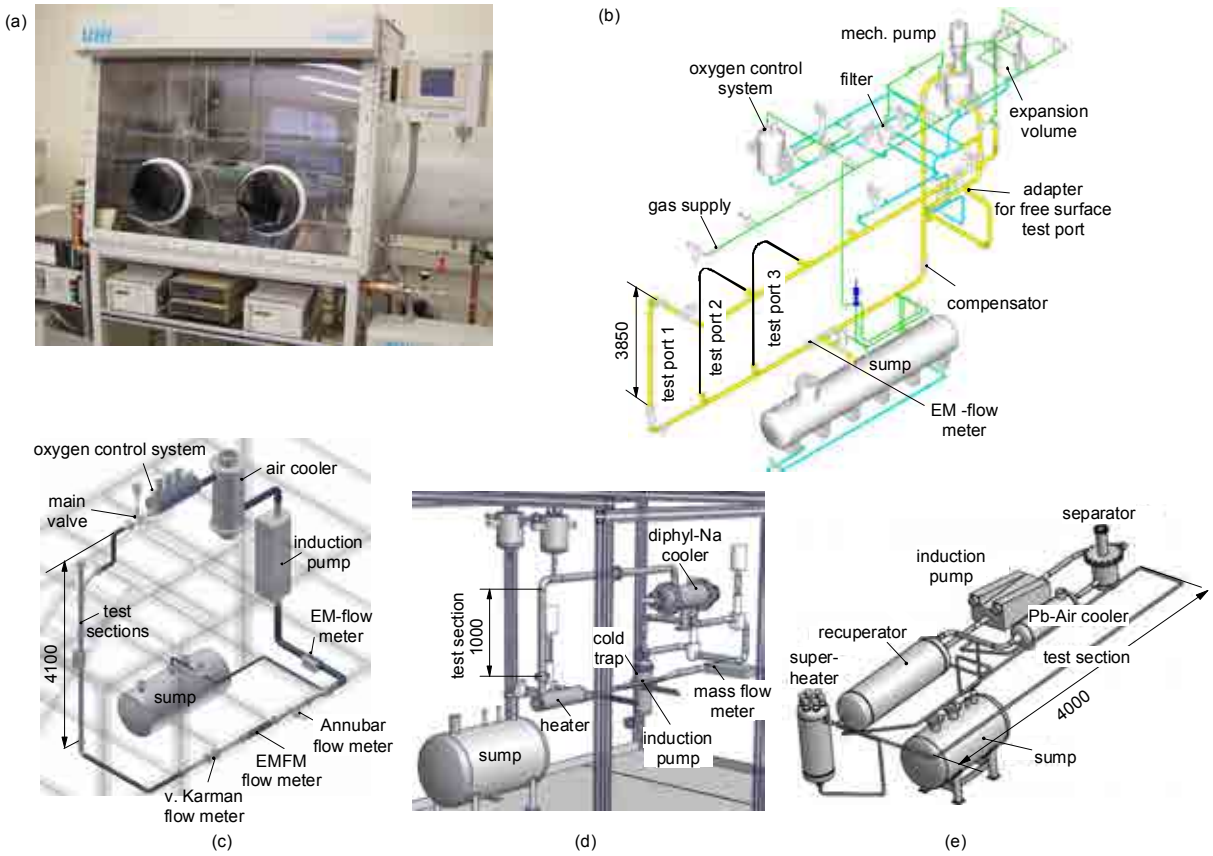


*FIG. 4.16. a.) OCEAN test stand, b.) THEADES loop, c.) THESYS loop, d.) ALINA facility, e.) Projected HT lead loop TELEMAT.*

TABLE 4.10. CHARACTERISTIC DATA OF LOOP EXPERIMENTS IN THE KALLA LABORATORY

| Header | THEADES | THESYS | CORRIDA | ALINA | TELEMAT |
|---|---|---|---|---|---|
| Operating liquid | $Pb^{45}Bi^{55}$ | $Pb^{45}Bi^{55}$ | $Pb^{45}Bi^{55}$ | Na (Li) | Pb |
| Pressure head [bar] | 5.9 | 3 | 2 | 3.5 | 2.3 |
| Max. flow rate [$m^3$/h] | 47 | 16 | 9 | 21 | 2.1 |
| Max. temp. [°C] | 400 | 550 | 650 | 400°C | 750° |
| Liquid metal inventory [litres] | 4000 | 300 | 280 | 150 | 200 |
| No. of test ports | 4 | 2(+2) | 2 | 1 | 2 |
| Max. size of test section [m] | 3.85 | 4.1 | 1.2 | 1.0 | 3.8 |
| Installed electric power [kW] | 1200 | 250 | 250 | 120 | 110 |
| Operation hours [h] | 3000 | 2000 | 17000 | - | - |
| Startup year | 2002 | 2005 | 2003 | 2006 | (2007) |

### 4.2.3. Technology experimental facility (India)

#### *4.2.3.1. Purpose and goal*

Design and construction of experimental facilities for development of technological details of lead-bismuth eutectic based spallation target subsystems and materials tests are in progress at BARC, Mumbai and VECC, Kolkata.

*4.2.3.2. Description of the facilities*

(a) LBE spallation target R&D and studies

The LBE liquid heavy metal target development programme that is being pursued mainly at BARC, involves solutions related to the following issues:

- Thermalhydraulics issues in high specific heating zone of target;
- Corrosion and erosion of the container material;
- Radiation damage of container materials (specifically, the beam window) by high energy protons and neutrons;
- Effects of spallation products on corrosion and radiotoxicity;
- Safety issues related to target performance under abnormal conditions.

— Window and windowless target systems

For the spallation target module configuration, two concepts are being studied. First is beam window concept, in which pump driven, buoyancy driven, and gas driven schemes are being studied through computer simulations for flow velocities, heat transfer and peak temperatures. The other one is the windowless concept, where the proton beam terminates on free surface of the molten LBE target at the operating temperatures < 4000°C.

For the beam window target studies, the proposed reference material is martensitic steel type T91. The maximum proton beam current density that the window will be subjected is ~50 μA/cm2. This puts a lower limit on the diameter of the target module for a desired accelerator beam intensity. In our simulations for 1 GeV proton energy, typically ~ 4kW of heat per mA of beam current is deposited in the window.

Even though windowless configuration seems convenient from material damage viewpoint, complex hydrodynamic instability problems are encountered in maintaining a very stable free surface in the presence of secondary flows, which also affect the heat transport capability of the flowing liquid metal.

A roadmap has been chalked out to develop various technologies associated with target sub-system in ADS. Under the ongoing R&D programme, a few liquid metal loops consisting of mercury, and LBE are being set up, computational tools are being developed and corrosion studies including mitigation methods for process system materials have been initiated.

— Mercury loop for diagnostic studies

In view of many fluid dynamical similarities between mercury and LBE, a mercury loop has been set up to study various special diagnostics methods; flow simulation studies and CFD code validations etc. Both beam window and windowless simulation concepts have been integrated in this loop. However, studies will be carried out without any heat input. The velocities simulated will be similar to that of actual target but flow pipe dimensions will be around one fifth of the actual one. In addition, flow circulation will be induced by nitrogen gas injection.

Special diagnostics like ultra sonic velocity profile monitor is being used for velocity mapping, and laser triangulation technique for free surface location measurements. The void fraction in the two phase flow will be measured by high energy gamma attenuation method. Some of these experiments are in progress in such a facility, which is shown in Fig. 4.17.

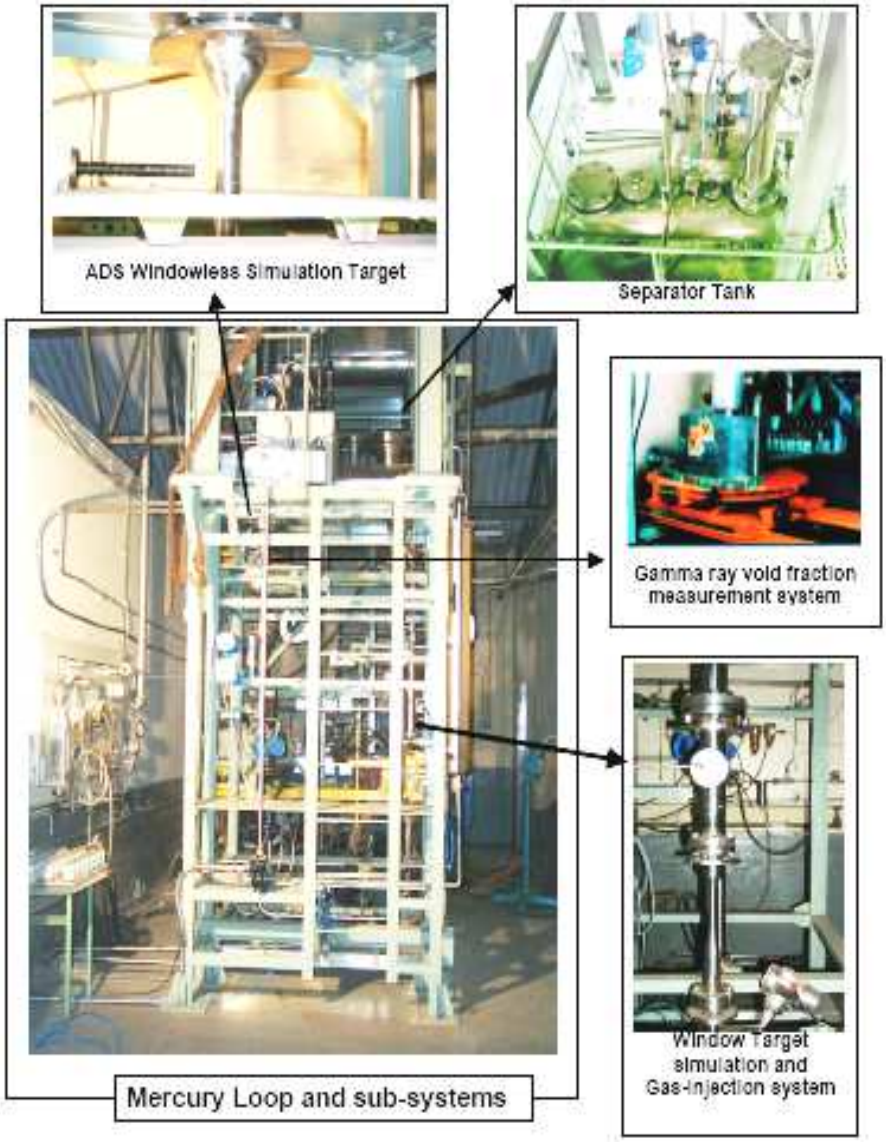


*FIG. 4.17. Mercury loop experimental facility.*

— LBE loop for thermalhydraulics simulation studies

An experimental LBE circulation loop is being set up at BARC to study both thermalhydraulic, and material issues of beam window as well as windowless target concepts. The 3-D layout of the proposed window simulation loop is shown in Fig. 4.18. A major components of the window simulation experimental loop consists of target module simulation region, separator, mechanical pump, heat exchanger, plasma torch and dump tank for LBE storage. The mass flow rate (maximum at 120 kg/s) and the geometry of the loop is ~ 1:1 scale of an actual target corresponding to a target of ~mA of proton beam current. The molten LBE loop will be operated at about $350^0$C.

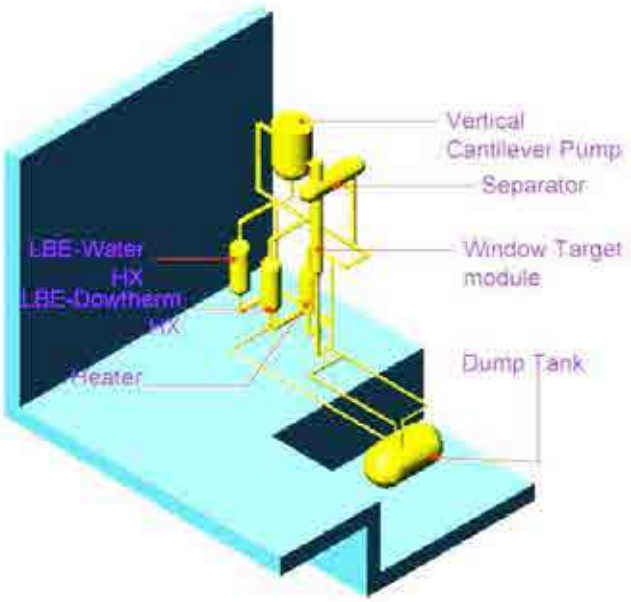


*FIG. 4.18. 3-D layout of the experimental loop being set up at BARC to study target concepts.*

A mechanical pump is used in this loop for obtaining the required flow rate, and a heat exchanger removes the heat deposited in the window. This facility is currently in the mechanical design stage. A plasma torch, with special arrangement to spread the beam, has been developed to simulate thermal loading in the window. This loop will also be used for the development of corrosion mitigation technology consisting of precise control and monitoring system of oxygen in the LBE. The loop will be operated at 4500°C in the second phase to test various loop subsystems for high temperature as required in a typical spallation target.

(b) LBE facility for proton and neutron radiation effects

— LBE Irradiation facility

A LBE loop is designed to study radiation effects on proton beam target and structural materials suitable for LBE systems by exposure to beam of tens of MeV energy and emitted neutrons. These studies would include helium and hydrogen generation, ductile to brittle transition temperature, and swelling, etc. Radioactive issues related to LBE like polonium generation, radioactive gas handling, remote handling of irradiated target module etc would also be addressed in this facility. The loop is likely to be ready for experiments in about 2–3 years time. The height of LBE circulation loop in this facility is ~ 7 m, which would operate at ~220°C with LBE flow rate of maximum ~25 kg/s that would be realized through nitrogen gas injection.

The liquid metal LBE (lead-bismuth eutectic of 45% lead and 55% bismuth, MP 123°C) will be used as target and cooling fluid. The target module (Fig. 4.19) consists of all the subcomponents of an actual spallation target. The low energy (~ tens of MeV) proton beam will simulate the thermal heat loads expected on the beam window like that with 1 GeV proton beam.

Major components of the module are the window, flow region near the window, proton beam pipe, annular riser pipe, separator, mixer (gas injector), downcomer pipe, heat exchanger and dump tank. The dump tank is provided at the bottom of the module, where the LBE is stored when the facility is not operated. Heaters are provided in the tank for melting the LBE. Nitrogen will be used for lifting the LBE in to the loop. Under emergency conditions, the LBE will be dumped in to the dump tank, which is based on gravity. Below the dump tank, a catcher tray will be provided for collecting LBE during any accidental condition.

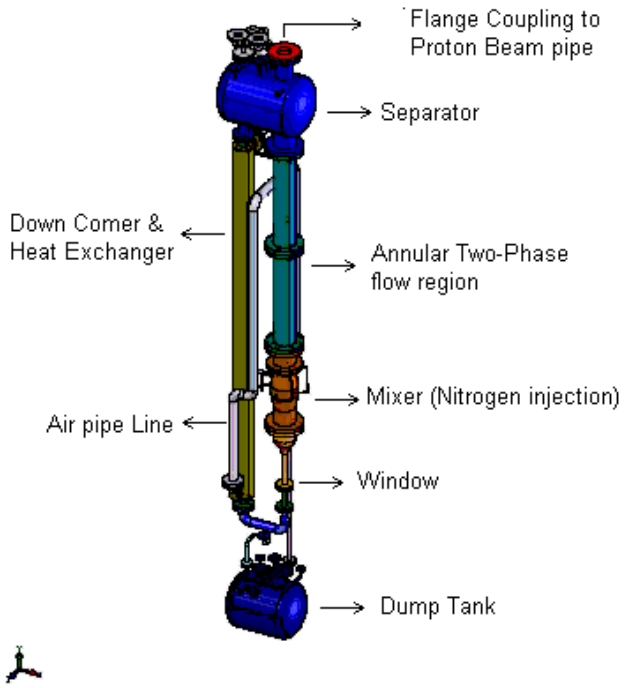


*FIG. 4.19. Gas driven LBE target module for coupling to low energy (tens of MeV and ~ hundreds of μA) proton beam.*

— Experimental plans

The beam window is a very important component of this loop. Typically, it is a hemispherical in shape, having a thickness of ~1.5 mm and 3 mm at the edges. One of the candidate materials that will be tested in this facility is T91 a martensitic type steel. The tens of MeV proton beam has estimated penetration depth of ~ 1mm in the T91 (based on FLUKA and LAHAT code), and almost the entire proton beam energy is deposited in the window.

The window in the target module would be irradiated by the incident proton beam and the liquid metal circulated around the window to extract the heat dissipated in window. Circulation of the liquid metal is achieved in the loop as follows:

- In the mixer, located below the riser pipe, nitrogen–argon gas is injected.
- This gives rise to two phase mixture and consequently to a density difference between the riser and downcomer pipes.
- This causes circulation of liquid metal in the loop. The riser height is designed in such a way that required flow rate of liquid metal is achieved. Both the phases enter the separator located at the top of the loop.
- Gas is separated here and taken to a gas pipeline. The liquid metal flows down through the downcomer pipe. In the middle of the downcomer, the heat exchanger is located which extracts the heat from the liquid metal.
- At the bottom of the downcomer the liquid metal flows through a connecting pipeline between the riser and the downcomer and enters the window flow region again.

(c) Target materials R&D programme

— LBE loops for corrosion studies

Two buoyancy driven LBE loops have been set up in BARC to study corrosion effects of LBE on candidate structural materials for spallation target module; like SS-316 L, 316 LN, SS-304 L, 9Cr-1Mo etc. The larger loops getting ready would be ~ 7 metre high and its riser and downcomer legs would operate at 5500°C and 4500°C respectively. The buoyancy head is estimated to provide a LBE mass flow rate of 1.7kg/s. The flow velocity around the sample is ~0.6 m/s. Material samples exposed in an already operational smaller corrosion loop were being evaluated by Charpy and Tensile tests after exposing the samples for 2000 hours in the flow with oxygen control. Provision is also being made in this loop to enhance the LBE flow by gas injection. Photographs of these operational facilities are shown in Fig. 4.20 and Fig. 4.21.

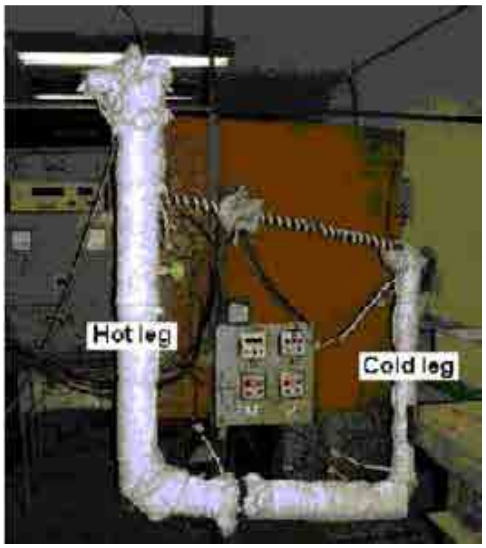


*FIG. 4.20. Prototype LBE thermo buoyancy loop.*


*FIG. 4.21. LBE Corrosion test loop at BARC.*

— *Corrosion mitigation studies*

Proper control of oxygen concentration in the LBE process system is imperative for safe and reliable operation of the spallation target loop. Dissolved oxygen monitoring and control strategies including corrosion mitigation techniques being envisaged for Indian ADS target development programme are outlined below. The major technological know-how that would be developed from these studies included the following:

- Development of zirconia based oxygen monitor.
- Oxygen control system.
- Development of protective coatings.

— Neutron activation analysis of structural materials

To assess the suitability of the available structural materials for manufacturing the mechanical components and support structure of LBE loop, we are presently carrying out neutron irradiation studies on analysis of neutron activation of structural materials like T91, SS304L, SS316L, mild steel, alumina wool, flame guard etc. These experiments are being carried out in BARC on beamlines from the 1 MW experimental reactor APSARA.

### 4.2.4. The CHEOPE, LECOR, LIFUS-5 & CIRCE Facilities in ITALY

#### *4.2.4.1. Purpose and goal*

CHEOPE (CHEmical and OPErational) and LECOR (LEad CORrosion) [4.15],[4.17], located at the ENEA Brasimone Reasearch Centre, Italy, are two facilities aimed at studying corrosion related phenomena in flowing lead and lead-bismuth under different operative conditions.

The main objective of the experiments going on in the two facilities is to study in a quantitative way the compatibility of the reference structural materials with the lead–LBE environment, under different operative conditions such as temperature, velocity of the flowing liquid metal, oxygen concentration.

The facilities are also used for studying technological aspects as impurity control and removal, oxygen measurement and control, thermalhydraulic measurement techniques, etc.

LiFUS 5 is a facility located at the ENEA Brasimone Reasearch Centre, Italy, designed and constructed to simulate LOCA accidents and operate in a wide range of conditions [4.16].

LIFUS 5 is presently operated to analyse the effects of mixing pressurised water (secondary coolant) with Lead-bismuth on the system behaviour in a SGTR scenario. The activity is relevant for XT-ADS design development.

CIRCE is a multipurpose facility, located at the ENEA Brasimone Research Centre, near Bologna (Italy) aimed at investigating the hydraulic, chemical and mechanical issues related to the development of the LBE cooled XADS in a pool configuration [4.18],[4.19].

#### *4.2.4.2. Description of the facilities:*

(a) CHEOPE loop

CHEOPE is a multipurpose facility, consisting of a section for thermalhydraulic experiments, a section for mass transport and chemistry studies and an oxygen control and corrosion section.

For what concerns the part of the facility dedicated to the corrosion tests, named CHEOPE III, it is used to perform corrosion tests at relatively high oxygen content in order to validate the technology of steel protection by in situ oxidation.

Fig. 4.22 shows CHEOPE III loop, which main characteristics are summarized as follows:

- Piping and components: AISI 316;
- Total volume of liquid metal: 50 litres;
- Maximum temperature: 500°C;
- Flow velocity within test section: 0.5–1 m/s;
- Oxygen concentration: $10^{-4}$–$10^{-7}$ wt%

(b) LECOR loop

LECOR (LEad CORrosion) is a non-isothermal, eight shaped forced Lead-bismuth loop, designed in order to perform corrosion tests in HLM. The reference working conditions during the experimental phase in LECOR, which schematic P&I (Fig. 4.23) and its characteristics (Fig. 4.24) are as follows:

- Piping and components: Ferritic and Austenitic (cold part) steels;
- Cold branch temperature: 250–350°C;
- Hot branch temperature (test sections): 350–450°C;
- Number of test sections: 3;
- Liquid metal velocity within test sections: 0.3–0.8 m/s;

— Liquid metal flow rate max.: 4 m3 /h;

— Lead bismuth volume: 0.480 m3;

— Oxygen content: < $10^{-9}$ wt/%

A special care is taken in operating the oxygen control system since the corrosion rate of the materials is a strong function of the oxygen concentration in the molten alloy.

(c) LiFUS 5 Facility

Fig. 4.25 shows a schematic P&I of LIFUS facility that mainly consists (Fig. 4.26) of:

— **a reaction vessel S1** with the water injection device; it is the tank in which the interaction between lead and water takes place. Its volume is 0.1 $m^3$, the design temperature and pressure are 500°C and 200 bar respectively. S1 contains a mock-up of U shaped cooling tubes made by ten tubes of 16.5 mm of external diameter and about 0.7 m in length. Therefore, a cross-section of the tube bundle sector close to the top flange shows twenty tubes with a pitch of 30 mm. This pipe bundle is located in one of the four sectors in which the vessel has been divided by two AISI 316 plates. The two plates are welded on the top flange and develop in the vertical direction up to 5 cm from the bottom of the vessel and in the radial direction up to 0.5 cm from the wall, so that the four sectors are communicating each other. On one side, the introduction of the tube bundle mock-up has been done in order to evaluate if an enhanced mixing between water and the liquid metal may produce relevant interaction effects. On the other side, on the plates and the tube bundle are placed different thermocouples used to detect the temperature and the shape evolution of the interaction zone. The upper flange has four connections to the Al 10 lines joining the reaction vessel S1 to the expansion vessel S5 and designed to simulate pressure drop in the liquid metal circuit. The reaction vessel wall is fitted with several nozzles for the insertion of the pressure transducers and some other thermocouples. All parts of the vessel are traced with heating cables and thermally insulated.

— **a pressurised water vessel S2**; It consists of a cylindrical tube with two flat heads. The shell is fitted with two socket thermocouples and a pressure transducer. Its design temperature and pressure are 350°C and 200 bar. It is electrically traced and thermally insulated. During the test the pressure in S2 is kept fixed by connecting directly this vessel to an Ar bottle charged at the test pressure.

— **a dump tank S3**, that is the safety vessel which allows to collect the gaseous and aerosol interaction products from S1 at the end of the test. If during the test the pressurization of the system exceeds 190 bar, the rupture disk D1 opens allowing to discharge the steam from S1–S5 to S3, decreasing pressure. Its volume is about 2 $m^3$ and the design pressure is 10 bar.

— **a storage tank S4** for melting the liquid metal and filling the reaction vessel S1and the expansion vessel S5. It contains an electromechanical pump for the filling procedure.

— **an expansion vessel S5** connected to the reaction vessel through four expansion tubes, one per sector. Depending on its filling level, the compressibility of the whole volume can be varied. S5 can be leaved completely in gas phase maintaining the liquid metal free level in S1 or can be completely disconnected from S1 and the other components of the plant.

The main qualified sensors of the facility are pressure transducers and thermocouples having quick response.

— Eight fast pressure transducers can be placed in different points of S1 and S5 vessel walls or in the water pipe before its entry in S1, depending on the system configuration chosen for the test.

— n. 8 K-type quick response thermocouples are placed into the tube bundle sector of S1 and fixed on the tubes at different height. Different socket thermocouples with a low response time can be also placed in S1 and S5.

— The water level in S2 is measured by a differential pressure transducer supplied by DRUCK company.

— Two meters are placed in S1 and S5 to measure the liquid metal level.

— Different design possibilities, depending on the water pressure chosen for the experiment, exist for the water injection device that is immersed in the liquid metal during the test phase. The water orifice can be protected by a cap, made by aluminium or brass and turned on a lathe along its circumference (different rupture pressures as a function of its radial thickness can be obtained), or by a suitable rupture disk. The orifice is placed on the top of a stainless steel tube that constitute the body of the water injection device. The water injection device is placed on the bottom of S1 in the sector containing the tube bank. Its penetration in the vessel can be varied.

— Only metal bellow sealed globe valves have been adopted in the facility, supplied by DESCOTE company. All valves are provided with pneumatic diaphragm actuator.

(d) CIRCE Facility

In Fig. 4.27 an isometric view shows P&ID of the facility. The facility can be considered as composed by two parts: the LBE containment and the auxiliary systems. Regarding the first part, the main components are the vessel S100 with a height of 8 500 mm and a diameter of 1200°mm, the storage tank S200 and the intermediate vessel S300, used during the handling of the LBE between the two other vessels. During the load operations of the facility, the LBE is gradually transferred from the storage tank to the S300 vessel. Then, by the pressurization of the S300 cover gas the liquid metal is gradually moved to the vessel S100.

The main vessel S100 is equipped with electrical heating cables, installed on its bottom and around its cylindrical surface. This heating system allows operation in the temperature range of 200–400°C. The main vessel houses different designs of test sections.

A sketch of the test section used to carry out the gas enhanced circulation tests is shown in Fig. 4.27. It consists of different components described in the following.

— Riser: it consists of only one pipe (diameter = 202.7 mm, height = 3854 mm) of the 22 pipes that form the reference XADS plant riser. Since this element is scaled 1:1, the flow mapping achievable by tests will be easily applicable to the full scale reference plant. Inside the riser the gas injection pipe is housed, ending with the injector; therefore, the influence of the liquid temperature on the expansion that the argon undergoes when injected into the bottom of the riser is unimportant, since the gas can be considered as already being at the same temperature of the LBE when injected.

— Dead volume: delimited by the test section support ferrule, it maintains the real height of the full scale dead volume, whereas the cross-section is scaled 1:22. At present the dead volume does not take active place in the test run; it is filled with argon and directly connected to the cover gas, in thermal equilibrium with it. In the future tests, the dead volume will be filled with liquid metal and connected to the flow path in order to study the coupled behaviour between the LBE stream and a stagnant region.

— Fitting volume: it consists of a cylindrical volume delimited by two circular plates (diameter = 982 mm), 225 mm spaced. It joints the feeding conduit to the riser. This element is designed and scaled to represent the upper plenum of the core, fitting the core outlet to the riser inlet.

— Feeding conduit: it is the lower part of the test section, immersed in the lower plenum of S100; a Venturi Nozzle flowmeter is installed on the conduit, as well as a drilled disc, downstream the flowmeter. The hole manufactured on this disc was calculated to provide a pressure loss suitable to simulate the one relevant to the full scale core, as defined in the ANSALDO XADS concept [4.20].

— Downcomer: is the outer side of the test section, interested by the descending path of the LBE during the test. It is scaled to represent 1/17 of the full scale downcomer, so it is characterized by a cross-section of around 0.7 $m^2$.

The test section is equipped by all the instrumentation suitable for performing all the required measurements, like thermocouples (accuracy 2%), differential pressure meters (accuracy 2%) and level meters (accuracy 2%). Bubble tubes have been installed on the test section to transfer pressure signals from the LBE to differential pressure cells operating with gas at room temperature. In particular, the LMS and the DPMS make use of the above instruments to perform their tasks. Both the DMPS and LMS, as well as the flowmeter, have been qualified and calibrated during dedicated experimental campaigns [4.21] [4.22].

*FIG. 4.22. The CHEOPE III loop.*

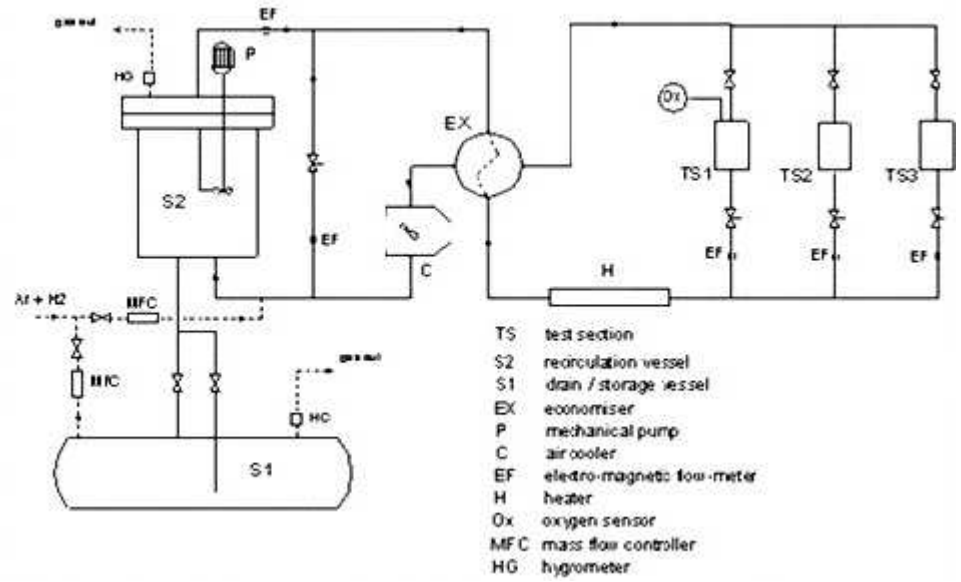


*FIG. 4.23. P&I of LECOR loop.*

*FIG. 4.24. The LECOR loop.*

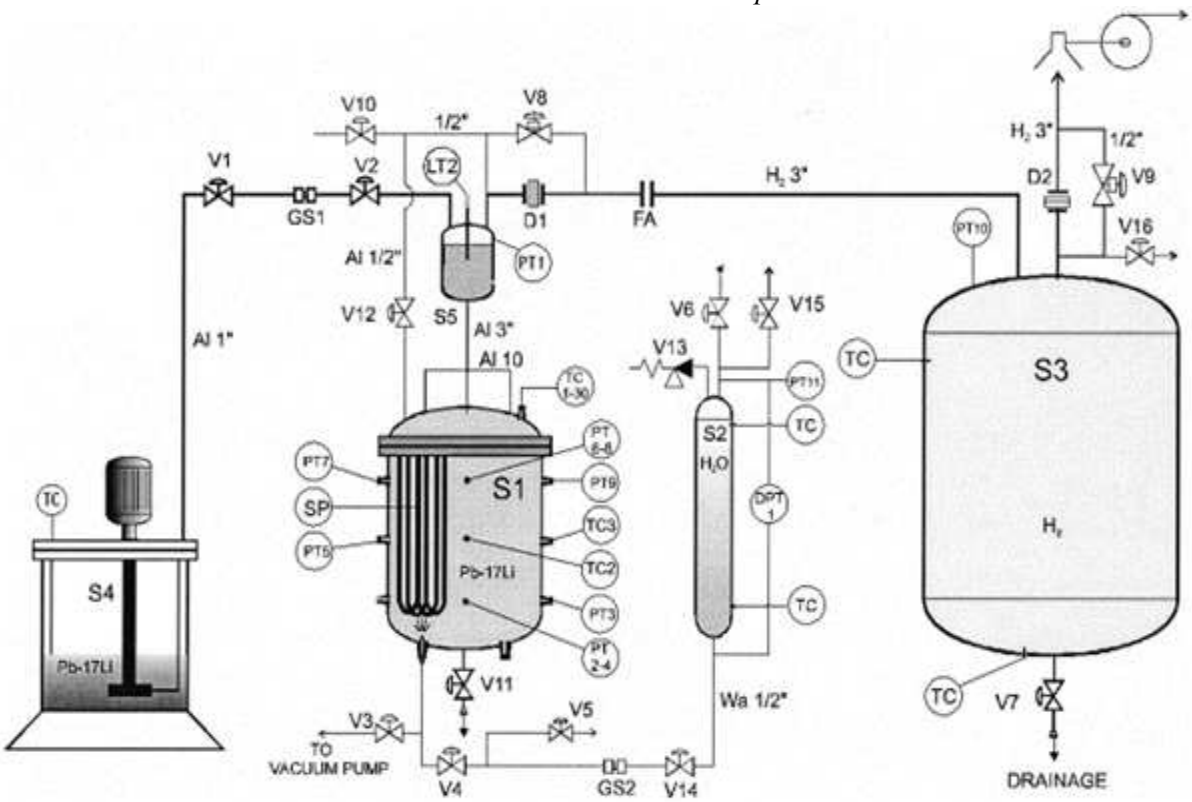


*FIG. 4.25. P&I of LiFUS 5 facility.*

*FIG. 4.26. LiFUS 5 facility.*

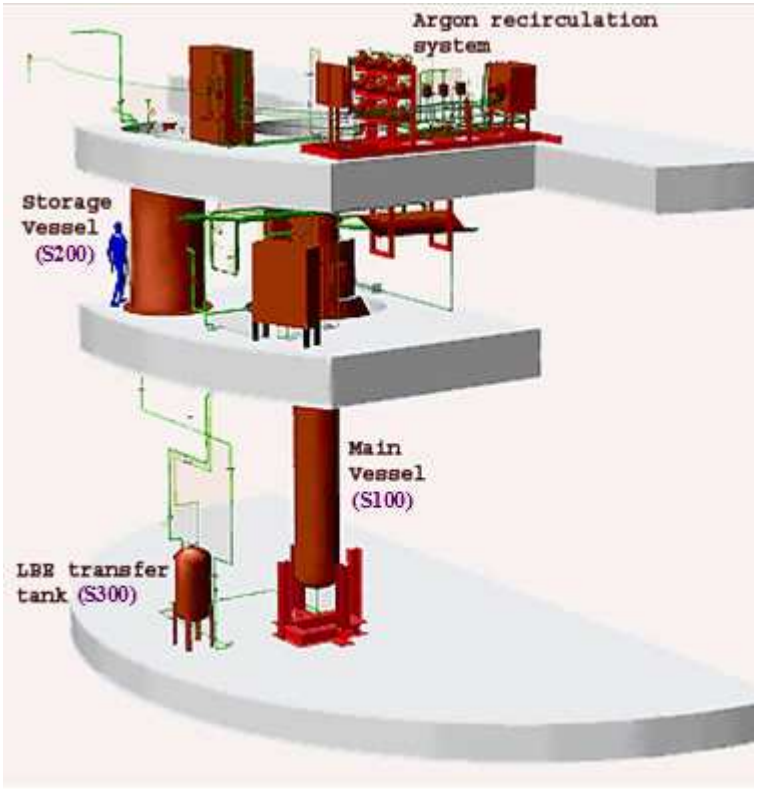


*FIG. 4.27. View of the CIRCE facility.*

*FIG. 4.28. View of the CIRCE facility.*

### 4.2.5. Existing experimental facilities in Japan

#### *4.2.5.1. Purpose and goal*

To examine the feasibility and applicability of the Lead-bismuth eutectic to accelerator driven transmutation systems, JAEA has one static corrosion experimental equipment and three experimental Lead-bismuth loops for corrosion–erosion examination, measurement device development and thermalhydraulic experiments around beam window [4.23].

#### *4.2.5.2. Description of the facility*

— JAEA Lead-bismuth static corrosion facility (JLBS)

The JLBS facility consists of four quartz pots, heaters and two oxygen control systems for corrosion tests of various materials. Ar-$H_2$-$H_2O$ or Ar-$O_2$ gas mixtures are used for oxygen control in LBE. The YSZ oxygen sensor with the Pt-air reference system has been mainly used to measure oxygen concentrations in LBE. The main operational parameters are as follows:

- Maximum temperature: 600°C;
- Number of pots: 4;
- Number of test pieces: 10/pot;
- Diameter of pot: 100 mm;

- Heavy metal weight: 7 kg/pot;
- OCS: Yes (partially);
- Heavy liquid metal: Pb-Bi.

The experiments carried out in the JLBS are dedicated to investigate mainly:

- Corrosion of materials for ADS components under static condition;
- Screening tests of materials for ADS components;
- Corrosion mechanism of various materials in Pb-Bi;
- Corrosion of surface treated materials;
- Effect of alloying elements and stress on corrosion in Pb-Bi;
- Effect of impurities in Pb-Bi.

— JAEA Lead-bismuth flow loop (JLBL-1)

The JLBS facility (Fig. 4.29) consists of two test sections, heaters, an air cooler, an electromagnetic pump, an electromagnetic flowmeter, a surge tank, a storage tank and three filters. The main operational parameters are as follows:

- Maximum temperature: 450°C;
- Maximum pressure: 5 bar;
- Maximum flow rate: 18 L/min;
- Maximum electrical power: 15 kW heaters;
- Number of test sections: 2;
- Oxygen control system (OCS): Yes;
- Heavy liquid metal: Pb-Bi;

The experiments carried out in the JLBL-1 are dedicated to investigate mainly:

- Corrosion study of ADS components in flowing Pb-Bi;
- Development of Pb-Bi flow control;
- Material corrosion proof test for ADS target test facility at JAEA.

— JAEA Lead-bismuth flow loop (JLBL-2)

The JLBL-2 is designed as a closed loop having double coaxial channels with hemispherical beam window. The facility consists of heaters, an electromagnetic pump, an electromagnetic flowmeter and a storage tank. The main operational parameters are as follows:

- Maximum temperature: <200°C;
- Maximum pressure: 2 bar;
- Maximum flow rate: 50 L/min;
- Maximum electrical power: 5 kW heaters;
- Oxygen control system (OCS): No;
- Heavy liquid metal: Pb-Bi;

The experiments carried out in the JLBL-2 are dedicated to investigate mainly:

- Flow study in horizontal Pb-Bi target including impinging jet flow at target head.

- Proof test of sealed annular tube type spallation target.
- Development of velocity measurement system for Pb-Biflow.

— JAEA Lead-bismuth flow loop-3 (JLBL-3)

The JLBL-3 facility consists of a test section with a beam window mock-up, heaters, an air cooler, a mechanical pump, an electromagnetic flowmeter, a calibration tank, a storage tank and a filter. The main operational parameters are as follows:

- Maximum temperature: 450°C;
- Maximum pressure: 7 bar;
- Maximum flow rate: 500 L/min;
- Maximum electrical power: 41 kW heaters (beam window mock-up: 6 kW);
- Number of test sections: 1;
- OCS;
- Heavy liquid metal: Pb-Bi;
- Total inventory: 450 litres;

The experiments carried out in the JLBL-3 are dedicated to investigate mainly:

- Thermal fluid test of beam window;
- Proof test of mechanical pump and massive Pb-Bi flow.

*FIG. 4.29. JLBL-1 loop.*

### 4.2.6. The Experimental facility KPAL-I in Korea

#### *4.2.6.1. Purpose and goal*

KAERI has been developing an ADS. The accelerator driven transmutation system developed by KAERI is called HYPER (HYbrid Power Extraction Reactor) [4.24]. Pb-Bi is adopted as the coolant target for HYPER. Most serious problem in using lead alloy is a corrosion of the steel structure materials in contact with the high temperature lead alloy. Therefore, it is requied to investigate the

corrosion behaviour of the structure materials such as HT-9, T91 and 316L at a high temperature. It is also need to find the methods to prevent corrosion if it is too severe. KAERI constructed a Pb-Bi corrosion test loop. The loop is named KPAL-I (KAERI Pb–Alloy Loop I) [4.25].

### *4.2.6.2. Description of the facility*

Fig. 4.30 shows the Pb-Bi corrosion loop which was installed at KAERI. The LBE loop is an isothermal loop. The flow velocity in the test section was designed to be around 2 m/s and the charging volume of the LBE is around 0.03 $m^3$. The temperature can be up to 600°C. The LBE loop is mainly composed of a main test loop, bypass loop for filtering LBE and a gas supplying system. The liquid metal in the main test loop circulates in the following order: EMP (Electromagnetic Pump), EM flowmeter, oxygen controller, test section, magnetic filter, EM pump. Major specifications of the KAERI's loop are summarized in Table 4.11. The oxygen concentration is controlled by the chemical equilibrium between the mixture gas of hydrogen–argon and the water vapour. The oxygen concentration in the LBE and mixture gas is measured with an oxygen sensor made of a Yttria Stabilized Zirconia. Test samples are installed in the test section with an annular cross-section. In order to treat the test samples in a regulated oxygen environment, the upper part of the test section is installed inside the glovebox. The KPAL-I was constructed and operated to perform the following experiments:

- Corrosion tests of ADS structure materials and fuel cladding materials;
- Development of oxygen control technology inside Pb-Bi;
- Test of oxygen sensors;
- Development and test of flowmeters;
- Study of corrosion products and their transport mechanism.

TABLE 4.11. MAJOR SPECIFICATION OF KPAL-I

| Parameters | |
|---|---|
| Temperature | Max. 600°C |
| Pb-Bi volume | 0.08$m^3$ |
| Test section | 3/4 inch SUS 316, $V_{mean}$=2m/s (at 45*lpm*) |
| Piping system | 1.5inch-Schedule 40, SUS316 pipe |
| Flow measurement | EM flowmeters |
| Pumping | EM-pump (60lpm-4bar-40kVA) |
| Oxygen control | $H_2$-$H_2O$ |
| Purification | Magnetic filter, mechanical filter |

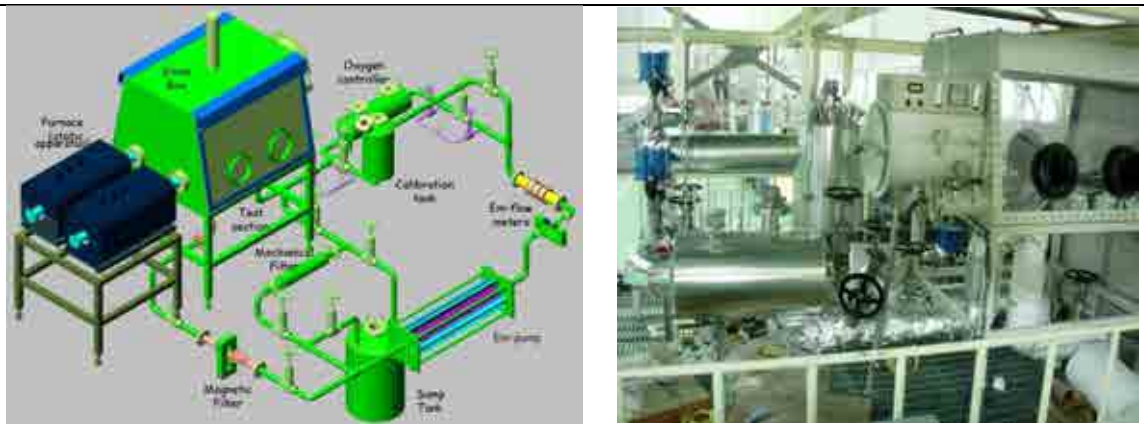


*FIG. 4.30. The Pb-Biloop KPAL-I.*

### 4.2.7. Experimental facilities with HLMC in Russian Federation

#### *4.2.7.1. Purpose and goal*

— Experimental facilities in IPPE

The significant experimental base on researches of HLM is concentrated in the IPPE (Obninsk). Researches were mainly carried out in substantiation of Lead-bismuth coolant (LBC). The wide spectrum of researches on various aspects of thermalhydraulics, coolant technology, problems of mass transfer and corrosion has been executed. Last years the certain researches with reference to lead coolant were executed.

— ILC in BOR-60 reactor

To justify the design features of fuel elements and fuel assemblies of the BREST-OD-300 reactor as regards the combined effect of lead coolant, radiation and temperature loads on fuel cladding and spacing grids, an experimental loop with lead coolant, so called independent lead cooled channel (ILC) was installed in sodium cooled fast reactor BOR-60 located in RIAR [4.26].

#### *4.2.7.2. Description of the facility*

— Experimental facilities in IPPE

The list of experimental facilities located in the IPPE and their basic parameters and directions of researches which are carried out on these facilities, is presented in Table 4.12.

— ILC in BOR-60 reactor

The channel components and a scheme of coolant flow are shown in Fig. 4.31, the main characteristics and parameters of the ILC are summarized in

TABLE 4.13.

The lead coolant circulation is arranged in accordance with Field's scheme and is provided by means of an axial centrifugal pump with motor speed being controlled by varying of frequency. To supply coolant to the sensing elements of ORS, the bypass pipes are used to arrange the auxiliary circulation circuit. A bubble tube for gas mixture supply is installed below the level of lead in order to maintain required thermodynamic reactivity of oxygen in the coolant and detect fuel cladding failure.

After implementation of prior to irradiation tests of the ILC, in 2002 a series of in-pile experiments of the ILC was carried out in BOR-60 reactor.Maximum values of the parameters obtained during the ILC tests are summarized in Table 4.14.

TABLE 4.12. EXPERIMENTAL FACILITIES WITH PB-BIAND PB COOLANTS IN IPPE

| No | Facility | Field of studies | Coolant | Temperature, °C | Coolant flow rate, $m^3/h$ |
|---|---|---|---|---|---|
| 1 | SVT-3M | Thermalhydraulics technology | Pb-Bi | 160–450 | 20 |
| 2 | SS-1 | Technology | Pb | 370–550 | 1.0 |
| 3 | TT-1M | Technology corrosion | Pb-Bi | 240–600 | 6.5 |
| 4 | TT-2M | Technology mass transfer | Pb-Bi | 250–550 | 5 |
| 5 | SM-1 | Corrosion mass transfer | Pb-Bi | 270–650 | 5 |
| 6 | SM-2 | Corrosion mass transfer | Pb | 350–650 | 2.5 |
| 7 | TsU-1 | Corrosion mass transfer | Pb | 350–620 | 5 |
| 8 | TsU-2M | Corrosionmass transfer | Pb-Bi | 270–650 | 2 |
| 9 | Sprut | Thermalhydraulics technology | Pb-Bi | 150–500 | 5.0 |
| 10 | FTM | Thermalhydraulics | Pb, Pb-Bi | 270–600 | 18 |

TABLE 4.13. THE MAIN DESIGN CHARACTERISTICS AND PARAMETERS OF THE ILC

| Parameter | Units | Value |
|---|---|---|
| Number of fuel elements | --- | 4 |
| Length of fuel containing part | m | 0.45 |
| Diameter of fuel cladding | mm | 9.4 |
| Relative pitch of fuel elements | --- | 1.25 |
| Power | kW | 53 |
| Linear heat rate | kW/m | 33.4 |
| Pump type | --- | axial centrifugal |
| Coolant | --- | C-00 lead |
| Coolant flow rate | $m^3/h$ | 1.3 |
| Pump head | MPa | 0.25 |
| Lead velocity among fuel elements | m/s | 1.1 |
| Lead temperature at core inlet/outlet | °C | 490/570 |
| Sodium flow rate | $m^3/h$ | 1.9 |
| Sodium temperature at channel inlet/outlet | °C | 330/420 |

TABLE 4.14. MAIN ACHIEVED PARAMETERS OF THE ILC

| Parameter | Units | Value |
|---|---|---|
| Fuel assembly (FA) power | kW | 43.4 |
| Coolant temperature at FA inlet | °C | 615 |
| Coolant temperature at pump and ORS inlets | °C | 540 |
| Design temperature on fuel element surface | °C | 645 |
| Damage inducing dose | dpa | 6.5 |
| Fuel burnup | % ha | 0.44 |

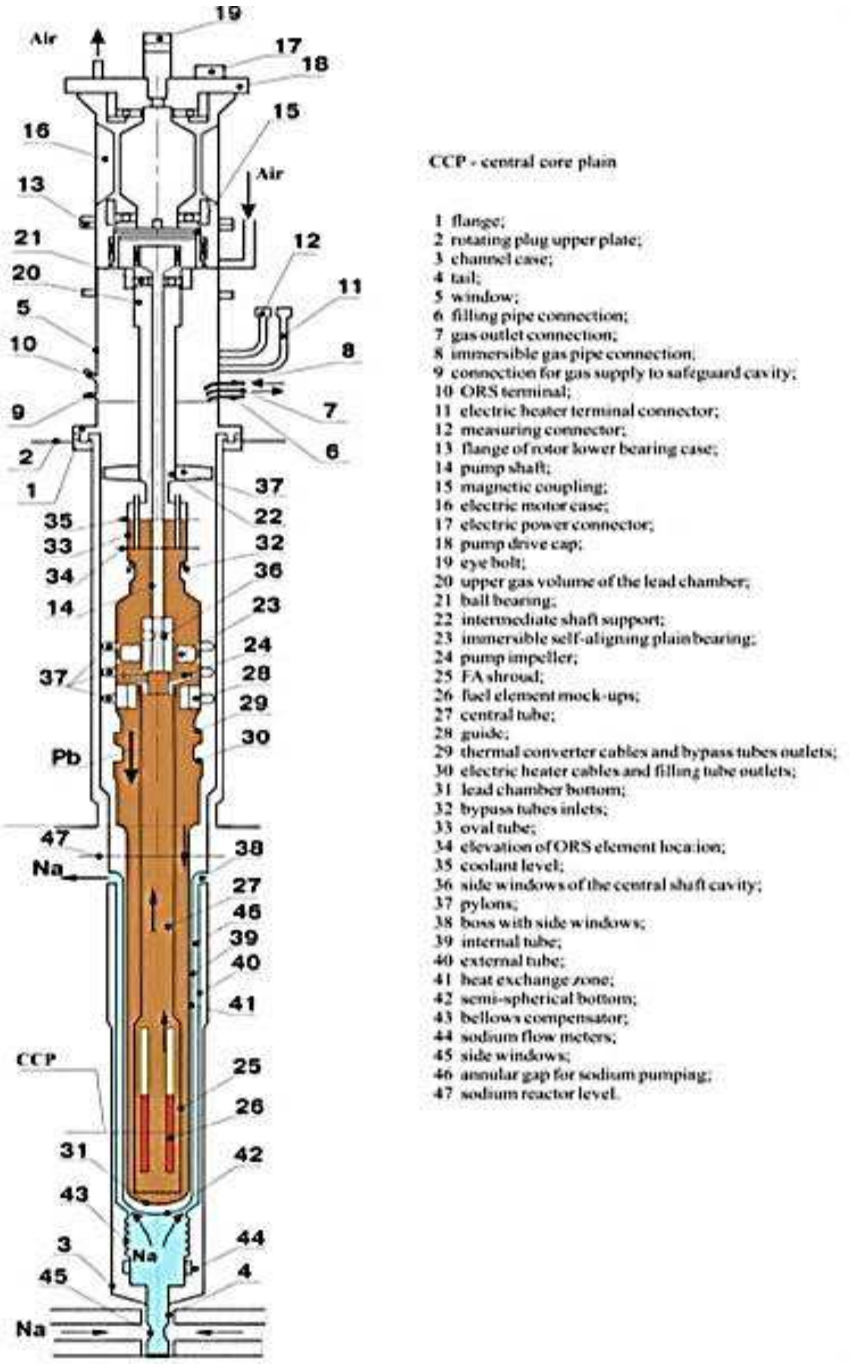


*FIG. 4.31. Scheme of the ILC.*

### 4.2.8. Corrosion behaviour of stainless steels in flowing lead-bismuth eutectic: the LINCE loop (Spain)

#### *4.2.8.1. Purpose and goal*

LINCE is an experimental facility, designed and built by CIEMAT to carry out corrosion studies of structural steels in contact with lead bismuth eutectic under non-isothermal conditions. LINCE is a forced convection loop with the following dimensions: 11 m length, 4 m width and 5 m height. It is supported on a metallic structure. The main objectives of LINCE operation are:

— Study of the long term corrosion behaviour of materials in liquid Lead-bismuth eutectic;

— Study of the oxygen control systems in flowing liquid lead-bismuth eutectic.

*4.2.8.2. Description of the facility*

Fig. 4.32 and Fig. 4.33 show a scheme of LINCE loop. It is composed of a vertical centrifugal pump (A), an exchange heater (B), a storage tank (C), a refrigerator (D), a heater (E), and two tests areas (cold (F) and hot (G)) and tubing to connect the previous components. The volume of LBE is 300 litres (3 Tm) and the flow rate approximately 1 m/s. The maximum temperature is 450°C and the minimum 300ºC, which means a temperature gradient of 150°C, and it is controlled by 25 temperature regulators. The electrical power is 80 kW. An OCS has been implemented in the loop. The oxygen activity in the loop is directly measured using oxygen sensors implemented in both test sections.

LINCE includes two test sections, hot and cold, with the possibility of by passing (Fig.4.35).These test sections are two vertical tubes with an inner diameter of 25 mm and 500 mm length. The samples are piled up in the test section and separated from each other. Threaded rods fix the specimens on the top of each test section.

The oxygen concentration in the range of 10–8wt% ~ 10–6 wt% is controlled by the chemical equilibrium between the mixture gas of hydrogen–argon and the water vapour. At present, the oxygen concentration in the LBE and the mixture gas is measured with an oxygen sensor made of Yttria Stabilised Zirconia as a solid electrolyte cell (Fig. 4.35). These oxygen sensors are placed at the entrance and exit of each the vertical tube of test sections. In Fig. 4.36 is shown the time evolution of temperatures in the hot and cold area, while Fig. 4.38 shows metallographic cross-section of T91 and 316L specimen tested in LINCE loop.

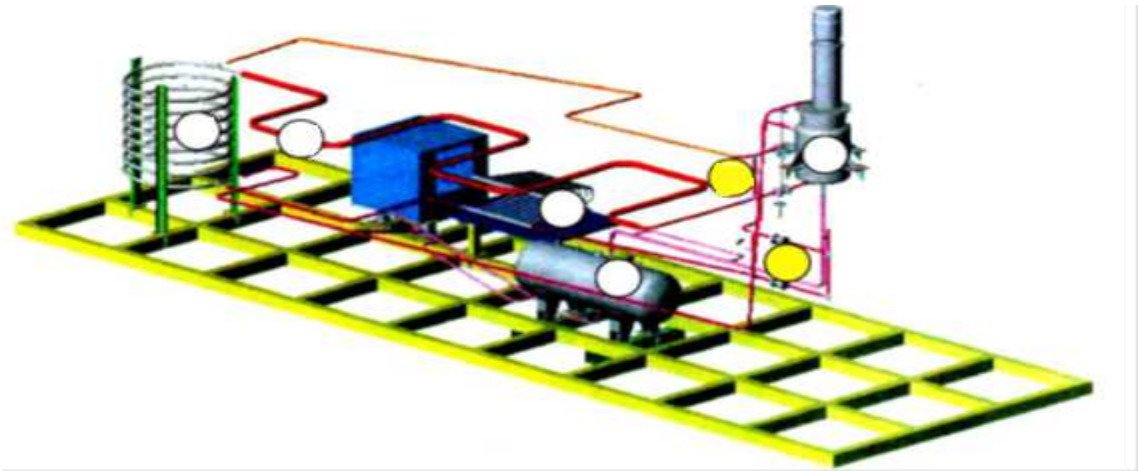

*FIG. 4.32. Scheme of LINCE loop.*

*FIG. 4.33. Photo of LINCE loop.*

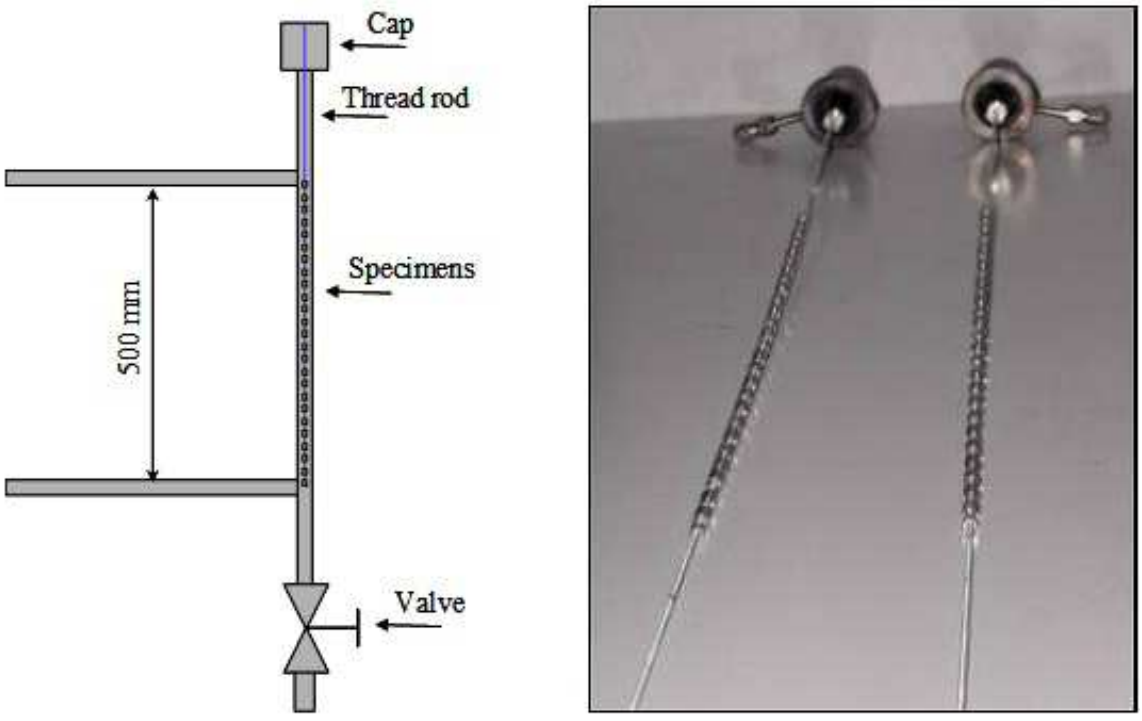


*FIG. 4.34. Scheme of the test section and photo of the corrosion specimens before the tests.*

*FIG. 4.35. Photo of oxygen sensor.*

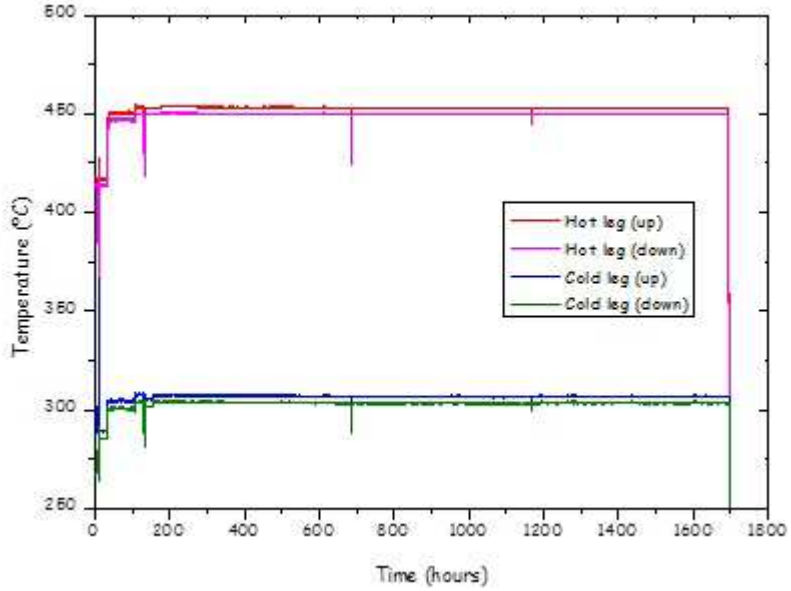


*FIG. 4.36. Evolution of temperatures in hot and cold area with time.*

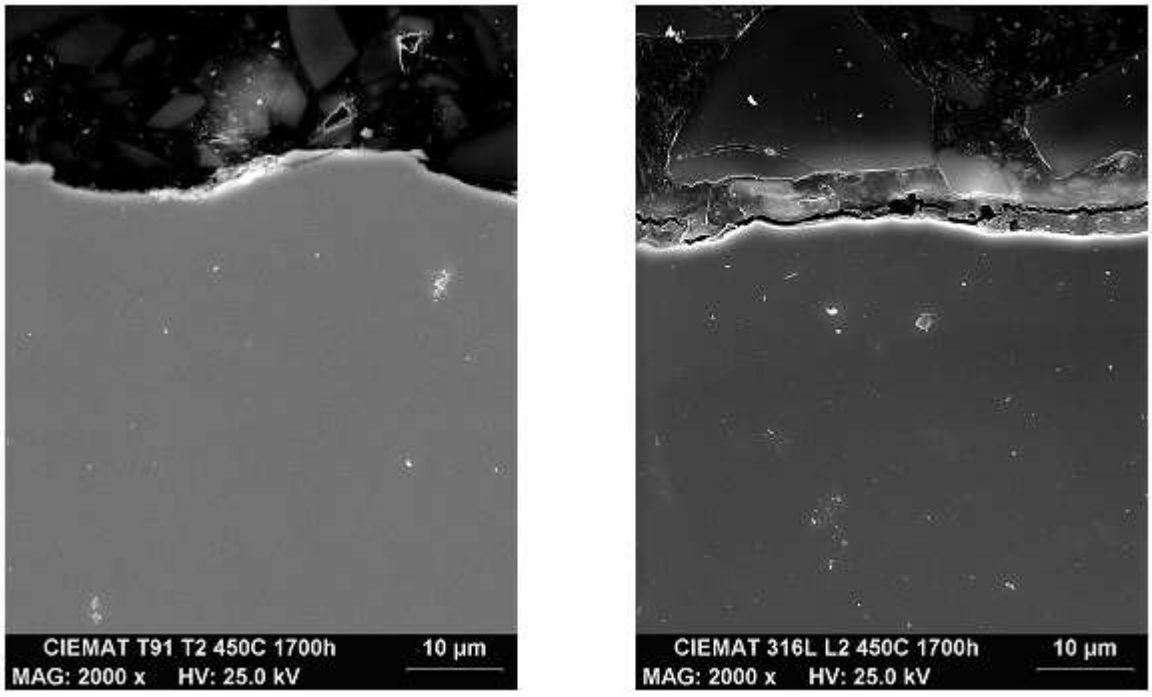


*FIG. 4.37. Metallographic cross-section of T91 and 316L specimen tested in LINCE loop, 450ºC from 1700 h.*

## 4.3. ACCELERATOR

Worldwide, there is at present a considerable experience accumulated that fulfill a primary requirement for an 'ADS class' accelerator, i.e. the ability to deliver beam powers at the multi MW level for proton beams energies of about 1 GeV. These accelerators have been called 'HPPA' for high power proton accelerators. A wealth of information can be found in dedicated conference proceedings organized by OECD-NEA [4.27] and other references quoted therein. For example, the new neutron spallation sources in Japan and the US, J-PARC [4.28] and SNS use the most modern HPPA.

In the subsequent sections there is reported the work that is ongoing in those countries or regions that have at present ADS specific accelerator developments under way. Namely, there have been collected contributions from China, Japan, India and Europe. Indeed, an accelerator suited to drive a subcritical reactor should not only be a generic HPPA, but need to fulfill rather unique and specific requirements with respects to reliability, operability and safety that shall be discussed below. These features demand for the focused and coordinated R&D programmes that shall be presented.

### 4.3.1. Status in China

#### *4.3.1.1. Accelerator specifications and associated R&D*

A basic research programme of ADS was launched in 2000 under the support of the Ministry of Science and Technology, China. In this programme some key technologies are studied for an intense beam proton LINAC, including construction of an ECR proton source and a pulsed beam RFQ accelerator. Further, Chinese Academy of Sciences also gave a support to LINAC research in the field of medium-β superconducting cavity.

#### *4.3.1.2. Accelerator components built in China and most important results*

An ECR proton source and LEBT have been built at CIAE as the injector of the RFQ. Fig. 4.38 shows the source and Table 4.15 its main performance parameters. Great efforts were made on the reliability and stability of the source operation. Problems associated with the breakdown of the RF input ceramic window resulting from electron back strike were successfully overcome. The electrodes have been optimized for minimum spark rate. At present a high reliability of 99.9% is achieved during a 120 hours continuous operation.

The main parameters of the RFQ are listed in Table 4.16. It is separated into two segments and each segment consists of two modules. On each module there are 16 tuners distributed on the 4 quadrants for frequency and field tuning. Dipole stabilizer rods on both the end plates and the coupling plate are applied. There are 20 cooling channels on the cavity body in each module. Four vane wall pieces are brazed to form a cavity for both RF and vacuum seals. This RFQ was fabricated in China and the cavity braze is very successful. Fig. 4.39 shows the installed RFQ before the connection of the cooling water ducts. Owing to the kind support from CERN, a set of RF power source of 352 MHz has been set up at IHEP for the RFQ accelerator. In the recent beam commissioning the RFQ output a pulsed proton beam of 43mA at 50 Hz repetition rate and 1.4ms pulse length. The measured beam transmission rate is larger than 92%. As the RFQ was designed for CW operation and the RF power source is also a CW, it is foreseen to upgrade the water cooling system and thus push forward to a high duty factor.

*FIG. 4.38. The ECR source and part of LEBT.*

TABLE 4.15. ECR PROTON SOURCE PARAMETERS

| Parameter | Units | Values |
|---|---|---|
| E | keV | 75 |
| I | mA | 70 |
| $f_{RF}$ | GHz | 2.45 |
| $P_{RF}$ | kw | 1 |
| $E_{n,rms}$ | πmm–mrad | 0.13 |
| $H^+$ Ratio | % | 80 |
| Raliability | % | 99 |

*FIG. 4.39. RFQ installed (prior to cooling connection).*

TABLE 4.16. RFQ MAIN PARAMETERS

| Parameter | Units | Value |
|---|---|---|
| Input energy | keV | 75 |
| Output energy | MeV | 3.5 |
| Peak current | mA | 50 |
| Structure type | --- | 4 vane |
| Duty factor | % | 6 |
| RF Frequency | MHz | 352.2 |
| Maximum $E_s$ | MV/m | 33 |
| Beam power | kW | 190 |
| Structure power | kW | 420 |
| Total power | kW | 610 |
| Total length | m | 4.75 |

The technology of superconducting RF cavities has been studied for the medium energy section of a 1 GeV proton LINAC for ADS. A superconducting single ellipsoid cell (1.3 GHz, β=0.45) was manufactured in China (Fig. 4.40). The measured $Q_0$ versus $E_{sp}$ is plotted in Fig. 4.41 (before electropolishing). An RF superconducting laboratory has been built at IHEP, Beijing for the RF cell processing and measurement. A cryostat for 1.3 GHz and 700 MHz cavity has been built for vertical measurement at the working temperature of 1.5~4.2K.

*FIG. 4.40. 1.3 GHZ, β= 0.45 single cells.*

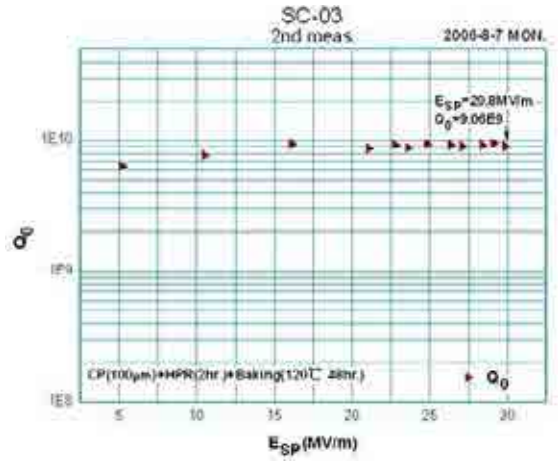


*FIG. 4.41. Measured Q0 with designed Esp/Eacc=5.13.*

### 4.3.2. Status in Europe

#### *4.3.2.1. The EUROTRANS research programme and its accelerator specifications*

The EUROpean research programme for the TRANSmutation of high level radioactive waste in accelerator driven systems (EUROTRANS) is funded by the European Commission within the 6th Framework Programme, and involves 31 partners (research agencies and nuclear industries) with the contribution of 16 universities [4.32]. EUROTRANS is a 4-year programme (2005–2009) extending previous activities (PDS-XADS, Preliminary Design Study for an eXperimental Accelerator Driven System) and paving the road towards the construction, during the next EC framework programmes, of an eXperimental facility demonstrating the technical feasibility of Transmutation in an Accelerator Driven System (XT-ADS).

Within the EUROTRANS programme, the activities are split into five main technical areas (called Domains), respectively devoted to: the design of the ADS system and its subcomponents; small scale experiments on the coupling of an accelerator, a spallation target and a subcritical core; studies on advanced fuels for transmuters; investigations on suited structural materials and heavy liquid metal technology; collection of nuclear data for transmutation. The main objective is to work towards a European Transmutation Demonstration (ETD) in a stepwise manner, i.e.:

— Provide an advanced design of all the components of an XT-ADS system, in order to allow its realisation in a short term view (~10 years);

— Provide a generic conceptual design of modular European Facility for Industrial Transmutation (EFIT) for the long term objective of the programme.

The XT-ADS machine that will be loaded with conventional MOX fuel is meant to be built and tested in the near future (before 2020 following the planning at the time of the EUROTRANS project) so as to fulfil three main objectives:

— Demonstrate the ADS concept (coupling of proton accelerator, spallation target and subcritical assembly) at significant but reasonable core power levels (50–100 MWth);

— Demonstrate the transmutation using some dedicated positions able to accept minor actinides assemblies;

— Provide a multi purpose irradiation facility for the neutron community in general, and for the testing of different EFIT components in particular (samples, fuel pins…).

The EFIT facility will be an industrial scale transmutation demonstrator system, loaded with transmutation dedicated fuel. Its characteristics are meant to maximize the efficiency of transmutation, the easiness of operation and maintenance, and the high level of availability in order to achieve an economical transmutation.

TABLE 4.17: BASELINE CHARACTERISTICS OF THE XT-ADS AND EFIT MACHINES

| | XT-ADS (ADS Prototype) | EFIT (Industrial Transmuter) |
|---|---|---|
| GOALS | Demonstrate the concept | Maximise the transmutation efficiency |
| | Demonstrate the transmutation | Easiness of operation & maintenance |
| | Provide an irradiation facility | High level of availability |
| MAIN FEATURES | 50–100 MWth power | Several 100 MWth power |
| | $k_{eff}$ around 0.95 | $k_{eff}$ around 0.97 |
| | 600 MeV, 2.5 mA proton beam (backup: 350 MeV, 5 mA) | 800 MeV, 20 mA proton beam |
| | Conventional MOX fuel | Minor actinide fuel |
| | lead-bismuth eutectic coolant & target | lead coolant & target (backup: gaz) |

Despite these sometimes contradictory objectives, the XT-ADS and the EFIT machines share the same fundamental system features. Especially, both designs use: (Table 4.17)

— Superconducting linac solution to produce the required high power proton beam; the main reasons for this choice are the power upgrading capability of this solution, and the perspectives of improvement of the beam reliability;

— Liquid metal core coolant and spallation target; the metal is pure lead for the EFIT design, and lead-bismuth Eutectic (LBE) for the XT-ADS, allowing lower working temperatures.

#### *4.3.2.2. The reliability oriented reference accelerator*

The European Transmutation Demonstration requires a high power proton accelerator operating in CW mode, ranging from 1.5 MW (XT-ADS operation) up to 16 MW (EFIT). The main beam specifications are shown in Table 4.18. At first glance, the extremely high reliability requirement (beam trip number) can immediately be identified as the main technological challenge to achieve.

TABLE 4.18. XT-ADS & EFIT PROTON BEAM ORIGINAL SPECIFICATIONS

| | XT-ADS | EFIT |
|---|---|---|
| Max. beam intensity | 2.5–4 mA | 20 mA |
| Proton energy | 600 MeV | 800 MeV |
| Beam entry | Vertical from above | |
| Beam trip (>1sec) number | < 5 per 3-month operation cycle | < 3 per year |
| Beam stability | Energy: ±1%, Intensity: ±2%, Size: ±10% | |
| Beam time structure | CW with 200μs low frequency 0-current holes | |

The reference design for the accelerator has been developed during the PDS-XADS programme [4.33], [4.34], [4.35] and is based on the use of a superconducting linac (see Fig. 4.42). Such a choice allows to obtain a very modular and upgradeable machine (same concept for prototype and industrial scale), an excellent potential for reliability, and a high RF-beam efficiency thanks to superconductivity (optimized operation cost). For the injector, an ECR source with a normal conducting RFQ is used up to 3 or 5 MeV, followed by an energy booster section which uses normal conducting H-type DTL or and superconducting CH-DTL structures up to a transition energy still under Optimization , around 20 MeV. This first part of the linac is duplicated in order to provide good reliability perspectives. Then a fully modular superconducting linac, based on different RF structures (spoke, elliptical), accelerates the beam up to the final energy (350, 600, 1000 MeV). Finally a doubly-achromatic beam line with a redundant beam scanning system transports the beam up to the spallation target.

The ADS accelerator is expected, especially in the long term EFIT scenario, to have a very limited number of unexpected beam interruptions per year, which would cause the absence of the beam on the spallation target for times longer than one second. This requirement is motivated by the fact that frequently repeated beam interruptions induce thermal stresses and fatigue on the reactor structures, the target or the fuel elements, with possible significant damages, especially on the fuel claddings; moreover these beam interruptions decrease the plant availability, implying plant shutdowns in most of the cases. Therefore, it has been estimated in the beginning of the project that beam trips in excess of one second duration should not occur more frequently than five times per 3 month operation period for the XT-ADS, and three times per year for the EFIT.

At the end of the EUROTRANS project, those figures have been revised; an acceptable beam trip is shorter than 3 seconds; the number of trips in excess has risen to 10 per cycle of 3 months in the case of XT-ADS.

To reach such an ambitious goal, which is lower than the reliability experience of typical accelerator based user facilities by many 2 or 3 orders of magnitude, it is clear that reliability oriented design practices need to be followed from the early stage of component design. In particular:

— Strong design practices are needed: every linac main component has to be derated with respect to its technological limitation (over design);

— Rather high degree of redundancy needs to be planned in critical areas; this is especially true for the identified poor reliability components: linac injector, and RF power systems, where solid state amplifiers should be used as much as possible;

— Fault tolerance capabilities have to be introduced to the maximum extent: such a capability is expected in the highly modular superconducting RF linac, from at least 20 MeV [4.36].

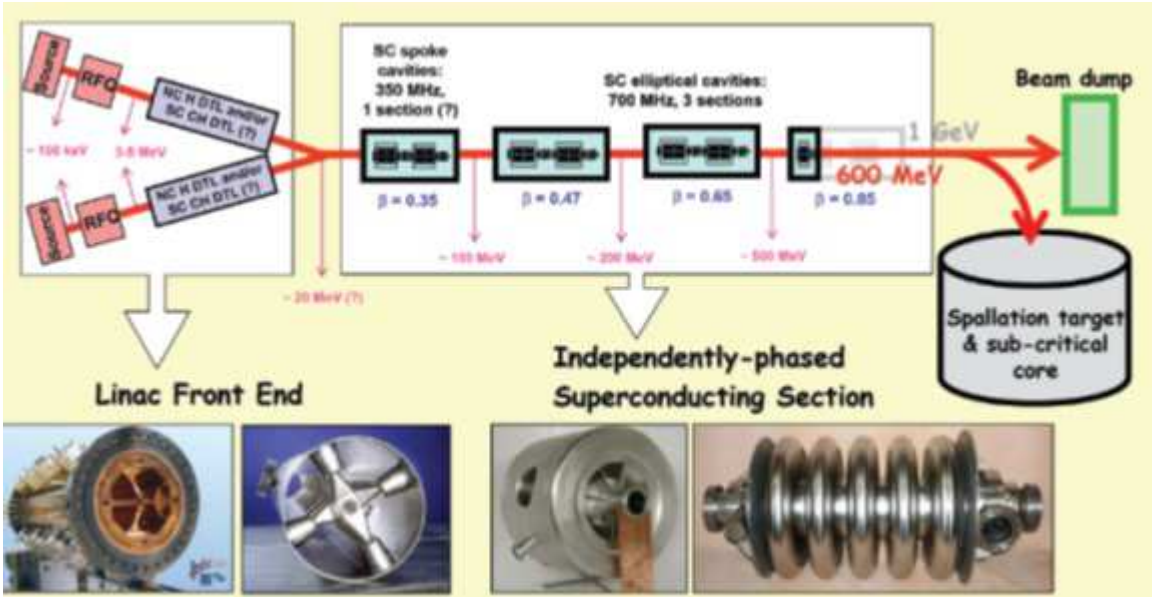


*FIG. 4.42. The reference accelerator scheme for the XT-ADS (& EFIT).*

A preliminary bottom up reliability analysis (Failure Mode and Effects Analysis, FMEA) has been performed in order to identify the critical areas in the design in terms of impact on the overall reliability [4.37]. This activity confirms the choice to provide a second, redundant, proton injector stage (composed of the source, RFQ and low energy booster), with fast switching capabilities. After the injector stage, the superconducting linac has a high degree of modularity, since the whole beam line is an array of nearly identical periods. All components are operating well below any technological limitation in terms of potential performances, and therefore a high degree of fault tolerance with respect to cavity and magnets can be expected in the superconducting linac, where neighbouring components have the potential to provide the functions of a failing component without affecting the accelerator availability. Clearly this approach implies a reliable and sophisticated machine control system, and in particular a digital RF control system to handle the RF set points to perform fast beam recovery in the case of cavity failures.

#### *4.3.2.3. EUROTRANS accelerator activities for ADS*

The EUROTRANS accelerator work package (WP1.3) is split in several tasks, focused to design the main subcomponents of the ADS linac in the different energy areas, and to identify their reliability characteristics. Activities are dedicated to:

- Experimental evaluation of the proton injector reliability, performed at the IPHI injector;
- Assessment of the reliability performances of the intermediate energy accelerator components, with particular attention to the comparison of different accelerating structures;
- Design and experimental qualification of the reliability performances of a high energy cryomodule tested at full power and nominal temperature;
- Design and test of a prototypical RF control system intended to provide fault tolerance operation of the linear accelerator;
- Update of the accelerator design, including beam dynamics issues and investigation of control strategies for fault tolerance, development of more reliability analyses and cost estimations for the XT-ADS and EFIT.

*4.3.2.4. Proton injector reliability tests*

The IPHI injector (see Fig. 4.43), developed in France at Saclay by CEA and CNRS, fulfills the specifications of the ADS proton injector, with wide margins in term of beam current capabilities. It is composed by the 95 keV SILHI ECR ion source, an already tuned low energy beam transport line, a 3 MeV copper RFQ under final completion, and the associated diagnostic beam line [4.38].

*FIG. 4.43. Scheme of the IPHI injector, and picture of the diagnostic beam line installation in Saclay.*

In the past years, the SILHI source has been successfully used for several week long reliability tests at currents of 30 mA, showing no beam stops and occasional sparks in the extraction region, causing no beam interruptions. In the EUROTRANS context, these tests will be extended, to include acceleration in the RFQ and propagation in the beam lines: the IPHI injector, once completed in 2008, will be used for a long run test (2 months), to demonstrate and assess, on a real scale, the reliability characteristics of this accelerator subcomponent.

Moreover, the possibility to achieve the sharp 200 μs beam holes at low repetition rate ($10^{-3}$ to 1 Hz), that is required for the subcriticality monitoring of the ADS core, has been successfully tested directly pulsing the SILHI source. Encouraging fall and rise time durations of less than 30 μs have been obtained. This test will also be extended to the full beam of the IPHI injector, at 3 MeV.

*4.3.2.5. RF structures for the intermediate energy section*

For the intermediateenergy region after the RFQ and up to approximately 100 MeV, several cavity types are considered as valid candidates. Studies and tests of prototypes are being developed in order to evaluate their feasibility and assess their potential reliability performances. In particular, activities concentrate on: 1. high shunt impedance copper DTL structures of the IH and CH type, using Konus focusing scheme (focusing elements outside the drift tubes) that provides high real estate gradients; 2. superconducting multigap CH structures, with Konus focusing scheme, ensuring both high real estate gradients and optimized RF to beam efficiency thanks to superconductivity; 3 superconducting spoke cavities, which are very modular, providing some fault tolerance capability, and can operate efficiently from very low energies (around 5 MeV) up to 100 MeV and more. The two first structures are meant to be part of the redundant injector front end, while the spoke structures will be part of the fault tolerant independently phased linac. At the present phase of the project, the transition energy is around 17 MeV, still to be optimized given the results of the ongoing R&D.

The first activity is carried out by IBA and IAP Frankfurt and is still in the design phase. Concerning the second activity, a 19-gap superconducting 350 MHz CH prototype has been successfully tested at IAP Frankfurt in vertical test (Fig. 4.44 left) with excellent results (more than 7 MV/m), and is ready to be installed in an existing horizontal cryostat, with an external driven mechanical tuner for further testing [4.39].

*FIG. 4.44. Pictures of the SC CH cavity during vertical test at Frankfurt (left) and of the spoke horizontal test cryomodule during its installation at Orsay (right).*

Concerning the spoke activities, CNRS-IPN Orsay is equipping an existing cryomodule (Fig. 4.44 right) with a 350 MHz β=0.15 spoke cavity, fully dressed with its stainless steel helium reservoir, its cold frequency tuning mechanism and its high power (20 kW) RF coupler [4.40]. The cavity, which has already reached the design goals in vertical tests, once completed with its ancillary RF components, will be operated in 2008 at nominal operating conditions in long tests to determine the reliability characteristics of the components.

#### *4.3.2.6. The high energy cryomodule*

The high energy part of the linac uses low beta elliptical cavities from energy of approximately 100 MeV, using 3 different beta sections (0.5, 0.65, and 0.85). Such a technology is already successfully used worldwide (e.g. at the SNS), but the full demonstration of the very low beta section is not yet fully accomplished. Excellent test results have been achieved with the β=0.47 TRASCO cavities at INFN Milano [4.41], but besides the development of the bare superconducting cavity, it is important to prototype and test each auxiliary system needed for the cavity operation in a real environment (power coupler, RF source, power supply, RF control system, cryogenic system, cryostat.

The goal of this EUROTRANS third task is thus to design, build and test before 2009 an operational prototypical cryomodule of the high energy first section of the proton linac [4.42], [4.43]. This cryomodule will host one of the existing β=0.47 TRASCO cavities, equipped with a cold frequency tuner, developed by INFN and a 150 kW CW RF coupler, developed by CNRS. This cryostat, under development at INFN and CNRS, will be assembled and tested at IPN Orsay under nominal 2K operating conditions, and extensive tests (without beam but at full 80kW RF power level) will be performed to qualify its reliability characteristics. Fig. 4.45 shows a conceptual layout of the module and of the RF power coupler.

#### *4.3.2.7. Low level RF control system and fault tolerance*

The scope of this activity is to develop a digital Low Level RF control system intended to provide the necessary field and phase stability (±0.5% in amplitude, ±0.5 in phase) and to identify and handle fast recovery scenarios for cavity failures in the superconducting linac, by means of local compensation at neighbouring cavities.

This local compensation method (Fig. 4.46, left), in which neighbouring components have the potential to provide the functions of a failing component, has been demonstrated on the beam dynamics point of view from 10 MeV [4.36]–[4.44] given that modular independently phased

accelerating cavities are used and that some RF power margin (up to 30%) is available. The remaining step is now to develop fast failure recovery scenarios to ensure that such a retuning is performed in less than 1 second. Two possible solutions, with and without stopping the beam during the recovery procedure, have been identified and analysed. The final choice will rely on the results of R&D activities to be performed on fast RF fault detection, fast cold tuning system management, and fast LLRF communication and data exchange.

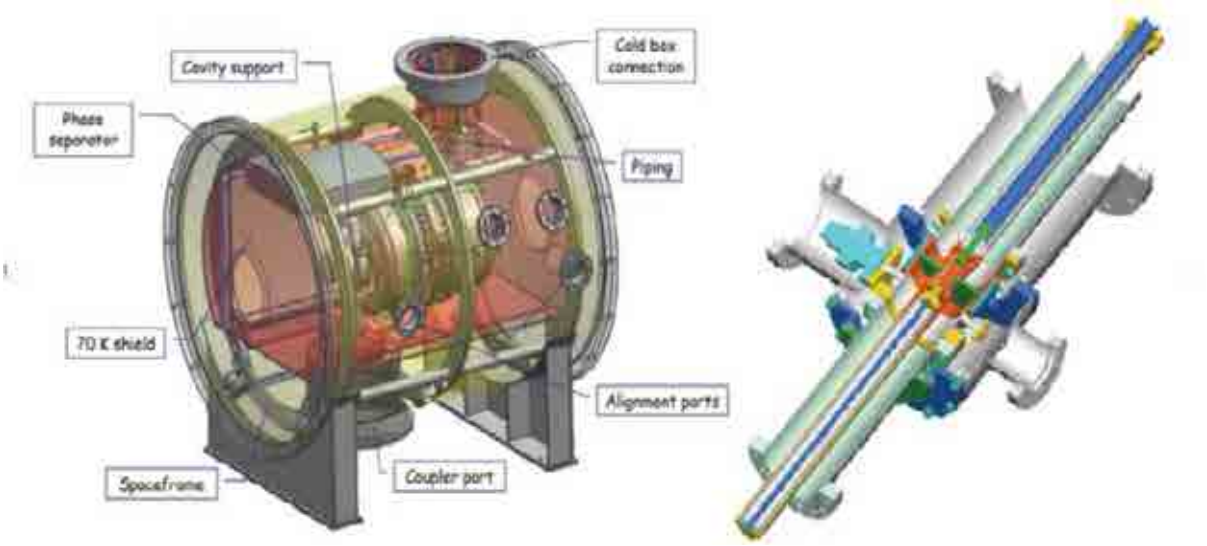


*FIG. 4.45. Conceptual layout of the single cavity module (left) and associated power coupler (right) for the testing of high energy components.*

Digital techniques become necessary to meet the speed and software configuration required by such a retuning procedure. A FPGA based digital LLRF control system, in which a number of key functionalities are implemented on a single chip, offers indeed a high grade reliability and flexibility. Developments are going on in CEA and CNRS at 704 MHz and 352 MHz respectively, with very encouraging preliminary results [4.40]. Fig. 4.46 (right) shows a picture of a first prototype developed by CNRS (LPNHE-IPNO).

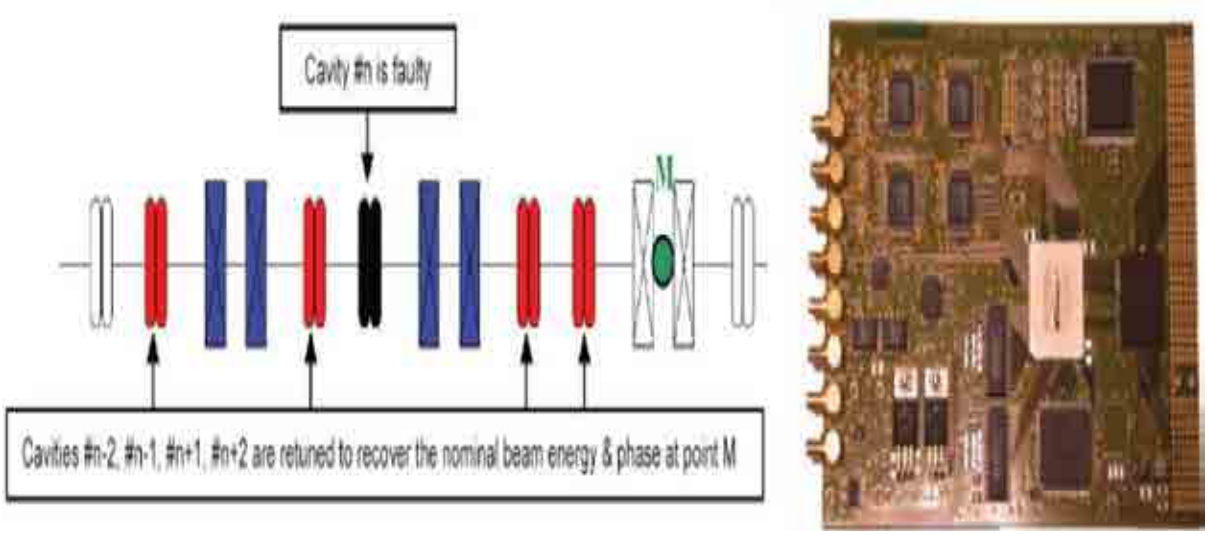


*FIG. 4.46. Principle of the local compensation method (left) and picture of a prototypical FPGA based digital LLRF control card developed at CNRS (right).*

#### *4.3.2.8. Global coherence of the EUROTRANS accelerator design*

The last task in the accelerator work package deals with the progress of the accelerator design and the characterization of its reliability characteristics, the final goal being to obtain in 2009 a frozen detailed conceptual design of the XT-ADS linac, with assessed reliability and costing.

Start end beam dynamics simulations are being performed, especially for the different options for the intermediate energy structures. The modelling also includes in the independently phased linac the effect of the beam transients induced by RF faults, and the final beam line injecting the beam in the reactor.

Furthermore, an integrated reliability analysis is being performed [4.45] to predict the reliability characteristics of the proposed accelerator, following the standard practices used in the nuclear energy applications (mainly failure mode and effects analysis and reliability block diagrams), and integrating the experimental results and demonstrated reliability numbers. This activity is the continuation of the PDS-XADS work, that already showed that a reliability oriented design can, without necessarily improving the 'Mean Time Between Failure' values (MTBF) of each subsystem, greatly improve the MTBF of the whole system by 1 or 2 orders of magnitude, especially with the implementation of redundancy, fault tolerance and corrective maintenance strategies in critical areas [4.37]–[4.44].

The 'less than a few beam trips per year' goal is still 2 or 3 orders of magnitude below present accelerator performance, but seems to be reachable. As a matter of fact, the concept of fault tolerance in a superconducting linac with independently phased cavities is now proven, at least at high energies (>200MeV), by the SNS experience, where a beam recovery system is successfully running, with recovery times of a few minutes [4.46]. An integrated reliability analysis of the whole system shows that this SNS proof of principle of the fault tolerance concept potentially improves the reliability figure by at least 1 order of magnitude already (given that we can implement it in less than the 1 second limit). The remaining order of magnitude will be gained by redundancy, corrective maintenance plans, careful design of auxiliary systems, and by improving the MTBF of individual components using the results from the on going R&D performed within EUROTRANS.

### 4.3.3. Status in India

#### *4.3.3.1. Specifications and roadmap for the accelerator*

Since India envisages the application as thorium–uranium breeder, the ADS must be operated with high beam power to maximize breeding potential. Since the thermalhydraulics issue in spallation target may restrict ~1 GeV proton beam current to ~10 mA on a single target module, an ADS core design is visualized with 3 or more spallation targets that would also help suppress the neutron flux peaking. With this assumption, the R&D objective is to realize a proton accelerator of 30 mA beam current (cw/average) within as short time as feasible. Of the two alternative accelerator types, cyclotron and LINAC, basic indigenous technological know-how, up to limited extent, exists for both.

The difficult and performance limiting part of high intensity proton accelerator for both these types, is low energy front end. So, the beginning of R&D programme has been made from there and efforts on development of appropriate ADS driver accelerator are initiated. The adopted roadmap of Indian ADS programme envisages deliverables related to development of LINAC technology over next 10–15 years as following:

— An ongoing 20-MeV high intensity proton LINAC project in BARC, Mumbai is due for completion by year 2011–12.

— Programme to develop ~ 100 MeV proton LINAC would be taken up in a five-year plan (2007–2012) in RR CAT, Indore as a H-/H+ injector to a 100 kW beam power, rapid cycling proton synchrotron (RCS) to be constructed there as spallation neutron source (SNS).

— Successful completion of above mentioned LINAC projects should lead to requisite technological developments for taking up construction of moderate to high energy (e.g. 100 to 250 MeV), high current accelerator in a new BARC campus at Visakhapattanam on the east coast of the country.

— The above mentioned planned accelerator for a demonstration ADS in Visakhapattanam would be further extendable in size and proton energy up to 1 GeV at the same site, so that construction of a full scale ADS power plant might be undertaken in future.

Initial design studies and work to set up technological facility for fabrication and characterization of superconducting RF cavities from bulk niobium have also been taken up in BARC, which will be expanded to include the expertise available in other Indian institutions notably in RRCAT, Indore and IUAC, New Delhi.

#### *4.3.3.2. Conceptual layout of a LINAC Driver*

The overall architecture has been studied through beam dynamics simulations. The proposed high current proton LINAC will consist of an ECR proton ion source (pulse and dc operation), 3 MeV RFQ, DTL up to 40 MeV, CCDTL up to 100 MeV and 5-cell Superconducting elliptical cavities to accelerate the beam to 1 GeV.

— In the 1-GeV beam dynamics design, the beam from the RFQ is accelerated to 40.12 MeV using 352.21 MHz DTL structure. A FFDD lattice is used in the DTL for transverse focusing. The total length of the DTL is 22.66 m and the RF power required is ~ 3 MW. The DTL will be built in 4 tanks. The axial electric field is kept constant at 2.5 MV/m in all the tanks.

— The 40.12 MeV beam from the DTL is then accelerated to 100.24 MeV using 2 gap CCDTL cavities operating at 704.42 MHz. The accelerating gradient is kept constant at 1.37 MV/m in the CCDTL. Its total length is 69.57 m and the RF power requirement is 6.45 MW.

— Above 100.24 MeV proton beam energy, superconducting elliptical cavities at 704.42 MHz are used to accelerate the beam to 1 GeV. The superconducting linac accelerates the beam using three different types of 5-cell elliptical cavities designed with their geometries corresponding to geometric beta values $\beta G$ = 0.47, 0.62 and 0.80. Length of this superconducting linac section would be 306.2 m.

#### *4.3.3.3. Activities at BARC, Mumbai*

The developments for a high current proton linear accelerator are progressing at BARC as five year plan projects (2002–07 & beyond). One can be distinguished between the LEHIPA project and the R&D programme on superconducting cavities.

The development modules for the LEHIPA project are an ECR proton ion source, a 3-MeV RFQ and 3–20 MeV DTL. The schematic of the ion extraction electrodes is also shown in Fig. 4.47. The extracted proton beam is matched to, and injected into the RFQ through a LEBT line.

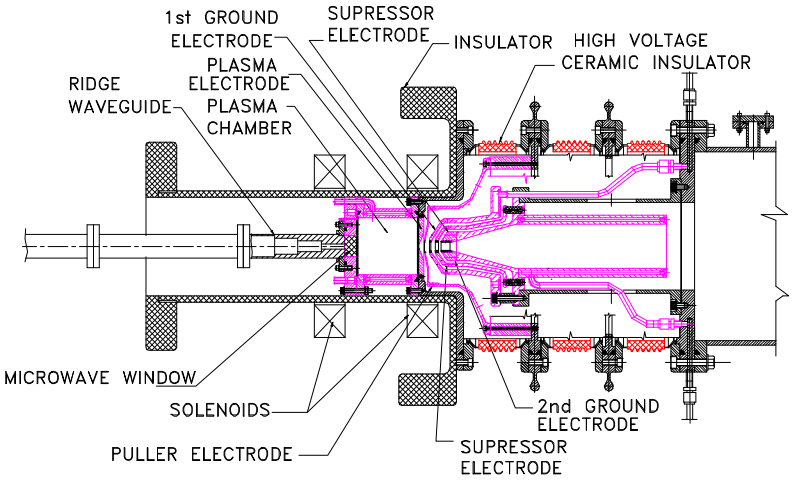


*FIG. 4.47. Schematic of ion extraction electrodes in ECR proton ion source.*

The RFQ operating at 352.21 MHz will accelerate the beam from 50 keV to 3 MeV. The 3 MeV beam is then matched into the DTL using a MEBT line, which consists of 4 quadrupoles for transverse matching and 2 RF gaps for longitudinal matching. The design of DTL for 20-MeV linac facility is slightly different from the DTL design studied for the 1 GeV linac. The DTL for 20 MeV linac facility will utilize four tank design and has slightly higher quadrupole field gradient than that for 1-GeV application.

Main power supplies for LEHIPA are the three 352.21 MHz RF power generator klystrons. The requirements for RF power input to the three acceleration modules are estimated as RFQ: 500 kW, 10-MeV DTL: 814 kW and 10–20 MeV DTL: 826 kW.

The 352.21 MHz klystron tube of cw rating 1 MW will be used as power source for each of the three accelerating modules. An additional 60 kW 350 MHz RF system module has been designed /configured around high power TH571 B tetrode tubes of Thales make. It is decided to develop two such RF systems, each feeding power of about 30 to 35 kW at two ports of a prototype RFQ being built under the RFQ development programme of LEHIPA for 400 keV deuteron beam. This RFQ accelerator will be commissioned for applications in 14 MeV neutron generator by using D-T reaction on a tritium loaded titanium target.

The LEHIPA in BARC will be set up in shielded enclosure at the basement of a building. Infrastructure for this facility is being created with provision for cooling water, electrical power, ventilation and radiological protection systems.

The overall design of mechanical assembly and procurement of major hardware of ECR ion source mentioned above are completed. Many of the subsystems including RF and high voltage power supplies, and diagnostics have been tested and characterized. The overall design of mechanical assembly and procurement of major materials of construction for RFQ are completed. Fabrication of prototype modules of RFQ is initiated with the in house workshop of BARC, and also by an industrial partner; whereby fabrication techniques of precision machining and vacuum brazing will be developed through a number of trials. One of the prototype as ‘hot RF test’ model would be used for accelerating deuterons to 400 keV and used for neutron generation by D-T reaction. The CAD models of the 3 MeV is shown in Fig. 4.48.

Preliminary mechanical design of four DTL tanks, to be made from forged, mild steel tubes with copper plated inside surface has been completed. Design calculations are in progress to freeze one of the two options of permanent or electromagnet quadrupole (PMQ/EMQ) magnets inside the drift tubes in FFDD lattice pattern. First stage operation 3-MeV RFQ and later with DTL up to 10 MeV energy beam at high power are scheduled by the end of 2010.

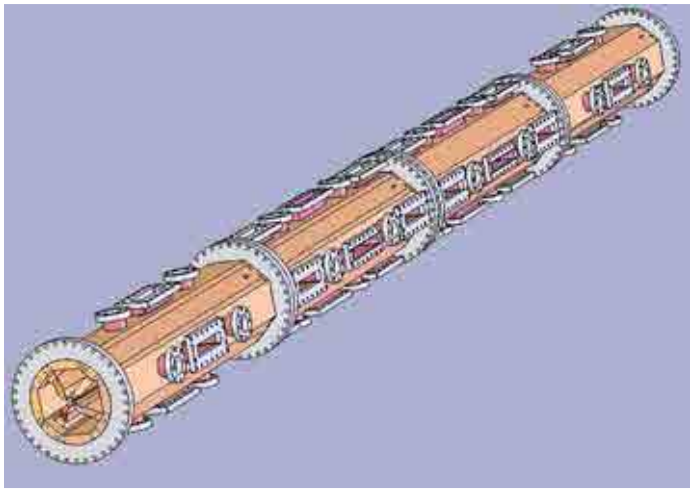

*FIG. 4.48. CAD Model of the BARC RFQ.*

The second programme aims at RF electrodynamics studies and mechanical design, fabrication and characterization of superconducting RF cavities for high energy (> 100 MeV) section of proton linac. Adopting the proven technology of elliptical, bulk niobium cavities of CERN-LEP as a feasible option; design, fabrication and the testing activities on superconducting RF cavities have been initiated for 700 MHz, β= 0.42 (~100 MeV Proton), and 1050/1056 MHz, β= 0.49.

RF electrodynamics analysis of single cell elliptical cavities of OFHC copper and bulk niobium have been performed for design frequency of 1050 MHz, by using standard design codes. A single cell cavity of this design and made of copper was fabricated (Fig. 4.49) for conducting RF measurements at room temperature.

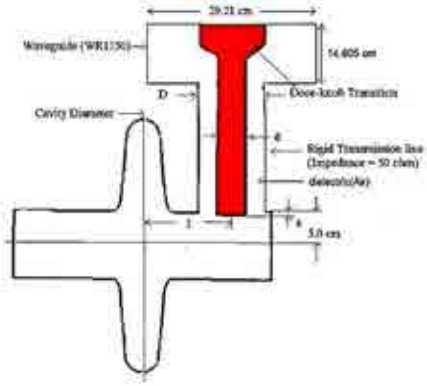


*FIG. 4.49. Scheme for 1050 GHz cavity and associated coupler.*

### *4.3.3.4. Activities at Raja Ramanna Centre for Advanced Technology, Indore*

R&D programmes initiated in RRCAT are oriented towards technological developments that are essential for design and construction of a SNS facility. This programme includes a high power proton linac injector, and the ongoing work so far centre around RF hardware and design studies of proton linac modules, a RFQ, development of high power RF load and solid state RF power amplifier (300W module).

### *4.3.3.5. Activities at Institute for Plasma Research (IPR), Gandhinagar*

A major activity contributing to ADS R&D relate to HV regulated DC power supplies for driving high power RF klystron at 95 kV and 24 A. This power supply design is based on series and controlled addition of number of smaller stages of voltages, in a phase synchronized fashion (Fig. 4.50 and Fig. 4.51). The components are rectifier transformers with multiple secondaries, switched

power units and a digital controller. The output is generated with addition of small stages of voltages. The output waveform shown in Fig. 4.52 explains about the additions during the turn on time.

The design and construction of first indigenously built power supply is complete and it is under tests in the IPR. Second version of the same design will be fabricated for use with the LEHIPA's RF system.

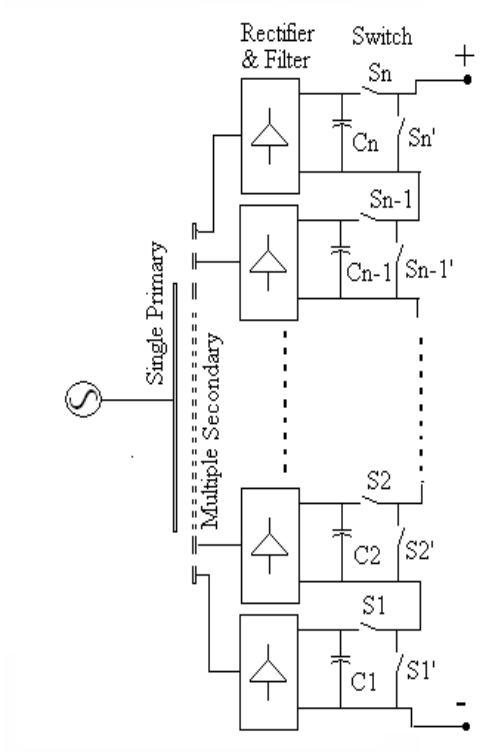


*FIG. 4.51. Scheme of regulated HV power supply.*

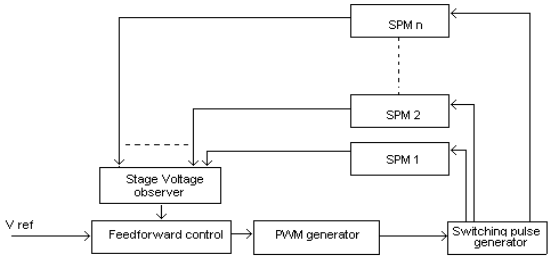


*FIG. 4.50. Control scheme for regulated HV power supply.*

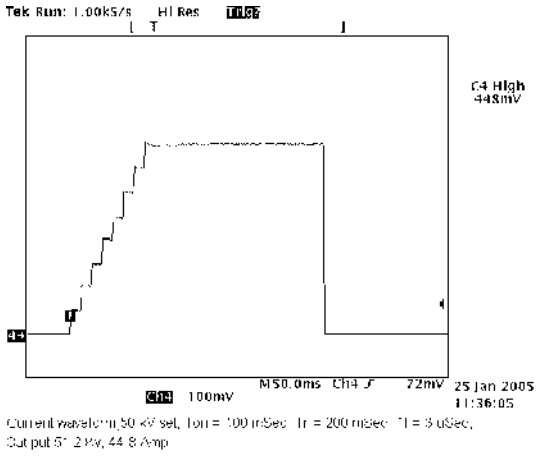


*FIG. 4.52. Typical waveform showing formation of output voltage.*

### *4.3.3.6. R&D activities on cyclotrons at VECC, Kolkata*

Beam dynamics studies of proton cyclotron have been carried out at VECC Kolkata for defining the maximum extractable beam current in 2 or 3-stage 1-GeV acceleration as to investigate the option of using cyclotron for ADS. Initial aim was to develop a 200/250 MeV, 5 mA SCC for accelerator target reactor coupling in a technology demonstration ADS. Activities are focused on the development of a 10 MeV, 5–10 mA compact radial sector proton cyclotron, and to study and resolve various physics and technological problems associated with the production, bunching, acceleration, injection, extraction, etc. of the high intensity proton beams. Presently ongoing work has concerns design and fabrication of an ECR proton ion source, and design of spiral inflector and beam buncher. The extracted beam will be first collimated using slits and then it will be bunched using a sinusoidal buncher (expected efficiency ~ 30% for space charge dominated beam). It will be injected axially in the central region of the cyclotron where a spiral inflector will place the beam on the proper orbit. Fig. 4.53 shows inflector positioning and turn pattern in the central region of the 10 MeV cyclotron.

A 2.45 GHz microwave ion source will produce ~30mA of proton beam at 100 keV. The plasma chamber of the source is a double walled water cooled cylindrical stainless steel chamber of 100 mm length and 90 mm diameter. The microwave power from the 2.45 GHz, 1.2 kW magnetron will be coupled through a three stubs tuning unit and ridged wave guide. Two motor controlled movable

magnetic coils with separate power supply will provide the desired magnetic field. There is a provision for adjustment of the resonance zone by moving these coils on-line with two motors. The overall design of mechanical assembly and procurement of major hardware are almost complete and the system integration is in progress.

Extracted 100 keV proton beam from the ion source will be injected axially in the central region of the cyclotron where a spiral inflector will bend the beam by 90 degree and placed it on the designed orbit. The spiral inflector has been designed analytically as well as numerically using CASINO code. The gap between the electrodes is chosen ~1.4 cm to ensure the loss free bending of the beam with size 5 mm and emittance 0.8π mm–mrad. The aspects ratio between the width and gap of the electrode is taken 2 to avoid fringe field effect and to tolerate the shift in beam trajectory inside the inflector.

Studies were made about the central region of 10 MeV cyclotron to optimize the central plug position and check the centering errors. All calculations of the beam centering have been performed with following parameters: injection energy 100 keV, Dee Voltage 125 kV, gap width between dee and dummy dee 2 cm, dee height 3 cm and homogeneous magnetic field 0.5 T in the plug region. A more detailed analysis and optimization of central region with computed electric and magnetic fields using computer codes RELAX3D and TOSCA are in the process.

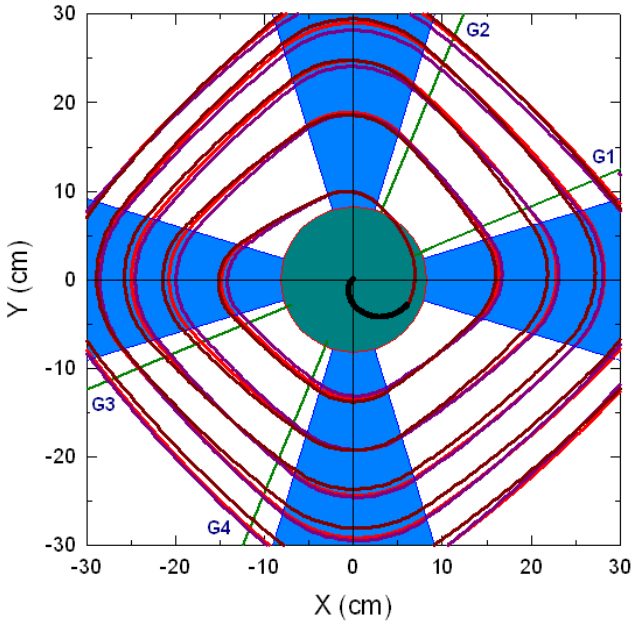


*FIG. 4.53. Inflector positioning and turn pattern in the central region of the 10 MeV cyclotron (ΔØ =±15° of RF).*

### 4.3.4. Status in Japan

#### *4.3.4.1. Accelerator specifications and scope of associated R&D*

In Japan, JAEA proposes an ADS which consists of a high power proton LINAC, a spallation target of lead-bismuth eutectic (LBE) and a subcritical core. In this proposal, the energy and beam power of the high power proton LINAC are 1.5 GeV and 20–30 MW, respectively. Other specifications of the high power proton linac are described in [4.28].

An important technical aspect that is considered in the JAEA work is the negative impact of very frequent beam trips as experienced in existing intense accelerator facilities. Frequent beam trips cause thermal fatigue problems for ADS components materials, leading to degradation of their structural integrity and reduction of their lifetime. They can also badly erode the availability or the capacity of

ADS, resulting in poor economics. In the development of accelerators for ADS, it is vitally important to establish the technologies to achieve a very high degree of reliability. On the other hand, JAEA considers that it is also important in the development of ADS to design structural components to withstand possible thermal fatigues and a power conversion system less sensitive to beam trips. The purpose of the JAEA study is the comparison of beam trip frequencies between requirement from ADS transient analyses and estimation from current experimental data of accelerators.

#### *4.3.4.2. JAEA study on beam trips*

As shown in Fig. 4.54, three parts of the reactor structure, i.e. the beam window, the inner barrel and the reactor vessel, were picked up as the representatives to discuss the effect of the thermal shock [4.29]. As for the beam window, a beam trip causes the rapid temperature drop, which causes the thermal stress owing to the temperature difference between the inner and the outer surfaces of the beam window. A transient analysis for a beam window showed that the maximum thermal stress of 179 MPa is expected with time lag of 0.5 seconds after the beam trip. The acceptable number of this thermal shock is estimated at about 105 times, which means that several beam trips per one hour may be acceptable for two years of the expected life time of the beam window. The inner barrel is a cylindrical structure and installed to straighten the LBE flow above the core. In the case of the beam trip, the inner surface of it is immediately cooled by the cold LBE, and the temperature difference between the inner and outer surfaces is expected to be caused. A transient analysis showed that the maximum temperature difference of 60°C will cause the maximum stress of about 130 MPa. Considering this stress, the acceptable frequency of the beam trip for the inner barrel ranges from 104 to 106 times. As for the reactor vessel, a beam trip causes the temperature change between the inner and the outer surfaces similarly to the inner barrel, and the formation of the temperature stratification and the LBE level lowering by thermal shrinkage will also cause the thermal stress. The thermal stress for the fatigue evaluation was estimated for the reactor vessel under the assumption that the beam is restated 400 seconds after the beam trip. It was found that the estimated stress range was about 270 MPa at maximum. Considering this magnitude of the stress range, the acceptable frequency of the beam trip for the reactor vessel was estimated at about 104 times.

The influence of the beam trip to the power generation system is also important from a viewpoint of the availability of the system because the restart procedure of the system usually takes long period of time, for example several hours, once the power generation turbine stops. The transient analysis on the saturated steam cycle with steam drums, adopted by JAEA's ADS design, showed that about 400 seconds of turbine operation may be possible without the beam. When the duration of the beam trip exceeds this limit, the pressure of the steam drum and the LBE temperature become too low to prevent its freezing.

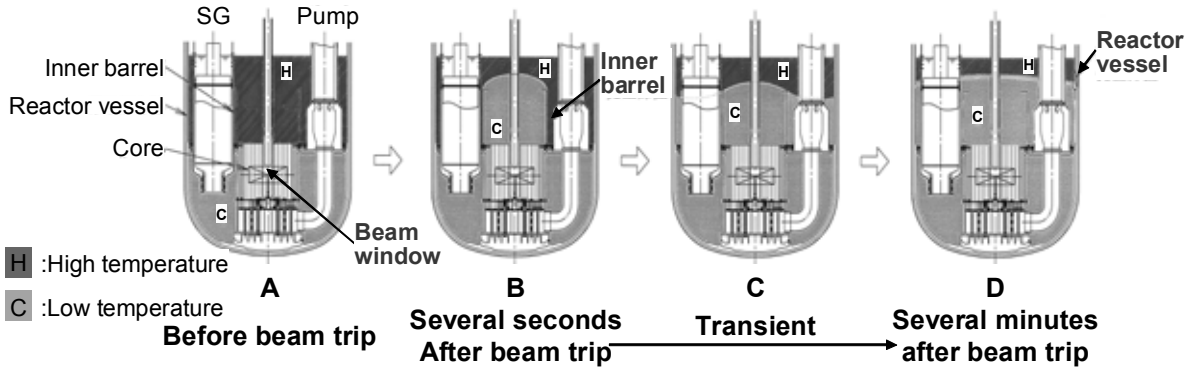


*FIG. 4.54. Influence of beam trip transient on reactor structure.*

*4.3.4.3. JAEA result and consequences for dedicated accelerator R&D*

As shown in Fig. 4.55, the acceptable frequency of the beam trip was obtained as function of the beam trip duration T:

— $10^6$ times per 40 years for short beam trips (T < 5 seconds) regarding the fatigue failure of the inner barrel;
— $10^4$ or $10^5$ times per 40 years for medium duration beam trips (5 seconds < T < 5 minutes) regarding the fatigue failure of the inner barrel and the reactor vessel; and
— once a week for long beam trip (T > 5 minutes) regarding the system availability.

In order to overcome this trip problem on ADS, it seems important to discuss the current level of the technology. Fig. 4.55 shows a diagram of the beam trip frequency and the duration based on the KEK electron–positron LINAC and LANSCE experiences together with above mentioned criteria depending on the beam trip duration [4.29] [4.30] [4.31]. Comparing the difference between the acceptable frequency of the beam trip and the current experimental data, about one order reduction of the beam trip frequency is necessary to satisfy the thermal stress conditions, except that the beam trip duration is less than ten seconds.

Two strategies are now being considered for this trip problem: (1) Reduction of the beam trip duration related the RF-reflection down to 5 seconds, and (2) Reduction of frequency for relatively long beam trips.

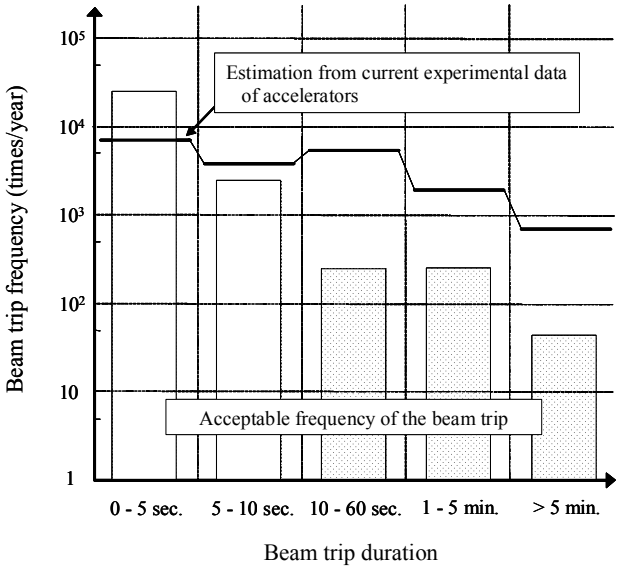


*FIG. 4.55. Comparison of current status of beam trip frequency based on the current experimental data of accelerators and criteria for ADS application.*

## 4.4. TARGET

The spallation target is a symbolic component of accelerator driven system (ADS) that generates spallation neutrons from high energy protons to drive the subcritical core.

Two design concepts are proposed worldwide: one is the target with window and the other is the windowless target. Generally, a beam window locates at the end of proton beam duct and forms a boundary between the vacuum zone (beam duct) and the target zone. The beam window faces several severe conditions such as mechanical stresses caused by the pressure difference, thermal stress caused by temperature gradient between accelerator side and reactor side and temperature distribution caused by injected beam profile, radiation damage by high energy particles, and corrosion–erosion by coolant flow. To avoid these technical difficulties, the windowless target is considered, where the beam window is removed and the free surface of the liquid metal target forms a boundary instead of beam

window. In the case of windowless type, other difficulties arises alternatively such as the control of the shape and position of free surface, liquid metal splash caused by high intensity beam injection, removal of volatile materials to keep vacuum condition.

In the decade since the previous report, an international experimental programme, MEGAPIE (MEGAwatt PIlot Experiment) was performed at Paul Scherrer Institute, Switzerland. A Pb-Bispallation target was successfully operated for about four months by a 590 MeV–1 MW proton beam. Through this programme, operation of liquid metal spallation target was demonstrated.

This section summarizes the activities for spallation target design and related R&D programmes including experimental target studies.

MEGAPIE is described in subsection 5.4.1 together with R&D performed by other countries (Japan, Russia) on target window.

### 4.4.1. Target with window

#### *4.4.1.1. The MEGAPIE programme (EU, Japan, Korea, Switzerland and United States)*

MEGAPIE (Megawatt Pilot Target Experiment) is an initiative launched by Commisariat à l'Energie Atomique, Cadarache (France) and Forschungszentrum Karlsruhe (Germany) in collaboration with Paul Scherrer Institut (Switzerland), to demonstrate, in an international collaboration, the feasibility of a liquid lead-bismuth target for spallation facilities at a beam power level of 1 MW. Such a target is under consideration for various concepts of accelerator driven systems (ADS) to be used in transmutation of radioactive waste and other applications world wide. It also has the potential of increasing significantly the thermal neutron flux available at the spallation neutron source SINQ for neutron scattering. SINQ's beam power being close to 1 MW already, this facility offers a unique opportunity to realize such an experiment with a reasonably small number of new ancillary systems. The basic features of the experiment are described together with the technical concept of the target.

(a) Background and goals

MEGAPIE (MEGAwatt Pilot Experiment) [4.47] [4.48] is a joint initiative by six European research institutions and JAERI, Japan, to design, build, operate and explore a liquid lead-bismuth spallation target for 1MW of beam power, taking advantage of the existing spallation neutron facility SINQ at PSI, Switzerland.

A liquid metal spallation target based on the lead-bismuth eutectic mixture with a melting point as low as 125°C and a boiling point as high as 1670°C is the preferred concept in several studies aiming at utilising accelerators to drive subcritical assemblies (ADS). The main goal in these efforts is to transmute long lived radioactive species into shorter lived isotopes in an effort to ease problems of long term storage and final disposal of radioactive waste. However, to date, such a target has never been operated. This lends a speculative element to all of these designs, which must be eliminated if serious consideration is given to the implementation of a demonstration facility. Apart from ongoing research into several of the underlying issues, a full demonstration of a working system is highly desirable. For obvious reasons such a feasibility demonstration should be carried out on an existing accelerator with suitable design features.

More specifically, the current orientation in France is a step by step approach towards a possible ADS demonstration experiment, as visualised in Fig. 4.56. In this context the test of a 1 MW liquid metal target is a crucial milestone, even if the final choice of the type of target (solid vs. liquid) has yet to be made. The MEGAPIE experiment will be an important ingredient in defining and initiating the next step, a dedicated ADS quality accelerator plus irradiation oriented target plus (at a later substage) a low power, subcritical blanket.

It is the goal of this experiment to explore the conditions under which such a target system can be licensed, to accrue a design data base for liquid lead-bismuth targets and to gain experience in operating such a system under the conditions of present day accelerator performance. Furthermore,

design validation by extensive monitoring of its operational behaviour and post-irradiation examination of its components are integral parts of the project. An extensive pre-irradiation R&D programme will be carried out in order to maximise the safety of the target and to optimize its layout.

The only accelerator in Europe which has a sufficiently high proton beam power to make the installation of such a target a meaningful experiment is the ring cyclotron at PSI with 590 MeV proton energy and a continuous current of 1.8 mA, being in the process of an upgrade to 2 mA. It is used for a large range of scientific research tools, the most prominent one being a spallation neutron source (SINQ) with its large number of different user facilities. Furthermore, the very existence of this spallation source with its heavy shielding and complete suite of ancillary systems makes this experiment much more easily affordable.

(b) Opportunities and boundary conditions at PSI

— Accelerator facilities and proton beam line

A large complex of research facilities at the Paul Scherrer Institut is based on a cascade of three accelerators that deliver a proton beam of 590 MeV in energy at a current up to 1.8 mA. A schematic floor plan of these facilities is shown in Fig. 4.57. The proton beam is preaccelerated in a Cockroft Walton column to the energy of 800 keV and is brought up to energy of 72 MeV in the 4 sector injector cyclotron. This has replaced the original Phillips injector cyclotron (Inj. 1) also shown in the figure, which is currently operating for different applications and is intended to be utilised also in the underlying research efforts for MEGAPIE, as discussed below (LiSoR experiment).

Final acceleration to 590 MeV occurs in the 8-sector main ring cyclotron, from which the beam is transported through the experimental hall in a shielded tunnel. A small fraction of the beam (20 μA) is split off early on to serve a proton irradiation and cancer therapy test facility. (PSI is in the process of providing a separate accelerator for the cancer therapy facility in the near future and thus taking off some operational restrictions on the main accelerator system that result from this additional use.).

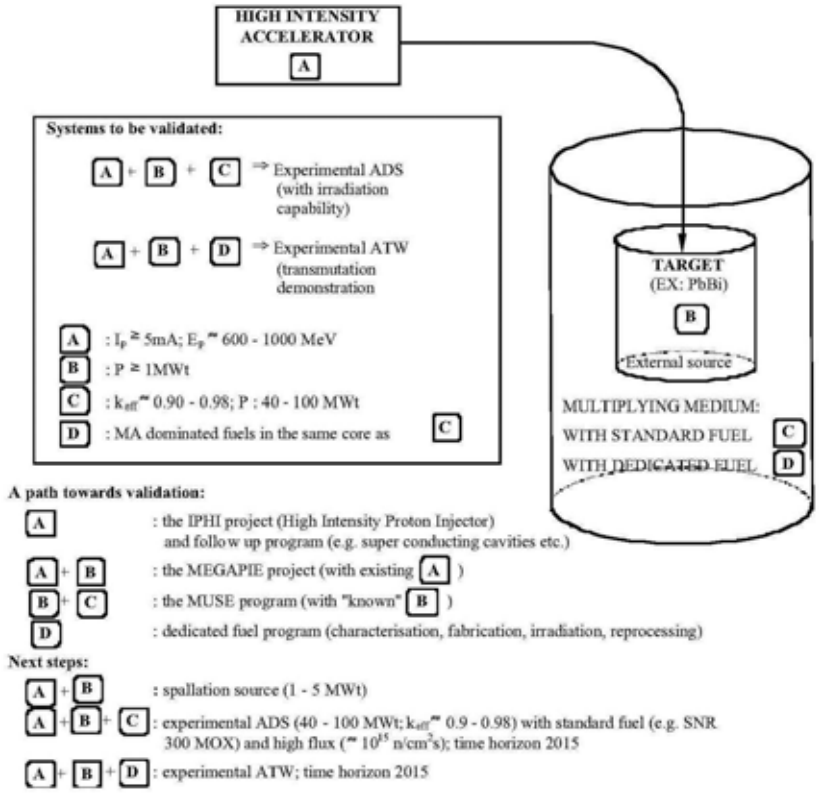


*FIG. 4.56. A step by step approach towards the validation and demonstration of the ADS concept.*

The main beam passes through two pion production targets (M and E), whereby its energy is reduced to 575 MeV. After passing through Target E the beam can either be dumped in a beam stopper or can be recaptured and bent downwards for onward transport to the spallation neutron source SINQ. Target

E, which is a 4cm long graphite target, causes some scattering of the beam. After this target 2/3 of the beam current (1.2mA) can be recaptured and transported to the SINQ target. The beam power presently available for SINQ thus is roughly 0.7MW and is expected to increase to 1 MW by 2004, the period for which the operation of the MEGAPIE target is planned.

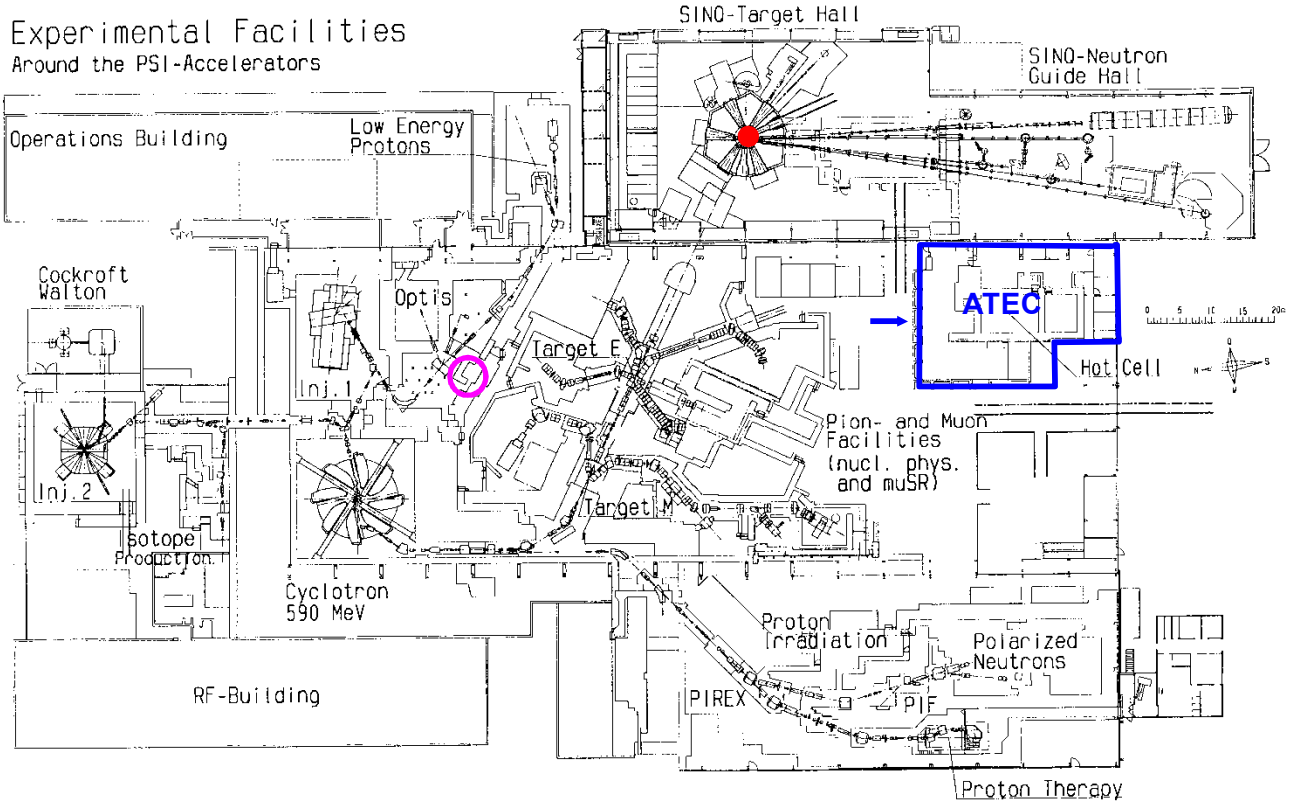


*FIG. 4.57. Schematic floor plan of the PSI accelerator complex and associated research facilities.*

— The spallation neutron source SINQ and its ancillary equipment

SINQ is designed as a neutron source mainly for research with extracted beams of thermal and cold neutrons, but hosts also facilities for isotope production and neutron activation analysis. Except for its different process of releasing the neutrons from matter, it resembles closely a medium flux research reactor for most of its users, since the neutron beams are extracted from a 2 m diameter heavy water moderator surrounding the target, as shown in Fig. 4.58. Beam injection into SINQ is from underneath and the target is inserted from the top and is suspended from the upper edge of the target shielding block.

Although the beam interaction region in the target is only about 30 cm long, the target unit is a 4 m long structure with 20 cm diameter in its lower 2 m, which widens to 40 cm in the upper half. These dimensions must also be adhered to with the MEGAPIE target. The present target is an array of solid rods cooled in cross flow by heavy water. Since it is essential to minimize neutron absorption in the region of the moderator tank in order to obtain a high neutron flux, the part of the target unit extending into the moderator tank is filled with heavy water, except for the rod bundle, which is about 40 cm long and is located in the centre of the moderator tank. The lower half of the target unit is enclosed in a double walled shell with separate heavy water cooling. This shell is presently made of aluminium alloy. Although it will be necessary to have such a shell surround the liquid metal container also in the case of the MEGAPIE target, it remains to be decided whether aluminium alloys

are still suitable or whether a material with higher strength at elevated temperatures needs to be chosen.

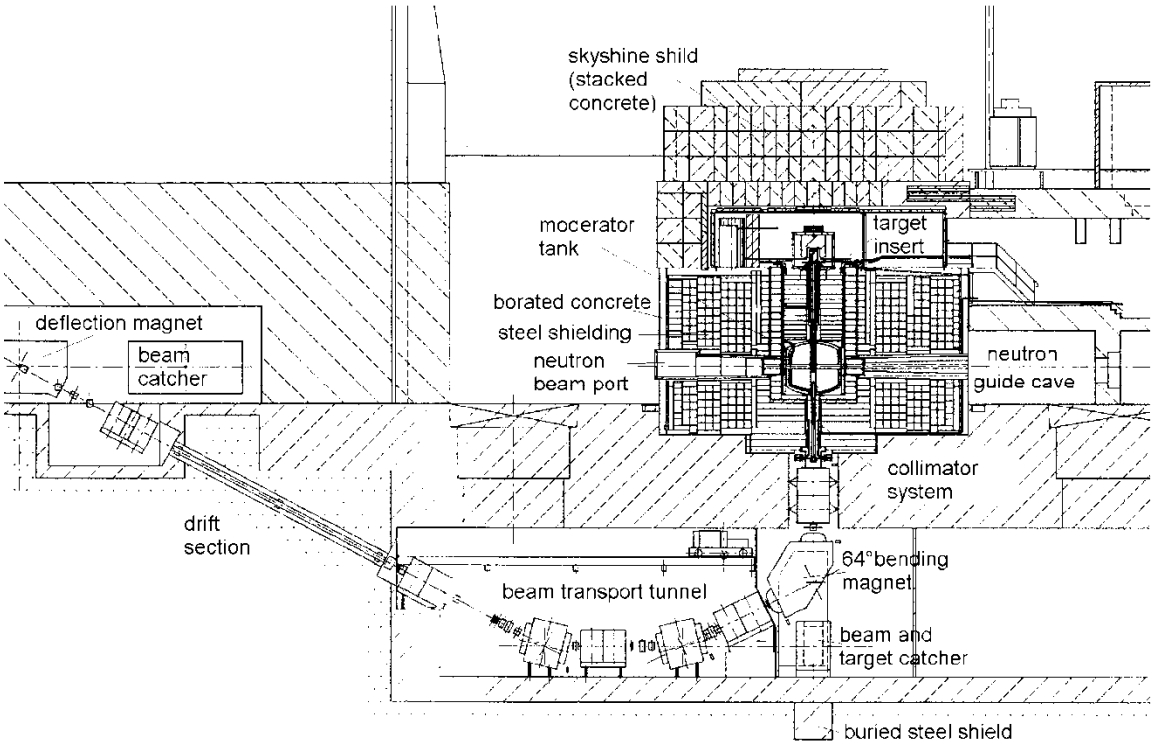


*FIG. 4.58. Vertical cut through the target block and part of the proton beam transport line of SINQ.*

The water cooling loop for the target has a heat removal capacity well above what is needed for either the solid or liquid metal target. It is, however, limited to operating temperatures below some 80°C and is not suitable for pressurisation to more than about 0.8 MPa. Hence, the water temperature of this loop cannot be raised to more than 125°C in order to prevent freezing of the PbBi. A different solution must be found for this problem.

The target is inserted into and removed from its operating position by means of a specially designed exchange flask which has an internal hoist to lift the target. This flask is transported by means of the overhead crane in the SINQ target hall, whose capacity is limited to 60 tons. The shielding of this flask is currently optimised for the solid target, which has its radioactivity concentrated in the bottom region. Although the specific activity of the liquid metal target will be much lower due to its significantly larger target mass, it remains to be examined whether the shielding in the upper part of the flask is sufficient. Possibilities for backfitting of the present flask are very limited due to both, its design and the weight limitations on the overhead crane.

— The active handling area ATEC

The area in the PSI Experiment Hall immediately adjacent to the SINQ Neutron Guide Hall (Fig. 4.57) is designed and equipped to handle large radioactive components and is generally used to service, repair and prepare for disposal all kinds of radioactive parts used in the operation of the facility. Its hot cell is equipped with a power manipulator, master slave manipulators and a movable heavy duty working table as well as several other items such as radiation monitoring, video cameras etc. Although access to the hot cell is possible through its roof, a specially designed port for horizontal access (arrow in Fig. 4.57) is used to insert the SINQ target, because limitations in height prevent vertical insertion with sufficient clearance for the manipulations required.

The SINQ targets No.1 and 2 were successfully dismantled and prepared for disposal in this cell. Samples from the target material and container shell were removed and one target was also reassembled in this hot cell. In principle this cell and its special equipment prepared for the handling

of the SINQ solid target should also be suitable to dismantle the liquid metal target. There are, however, some severe boundary conditions, the most important one being the fact that this hot cell is not equipped and licensed to handle α–activity. Thus, even if a method is developed to drain the liquid metal from the target before opening it, as is desirable for a variety of reasons, one must still be able to guarantee that no α–active isotopes are released into the cell during the manipulations foreseen.

Alternatively, the cell might be retrofit for handling α–active parts, but this would not only mean a significant additional expense, it would also make access much more difficult and would shut down the area for an extended period of time. The latter is a particular problem because the cell is more or less continuously utilised and must be available on short notice in case any of the vital components in the accelerator or beam transport systems fail. It shall, therefore, be an important task in the MEGAPIE design phase to develop a procdure for use inside the hot cell that guarantees that no α-activity is released into the cell when the target is opened to remove those parts on which post use examinations are foreseen.

— PSI hot cell facilities and PIE equipment

PSI is operating well equipped hot cells in which post-irradiation examinations (PIE) can be carried out with a large variety of different methods. Final definition of the PIE programme will be a relevant part of the project activity during the R&D and engineering design phase.

— Operation of the MEGAPIE target

The MEGAPIE target will, for a period of time of up to one year, replace the neutron production target in SINQ while utilisation of the facility will continue. This means that a high reflector flux and reliable operation are important issues in the project.

— Target development for SINQ in view of the MEGAPIE initiative

The first target (Mark 1) used for commissioning the SINQ facility was made up from simple Zircaloy rods. While this is a relatively well proven material in nuclear applications, its neutron yield is not optimum. It has, therefore, been an important goal of the SINQ target development programme to improve the neutron flux in the moderator and to maximise the time of reliable operation of the targets. In order to establish a data base for the design and operation of future targets, the first target was removed after half a year of operation (500 mAh total charge delivered). It was replaced by another one (Mark 2) which, while still being essentially a Zircaloy rod bundle, incorporated several test elements designed to provide data for future target concepts.

Apart from a large number of test specimens which will allow examining the radiation effects in a mixed proton fast and thermal neutron spectrum under varying load for the first time (STIP-collaboration, see below), the target also contained rods made from lead filled steel tubes. Although results from post-irradiation examinations are not yet available, the fact that no problems were encountered up to a total charge of 6.8 Ah (at which point the target was removed) seemed to justify the use of a target made up of lead filled steel tubes. In this way the thermal neutron flux increased by a factor of 1.45 relative to zircaloy. This target (Mark 3) is again loaded with test specimens. Following the investigation of the material from the Mark 2 target it is intended to decide whether or not Zircaloy can be used as a tube material for the lead rods, in which case another gain factor of 1.3 would be expected for the thermal flux. Currently the projected operating life for each target is 2 calendar years.

As for the MEGAPIE target, a period of 2 years (2000–2001) has been allotted to carry out the research and engineering work necessary to decide what the final design should be and to prepare the preliminary safety analysis report. At the end of this period a decision will be made whether to go ahead with the detailed design and construction, for which another two years are foreseen, including testing without beam. This sets the beginning of the year 2004 as the goal for putting the MEGAPIE target into SINQ. A standby target will be ready in case some unforeseen difficulty arises in the last minute. This target will be used at the end of the operating period of the MEGAPIE target, unless a follow-up liquid metal target will be available. The duration of the irradiation period will be decided

upon, based on the results obtained up to that point from supporting research, but the design goal was set to 6000 mAh, which corresponds to 1 year of full power operation at 1 MW. A rough schedule of the MEGAPIE project is shown in Fig. 4.59.

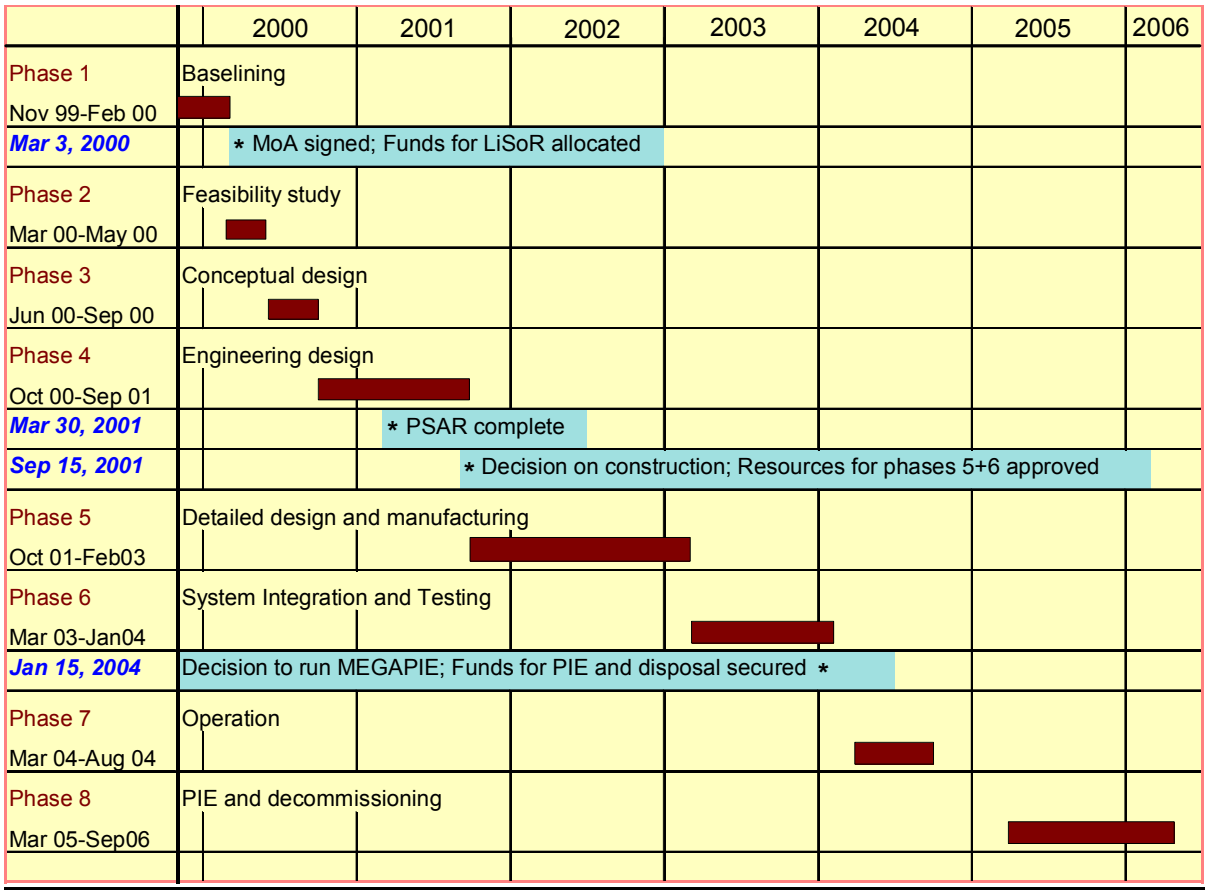


*FIG. 4.59. The MEGAPIE project phases and major mile stones.*

(c) Baseline of the MEGAPIE project

The overall (level 0) project baseline as agreed upon as a basis to draw up an Agreement of Collaboration between the partners is as follows:

— MEGAPIE is an experiment to be carried out in the SINQ target location at the Paul Scherrer Institut and aims at demonstrating the safe operation of a liquid metal spallation target at a beam power in the region of 1 MW. It will be equipped to provide the largest possible amount of scientific and technical information without jeopardising its safe operation. The minimum design service life will be 1 year (6000 mAh).

— MEGAPIE is an international collaboration in pursuit of common interests and in order to pool existing know-how and resources. The experiment will not constitute a major disruption to the primary mission of SINQ, namely the supply of neutrons to the user instruments. No specific new requirements will result for the operation of the PSI accelerator system.

— The maximum incremental total project cost (ITPC, total project cost over and above efforts going on in the participating laboratories or funded by other sources, e.g. EU-programmes), to be shared by the participants, shall be 10 MSFr, including final disposal. No charge will be levied by PSI for the proton beam. Start of irradiation will be March 2004; the duration of the project will be though 2006, including PIE and decommissioning.

— Target material will be the PbBi eutectic mixture. The design beam power is 1 MW at 600 MeV. Existing facilities and equipment at PSI will be used to the largest possible extent. Cooling water loops of the target station will be left largely unchanged and will be ready for use with a solid target again within less than 1 month after termination of the MEGAPIE irradiation.

— The overall project leadership rests with CEA, while PSI takes charge of the technical coordination, since the experiment will be licensed under Swiss authority. The project will be overseen by a Project Steering Committee (PSC) in which the participating laboratories are represented. Each participating laboratory will nominate a responsible Local Coordinator (LC), who will be a member of the Project Management Group (PMG) and will be given the executive power to see to it that the laboratory fulfils its technical commitments in accordance with the overall project needs. The PMG will be chaired by the Project Director (PD). Task leaders (TL) will be nominated for specific subunits of the project. The TL and the PMG will form the Project Control Team (PCT).

(d) The MEGAPIE collaboration

Originally proposed by three laboratories, CEA Cadarache (F), FZ Karlsruhe (D) and PSI (CH), the MEGAPIE collaboration has since been joined by four more institutions, namely ENEA (I), SCK•CEN (B), JAEA (J) and CNRS (F) jointly with SUBATECH and later by the EU, the DOE (USA) and KAERI (Korea). An Agreement of Collaboration (AoC) was worked out in which the terms of the collaboration are laid down. In accordance with the general project baseline (see above), a Project Steering Committee (PSC) was formally established as the controlling body of the project. All participating institutions are represented in the PSC. Its main tasks are to ensure the necessary support from the different parties, approve the project planning, authorise the project spending plan, monitor progress and decide on corrective actions. The Collaboration is open to new members who are willing to contribute actively to the funding and realisation of the project. The PSC will decide on the use of additional funds from new partner or research programmes.

A Common Funding was agreed upon as joint funding for the project to cover the amount of new money (money to be spent specifically for the execution of the project, not including own man power and direct or indirect cost of related R&D — as opposed to supporting developments — at the parties). This Common Funds will be controlled by the PSC. While a fixed distribution key has been agreed upon for this common funds, the supporting R&D work is carried out on a best effort basis by the participating laboratories and all results are made available to all participants.

(e) Technical baseline of the MEGAPIE target

— Introduction

The MEGAPIE target will be used in the existing target block of SINQ. A vertical cut through this target block and parts of the proton beam line is shown in Fig. 4.58.

The beam enters the target block from underneath and passes through a collimator system which, on the one hand prevents the proton beam from hitting the central tube of the moderator tank surrounding the target and, on the other hand limits the intensity and angular divergence of the evaporation neutrons streaming back from the target into the beam transport system. A specia, heavily shielded catcher device is located beneath the last bending magnet to avoid soil activation by the remaining neutrons and, in case of a catastrophic target failure, hold the debris that would eventually fall down. This part of the beam line is designed for use with a solid target only and some retrofitting will become necessary for use with a liquid metal target.

— Technical baseline

The technical baseline of the MEGAPIE target developed in view of the above boundary conditions is schematically represented in Fig. 4.60, showing the main components of the target unit and the required new auxiliary systems.

— The target unit

The original concept for the SINQ target was to move the liquid metal from the beam interaction zone to the heat exchanger by natural convection [4.49]. This has the benefit of being a completely passive system and it was shown that, in an equilibrium situation, is also sufficient to establish the necessary flow of about 4 l/sec/MW. However the situation during transients is difficult to control. In order to avoid the risk of local overheating it would be necessary to restart the beam after each trip with a

carefully controlled ramp. In particular the flow configuration at the beam entrance window becomes very unpredictable.

In order to rectify this latter problem tests were carried out at the large mercury loop of the University of Latvia in Riga, using a pumped bypass flow across a hemispherical window in a full scale mock-up of the SINQ target [4.50] [4.51]. It was shown that, even in a non-wetting condition inverse heat transfer coefficients of 0.5 K/W/cm$^2$ could be obtained, which is a factor of 5 lower than without a bypass flow. For this reason the concept of a pumped bypass flow of 1 l/sec to cool the window was adopted as a reference for MEGAPIE. Although this flow from the bypass pump might be sufficient to avoid overheating during transients, the technical baseline for MEGAPIE was chosen to include a pump also for the main flow. Its estimated capacity should be 4 l/sec at a pressure head of less than 0.01 MPa. Although an EM-pump has been selected as reference concept, other alternatives will still be evaluated.

The heat exchanger system must be designed such that freezing of the liquid metal can be safely avoided everywhere in the system even in cases of variable beam power or extended shutdown periods (e.g. the weekly 1–2 days of accelerator maintenance and beam development). Several options to achieve this have been identified. The one selected as the reference concept includes a double walled heat exchanger with an intermediate heat transfer fluid whose level can be varied (e.g. by pressurising a gas volume connected to it).

Since the existing target exchange flask is shielded to handle solid targets, i.e. has most of its shielding in the lower part, it is important to keep the amount of PbBi in the upper part of the target small. To this end displacement bodies of steel are foreseen around the heat exchanger pins and below the heat exchanger — pump unit. The main flow guide tube which serves to separate the upward flow in the centre of the target from the downward flow in the outer annulus is planned to form one unit together with the pump system. It will have a ceramic insulated heater system attached to it in order to facilitate initial filling of the target and as a second means of preventing the liquid metal from freezing. A gas filled expansion volume will be located above the liquid metal level.

The structural material for the target container is foreseen to be martensitic (French designation T91 type) steel, at least in its lower part. For the upper part the use of austenitic (316L type) steel is being considered, which is more readily available and easier to weld. This is contingent upon sufficiently high liquid metal corrosion resistance, because the highest temperature gradient in the system will occur along the heat exchanger. In order to facilitate the transition between two different materials the two parts will be joined by a flange system. The whole target container will be surrounded by a second enclosure with an insulating vacuum between. In the lower part this enclosure will be double walled with heavy water cooling as is the present target shell. The material for this part will be chosen for minimum neutron absorption and sufficient strength at any temperature the shell might reach in the case of a breach of the target container. Presently zircaloy 2 is the favoured material, but this needs to be studied in detail. Again, as in the present target concept, the upper and lower parts of the outer shell will be joined by a flange. The upper part of the outer shell will be stainless steel. Sufficient shielding shall be provided in the top part of the target to avoid excessive radiation levels in the target head room from direct gamma radiation from the liquid metal. Whenever possible, the feeds through this shield should be designed to avoid direct sight.

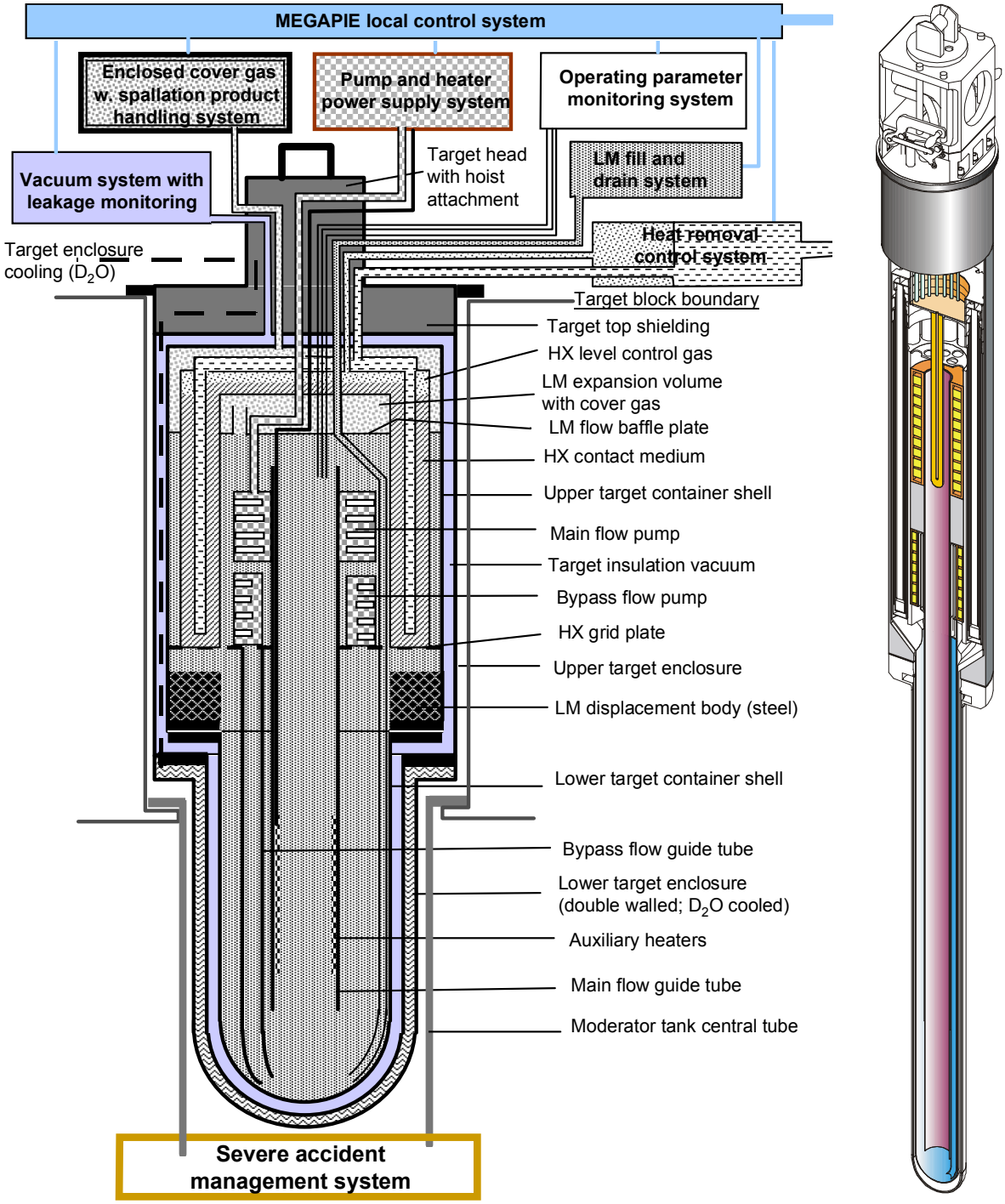


*FIG. 4.60. The basic concept (left) and conceptual design (right) of the MEGAPIE target.*

— Auxiliary systems

While changes to existing auxiliary systems of the SINQ target shall be kept to a minimum, there will be a number of additional auxiliary systems required for the safe operation of the MEGAPIE target. They are schematically indicated in Fig. 4.60.

- Cover gas and spallation product handling system

Volatile spallation products will enter the cover gas of the expansion volume during operation of the MEGAPIE target. This will include light species (isotopes of hydrogen, helium) as well as noble gases and possibly mercury. An assessment of the production rates can be found in [4.52]. All condensable species should be trapped either inside the expansion volume (e.g. by a water cooled baffle) or in a specially enclosed cover gas handling system. The question of tritium treatment needs

still to be evaluated. It can either be released under controlled conditions into the ventilation system or retained in special getters.

- Liquid metal fill and drain system

Filling the target must be effected in a very careful manner, making sure that all surfaces and the target material are in the required conditions. It remains to be decided whether the PbBi will be drained from the target or whether it will be allowed to solidify after the end of the irradiation period. This decision will have a strong effect on the design and location of the LM fill and drain system. In any case this work package will include the liquid metal technology system. There will also be a close interrelation with the expansion room cover gas system, since this will be used to preheat the structure for filling and, eventually, to push the PbBi out of the container. Filling and draining must also be provided for the heat exchanger intermediate fluid with precautions taken for potential radioactivity of the fluid after use.

- Vacuum and leakage monitoring system

A new vacuum system with controlled exhaust will be required to maintain the insulating vacuum between the LM container and the outer target shell. This vacuum will be continuously monitored for spallation products and water vapour in order to detect any leaks in the system. The question, whether or not a continuous stream of a small amount of carrier gas is desirable to speed up the response time of this monitoring system needs yet to be decided. It is intended to have also other, redundant, leakage monitors such as electrical contacts in this volume.

- Heat removal and liquid metal temperature control system

As mentioned before, heat removal from the target needs to be closely controlled in order to avoid freezing of the LM anywhere in the system. Various concepts have been identified which can be implemented individually or in combination. These include:

- Activating the auxiliary heater system in the guide tube;
- Using an economiser second heat exchanger, eventually with water preheating in a bypass stream, to keep the water temperature level in the heat exchanger pins higher than in the existing cooling loop;
- Controlling the heat transfer in the primary heat exchanger, for example by varying the level of an intermediate heat transfer fluid;
- Varying the efficiency of the EM-pump through the frequency of its current supply.

The economiser secondary heat exchange system will have to be installed in the room above the target head.

Pump and heater power supply system:

The power supplies for the pumps and heaters will have to be installed outside the target head room for easy access and space. This requires new cabling into the target head room.

- MEGAPIE local control system

All additional parameter monitoring and controlling required to operate the MEGAPIE target will be handled by a local control system which will be located outside the target head room and will be connected to the main SINQ control system.

- Operating parameters monitoring system

All operating parameters which need to be monitored (temperatures, pressure, flow rates etc.) in order to verify design predictions but are of no or little safety relevance will be collected in this system and will be transferred to the SINQ control system for data logging. Details of the parameters to be surveyed need yet to be defined.

- Severe accident management system

Every possible precaution will be taken to avoid severe accidents during the operation of the MEGAPIE target. As far as the target block is concerned, the necessary precautions against the consequences of an earth quake or an air plane crash have already been implemented. A breach of the outermost shell or both shells of the lower, D2O cooled enclosure is equivalent to the same accident in the present situation and need not be discussed further. Similarly, a breach of the LM container alone would not constitute a severe accident because the target could still be removed by the normal procedure. The one potential severe accident that needs to be studied in detail for the liquid metal target as opposed to the solid target is the simultaneous breach of all three shells separating the liquid metal from the beam line vacuum.

Since the three shells of the target containment are exposed to different environments during operation and are likely to be made of different materials, the only credible common cause of failure would be an inadvertent focusing of the proton beam and consequent overheating of all three shells. The collimator below the target and several monitors along the beam line are in place to guard against this situation, but there is no passive system to avoid it in the event of a loss of Target E. In this case liquid metal would enter the proton beam vacuum and would severely contaminate parts of the beam vacuum tube. While this is not an accident which would pose an immediate risk to the public, its consequence might be a very long shutdown of SINQ and significant radiation exposure of workers during the cleanup operation. It is, therefore, a question of risk management within PSI, whether and to what extent modifications to the existing system (vacuum pipe, catcher and collimator below target) shall be implemented to shorten a potential shutdown period in the unlikely case of such an event. The present position is to study possible measures and their implications and to decide about their realisation on the basis of a serious analysis. This decision will have to be made at latest in the early months of the engineering design phase before submission of the safety analysis report.

(f) Conclusions on the design and construction

The MEGAPIE project will be an essential step towards demonstrating the feasibility of the coupling of a high power accelerator, a spallation target and a subcritical assembly. It will specifically address one of the most critical issues, namely the behaviour of a liquid metal target under realistic operating conditions. As an intensely instrumented pilot experiment it will provide valuable data for benchmarking of frequently used computer codes and will allow gaining important experience in the safe handling of components that have been irradiated in contact with PbBi.

The supporting R&D activities focus ongoing research and streamline efforts in several European laboratories.

MEGAPIE will also be a valuable contribution to potential collaborations with partners outside Europe, and can help to establish an effective sharing of work.

The envisaged target date (irradiation in 2004) is consistent with development plans in the Accelerator Driven System domain and with the milestones of the 5th and 6th European Union Framework Programmes, as well as with upgrade plans in the SINQ facility.

The results obtained in this pilot experiment will also help PSI to decide whether or not it wants to go ahead with the development of a liquid metal target for routine use in its spallation neutron source. If the answer is positive, this will be a continuous source of experience and information which will benefit the ADS activities of all participating parties.

(g) Operational experience

Meanwhile the MEGAPIE target has been operated in SINQ from mid August 2006 until December 21st, 2006. Over that period, the routine proton current received by MEGAPIE was at about 1300 μA, corresponding to a beam power of 0.78 MW.

The section presents in brief the main features of the target and the ancillary systems and summarizes the general performance and the operational experiences, including new beam and target safety

devices, the general functionality and lessons learned. For more details on design, operation and system performance we refer to [4.53].

The first beam on Megapie was received on Aug. 14th, 2006 with a beam current of 40 μA, which corresponds to about 25 kW. The second phase of the startup procedure was successfully accomplished the following day, where the power was stepwise increased to 150 kW (250 μA proton current). Normal user operation with MEGAPIE started on August 21st, and was continued until the normal annual winter shutdown starting on December 21st, 2006. All over this period the availability of SINQ, relating accepted to offered proton beam, was at satisfactory ~95%. The total proton charge accumulated at the end was 2.796 Ah.

During the MEGAPIE irradiation experiment the target experienced 5500 beam trips (<1 min) and 570 interrupts (< 8 h) with the consequence of temperature transients (see Fig. 4.61) and related variable stresses. Even so the behaviour was found excellent. The temperature distributions and transients were as expected, very close to predictions.

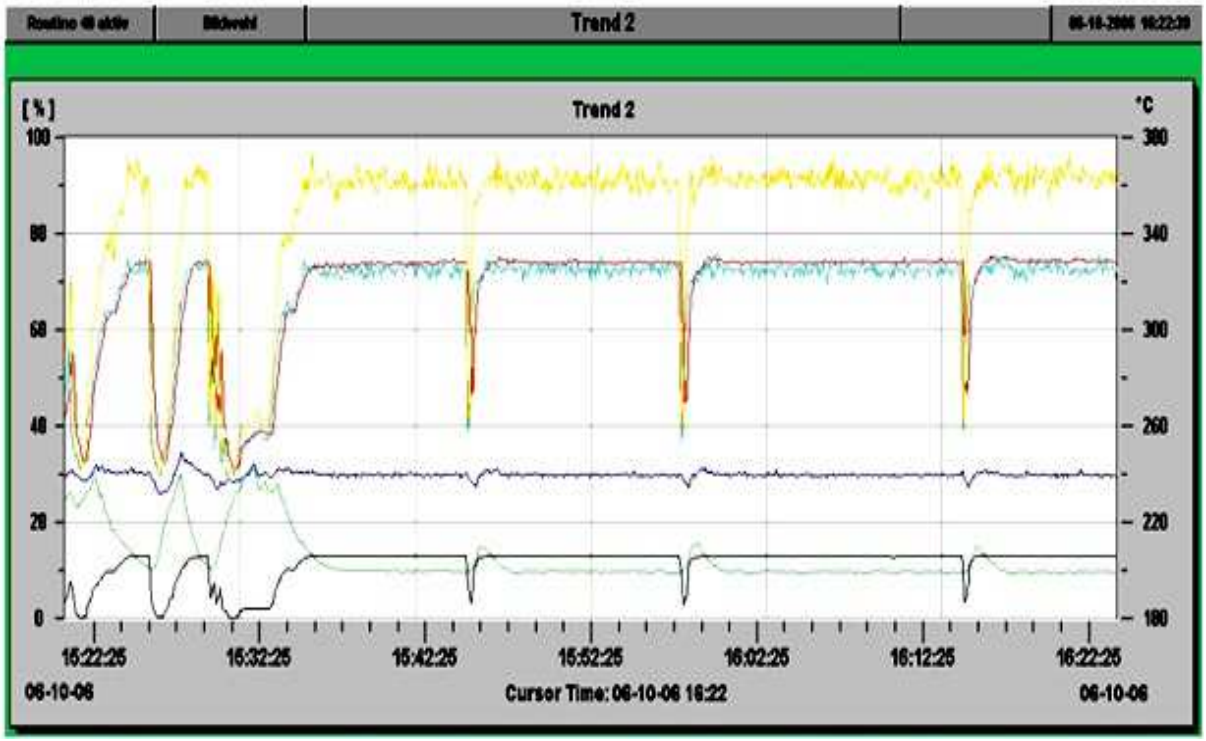


*FIG. 4.61. Time history of relevant temperatures responding to beam trips from full power.*

The electromagnetic pumps operated stable and reliably, without any indication of degradation. For the operational experience with the MEGAPIE ancillary systems see the special chapter below. All in all, the MEGAPIE systems worked reliably according to specifications, exceeding our rather cautious expectations.

Ancillary systems functional experience and lessons learned

The main MEGAPIE ancillary systems directly necessary for the target operation are the heat removal system (HRS), the cover gas system (CGS), the insulation gas system (IGS) and the fill and drain system (F&D). Fig. 4.62 shows the systems installed in the target head enclosure chamber (TKE), shortly before final commissioning. For the basic functional requirements and the technical layout refer to [4.54]–[4.58]. The present description mainly focuses on the experience gained during the design and operational phases.

*FIG. 4.62. View into the TKE which is on top of the SINQ main shielding block (situation of April 2006). The target head is in the centre, still without the cables connected which are in preparation in the rear, the oil loop of the HRS is at the right, the F&D system at the left, and the CGS in the left rear corner (partly hidden).*

The Heat Removal System HRS [4.54] consists of two subsystems: an intermediate cooling loop with oil Diphyl THT as cooling medium (ICL), connected to the heat exchanger pins in the target, and second a back cooling water loop (WCL). The ICL, operating between 160°C and 230°C, is primarily necessary to remove the about 0.6 Megawatt of heat load deposited in the liquid LBE by the proton beam. As a second function it must also be capable to manage a controlled hot standby operation after beam trips or scheduled beam interruptions to prevent freezing of the target.

The general layout of the system proved to be sound. Oil as cooling medium turned out to be a reasonably good choice. The heat removal capacity of the system was rather over dimensioned. Oil degradation by radiolysis and pyrolysis was found to be much less than anticipated. The main drawback of using oil is the need for fire protection which was achieved by inertization of the atmosphere in the TKE and in the beam transport vault.

The Cover Gas System CGS [4.55] must handle the volatile radioactive and non-radioactive inventory of spallation products released from the LBE in the target. Handling of radioactive gases and volatiles imposes stringent requirements on safe and remote operation, on retention of radioactivity, like second containment and tightness, and on shielding. The schematic layout is shown in Fig. 4.63, together with a photo of the shielded decay tank box.

The chosen design, in principle, proved sustainable; in practice, meeting the stringent requirements turned out to be rather complex and expensive. One lesson learned with the system was, that 'leak tightness' for gases in the conventional definition is not the same as for radioactive gases: In spite of successful He leak tests according to specification a leak from the decay tank into the 2nd containment was detected by the very sensitive detector controlling the circulating gas. Although clearly detectable, the leak was sufficiently small such that the inventory could be released weekly by venting of the 2nd containment through the controlled exhaust system. A further lesson was to care for redundancy (if possible double) of vital sensors in such a delicate system: one pressure transducer inside the enclosure controlling and recording the plenum gas pressure failed, most likely due to

radiation damage, although qualified for radiation resistance up to a total gamma dose of 1 MGy. Switching to the remaining redundancy solved the problem, but after that no redundancy remained.

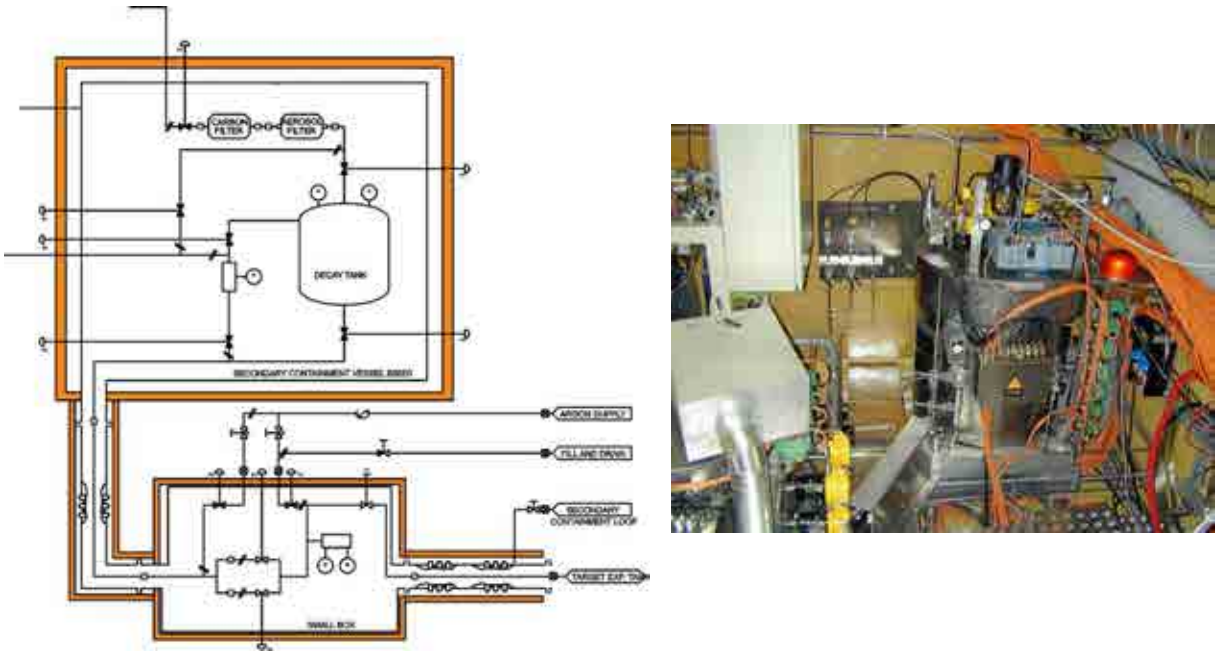

*FIG. 4.63. Schematic layout of the CGS, including second containment and shielding (left) and photo of the decay tank box in the TKE (right).*

A further critical issue is gas sampling, indispensable to control the inventory before venting. Reliable and quantitative gas sampling is a difficult action and can be a hazardous job which needs special precautions, not at least to prevent or minimize radioactive exposure of the executive personnel. A qualified steel gas mouse with easy to handle valve and flange connection is a minimum requirement.

The Insulating Gas System IGS [4.56] fills the volume between the inner hot part of the target and the outer cold hull by an insulating gas. The concept envisaged was filling with He at a pressure of 0.5 bar, benefiting from lower activation on the expense of a higher heat loss compared to filling with Ar. During preheating the empty target it turned out that evacuation was necessary to prevent excessive heat loss. After the target was filled with liquid metal, during refilling the isolation volume with He we experienced that 4 out of 7 electric heaters in the lower central target were damaged, probably caused by electric discharges. The loss of heaters did not hamper or inhibit further operation, but another draining and refilling with liquid metal would not have been possible any more.

One of the accident scenarios which needed to be safely handled was water ingress from a leaking safety hull into the insulating gas volume with the consequence of steam production and possible pressure buildup. This was accomplished by installing a 40 mm exhaust pipe combined with a rupture disk and a steam condenser vessel outside the insulation volume.

Designed as closed volume the pressure in the IGS was expected to remain constant during target operation, only reacting to temperature variations. Instead, starting with the first beam a continuous gas pressure increase of about 5 mbar/h was observed. Thorough analysis gave evidence that most likely oil from the HRS was leaking into the IGS volume and decomposed by radiolysis during beam operation. The gas produced further contained small amounts of (radioactive) cover gas, entering through a second (small) leak. The gas production urged a weekly venting of the IGS. The measures taken to cope with this problem were the installation of a 180 l decay vessel in the cooling plant and regular (weekly) venting into the exhaust system after a sufficient decay period and gas sampling. The lessons learned: do not rely on closed volumes, expect radioactivity everywhere and provide devices to handle that.

The initial baseline for the Fill and Drain System F&D required draining of activated LBE from the target after the operation period. A detailed design for that was elaborated; however, the draining option was recognized to bear considerable risks, immediate ones for accessing the TKE and more general ones related to licensing. As well, it had required considerable extra expenditure in the technical realization: the active draining option would have imposed the need of radiation shielding, second containment, radiation hard components and remote operation, similar to the CGS.

Viewing these difficulties the decision was taken to abandon the initial concept in favour of only inactive draining and final freezing of the LBE in the target after completion of the irradiation experiment [4.57] [4.58] The inherent final freezing imposes mechanical stressing of the hull and window material due to the well known volume expansion of solidified LBE. Hence, postirradiation alterations of the materials properties are not completely excluded. This drawback is handled by controlled slow freezing of the LBE in the lower target volume.

The finally realized concept is sound; the system is reasonably safe and easy to operate. The experience during commissioning recommends providing sufficient trace heaters and place controlling thermocouples at the coldest points to prevent clogging. The missing oxygen control did not impose a problem.

Beam monitoring and LBE leak detection system which make sure that no liquid metal can leak out of the target are of utmost importance for the safety of the MEGAPIE experiment. In the case of breaking the integrity of the lower target enclosure in the SINQ, LBE would spill into the beam line and cause a major accident. While the impact to the environment could be kept within acceptable limits, the situation for the PSI SINQ installations would be very serious.

For safe target operation a sufficiently broad footprint of the incident proton beam on the SINQ target is mandatory. With a focused beam at the resulting high current density it would take only 170 ms until a hole is burned through both the liquid metal container inside the target and the lower target enclosure (double walled safety hull) with the fatal consequences cited above. In order to prevent an insufficiently scattered beam from reaching the SINQ target three independent safety systems have been installed: a dedicated current monitoring system, a beam collimating slit and a novel beam diagnostic device named VIMOS [4.59]. The latter monitors the correct glowing of a tungsten mesh closely in front of the liquid metal target. Fig. 4.64 shows a Photo of this device taken before installation. All these systems have to meet the basic requirement to switch off the beam within 100 ms when they respond to off normal situations.

Similarly to an improper beam density also LBE leaking from the container requires tripping of the proton beam. Two different types of leak detectors have been developed: one employing thermocouples and an ancillary device monitoring the electrical impedance between special electrodes. The assembly at the lower end of the liquid metal container is shown in Fig. 4.65. During the operation of the MEGAPIE target the temperature based leak detector proved its robustness and showed the expected response to beam-on operation and transients. Its response to a leak had been monitored in an earlier full scale leak test; in the real experiment, fortunately, no leak occurred.

*FIG. 4.64. VIMOS head with a Tungsten wire mesh to be installed close in front of the target window.*

*FIG. 4.65. MEGAPIE leak detector mounted at the beam entrance calotte of the liquid metal container.*

Neutronic performance of MEGAPIE

During the startup phases, several neutronic measurements were performed, i.e. measurements of delayed neutrons in the target head area, Bonner spheres and chopper measurements for spectral resolution at the ICON beam port, fission chamber measurements from inside the target and neutron flux measurements inside the $D_2O$ moderator and at selected instruments and beam ports. Stimulated by these early measurements, a new campaign of simulations started to calculate the neutron fluxes at the actual positions were the measurements were performed. The main results are given in Table 4.19. Results for the solid target Mark IV are also included in the table. The data show that: i) the agreement between absolute flux values is rather good for most of the measurements. This indicates that the fluxes with the MEGAPIE target model are correctly calculated; and ii) the measured increase of the flux performance is of a factor 1.78–1.85, which is somewhat higher than the predictions. The difference is mostly understood in light of the newer calculations of the solid target, which include the STIP samples and the fact that the lead occupies only 90% of the volume inside a rod.

Complementary to the external flux measurements, the inner neutron flux was measured and monitored during the whole target irradiation by an array of miniaturized fission chambers placed in the central rod right above the spallation zone. First results are reported in [4.53].

TABLE 4.19. CALCULATIONS AND MEASUREMENTS FOR RELEVANT THERMAL NEUTRON
(Calculated values are the integral between 0 and 1 eV. Systematic uncertainties on the experimental fluxes are of the order of 10%. Uncertainties on the experimental data are of about 8%).

| | SINQ target 6 (2005) | | MEGAPIE (2006) | | RATIO | |
|---|---|---|---|---|---|---|
| | EXP | CALC (E<1eV) | EXP | CALC(E<1eV) | EXP | CALC (E<1eV) |
| NEUTRA (30) | $2.55\times10^{7}$ | $2.43\times10^{7}$ (3%) | $4.80\times10^{7}$ | $3.81\times10^{7}$ (2%) | 1.85 | 1.57 |
| ICON (50) | $4.27\times10^{8}$ | $4.77\times10^{8}$ (1%) | $7.73\times10^{8}$ | $8.0\times10^{8}$ (2%) | 1.81 | 1.68 |
| NAA | $5.06\times10^{12}$ | $6.43\times10^{12}$ (2%) | $9.01\times10^{12}$ | $1.14\times10^{13}$ (2%) | 1.78 | 1.77 |

(h) Conclusion

The very challenging milestone to operate a representative, high power heavy liquid metal spallation target on the road towards a possible ADS development has been effectively achieved. Indeed, the MEGAPIE target, which is of significant power, has been operated successfully from August 2006 to December 2006 in the SINQ facility at PSI, producing innovative know-how and expertise on the different components and materials of a heavy liquid metal spallation target.

The results achieved so far within the MEGAPIE project clearly indicate that a step forward has been made in the neutronics and thermalhydraulics code validation for HLM systems. Moreover, an increased confidence has been gained in the procedures needed to assess structural material performances, in the area of component (e.g. pump systems) testing and on the crucial issue of the beam window coolability.

For instance, the analysis of the neutronics data gathered during the irradiation of MEGAPIE confirmed the expected increase in neutron flux obtained with the MEGAPIE target with respect to the performance of previous solid targets irradiated in SINQ.

Moreover, the integration of the target and of the ancillary systems, the execution of the integral test, the first operation and the irradiation, allowed getting confidence with the startup and routine operation of this innovative system.

As next steps of the MEGAPIE project, after the dismantling of the target, an extensive PIE is foreseen to complete the evaluation on the components and materials performance under irradiation completing the assessment of a first of a kind high power liquid metal spallation target.

#### *4.4.1.2. The Japanese programme*

(a) Design Study of solid tungsten target for sodium cooled ADS

— Purpose and goal

In order to achieve the effective transmutation of MA, fast neutron spectrum field formed with sodium coolant is one of the hopeful options. For the sodium cooled ADS, heavy metal spallation target is indispensable. The solid tungsten is selected because of its good compatibility with liquid metal coolant and its good performance in the past experiences [4.60].

— Theoretical explanation and results

To flatten the power density distribution in the fuel region, uniform neutron emission distribution is desirable for the spallation target of ADS. According to the experience in fast reactor development, tungsten has a good compatibility with liquid sodium in a neutron flux field. The target is composed of the multi layered tungsten disks. Each target disc has several coolant flow holes and these holes are located in a staggered manner from layer to layer to suppress the streaming of the high energy particles throughout the target.

For the reference design of sodium cooled ADS with 800 MW of thermal output, an effective diameter and length of the target is 50 cm and 85 cm, respectively. The diameter of the target is determined by the allowable beam current density of the beam window. The length of the target was determined by the stopping length of primary proton beam power.

To define the detail configuration of target disc layout, incident proton beam condition was assumed to have energy of 1.5 GeV, the same radius as that of the target, and a flat profile. From the comparison of optimum multilayer disc type target and bare target, a bulk target has a higher number of neutron yield by about 10% more than that of multi layered target, but it also gives two times higher peaking of neutron emission distribution from the target than that of the multi layered one. Fig. 4.66 shows the comparison of the axial neutron emission distributions from the multi layered target model and the bulk target model.

Based on the optimum configuration of target disks, target subassembly is designed as illustrated in Fig. 4.67. In this figure, coolant flows from right hand side to left hand side (upward direction in reactor vessel) and proton beam is injected from left hand side direction. The thickness of the disc becomes thick according to the beam direction to suppress the higher neutron yield at beam injection part and leakage of primary proton from the bottom of the target.

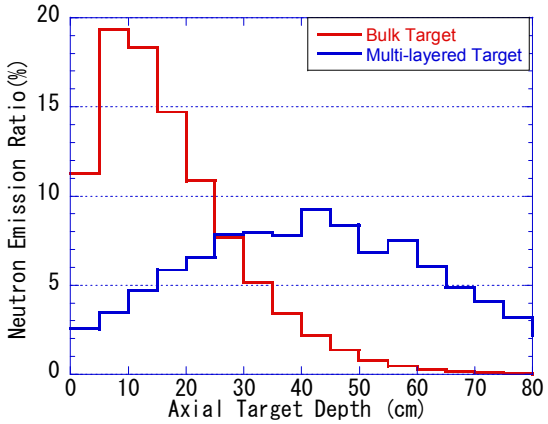


*FIG. 4.66. Comparison of axial neutron emission distribution.*

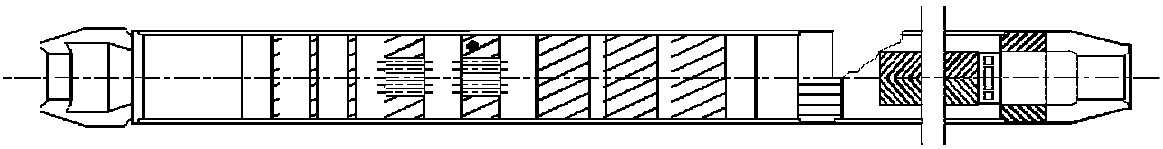

*FIG. 4.67. Conceptual drawing of tungsten disc target subassembly.*

(b) Design study of TEF 200kW Pb-Bi target

— Purpose and goal

The 200kW Pb-Bi spallation target installed in ADS Target Test Facility (TEF-T) on J-PARC project is planned to use following purposes, mechanical tests for structural materials under the proton–neutron irradiation condition in flowing Pb-Bi environment and engineering tests for Pb-Bi liquid spallation target system (see Fig. 4.68) [4.61].

— Instruments description

A primary Pb-Bi loop which acts as a spallation target is designed to allow Pb-Bi flow with 2 meter per second of a maximum velocity and 450 degree centigrade of maximum temperature. A type 316 stainless steel is tentatively assigned as a structural material of the target vessel. Target vessel is a sealed double annular cylindrical tube with a 90 degree bend section. Pb-Bi is circulated by electromagnetic pump that is completely separated from the target tube. By using this newly designed target, target can be replaced quickly and easily by withdrawing the target tube in upward direction from heat exchanger, electromagnetic flowmeter, and electromagnetic pump. Several electronic measuring equipments such as thermocouple are needed for operation but these items can be disconnected easily by remote handling devices. The maintenances of the spent-new target tube will be done at the access cell which has functions to clean up residual Pb-Bi to reduce exposure dose by the spallation products, and to pick up irradiated material test pieces by using remote handling devices.

According to the preliminary analysis of the Pb-Bi target neutronics, the radiation damage of type 316 stainless steel samples which are put in the liquid Pb-Bi target with 400 degree centigrade partially becomes more than 10 DPA (Displacement per Atom) per year. It is expected that the Pb-Bi target of TEF-T has enough performance to irradiate samples at ADS operating condition by adjusting the beam profile.

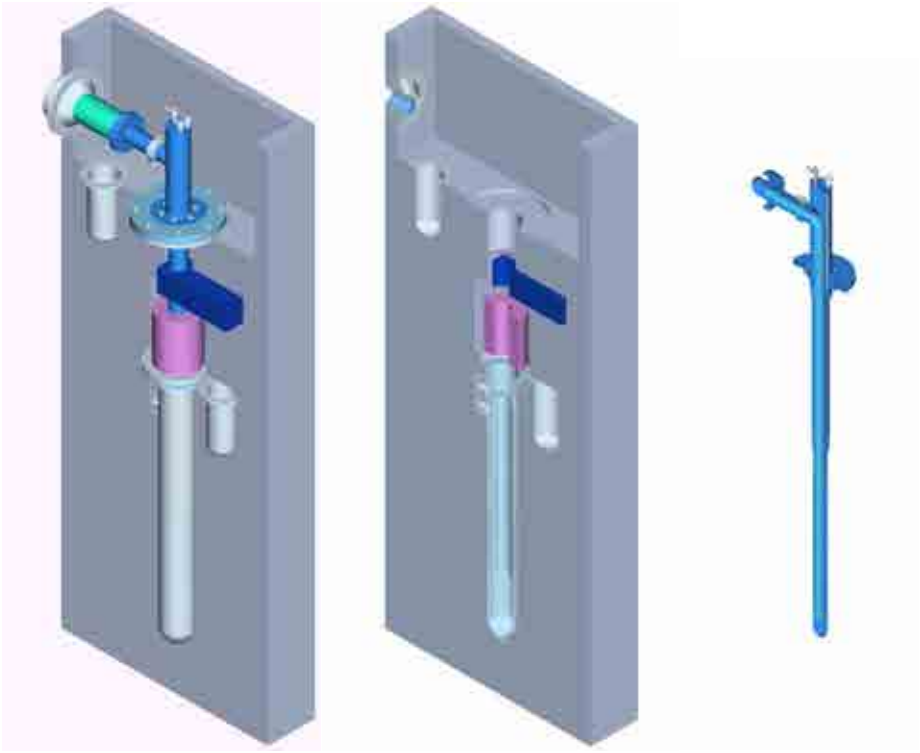

In operation Facility side device layout Target unit

*FIG. 4.68. Sealed annular tube type spallation target for TEF-T.*

*4.4.1.3. Researches on ADS window target in Russia*

(a) Introduction

This section is devoted to experimental and numerical studies of thermal and hydrodynamic processes realized in an ADS window target. These studies are related to design of a target system TS-1.

Target System TS-1 is a component of experimental facility created in Los-Alamos National Laboratory for testing in proton beam, which is generated in accelerator LANSCE. Eutectic lead-bismuth alloy (Pb-Bi) is used as a target material. Volume of ion-conductor and volume of target are separated by thin metallic membrane. A beam of high energy neutrons is generated in the target, when proton beam interacts with target material. This process is accompanied by volumetric power generation in 600 kW that creates tense working conditions as for membrane, and for other structural elements. Flow of Pb-Bi alloy has to provide required heat transfer from membrane surface and heat removal from the target volume in nominal, transient and accident conditions.

Target working regimes are based on numerical and experimental researches [4.62]. Experimental researches of hydrodynamic and thermal processes were performed in the SSC RF IPPE on specially developed models.

In 2004 benchmark problem on heat transfer in the target model was presented on the meeting of International Working Group on Advanced Nuclear Reactor Thermohydraulics held in the frame International Association for Hydraulic Engineering and Research (IAHR). The general objective of the benchmark problem was to analyze temperature behaviour of liquid metal coolant and target membrane and to examine the reliability and precision of thermohydraulic codes used by authors from different countries for computations. Specialists from Japan, Spain, China, Italy and Russia participated in calculations [4.64] [4.65] [4.66] [4.67].

(b) Experimental target models

There were developed hydraulic and thermal target models of TS-1. The circuits of flow parts of the experimental target models completely coincide to the target structure. Models were manufactured in scale 1:1.

Hydraulic target model (HTM). Hydrodynamic processes in ADS target have been studied on the full scale model mounted on air test facility. HTM was designed and fabricated as sectional one. Combinations of separate sections gave the possibility to measure parameters as in the whole model and in some elements of flow part. HTM includes a half of annuli, turning in step of 180°, and central channel with distributing grid. Design of HTM allowed varying distance between membrane and distributing grid from 1 to 10 mm.

Thermal target model (TTM). Thermal experiments were performed with eutectic sodium–potassium alloy (78%K, 22%Na) as a coolant. Theoretical foundation to the use of this coolant lies in the fact that Prandtl numbers of Na-K (Pr=0.031 under experimental conditions) and Pb-Bi (Pr=0.03 at working temperature in the target) are coincident, practically.

Longitudinal view of the TTM is shown in Fig. 4.69. Target membrane represents a figured thin plate made of stainless steel, with the thickness being 1.5 mm. With the use of the copper block of 65 mm in diameter soldered to the membrane surface a heat flux at the membrane surface was generated. Heat flux in experiments may run to q=86 W/cm$^2$.

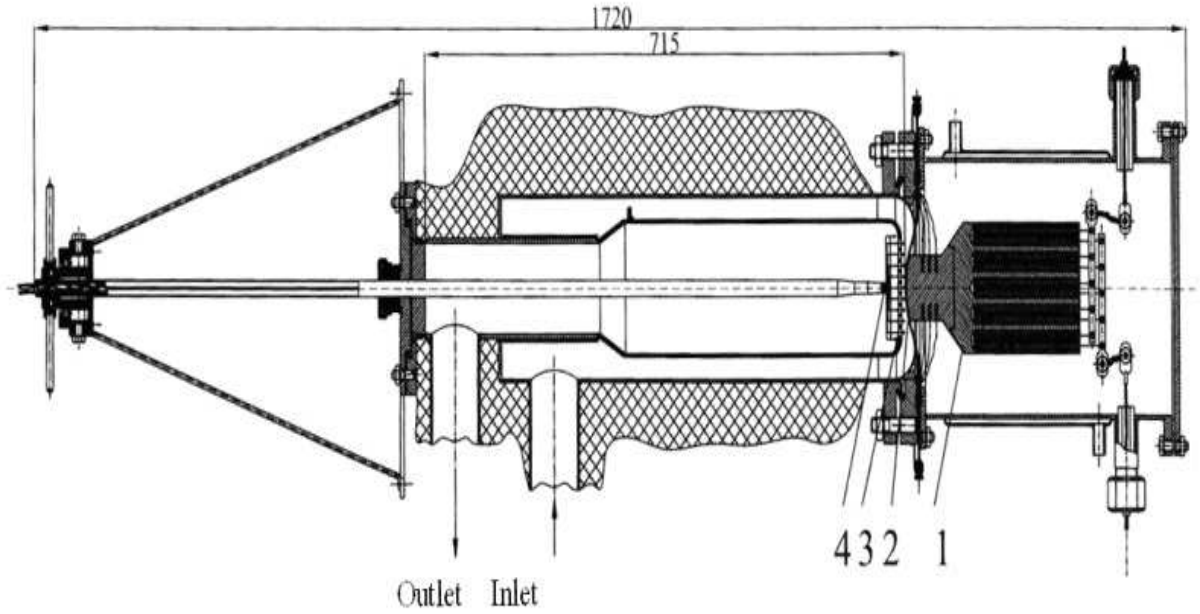


2 - Target membrane, 3 - Distributing grid, 4 - Thermocouple probe.

*FIG. 4.69. Schematic view of the TTM: 1- copper block with heaters.*

Parameters of experimental models and real target system TS-1 are summarized in Table 4.20. A detailed description of target models, measurement devices and modeled modes is presented in [4.62] [4.63].

TABLE 4.20. PARAMETERS OF EXPERIMENTAL MODELS AND TARGET SYSTEM TS-1

| Parameter | Target System TS-1 | Hydrodynamic target model (HTM) | Thermal target model (TTM) |
|---|---|---|---|
| Working liquid | Pb-Bi | air | Na-K |
| Power generation in membrane | Heat flux from the membrane peak qf(max)=64 W/cm$^2$ | Isothermal flow | Heat flux from membrane surface<br>qf=86 W/cm2=const<br>Total power Qf=2.63 kW |
| Power generation in coolant flow | ~600 kW | Isothermal flow | - |
| Inlet temperature | 320°C | 25 ± 1°C | 35 $^o$C |
| Outlet temperature | 220°C | 25 ± 1°C | 35 + (1÷2)°C |
| Flow rate | 15.0 m$^3$/h | < 1100 m3/h | 7 m$^3$/h |
| Pr number | 0.03 | not taken into account | 0.031 |
| Re number | 177000 | 40 000–180 000 | 23750 |
| Pe number | 5310 | not taken into account | 700 |

(c) Hydraulic and thermal experiments

The hydraulic resistance of target circuit was investigated in detail in the HTM. Side input of the coolant into collector results in the non-uniform velocity distribution in azimuthal direction to be formed at the collector output. This non uniformity is retained over all length annuli. With the purpose to equalize velocity field over the annular channel of the target, its design was optimized. It allowed reducing a maximum deviation of local coolant velocity from its average value up to 11%.

Experimental researches of velocity fields in the central tube of the HTM were performed with the purpose to develop database for verification computer codes and to test effectiveness of distributing grid in the process of generation of needed liquid metal coolant flow. Obtained results revealed practically symmetric coolant velocity distribution relatively to the central tube's axis and its monotonic behaviour at the distance more than 50 mm from the membrane surface. It was observed non-monotonic behaviour of coolant velocity with significant pulsations near membrane surface. Thus, it was confirmed that distributing grid provides a formation of required velocity field in the target model with enhanced velocities near the axis of central tube.

Temperature field in TTM was investigated under conditions of the constant heat flux at the membrane surface, which was equal to 86 W/cm$^2$. This value was by 30% higher then local heat flux from the peak point of target membrane.

Instantaneous values of liquid metal coolant temperature were measured in the cross-sections spaced by the distance from 1 to 300 mm from the membrane surface.

Analysis of obtained radial distributions of coolant temperature shows that narrow jet of hot coolant is formed in the central tube (Fig. 4.70). As the coolant moves from the membrane the jet is washed up. A very important fact agreed with results of hydrodynamic experiments was the availability of significant fluctuations of coolant temperature. So, at the distance 15 mm from the membrane surface they achieved 13–18°C that is about 50% of coolant temperature rise in the model.

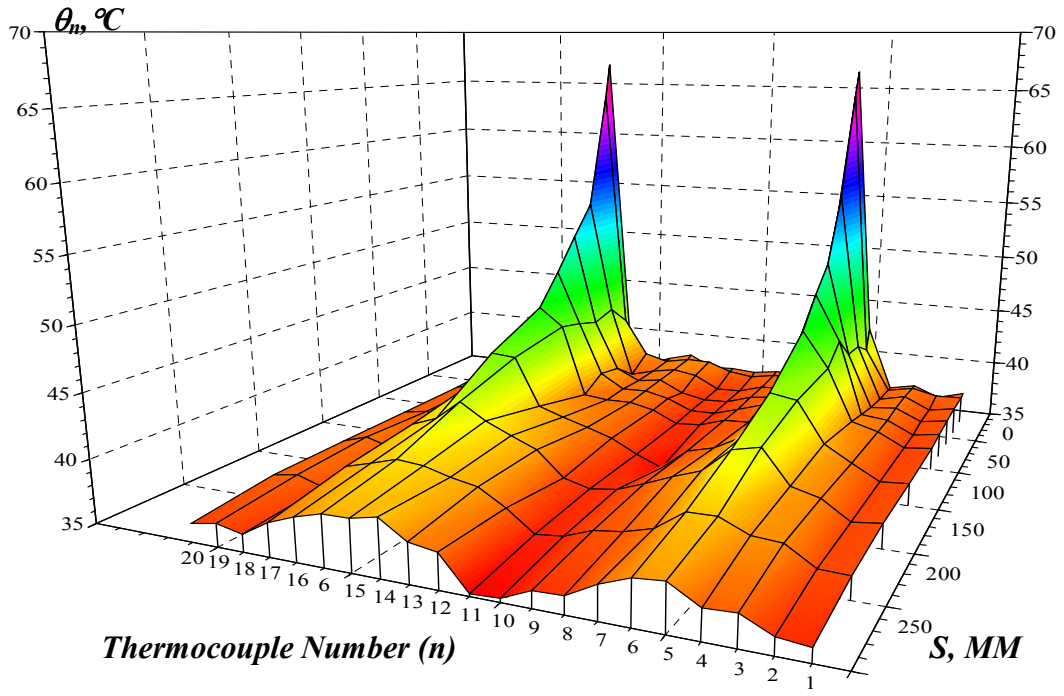


*FIG. 4.70. Volumetric presentation of temperature field in the coolant.*

Thus, the availability of significant pulsation amplitudes for membrane surface temperature measured in experiments requires the integrity characteristics of the target membrane to be analyzed in experiments with cyclic temperature regimes.

(d) Benchmark results

Specialists from Japan [4.64] Spain [4.65] China [4.66], Italy and Russia [4.67] were participated in numerical studies in the frame of benchmark problem. Codes, as well as numerical models for modeling geometry and turbulence are given in Table 4.21. 2-D approximation is also used in parallel with 3-D one.

Analysis of numerical and experimental data on membrane surface temperature distribution has shown that there is significant discrepancy both as between results predicted with different codes and between the predicted and experimental values (Fig. 4.71). For more exact prediction of membrane temperature the more detailed approaches to modeling of distributing grid and power generation at the membrane surface are needed. Predicted and experimental values of coolant temperature are practically coincident in all calculations, except area near the channel axis (Fig. 4.72 and Fig. 4.73). The reason of discrepancy of coolant temperature predicted by different authors is likely to be asymmetric real flow in the central tube of the model.

TABLE 4.21. CODES AND MODELS APPLIED IN BENCHMARK CALCULATIONS

| Researchers | Mikhin V.I. Vecchi M. | Chen H.Y. | Pena A., Castro A. | | Takata T., Yamaguchi A., Hachimoto A. | |
|---|---|---|---|---|---|---|
| Computer code | ANSYS version 5.7.1 | Phoenics 3.2 | FLUENT version 5.5 | STAR-CD | AQUA | FLUENT version 4.8 |
| Code owner | ANSYS Inc. | CHAM | FLUENT Inc | CDL | JNS | FLUENT Inc |
| Dimension | 2 | 2 | 3 | 2 | 3 | 3 |
| Turbulence model | RNG k-ε | LVEL | k-ε | RNG k-ε | ASM | RSM |
| Geometry model | Grid with holes | Porous body model | | | 3-D | 2-D |

Experimental and numerical results have been used for development of target construction, for verification computer codes, for analysis of integrity and thermal stresses in structural elements.

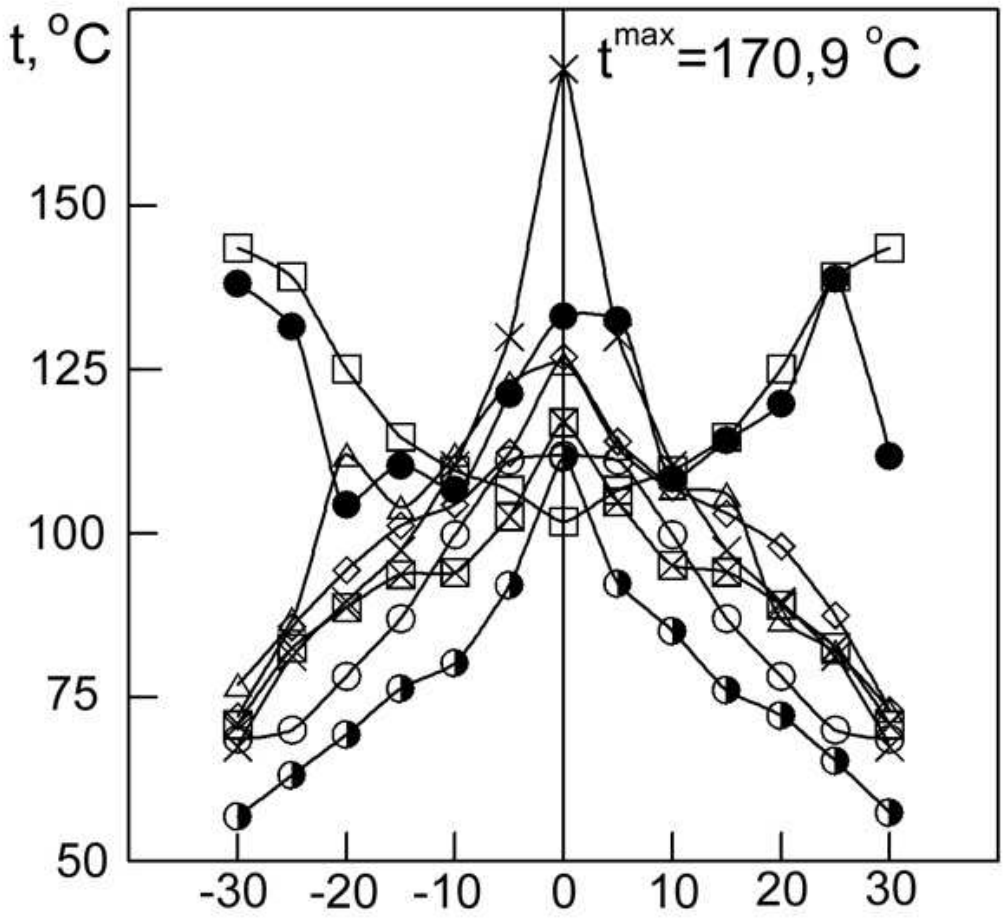


*FIG. 4.71. Experimental and benchmark numerical distributions of the membrane surface temperature (y - distance from membrane axis): ● - experiment; △ - FLUENT RNG; □ - STAR-CD; ◇ - AQUA-TM; ⊠ - AQUA-ASM; ◑ - FLUENT-RSM; ○ - Phoenics 3.2; ✕ - ANSIS version 5.7.1.*

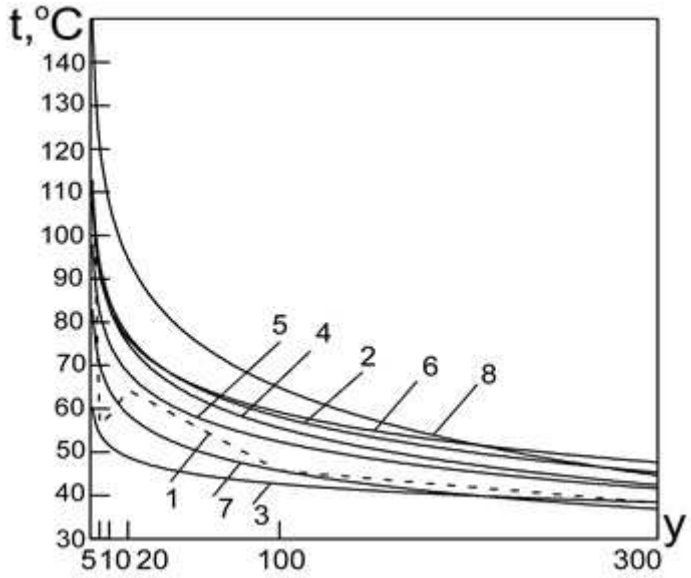


*FIG. 4.72. Experimental and benchmark numerical results on axial coolant temperature distribution: 1 - experiment (central thermocouple of the thermocouple probe); 2 - FLUENT RNG; 3 - STAR-CD; 4 - AQUA-TM; 5 - AQUA-ASM; 6 - FLUENT RCM; 7 - Phoenics 3.2; 8 - ANSIS.*

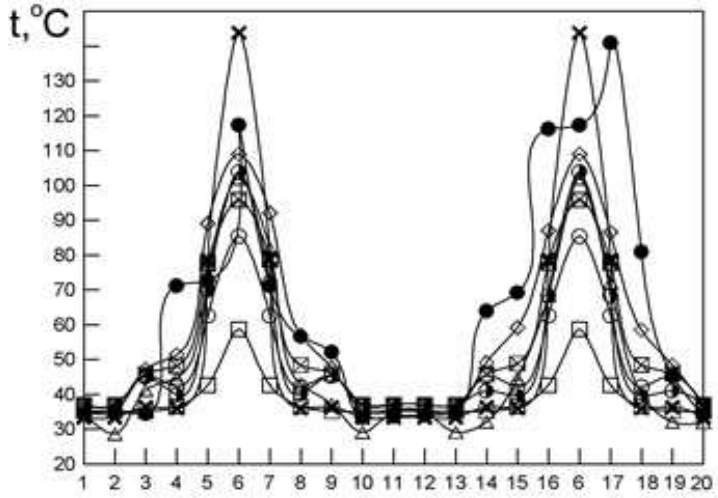


*FIG. 4.73. Experimental indications of thermocouples in the thermocouple probe and appropriate benchmark numerical results (distance between central thermocouple and membrane 1 mm): ● - experiment; △ - FLUENT RNG; □ - STAR-CD; ◇ - AQUA-TM; ⊠ -AQUA-ASM; ◑ - FLUENT-RSM; ○ - Phoenics 3.2; ✕ - ANSIS version 5.7.1.*

### 4.4.2. Windowless target

#### *4.4.2.1. Summary*

The design of the XT-ADS spallation target is performed within the European integrated project EUROTRANS (FP6 Contract FI6W-516520) [4.68] that has started in April 2005. At the current status of the spallation target design process, the boundary conditions for the spallation target loop with respect to the XT-ADS performance requirements and the design of the subcritical core and

primary system have been established. The next steps will concentrate on further development of the spallation target nozzle, the vacuum and spallation product confinement system and the pumping, LIDAR and cooling system.

#### *4.4.2.2. Spallation target specifications and boundary conditions*

The first major requirement of the spallation target of the XT-ADS [4.69] is that it should produce a sufficient amount of neutrons to feed the subcritical core at its specific $k_{eff}$ value. The precise number of neutrons that is required both depends on the required flux levels in the core and design details of the core where the envisaged value of $k_{eff}$ in particular plays an important role. With the desired flux levels mentioned above and a reference $k_{eff}$ value in the core of 0.95, the spallation target will need to produce about $10^{17}$ neutrons/s.

The second major requirement is that the neutron source provided by the spallation target must be placed in the centre of the subcritical core. Because of the compact design, the space available into which the target must fit is limited. Furthermore, for simplicity of design of the core, the room for the spallation target must be created by leaving an integer number of fuel assembly positions in the centre of the core empty. In the reference design, the target space is created by removing three of the hexagonal fuel assemblies. With a fuel assembly pitch of 96.2 mm, the maximum circular space vacant for the target is 109.5 mm. However, additional space for supporting features of the target loop (e.g. target material feeder lines) is available in three lobes surrounding the central circle.

The production of neutrons in the spallation target is done by impinging a high power proton beam on a target material with a sufficiently high neutron number. In order to reach the required neutron yield in the target, a proton beam power of about 1.8 MW is needed depending on the choice of beam energy and current.

For this purpose, the spallation target must accept the appropriate high power proton beam that is currently set at a maximum value of 3 mA at energy of 600 MeV. Because the thermal energy of about 1.24 MW that is deposited by the proton beam requires forced convection cooling, liquid lead-bismuth eutectic (LBE) is chosen as target material. As already presented in chapter 4, LBE is likewise the coolant of the main vessel although both circuits are separated.

Furthermore, the design of the target should not hamper the fundamental role of XT-ADS as a flexible high intensity experimental irradiation device. Consequently, the spallation target loop should inhibit the free access to the core as little as possible.

Finally, although a replacement of the spallation target within the envisaged lifetime of the XT-ADS is unavoidable, this operation should not be required too often. Thus, the spallation target unit should be able to survive operation within the ADS system for a reasonable amount of time.

#### *4.4.2.3. Reference spallation target design*

(a) Spallation target design concepts

Due to the functional similarity between the XT-ADS and the original MYRRHA concept that was developed earlier at SCK•CEN, the design of the latter spallation target was chosen as a starting point for the development of the XT-ADS target loop. As was the case with MYRRHA, the functional and spatial constraints mentioned above compel the selection of some fundamental design concepts. Firstly, the limited space available in the core and the high proton current lead to very high proton beam densities of about 150 μA/cm2. No structural material is expected to withstand these conditions at elevated temperatures during a reasonable lifetime of the spallation target (≥ 1 year). Thus, the spallation target is being designed without a hot window between the target area and the vacuum of the beam line albeit that a cold window further upstream is envisaged. It may be noted here that the focus of the EUROTRANS project on a windowless design is complementary to the work that was carried out in the FP5 programme PDS-XADS and the MEGAPIE initiative in which a window concept for a high power spallation target was studied.

A result of the windowless target option is that at the interaction point, the spallation target is formed by a free liquid surface that must be properly shaped by careful design of the LBE flow. As before, the limited space is responsible for the choice of a vertical confluent flow as formation mechanism for the target free surface (Fig. 4.74). The liquid LBE is fed to the target nozzle via a vertical three-lobed annular pipe to optimize the use of the available space in the core. The target nozzle itself is designed to ensure a stable free surface flow. In addition, monitoring of the free surface level is mandatory. The design and R&D efforts on this topic will be discussed below. The compact core of the XT-ADS only allows a passage of the LBE target material in one direction from top to bottom. The feeder line passes above the core and the return line underneath it thus interlinking the core. In this configuration, the spallation target loop has off-axis housing for all active components. A split core base plate is necessary to allow removal of the spallation loop from the main vessel. The off-axis design of the spallation loop leaves the top and bottom of the subcritical core accessible for fuel manipulations and the installation of irradiation experiments. In addition, the main part of the spallation loop is moved away from the high radiation zone which is beneficial for its lifetime.

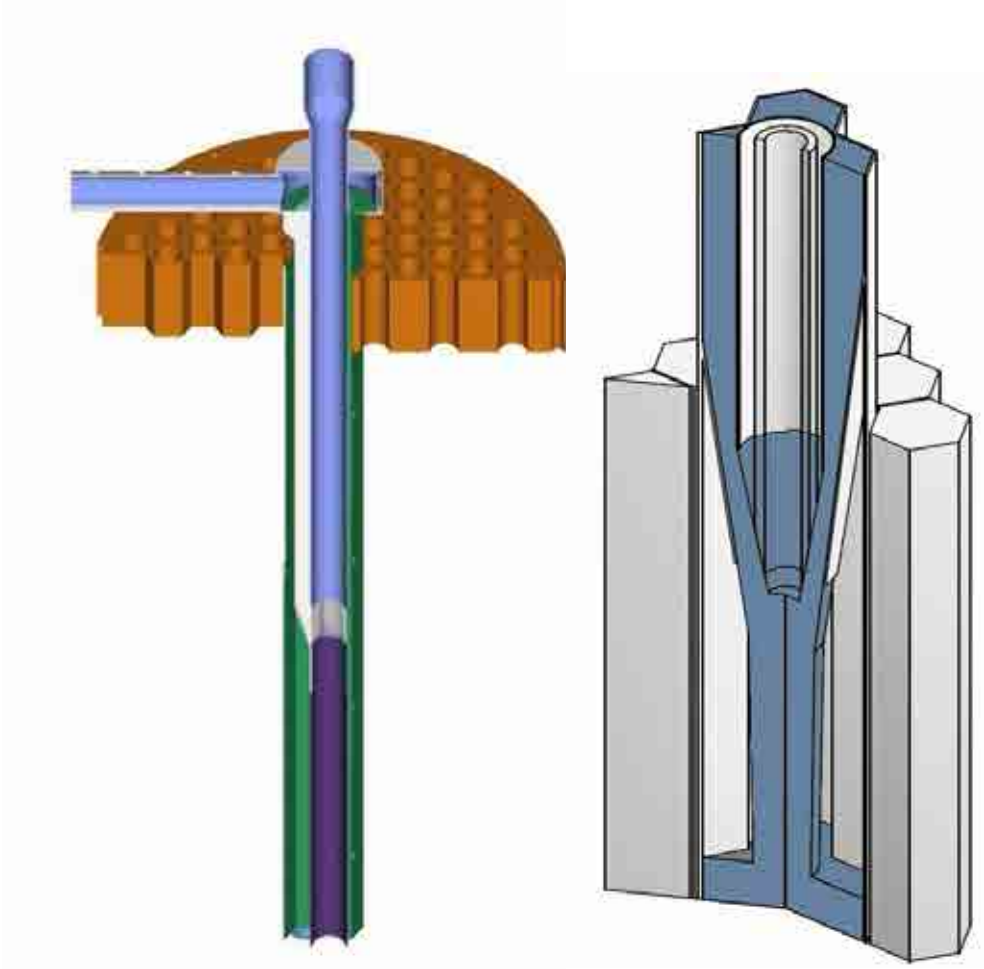

*FIG. 4.74. Schematic drawing of the vertical confluent flow concept.*

The common vacuum of the target zone and the proton beam line puts requirements on the vacuum system. Firstly, the pressure directly above the spallation target should be below the $10^{-5}$–$10^{-6}$ Pa range to guarantee compatibility with the vacuum of the proton beam line and to avoid plasma formation caused by the interaction between the rest gas above the target and the proton beam. The pressure condition implies that the outgassing of the spallation target material must be limited and that care should be taken in the design of the vacuum system to ensure sufficient vacuum conductance and pumping capacity. The second essential function of the vacuum system is the confinement of volatile radioactive spallation products. Due to the spallation interaction of the proton beam with the target material, radioactive elements with a high vapour pressure (e.g. Hg isotopes) are produced. These

products could possibly emanate from the free surface of the target and should be confined, either within the spallation loop or in the vacuum system. For this purpose, the latter is equipped with a closed back end composed of sorption and getter pumps. In order to minimize emanation of spallation products into the proton beam line, a large second free LBE surface is foreseen in the servicing vessel, directly underneath the main vacuum pumps.

The spallation target is designed to be capable of handling the heat deposited in the spallation target by a 3 mA, 600 MeV proton beam that amounts to about 1242 kW [4.70]. Forced convection by circulating liquid target material is used to evacuate the heat trough the spallation target heat exchanger situated at the bottom of the off-axis part of the loop. The secondary side of the heat exchanger is cooled by the main vessel coolant. The flow rate of the LBE is about 10 l/s. The lower limit of this value is determined by the maximum temperature allowed in the target. In order to limit LBE evaporation and corrosion of structural materials in the target loop, this temperature is set at about 430°C. Because the spallation target material is cooled against the main vessel coolant, the lowest achievable temperature during normal operation of 330°C is mainly determined by the inlet temperature of the core (300°C).

The XT-ADS spallation target system has been designed to be compatible with the remote handling scheme envisaged for the entire XT-ADS. The full loop can be removed from the main vessel after unloading of the core. The prior unloading of the core is to avoid criticality issues, for general safety and to allow in situ commissioning of the target unit. In addition, all active elements are placed in a separate subunit which allows servicing of these parts without removal of full the spallation loop. The closed outer housing allows regular (yearly) replacement of the spallation target zone that will be required because of radiation induced embrittlement and possible replacement of the heat exchanger. Maintenance, inspection and repair of the spallation unit are foreseen to be performed in the XT-ADS hall, outside the main vessel pool under cover of a protective inert atmosphere. This includes disconnection and reengagement of all service jumpers, replacement of the embrittled loop parts close to the target zone and removal and re-installation of the interior column with all active parts. Also the replacement of the heat exchanger fits into the scheme. Before and after maintenance, the LBE loop is drained and later refilled into and from a special container. This allows save storage of the LBE during maintenance and simultaneously permits conditioning of the material in a dedicated off line system.

(b) Spallation loop layout & operation

Fig. 4.75 shows the subunit and outside housing of the spallation loop. All components are indicated and their layout reflects the design status of the original (2005) MYRRHA concept. The target LBE is fed from the off centre spallation unit and traverses to the central axis of subcritical core. It comes down through the three feeders (forming what is called the downcomer) surrounding the beam transport line. The target free surface is formed at the confluence point of the target nozzle in the centre of the subcritical core. Here the proton beam impinges from the top. The LBE subsequently flows away from the beam impact zone through the central tube, the lower U-bend and the heat exchanger to the pumping unit in the spallation housing.

For proper operation of the liquid target, the formation of the target free surface and a firm control over the size of the recirculation zone that is formed in the centre of the target free surface is essential. When the recirculation zone is too small, LBE droplets are ejected from the LBE confluent zone that may cause metal evaporation when hit by the beam. If the recirculation zone is too large, it will be directly heated by the proton beam causing the temperatures to increase very rapidly which would also lead to excessive evaporation of LBE and other volatiles.

The size of the recirculation zone can be determined indirectly by its height. In the 2005 concept, the target free surface height is given by the balance between the nozzle in and outflow. The height of the recirculation zone is measured by a laser based level measurement device (LIDAR) positioned in line with the beam. This level measurement is used to control the pumping power of the magneto hydrodynamic (MHD) pump in order to keep the height of the recirculation zone at a fixed level.

The free surface level is particularly difficult to maintain under the dynamics changes caused by beam trips and during the startup-shutdown procedures. In order to cope with these dynamics, a second free surface in the spallation loop main unit is maintained at about 2.5 m above the target free surface. The mechanical pump lifts the LBE that has passed the heat exchanger to the level of the second free surface. From here, the LBE flows through the feeder line to the target nozzle by gravity. The MHD pump in the feeder-line provides the fine tuning of the gravity fed inflow in 2-quadrant acceleration–deceleration operation. Normal operation of the pump, however, is slightly biased towards an accelerating action to avoid frequent reversal of the travelling wave. The three feeders are drag limited, exceeding the minimum drag of 1 bar/m necessary to compensate for the hydrostatic pressure, to prevent the spallation LBE to tear off and reach the target nozzle in free fall.

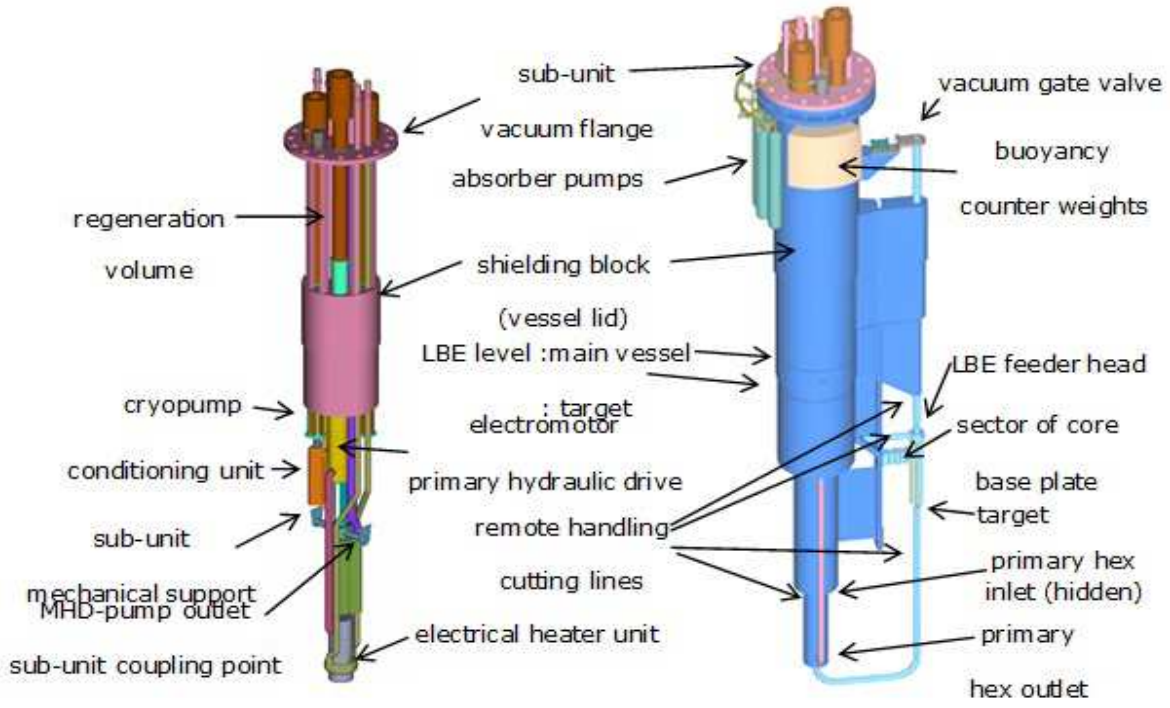


*FIG. 4.75. Spallation subunit and outside housing of the spallation loop (2005 concept).*

(c) Spallation target components

— The nozzle

Within the XT-ADS spallation target design work of the EUROTRANS project, a specific effort is put on the development of the target nozzle. As stated above, in the MYRRHA 2005 concept that serves as the input for the XT-ADS, the target nozzle was designed to have a straight LBE flow, without detachment of the LBE from the nozzle walls. However, experiments at UCL and FZK have shown that a more stable flow is achieved if detachment of the LBE flow is allowed. Also, introducing a mild swirl has a stabilising effect. These results are now used as input for further development of the target nozzle. In this respect, three tracks are investigated.

Firstly, the feasibility of a target nozzle that explicitly forces flow detachment is studied. In order to achieve detachment at the right position and nowhere else, a rig in the nozzle wall is created. In addition, the nozzle shape and the in and outflow cross-sections must be optimised. For this purpose, several nozzle proposals are looked into with CFD calculations, followed by experimental tests using water and LBE flow experiments at UCL and FZK respectively.

A similar strategy is being followed for the investigation of the influence of swirl on the target flow. Here, numerical and experimental results show that in the current geometry, the application of a mild swirl of 5%, corresponding to a 1/20 ratio of the tangential relative to the axial LBE velocities, has a small but stabilizing effect on the target free surface. Application of a swirl strength of 10% or higher

leads to undesirable free surface behaviour, ultimately leading to an unacceptable strong vortex in the central tube.

The third modification in the target nozzle that is being studied in more detail is the 3-feeder option for the LBE downcomer which has the advantage that optimal use is made of the available space in the ADS core. Next to the three main design modifications, design activities are performed addressing the flow distribution into the downcomer and drag enhancement in the downcomer itself. The strategy of the project is to investigate the three design modifications separately before they are integrated in one nozzle. The combined nozzle will be further studied using the water flow experiments and fine tuned in LBE flow experiments at KALLA.

— LBE pumping system

In the 2005 concept the mechanical pump is powered by an indirect hydraulic drive that avoids the use of a long shaft. A canned electric motor drives a pump that transmits its power to the hydraulic drive and hydraulic pump in the lower part of the column. The hydraulic transmission fluid is taken to be the same as the LBE that it is circulating in the spallation loop (although at higher pressure).

One option for the design of the pump-drive tandem is based on common impeller technology. The impeller direction of drive and pump are opposite in order to ease the axial bearing requirements. This design is shown in all pictures of the spallation loop. Another option is to design the pump-drive tandem based on a screw spindle technology. In this option the fluid smoothly follows the spindle motion without being subject to the accelerating or decelerating phases of impeller pumps. Such a smooth flow is assumed to be less bothered by corrosion and cavitation problems. Although the hydraulic drive pump is the reference design in the 2005 concept, the long shaft option has not been ruled out. Here however, the proper design and testing of the shaft bearings is the most crucial point. The basic concept for the annular linear induction pump or MHD pump is similar to the one used for the MEGAPIE Project at PSI (Switzerland). The MEGAPIE pump is constructed at IPUL (University of Latvia). The MHD pump envisaged in the 2005 concept differs from this pump in certain respects in order to obtain the pressure gain of 1.2 bars as required by the spallation loop dynamics. The pump efficiency is almost doubled by better matching the LBE velocity to the mean magnetic field velocity thus decreasing the slip ratio. Furthermore, the pump length is increased to 1.2 m, including an integrated annular magnetic flowmeter and the number of poles is increased accordingly. Taking into account the MEGAPIE model findings, the efficiency could be increased even more by grading the magnetic core flux over its length.

In the present design with flow detachment, the MHD pump for fast flow regulation in the 2005 concept is obsolete. As described above, different configurations are now possible for the main pumping system consisting of one or two mechanical or MHD pumps. The decision on which configuration to use has not yet been taken.

— Heat exchanger

In the heat exchanger (HEX), the LBE from the spallation loop exchanges heat with the LBE from the primary system. The basic option for this component is a counter-current shell and tube heat exchanger with the LBE spallation loop passing through the tubes. The LBE from the primary system is taken from the lower plenum in the reactor vessel and is released above the vessel diaphragm. In this way, it is driven through the HEX by the pressure difference between the lower and upper core plenum (i.e. the pressure drop across the subcritical core). The HEX is designed in such a way as to minimize pressure losses at the spallation side in order to keep sufficient suction head for the pump downstream.

— LIDAR

In the 2005 concept with an active control of the target height using a feedback loop with the LIDAR and MHD pump, LIDAR update rates of several kHz and accuracies in the mm order were necessary. Such systems are not available on the market today and require significant R&D effort.

In the new flow configuration, the LIDAR system has not completely disappeared but the timing and accuracy requirements have changed by several orders of magnitude and have come into reach of

commercially available devices. Update rates of 2 Hz and accuracies of 10 cm (with a resolution of 1 cm) are now relevant [4.71].

— Vacuum system

The absence of the window implies that the target needs to be under vacuum to accommodate the vacuum of the accelerator. Thus, a vacuum system must be provided that maintains sufficiently low pressures to avoid plasma formation. In addition, it must ensure sufficient confinement of volatile radioactive spallation products that may emanate from the target. In the 2005 concept, the spallation unit is connected to the central beam line via a duct and is being pumped as an integrated vacuum system to a pressure of less than 10–5 Pa. At the backend of the system, all radioactive volatile emanations are collected in absorption pumps from where they can be batch wise removed. Because of the target vacuum, the LBE flow is optimised to keep the temperature of the free surface low in order to prevent excessive LBE evaporation into the beam line.

During target nozzle experiments it was observed that the fast flowing LBE in the spallation target zone has a significant vacuum pumping effect since the pressure in the target module was reduced to two orders of magnitude below the minimum pressure reachable by the vacuum pump installed at that time. Although the effect has not been duly quantified in the present target geometry, it does open possibilities for a modification of the vacuum system design. Indeed, the vacuum pumping effect of the LBE may be sufficient to reduce the vacuum pressure in the target zone during normal operation to below the level required. In that scenario, the confinement of the spallation products can be improved by abandoning the vacuum duct between the beam line tube and the servicing vessel. In this way, the vacuum chamber above the free surface in the main vessel has no contact with the beam line and thus migration of volatile radioactive spallation products that were emanated from this free surface to the beam line is prevented. Separation also allows operating the vacuum vessel at higher pressures of the order of 1–100 Pa which would simplify the vacuum system without changing the LBE flow behaviour significantly. In addition, the higher operating pressure allows envisaging a room temperature vapour trap in the vessel that would immobilise the bulk of the volatile spallation products, so that the load on the absorption pumps is reduced.

— LBE conditioning

Conditioning of the LBE eutectic in the spallation loop is required for two main reasons: corrosion inhibition and the need to prevent conglomeration of insoluble impurities that may lead to a blocking of the flow. In the design of the MYRRHA ADS, the main corrosion inhibition strategy followed is by controlling the oxygen content in the LBE target material to the level of $1.10^{-6}$ wght%. For this, a hydrogen and water vapour gas treatment system is foreseen to reduce the amount of oxygen in the LBE when required. However, since the spallation unit is a vacuum system the treatment is only possible during maintenance times. Because of the generally reducing nature of the spallation products and the hydrogen from the proton beam, the opposite reaction for adding oxygen is also included. For this purpose a dedicated conditioning unit is foreseen. Its active component is a heated basket with PbO pebbles housed in an insulated vessel. The exchange rate between the pebbles and the bypass LBE flow is governed by controlling the temperature of the basket. In addition, magnetic filtering is foreseen at the entrance of the MHD pump to extract magnetic corrosion products (mainly Fe and Ni compounds) that could otherwise block the MHD pump. Finally, at the top of the second free surface filtering skimming is envisaged to remove floating debris.

## 4.5. FUEL

The section gives an overview on the characteristics of the different fuel candidates considered for the ADS design under development.

### 4.5.1. Fuel development in France

#### *4.5.1.1. Specifications of fuel candidates*

Fuel used in an ADS for transmutation in a fast spectrum can be described as a highly innovative concept in comparison with fuel used in a critical core. ADS fuel is not fertile, i.e. there is no uranium, so as to improve the transmutation performance. It necessarily contains a high concentration of Am+Cm actinides (about 45%–70%) and plutonium (30%–55%) whose isotopic vector consists of 80%–90% of even isotopes $^{238}$Pu, $^{240}$Pu and $^{242}$Pu, 10%–20% of odd isotopes $^{239}$Pu and $^{241}$Pu. Table 4.22 provides a list of Actinides compounds and their properties.

This unusual fuel composition results in high gamma and neutron emissions during its fabrication, as well as degraded core performance. This is due to: 1) the thermal and thermodynamic properties of the minor actinide (MA) compounds which are poorer than those of major actinides, 2) the volatility of the americium species, and 3) the significant production of helium during irradiation. Furthermore, we still have very little information on the in-pile behaviour of these compounds. A relatively comprehensive review of the minor actinides likely to be considered for the composition of ADS fuels was carried out under the CAPRA-CADRA project [4.72], and then under the Fuel Fabrication and Processing Working Group [4.73] to meet the Technical Working Group requirements for the elaboration of a European ADS development plan[4.74] The main selection criteria retained were:

— Thermal properties;

— Thermodynamic stability;

— Density of heavy atoms (high densities contributing to spectrum hardening and favouring transmutation);

— Cubic or highly symmetrical crystal lattice structures (known for their high resistance to neutrons) not subjected to phase transformations and isomophisms, for all transuranium elements.

TABLE 4.22. LIST OF ACTINIDE COMPOUNDS AND THEIR PROPERTIES

| Actinide compounds | Melting or decomposition temperature (°C) | Density ($g/cm^3$) | Thermal conductivity 1273K ($W.m^{-1}.K^{-1}$) | $\Delta G^o_f$ - 298K ($kJ.mol^{-1}$) |
|---|---|---|---|---|
| Pu-Am-Cm-40Zr | 1327 | 9.61 | 22 | - |
| $NpO_2$ | 2550 | 11.14 | - | -720 |
| $PuO_2$, $Pu_2O_3$ | 2390, 2360 | 11.46 | 3 | -730 |
| $AmO_2$, $Am_2O_3$ | 2175, 2205 | 11.71 | - | -620 |
| $Cm_2O_3$ | 377 | - | - | - |
| NpN | 2830 ( 12atm $N_2$) | - | 17 | - |
| PuN | 2675 (1atm $N_2$) | 14.24 | 13 | -150 |
| AmN | 2570(1atm $N_2$) | 13 | - | - |
| CmN | - | - | - | - |
| $NpC_{1-x}$ | >1400 | - | - | -90 |
| $PuC_{1-x}$, $Pu_2C_3$ | 1654, 2050 | 13.6 | 11 | -70, -100 |
| $Am_2C_3$ | - | - | - | -70 |
| NpS | - | - | - | -342 |
| PuS | 2347 | - | - | -360 |

| Actinide compounds | Melting or decomposition temperature (°C) | Density ($g/cm^3$) | Thermal conductivity 1273K ($W.m^{-1}.K^{-1}$) | $\Delta G^o_f$ - 298K ($kJ.mol^{-1}$) |
|---|---|---|---|---|
| AmS | - | - | - | - |
| CmS | >1550 | - | - | - |

The optimal minor actinide composition in ADS fuels is based on finding a compromise between constraints of thermal nature (margins in relation to melting or decomposition/vaporisation), mechanics (cladding failure through fuel cladding interactions, and internal pressure), and chemistry (cladding corrosion, fuel cladding eutectics) associated with the fuel and its cladding on the one hand, and the neutron and technology related constraints associated with subcritical cores (themselves defined by the core's level of subcriticality and the power of both the accelerator and the spallation target) on the other hand.

(a) Metal fuel

— Main characteristics of metal alloys [4.75] [4.76]

As defined within the scope of the Advanced Accelerator Applications (AAA) and the Advanced Fuel Cycle Initiative (AFCI) programmes in United States [4.77], Pu-MA-Zr metal fuels have a rather complex metallurgy with several phase transitions, and the mutual solubility of poorly understood transuranium elements, though with excellent thermal and mechanical (creep) properties. Their density is also one of the highest. Lastly, they are compatible with pyrochemical processes in molten salts that are generally preferred for the reprocessing of 'hot' fuels. However, the volatility of metal americium is high (4 times higher than that of plutonium). Special precautions also have to be taken in terms of the pyrophoricity of the metal components. The melting temperature is relatively low and there is a high risk of chemical interaction between the fuel and the cladding as early as 725°C.

Therefore, they can not be used in the same way as standard American U-Pu-Zr fuel with a metal sodium bond. This bond is an excellent conductor which produces a great fuel cladding gap and strong gaseous swelling to which metal alloys are prone. In the case of standard integral fast reactor (IFR) fuel, the filling density drops to 75% of the theoretical density but still remains higher than that of refractory fuels. This design can therefore accommodate for free swelling of 30 vol% which is reached with a burnup of about 2 at%. An interconnected network of pores forms above this limit. This porous network is incapable of exerting any mechanical stress on the cladding which thus releases over 80% of its gas. Metal fuels are therefore intrinsically designed to release gases, which is an advantage in terms of helium production. The problem with helium can be solved by designing a large enough plenum to avoid cladding pressurisation.

The metal fuel that the Americans chose for a sodium cooled accelerator driven system (ADS) is not ideal for a Pb or Pb-Bi cooled ADS, owing to its probable incompatibility with the coolant. Pu and Zr are compatible with sodium but not with lead or bismuth. They form intermetallic compounds with these metals, or can be partially soluble. However, this disadvantage does not necessarily rule out this solution completely. The reaction kinetics can be slow enough so that the faulty fuel assembly can be removed in the event of cladding failure, as is currently foreseen in certain experimental reactors.

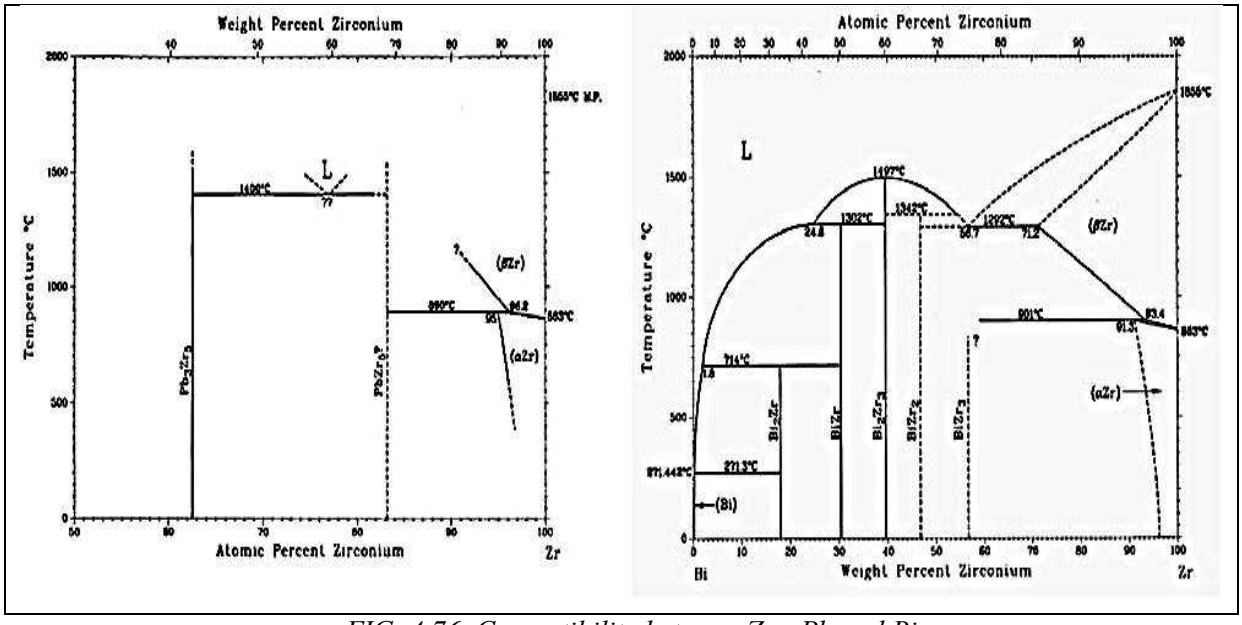


*FIG. 4.76. Compatibility between Zr - Pb and Bi.*

— Optimization of fuel composition for ADS [4.78]

American studies have made possible an optimised composition of a non-fertile metal fuel. The alloys involved contain 30% to 40 wt% of zirconium. According to the results of irradiation on an extruded Pu-35Zr alloy up to 0.8 at% at 500°C (Fig. 4.79), this composition stabilizes the δ-Pu face centred cubic phase with only low swelling of 6.5%–at%. Furthermore, americium stabilizes this δ-Pu phase over a large range of compositions. There is nevertheless uncertainty on neptunium: it is completely soluble in the ε-Pu phase but hardly so in the δ-Pu phase. We have contradictory information on its alloying with zirconium. The formation of phases with low melting points, if confirmed, would require improving the alloy by adding additional minor elements. Fig. 4.77 and Fig. 4.78 show the Pu-Zr and Pu-Am phase diagram, respectively.

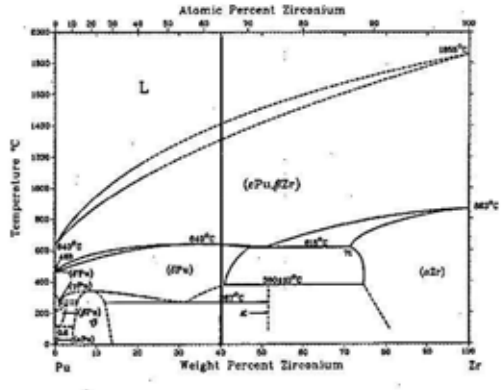


*FIG. 4.77. Phase diagram Pu-Zr.*

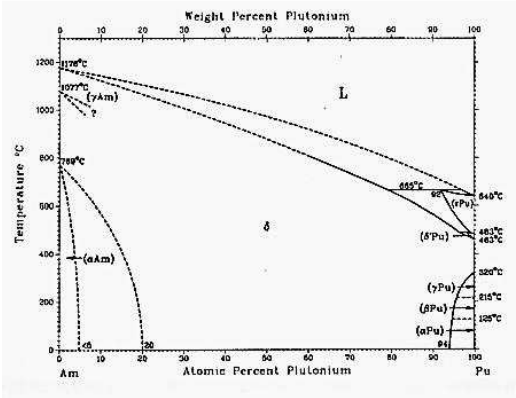


*FIG. 4.78. Phase diagram Pu-Am.*

Above 40% Zr, a two phase system composed of δ-Pu and a hexagonally structured α-Zr phase forms below 597°C. This α-Zr phase is detrimental owing to its tendency for anisotropic swelling, as demonstrated by the irradiation of two alloys, Pu-95Zr (Fig. 4.80) and Pu-97Zr α-Zr prepared by cold rolling. They experienced very little swelling but did show 200% to 500% axial strain following irradiation at 430–530°C without exceeding a burnup of 0.8–1.3 at%. Above the limit defining the δ-Pu phase, there is complete miscibility of plutonium and zirconium in a centred cubic phase (ε-Pu, β-Zr).

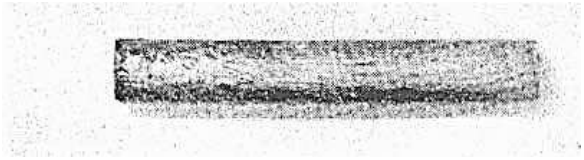

*FIG. 4.79. Pu-35Zr extruded bar of δ-Pu structure irradiated at 500°C up to a 0.83 at% burnup.*

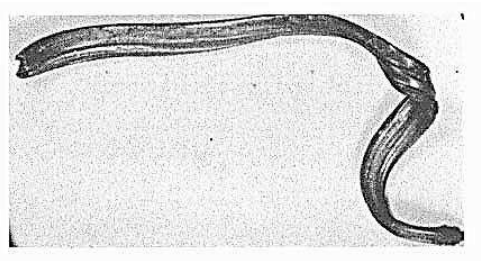

*FIG. 4.80. Pu-95Zr rolled plate of α-Zr structure irradiated at 530°C up to a 0.9 at% burnup.*

The synthesis tests for δ-Pu type alloys containing americium performed by ANL confirmed the close similarities expected between the Pu-Zr diagram and the Pu-Am-Zr diagram, at least for the Zr contents at 40 wt%.

(b) Nitride, carbide and sulphide fuels

— Main characteristics of nitrides and carbides [4.81]

Among the refractory ceramic compounds which all have mutual solubility over a large range of compositions, carbides and nitrides are more interesting than oxides due to their high density and thermal conductivity. However, their significant swelling under irradiation calls for low filling densities (75–85%) to avoid fuel cladding mechanical interactions that could result in failure: this puts a significant burden on the heavy atom balance and reduces thermal conductivity owing to the creation of pores. Furthermore, their compatibility with liquid metals such as lead or sodium means that fuels with metal bonds can be used, thereby offering a large safety margin in terms of meltdown accidents.

Despite very similar behaviour patterns, nitrides are generally preferred to carbides as they are not as pyrophoric, they are easier to synthesise (mononitride accepts a broader stoichiometric range in comparison with monocarbide), they swell less under irradiation, and they show greater thermodynamic stability.

Therefore, during the carbothermic fabrication of mixed uranium and plutonium carbide (U, Pu)C, significant americium losses have been observed due to the ageing of plutonium and the decay of $^{241}$Pu into $^{241}$Am. The low thermodynamic stability of $Am_2C_3$ implies its decomposition at relatively low temperature, and the evaporation of metal americium whose vapour pressure is very high. Nitride is also compatible with PUREX and pyrochemical processes, whereas carbide forms chemical complexes that are problematic in nitric acid media.

However, nitride produces $^{14}$C under a neutron flux via (n, p) reactions with $^{14}$N. To reduce releases from reprocessing plants, nitrides could be enriched with $^{15}$N. Enrichment of nitrides to 97% $^{15}$N to avoid producing more $^{14}$C in the first stratum than in the second would represent a heavy economic constraint [4.82].

Lastly, large uncertainties remain on the thermal stability of nitrides at high temperature, especially that of americium nitride [4.83]. The vaporisation of americium nitride proved to be a major problem when the Japanese and Americans lost significant quantities of americium in their sintering furnace while performing the first carbothermic synthesis of americium nitride. Adding extremely refractory ZrN has become the best solution for mitigating this phenomenon as it is stable in air and at high temperature, while showing excellent physical properties. YN nitrides (very hygroscopic) and HN nitrides (very absorbing) do not share the same advantages despite their equally refractory nature.

Actinide sulphides (and phosphides) that share a lot of similarities with nitrides and carbides do not actually offer any major advantages that could justify developing them for nuclear fuels. They would also be difficult to manufacture as they are hygroscopic. There is little feedback on these actinide compounds in comparison with nitrides and carbides, which is why they weren't chosen.

— Optimization of fuel composition for ADS [4.84][4.85]

When ZrN is combined with actinide nitrides, it forms a solid solution over the entire range of possible compositions. Its content must therefore be as high as possible to ensure greater fuel thermal stability. Therefore, it is mainly neutron related considerations that determine the fuel composition, contrary to metal whose composition is determined by its metallurgy.

The inert matrix content is adjusted to obtain an initial subcritical level of 3000 pcm ( $k_{eff}$ = 0.97). Fig. 4.81 shows the volume contents of ZrN as a function of the P/D ratio, where P is the pitch of the pin bundle, and D is the pin diameter (hydraulic parameter). Two pin diameters were used as parameters. Small diameters were chosen (D = 5.0 and 7.0 mm) to reduce the irradiation time required to reach a burnup of 20 at% while avoiding cladding corrosion by the Pb-Bi coolant. The fraction of plutonium and minor actinides was adjusted to minimize the decrease in reactivity. For the first cores, reactivity losses below 1,800 pcm were possible at a burnup of 20 at%, with Pu/Am/Cm actinide contents of 40, 50 and 10 respectively. For P/D ratios above 1.7 (the minimum ensuring cladding integrity in the case of a loss of flow accident), it can be seen (figure 4.85) that the contents range between 40–60%, with the large pins making it possible to increase the acceptable content by about 4–7%.

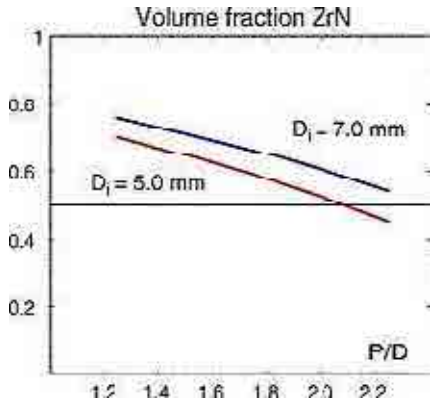


*FIG. 4.81. Requested ZrN volume fraction for $k_{eff}$=0.97 (800MWth ADS reactor Pb-Bi coolant fuel density ratio:85%).*

(c) Oxide fuels

— Main characteristics of oxides (Fig. 4.82,Fig. 4.83)

The properties of actinide oxides do not appear to be the most advantageous in comparison with alloys or nitrides, but our level of knowledge on the technology and the behaviour of both standard fuels [4.86][4.87] and minor actinide oxides under irradiation is unequalled. This reduces the number of uncertainties and provides a confidence level that neither metal alloys nor minor actinide nitrides have reached. Minor actinide oxides generally have poorer thermal properties than UOX or MOX fuels, with a melting point that continuously decreases from $UO_2$ to $Cm_2O_3$ and a high oxygen potential that can result in 1) serious cladding corrosion problems, especially at high burnups, and 2) increased volatility of the americium species in certain oxygen potential conditions. The thermal conductivity is not necessarily lower than that of major actinide oxides, but it remains mediocre and highly penalising, especially if swelling imposes a big fuel cladding gap to act as a thermal barrier between the coolant and the cladding.

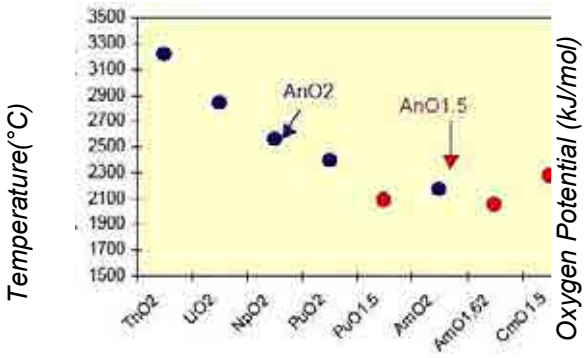


*FIG. 4.82. Melting temperature versus the nature of the actinide for oxide compounds.*

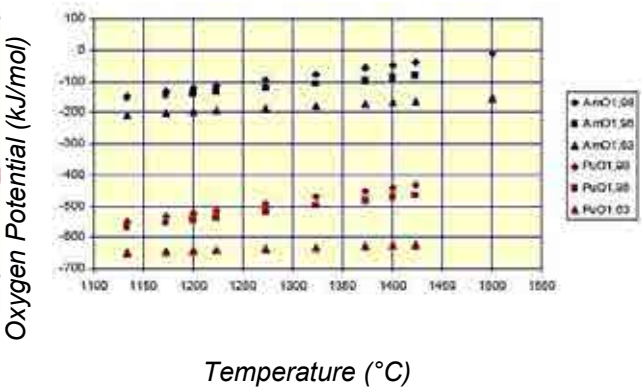


*FIG. 4.83. Oxygen potentials versus temperature forr plutonium and americium oxide compounds.*

However, the dispersion of actinide oxides in a carefully chosen inert matrix makes it possible to overcome most of these problems. Whether dispersed in a refractory ceramic matrix or metal matrix, composite fuels offer good failure resistance up to very high burnups. Experiments performed in the 60s on $PuO_2$+MgO [4.88] and $UO_2$+steel demonstrated the feasibility of such concepts up to high burnups.

— Optimization of fuel composition for ADS

Ideally speaking, fuels must form a network of uniformly distributed particles in the inert matrix. Each particle is thus under pressure and the continuous network in the inert matrix (with good thermal conductivity) ensures acceptable fuel temperatures. The performance of dispersed fuel greatly depends on its microstructural characteristics, which is why much effort has been devoted to perfecting fabrication processes. From a process viewpoint, the inert matrix volume content must not be below 50%. Tests performed by ITU on molybdenum and steel CERMET showed that beyond this limit, the fuel density drops, the pellet surface becomes rough, actinide oxide inclusions show on the surface, and particles become interconnected. This content is currently limiting the performance of oxide fuels for ADSs.

Fig. 4.84 illustrates the importance of choosing matrices that are transparent to neutrons such as $ZrO_2$, rather than neutron absorbing matrices such as W. With the latter material, it is impossible to reach the level of subcriticality required for such high matrix volume contents. The first material provides a certain degree of flexibility in the assembly design, particularly in terms of choosing the bundle pitch and the pin diameter.

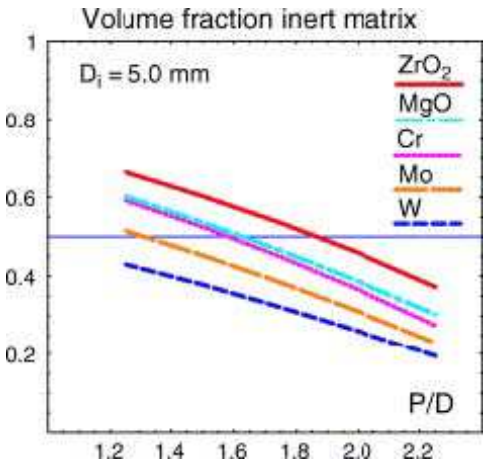


*FIG. 4.84. Inert matrice volume fraction for $k_{eff}$=0.97 (reference: 800MWth ADS reactor Pb-Bi coolant fuel density ratio:90%).*

From a neutron viewpoint, the matrices retained for ADS fuels that have been studied in Europe since the 5th European Framework Programmes are: $ZrO_2$, MgO, Cr, V and $^{92}$Mo (captures less than natural molybdenum). Taking into account of physic chemical properties and reprocessing criteria, the 6th European Framework Programme EUROTRANS [4.89] focuses on MgO and 92Mo matrices for fuel developments.

### *4.5.1.2. Behaviour under irradiation*

(a) Introduction

The design studies for ADS fuel pins have only reached a preliminary phase, considering that the modelling of their behaviour has yet to be compared with feedback from irradiation experiments conducted in experimental reactors. The first irradiation experiments designed to study the behaviour of fuels (AFCI programme in the US and FUTURIX-FTA collaboration between CEA–DOE–ITU–JAEA) are under way. However, based on studies by the CEA and its partners on the behaviour of transmutation targets [4.90][4.91][4.92] whose compositions are similar to that of ADS fuel matrices, it is possible to anticipate certain fuel behaviour patterns and design constraints. Among these are: the release of fission gases (Xe+Kr), the helium produced by the alpha decay of $^{242}$Cm, and the swelling of the fuel material. Other phenomena such as internal cladding corrosion, the redistribution of volatile species, and the restructuring and densification at the beginning of life are also important parameters as they are capable of impairing the transmutation performance.

(b) Fission gas releases

In depth analysis of the irradiation results for composite targets with inert matrices and $UO_2$ showed gaseous releases of xenon and krypton below 10% up to burnups of 20–30% at (Fig. 4.85), regardless of the material's microstructure (macrodispersion, microdispersion or solid solution) and the type of matrix ($CeO_2$, MgO, Mo, $MgAl_2O_4$, $Y_2O_3$), and this up to about 1500°C (Fig. 4.86). Above this temperature, the releases increase and are capable of exceeding 20% for macro or microdispersed composite fuels. Several experiments were performed at abnormally high releases whose causes were identified: degradation of the spinel matrix heated at excessively high temperature and significant cracking of the spinel and YAG macromasses. This resulted in a poorer plasticity compared with the other matrices at a relatively low irradiation temperature of 730°C. Generally speaking, solid solution type fuels tend to have more trouble releasing their gases.

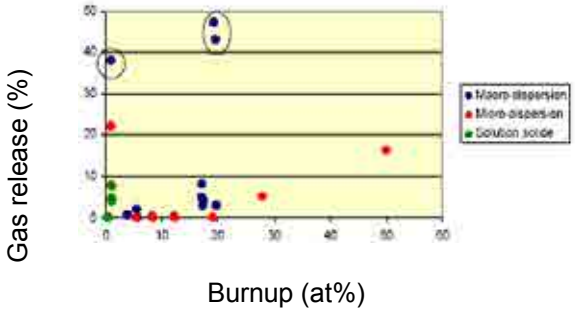


*FIG. 4.85. Xe+Kr release data of all the irradiated samples versus burnup.*

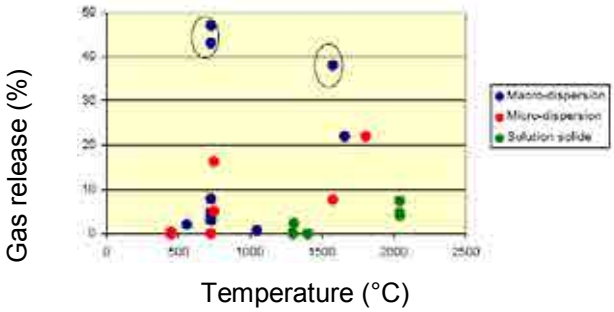


*FIG. 4.86. Xe+Kr release data of all the irradiated samples versus temperature.*

These are relatively low release rates in comparison with a fast reactor fuel (closer to 60%). However, the latter fuel operates at much higher temperatures (>2000°C) than the targets. The release rates are also just as high as those measured in PWR MOX fuels (<3%) up to burnups of about 8–9at%.

(c) Helium releases

The production of helium is proportional to the quantity of americium in the fuel. The fuel can contain very large quantities of americium, about 12 litres TPN, as shown in Fig. 4.87. These values were calculated for a CERCER fuel volume of 150 $cm^3$ up to a burnup of 20 at% and containing 60 vol% of actinide oxides. In this calculation, the isotopic compositions of the actinides are representative of a double strata scenario.

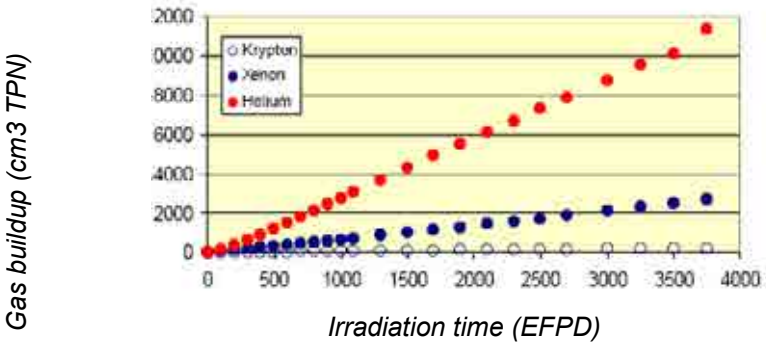


*FIG. 4.87. Fission gas buildup of a composite fuel (Pu,Am)O2+MgO in an ADS core.*

Except for the EFTTRA-T4 [4.90], EFTTRA-T4bis [4.93] and SUPERFACT [4.94] experiments, very few irradiation experiments on americium-based samples are available. EFTTRA-T4 and EFTTRA-T4bis used a microdispersed spinel composite and $AmO_2$ (11 wt%) respectively, whereas SUPERFACT used mixed actinide fuels with low and high contents: (U, $Pu_{0,20}$, $Am_{0,02}$)$O_{2-x}$ and (U, $Np_{0,20}$, $Am_{0,20}$)$O_{2-x}$ respectively.

The SUPERFACT fuel operated at about 2370°C and 1920°C. It released all of the helium produced, whereas the spinel composites which operated at about 750°C only released 20% of helium after 28% of the burnup (48% after 50% of burnup). As helium is more mobile than xenon and krypton, we can expect a total gas release at the operating temperatures of ADS fuels. The size of the plenum must be big enough to hold this large quantity of gas, which can be 6 times greater than that of fission gases. It is worth pointing out that the production of helium continues out of pile via the natural decay of 242Cm. According to the SUPERFACT experiment, only 50% of the helium is released at ambient temperature. The retention of helium in the fuel during its interim storage can therefore contribute to material swelling and increase the risk of pin failure even after irradiation.

— Swelling due to matrix damage caused by fission products (Fig. 4.88, Fig. 4.90)

One of the main uncertainties related to the pin design concerns the swelling of material containing high MA contents (Fig. 4.89, Fig. 4.91). This is design basis data considering that it determines the thickness of the fuel cladding gap that has to be included to avoid strong fuel cladding interactions. As the margins are relatively small for hot fuels such as oxide composites, this can therefore have a direct impact on the transmutation performance.

Different causes of swelling were analysed. The first cause depends on the type of material and concerns inert matrix damage caused by the fission products. The high propensity of spinel to swell was demonstrated during the THERMHET and TANOX experiments [4.91]. Swelling can reach about 15 vol% in the worst case scenario and seems to be related to the amorphization of the crystal lattice structure under relatively cold temperature conditions (600°C). The thermal cycling of the material (600–1200°C) induces a recrystallisation and amorphization phenomenon. Recrystallisation on a nanometric scale also includes redensification and significant cracking. The same material that has been irradiated for the same duration at a higher temperature (> 1400°C) does not undergo any microstructural change or swelling. Excepting YAG, the other matrices ($CeO_2$, MgO, $Y_2O_3$, $Al_2O_3$) show better resistance to fission products. Composite swelling is therefore practically linear with an actinide content and does not exceed 5 vol% for contents of about 2–2.5 g/cm$^3$.

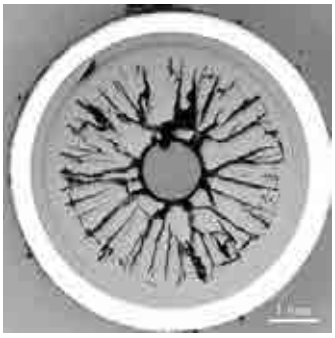

*FIG. 4.88. $MgAl_2O_4$+$UO_2$ composite swelling due to fission products (1.3at%burnup).*

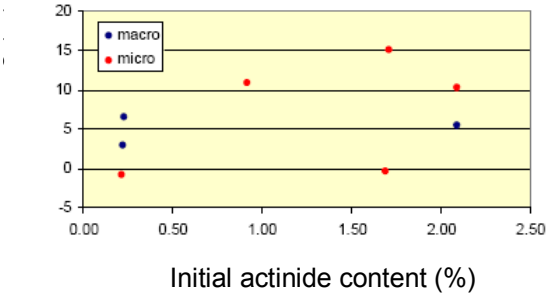


*FIG. 4.89. Swelling of $MgAl_2O_4$ composites versus initial actinide content.*

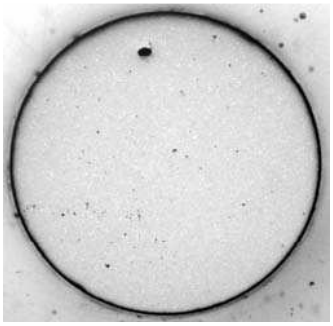

*FIG. 4.90. Microstructure of an irradiated MgAl2O4+UO2 microdispersed sample (Phenix reactor, 1400°C, 1.3at%).*

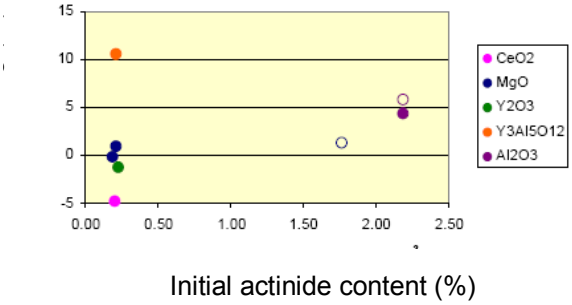


*FIG. 4.91. Swelling of composite targets versus initial actinide content (o: macrodispersion; □: microdispersion).*

The material's microstructure (whose effect on thermal conductivity has already been discussed) also has an impact on the fuel resistance to fission products. An aerated network of particles free of interconnections and well distributed in the volume limits damage to the inert matrix by the fission products and alpha particles emitted by actinides (Fig. 4.92, Fig. 4.93).

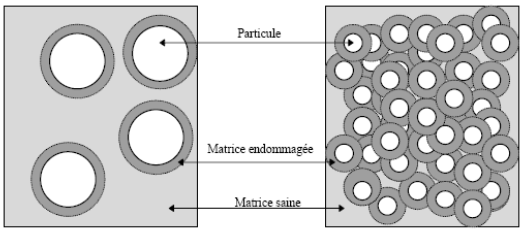


Same volume content of particles in the both pictures.

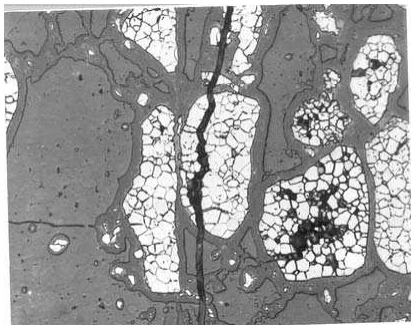

*Damaged area around particles of an irradiated sample.*

*FIG. 4.92. Behaviour of the microstructure versus volume content and size of particles*

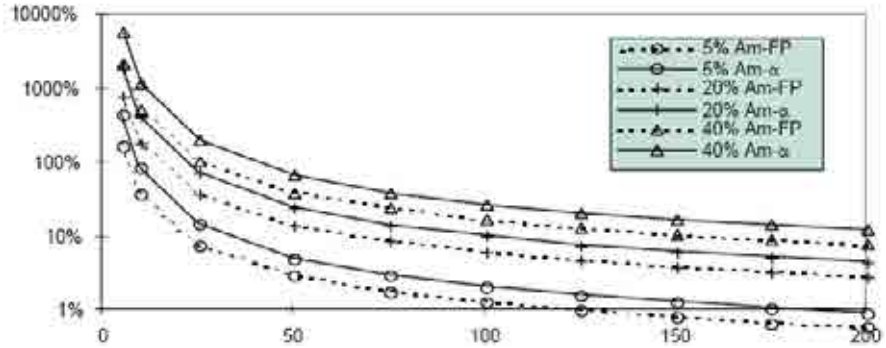


*FIG. 4.93. Damaged matrice content (vol%) versus particle diameters (μm) for several actinide content.*

Though very difficult to manufacture under the conditions required by the presence of MA, this type of microstructure has demonstrated its efficiency for spinel fuels. The $MgAl_2O_4$+$UO_2$ composite proves to have poor resistance to fission products when microdispersed, but shows excellent resistance under the same irradiation conditions when macrodispersed (Fig. 4.94).

*FIG. 4.94. Comparison of the microstructure of macrodispersed and microdispersed particle composites after irradiation: initial central hole remains in the macrodispersed sample (left side where as it disappeared in the microdispersed sample (right side).*

— Swelling due to helium

Helium's contribution to swelling has been demonstrated in the EFTTRA-T4, EFTTRA-T4bis and SUPERFACT experiments (Fig. 4.95, Fig. 4.96). They also showed pellet–cladding interactions without cladding failure, though these interactions were pronounced in the case of the target. Whereas swelling due to fission products can be controlled by choosing the right matrix or by optimising the microstructure, swelling caused by helium is a phenomenon inherent to transmutation.

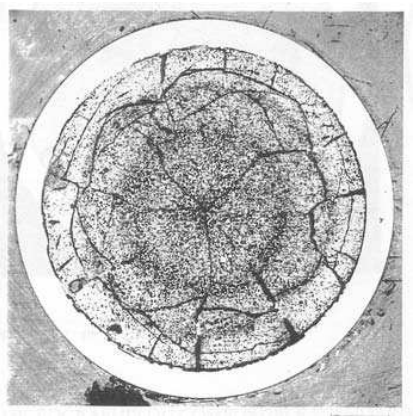

*FIG. 4.95. Ceramography of a SUPERFACT irradiated sample with 40% Am and Np content.*

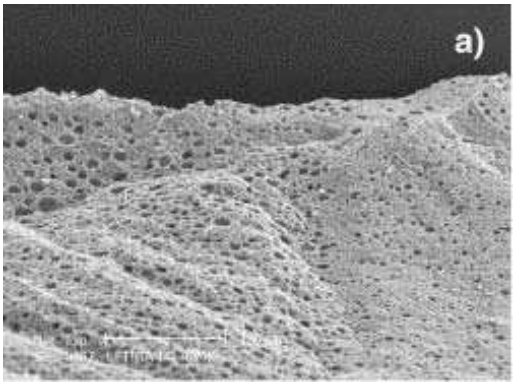


*FIG. 4.96. Porous microstructure of a $AmO_2$ microdispersed sample after irradiation (T4 test in HFR reactor).*

Swelling of 28 vol% was measured on the target that operated at temperatures of about 700°C with a burnup of 50 at%. Swelling in SUPERFACT — whose maximum temperature was 1,900°C at a burnup of 4.1 at% corresponded to the gap closure. It is possible to improve gas releases by organising preferential routes for removing helium such as those provided by open porosity and by systematically operating at high temperature. Such solutions are currently being explored in an attempt to reduce helium related swelling. Irradiation tests are currently being prepared for the HFR with the intention of validating them. It is important to determine the swelling rates and amplitudes under typical ADS conditions if we want to integrate such swelling into the fuel design.

#### *4.5.1.3. Impact on design*

Considering the characteristics of the materials and their expected behaviour under irradiation, three types of concepts are worth comparing in terms of their reactor performance:

— Hot fuels whose operating temperature allows for the release of fission gases and helium. This is the case of refractory ceramic fuels with helium bonds. (Pu, Am)$O_2$ based oxide fuels with inert matrices fall into this category. The (Pu, MA) N based nitride fuel with an inert matrix and a helium bond can also fall into this category. The thermal margins available with this fuel due to its excellent thermal conductivity are used to take on higher minor actinide concentrations than those in oxide fuel. The inert matrix in this case is generally ZrN.

— Cold fuels with low gas releases such as nitride fuels with sodium bonds. The molten metal bond enables the heat to flow easily from the fuel to the coolant. The temperature level and the temperature gradient between the core and the fuel surface must remain low, which is essential for safety. However, the effect of probable gas retention in the fuel upon swelling and its impact on the fuel's transient behaviour must be assessed. The Americans have chosen this concept.

— Cold fuels with high gaseous releases such as Pu-MA-Zr metal fuels with sodium bonds. The low operating temperatures produce significant swelling in the metal alloy, which is easily compensated by designing a big fuel cladding gap. This swelling quickly (as early as 2 at% burnup) results in the interconnection of pores and the formation of canals emerging on the surface. These canals act as pathways for the gas releases. This is an American concept based on their knowledge of metal fuel from the IFR programme.

#### *4.5.1.4. Manufacturability*

(a) Thermal and radiological stress

ADS fuels contain quantities of transuranium elements capable of amounting to more than 6 g/cm$^3$. Table 4.23 lists radionuclides of interest and their main nuclear properties. The highest MA concentration can reach more than 3 g/cm$^3$. The fabrication of such objects is made complicated by alpha, beta, gamma and neutron emissions from most of the isotopes involved in their composition, as shown in the table listing various characteristics of heavy nuclei composing the fuels and targets.

TABLE 4.23. LIST OF RADIONUCLIDES AND THEIR PROPERTIES

| Radionuclide | Half-life time (year) | Activity (xE10Bq.g$^{-1}$) | Neutron emission (n.g$^{-1}$.s$^{-1}$) | Thermal power (W/g) | Ingestion dose factor (xE3 Sv.g$^{-1}$) |
|---|---|---|---|---|---|
| Np-237 | 2.14xE6 | 0.00261 | 0 | 0 | 0.028 |
| Pu-238 | 87.7 | 63.4 | 2511 | 0.568 | 630 |
| Pu-239 | 24390 | 0.227 | 0.02 | 0.002 | 2.6 |
| Pu-240 | 6540 | 0.843 | 905.6 | 0.007 | 9.8 |
| Pu-241 | 14.3 | 382 | 0 | 0.003 | 90 |
| Pu-242 | 3.87x E5 | 0.0141 | 1678 | 0 | 0.15 |
| Am-241 | 432 | 12.7 | 1.2 | 0.115 | 150 |
| Am-242m | 152 | 36.0 | 150 | 0.004 | 410 |
| Am-243 | 7380 | 0.736 | 0 | 0.007 | 8.8 |
| Cm-242 | 0.446 | 12300 | 2.08x E7 | 122 | 4300 |
| Cm-243 | 28.5 | 170 | 0 | 1.685 | 1300 |
| Cm-244 | 18.1 | 299 | 5892 | 2.825 | 1800 |
| Cm-245 | 8530 | 0.633 | 5448 | 0.006 | 7.6 |

Curium is without a doubt the most problematic isotope for fuel fabrication plants. It is a powerful source of neutrons, and its major isotope, $^{244}$Cm, naturally gives off 2.8 W/g, which is why handling poses technological problems at each stage of the fabrication process. The second most problematic isotope is $^{238}$Pu, whose accumulation during recycling poses similar problems, though on a smaller scale than curium. After plutonium comes $^{241}$Am. Other than suitable protection against neutron and gamma radiation (thick walls of concrete or light materials such as polyethylene or water to stop neutrons) which imply remote handling, the permanent cooling of the tools and vessels is essential from the conversion phase (transition from a liquid solution containing the actinides, to a solid actinide compound) right through to the assembly and storage phases (also in shielded cells). The transport of fuel assemblies and their handling in reactor are also affected by these thermal and radiological constraints.

Aspects such as the compactness of the plant, and the simplicity and robustness of the fabrication process for curium fuel and targets are absolute necessities when it comes to limiting the economic cost of automatic fabrication in shielded cells. Limiting the volume and number of cells, simplifying equipment maintenance, reducing the volume of contaminated waste, shortening the duration of fabrication and inspection operations, and making scrap recycling easy, are all major requirements. The consequences can be detrimental on the fuel or target performance.

The search for improved microstructures, e.g.: macrodispersion, to meet the ambitious transmutation objectives does complicate the process. A granule making stage is required for which the size, composition and distribution the granules (macromasses) in the inert matrix must be checked. A good compromise between performance and manufacturability must be found. A systematic study of the process's impact on the microstructure and inpile performance therefore seems essential in order to reach this compromise.

The constraints involved for americium are especially radiological. The remote handling in stainless steel or lead cells is generally sufficient. Furthermore, certain stages of the process (e.g.: quality control of small volume samples) can be performed using pincer boxes. In this case, using complex processes to obtain fuels with improved microstructures seems more reasonable on a technical & economical viewpoint.

The economic gain associated with improved in reactor performance could compensate for the additional cost of fabrication. However, Pu-238 can be found in significant quantities in ADS fuels after several combined recycling operations of plutonium and americium. This can engender constraints requiring us to rethink the process, as for curium based fuels.

Last of all, neptunium is the only minor actinide that is relatively transparent in terms of fabrication: the standard handling conditions (gloveboxes) for (U, Pu) O2 fuels are sufficient for recently purified neptunium. However, aged neptunium requires reinforced biological protection owing to protactinium generated by decay.

(b) Impact of thermodynamic properties of minor actinides

The physicochemical properties of minor actinides are remarkably different from those of major actinides (U-Pu), and they have an impact on the synthesis and storage conditions. Regardless of the chemical nature of the actinide compound (nitride, oxide or metal), the pronounced volatility of americium species can be observed. Fig. 4.97 illustrates this point for metals and oxides.

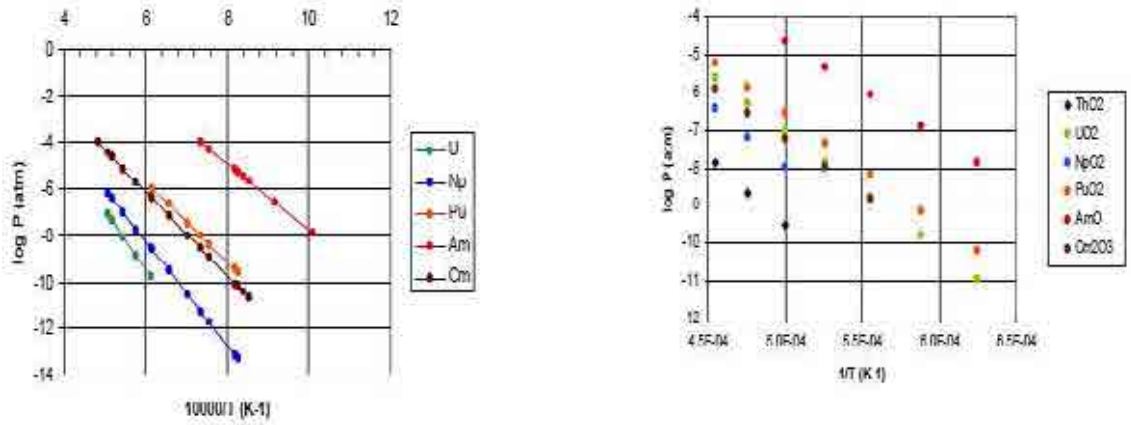


*FIG. 4.97. Vapour pressure of actinide elements and oxides versus temperature.*

For oxides, the vapour pressure of the minor actinides is as high as the actinide valence is low [4.95]. This high vapour pressure can result in the vaporisation of species and a change in the respective concentrations of elements during the heat treatment such as sintering. This phenomenon can nevertheless be minimised by controlling the oxygen potential of the sintering gas, and by applying a suitable thermal cycle. For nitrides such as carbides, the loss of americium (often resulting from the ageing of Pu-241) proved to be significant at heat treatment temperatures above 1500°C. Thermal stability tests on AmN and (Am, Zr)N [4.96] showed that AmN decomposes from 1300°C and undergoes selective vaporisation at higher temperature. The amplitude of the phenomenon at high temperature, and the significance of the gas during the heat treatment are illustrated in Fig. 4.98.

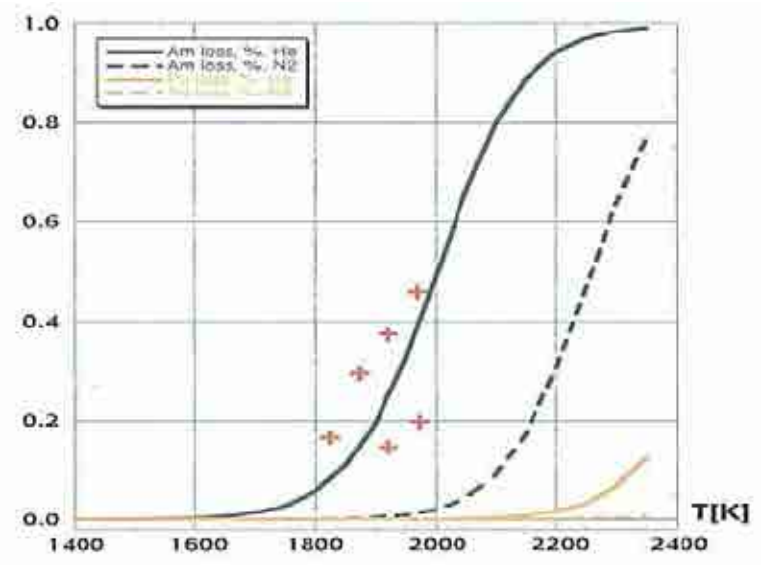


*FIG. 4.98. Americium and plutonium loss versus temperature and gas atmosphere (He or Ne: 1 bar), calculated from free energy of vaporization of AmN and PuN.*

Losses can be practically total for the metal, which implies a fast flash heat treatment for the casting of metals and their homogenisation.

(c) Fabrication processes

Power metallurgy processes, such as those used on an industrial scale for PWR MOX fuels, are well suited for the laboratory fabrication of a broad range of fuels and transmutation targets. These processes are flexible and universal, meeting quality requirements related to reactor performance. They have demonstrated their capacity to implement elaborated microstructures (solid solution, macro and microdispersed composites with inert matrices).

For minor actinide nitrides, the volatility of americium nitride at temperatures below the usual sintering treatment temperature raises a problem that has yet to be solved.

The main disadvantage that may compromise its use for the industrial scale fabrication of fuels and americium targets is the problem of managing fines resulting from milling (and possibly rectification) which occur downstream of the pressing phase. They accumulate in the filters of the shielded cells and on the walls of the plants, which raises a radiological problem considering the characteristics of the isotopes involved.

The possibility of removing these penalising stages would be a major industrial breakthrough. This is the objective of the synthesis processes by co-precipitation or solgel, which would make it possible to directly obtain the required composition of the mixtures with a controlled grain size distribution, therefore removing the milling and granulation stages. Development of the VIPAC-SPHEREPAC process by means of directly filling the pins with granules would allow us to optimize the process even further by removing the pressing stage. Each stage removed would also simplify the control operations.

(d) Co-precipitation processes [4.97]

Precipitation or co-precipitation are the most frequent methods used to obtain a solid from actinide solutions resulting from extraction and purification operations involved in treating spent fuels (based on a hydrometallurgy method). Furthermore, even in the case of fuel or target fabrication using a dry process (powder metallurgy), this precipitation stage combined with a heat treatment would be required to temporarily solidify the different minor actinides resulting from the spent fuel treatment.

Though the implementation of this precipitation stage seems straightforward (mixture of reagents), controlling it requires taking into account all of the physicochemical and chemical engineering

parameters. The main properties affected by these parameters are 1) the chemical composition of the precipitate and its physical characteristics (castability, grain size distribution, filterability, and microstructure), 2) the possibility of reproducing these characteristics, and 3) the actinide concentration in the effluents.

To illustrate the importance of the operational parameters to be taken into account, the composition of the precipitate and its physicochemical properties greatly condition those of the ceramic phase produced following heat treatment, i.e.: the precursor of the fuel material.

This approach to understanding and controlling the different stages of precipitation began about ten years ago within the scope of studies on the oxalic conversion of plutonium. Each time progress is made, it is applied to the co-precipitation of several actinides and possibly an inert element. In the end, progress made in this modelling approach should enable us to play around with these parameters to more systematically obtain a solid compound with targeted or original characteristics, especially in terms of the grain size distribution and microstructure. For the time being, these characteristics tend to be obtained randomly. This compound could therefore be used as a direct fuel precursor, simplifying its fabrication, e.g.: by removing upstream stages of mixing and comilling of the oxide powders of each actinide.

However, the issue of managing the high level effluents generated by certain co-precipitation processes (especially those using ammonia or carbonate) remains to be solved. In terms of oxalic co-conversion, feedback collected from the oxalic conversion of plutonium on an industrial scale has subsequently helped develop this process. Furthermore, these processes generally result in powders, and certain fuel or target concepts (e.g.: based on spherical particles) can require additional forming stages (agglomeration, pressing, etc.). The solgel processes have the advantage of having integrated these stages into the cogelation phase.

It is worth pursuing R&D on co-precipitation processes in order to broaden solid forming possibilities (increase in particle size, improvement of powder castability, wet agglomeration process) and to continue simplifying subsequent fuel fabrication stages, while remaining within the limits inherent to the principle of these processes used to obtain solid powders.

(e) Solgel processes [4.98] [4.99]

In the 1980s and 1990s, several solgel processes were tested for the fabrication of actinide materials (mixed oxides, carbides and nitrides). The main advantage of any solgel process lies in the easy forming stage performed during gelation thanks to the fluidity of the initial solution. A great deal of research describes the controlled fabrication of dense or porous microspheres depending on their subsequent use, for example, as particle fuel or pellet fuel.

Apart from the main advantage of forming the solid synthesised compound, the very principle of gelation generally makes it possible to obtain homogeneous compounds thanks to the perfect initial mixture of the elements in solution. The formation of solid solutions is thus simplified during the subsequent heat treatment phase.

Once optimised, this technique can be used to obtain — after washing, drying and calcining — spherical particles of a homogeneous composition resulting from the co-condensation of the heavy metals involved. The different variations of this process are especially well suited to the coconversion of several actinides, or an actinide with an easily hydrolysable inert element (e.g.: Zr), including the forming of the material.

The main disadvantages are associated with the lack of R&D data and know-how in terms of:

— Preparing the initial actinide solution which must be concentrated (about 1 mol.l, 1 of heavy metals), and partially denitrided;

— Recycling (or eliminating) additives and the relatively complicated management of degradation products and effluents;

— Taking into account heat and radiolytic effects.

The current lack of experience in elaborating materials containing minor actinides, elements that are more difficult to hydrolyse than the more common actinides, and that also provoke pronounced radiolytic and heat effects prevents us from concluding on the possible transposition of these processes to manufacture fuel or transmutation targets.

However, considering the potential of these processes, the main recommendations are to continue recently launched R&D so we can improve their application to MA-based compounds, especially in terms of the following key points:

— Better control over the preparation of concentrated and partially denitrided actinide solutions upstream of the gelation stage;

— Forming of solids containing significant contents of An(III) or even An(V) which are difficult to hydrolyse (the actinides involved are Am-Cm and Np respectively);

— Specific treatment of aqueous effluents containing ammonium nitrate.

There are several solutions to be tested for effluents that could eliminate ammonium nitrite, either by recycling as ammonia and nitric acid solutions (by electrolytic treatment or by extraction using an ion exchanger), or by breaking it down directly by photochemistry. Furthermore, microwaves have already been used for internal gelation in several laboratories (ORNL, PSI, JAERI) to avoid using silicon oil and to simplify the washing stages: this simplification remains to be assessed for the gelation of solutions containing MAs.

(f) VIPAC-SPHEREPAC process [4.100]

VIPAC-SPHEREPAC is a pin filling process based on the vibrocompaction of dense granules. Densification of the column of powder is obtained by rearranging the different grain sizes of the granules by means of vibration.

This technique is interesting for transmutation fuels as it significantly simplifies the fabrication process right up to cladding, and also does away with the dust producing steps: milling, granulation, pressing and rectification.

The success of such a process depends on two specific points:

— Manufacturability of the granules whose grain size must be perfectly controlled in order to obtain a filling density that is compatible with the reactor specifications and mechanical resistance that is capable of withstanding the filling and vibration operations. The studies described in §8.5.3.2 also mention this problem.

— The pin filling quality, characterised by the final compactness of the fissile column and the homogeneity of the actinide distribution and density throughout the fissile column. The final objective is to obtain a high powder density so as to minimize inpile redensification phenomena at the operating temperature. The linear density and the distribution of the fissile material must be as homogeneous as possible to ensure identical neutron behaviour throughout the pin. The rod transport in a horizontal position must not affect the density either, especially at the ends of the fuel column.

Several irradiation experiments on vibrocompacted fuels have been performed worldwide since the concept appeared about 40 years ago, demonstrating their feasibility. The Russians are still using the BOR-60 and BN-600 fast reactors to irradiate full assemblies of vibrocompacted rods containing $(U,Pu)O_2$ obtained from pyro-electrical reprocessing. The particle size varies between 30 μm and 1200 μm. The granule density is very close to the theoretical density (98%) and that of the fuel column is 88%MVTh.

#### *4.5.1.5. Conclusion*

Transmutation fuels are very innovative and have not so far been developed. Experimental programmes are going on to provide properties of materials both inpile and out of pile, and to develop

the first models to predict fuel behaviour under irradiation on the basis of national programme results and collaborative agreements on transmutation targets and fuels for reactors using validated technologies.

A preliminary assessment carried out within a European framework in collaboration with the US DOE and JAERI have made possible to test three types of uranium free fuel highly loaded in transuranium elements. These fuels are:

— A Pu-MA-40Zr metal fuel with a sodium bond;

— A (Pu, MA, Zr)N nitride fuel with a helium or sodium bond;

— A (Pu, MA)$O_2$+MgO or $^{92}$Mo oxide composite fuel.

Their irradiation in the Phenix reactor (FUTURIX-FTA programme) which is going on should allow us to compare the different hot and cold fuel concepts, especially their swelling caused by fission product damage or by the significant production of helium *in situ*. In addition to this programme, the irradiation of ADS fuel precursors without minor actinides in the BOR 60 fast reactor (BORA-BORA) or in the HFR should also provide a great deal of information.

Moreover, as the first conceptual overall designs for ADS industrial transmuters have been recently described within European (EUROTRANS) and Japanese programmes, the fuel development studies comes into a technological stage of assessment.

### 4.5.2. Nitride fuel development in Japan

#### *4.5.2.1. Purpose and goal*

Nitride fuel for ADS has been developed by Japan Atomic Energy Agency (JAEA) under a double strata fuel cycle concept. In this case the nitride fuel contains MA elements as a principal component and is diluted by inert materials in place of U, which is totally different from the fuel for power reactors. So the fuel fabrication manner, fuel properties and irradiation behaviour have to be investigated in detail as well as the treatment of spent fuel. Through the experimental R&D, technical feasibility of nitride fuel cycle for the transmutation of MA will be demonstrated [4.101]–[4.105].

#### *4.5.2.2. Theoretical explanation*

Uranium–plutonium mixed nitride fuel has been developed for an advanced fuel for FRs because of superior thermal and neutronic properties of nitride fuel. In addition, the formation of mononitride solid solution including MA elements is possible in wide range of actinide combination and composition, which leads to a big advantage of the dedicated fuel for ADS. These characteristics enable us to design the MA transmutation cycle, in which MA elements from the partitioning plant is transmuted by 0.25 ton/year using one ADS with 800MWt. One of the drawbacks of nitride fuel is that N-15 enriched nitrogen has to be used for preventing the formation of long lived C-14. So the development of economical enrichment of N-15 and its recycling technology in fuel fabrication process is inevitable.

#### *4.5.2.3. Instruments description*

Experiments on MA nitride fuel have been carried out in JAEA Tokai and Oarai. Since MA nitride fuel is easily hydrolyzed and oxidized in air even at room temperature, inert gas atmosphere is necessary for handling nitride samples. In JAEA Tokai, experiments are carried out in hot cells and gloveboxes of Nuclear Fuel Cycle Safety Engineering Facility (NUCEF) and Waste Safety Testing Facility (WASTEF), while experiments are carried out in gloveboxes of Plutonium Fuel Research Facility (PFRF) in JAEA Oarai. The experimental apparatus for nitride fuel includes reduction and sintering furnace, X ray diffratometer (room temperature and high temperature), TG/DTA/DSC,

chemical analysis apparatus, laser-flash apparatus, drop calorimeter, quadrupole mass spectrometer, electron microscope, molten salt electrorefiner, cathode processor, fuel pin welding apparatus and so on. An appearance of a modular facility for TRU high temperature chemistry, called 'TRU-HITEC', constructed in NUCEF, is shown in Fig. 4.99.

#### *4.5.2.4. Most important results*

Solid solutions of MA bearing nitride were prepared by carbothermic reduction of their oxides. Fig. 4.100 shows an X ray diffraction pattern of (Np, Pu, Am, Cm) N solid solution prepared by carbothermic reduction. Main concern focused on preventing the loss of Am by evaporation and reducing the oxygen and carbon impurities in the product of carbothermic reduction. Further, MA nitride fuel with possible diluents such as ZrN and TiN were prepared and characterized.

Thermal diffusivities and thermal expansions of MA nitrides and their solid solution were measured and thermal conductivities were evaluated. It was found that thermal conductivity of actinide mononitride decreased with the atomic number of actinides. Measurements of specific heat capacities of MA nitrides are also in progress. Further, evaporation behaviour of MA elements and thermal properties of UN-based burnup simulated samples were measured.

With regard to pyrochemical process for the treatment of spent nitride fuel, anodic dissolution behaviour of nitride fuel in LiCl-KCl molten salt was investigated mainly by electrochemical measurements. Recovery of actinides into liquid Cd cathode by electrorefining and nitride formation of actinides in liquid Cd by nitridation distillation combined manner was demonstrated.

Following the irradiation tests of (U, Pu) N fuel in JOYO and JMTR, U-free nitride fuel pin containing (Pu, Zr) N and PuN+TiN pellets was irradiated in JMTR and post-irradiation examinations were completed in Reactor Fuel Examination Facility. Appearances of (Pu, Zr) N and PuN+TiN pellets before irradiation, and cross-sections of the irradiated pellets are shown in Fig. 4.101 and Fig. 4.102, respectively. For the moment no detrimental effects on the irradiation behaviour of nitride fuel has been found by the addition of ZrN or TiN.

*FIG. 4.99. Appearance of TRU-HITEC in NUCEF of JAEA Tokai.*

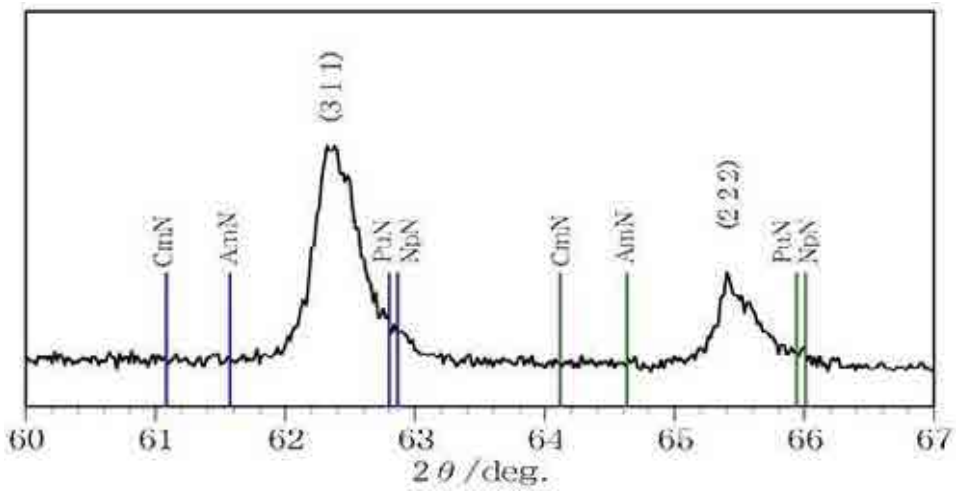


*FIG. 4.100. X ray diffraction pattern of (Np,Pu,Am,Cm)N prepared by carbothermic reduction.*

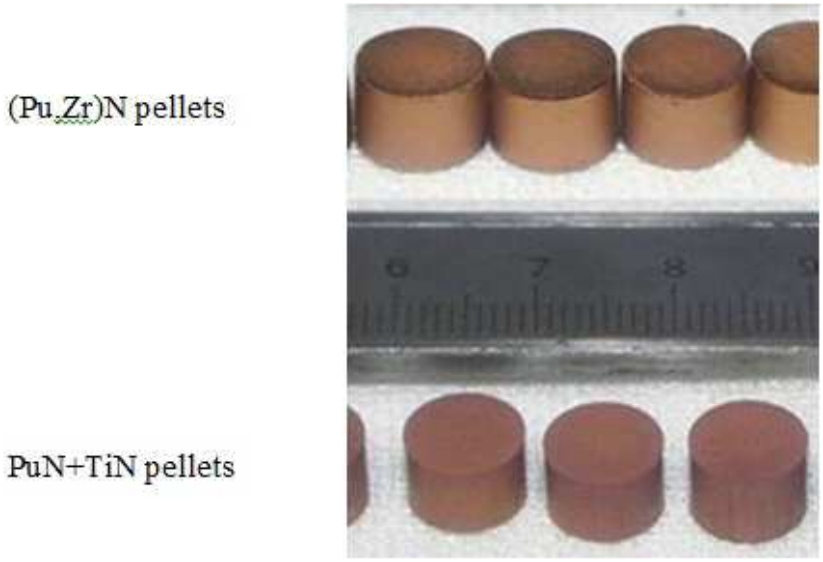


*FIG. 4.101. Appearances of (Pu,Zr)N and PuN+TiN pellets used for the irradiation test.*

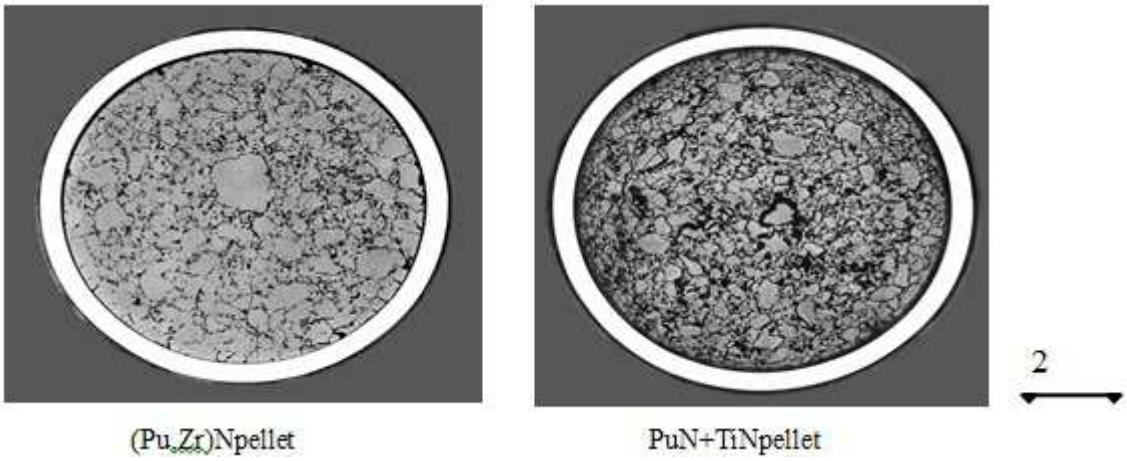


*FIG. 4.102. Cross-sections of (Pu,Zr)N and PuN+TiN pellets after irradiated in JMTR.*

The section presents an overview of the main R&D activities on coolant technologies ongoing at international level, in support to the development of ADS systems.

## 4.6. COOLANT

The section gives an overview on the Coolant technology considered for the ADS design under development.

### 4.6.1. Coolant technology experience at FZK Germany

#### 4.6.1.1. *Purpose and goal*

The measurement and adjustment of the oxygen activity in liquid lead and lead alloys is a critical issue when applying these materials as coolant in nuclear facilities. On the one hand, the oxygen concentration must be high enough for establishing a protective oxide scale on the surface of the structural materials (e.g. steels) in order to prevent their dissolution in the liquid metal. On the other hand, a certain threshold must not be exceeded, so that precipitation of coolant oxides within the flow paths of the plant is prevented. For measuring and keeping the concentration of dissolved oxygen in liquid lead alloys at the appropriate level, electro-chemical sensors and an oxygen control system based on $H_2$-$H_2O$ were developed at FZK.

#### *4.6.1.2. Description of theory (oxygen sensor)*

The measuring principle of electrochemical (or solid electrolyte) oxygen sensor for the use in liquid metals is shown in Fig. 4.103 [4.108]. It consists of a reference electrode that is separated from the liquid metal by a solid electrolyte which, in the ideal case, is an electric insulator, but conducts $O^{2-}$ ions. The second electrode of the electrochemical cell is the liquid metal itself which is in electric contact with the housing of the sensor. The difference in the electric potential on both sides of the solid electrolyte, i.e., the potential difference between the sensor housing and the electric lead of the reference electrode, is measured via a high impedance voltmeter at zero current, which gives the electromotive force (EMF or E in mathematical equations) of the electrochemical cell. The EMF is proportional to the difference of the chemical potential of gaseous oxygen at the reference electrode and in the liquid metal. Usually this difference is substituted by the natural logarithm of the ratio of the respective oxygen partial pressures in the reference and in the liquid metal. The latter can be interpreted as the oxygen pressure above the liquid metal phase and depends on the oxygen content of the liquid metal.

$$E = \frac{RT}{zF} In \frac{P_{O_{2;Ref}}}{P_{O_{2;LM}}} \qquad \text{(Eq. 4.1)}$$

Where $R$ is the universal gas constant ($R$ = 8.31451 J/(mol K)) and $T$ is the thermodynamic temperature in Kelvin, $z$ is the number of electrons per oxygen molecule which is produced and consumed at the anode and cathode, respectively, of the electrochemical cell and $F$ is the Faraday constant ($F$ = 96485.31 C/mol). By convention, the EMF is positive if the oxygen potential at the reference electrode is higher than the oxygen potential in the liquid metal.

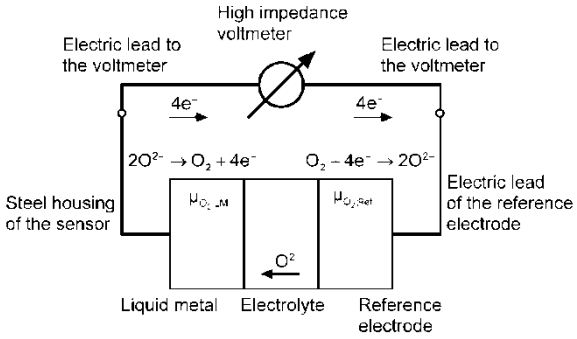


*FIG. 4.103. Measuring principle of electrochemical oxygen sensors.*

*4.6.1.3. Oxygen control system*

The oxygen potential that is required to protect the steel surface by formation of stable oxide layers is here established by control of the $H_2 - H_2O$ ratio in the gas atmosphere above the liquid lead alloy [4.107]. It is known from Gromov [4.106] that the oxygen partial pressure in the gas phase must be higher than that required for oxidation of iron, the main steel component, and lower than that for $PbO$ formation. Formation of $PbO$ would lead to plugging of the loop. In terms of the Gibbs energies of formation of $Fe_3O_4$ and $PbO$ this condition is given by

$$2\Delta_f G^0(PbO) > RTInp_{O2} > 0.5\ \Delta_f G^0\ (Fe_3O_4) \qquad \text{(Eq. 4.2)}$$

where $p_{O2}$ gives the oxygen partial pressure in the gas atmosphere in equilibrium with the metal melt. The relation between $H_2 - H_2O$ ratio and the oxygen partial pressure is given by

$$P_{O_2} = \frac{P^2{}_{H_2O}}{P^2{}_{H_2}} \exp(2\Delta_f\ G^0\ /RT) \qquad \text{(Eq. 4.3)}$$

In order to calculate the oxygen concentration in equilibrium with the oxygen partial pressure $P_{O_2}$, the activity coefficient has to be known. The activity coefficient can be calculated from the relation for the oxygen activity in $Pb$ and LBE.

The theoretical principles related to the oxygen potential adjustment in the liquid metal via the $H_2 - H_2O$ relations is summarized in Fig. 4.104.

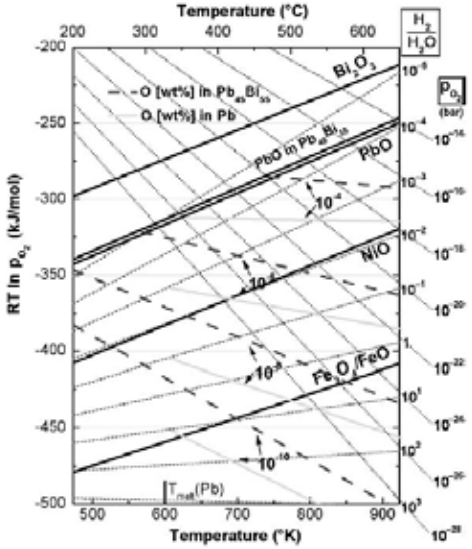


*FIG. 4.104. Ellingham-Richardson diagram. Lines of constant oxygen concentrations in Pb and LBE melt indicate the stability regions of iron oxide without PbO precipitation in the temperature gradient.*

The diagram in Fig. 4.104 shows in which region the stable conditions exist and how they can be established. The ordinate shows the partial Gibbs energy of oxygen expressed by the oxygen partial pressure, the abscissa the temperature. The lines of constant $H_2 - H_2O$ ratios and those of constant oxygen partial pressures, $p_{O2}$, show the ratios which must be established in the gas phase to attain a certain oxygen partial pressure. Those lines intersect at absolute zero temperature, the $P_{O_2}$ lines at $RT$ ln $P_{O_2} = 0$ and the $H_2 - H_2O$ lines at $RT\, Inp_{O_2} = 2\Delta_f G^0\,(H_2O)$. The important region with protective oxide scale formation is the one between the lines for PbO and $Fe_3O_4 - FeO$ in the temperature region of 200–650°C, which is relevant for loops with liquid LBE and Pb. The diagram also contains lines of constant oxygen concentration in Pb and the LBE melt in equilibrium with the corresponding oxygen partial pressure and $H_2 - H_2O$ ratios.

### *4.6.1.4. Major results*

The design of the oxygen sensors which were developed at FZK for use in liquid lead and lead alloys is schematically shown in Fig. 4.105. Two versions of these sensors exist, one working with Pt/air as a reference system for the measurement of the oxygen potential and the other working with a metal–metal oxide pair, i.e., Bi-$Bi_2O_3$. In both cases, the solid electrolyte is zirconia partially stabilized with yttria.

In the case of the Pt/air sensors (Fig. 4.105, left), the reference electrode inside the electrolyte tube consists of a stainless steel wire with a platinum tip. The head of the Pt/air sensors is provided with two open tubes which allow for the ingress of air into the inside of the electrolyte tube. In the case of the Bi-$Bi_2O_3$ sensors (Fig. 4.105, right) which are designed for operating temperatures above the melting point of bismuth (271°C), the electric lead of the reference electrode is a molybdenum wire submerged in the, at the operating temperature, liquid metal oxide mixture. The housing of the sensors is made of stainless steel and consists of the sensor head and a sheath that is screwed together with the sensor head (Fig. 4.105). The bottom part of the sheath is perforated, so that the liquid metal, the oxygen content of which is measured, can encounter the closed end of the electrolyte tube.

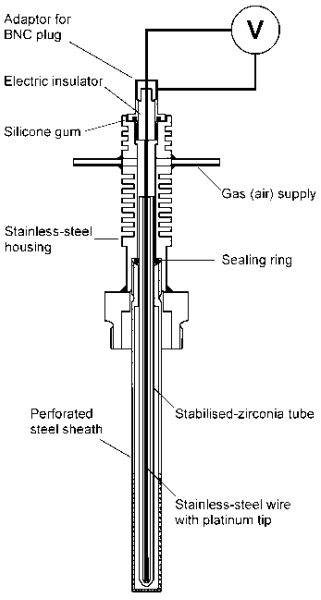


Left: Sensor with Pt/air reference system.

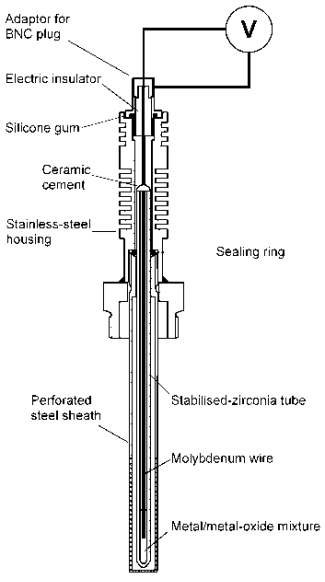


Right: Sensor with metal-metal oxide (Bi-$Bi_2O_3$) reference system.

*FIG. 4.105. Schematic illustration of the electrochemical sensors developed at FZK for the measurement of the oxygen potential in liquid lead alloys.*

The oxygen control system developed at FZK is reported in Fig. 4.106. The gases Ar and Ar/5%$H_2$ are mixed in an oxygen control system by two flow controllers to obtain the required hydrogen concentration in the cover gas. The gas passes through a moisturizer, the water vapour pressure of which is controlled by a precision thermostat. The oxygen control by equilibration between gas phase and liquid metal in the reaction tube is sketched in the shaded area of the picture. The incoming and outcoming gas is checked by a moisture sensor and finally by an oxygen partial pressure detector.

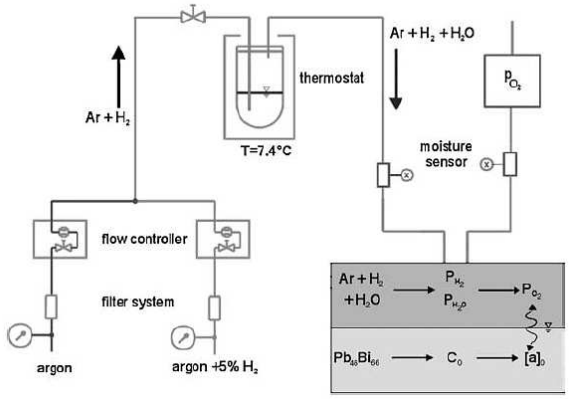


*FIG. 4.106. Scheme of an oxygen control system with gas conditioning and control.*

On the principle described above, the oxygen control system and the oxygen sensors were developed and build to control the oxygen concentration in the KALLA loops at FZK. In Fig. 4.107 the output of the oxygen sensors, during 8000h of continuous operation at the CORRIDA loop of KALLA is reported.

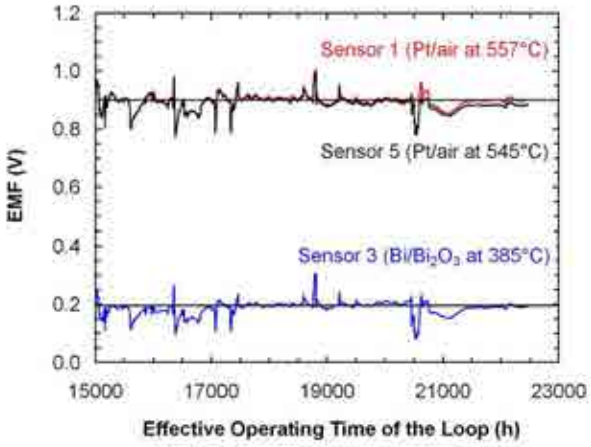


*FIG. 4.107. Output of oxygen sensors (Sensors 1, 3 and 5) during the last 8000 h of effective operation of the CORRIDA loop.*

Sensor 1 is a Pt/air sensor that resides at a nominal temperature of 550°C at the inlet of the first test section of the loop.

Sensor 3 is a Bi-$Bi_2O_3$ sensor that resides in the cold leg of the loop at a nominal temperature of 380°C.

Sensor 5 is a Pt/air sensor that resides at a nominal temperature of 540°C at the outlet of the oxygen box.

The oxygen concentration has been successfully kept and measured at the requested level to build oxide scales on the corrosion test samples installed in the CORRIDA loop.

### 4.6.2. Coolant technology experience in Italy

#### *4.6.2.1. Purpose and goal*

The goal of this document is to summarize and describe the ENEA experience in the frame of oxygen monitoring in HLM systems.

#### *4.6.2.2. Description of theory and-or instruments*

The development of the heavy liquid metal chemistry control and monitoring is one of the issues that is critical for nuclear systems using lead alloys either as a spallation target or as a coolant [4.109]–[4.119]. Indeed, the chemistry interacts with at least three operating specifications of any nuclear system, such as the contamination control the corrosion control and the radioactivation control, to ensure a safe management of the operations and maintenance phases;

These three requirements refer all to the chemistry control in lead alloys systems as regards the oxygen and others relevant impurities such as the corrosion products, spallation and activation products.

The use of the ionic conduction properties of some solid electrolyte, and in particular the zirconia based ceramic, allow to make electrochemical cell assembly that enables the measure of dissolved oxygen in liquid metal system. This is known as the electromotive force measurement in open circuit or as the galvanic cell method.

This technique presents several well known advantages such as:

— Specific to the dissolved oxygen, but the bounded oxygen, such as in oxide, is not taken into account;

— Rapid and continuous sensor, that is able to be implemented directly on the system, provided the leak tightness of the seal in between the liquid metal and the ceramic;

— Wide concentration range covered by one single sensor as well as it potential operating temperature range;

— No relation with the size and contact area of the electrodes.

In addition, the sensor makes hardly any disturbance on the measured system and it can be used on a number of applications.

The main requirements for an on-line oxygen sensor are as follows: accurate in such a low oxygen concentration range, reliable, predictable and safe for long term nuclear operation. However, some limitations appeared on some sensors [4.109], such as the ceramic relative fragility, as well as the time drift that is often observed that will delay for a while their direct implementation on nuclear system.

#### *4.6.2.3. Principle & theory*

Sensors are based on the electromotive force (EMF) measurement method at null current for a galvanic cell. This cell is built with a solid electrolyte: zirconia doped with either magnesia or yttria as this doping element stabilizes the ceramic into the tetragonal form, which allows oxygen ions to cross the electrode and to conduct (temperature and oxygen concentration fixed).

In Fig. 4.108 the working principle of the galvanic cell is described: (1) is the reference electrode, with a constant oxygen concentration ($CO_2$), while (2) shows the working electrode) which is the liquid metal phase where the unknown $CO_2$ is.

The method of the electromotive force (EMF) measurement with null current can be applied to the measurement of the dissolved oxygen in liquid lead-bismuth alloys. A typical electrochemical galvanic cell that will be subsequently referred to as EC sensor, is as follows:

Mo, Metal + metal oxide (reference) // $ZrO_2 + Y_2O_3$ //$Pb + PbO$ (lead alloys solution), steel (Eq. 4.1)

where the yttria stabilized zirconia (YSZ) ceramic, which conducts specifically oxygen ions, separates 2 medias showing different oxygen activities : an electromotive force is then formed across the solid electrolyte. If one of the media is defined to act as a reference, so as to maintain constant the oxygen partial pressure to a defined value, then the EMF is a function of the oxygen activity in the other medium.

Assuming pure ionic conduction in the solid electrolyte, and assuming that all transfers at the various interfaces developed in the electrochemical cell are reversible, the Nernst relation giving the theoretical EMF. can be written:

$$E_{th} = \frac{RT}{4F} \ln \frac{P_{O2(reference)}}{P_{O2}} \quad \text{(Eq. 4.2)}$$

With:

$E_{th}$ in Volts,

$R$ the perfect gas constant (8.31441 J/mol/K),

$F$ the Faraday constant (96484.6 C/mol), T the temperature (Kelvin),

$P_{O2}$ the oxygen partial pressure in the media.

The choice of the reference system depends widely on various parameters, such as for instance the gas or liquid phase, liquid metal are known to provide a better contact with the solid electrolyte, and then a lower cell resistance at comparatively lower temperature. The use of low melting point metal allows favour the use of the sensor in a higher temperature range. In addition, the contact lead wire must be compatible with the liquid metal melt of the reference. The chemical compatibility with the solid electrolyte must be correct as well.

The ceramic electrolyte, which should be in contact with le melt alloy, is of a cylindrical shape. Its bottom is semi spherical. The reference electrode and the metallic wire are hosted inside the electrolyte . The metallic wire is joint to the voltmeter. It is possible to use different kind of reference electrode:

— $Bi - Bi_2O_3$ (mp. 271°C), Mo lead wire;

— $In - In_2O_3$ (mp.157°C), Mo lead wire;

— Air, Pt lead wire;

Due to signal amplification problems detected for the Air/Pt sensor, the research programme was focused on the calibration of a $Bi - Bi_2O_3$ (Fig. 4.109) sensors supplied from IPPE, Obnisk (Ru) and the design and calibration of a $In - In_2O_3$ sensor (Fig. 4.109). This analysis was performed for pure lead as well as for the lead-bismuth (55% in weight) eutectic.

#### *4.6.2.4. Calibration experimental procedure*

(a) Oxygen fine measure experimental device

The OFM calibration facility is a device built in order to test and improve electrochemical oxygen sensors for liquid metals in stagnant conditions. It consists of a cylindrical vessel, a heating system, an inert atmosphere gas bubbling system and an electronic multimeter. The recorder registers the temperature of the vessel, the sensor signal and the gas pressure. The bubbling is performed with Ar coming from a pressured tank. The vessel has an interchangeable top with a swagelock sealing for the gas pipes and the sensor itself. There are two kinds of vessel tops: a simple one for measures in reducing conditions and a more complex one for oxidizing conditions tests.

(b) Test parameters

Two $B_i - B_{i2}O_3$reference oxygen sensors, as described above, made by IPPE [4.110], Obnisk, RU, were calibrated in the OFM facility, recording the EMF signal and their behaviour in different temperatures. For simulating the CHEOPE III loop oxidizing conditions, i.e. an oxygen concentration of $10^{-5}$–$10^{-6}$ wt %, solid Fe was added to the liquid Pb-55.5 Bi eutectic; for simulating the reducing LECOR environment, solid Mg was added and an oxygen concentration of $10^{-8}$–$10^{-10}$ wt % was reached. The atmosphere was kept inert via an Ar bubbling inside the vessel. The calibration process followed the scheme summarized in Table 4.24.

Two temperature loops were performed in order to check the reputability of the electrode signals. The acquisition system for the CHEOPE III sensor was a digital one, while the one for the LECOR sensor signal was an analogical data recorder. This is why the EMF graphics are different and the calculation of a tendency line for the analogical graphics was necessary.

(c) Calibration experimental results

After the calibration campaign, the data collected were plotted in order to compare the behaviour of the sensors in different environmental conditions. They show a quite linear behaviour of the two sensors, in stagnant condition. Fig. 4.110 summarizes the experimental results, comparing them with the calculated theoretical curves of EMF at fixed oxygen concentration. The iron oxide curve and the magnesium oxide one are emphasized. It is possible to underline the good behaviour of both the sensors at different temperature plotting the output EMF signal parallel to the temperature variations.

Fig. 4.111 shows the sensor signal of the LECOR and the CHEOPE III loops.

(d) Calibration conclusions

Both Bi–$Bi_2O_3$ sensors gave good accordance between expected and experimental data, in stagnant conditions. The EMF measured values were consistent with the predicted calculated ones giving an accurate behaviour, with an excellent agreement with the calibration standard for further work. During the calibration campaign in lead, it has been noted that the outcome signal does not vary too much then the one in LBE. Usually it is, at least,10–20nV less then the previous one for the same testing temperature.

### *4.6.2.5. Experimental data*

After the calibration procedure the sensors were mounted in the LECOR and CHEOPE loops.

(a) LECOR loop data

— $Bi - Bi_2O_3$

The historical reconstruction of the oxygen sensor signal during the four experimental runs ($T = 637\ K$, constant) is shown in Fig. 4.112. In the first run, before starting exposure tests, 130.8 g of Mg were added in 400 l ca. of LBE in order to guarantee the reducing conditions. In the second run, after the conditioning in the storage tank with $Ar + H_2$ (3%). the oxygen signal stands near 500±100 mV. In the third run, shows an oscillatory path near 500±30 mV, even thought there had been a plant stop. In the fourth run the oxygen concentration grew up consistently; for lowering this, a gas bubbling was performed, without success, and then Mg was added again.

It is noticeable how the oxygen concentration has an oscillating behaviour. This result has to be considered excellent, being these variations very small. In particular, after the LBE conditioning the sensor signal starts from very high mV values and later lowers towards the acceptable value of 500 mV ca, indicating slightly more reducing conditions than the minimal required signal (>350 mV).

— $In - In_2O_3$

After the first 1400 h a historical reconstruction of its signal is possible. In FIG. 4.113 it is clearly visible the reducing action performed in the first days in the storage tank. When the test campaign started the injection of $Ar - H_2$ was stopped. In the graph it is possible to see how the oxygen content

slightly increases. This is caused by the mass transfer between the passivated pipe walls and the reduced LBE. A comparison between the behaviour of the two different sensors is shown in Fig. 4.114.

As it can be observed the output signal is in the first case positive and it grows up to a constant value (~ 500mV). Two slopes are clearly identified. They show two $Ar + H_2$ bubbling series. After the first one the $O_2$ content increased a little, while after the second one the oxygen content remains almost constant. The second case the signal is negative and changes to positive values due to gas bubbling. The two sensors, with a very good agreement, show that the $H_2$ bubbling method is effective in order to reduce the oxygen content.

(b) CHEOPE III loop data

In the CHEOPE III loop were performed 10000 hours of corrosion tests in lead-bismuth. During the hole duration of the campaign the $O_2$ content was measured with a $Bi - Bi_2O_3$ sensor and recorded. After the conclusion of the tests the loop was emptied cleaned and refilled with pure lead, in order to start another 10000 hours material compatibility test with a different liquid metal.

— $Bi - Bi_2O_3$ in LBE

The historical reconstruction of the oxygen sensor ($Bi - Bi_2O_3$) signal of CHEOPE III loop ($T = 637K$, constant) is shown in Fig. 4.115. The operation oxygen concentration range is $10^{-5}$–$10^{-6}$ wt%, corresponding to a 150–200 mV signal ca. These conditions is very close to the saturation value for $PbO$ ($10^{-4}$ wt%, i.e. 76 mV ca.) and for this reason are very difficult to be exactly controlled. This could be seen comparing the two historical pictures of the two facilities: in the CHEOPE III one, plant stops and technical problems are much more frequent, where the following analyses of the impurities gave $PbO$ as the main result. From this behaviour it is possible to infer that the sensor signal, even so near to the lead oxide saturation, is reliable. The sensor response to the on-line gas bubbling is not immediate. Some weeks are necessary to stabilize the signal, as depicted in Fig. 4.116, showing the sensor signal after one month while some bubbling were performed.

— $Bi - Bi_2O_3$ in lead

After the conclusion of the corrosion tests in LBE, in the frame of the 6the framework programme, the PbBi was substituted with pure lead. This in order to perform new compatibility tests. The $Bi - Bi_2O_3$ sensor installed in the plant was recalibrated and set in the third test section in order to monitor the content of the oxygen dissolved in the lead, during the tests.

In Fig. 4.117 the first 2000 hours are graphed. It is possible to see that during the first 500 hours the oxygen dissolved increased and how it decreased after the injection on $Ar - H_2$. The gas mixture was bubbled for 105 minutes at a flow rate of 0.5 litres/min. When the bubbling of the mixed gas was suspended the oxygen content increased. It is possible to graph also the start up of the facility. During the first seconds the signal oscillates then after the pump started to work it grows up to 300mV. The signal becomes constant when the loop reaches the test temperature.

### *4.6.2.6. Conclusions*

In $PbBi$, the two $Bi - Bi_2O_3$ sensors gave signals which were in good accordance with the theoretical ones in both plants. Also the $In\text{-}In_2O_3$ sensor gave outcome signals coherent with the theoretical data. Moreover the two sensors gave coherent signals in similar working conditions, allowing to start the design of a sensor for a pool configuration. That leaded to the design and construction of an oxygen sensor adapt to pure lead. In this case it was a technological innovation since, up to now, few data are available. The $Bi - Bi_2O_3$ sensor was recalibrated in pure lead and showed behaviour comparable to the one in PbBi. Only the magnitude of the outcome signal is slightly lower than in the LBE case.

The next step is to design and construct an oxygen sensor for a pool type reactor. This sensor will be tested in the frame of experimental campaigns, which are now (2009) in progress in the CIRCE facility. For the new pool sensor some obstacles should be overcome, such as the higher pressure filed, the temperature variations and the insulation of the electrical cables. As a matter of fact, in order

to monitor the oxygen content in a pool deep nine meters, it is necessary to install some sensors. Due to the different deepness they are loaded differently along their length and this can affect the ceramic glove. Moreover the temperature gradient along the pool affect both the ceramic and the electrical cables with the possibility to break the sensor.

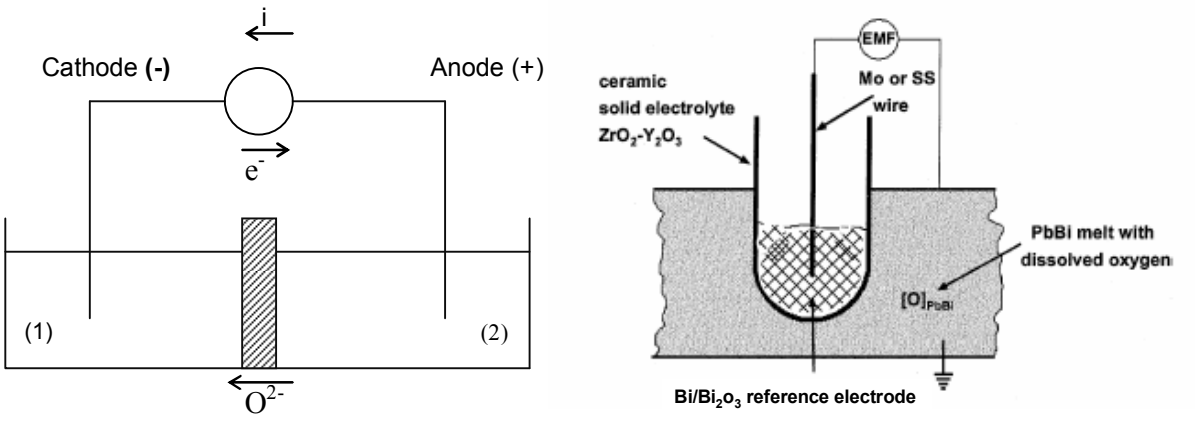


*FIG. 4.108. Galvanic cell principle.*

*FIG. 4.109. Russian sensors ($Bi\text{-}Bi_2O_3$), produced at IPPE, Obnisk (sx) $In\text{-}In_2O_3$ sensor home produced (dx).*

TABLE 4.24. SUMMARY OF EXPERIMENTAL PROCEDURES

| Step | Value |
|---|---|
| Temperature gradient | 673K – 813K |
| Temperature step | 20K |
| Gas inlet | $Ar+H_2$ (3%) |
| Number of temperature tests | 2 |
| Total LBE volume | 0.5 l |
| Vessel material | AISI 316L |

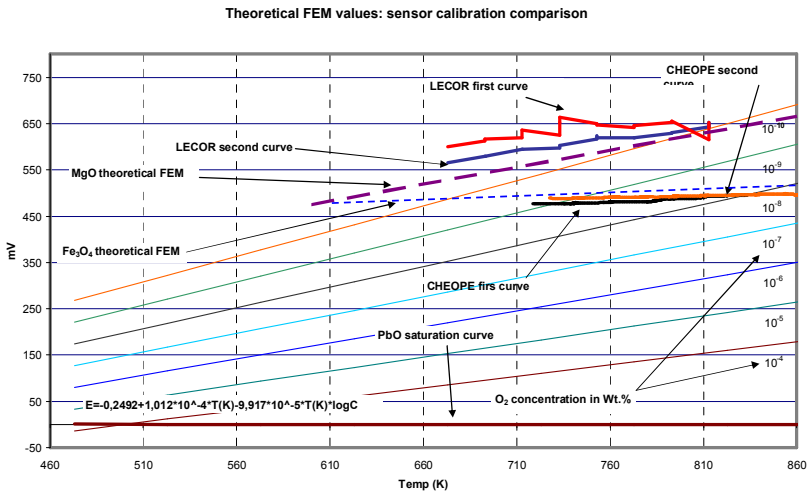


*FIG. 4.110. Summary of experimental data and comparison with theoretical oxygen concentration-EMF curves.*

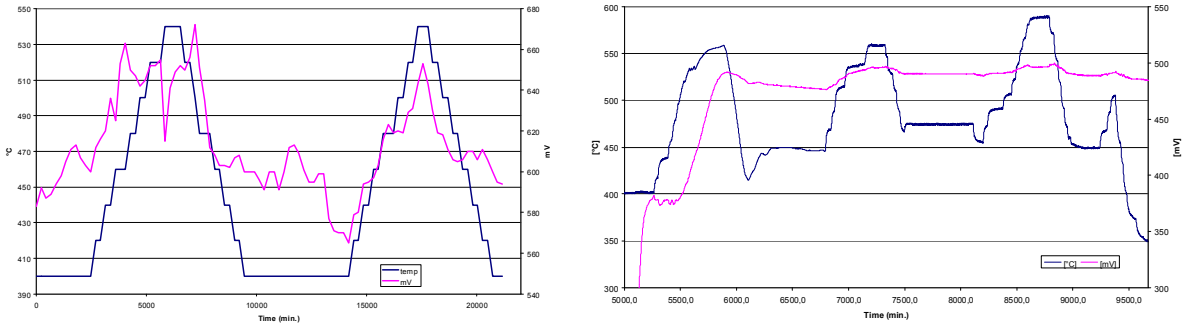


*FIG. 4.111. EMF signal of the LECOR (sx) and CHEOPE III (dx) sensors and temperature variations.*

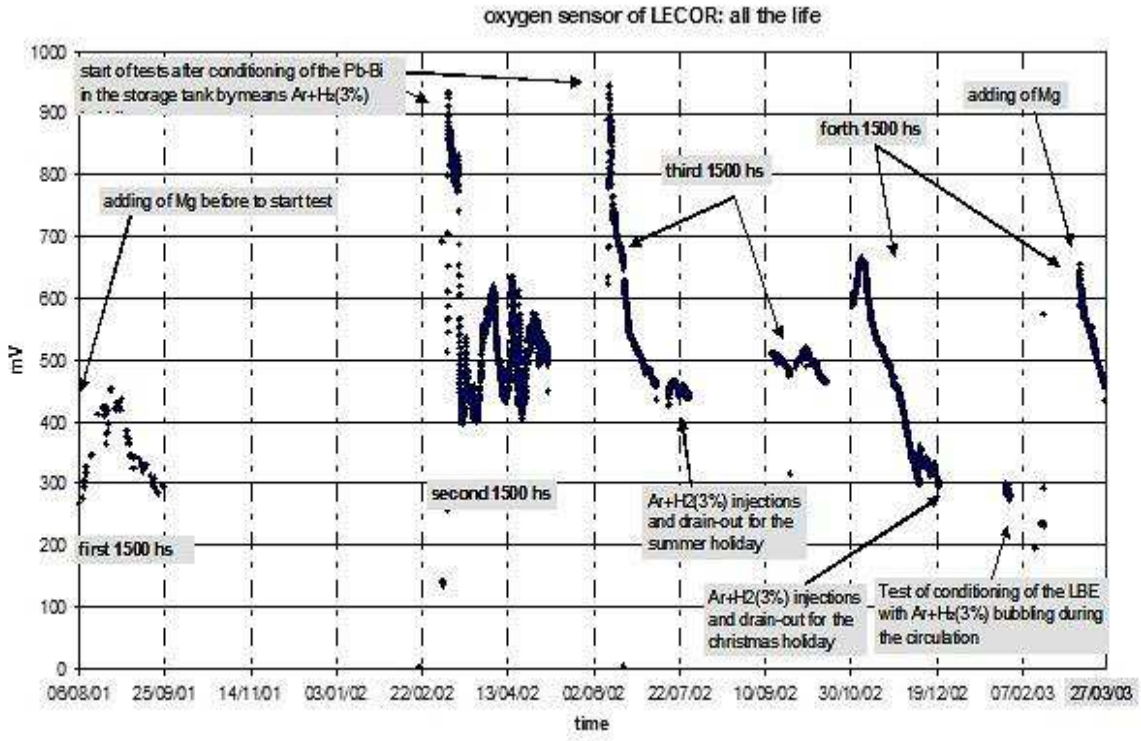


*FIG. 4.112. Reconstruction of whole activity of LECOR sensor.*

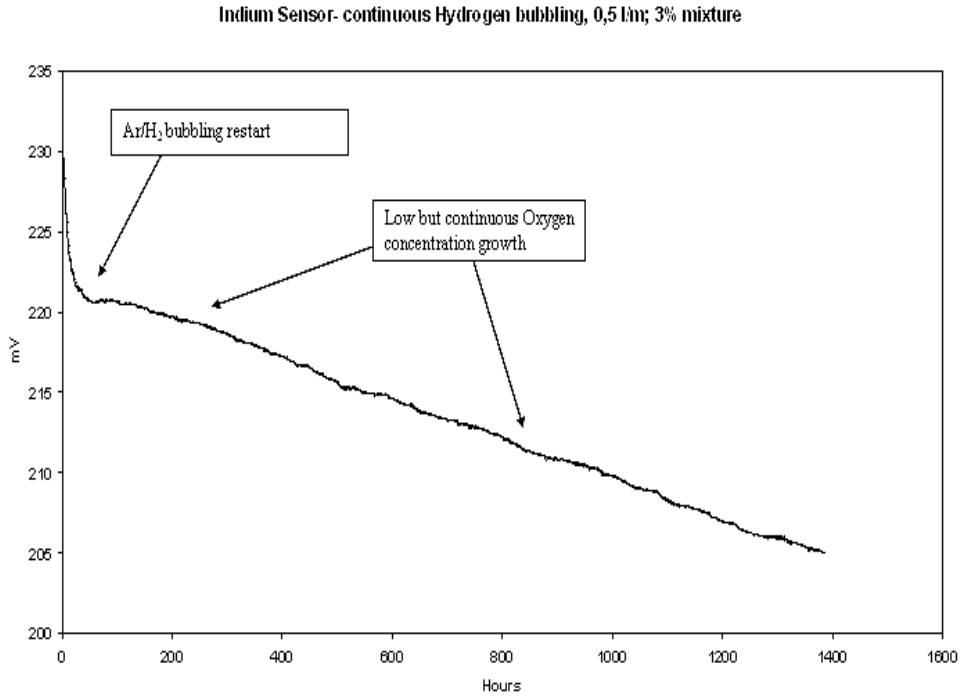


*FIG. 4.113. Conditioning of LBE via bubbling of Ar-$H_2$ (3%) in the storage tank, with a flow of 0,5 l/h*

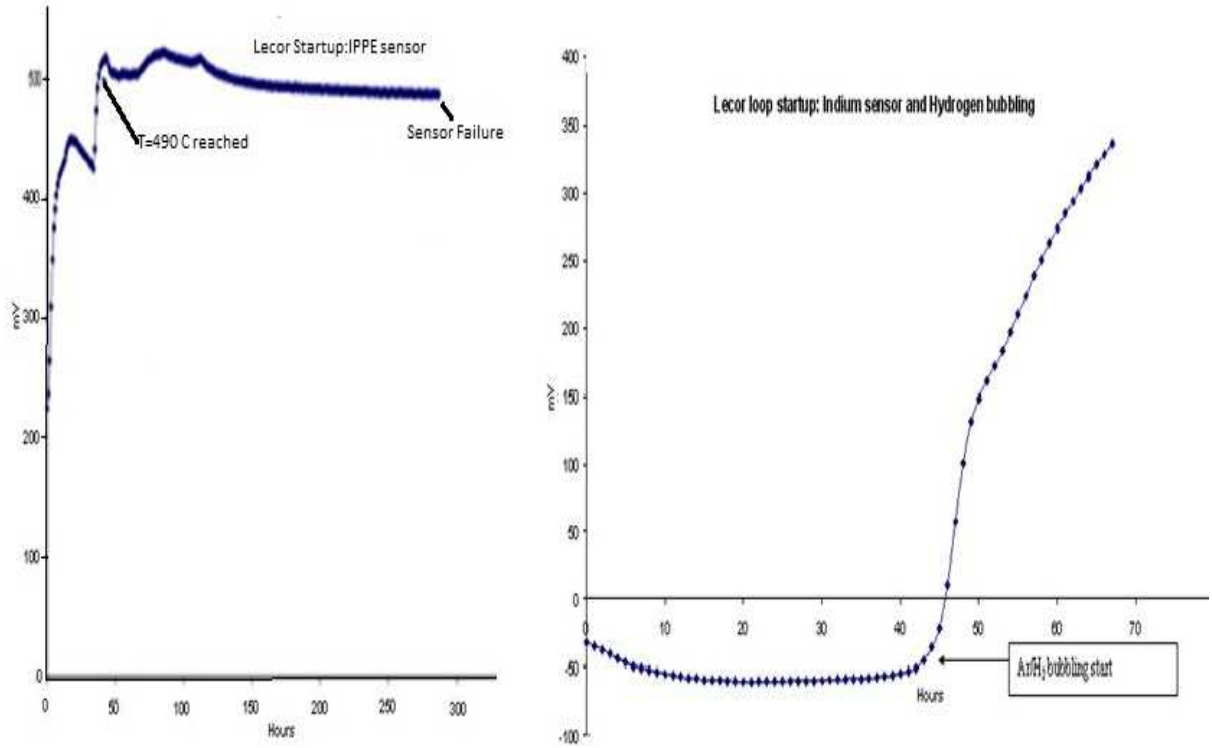


*FIG. 4.114. Comparison between the start up of the Russian sensor and the ENEA's one.*

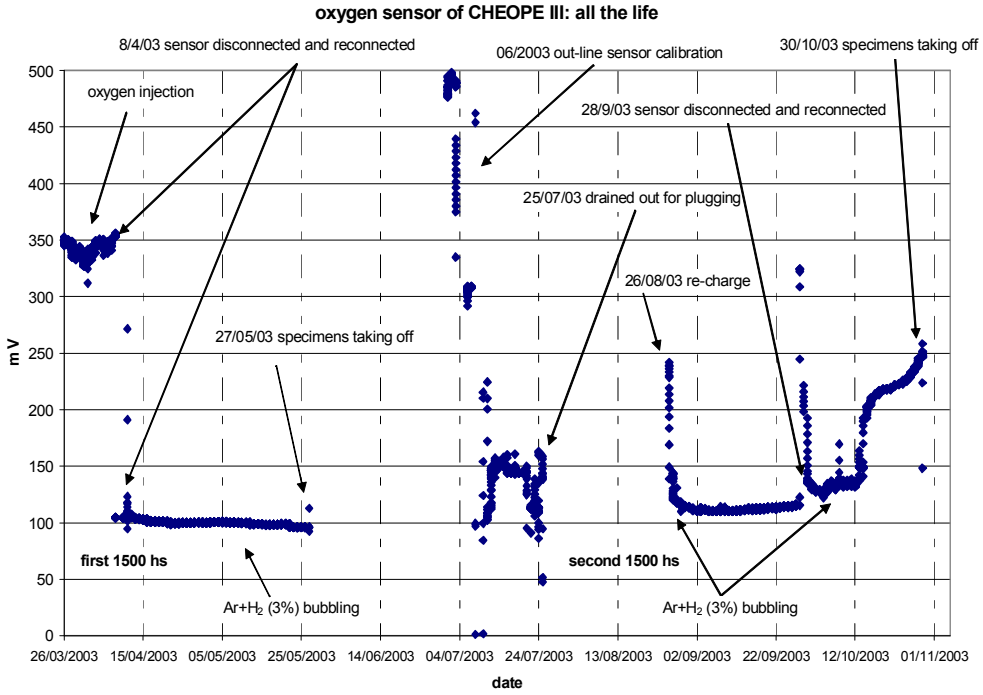


*FIG. 4.115. Reconstruction of whole activity of CHEOPE III sensor.*

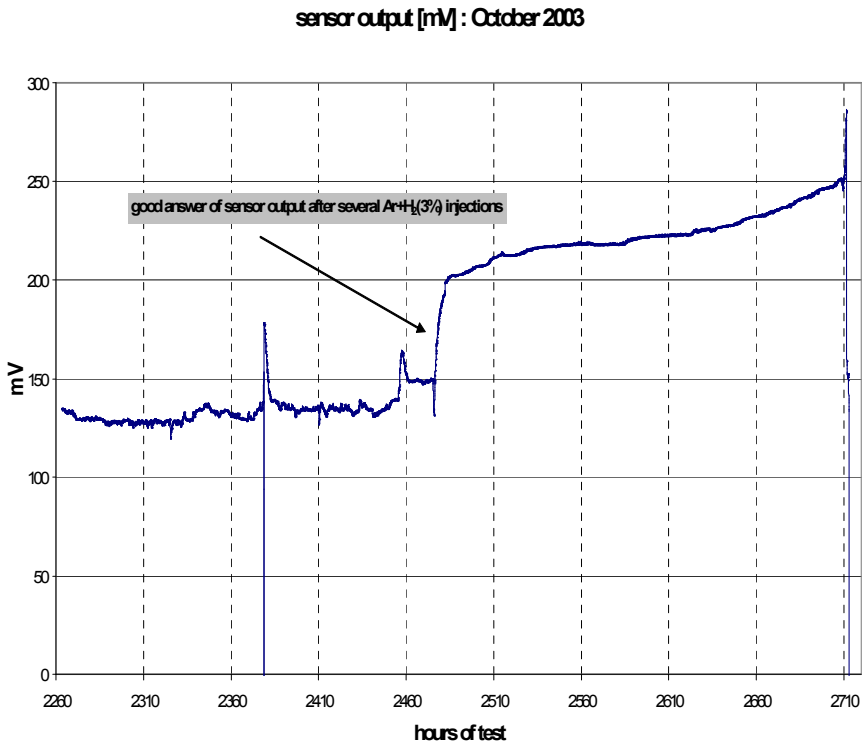


*FIG. 4.116. Answer of the sensor output after several gas bubbling within one month.*

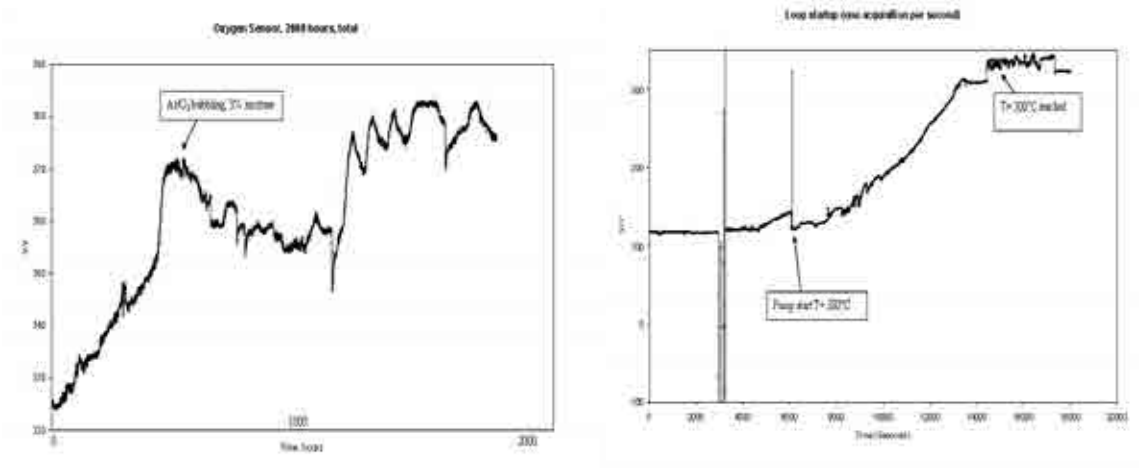

*FIG. 4.117. Cheope III sensor historical outcome signal and start up.*

### 4.6.3. Coolant technology experience in Japan

#### *4.6.3.1. Purpose and goal*

One of important issues is the generation, accumulation and evaporation of polonium when the use of LBE is considered in nuclear systems.

First of all, an experimental study on the equilibrium evaporation of LBE was made to obtain essential and fundamental knowledge of LBE [4.123]. Furthermore, experimental works were conducted to investigate equilibrium evaporation behaviour of polonium and tellurium in liquid LBE [4.124][4.125].

The goal of the study on evaporation is to obtain fundamental data and empirical equations such as partial vapour pressure and gas–liquid equilibrium partition coefficients of polonium.

The baking method for removal of polonium from materials surfaces was investigated by an evaluation method using Langmuir's equation and baking experiments for quartz glass [4.122] and Type 316 stainless steel [4.121] contaminated by neutron irradiated LBE.

#### *4.6.3.2. Theoretical explanation*

The principle of equilibrium evaporation measurement adopted is the transpiration method [4.123]. The vapour is transported by carrier gas from an isothermal evaporation pot to an outside collector through a capillary tube. This method enables us to make the quantitative analysis of saturated Po and LBE vapour at the same time.

In the baking experiments [4.121], the evaporation rate of a metal is estimated by Langmuir's equation, which shows the amount of evaporated metal in a unit area and time from the melted surface of single metal in an equilibrium state.

#### *4.6.3.3. Instruments description*

The test apparatus [4.123] consists of an evaporation pot, an electric heating furnace, an argon gas supplying line, a sampling line and a data acquisition system as shown in Fig. 4.118. The evaporation tests were conducted in the temperature range from 450 to 750°C. Po-210 was produced in the LBE specimen by neutron irradiation at JMTR (Japan Material Testing Reactor). The method of Po-210 quantification was a liquid scintillation measurement. The POLEX was used as polonium extractant and scintillator.

In the baking experiments for the contaminated quartz glass plate, an infrared furnace was used. An electric furnace with good accuracy of temperature measurement was developed for the baking experiments for contaminated Type 316SS as shown in Fig. 4.119 [4.121]. Both evaporation experiments were conducted under a vacuum condition. The temperature range was from 200°C to 600°C. Po-210 was produced by neutron irradiation of LBE and its specific activity was about 30 Bq/g at the time of the baking experiments.

#### *4.6.3.4. Major results*

Data on the saturated vapour pressure of LBE and the LBE vapour pressure equation were obtained from LBE evaporation experiments [4.123].

From the evaporation tests of Po-210 in LBE, we obtained fundamental test data and empirical equations such as Po partial vapour pressure, gas–liquid equilibrium partition coefficient of Po in LBE [4.124] [4.124]. Fig. 4.120 shows the Po-210 partial pressure as the value in a mole fraction of Po, ($\chi_{Po}$=2.0x10$^{-10}$ where $\chi_{Po}$is mole fraction of $Po$). Experimental data by Buongiorno et al. [4.120] were also plotted in this figure. General expression of $Po$ partial vapour pressure, $P_{Po-LBE}$ is represented by the following equation:

$$log\ P_{Po-LBE} = 10.5357 + \log \chi_{Po} - 8348/T$$

where $T$ is absolute temperature.

Gas–liquid equilibrium partition coefficient of Po in LBE, $Kd_{Po-LBE}$ is correlated against $T$ as shown in Fig. 4.121.

$$logKd_{Po-LBE} = 1.079 + \frac{1101}{T}$$

Activity coefficient of $Po$ in $LBE$, $\chi_{Po-LBE}$ is also derived:

$$log\chi_{Po-LBE} = 1.079 - \frac{2908}{T}$$

Concerning chemical form of vapour in gas phase, the possibility $PbPo$ formation is implied from the observed results in the evaporation experiment of Te in LBE.

Experimental data for removal of Po were obtained from the baking experiments. In case of the contaminated quartz glass plates, polonium evaporated at the temperatures 300°C and above. On the other hand, as shown in Fig. 4.122, the experimental results indicted that the baking method was effective for polonium decontamination when the baking temperature was higher than 500°C in a vacuum condition (0.4Pa) for Type 316 stainless steel [4.121]. From comparison of the experimental results and calculation of evaporation rare of polonium compounds using Langmuir's equation, it is considered that the difference in effective temperatures was due to the different chemical forms of polonium, i. e., elemental polonium and lead polonide.

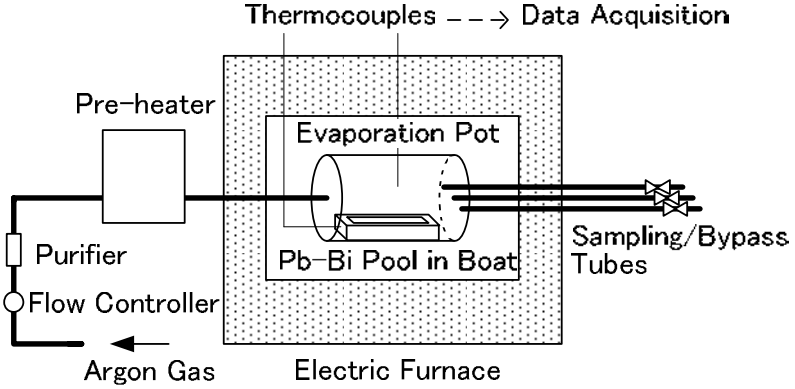


*FIG. 4.118. Schematics of evaporation experiment apparatus using the transpiration method.*

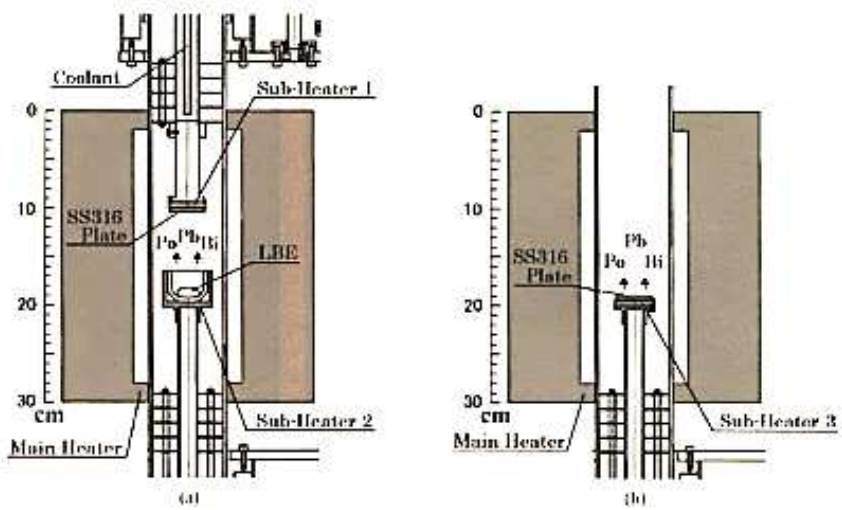


*FIG. 4.119. Electric furnace: (a) for evaporation of neutron irradiated LBE and preparation of contaminated Type 316 plate and (b) for baking contaminated Type 316 plate.*

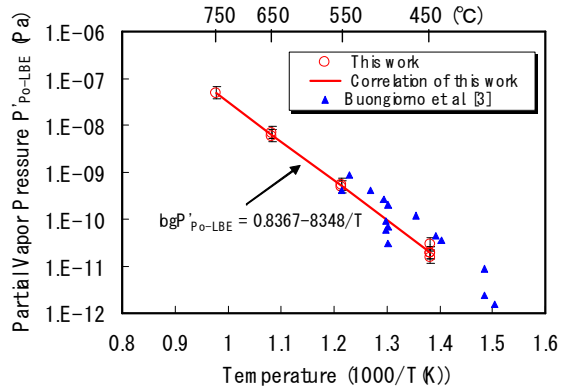


*FIG. 4.120. Po-210 partial vapour pressure in gas.*

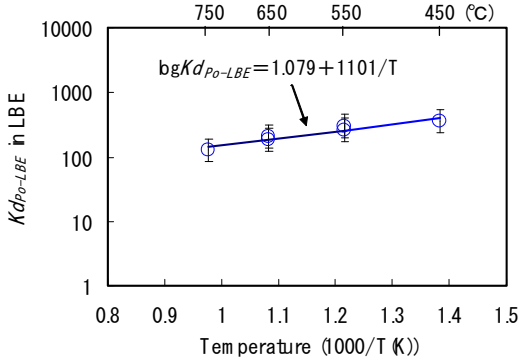


*FIG. 4.121. Gas–liquid equilibrium coefficient of Po-210 in LBE.*

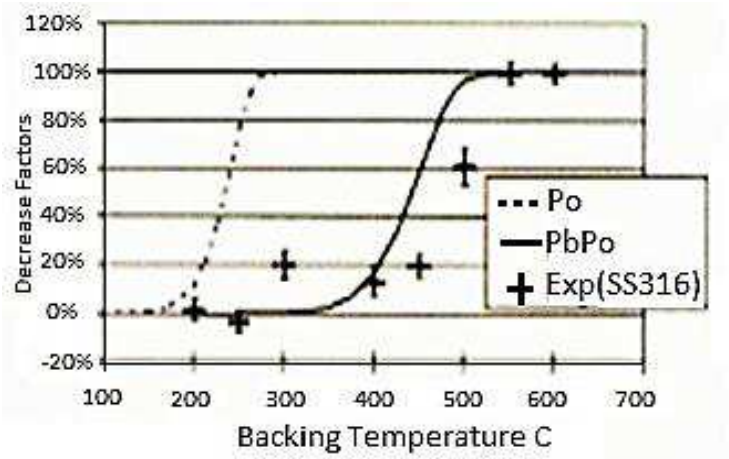


*FIG. 4.122. Comparison of DFs (Decrease Factors) from calculation using Langmuir's equation and from results of baking experiments on contaminated Type 316 plate.*

### 4.6.4. Coolant technology experience in Russia

In the early 1950s, the researches on substantiation of nuclear power facilities cooled with lead-bismuth eutectic alloy were started in Russia under the proposal made by A.I. Leipunsky.

The choice of this alloy as a coolant was determined by its some positive physical-chemical thermal-physical properties.

Low chemical activity of lead and bismuth at interaction of the alloy with air, water, steam excludes an opportunity of explosion and fire. The high level of coolant boiling temperature prevents an opportunity of its boiling in high power density parts of facility. The low working pressure in a coolant circuit increases a reliability and safety, simplifies a design and manufacturing of the equipment, essentially facilitates operational conditions of the equipment in the primary circuit.

However lead-bismuth coolant is rather aggressive in relation to structural materials; it can contaminate itself with solid impurities by interacting with structural materials and oxygen during facility operation. Therefore for long safe operation of facilities with Pb-Bi coolant it was necessary to solve two basic problems:

— Provide a necessary purity both the coolant and internal surfaces of the equipment of a circulation circuit;

— Ensure a corrosion resistance of structural materials contacted to the alloy.

In Russia, for the decision of these tasks a programme of researches of lead and lead-bismuth alloy properties, physical chemical processes occurring in non-isothermal circuits, corrosion resistance of structural materials, impurity sources and their influence on serviceability of facilities was widely developed.

Contents and amount of impurities in the coolant depend on a set of used structural materials, modes of operation, design and purpose of facilities. Impurities are formed in the coolant under operational conditions of facilities by the following processes:

— Diffusive release of components of structural materials through protective oxide coating;

— Corrosion and erosion of structural materials under coolant influence;

— Formation of new elements after an irradiation of coolant by neutrons and protons.

The incoming of impurities from cover gas into the circuit is possible due to depressurization of circuit gas volume, core refueling, various repair work, steam generator leaks etc. Impurities can be in both forms dissolved form and as solid small dispersed particles. During operation impurities basically consisting from oxides of coolant and structural material components interact each other, with coolant and materials of the circuit. Therefore there are constant mass transfer processes in the non-isothermal circuit.

For maintenance of corrosion resistance of structural materials there was used a method of oxygen inhibition in liquid metal medium.

At the first stage there were attempts to use various inhibitors ($Zr$, etc.). However results of these researches were negative, basically due to accumulation of impurities which are thermodynamically steady and hardly removed from the circuit. Therefore use of oxygen as inhibitor that naturally presents in the alloy, was the completely correct decision. This decision determined further direction of researches, structure of systems and methods of coolant technology and positive results of operation of facilities with $Pb-Bi$ coolant.

Since a protective covering in the accepted method is based on oxide compounds of steel components, its stability depends on thermodynamic activity of oxygen in $Pb-Bi$ alloy and $Pb$. Thus, an iron oxide $Fe_3O_4$ is basis of protective covering. On the one hand, operational experience shows a possibility of decrease of concentration of the dissolved oxygen in the alloy up to value equal or smaller equilibrium with $Fe_3O_4$. On the other hand, the presence of significant amount of oxygen in the circuit is undesirable, because it can result in accumulation of invalid amount of the coolant

oxides. Therefore it is necessary to control a quality of the coolant during facility operation by supporting the contents of the dissolved oxygen at the certain level.

On the basis of results of theoretical and experimental researches and operational experience of transport facilities there are determined the basic processes of the coolant technology providing a normal facility operation from the point of view of the coolant [4.126]. They include:

— Hydrogen cleaning of the circuit from impurities on a basis of lead oxide;

— Cleaning of the coolant from the weighed impurities by filtration;

— Oxygen enrichment of the coolant for maintenance of the fixed level of its oxidation potential;

— Cleaning of protective gas from aerosols;

— Control of parameters of the coolant.

In Russia last decades the researches of technology of heavy liquid metal coolants Pb-Bi and Pb with reference to stationary fast reactors (SVBR, BREST etc.) and ADS are conducted. Besides lead-bismuth alloy it is offered to use a pure lead as the coolant. Lead is attractive due to its indeficiency and inexpensiveness; its polonium activity is less by ~3 order than Pb-Bi alloy. However, high meltdown temperature of lead (327°C) causes a number of difficulties of its use as coolant. The affinity of the basic physical-chemical processes proceeding in the circuits with lead and lead-bismuth coolants is experimentally confirmed. It allows using an experience gained at a substantiation of lead-bismuth coolant for development of lead coolant technology.

There are developed and used the various methods and devices for control of coolant quality. There are sample takers (devices) for coolant and cover gas, continuous or periodically acting analyzers of impurities in cover gas and other devices. Sample taking is made periodically with their subsequent analysis by various methods in laboratory conditions.

For the control of concentration of the oxygen dissolved in the alloy specialists of the IPPE developed and created a gauge of thermodynamic activity of oxygen (activometer) that is based on a principle of galvanic concentration cell with solid electrolyte. Creation of activometer and equipping of all experimental and industrial facilities by this device allowed qualitatively increasing value and reliability of researches. The results of the theoretical analysis on definition of optimum thermodynamic conditions of operation of non-isothermal facilities were confirmed by activometer. It allows controlling all processes of the coolant technology. Last years the works on improvement of activometer were executed that allowed increasing reliability of its indications.

The main purpose of cleaning system is a maintenance of necessary purity both coolant and internal surfaces of the circuit equipment. Now various ways of cleaning have been developed. They can be divided into two groups.

The first group joins ways providing transformation of impurity with return of a product of transformation to the coolant. Here a cleaning of the circuit from impurities by use of oxides of the coolant components $PbO$ and $Bi_2O_3$ can be mentioned. The second group contains ways providing removal of solid non-restorable impurities from the circuit with gathering them in special devices which can be removed and replaced or placed in the circuit during all facility's lifetime.

The most effective method of the first group is reduction of lowest oxides by hydrogen

$$Me_xO_y + yH_2 \leftrightarrow xMe + yH_2O$$

The effective cleaning is implemented by introduction of a gas mixture consisting of hydrogen, water steam and inert gas into the coolant flow [4.127]. Gaseous bubbles with hydrogen are transported with the coolant flow to places of a congestion of impurities where a reduction of solid lead oxides up to pure lead by hydrogen is implemented with return of pure lead into the coolant. The chosen conditions of implementation of this reaction exclude an opportunity of reduction of oxides in protective covering on structural materials.

The organization of twocomponent flow 'liquid metal gas' in all parts of the circulation circuit is provided by special devices called dispergators. Dispergators produce a small dispersed gas mixture with the size of gas bubbles up to 10 to 100 μm which is transported by the coolant even in downward parts of the circuit with low velocity (~0.2–0.3 m/s).

Filtration is the most effective way of the second group [4.128]. Its application provides two basic mechanisms of filtering process mechanical retention of impurity particles from the alloy flow and adhesive capture of impurities by all volume of a filtering material. The filters have a certain capacity on impurities. Accumulation of impurities in the filter decreases its cleaning efficiency, but the coolant flow rate through the filter does not stop. This feature of the developed filters is very important, since provides an opportunity of use of hydrogen cleaning. Bubbles of a gas mixture with hydrogen enter the filter with the coolant flow, they reduce lead oxides up to pure lead and thus clean the filter. Finally the filter only accumulates those impurities which can not be reduced by hydrogen. There are iron oxides, particle of structural materials and welding produced by friction and other impurities which can be formed in the circuit during its long operation.

Thus, simultaneous use of hydrogen regeneration and filtration provides cleaning internal circuit surfaces from slag materials, return of lead from slags into the coolant and localization in the filter of slag residua non-reduced by hydrogen.

There are developed and investigated filtering dress type materials having low hydraulic resistance, high porosity, rather high capacity on impurities, sufficient mechanical durability and thermal stability. Dress type materials made of glass, metal or carbon fibres meet in the greatest extent to the present requirements.

The various systems and devices are developed for regulation of the dissolved oxygen concentration in the coolant. They are based on the following processes:

— Delivery of gaseous oxygen into the circuit;

— Delivery of water steam hydrogen mixture into the circuit;

— Dissolution of solid oxides of $Pb$ or $Bi$.

Delivery of gaseous oxygen (gas mixture of oxygen with inert gas) into gas volume or directly into the coolant provides dissolution of the part of oxygen in the coolant only. The most part of oxygen interacting with coolant forms solid lead oxides which are located in various sites of the circuit. Therefore this method is recommended to be used only in emergency cases at sharp deoxidization of the coolant.

Changing ratio $PH_2O/PH_2$ in mixture of hydrogen and water steam delivered into the circuit allows decreasing or increasing concentration of the dissolved oxygen in the alloy. This method excludes a formation of solid oxides of coolant components.

Most effective is the method based on use of solid lead oxides ($PbO$) preliminarily past special technological treatment as means of oxidation. Changing coolant temperature and-or flow rate in reactionary capacity, it is possible to manage velocity of dissolution of lead oxides in accordance with needs.

Now is observed a significant interest to ADS, where lead or lead-bismuth eutectics are considered as a target and coolant.

The new elements generated by a proton beam in the coolant can take part in various chemical reactions breaking a chemical balance in the circuit. Most important are redox reactions that can proceed with formation of insoluble oxides and reduction of iron oxide $Fe_3O_4$, being a basis of a protective film on structural materials.

The elements having oxidation potential smaller than lead will be dissolved without formation of oxides ($Au, Ag, Pt, Hg, Os, Cu, TI, Pb\ Bi$).

The elements having oxidation potential between values for lead and iron will be dissolved or oxidize depending on thermodynamic activity of oxygen ($Re, As, Te, Sb, Co, Ni, Mo, Sn, Fe$).

The elements, (lanthanides, halogens, alkaline elements,$Be$, $Y$, $Sc$, $Al$, $Ge$, $Ti$, $Hf$) having oxidation potential higher than iron will be capable to reduce iron oxide $Fe_3O_4$ and to destroy a protective film under some conditions.

It is also necessary to take into account an opportunity of origination of new solid phases by means of formation of new chemical compounds, in particular intermetalloids, under interaction between impurities of all groups and components of the coolant.

Thus, during ADS operation the coolant and the gas volumes contaminate themselves by impurities incoming from structural materials, protective gas, and also generated owing to influence of proton beam. This contamination increases with increase of lifetime and capacity of ADS and with decrease of amount of the coolant in the system.

In the whole analysis has shown that the influence of impurities produced by proton beam in the circuit on mass transfer processes can be significant for targets by capacity of 10–20 MW and it requires special attention.

Now technology of HLM coolants has been developed with reference to conditions of conventional NPP and it is aimed at maintenance of required purity of coolant and circuit surfaces, and also corrosion resistance of structural materials. This technology basically includes a series of processes for decontamination of the circuit and coolant from excess of oxide phases and maintenance of the exact level of concentration of oxygen dissolved in the coolant.

The accumulation of radioactive nuclides in the circuit owing to spallation and fission reactions creates the new requirements to conditions of implementation of the developed processes, and also provides a necessity of development of additional processes and measures.

So, the realization of conventional technology mainly based on replacements of cover gas, removal and delivery of gas mixtures in the circuit becomes complicated and, at least, requires development and application of devices of cleaning of removed gases and radiation shielding of these devices. Such developments are especially urgent in application to the ADS designs where coolant circulation is carried out by gas lifting.

The conventional technology can not solve a series of problems related to removal of electropositive impurities ($Au$, $Ag$, $Hg$ etc.) which make the essential contribution to change of contents and radioactivity of coolant in ADS. The task of removal of such impurities did not exist for conventional NPP and the appropriate researches have started last years only.

Implemented researches have not revealed new processes, which could replace already developed ones, though there are opportunities of use of new means of their realization.

The decision of a set of problems can be assigned to the coolant technology, in particular, localization of radioactive impurities inside ADS circuit, restriction of radioactive release at normal operation of ADS, decrease of radioactivity of the coolant and circuit as a whole.

The most probable ways of development of technology of HLM with reference to ADS are:

— Development of new processes and devices for removal of electropositive impurities from the coolant and their localization in the circuit (sorbing filtration, evaporation, condensation etc.);

— Development of highly effective means of cleaning of gases removed from the circuit;

— Adaptation of the developed processes with reference to ADS;

— Adaptation of devices of realization of processes based, mainly, on use of external systems of feed and removal of chemically active gases;

— Development of new devices of realization of processes without use of external gas systems.

Implementation of research works in all above mentioned areas for definition of prospects of each of them now is expedient.

## 4.7. BEHAVIOUR OF STRUCTURAL MATERIALS

The international R&D activities related to the structural materials development and selection and their performance assessment are mainly focussed on ADS concepts, where the spallation target and the subcritical core are cooled with Heavy Liquid Metals (HLM) as lead ($Pb$) and lead-bismuth Eutectic (LBE). In this frame synergy with R&D structural materials issues addressed within the Generation IV Pb cooled fast reactors (LFR) have been pointed out.

Some alternative ADS concepts with solid metal (W-based alloys) target are as well investigated.

### 4.7.1. Structural materials selection and development

For the design of a given component, considering e.g. the heat load-neutron fluence and the envisaged operational stress and temperature regime, the materials selection is based on properties as:

- Thermo-physical (e.g. thermal stress response or power density capability which determines the maximum allowable heat load);
- Mechanical (tensile, creep-rupture, fatigue, creep-fatigue and fracture toughness);
- Corrosion and compatibility data (including synergistic effects);
- Behaviour under irradiation;
- Technical maturity, i.e. qualified fabrication and welding technology and a general industrial experience.

All R&D teams contributing to this status report have selected commercially available materials in order to assess their performance under HLM-cooled ADS relevant conditions. In particular, steels belonging to the ferritic, ferritic–martensitic (F-M) and austentic classes are considered. Among the different options of these classes of steels, the most investigated are the high $Cr$ Ferritic–martensitic steels and the austenitic steels developed in the past for the claddings of Fast Breeder Reactors (FBR).

Newly developed materials are also taken into account. Especially, experimental activities are conducted on:

- The low activation F-M steels developed in the frame of the fusion technology programme;
- The Oxide Dispersion Strengthened alloys (ODS) for applications at higher temperature and higher burnups.

Finally, in order to enhance the corrosion resistance of the structural materials, and in particular of the cladding, a surface alloying technology is under development.

### 4.7.2. Structural materials performance assessment

The experimental activities presented by the R&D teams contributing to this status report, address the following issues:

- Corrosion and mechanical performance in HLM;
- Mechanical performance in proton and neutron irradiation fields;
- HLM and irradiation fields combined effects.

The corrosion studies are conducted within experimental configurations where the HLM is either in static or flowing conditions. In any case, particular attention is put on the oxygen activity in the HLM, since this activity can affect the corrosion mechanism of the structural materials (both the austenitic and F-M steels), which can change from oxidation to dissolution by decreasing the oxygen activity at

a given temperature. The experiments are conducted within a range of temperature between 400°C and 650°C.

The experimental results show that at temperatures of 500°C in oxidising HLM, the buildup of an oxide layer can be protective and can avoid a corrosive liquid metal attack, where steel elements can dissolve in the liquid metal and the mechanical properties of the steel can change negatively. However, at higher temperature the oxide layer protection system has some disadvantages:

— Oxide layer growth in a less compact way, so that the liquid metal can penetrate within the steel matrix inducing dissolution;

— Oxide layer thickness after a certain period of time can be such to worsen the heat transfer capability of the structural material.

Therefore alternative protection methods are under investigation. In particular, the surface alloying with the GESA technology is developed and the surface modified steels are tested in the liquid metal. First results have shown the effectiveness of this system.

The performance assessment of the structural materials in irradiation fields are investigated at:

— BR2 reactor at SCK•CEN (neutron irradiation, mixed spectrum);

— SINQ facility at PSI (proton irradiation);

— BOR60 reactor in Russia (neutron irradiation, fast spectrum);

— Heavy ion irradiation facility in China.

The Post-irradiation Experiments (PIE) are aimed at understanding the material behaviour under irradiation and complementing the existing database on the different steels tested, To achieve these objectives, mechanical tests, metallurgical and microstructural investigations are conducted.

Finally, in order to investigate the materials response when in contact with HLM and a neutron irradiation field, a very challenging experiment has started at the BR2 reactor (SCK•CEN).

Further activities in the area of irradiation studies are multiscale physical-model development to predict irradiation damages and their effect on the material behaviour and the development and testing of miniature specimens. Both topics have an increasing importance in this area.

### 4.7.3. Belgium

#### *4.7.3.1. Purpose and goal*

For the development and qualification of structural materials for advanced and sustainable nuclear systems, the efforts are concentrated on the systems which are considered as priority for the Institute for Advanced Nuclear Systems [4.129]–[4.135]. These are: accelerator driven systems where both the spallation source and the cooling medium is the liquid lead-bismuth eutecticum, lead cooled fast reactor (LFR) as a serious option for GEN IV systems. The material development and qualification activities are primarily concerned with the chemical and physical integrity of the selected materials when subjected to the expected but new harsh conditions. The issues that are being addressed and will be pursued in the future are: 1) the effects of irradiation on the material performance including spectrum, temperature and flux variations, 2) the specific compatibility issues related to application of these materials in the foreseen reactor environment especially under the synergetic effect of irradiation and 3) the modeling of these effects in order to be able to extrapolate the validity of the data to cover relevant operation conditions as no irradiation facility exist now a days that is able to reproduce the expected environment. The definition of these priority reactor systems focusses the research efforts on the high chromium ferritic–martensitic steels, austenitic stainless steels and oxide dispersion strengthened steels and alloys with emphasis on their fabricability, weldability and performance.

This goal relies on the expertise, available from the activities along the research into radiation and ageing effects on structural materials for the currently operating nuclear power plants. This expertise covers databases on the behaviour of irradiated materials, validated test methods for evaluation of mechanical properties and environmental assisted cracking and models for prediction of radiation damage effects on the microstructure of the material and its effect on the material behaviour. The extrapolation of the expertise from the existing ones shall be validated by dedicated experiments for which the required infrastructure is being developed.

#### *4.7.3.2. Instrumentation description and most important results*

The activities concerning the development of materials for accelerator driven systems and fast reactors have been focused on the following areas:

— Fabricability, workability and welding methods of candidates steels for ADS and fast neutron reactors (cladding, coating & welding);

— Chemical and mechanical compatibility of steels with liquid PbBi eutectic coolant;

— Effect of irradiation on the microstructure and mechanical behaviour of material.

The main achievement of the past years has been the startup of a dedicated research group and the construction of appropriate facilities for addressing the relevant issues. This has resulted in the construction of dedicated testing equipment for liquid metal embrittlement testing of steels in liquid lead alloys before and after irradiation, this task has been the subject of a PhD thesis that has been defended at KUL in 2006. Also, an important effort was made to identify Belgian partners (industry and research) to improve the capability of SCK•CEN facing the challenge to provide relevant materials to the ADS community. Last but not least, a substantial breackthrough has been achieved in the development of the technology for performing irradiations in lead-bismuth filled capsules in the BR2 reactor under controlled chemistry, temperature and dose rate. Also, these tasks are being parts of the two PhD thesis that are ongoing at SCK•CEN in collaboration with industry and university.

#### *4.7.3.3. Conclusions*

In order to reach our main objectives, the following activities are being performed:

— Complementing of the existing database on irradiation performance of ferritic martensitic steels for irradiation conditions, relevant to the selected reactor concept. These activities will include mechanical tests on irradiated materials, analysis of the microstructural changes, induced by irradiation and evaluation of the compatibility between the material and liquid metal environment before and after irradiation. The main deliverables for this task are the following:

  - Post-irradiation mechanical tests of irradiated materials; irradiation sources: BR2 (dose up to 2.5 dpa, irradiation temperature 325–450°C), MEGAPIE (spallation spectrum), BOR-60 (450°C–550°C, 16 dpa). The objective of the test programme is to verify the occurrence of liquid metal embrittlement and the eventual synergy of irradiation and liquid metal embrittlements.
  - Evaluation of irradiation creep at low to intermediate dose levels for candidate fuel cladding materials (450°C–550°C, 2.5–16 dpa).
  - Evaluation of corrosion rates of structure material and cladding under irradiation; measurement of corrosion layer thickness after long term exposure to liquid metal and irradiation (identical conditions as creep experiments).
  - Investigation of irradiation damage: characterisation of irradiation induced damage in structural materials as a function of dose, spectrum and irradiation temperature. The main target of characterisation is the swelling behaviour of materials under irradiation.

— Further development and validation of models for prediction of irradiation damage and its effect on the material behaviour. This activity will contain the extrapolation of multiscale models for the existing reactor types, validated using the database from the existing reactors and validating the extrapolations by a similar approach as applied before. The objectives of the modelling work are

  - To develop models describing the microstructure evolution in FeCr alloys under thermal ageing and irradiation in terms of phase transformation (ordering, clustering) and damage accumulation, as functions of Cr content, temperature and dose.
  - To correlate the microstructural changes to changes in the mechanical properties of these alloys, focusing on a quantitative prediction of radiation induced hardening, and define a mechanistic framework for the development of future, more comprehensive predictive models.

— Maintain and expand the capability of testing highly irradiated materials, including the development of testing on miniature specimens.

  - Installation of small punch test in hot cell for mechanical tests on irradiated materials.
  - Develop the handling capability of materials, contaminated with typical spallation transmutation products from the irradiation in Pb-Bi environment (such as polonium).
  - Develop-expand the capability of evaluating the compatibility of structural materials with the expected environment (liquid metal, high temperature, etc.) for unirradiated and irradiated materials.
  - Develop-expand the capability of chemical and radiochemical analysis of materials, especially focusing on the issues related to liquid lead alloy coolant and its interaction with structural material under irradiation.

— Identify suppliers of representative materials products and interact with these to optimize production methods and product properties and quality.

### 4.7.4. China

#### *4.7.4.1. China ADS material programme*

(a) Purpose and goal

Since accelerator driven system (ADS) will be used as the facility for long life radioactive waste transmutation, some issues in structure materials of ADS are being paid attention, such as the compatibility of the materials and coolant, the development and selection of materials which are irradiation resistance to neutron and high energy proton, and corrosion resistance to Pb-Bi. In China, ADS material programme was proposed in 2000, started in 2001, and the compatibility project is focused on three topics:

— The compatibility studies of tungsten with sodium and with water;

— The development and investigation of the structure materials;

— The primary tests of the complex technologies for W–S.S. and W–Zr cladding.

Some primary results from these researches have been obtained, and some investigations are being performed. Since our investigation is in an early step, a lot of issues on materials have to be studied further in the near future.

(b) Instruments description and most important results

— The compatibility studies on tungsten with sodium and with water [4.136]

Tungsten will be the solid target material of ADS, and sodium or water are to cool the solid target. Therefore, it is necessary to study the compatibility between tungsten and sodium or and water. The test conditions of compatibility studies for tungsten and sodium are shown in Table 4.25, for tungsten and water are shown in Table 4.26.

TABLE 4.25. TEST CONDITIONS OF COMPATIBILITY STUDIES FOR TUNGSTEN AND SODIUM

| | | |
|---|---|---|
| Temperature | °C | 500, 600, 700 |
| Test periods | h | 200, 400, 600, 1000, 1500 h[a] |
| | | 200, 400, 600, 1000, 1500, 2000, 3000h[b] |
| Oxygen content in sodium | μg/g | 12.6, 32.2 |
| Carbon content in sodium | μg/g | 7 |

[a] For rotary swaged W.
[b] For polished W.

TABLE 4.26. TEST CONDITIONS OF COMPATIBILITY STUDIES FOR TUNGSTEN AND WATER

| | | |
|---|---|---|
| Temperature | °C | 100 |
| Test periods | h | 100, 200, 500, 800, 1500, 2000, 3000 |
| Removing method of oxygen | | Bubbling with N2 for 3 hours |
| Impurities content in water | μg/kg | SO4-2 < 80 , Cl -1< 20 , Cu+2 < 0.2 |
| Water quality | | |
| pH | | 5.9–6.8 |
| Electric conductivity | μS /cm | > 1.00 |

Main results are here summarized:

- The different original surface states of tungsten which are due to the different processing technology resulted in the different corrosion behaviour, microstructure, and fracture characteristics.
- The corrosion resistance to high temperature sodium and water are good under above static test conditions. There is no sodium penetration was observed at the grain boundaries for both kinds of W-samples.
- Both original W-samples show inter-granular brittle fracture mode before test and inter-granular or trans-granular brittle fracture mode after the tests.

— The developing and investigation of the structure materials [4.137]

The ferritic steel 12CrWTi-ODS and austenitic stainless steel 316LN was developed by Institute of Steel and Iron Beijing in passed years. The China Low Activation Martensitic Steel-9Cr2WVTa (CLAM) was developed by CIAE in the collaboration with University of Science and Technology Beijing. The chemical compositions of these steels are show in Table 4.27, Table 4.28 and Table 4.29, respectively.

TABLE 4.27. CHEMICAL COMPOSITION OF 12CRWTI-ODS STEEL (WT. %)

| Alloy | Fe | Cr | W | Ti | O | Y2O3 | C |
|---|---|---|---|---|---|---|---|
| 12CrWTi-ODS | Bal. | 12.83 | 2.0 | 0.71 | 0.26 | 0.52 | 0.018 |

TABLE 4.28. CHEMICAL COMPOSITION OF 316LN STEEL (WT. %)

| Alloy | Fe | Cr | Ni | Mo | Mn | S | C | P | Si | N |
|---|---|---|---|---|---|---|---|---|---|---|
| 316LN | Bal. | 17.17 | 12.5 | 2.6 | 0.97 | 0.013 | 0.016 | 0.033 | 0.17 | 0.12 |

TABLE 4.29. CHEMICAL COMPOSITION OF CLAM STEEL (WT. %)

| Alloy | Fe | Cr | W | V | Ta | Mn | C | Y | Si |
|---|---|---|---|---|---|---|---|---|---|
| A | Bal. | 8.8 | 1.49 | 0.20 | 0.059 | 0.68 | 0.13 | -- | -- |
| B | Bal. | 9.11 | 1.51 | 0.21 | 0.16 | 0.41 | 0.10 | -- | 0.46 |
| C | Bal. | 7.78 | 1.93 | 0.20 | 0.24 | 0.41 | 0.10 | 0.25 | -- |

CLAM was designed based on 9Cr1.5WVTa. The effect of tempering temperature on the properties of steel was studied. The effect of silicon and yttrium addition on the mechanical properties of steel was investigated too. The results show that the strength of CLAM steel was increased by silicon addition, and the ductility is still good, while yttrium addition led to the CLAM steel keeping good ductility, but lost much of the strength.

CIAE is collaborating with PSI in Switzerland to study the irradiation resistance of the materials. The samples of 12CrWTi-ODS ferritic steel have been irradiated to19 dpa at 450°C in STIP-4, its properties post-irradiation will be examined in 2007. The 316LN and 9Cr2WVTa steel will be irradiated in STIP-5.

Electron irradiation behaviour of CLAM steel was tested in high voltage electron microscope. Many voids formed in CLAM steel with basic composition by electron irradiation at 450°C, while no void can be found in silicon added CLAM steel. Silicon is a good alloying element for increasing the irradiation swelling resistance of CLAM steel, and some slice shape precipitates formed by electron irradiation at 450°C in silicon added CLAM steel [4.137].

CIAE is collaborating with Brasimone Research Center in Italy to investigate the corrosion resistance to flowing Pb-Bi and Pb. The samples of 12CrWTi-ODS were tested in LECOR Pb-Bi loop with lower oxygen for 2000h, and its properties post-test will be measured in 2007. The samples of 316LN and 9Cr2WVTa steel are testing in Pb loop CHEOPE III now.

— The primary tests of the complex technologies for W–S.S. and W–Zr [4.138]

As all know, tungsten is always used as the material of solid metal target. It will be embrittle under irradiation at high temperature, and will be attacked by the flowing coolant. Therefore, another material which is irradiation resistance, corrosion resistance and excellent neutron properties has to be used as the cladding of solid tungsten. In our project, Zr alloy and stainless steel were selected as the cladding material of tungsten, respectively due to the Zr alloy is the cladding material of the fuel elements for water reactor, stainless steel is that for sodium cool FBR, and water reactor or FBR will be an option of the subcritical reactor.

On the other hand, in order to increase the life of tungsten target, the cladding of W target has to be able to transfer the heat from W body to coolant quickly and efficiently. Therefore, the bonding of W and its cladding should be very well. The Hot Isostatic Press (HIP) process seems to be the most promising and attainable method to get good bonding of W and its cladding. The purpose of this research is to look for a proper bonding method of W-cladding materials and try to find their optimum conditions of the HIP process.

The electric beam weld was used to prepare the W–Zr and W–S.S. small samples for HIP. The size of samples is following:

- Polishing tungsten bar: Ø8×30; Ø5×30;
- Zirconium cladding: Ø9.6×0.75×30;
- Stainless Steel cladding: Ø6.0×0.4×30.

The Parameters of HIP Process are shown in Table 4.30 and Table 4.31.

TABLE 4.30. HIP PROCESS FOR W–ZR CLADDING

| Temperature (°C) | Pressure (MPa) | Duration (h) | Rate of T increase (°C/h) | Getter material | Container | Cover gas |
|---|---|---|---|---|---|---|
| 1200 | 180 | 4 | 300 | sponge Zr | $Al_2O_3$ crucible with Zr lid | Ar (5N) |
| 1300 | 180 | 4 | 300 | sponge Zr | | |
| 1400 | 180 | 4 | 300 | sponge Zr | | |

TABLE 4.31. HIP PROCESS FOR W–S.S. CLADDING

| Temperature (°C) | Pressure (MPa) | Duration (h) | Rate of T increase (°C/h) | Getter material | Container | Cover gas |
|---|---|---|---|---|---|---|
| 1200 | 180 | 4 | 300 | no | $Al_2O_3$ crucible[a] | Ar (5N) |
| 1300 | 180 | 4 | 300 | sponge Zr | $Al_2O_3$ crucible[b] | Ar (5N) |

[a] without lid
[b] with Zr lid

Following results were investigated;

— The bonding of W–Zr and W–S.S is very well under the testing conditions. No any pores or micro cracks can be observed in the interface.

— The diffusion of Zr to W in HIP process is preferred. The diffusion depths are 7–13 μm and increase with the increasing of the HIP temperature; In case of W–S.S, the diffusion of Fe to W is considerable, its depth is about 13μm.

— The oxygen absorber Zr can not be used in the HIP for W–S.S., because Zr reacts with S.S. under the test conditions, and to form $FeZr_2$ and $NiZr_2$ metal compounds whose melting point is less than 1000°C, and to result in the melting of the cladding.

— There is a hardness peak in the diffusion layer of both W–S.S. and W–Zr, it may be resulted from the formation of the Fe–W and Zr–W metal compounds respectively in the diffusion layer.

— Some issues on HIP process, such as the inspection methods for the bonding, and the bonding technology for the practical components have to be studied further in next step.

#### *4.7.4.2. China contribution to the radiation damage in ADS materials*

(a) Purpose and goal

This section describes the research activities of radiation damage in the ADS materials at China Institute of Atomic Energy. As mentioned above, the irradiation dose can reach a couple of hundred dpa per year for the ADS materials. In order to fulfill the radiation damage investigation at such a

high dose, the heavy ion irradiation simulation method and the related facilities have been established at the HI-13 tandem accelerator in China Institute of Atomic Energy. Before doing the radiation damage investigation by it, the verification experiment of heavy ion irradiation simulation method was performed to show its validity and reliability. Also, the positron annihilation lifetime spectrometer has been set up for the microscopic investigation of the produced radiation damage and its evolution with irradiation dose and-or temperature. Finally this paper reports on the investigation of radiation damage in the ADS materials such as stainless steel, tungsten, tantalum, etc, which are important candidate materials used for the target and window of the spallation neutron source and the structural components in ADS.

(b) Instruments description

The heavy ion irradiation facilities have been established at the HI-13 tandem accelerator in China Institute of Atomic Energy. The improved HI-13 tandem accelerator has a terminal voltage of 15 MV and can provide the heavy ions up to Au. Table 4.32 shows some radiation damage rates for stainless steels that can be achieved at the HI-13 tandem accelerator.

A multi sample and variable temperature irradiation chamber is constructed. Six samples can be irradiated in turn. The irradiation temperature ranges from room temperature to 800°C with an accuracy of ±5 oC. The sample was heated by a electric heater during irradiation. The heating was fully controlled by a temperature controller. The irradiating beam also deposits a certain amount of heat in the sample, and thus the beam current was kept stable around ~ 1 μA for an easy control of the temperature. A high beam current irradiation chamber for room temperature irradiation is set up in which the sample to be irradiated is directly cooled by flowing water. In addition, a multi sample and room temperature irradiation chamber is established. Fig. 4.123 shows the heavy ion irradiation chambers constructed at the beam terminal of the HI-13 tandem accelerator. The irradiation dose is up to hundreds of dpa with an accuracy of ±0.1 dpa.

TABLE 4.32. PART OF RADIATION DAMAGE RATES OBTAINED WITH HI-13 TANDEM ACCELERATOR FOR STAINLESS STEELS

| Ion specimen | Ion energy (MeV) | Irradiation depth (μm) | Radiation damage rate (dpa/μAh) |
|---|---|---|---|
| C-12 | 70 | 41 | 2.1 |
| F-19 | 80 | 21 | 3.9 |
| Cl-36 | 70 | 7.7 | 11.7 |
| I-129 | 100 | 6.6 | 26.5 |

*FIG. 4.123. Multi sample and variable temperature irradiation chamber (right), multi sample and room temperature irradiation chamber(middle) and high beam current irradiation chamber (left).*

(c) Most important results

— Comparison of radiation damage in stainless steels and tungsten [4.143]–[4.153]

A comparison of radiation damage has been made at irradiation doses up to 20~30 dpa for the modified 316L stainless steel (MSS) and the commercially available stainless steel (SS) and tungsten [4.139], which are important candidate materials for the spallation neutron source target and beam

window.SS was the 18Cr-9Ni-Ti stainless steel. The purity of W was 99.9%. The size of all the samples was Ø 23 mm × 0.5 mm.

The samples were irradiated at room temperature by 80 MeV 12C or 85 MeV 19F ions, using the multi sample and room temperature irradiation chamber. In order to ensure that the irradiation was carried out at room temperature, the irradiating beam current was limited to ~0.3 μA and the samples were firmly contacted with the irradiation chamber wall of metal that was cooled by an electric fan. The irradiation doses were 2.0 dpa and 20.0 dpa for W, 2.28 dpa and 22.8 dpa for SS, 30.0 dpa for MSS.The extracted lifetimes τ1 and τ2 and their relative intensities I1 and I2 for MSS, SS and W are shown in Fig. 4.124 as a function of irradiation dose.

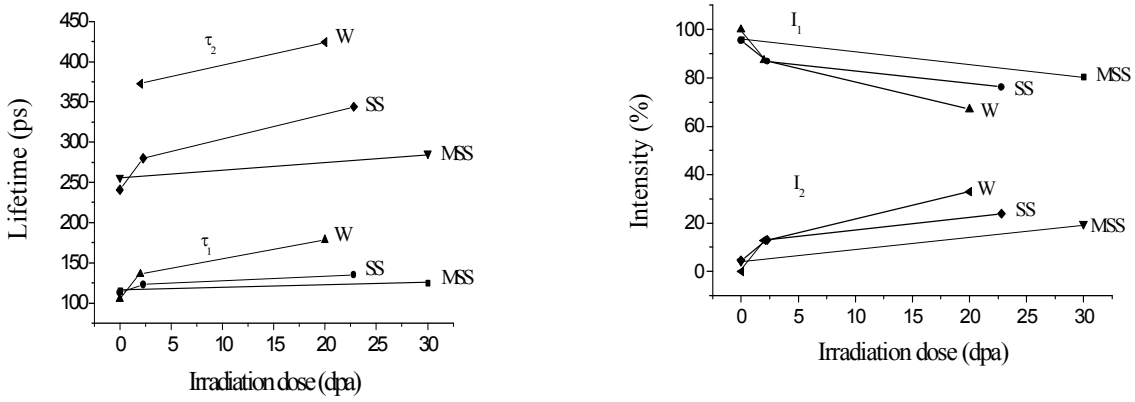


*FIG. 4.124. Dependence of positron lifetimes (left) and their intensities (right on irradiation dose in MSS, SS and W.*

The annihilation lifetime τf of free positrons is ~110 ps in stainless steel and ~105 ps in tungsten. The positrons trapped at vacancy clusters or voids give much longer annihilation lifetimes. Usually, the larger the vacancy cluster, the longer the annihilation lifetime. It can be seen from FIG. *4.124* that only τ1 was obtained for the unirradiated W the value of which is in good accord with the free positron annihilation lifetime, and τ1 = 112.9 ps and τ2 = 240.0 ps and τ1 = 115.0 ps and τ2 = 256 ps were observed for the unirradiated SS and MSS, respectively. The τ1 values of 112.9 and 115.0 ps are a little larger than the free positron annihilation lifetime, indicating there are a very small amount of mono and divacancies and dislocations. τ2 is related to the small vacancy clusters, and vacancy cluster is a bit larger in MSS than in SS. The above measured data show that before irradiation W is defect free and SS and MSS contain vacancy clusters. MSS is treated by the cold working which produces vacancies, vacancy clusters and dislocation in it [4.140]. Even after thermal annealing at 800 $^{o}$C the vacancy clusters still exist [4.141]. τ1 = 108.8 ps and τ2 = 255.7 ps were obtained for the MSS annealed at 800 $^{o}$C for about 40 min., demonstrating that the mono and divacancies and dislocations were annealed away, and the vacancy clusters are not annealed.

Both τ1 and τ2 increase for the SS irradiated to a dose of 2.28 dpa. Their values indicate that the mono vacancy was mainly produced and that the vacancy cluster becomes larger and its intensity increases by ~9%. In the case of W irradiated to 2.0 dpa τ1 = 136 ps reveals the production of the mono and divacancies, and the rapid increase of τ2 to 372.6 ps indicates the formation of rather large vacancy clusters. In W irradiated to 20.0 dpa τ1, τ2 and I2 arrive at the values of 178.4 ps, 424.1 ps and 33%, respectively. 1 = 178.4 ps illustrate the generation of the trivacancies and quadrivacancies besides the mono and divacancies, otherwise, one can't obtain such a large τ1. Here, τ1 is the average value of lifetimes of free positrons and positrons trapped at the mono, di, tri and quadrivacancies. In metals the positron lifetime of ~500 ps means a zero density limit of electron density. τ2 = 424 ps clearly demonstrates the formation of large size voids the intensity of which is 33%. In SS irradiated to 22.8 dpa τ1, τ2, and I 2 are 135.1 ps, 343.9 ps and 23.8%, respectively. τ1 = 135.1 ps shows the creation of the monovacancies and divacancies. The lifetime τ2 of 343.9 ps, the intensity of which

reaches 23.8%, can be explained by the generation of the ~10 vacancy cluster [4.142]. For the MSS irradiated to 30 dpa $\tau 1$ increases to 125 ps, indicating the production of the monovacancies, and $\tau 2$ increases to 286 ps with an intensity of 19.6%. This value of $\tau 2$ is corresponding to the lifetime of positrons trapped at the 5 vacancy cluster [4.142].

TABLE 4.33. COMPARISON OF THE LIFETIME $\tau 2$ IN MSS, SS AND IRRADIATED TO ~20 OR 30 DPA

| Sample | MSS | SS | W |
|---|---|---|---|
| Irradiation dose (dpa) | 30.0 | 22.8 | 20.0 |
| Lifetime $\tau 2$ (ps) | 286 | 343.9 | 424.1 |

TABLE 4.33 shows the comparison of the lifetime $\tau 2$ in W, SS and MSS irradiated respectively to 20, 22.8 and 30 dpa. It can be seen that radiation damage is very severe in W, sizeable in SS and very small in MSS. The irradiation induces large size voids in W, 10 vacancy clusters in SS and 5 vacancy clusters in MSS and their relative intensities are in turn 33%, 23.8% and 19.6%. Therefore, from our positron lifetime data, one can say that among the three samples investigated in the present experiment the modified 316L stainless steel (MSS) has the best radiation resistant property, and the radiation resistant property of the commercially available tungsten (W) is worst. The present experimental results demonstrate that the commercially available stainless steel is better than the commercially available tungsten for a beam window material of an ADS spallation neutron source system, and the modified 316L stainless steel is the best among the three.

— Comparison of radiation damage in stainless steels CLAM, F82H and T91

Low activation ferritic–martensitic steels are the most promising materials used as structural components for ADS, ITER, etc. due to their superior irradiation resistance in physical and mechanical properties.

China Low Activation Martensitic steel (CLAM) added with a rare earth element Y has been developed, the chemical composition of which is listed in Table 4.34.

In order to understand its radiation resistant property a comparison experiment was carried out for three stainless steel types of CLAM, F82H and T91.

TABLE 4.34. NOMINAL COMPOSITION OF CLAM (WT%)

| Element | C | Cr | W | V | Ta | Mn | Y | Fe |
|---|---|---|---|---|---|---|---|---|
| Content | 0.1 | 9.0 | 1.5 | 0.20 | 0.15 | 0.45 | 0.2 | Bal. |

The samples of CLAM, F82H and T91 were irradiated at room temperature by 80MeV 19F ions to a dose of 10.0 dpa with a damage rate of 1.0 dpa/h. The results of positron lifetime measurements are shown in Fig. 4.125.

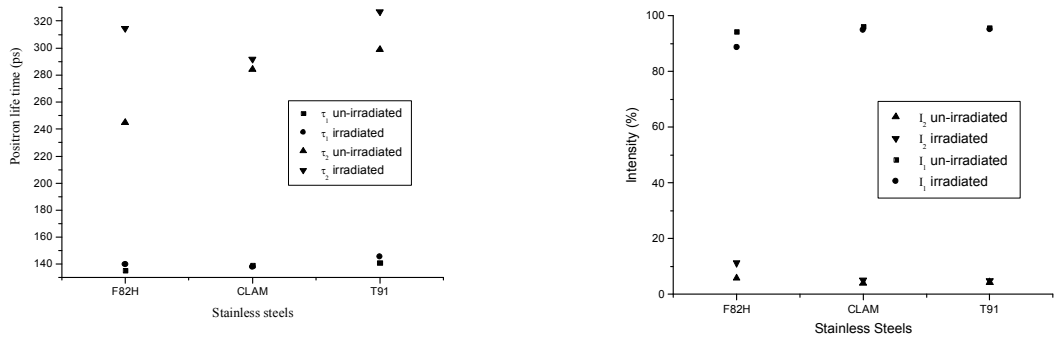


*FIG. 4.125. The positron annihilation lifetimes and their intensities before and after irradiation.*

For the samples before irradiation, τ1 and τ2 are 139ps and 284ps for CLAM, 135.3ps and 245ps for F82H and 140.9ps and 291.2ps for T91. It is clear that the amounts of mono and divacancies and dislocations are similar for these three types of samples, while F82H has the least vacancy clusters or voids before irradiation.

For the samples after irradiation, τ1 is 138ps for CLAM, which is almost the same as that of the unirradiated one, and τ2 is 292ps; while τ1 and τ2 are 139.9ps and 314.4ps for F82H and 145.5ps and 327ps for T91. It shows that the difference of τ1 is very small for all three samples, while the variation of τ2 is much larger for F82H and T91 than that for CLAM before and after irradiation. According to the rule that the longer annihilation lifetime τ2 means the larger vacancy cluster, the irradiation generates larger vacancy clusters or voids in F82H and T91 than in CLAM. It reveals that the CLAM steel has better irradiation resistant property compared with F82H and T91 and illustrates the role of the addition of Y in CLAM. Further investigations of irradiation effects for CLAM are still on going.

## 4.7.5. Germany

### *4.7.5.1. Purpose and goal*

One of the key problems for heavy liquid metal (HLM) especially lead or LBE cooled prospective nuclear and transmutation reactors is the compatibility of structural and cladding materials with the coolant. Unprotected steels are attacked by dissolution of their components in the liquid lead alloys. One measure that is widely being used is dissolution of oxygen in HLM until the oxygen content reaches a level at which oxidation of steel components occurs and protective oxide scales develop on the steel surface [4.156] [4.157]. An alternative protection methods is as well investigated and hereafter described

Protection by oxide scale formation requires control of the oxygen concentration. The concentration must be high enough to oxidize iron, the main component of the steels that are considered for application, but should not exceed the value at which oxidation of lead occurs. The concentration range that must be kept to fulfill these conditions is depicted in Fig. 4.126. The Co,s line indicates the upper boarder for the HLM oxygen concentration which extends in the temperature region of interest over 4 orders of magnitude. The same holds for the Co($Fe_3O_4$-FeO) line that indicates the minimal concentration at which iron is oxidized. Since there will be a temperature gradient of about 250°C, the oxygen concentration has to be controlled in a range that stays away from the boarder concentration lines in this temperature range.

### *4.7.5.2. Instrument description and summary of major results*

The compatibility tests have been performed in the COSTA and CORRIDA facilities of KALLA. These facilities are described in Chapter 5.2.

(a) Compatibility studies

During the last year's researchers in several laboratories examined the suitability of austenitic and ferritic steels as structural and cladding materials in liquid LBE at temperatures relevant for nuclear fission and transmutation reactors [4.156] [4.157]**Error! Reference source not found.**. Corrosion tests in static and flowing LBE covered the temperature range from 400 to 650 °C. In most cases the HLM contained around $10^{-6}$wt% of oxygen to allow formation of protective oxide scales on the steel surface. Below temperatures of 500°C no difficulties arise with the protection of steel surfaces by formation of an oxide scale. Martensitic steels develop thick multilayer oxide scales growing with the exposure time which probably split off after long times. Austenitic steels have thin, stable, protective spinel scales on the surface. Early experiments on the compatibility of steels and HLM without oxygen showed catastrophic dissolution attack of the HLM onto the unprotected steel [4.158]. In summary, steels can be used in HLM with an oxygen concentration of 10–6wt% at temperature ≤ 500°C without any further measures. However, ferritic–martensitic steels form under such conditions already thick oxide scales. On parts of a reactor at which heat removal is a crucial point like claddings or heat exchangers formation of thick oxide scales is not acceptable. Preliminary calculations of the inner clad temperatures [4.159] show a 10K increase each 10 µm of oxide scale considering a thermal conductivity of 1W/mK (which is close to that of magnetite and spinel). Moreover, above 500°C the HLM penetrates the oxide scale and starts to attack the steel.

Corrosion resistance of structural materials can be enhanced by their surface modifications with coating or surface alloy. These surface modifications should eliminate–mitigate dissolution and oxidation attack of both austenitic and martensitic steels that can occur in HLM environment above 500°C. Therefore, the protective layer has to fulfill following requirements:

— Prevention of dissolution attack;

— Tolerable oxidation rate during oxide scale formation;

— Long term high temperature stability of the system also under abnormal conditions;

— Tolerable influence of the coating and surface alloy on the mechanical properties of the steel;

— Durability under irradiation;

— Long term mechanical stability of the surface coating and alloy layer;

— Industrial feasibility;

— Self-healing capability of the oxide scale.

(b) Behaviour of steels with modified surface

FeCrAlY coatings are well known for their excellent oxidation resistance at high temperatures by forming alumina layers due to selective oxidation**Error! Reference source not found.**. Bulk FeCrAl alloy (15%Cr, 4% Al, Fe balance) is already examined by Asher et al, 1977 [4.154] in flowing Pb at 700°C and did not show any visible attack also after 13000h of exposure at low oxygen potential. Alumina scales forming on such MCrAlY's are an effective barrier against diffusion of cations as well of anions and prevent, thus, a fast growth of the scale like it is observed with the magnetite and spinel layers on FeCr steel.

Bulk Al containing alloys or thick coatings can not be considered for the envisaged parts (e.g. cladding tubes) to be protected. Only the surface of steels should be enriched with Al. Two methods, alloying an Al layer into the steel surface and coating the surface with an Al–alloy with subsequent GESA treatment, are applied [4.160].

(c) Surface modification by the GESA process

The GESA process uses pulsed electron beams with a kinetic energy in the range of 50±400 keV, with a beam power density up to 6MW/cm$^2$ at the target and pulse duration up to 40µs [4.155]. The energy density absorption of the target is up to 80J/cm$^2$, which is sufficient to melt metallic materials adiabatically up to a depth of 10–50µm. Due to the high cooling rate in the order of 107K/s, very fine

grained structures develop during solidification of the molten surface layer. This is a suitable basis for the formation of protective oxide scales with good adhesion [4.155]. To surface alloy cladding tubes a special GESA the GESA IV with a cylindrical cathode was designed. This facility allows the treatment of an entire tube of about 30 cm length with a single pulse. Detailed description of surface modification with the GESA treatment is given in [4.160].

(d) Corrosion, erosion and mechanical testing on GESA surface alloys and coatings

Coating the surface of T91 steel specimens with FeCrAlY leads to positive results. Indeed, those specimens exposed for 2000 h to LBE with 10–6 wt% oxygen at 480, 550 and 600°C flowing at 1m/s [4.161] showed no dissolution attack, no scale damage and no additional oxide formation. The result of the surface examination with SEM-EDX showed that alumina is formed while Cr does not seem to oxidise. The EDX shows also that at the interface between coating and steel, the Al content drops down and some Cr precipitated at the grain boundaries of the coating.

Other experiments with FeCrAlY coated steel 1.4970 support the suitability of this coating for high temperature application. No corrosion attack could be observed in 5000 h tests in LBE with $10^{-6}$ wt% oxygen at 500, 550 and 600°C, respectively (25). Corrosion experiments with alloyed steels show that 4wt% Al is necessary to achieve selective alumina scale formation. For concentrations above 20 wt%, however, the Al activity gets too high and dissolution attack will occur. From experiments performed up to now prevention of dissolution attack, tolerable oxidation rate and long term high temperature stability seems to be fulfilled requirements of the above presented protective layers.

Furthermore, an experiment has been performed in order to investigate the enhanced flow corrosion erosion of T91 with and without surface modified layer [4.161][4.162]. A special test section was designed and implemented in the IPPE loop in Obninsk where samples with and without surface modification were exposed to 1, 1.5 and 3 m/s.

The results showed that by increasing the flow velocity from 1 m/s–1.5 m/s the magnetite scale is not anymore homogenously present at the sample surface and at 3m/s the magnetite scale is entirely removed. All three oxide scales are, beside the upper magnetite layer, almost identical in composition and thickness. Therefore, instantaneous removal of the fragile magnetite layer by the flowing LBE is responsible for this behaviour and not a difference in scale growth. On the other hand, T91 with surface modified layer do not show any difference in scale growth depending on flow velocity. Thin protective alumina scales like described above cover the steel surface at all investigated flow velocities.

(e) Mechanical properties

The effect of the protective layers on mechanical properties has been as well investigated. In particular the influence of LBE and steel coating was addressed in low cycle fatigue (LCF) tests at 550°C with 0.5 Hz and elongations $\Delta\varepsilon t$ between 0.3–2.028. The result was that no influence could be observed neither of the LBE with 10–6 wt% oxygen nor with a FeCrAlY coating.

A further test has been performed on the T91 cladding tubes with and without surface alloyed FeCrAlY layer, where the tubes are tested under internal pressure at 550°C in flowing LBE with appropriate oxygen concentration. The results have shown that if an internal pressure of 15 MPa is supplied to the specimen tubes, which causes a strain of 0.7%, the steel surface is still protected but the magnetite layer however the oxide layer growth is accelerated with respect to tests performed under not pressurised conditions. On the other hand surface alloyed tubes do not show any difference in oxidation at such conditions.

(f) Outlook

The still open requirement regarding durability under irradiation is addressed in irradiation studies of T91 with and without surface modified layer in the Phenix reactor. Further irradiation experiments also in contact with LBE will be conducted in the near future.

Open questions for a final judgment of the surface alloyed layers and which will be addressed in the near future are:

— Long term high temperature stability of the system also under abnormal conditions;
— Durability under irradiation;
— Long term mechanical stability of the surface alloyed layer;
— Industrial feasibility.

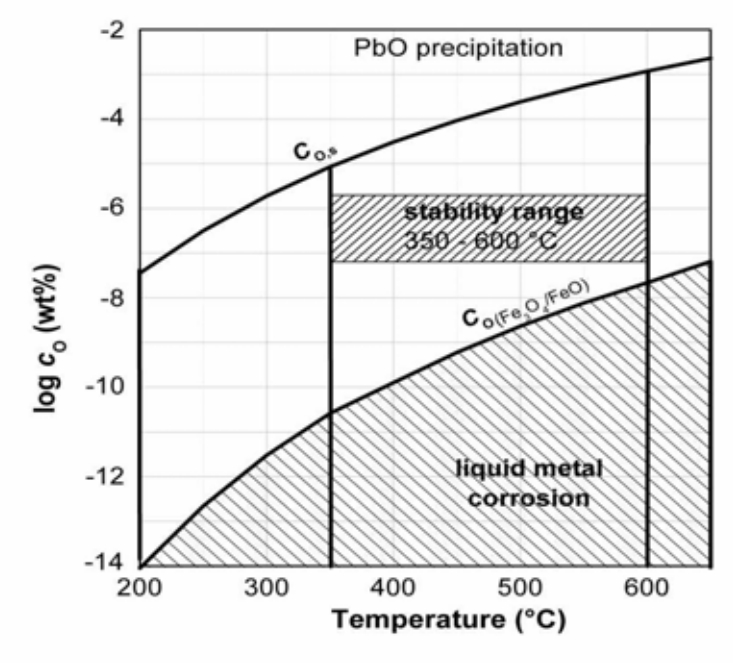


*FIG. 4.126. Range between the solubility limit Co and the oxygen concentration at which decomposition of iron oxides takes place. The area between the curves indicates the concentrations for which stable conditions are expected.*

The oxygen control system developed at FZK is described in Chapter 5.6.

### 4.7.6. India

#### *4.7.6.1. Purpose and goal and major results*

Two buoyancy driven LBE loops have been set up in BARC to study corrosion effects of LBE on candidate structural materials for spallation target module; like SS-316 L, 316 LN, SS-304 L, 9Cr-1Mo etc. The larger loops getting ready would be ~ 7 metre high and its riser and downcomer legs would operate at 5500°C and 4500°C respectively. The buoyancy head is estimated to provide a LBE mass flow rate of 1.7kg/s. The flow velocity around the sample is ~0.6 m/s. Material samples exposed in an already operational smaller corrosion loop were being evaluated by Charpy and Tensile tests after exposing the samples for 2000 hours in the flow with oxygen control. Provision is also being made in this loop to enhance the LBE flow by gas injection. Photographs of these operational facilities have been shown in Fig. 4.127 and Fig. 4.128.

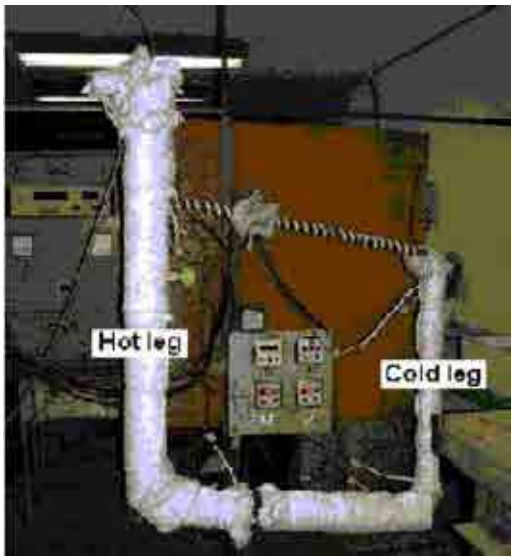


FIG. 4.127. Prototype LBE thermo buoyancy loop.


FIG. 4.128. LBE Corrosion test loop at BARC.

#### *4.7.6.2. Corrosion mitigation studies*

Proper control of oxygen concentration in the LBE process system is imperative for safe and reliable operation of the spallation target loop. Dissolved oxygen monitoring and control strategies including corrosion mitigation techniques being envisaged for Indian ADS target development programme are outlined below. The major technological know-how that would be developed from these studies includes the following:

— Development of zirconia based oxygen monitor;
— Oxygen control system;
— Development of protective coatings.

#### *4.7.6.3. Neutron activation analysis of structural materials*

To assess the suitability of the available structural materials for manufacturing the mechanical components and support structure of LBE loop, we are presently carrying out neutron irradiation studies on analysis of neutron activation of structural materials like T91, SS304L, SS316L, mild steel, alumina wool, flame guard etc. These experiments are being carried out in BARC on beamlines from the 1 MW experimental reactor APSARA.

### 4.7.7. Italy

#### *4.7.7.1. Purpose and goal*

Lead and lead-bismuth eutectic (LBE) are foreseen as spallation target and coolant in ADS system, due to their favourable physical, chemical, thermodynamic and neutron properties. However, besides the above mentioned advantages, they present high corrosion potential with respect to the most of the considered structural materials.

Therefore, the compatibility of the structural materials with the coolant is an issue of major concern, as well as the role played by the neutron irradiation. To establish the system feasibility, then, among all the other R&D needs, it is of fundamental importance to carry out suitable experimental campaigns in order to acquire a complete knowledge of the structural materials behaviour in Pb-LBE

environment, also in presence of fast spectrum neutron irradiation. Particular attention has to be paid to austenitic and ferritic martensitic steels

#### *4.7.7.2. Corrosion*

Some experimental campaigns dedicated to characterize the corrosion behaviour of several steels already available (mainly AISI 316 and T 91) in lead-LBE have been done. In this framework, a large effort has been dedicated to short–medium term corrosion experiments in stagnant and flowing Pb-Bi and few experiments have been carried out in pure Pb of the ADS reference materials but knowledge is still missing on medium–long term corrosion behaviour, mainly in flowing lead. In particular, exploiting the capabilities of the facilities LECOR and CHEOPE; located at the ENEA in Brasimone research centre, several experimental campaigns aimed at characterizing in lead the reference materials (nuclear grade steels, refractory metals), in order to assess their corrosion properties and to investigate the possibility of protecting them by in situ oxidation

#### *4.7.7.3. Irradiation*

Some irradiation studies to determine the structural material behaviour under thermal neutron irradiation in Pb-Bi are part of the currently going on research projects (i.e. EUROTRANS_DEMETRA). What is still missing is a characterization of the reference materials in pure lead under fast neutrons irradiation, referring in particular to phenomena such as corrosion and liquid metal embrittlement (LME), for which the knowledge is limited. Only few and incomplete data are available up to now, from which the necessity to carry out an adequate experimental campaign. An experimental campaign investigating the LME under fast neutron irradiation on EUROFER 97, in the liquid eutectic alloy Pb-17Li has been successfully carried out by ENEA in recent times (LEXUR I Project), highlighting some characteristics of the phenomenon.

On the basis of the preliminary knowledge gained, a second irradiation campaign (LEXUR II) is envisaged, in lead, with the main goal to characterize the behaviour of the materials of interest under fast neutron irradiation, in pure lead, in a significant temperature range.

#### *4.7.7.4. Description of theory and-or instruments*

(a) Corrosion

Several experimental campaigns have been carried out in LECOR and CHEOPE facilities, for testing at different temperatures, under different oxygen contents, the corrosion behaviour of the reference structural materials.

AISI 316L and T91 steels and the refractory metals tungsten and molybdenum have been extensively tested in LECOR loop, at 400°C, at a velocity of about 1 m/s and oxygen content of $10^{-8}$–$10^{-10}$ wt%. To perform the corrosion tests in the LECOR loop using liquid metal with a low oxygen activity, 80 wppm of pure Mg were added to the eutectic lead-bismuth. In addition, pretreatment with hydrogen gas was performed in the storage tank for a few days at 330°C.

The eutectic alloy used for the loops has been supplied by the Stachow GMbH firm (Germany), with a composition of LBE as follows: 44.4wt.% Pb and 55.6wt.%Bi with few ppm of impurities (Ag, 4; Zn, <0.2; Cu, <0.5; Sb, <3; Sn, <9.5; Mg, <1; Cd 0.2; Fe, <0.6; Ni, <0.9) (Fazio, 2003).

T91 and AISI 316 have also been tested in CHEOPE loop, at a temperature of 400°C, a velocity of about 0.8 m/s and an oxygen content of $10^{-5}$–$10^{-6}$ wt %.

Further experiments with Pb-Bi at higher temperatures (450°C) and with longer exposure time in LECOR, and tests on pure Pb in CHEOPE III at 500 °C, are now going on. The use of aluminised coatings and/or the use of modified steels (i.e. martensitic steels with high Si content) are under investigation.

(b) Irradiation

Investigations of reactor irradiation influence on LME of steel EUROFER 97 have been carried out in the Lexur 1 experiment for samples irradiated in the fast reactor BOR-60. Tensile specimens were placed in ampoules filled with the eutectic alloy Pb-17% Li, irradiated and tested. Irradiation temperature was 310–340°C and damaging dose was 0,2–5,9 dpa depending on disposition throughout the height of the core region. Tensile tests of samples have been performed out of pile in the same alloy at the same temperature at which irradiation was carried out. Specimens were realized in Eurefer 97, the reference European low activation martensitic steel, produced by Boehler Edelstahl GMBH. The material was delivered normalized and tempered, and machine worked as received. Each irradiation ampoule, filled with lead lithium, contained one specimen. After irradiation the material testing assembly was extracted from the reactor. Some standard procedures, such as washing of the assembly from sodium coolant and decontamination, were performed. The assembly was opened and the irradiated specimens were transported to the material test hot laboratory. The low strain rate tensile tests of irradiated samples were carried out in liquid metal environment. Tests have been performed at the calculated irradiation temperature of samples. The strain rate was $1 \times 10^{-4}$ $s^{-1}$. Calculations of mechanical characteristics of irradiated samples were carried out according to the standard procedure with test diagrams. All calculations were performed for the mean diameter of the sample effective part. The obtained results in terms of YS ans UTS are allined to the ones available in literature. This testifies that irradiation in the liquid alloy has not most likely resulted in liquid metal embrittlement (LME) of the steel, and radiation hardening made the main contribution to mechanical characteristics change. This is in good agreement with out of pile experiments of LME performed on martensitic steels with temepred fully martensitic state. However, to fully understand the effect of lead lithium it could be useful to explore the behaviour of the material at higher doses and different temperatures.

Taking into account the results obtained in the LEXUR I project, a second irradiation campaign will be carried out in the BOR 60 experimental fast reactor of SSC RF RIAR, in stagnant lead environment.

Corrosion, tensile, CT specimens and creep tubes, sealed in a lead filled capsule, will be irradiated at different temperatures and doses and then analyzed. Virgin/coated/welded specimens of AISI 316L and T91, as well as 15-15Ti and ODS steel samples will be considered for analysis. The tests will be performed at two temperature values relevant for the systems under investigation and two values of dose, preliminarily 8 and 16 dpa.

A comparison of the results obtained with out of pile experiments is also envisaged, to outline the effects not only of the fast neutron irradiation but also of the simultaneous presence of lead coolant and neutron irradiation.

#### *4.7.7.5. Major results*

(a) Corrosion

The results of corrosion tests performed revealed a strong influence on the corrosion mechanisms of the oxygen concentration in Pb-LBE [4.163]–[4.172].

For what concerns the reference steels (martensitic and austenitic stainless steels) it has been noticed how at low oxygen concentration both steels exhibited weight loss, and the corrosion was due to the dissolution of alloy elements, while at high oxygen concentration both steels exhibited weight gain, and the formation of protective thin oxide layer on the surface of specimens has been detected.

At low oxygen concentration the austenitic steel was affected by preferential dissolution of Ni and Cr in the LBE, and the grew of a ferritic layer on the surface has been detected. Under the same condition the martensitic steel was affected by uniform corrosion, and no preferential dissolution has been noticed [4.163]. There was no oxide scale on the surface of specimens, so the corrosion depths of AISI 316L and T91 steels has been estimated by the weight change of specimens. In this situation, the

corrosion depth of specimen stands for the thickness of material which was corroded (or dissolved) by the liquid metal.

In Fig. 4.129 are shown the curves of the corrosion depths versus test time for AISI 316 and T91 steels which were exposed to low oxygen content, flowing LBE, at 450°C. It can be noticed as the corrosion depth for T91 specimen is higher than for AISI 316L specimens: the value of corrosion depth for T91 reaches 23.8 μm after 4500 hours exposure, while the corrosion depth of AISI 316L is about 19.5 μm.

The so called 'in situ oxidation' technique seemed to be effective in the range between 300 and 550°C for EU nuclear grade conventional steels. Steels with higher chromium content presented thinner oxide layer in oxidising environment.

In Fig. 4.130 is reported the corrosion depth of the T91 and AISI 316 specimens tested in CHEOPE loop, at 450 °C, in LBE, at higher oxygen content.

It should be noted that the formula was established under the assuming that we supposed the oxidation is uniform. Since the oxide layer formed on the surface of AISI 316L steel was not very uniform, there was leaching occurred both in the oxide layer and bulk material, the calculated corrosion depth of AISI 316L should not be so precise. An apparent 'threshold limit' (550–600°C), above which the oxide layer onto the steels could become non-protective, seemed to exist for the European steels tested; The aluminised coatings seemed to be able to protect both austenitic and martensitic steels up to 550°C. Pure metals (Ta, W, Mo) have shown a good behaviour in reducing environment.

All the refractory materials tested exhibited a weight loss after 1500 h and 4500 h exposure in LECOR except Ta. The weight loss of refractory metals is by two orders of magnitude smaller than that of steels. The assumption of the growth of a thin oxide layer on the Ta specimens could explain the weight gain found, and is consistent with the experimental condition adopted.

(b) Irradiation

The experimental campaign LEXUR I, investigating the LME under fast neutron irradiation on EUROFER 97, in the liquid eutectic alloy Pb-17Li, successfully carried out in recent times, highlighted some characteristics of the phenomenon[4.163] [4.170]. The main consequences associated to LME have been shown to be a high crack propagation rate, a drastic reduction of strain to rupture and a modification of stress-strain curve. On the other hand, typical effects of irradiation have appeared to be the hardening of steel and a reduction of the plastic strain and of the energy to rupture.

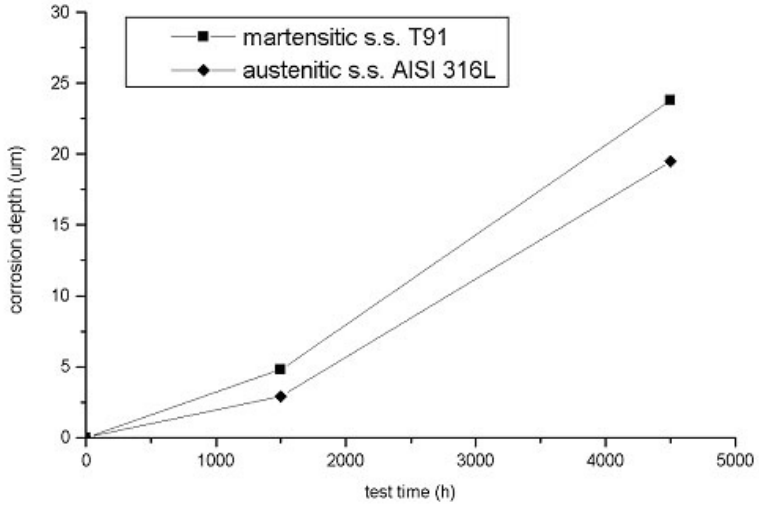


*FIG. 4.129. Calculated average corrosion depths of the steels tested in the LECOR loop. (T=400˚C, Co2=$10^{-10}$ ~ $10^{-8}$wt.%, vLBE=1.0 m/s).*

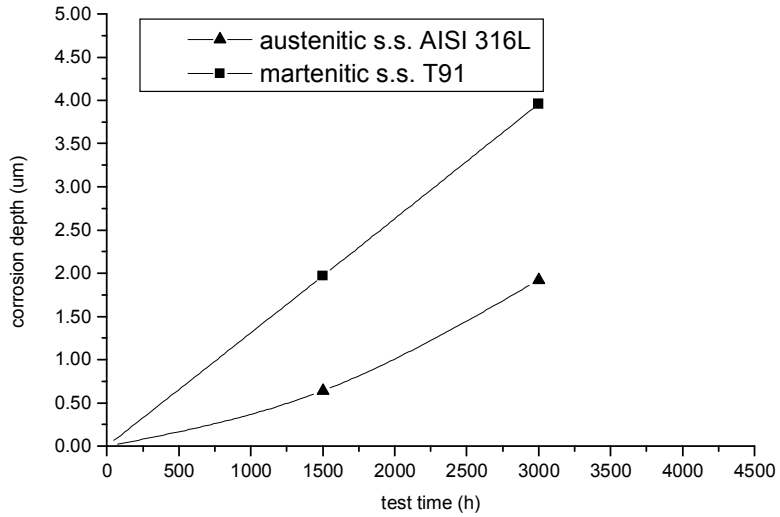


*FIG. 4.130. Corrosion depth of the steel tested in the CHEOPE III loop (T=450˚C, Co2=10-5 ~ 10-6wt.%, vLBE=1.0 m/s).*

### 4.7.8. Japan

#### *4.7.8.1. Purpose and goal*

One of main problems to use lead alloys for nuclear systems such as ADS (Accelerator Driven Dystem) and FBR (Fast Breeder Reactors) is compatibility of steels with lead alloys. Mainly approaches from the following two directions have been made: 1) basic investigation on effects of various parameters to corrosion behaviour in liquid LBE (lead bismuth eutectic) [4.175] [4.176] [4.177] and 2) investigation on applicability of candidate steels developed for FBR to LBE environment [4.173] [4.174].

Effects of temperature, oxygen concentration in LBE and contents of alloying elements, Cr, Ni, Si and Al in steels on corrosion behaviour are investigated in static liquid LBE. Drawing up the corrosion map in liquid LBE is the main goal in this study.

In order to examine the applicability of candidate steels to LBE environment, some steels developed for FBR are used for corrosion tests in LBE. Furthermore, estimation of the predicted curves of the corrosion depth is the main goal.

#### *4.7.8.2. Instruments description*

The static corrosion test apparatus at JAEA was used for basic research of corrosion behaviour in LBE. Corrosion tests were conducted using pots where corrosion specimens were soaked in liquid LBE. The static corrosion test apparatus was composed of a furnace, a quartz pot containing LBE and specimens, and a gas control system. Corrosion tests were conducted in liquid LBE under oxygen-saturated condition) [4.175] [4.176] and low oxygen condition [4.177] at 450°C and 550°C for 3000 h. Materials used in the experiment were F82H, Mod.9Cr-1Mo steel, 410SS, 430SS, 2.25Cr-1Mo steel, pure iron, 14Cr-16Ni-2Mo steel (JPCA), 316SS and SX containing 5%Si. The size of corrosion specimens was 15 mm × 30 mm × 2 mm.

The corrosion tests to examine the applicability of candidate steels developed for FBR were conducted under cooperation with FZK in Germany. Corrosion tests were made at FZK using small

crucibles in which corrosion specimens were put with liquid LBE. The corrosion test apparatus was composed of a furnace, $Al_2O_3$ crucibles containing LBE and specimen, and a gas control system. oxygen concentrations in the LBE were controlled and calculated from $H_2$-$H_2O$ ratio of the supplied Ar-$H_2$-$H_2O$ gas. The corrosion tests were conducted in stagnant LBE containing $10^{-6}$ wt% oxygen at 500–650°C up to 10000 h. Experiments with $10^{-4}$ wt % and $10^{-8}$ wt % oxygen were also conducted at 650°C up to 5000 h. Materials used in the experiment were 316FR, 12Cr steel and ODS steel. The size of corrosion specimens was 6mm × 27mm ×2mm.

#### *4.7.8.3. Main important results*

Effect of test temperatures and contents of alloying elements were studied in corrosion tests in oxygen saturated LBE) [4.175] [4.176]. Corrosion depth decreased at 450°C with increasing Cr content in steels regardless of ferritic–martensitic steels or austenitic steels. Appreciable dissolution of Ni and Cr did not occur in the three austenitic steels at 450°C. Corrosion depth of ferritic–martensitic steels also decreased at 550°C with increasing Cr content in steels whereas corrosion depth of austenitic steels, JPCA and 316SS became larger due to ferritization caused by dissolution of Ni at 550°C than that of ferritic–martensitic steels. An austenitic stainless steel containing about 5%Si exhibited fine corrosion resistance at 550°C because the protective Si oxide film was formed and prevented dissolution of Ni and Cr. These characteristics of corrosion behaviour are shown in Fig. 4.131.

Corrosion tests in liquid LBE with low oxygen concentrations were conducted under the condition of an oxygen concentration of $5x10^{-8}$ wt% at 450°C and an oxygen concentration of $3x10^{-9}$ wt% at 550°C [4.177]. Decrease in oxygen concentration generally caused increase in corrosion depth. Fig. 4.132 shows the corrosion rate per year calculated from the measured corrosion depth for 3000h assuming a linear rule. Although significant corrosion was not observed at 450°C for ferritic–martensitic steels, F82H, Mod.9Cr-1Mo steel, 410SS, 430SS except 2.25Cr-1Mo steel, ferritization was found at 450°C for austenitic stainless steels, 316SS and JPCA. Pb-Bi penetration into steels and dissolution of elements into Pb-Bi were severe at 550°C even for ferritic–martensitic steels. Typical dissolution attack occurred for pure iron both at 550°C without surface $Fe_3O_4$ and at 450°C with a thin $Fe_3O_4$ film. Feritization due to dissolution of Ni and Cr, and Pb-Bi penetration were recognized for austenitic stainless steels, 316SS and JPCA at both temperatures of 450°C and 550°C. The phenomena were mitigated for austenitic stainless steel with 5%Si. It was found that oxide films could not be an effective corrosion barrier in liquid LBE in some cases.

Long term corrosion test data were obtained in corrosion tests to examine the applicability of candidate steels developed for FBR [4.173] [4.174]. Martensitic steels containing Cr to more than 9% presented good corrosion resistance by the formation of spinel oxide layer in $10^{-6}$ wt % oxygen LBE at temperatures below 550°C. 9%Cr ODS steel exhibited similar corrosion behaviour to the martensitic steel. Fig. 4.133 shows results of measurement of the oxide thickness formed on ODS steel at 550°C at different positions on each specimen and of the Fe-Cr spinel layer thickness. At temperatures above 600°C, the oxide layer thickness diminished with increasing temperature. The behaviour seems to be ascribed to change in the stable form of iron oxide. Some data between thickness of oxide layer and exposure time up to 10000 h were obtained. Estimation of the predicted curves of corrosion depth is also tried using these data. Effect of oxygen concentration on corrosion behaviour in LBE at 650°C was very complicated: $10^{-4}$wt% and $10^{-8}$wt% oxygen were favorable for good compatibility, however, not $10^{-6}$wt% oxygen.

#### *4.7.8.4. Outlook*

While effect of Si was confirmed, it is expected that Al addition has more influence on improvement of corrosion resistance in liquid LBE. Effects of Al-alloy and ceramics coatings will be studied for this purpose. In the study on application of steels developed for FBR, it was found that usage of these steels at higher temperatures than 600°C in liquid LBE is difficult. Development of ODS steel with Al addition is being continued as an extension of the study.

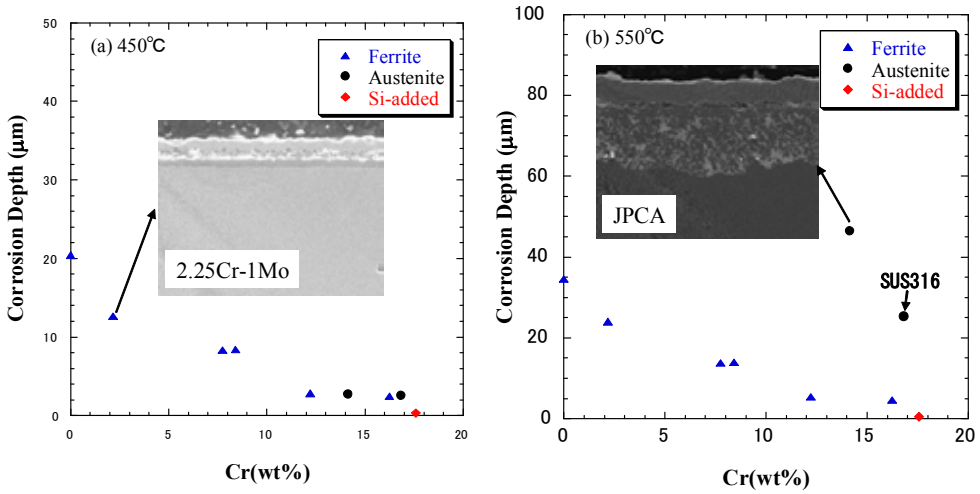


*FIG. 4.131. Relationship between corrosion depth and Cr content in steels. Some SEM images of cross-section of specimens after the corrosion test are shown. The corrosion test was conducted in oxygen saturated LBE at (a) 450°C and (b) 550°C.*

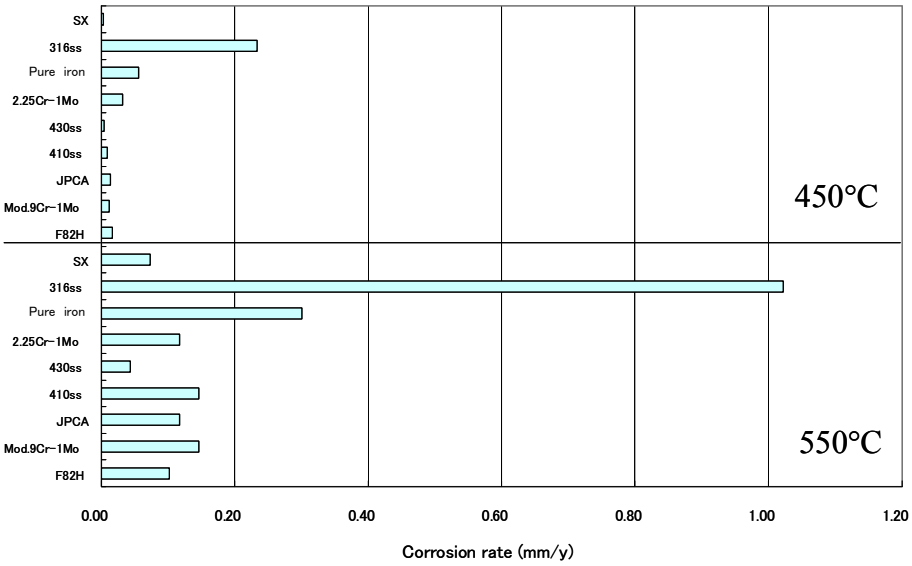


*FIG. 4.132. Estimated corrosion rates per year of various steels in liquid LBE with low oxygen concentrations.*

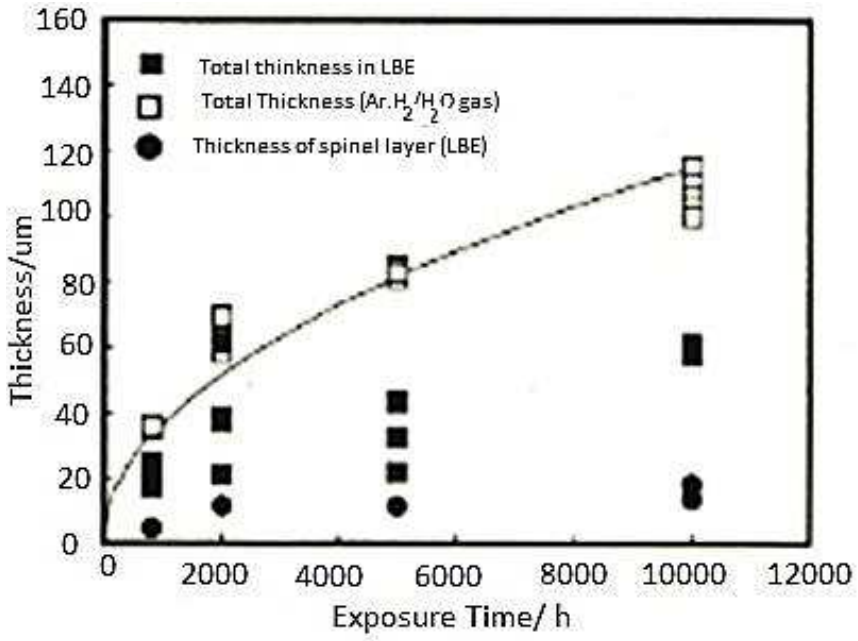


*FIG. 4.133. Results of measurements of the oxide thickness formed on ODS steel at 550°C at different positions on each specimen and of the Fe-Cr spinel layer thickness. The corrosion test in liquid LBE was conducted under the condition of 10–6 wt % oxygen.*

## 4.8. NUCLEAR DATA

The section presents an overview on the ongoing studies on nuclear data.

### 4.8.1. India

#### *4.8.1.1. Spallation target simulations and analyses*

There are a few Indian teams studying ADS target reactions, thermalhydraulics and materials behaviour through simulations and analytical studies. There are also experimental programmes to validate the results from these studies.

(a) Heat deposition calculations by CASCADE.04.h and FLUKA code

The heat deposition due to nuclear and ionization losses of primary proton and secondary particles have been estimated for thick targets of Be, C, Al, Fe, Cu, Pb, Bi and depleted U, by using CASCADE.04.h and FLUKA Monte Carlo codes [4.178]. The results obtained from both codes show good agreements with the experimental data verification for the light elements would be necessary. Remeasurements of the heat deposition data for the Iron, which is a strong candidate as target window material, are needed. CASCADE.04.h code has been improved to take into account the quasi-continuous heat deposition by reducing the incremental distance between energy loss points so that not more than 2–3% energy loss can occur between these points. The results of heat deposition by using CASCADE.04.h were found better than the results obtained by using its precursor CASCADE.04 [4.179] near the target window.

The loss of proton beam energy within the target module (for the given geometry and flow conditions) due to interaction of 1 GeV protons, and consequent heat deposition rates have been calculated using both the codes. The calculated data were also integrated with CFD codes (as given in next section) for obtaining detailed temperature profile in the beam window, target and other components near the

spallation zone in the liquid LBE metal flow stream. It was found that CASCADE.04.h code gives the higher temperature (TWM = Maximum Window Temperature) inside the window as given in Table 4.35, which gives total heat deposited and maximum temperature inside the T91 window for different LBE flow rates. The data inside the brackets show heat deposition when LBE is not filled.

TABLE 4.35. TOTAL HEAT DEPOSITED IN THE LEAD TARGET OF RADIUS 10 CM FOR PROTON ENERGY OF 1GEV

| Flow Guide inner diameter (9.7cm), total heat deposited in target=1252 (kW/2 mA) | | | |
|---|---|---|---|
| LBE flow rate, kg/s | Simulation code | Total heat, kW/2mA | TWM, (K) |
| 91 | CASCADE.04 | 8.2 (7.8) | 759 |
| | FLUKA | 8.4 (7.6) | 800 |
| | CASCADE.04.h | 9.4 (7.8) | 855 |
| 136 | CASCADE.04 | 8.2 (7.8) | 696 |
| | FLUKA | 8.4 (7.6) | 716 |
| | CASCADE.04.h | 9.4 (7.8) | 779 |

(b) Neutron Yield Calculations by CASCADE.04.h code

Comparison of neutron yield from thick and thin targets was made for different target materials; and distributions of neutrons along the target radius and length were estimated. Angular and energy spectra of emitted neutrons from the LBE target were also generated by using both the codes. The results were found within 10% accuracy for these parameters. The energy dependence on neutron yield, energy and angular spectra were analyzed. Percentage of high energy neutrons (En > 20 MeV) remains within 5–7% with increase in the proton energy as shown Fig. 4.134. Similar observations were also reported in ref. [4.180].

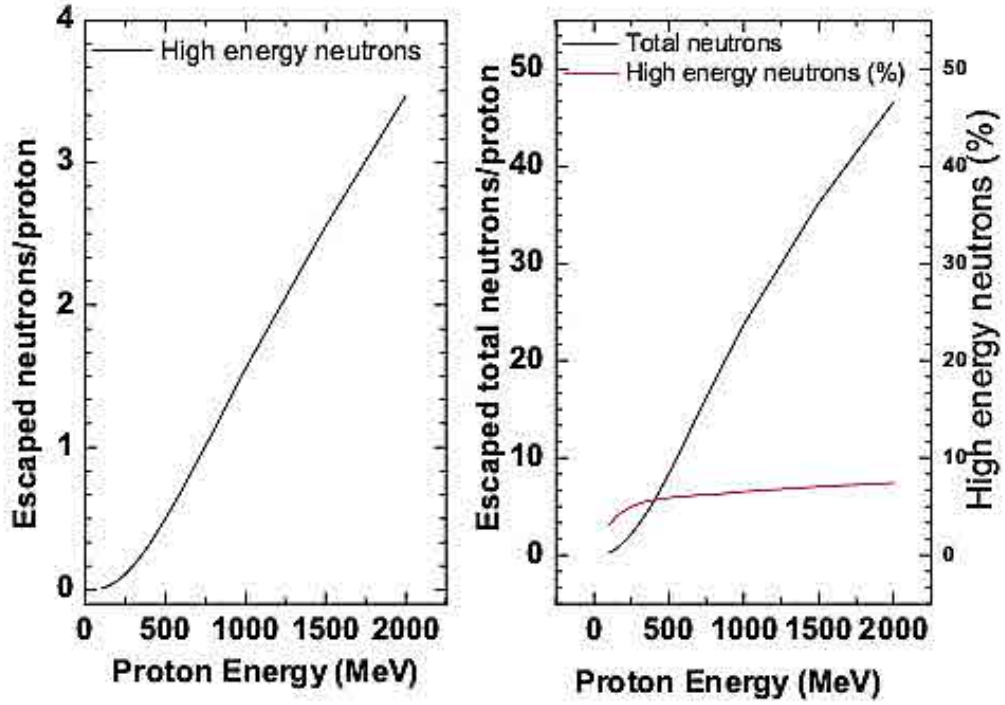


*FIG. 4.134. Total and high energy neutron yield & percentage neutrons at energy > 20 MeV from LBE as a function of proton energy.*

The CASCADE.04.h code uses 26 group library for the low energy (< 10.5 MeV) neutron transport. We have coupled the high energy part of the CASCADE.04.h code to the low energy code developed at BARC which uses the point data library to study transmutation and burnup of the ADS reactor assembly.

#### *4.8.1.2. Computational tools for LBE target design*

(a) One dimensional codes for loop design and optimization

We have developed computation codes for complete LBE loop design (including 2 phase flow region for gas driven target system). Specific codes have also been developed for buoyancy (window target) as well as gas driven target loops for window as well as windowless target systems.

(b) CFD codes for flow and temperature analysis

We have developed 2 Dimensional CFD codes based on FEM, which can handle complex geometries, buoyancy effects, turbulent flow and conjugate heat transfer etc. The numerical method is based on Streamline Upwind Petro-Galerkin (SUPG) technique and following the Eulerian Velocity correction approach. Time dependent governing equations for conservation of mass, momentum and energy in the fluid are solved. For conjugate analysis, the conduction equation in the solid is solved. Structured grid has been generated using partial differential equation technique (Laplace equation). Higher grid refinement was ensured for the fluid zone near the window, which is the region of interest.

Based on these codes, thermal design of a target has been carried out for one way coupled Indian ADS reactor concept. A preliminary design of this ADS reactor consists of fast and thermal reactor zones producing about 100 MW(th) and 650 MW(th) respectively. The typical velocity and temperature distributions obtained in the spallation region for a 1 GeV and 2 mA proton beam current are shown in Fig. 4.135.

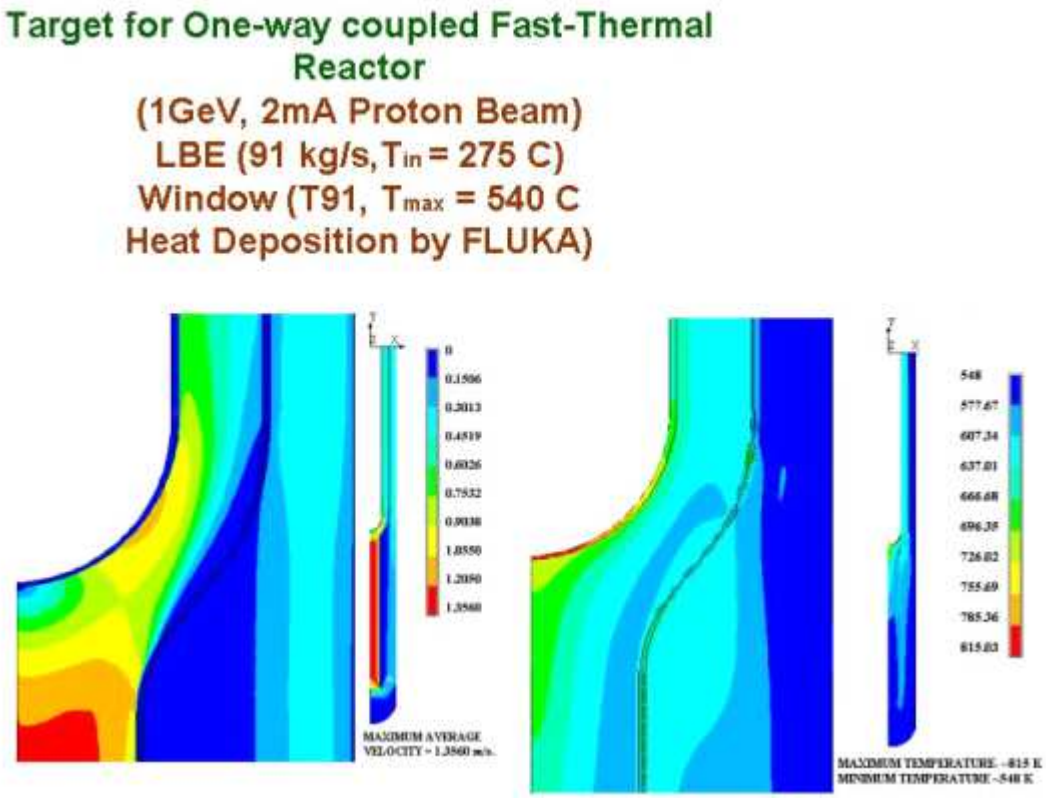


*FIG. 4.135. Typical velocity and temperature distributions obtained in the spallation region for a 1GeV and 2 mA proton beam current.*

### 4.8.2. Japan

#### *4.8.2.1. Purpose and goal*

The goal is to provide nuclear data for ADS design and feasibility study. The neutron nuclear data for minor actinide (MA) and long lived fission product (LLFP) nuclides below 20 MeV are prepared for estimation of subcriticality, transmutation rate, etc. The neutron and proton nuclear data for target and structural nuclides up to 3 GeV are also given for the calculations of transport, shielding, etc.

#### *4.8.2.2. Theoretical explanation*

For the neutron nuclear data below 20 MeV, used are the evaluation tools which are the nuclear model calculation codes with optical model, statistical model with preequilibrium correction, fission model, and so on. For this purpose, the codes of POD [4.181] and CCONE have been developed.

For the neutron and proton nuclear data above 20 MeV, nuclear data evaluation codes, such as GNASH have been extended and performed evaluation below 200 MeV. Above 150 MeV we have adopted simulation codes, such as JQMD which applies quantum molecular dynamics and statistical decay mode, JAM [4.182] which applies intranuclear cascade and generalized evaporation models. Recently PHITS [4.183] code has been developed and implemented functions of both JQMD and JAM. PHITS has not only nuclear data evaluation function but also all particle transportation calculations. The calculated results by above two method is combined at the suitable energy point between 150 and 200 MeV.

#### *4.8.2.3. Most important results*

— JENDL-3.3 [4.184]: the latest Japanese general purpose nuclear data file, which includes neutron nuclear data for 337 nuclides below 20 MeV;

— JENDL/HE-2004 [4.185] : the intermediate energy nuclear data file, which includes neutron and proton nuclear data for 66 nuclides below 3 GeV;

— JENDL/PD-2004 [4.186]: the photonuclear data file, which includes photonuclear data for 68 nuclides below 140 MeV;

— POD and CCONE: the model calculation codes for nuclear data evaluation below 20 MeV.

### 4.8.3. Russia

#### *4.8.3.1. Measurement of nuclear data on minor actinides*

One of the most important directions of researches on substantiation of ADS as burner of minor actinides (MA) is the measurement of neutron cross-sections for fissile and fertile materials, first of all, for MA. Available experimental data for the majority of MA have a wide dispersion of values, and they are practically absent in the neutron energy range over 5–7 MeV.

It is necessary to mention the following works carried out in this area:

— Participation of the experts from IPPE in experimental researches aimed at obtaining nuclear data for minor actinides and fuel compositions including thorium cycle, which are carried out in CERN with reference to the European ADS Project (researches are implemented at the proton accelerator PS24 using lead target, within energy range from 0.01 eV up to 1 GeV);

— Experimental researches of mechanisms of nuclear reactions within neutron energy range up to 30 MeV using the tandem generator EG-15 located in IPPE;

— Creation of validated libraries of evaluated nuclear data on interaction of protons and neutrons with energy up to 3 GeV with materials of ADS window, target, accelerator and blanket;

— Studies of accumulation and fission parameters of MA under irradiation (Np237, Pu238, Pu240, Am241, Cm244), executed on the basis of samples previously irradiated in BN-350 reactor;

— Irradiation of samples with isotopes Np237, Pu238, Pu239, Am241 under conditions simulating ADS parameters (JINR, Dubna);

— Analytical studies of neutron cross-sections of various isotopes in energy range more than 20 MeV.

Now a coordinated programme of researches on measurement and estimation of nuclear data for 22 isotopes of U, Pu, Np, Am, Cm, Bk and Cf in neutron energy range from 0.05 eV up to 30 MeV has been prepared:

— BOR-60 and SM-3 reactors located in RIAR (Dimitrovgrad) are supposed to be used for integral in-pile experiments;

— Differential measurements of neutron cross-sections of MA are planned being carried out at the linac LU-50 (VNIIEF, Sarov) and pulse electrostatic accelerators EG-1 and EG-15 (IPPE, Obninsk);

— Measurements of fission cross-sections of $^{241}$Am, $^{242m}$Am, $^{243}$Am, $^{243}$Cm, $^{244}$Cm, $^{245}$Cm, $^{246}$Cm, $^{247}$Cm, $^{248}$Cm, $^{236}$U in resonance neutron energy range (0.05–30 keV) where dispersion of nuclear data is especially large, are carried out with using lead slowdown spectrometer (lead mas 100 t) at the base of linear proton accelerator of 'Moscow meson factory' (IYaI RAN, Troitsk; IPPE, Obninsk);

— Benchmark experiments are scheduled to be implemented at the critical facilities BFS-1 and BFS-2 (IPPE, Obninsk);

— Total and relative outputs of delayed neutrons for a number of nuclides including $^{241}$Am, $^{243}$Am will be measured at the accelerator EG-2.5; a database systematizing time and energy spectra of delayed neutrons in reactor neutron energy range will be created for all set of U, Np, Pu, Am isotopes.

#### *4.8.3.2. Neutron physics researches at BFS facilities*

(a) Description of BFS facilities

There are unique zero power critical facilities BFS-1 and BFS-2 in IPPE. They are constructed, first of all, for implementation of neutron physics researches in fast reactor area (FR) [4.187]. These experimental facilities can also be used for carrying out neutron physics researches in ADS area.

BFS-1 fast critical facility has been constructed to simulate FR cores of small and medium power. A fundamental construction of the facility is a set of metal (stainless steel, as a rule) tubes of 50 mm in diameter and vertically positioned with a pitch equal to 51 mm in a tight hexagonal structure inside a cylindrical tank and fastened with their end details in a supporting slab. The tubes are filled with pellets of fuel, structural and coolant materials in fractions the materials constitute reactor cores and reflectors. There are two additional volumes being attached to the tank. The first volume is a graphite thermal column and the second one is a metallic column of parallelepiped shape filled with metal tubes. The maximal sizes of reactor basket are: diameter 2 m, height 2.2 m.

BFS-1 is united with a microtron — a pulsed resonance cyclic accelerator of electrons that allows to carry out ADS modeling and to implement the appropriate neutron physics researches. The basic microtron parameters are: pulse duration 0.2–2 μs, frequency 100–1000 pulses per second, energy of accelerated electrons up to 30 MeV, pulse current strength up to 100 mA. In reactor physics researches, the electron beam hits on a tungsten (or another material) target installed in the center of the BFS-1 facility and beats out neutrons from it. They are getting the core of the facility and initiate

neutrons multiplication. The arising neutrons flashes allow determining neutrons energy spectrum of the reactor using time of flight approach on a base of 50 m and 250 m.

A design of BFS-2 facility is similar to the design of BFS-1 facility. However, its sizes are much more than sizes of BFS-1: the reactor basket diameter is equal to 5.0 m, height of pipes with various materials is equal to 3.0 m. Such characteristics of the facility have made possible neutron physics investigations of full scale mock-ups of cores, blankets, shielding and in-vessel storages of large power fast reactors (up to 3500 MWt). The facility is equipped with graphite and metal columns, forced air cooling system with a gas purifier and elevating system. A significant quantity of tools providing a fast and convenient experimental activity, particularly, a computer controlled semi-automatic fuel rods reloading and detectors moving machine is used at the facility.

Both facilities are equipped with sufficient stocks of reactor materials:

— Metallic plutonium with various isotope composition;

— Metallic uranium (with enrichment of 90%–36%);

— Uranium dioxide;

— Plenty of raw materials (~250 t);

— Disks from pure lead, alloy Pb-Bi (~200 t) and metallic sodium;

— Plenty of construction materials, absorbers and moderators.

Basic experimental research methods used at BFS-1,2 facilities are:

— Measurement of spatial fission reaction rates distribution by miniature fission chambers;

— Measurement of integral capture cross-sections ratios by activation of detectors;

— Coolant void reactivity worth measurement;

— Doppler effect measurement by means of oscillation of hot and cold sample in the core;

— Reactivity worth measurement for one or several rods using either so-called ‘long rod’ method or just usual replacement of staff rods (for instance, simulation of safety and control rods system);

— Integral fission cross-section ratios measurement by absolute, miniature and segment fission chambers as well as by solid track detector method;

— $K\infty$ measurement by oscillation method of elementary cell and its constituents;

— Measurement of central reactivity coefficients of materials by small samples oscillation method.

Besides modeling cores of the concrete FR designs, implementation of the problem oriented researches including various benchmarks is also possible.

(b) Researches implemented with reference to ADS

Among researches carried out at BFS facilities which can represent the certain value for a substantiation of ADS, it is necessary to mention the following experimental works:

— Within the framework of a substantiation of BREST-OD-300 reactor design, the modeling of FR with lead coolant and mixed nitride fuel was carried out on a series of assemblies (BFS-61, BFS-64 etc.);

— The researches of influence of plutonium isotope composition on the basic core neutronic characteristics were carried out. A special attention was given to investigation of coolant void reactivity effect as well as the opportunity of MA transmutation in such cores. In particular, there have been measured:

  - Ratios of fission cross-sections of Np237, Am241, Am243, Pu and Cm isotopes to referenced isotope U235;

- Central reactivity coefficients of Np237 with Am241 and Am241;
- Doppler effect for Np237 etc;

— A series of benchmarks for testing neutron data was created (BFS-85, BFS-87 assemblies). These assemblies represent critical ensembles with maximum simple geometry and two types of the coolant Pb and Pb-Bi.

As a perspective direction of researches at BFS facilities, it is necessary to mention an opportunity of implementation of integral experiments for substantiation MA transmutation.

## 4.9. REACTOR PHYSICS AND CORE DESIGN, INCLUDING NEUTRONICS, THERMAL HYDRAULICS AND THERMOMECHANICS

The section presents an overview of the studies ongoing at international level on reactor physics and core design.

### 4.9.1. The GUINEVERE project in Belgium

#### *4.9.1.1. Purpose and goal*

The GUINEVERE project (**G**enerator of **U**ninterrupted **I**ntense **NE**utrons at the lead **VE**nus **RE**actor) is a European project in the framework of FP6 'IP-EUROTRANS'. The IP-EUROTRANS project aims at addressing the main issues for Accelerator Driven System (ADS) development in the framework of partitioning and transmutation for radioactive waste volume and radiotoxicity reduction.

The GUINEVERE project is carried out in the context of domain 2 of IP-EUROTRANS, ECATS, devoted to specific experiments for the coupling of an accelerator, a target and a subcritical core. These experiments should provide an answer to the questions of on-line reactivity monitoring, subcriticality determination and operational procedures (loading, startup, shutdown) in an ADS by 2009–2010.

The GUINEVERE project will make use of the VENUS reactor, serving as a lead fast critical facility, coupled to a continuous beam accelerator. In order to achieve this goal, the VENUS facility has to be adapted and a modified GENEPI-C accelerator has to be designed and constructed. During the years 2007 and 2008, the VENUS facility will be modified in order to allow the experimental programme to start in 2009.

#### *4.9.1.2. Description of theory and-or instruments*

(a) The VENUS reactor

The VENUS reactor (Fig. 4.136) was built in 1963–1964 in the framework of the Vulcain project. This explains the name VENUS, which is an acronym for Vulcain Experimental Nuclear Study. The purpose of the Vulcain project was to demonstrate the feasibility of a reactor concept with a variable neutron spectrum. In 1966–1967, the facility was adapted and improved to study new applications, more in particular the study of Light Water Reactors (LWR). In 2000–2001 the internal parts of the VENUS reactor vessel were modified to allow the loading of 1m active length fuel rods, thereby broadening the field of possible applications [4.188].

The VENUS reactor is a water moderated reactor (zero power critical facility). The reactor consists of an open vessel (without pressure) inside a concrete protection (called casemate) which can only be entered when the reactor is not working (no water and fissile fuel in the vessel).

The fissile fuel is contained in fuel pins which are manually loaded in the reactor according to a configuration with a square pitch. The fuel pins used in VENUS are of PWR type and can contain either uranium oxide or MOX. The configuration of fuel pins is contained by means of a set of stainless steel grids. A large variety of configurations can be loaded as a function of the experimental programme.

*FIG. 4.136. Top view of the VENUS reactor.*

The reactor is made critical by increasing the water level in the reactor. At one specific water level the reactor loaded with that specific configuration becomes critical. The power level and reactivity can be changed by varying the water level. To control the reactor, one uses control bars which displace water and thereby change the water level. The reactor is shut down by a fast water dump system.

For the execution of de GUINEVERE project two main type of modifications at the SCK•CEN site are necessary. First of all, the modifications which are connected to the installation of a new GENEPI-C accelerator, working in continuous and pulsed mode, at the VENUS critical facility and its coupling to the core. The second type of modifications is linked to the adaptation of the VENUS critical facility to host a fast lead core, further on referred to as VENUS-F.

(b) The GENEPI-3C accelerator

The GENEPI-3C neutron source is the third of a series of machines designed for reactor physics. It consists of a 250 keV deuteron accelerator producing neutrons by the D(d, n)3He or T(d, n)4He nuclear fusion reactions in a target.

The first GENEPI (GEnérateur de Neutrons Pulsé Intense) was designed and built for the MUSE programme [4.189] devoted to ADS studies. It was coupled to the MASURCA reactor with a horizontal insertion in the mid plane of the core (Fig. 4.137). This programme [4.190] investigated particularly reactor kinetics measurement techniques aiming at subcriticality determination, to provide recommendations for the operation of a nuclear reactor coupled with an accelerator. It required a pulsed neutron source with very short pulse duration (< 1μs), short leading and lagging fronts (100 ns) and a high intensity (deuteron peak current ~ 40mA).

For the GUINEVERE project starting from the experience gained with GENEPI 1-2, a new GENEPI-3C accelerator operating both in the continuous and pulsed mode will be designed to be coupled to VENUS-F. In the pulsed mode it should work with characteristics as close as possible of that of the GENEPI 1-2. In the continuous mode, deuteron currents to be reached should be in the 100 μA to 1mA range. It is recalled that a 1μs peak of 40 mA intensity at 4 kHz is equivalent to a continuous beam of 160 μA, resulting in the same quantity of source neutrons per second (around $10^9$–$10^{10}$n/s), i.e. the conditions of the MUSE experiment. To achieve the 'beam trips'part of the experimental programme, prompt beam interruptions should be performed with a repetition rate of a fraction of Hz and with a duration between a few hundreds of microseconds and a few tens of milliseconds.

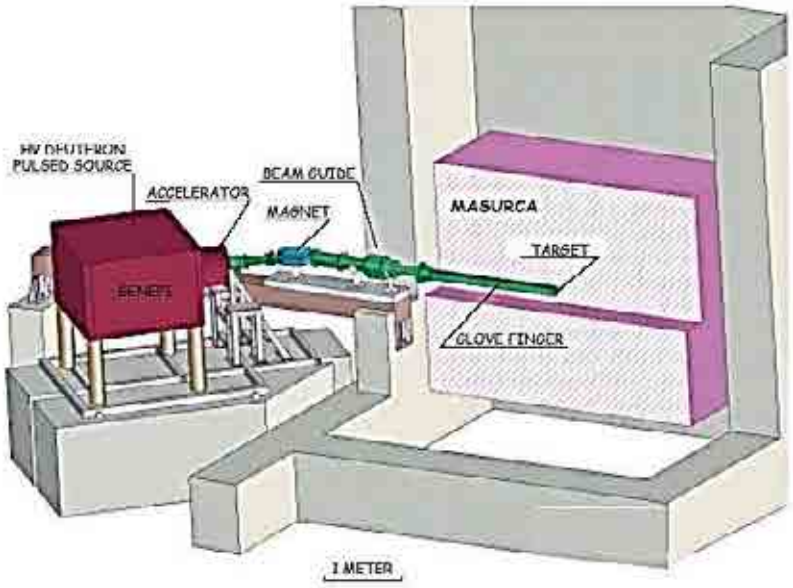


*FIG. 4.137. GENEPI-1 implantation at the MASURCA facility.*

### *4.9.1.3. Major results*

The start of the experimental programme is scheduled for the beginning of 2009. At the moment the main activities are dedicated to the design of the modified GENEPI-3C, the modification of the VENUS reactor and de design of the fast core of VENUS-F. A brief summary of those activities is given below.

(a) Design of the GENEPI-3C accelerator

For the coupling of the GENEPI-3C accelerator with VENUS-F, a vertical insertion of the thimble with a 90° bending magnet above the reactor surface was chosen (Fig. 4.138). This choice frees the reactor room from heavy devices, and will simplify detector operation during the experiment, especially in the reduced fuel zone (60 cm in diameter) around the beam insertion. One of the challenges of the GENEPI-3C machine is to perform both pulsed and continuous modes with the same ion source. The ion source used for the pulsed mode of the GENEPI accelerators is a duoplasmatron source [4.191]. The operation in continuous mode has been investigated on a dedicated source test bench built at LPSC for the GUINEVERE project.

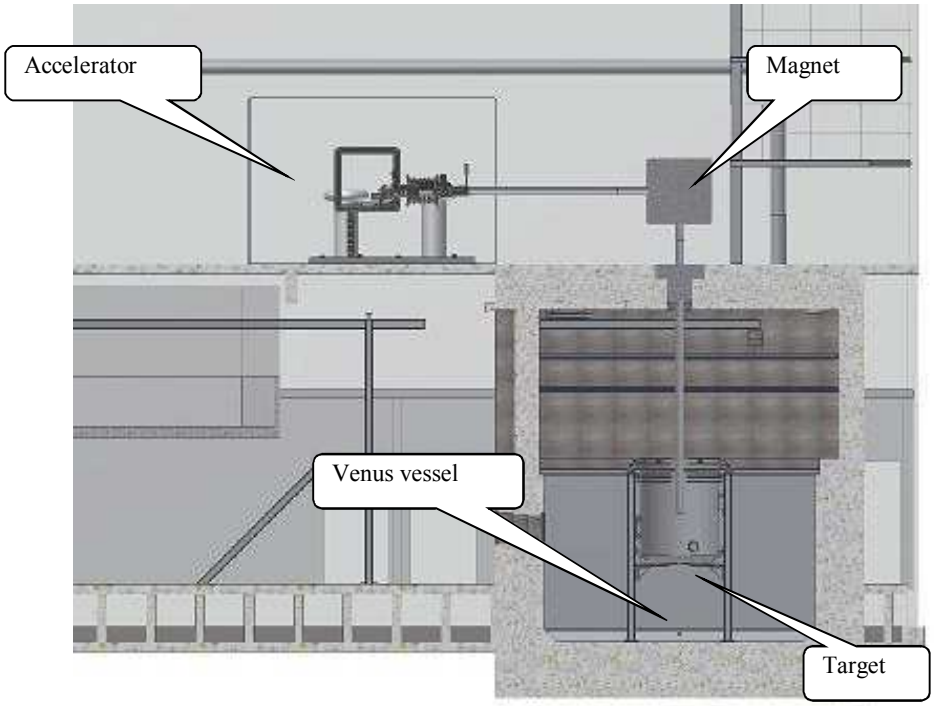


*FIG. 4.138. GENEPI-3C implantation at the VENUS facility.*

The 90° magnet has a 'C' design with a radius of 0.6m, 30° faces and a magnetic field of 0.2T. It is cooled by several water loops, and the heat exchanger unit is separated from the magnet to keep the main amount of water far from the hole above the reactor. It is one of several precautions taken to avoid water leakage in the reactor which could drive it critical. The target module ending the thimble is rather similar to those of the GENEPI-1 and GENEPI-2 accelerators. A first design of the target is available. It is a TiT2-target and it is designed to be easily removable from the thimble and to allow target handling and mounting operations in a glovebox in order to minimize tritium contamination. Other works in progress are de design of the vertical beamline handling and the evaluation of the most reliable methods for direct neutron source monitoring.

(b) Modification of the VENUS reactor

As mentioned in the above section the GENEPI-3C accelerator will be installed above de bunker of the VENUS-F reactor. Since such a room does not exist at present, modifications to the existing building are required. For that purpose an engineering office has been contacted to verify the stability of the building. Measurements of the soil resistance have been carried out with positive results. The construction permit is now submitted to the proper authority.

In March 2007 the VENUS reactor was started up for the last time in its water moderated configuration, after which the dismantling of this configuration was started. All the internal components in de vessel have been removed and safely stored in such a way that a future return to the water moderated configuration remains possible [4.192].

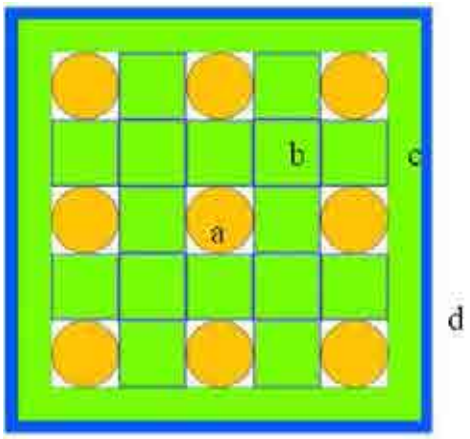


*a) lead element; b) fuel rod; c) lead plate; d) square profile in stainless steel.*
*FIG. 4.139. Cross-section of the loading pattern of a standard fuel assembly.*

The typology of the fuel assembly of the new fast configuration has been fixed Fig. 4.139). It will consist of a square profile of stainless steel, binding together 9 fuel elements of 30% enriched U, 16 lead elements and 4 lead plates. Apart from this standard typology, some other special assemblies will be designed to host nuclear instrumentation. A first dummy assembly was produced in order to validate the design (Fig. 4.140). The test has given a positive result.

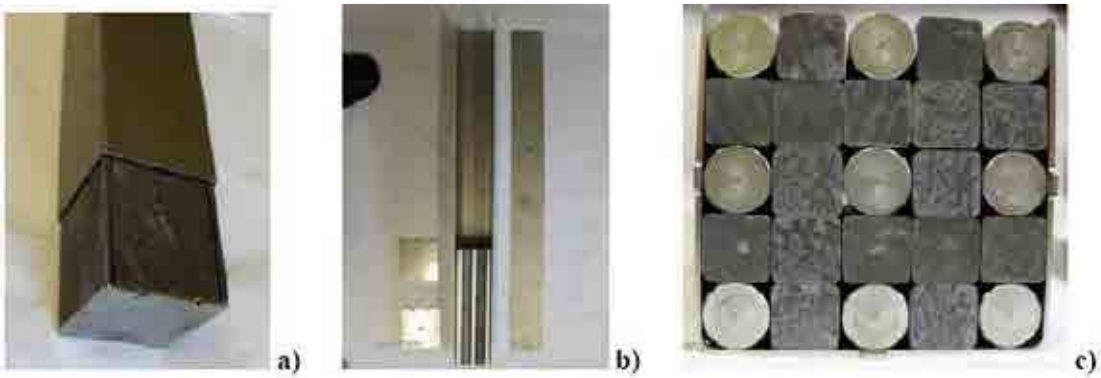


*a) stainless steel tube, and lead plates; b) longitudinal view of the fuel and lead elements; c) cross-section of the loading pattern with fuel and lead elements.*
*FIG. 4.140. Pictures of the dummy fuel assembly.*

(c) Design of the core

The various studies of the core configuration have converged to a critical configuration made of 88 subassemblies as shown in Fig. 4.141 [4.193]. The six B4C safety rods placed close to the center of the core have a fuel assembly follower. Because of this the neutron flux in the core won't be locally distorted when the rods are withdrawn from the core. Moreover during a scram the efficiency of the safety rods will be very high since the fuel is replaced by a neutron absorber.

For the coupling experiment the subcritical configuration will be obtained from de critical one by removing the four central assemblies. The empty central room will host the thimble of the GENEPI-3C accelerator.

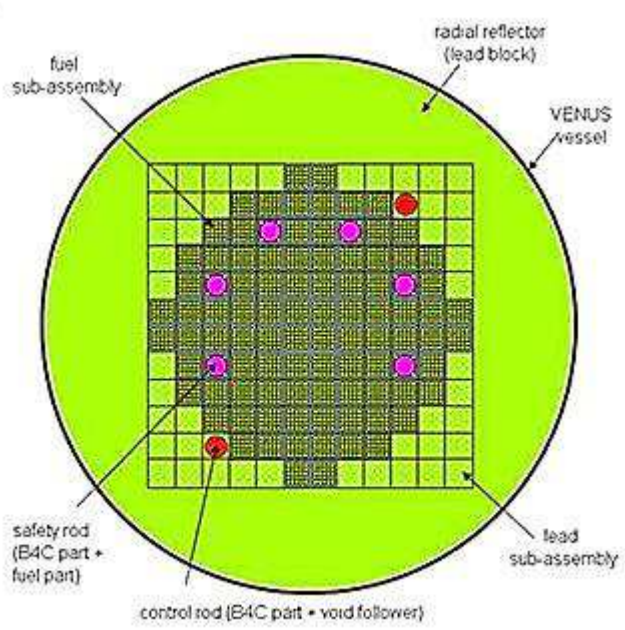


The purple circles indicate the position of the B4C safety rods with a fuel element follower.
The red circles indicate the positions of the control rods.

*FIG. 4.141. Core layouts with 90 fuel subassemblies.*

### 4.9.2. The Venus-1 subcritical experimental assembly and experiment results

#### *4.9.2.1. Purpose and goal*

In 1995, a research group is established in China, focusing on the topic of 'Accelerator Driven System' and the conceptual studies [4.195]. In 2000, a project of 'major state basic research programme (973)' in energy domain sponsored by the Ministry of Science and Technology (MOST) started to investigate the ADS physics and the related technologies. At the present, the design, construction and preliminary experiments of the China's ADS subcritical assembly (Venus-1) have been completed. Detailed description of the design parameter of Venus-1 and experiment results is given below.

#### *4.9.2.2. Instruments description*

According to the above mentioned design objectives and requirements, as well as the conceptual study on the reactor core physics for an accelerator driven subcritical reactor [4.196], the core of Venus-1 subcritical assembly [4.197] is designed to be coupled core by a fast neutron spectrum zone and a thermal neutron spectrum zone. The fast neutron spectrum zone (including external neutron source) is located at the center of the core and the thermal neutron spectrum zone is surrounding the fast neutron spectrum zone. The Venus-1 is driven by several different energy external neutron source [4.198] which are Am-Be neutron source, Cf-252 spontaneous fission neutron source, D-D reaction neutron source, D-T reaction neutron source and so on steady neutron source to study the effect of external neutron source and D-T pulsed neutron source through CPNG (CIAE Pulsed Neutron Generator) to study dynamic characteristic.

There are no safety rod and control rod in the core, excepting the aluminum structure used for modeling sodium coolant in the fast neutron zone and the polyethylene structure used for modeling water coolant and moderator in the thermal neutron zone, thus satisfying the requirement for simple structure of the core. The maximum $k_{eff}$ is designed less than 0.98, which is smaller than the

shutdown margin of a PWR. On the other hand, a subcritical assembly depends on external neutron sources for its operation and can be shut down by cut off deuterium ion current (for D-D or D-T reaction steady external neutron sources and D-T reaction pulsed neutron source) or by removing steady external neutron source (Am-Be isotope neutron source or Cf-252 spontaneous fission neutron source), thus exempting concerns in nuclear criticality safety for Venus-1 subcritical assembly, unlike critical reactors depending on safety rods and control rods for operation.

Natural uranium is used as the fuel for the fast neutron zone and low enriched uranium ($UO_2$ with 3% enriched U-235) is used as the fuel for thermal neutron zone. The parameters of these fuels are listed in Table 4.36.

TABLE 4.36. PARAMETERS OF REACTOR CORE

| Item | Fast zone | Thermal zone |
|---|---|---|
| Fuel material | Natural U | LEU(3% $UO_2$) |
| Fuel elements diameter, mm | 20 | 6.5 |
| Fuel density, g/cm$^3$ | 18.6 | 10.5 |
| Fuel length, mm | 1000 | 700 |
| Cladding material | Al | Zr-2 |
| Cladding diameter, mm | 22 | 8 |
| Fuel element weight, kg | 6.2 | 0.25 |

After optimized calculation a suitable fuel arrangement is given. In the fast neutron spectrum zone of Venus-1 subcritical assembly, hexagonal aluminum structure with Natural U fuel rods arranged in equilateral triangle and rod pitch being 25 mm.

In the thermal neutron spectrum zone of Venus-1 subcritical assembly, LEU fuel rods with 3% enriched U-235 are inserted in the polyethylene with fuel rods arranged in pattern of equilateral triangle. An optimized calculation fuel rod pitch is 12mm when thermal zone surrounding the fast zone exists ( $k_{eff}$ value is measured by experiment to satisfy requirement in the 0.90–0.98).

The final dimensions of Venus-1 subcritical assembly are determined: 1600mm in diameter, 1800 mm in length, and 1000 mm from the center of the core to the floor surface. The subcritical assembly is laid on a chassis, which can be moved vertically or horizontally when coupled to CPNG. The following describes the main parameters of the assembly.

The neutron source is sealed in an aluminum tube of 50mm diameter, which is vacuumed and inserted in the center hole of the subcritical assembly core. The center hole is formed by removed 7 fuel elements from the fast neutron zone. As the neutron source aluminum tube occupies only half length of the hole, 7 fuel rods of half length can be loaded into the other section of the hole.

Table 4.37 shows amounts of natural uranium fuel rods in each layer of fast neutron zone, there are 7 fuel rods of length half in the 1st to 2nd layer, there are 264 fuel rods of full length in the 3rd to 10th layer. Fig. 4.142 shows the Arrangement for neutron source zone and fast neutron zone.

TABLE 4.37. NATURAL URANIUM FUEL RODS IN EACH LAYER

| Layer | 1 | 2 | 3 | 4 | 5 | 6 | 7 | 8 | 9 | 10 |
|---|---|---|---|---|---|---|---|---|---|---|
| Fuel element | 1 | 6 | 12 | 18 | 24 | 30 | 36 | 42 | 48 | 54 |

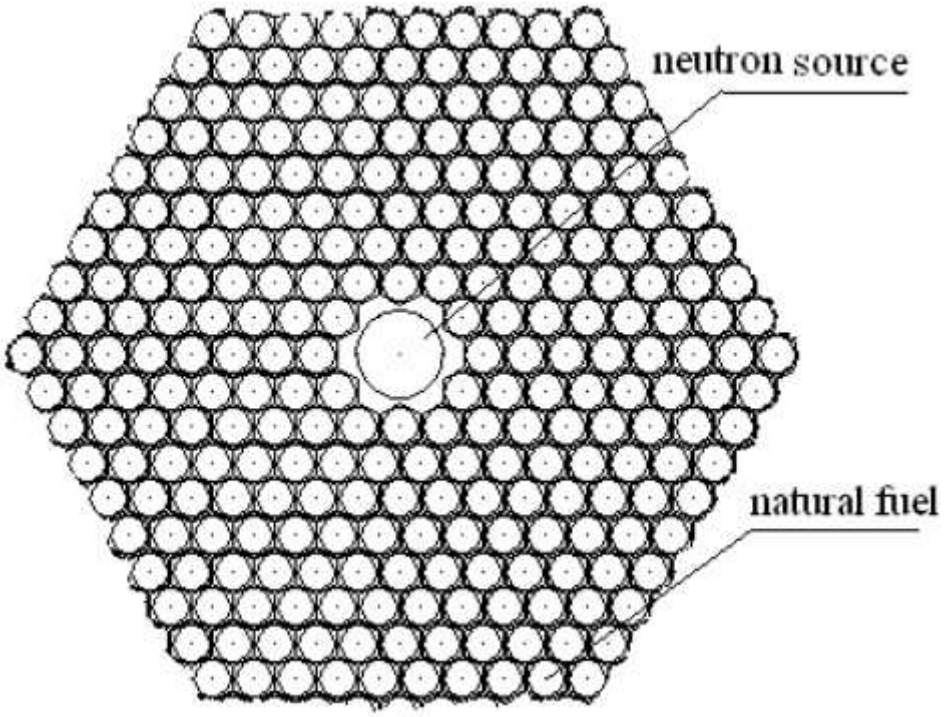


*FIG. 4.142. Arrangement for neutron source zone and fast neutron zone.*

Table 4.38 shows amounts of $UO_2$ fuel rods in each layer of thermal neutron zone, total of 2268 fuel rods can be arranged in 15 layers. The calculated efficiency of each fuel rod in the outermost layer is $1\times10^{-4}\Delta k/k$, and the final fuel loading of the thermal zone is determined through experiments.
As the core will take a quasi-cylindrical form, the amounts of fuel rods inserted in the outer three layers are less than those in the inner 11 layers of this zone.Fig. 4.143 shows the arrangement for the thermal neutron zone (local).

TABLE 4.38. [3% UO2] FUEL RODS IN EACH LAYER

| layer | 1 | 2 | 3 | 4 | 5 | 6 | 7 | 8 | 9 | 10 | 11 | 12 | 13 | 14 | 15 |
|---|---|---|---|---|---|---|---|---|---|---|---|---|---|---|---|
| Fuel elements | 126 | 132 | 138 | 144 | 150 | 156 | 162 | 168 | 174 | 180 | 186 | 174 | 156 | 126 | 96 |

The reflector zone is formed by polyethylene in approximate 220 mm thickness. Its side surface is cylindrical. The final thickness of the reflector is decided after the fuel loading of the thermal neutron zone.

The shield is a cylinder made of polyethylene with boron in thickness of 200mm. The outer shell of the assembly is a 10 mm thick stainless steel.

At present, neutrons in Venus-1 assembly are two way coupled, i.e., if aluminum plate is filled in the gap between the fast zone and the thermal zone, thermal and fast neutrons can travel to and from these two zones. If Cd or B absorber is inserted in the gap, fast neutrons can travel to and from these two zones, but thermal neutrons moderated by polyethylene in the thermal zone can not travel to the fast zone, which means neutrons in the assembly are one way coupled, hence characteristics of a reactor core with one way coupled neutrons can be studied.

Fig. 4.144 is the longitudinal section arrangement of Venus-1 assembly and Fig. 4.145 is the cross-section arrangement of Venus-1 assembly.

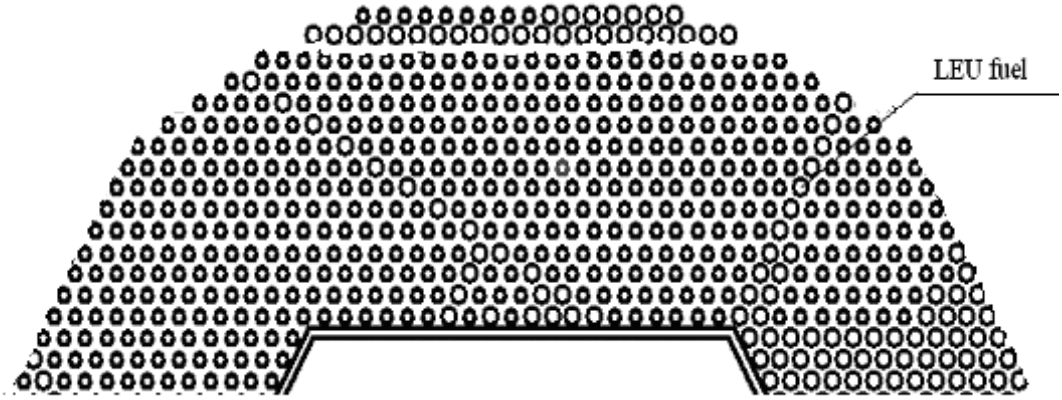


*FIG. 4.143. Arrangement for thermal neutron zone (local).*

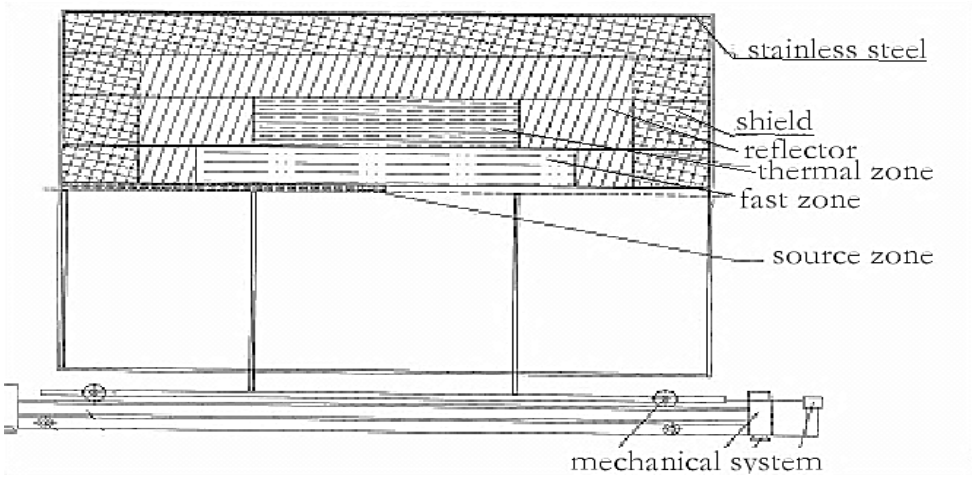


*FIG. 4.144. Longitudinal section arrangement of Venus-1 assembly.*

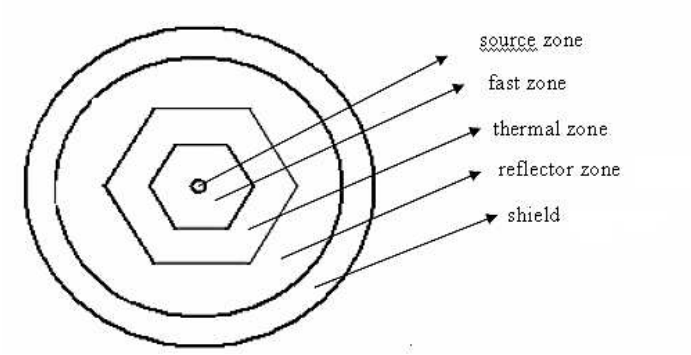


*FIG. 4.145. Cross-section arrangement of Venus-1 assembly.*

From Jan 1, 2005 to July 18, 2005, the Venus-1 subcritical assembly is installed in CIAE. Following pictures are taken during the installation and adjustment.

Fig. 4.146 shows the honeycombed hexagonal aluminum structure. Fig. 4.147 shows the saddle shaped chassis. Fig. 4.148 shows the appearance of Venus 1 subcritical assembly. Fig. 4.149 shows the appearance of Venus 1 subcritical assembly is coupled to the CPNG.

*FIG. 4.146 .Hexagonal aluminum structure.*

*FIG. 4.147. Photograph of the chassis.*

*FIG. 4.148. Photograph of Venus-1.*

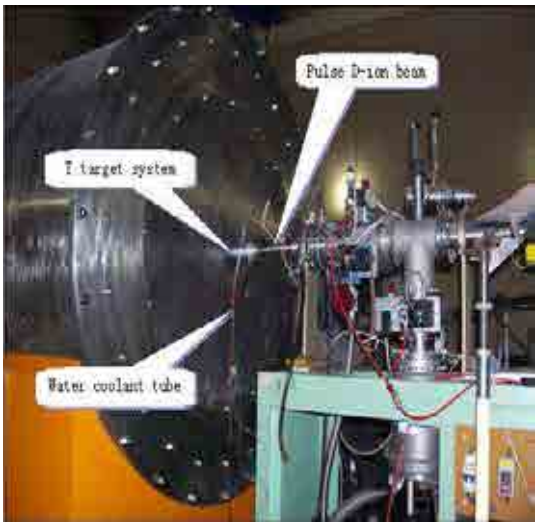


*FIG. 4.149. Venus 1 coupled to the CPNG.*

The gap between the fast zone and thermal zone is filled with polyethylene. Fig. 4.150 presents calculated neutron flux distributions with MCNP code in the fast neutron zone and the thermal neutron zone without external neutron source. Fig. 4.151 presents the calculated neutron flux distributions on the boundaries of the fast neutron zone and the thermal neutron zone without external neutron source, respectively. It is shown in these spectra that fast neutron flux is higher than thermal neutron flux in the fast zone and on its outer boundary, while in the thermal neutron zone thermal neutron flux is higher than fast neutron flux.

Table 4.39 presents the average neutron energy at different places calculated with MCNP code and TWODANT code, respectively.

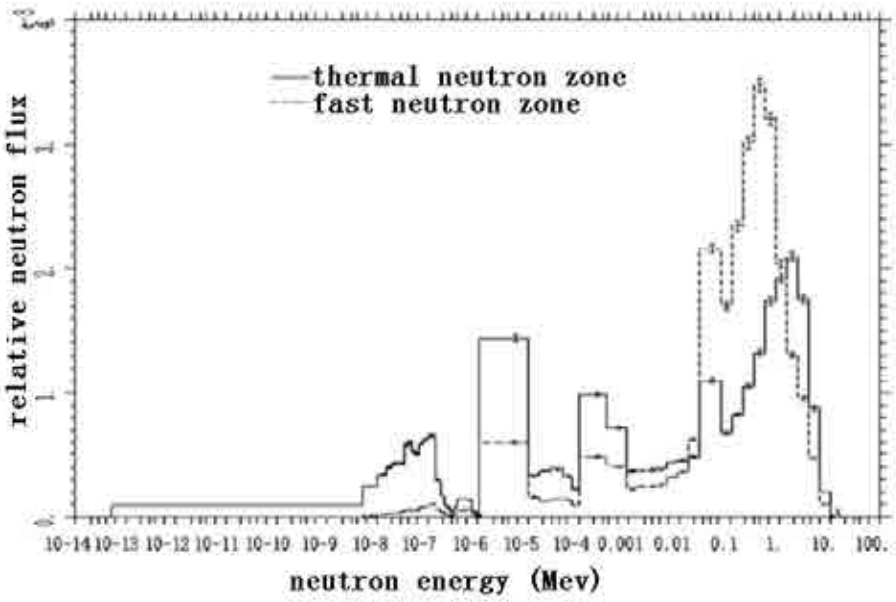


*FIG. 4.150. Calculated neutron flux distribution.*

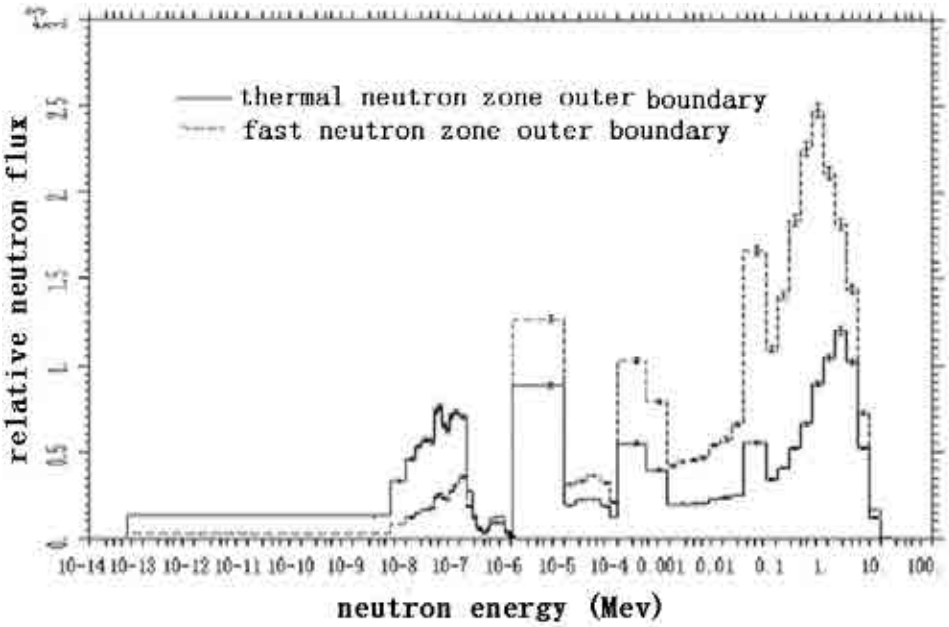


*FIG. 4.151. Calculated neutron flux distribution in different zone boundary.*

TABLE 4.39. AVERAGE NEUTRON ENERGY AT PLACES OF DIFFERENT DISTANCES

| Distance from center | cm | 4 | 15 | 21 | 26 | 31 | 36 |
|---|---|---|---|---|---|---|---|
| Average neutron energy (MCNP) | keV | 4820 | 968 | 656 | 617 | 683 | 681 |
| Average neutron energy (TWODANT) | keV | 3630 | 722 | 690 | 655 | 716 | 734 |

*4.9.2.3. Most important results*

On July 18, 2005, the first fuel element was loaded into Venus-1 subcritical assembly and the following experiments were subsequently conducted: subcriticality determination, neutron importance

relative distribution of external source, thermal neutron flux distribution in fast zone, neutron count changing with the loading, effect of the external neutron source with different energies, prompt neutron decay constant in the different point of the core and so on.

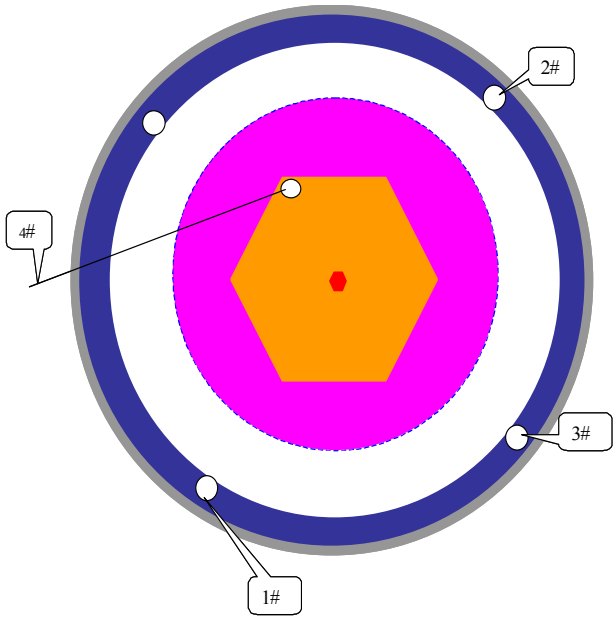


*FIG. 4.152. 1#, 2#, 3# and 4# neutron detectors position.*

During the experiment, detectors were placed at the outer of polyethylene reflector and in the outer layers of the fast zone respectively, as is shown in Fig. 4.154.

The detectors are 3He counter with dimensions of Ø10×150mm as 1# and 4# detector, two BF3 counter of Ø65×780mm as 2# and 3# detectors, they were used for inverse multiplication measurement (critical approach). 4# detector was used for neutron counts vs. loading in different neutron source.

(a) Subcriticality determination—extrapolating criticality

The total fuel element loading of Venus-1 subcritical assembly was determined by the experiment of source multiplication method [4.198] (i.e. inverse multiplication measurement). An Am-Be steady neutron source was used in the experiment.

Fuel rod is one by one loaded in to core in extrapolating criticality experiment. The determined final loading of fuel rod for Venus-1 ADS subcritical assembly is 264 rods+7 half rods of natural uranium fuel in the fast zone and 2046 rods of 3% enriched U-235 in the thermal zone.

As the efficiency of a fuel rod in the outmost layer of the thermal zone is 0.0001, $k_{eff}$ of the assembly with and without end reflector was obtained through the difference between the extrapolated critical loading (2312 or 2333 rods in the thermal zone with or without end reflector) and the actual loading (2046 rods in the thermal zone), which was 0.9741 or 0.9721. It seemed that the efficiency of the end reflector (~ 0.0020) was somewhat small. Accurate $k_{eff}$ values of the above two loadings are planed to measure by other methods in the future.

(b) Neutron importance relative distribution of external source

Table 4.40 shows neutron importance relative distribution of external source in different position of core. To measure the relative importance of external source neutron, an Am-Be steady neutron source was placed at different axial positions along the central hole. The distance of these positions to the center point are 0 cm, 17.5cm, 35.0cm, 50.0cm, 60.0cm along axial respectively. It can be seen that the position of 50.0cm from center point is at the boundary of the fast zone, while the position of

60.0cm is outside of the boundary. The neutron counts are measured with $^{3}He$ proportional counters and normalized to give the relative importance of the external neutron source.

TABLE 4.40. RELATIVE IMPORTANCE OF EXTERNAL SOURCE NEUTRON

| External source location (cm) | 0 | 17.5 | 35 | 50 | 60 |
|---|---|---|---|---|---|
| Relative importance | 1.000 | 0.847±0.005 | 0.486±0.045 | 0.168±0.017 | 0.055±0.010 |

### 4.9.3. The various programmes within the EU

#### *4.9.3.1. Introduction*

Partitioning and transmutation aims at reducing the amount of minor actinides, and thus the radiotoxicity of the high level waste going to disposal. One way to handle minor actinides is to concentrate them in a specific stratum using systems which are dedicated to transmutation. The subcritical systems known as hybrid systems or Accelerator Driven Systems (ADS) are able to burn these actinides at a high level of concentration in the core. The development of ADS for radioactive waste transmutation is envisaged from the mid-1990s in a European context under the encouragement of Professor Carlo Rubbia. This development aims at placing the role of ADS within a double strata fuel cycle strategy. The roadmap [4.199] includes several years of R&D on the acquisition of the physical and technological data needed for the operation of a fast neutron ADS. During the 5th Framework programme, from 2000 to 2004, the MUSE experiments were realized in the MASURCA facility (Fig. 4.153) of the CEA-CADARACHE. After MUSE, and in the frame of the 6th Framework programme running now, researches in this domain are mainly focused on five topics:

*FIG. 4.153. Bottom view of MASURCA core.*

— Qualification of subcriticality monitoring;

— Validation of the core power-beam current relationship;

— Startup and shutdown procedures, instrumentation validation and specific dedicated experimentation;

— Interpretation and validation of experimental data, benchmarking and code validation activities;

— Safety and licensing issues of different components and for the integrated system.

New experiments named: RACE-T in the TRIGA reactor of ENEA-CASACCIA, RACE-LP-IAC in the subcritical assembly of the Idaho Accelerator Center in US, YALINA in the subcritical assembly of MINSK in BELARUS, and the new proposal GUINEVERE in the VENUS reactor of SCK•CEN are supported. On following, after the recall of the MUSE main results, the outlines of these experiments and the main results when available are reported.

#### *4.9.3.2. The MUSE results*

The main topics of the MUSE programme were:

— Defining subcritical experimental configurations of interest (in terms of fuel, geometric arrangement, external source type and operating modes);

— Developing new specific experimental techniques mainly in support to the operation of subcritical systems, but also for standard integral parameters to obtain a wide range of experimental results to define accurate experimental uncertainties;

— Experimentally characterizing these configurations (in terms of reactivity level and neutron spectra) by integral experiments using standard or new experimental techniques;

— Analyzing these experimental results by use of different nuclear data files and calculation methods (deterministic and Monte Carlo tools) with the objective of evaluating the performances of current neutronic code systems and to contribute to the definition of reference calculation routes (including nuclear data and calculation tools) for the neutronic predictions of an ADS;

— Proposing new strategies allowing the determination of the reactivity level of subcritical configurations without the need of a critical configuration.

The MUSE cores (2001–2004) are based on a basic fuel cell, composed of two Mox rodlets for two sodium rodlets, representative of a fast Pu burner core (Pu enrichment of 25% with 18% content of 240 Pu) with sodium coolant. This pattern is reproduced sixteen times in each fuel subassembly (FIG. 4.154. Radial cuts of the fuel and reflector assemblies). The fuel zone is radially and axially reflected by a stainless steel–sodium (75%–25%) shielding. The fuel zone is radially and axially reflected by a stainless steel–sodium (75%–25%) shielding.

The GENEPI (see the description later on) deuteron guide was horizontally introduced at the core midplane and the deuterium or tritium target will be located at the core centre (see Fig. 4.155). To compensate the spatial effect due to the presence of the GENEPI guide in the north part of the loading, the south symmetrical part was loaded with pure lead (99.99% of Pb) simulating the Pb circulation of the target. To simulate the physical presence of a Pb spallation source, a pure square (10 cm thick) lead zone is placed around the GENEPI target. Full details of these configurations and the materials used are reported in [4.200].

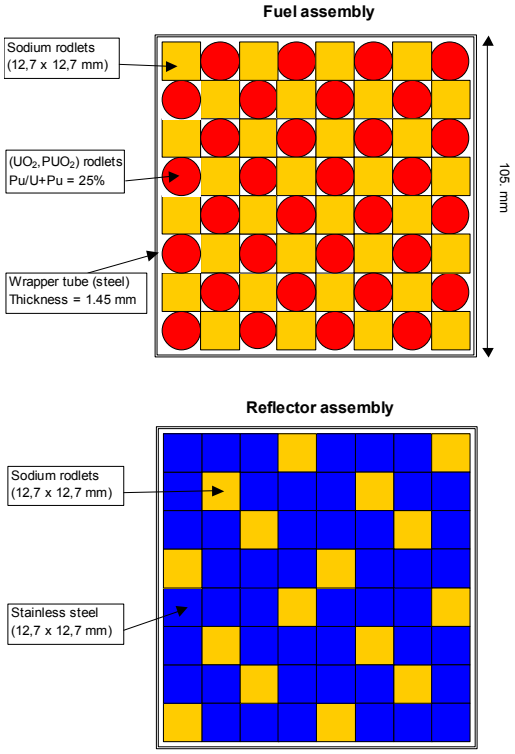


*FIG. 4.154. Radial cuts of the fuel and reflector assemblies.*

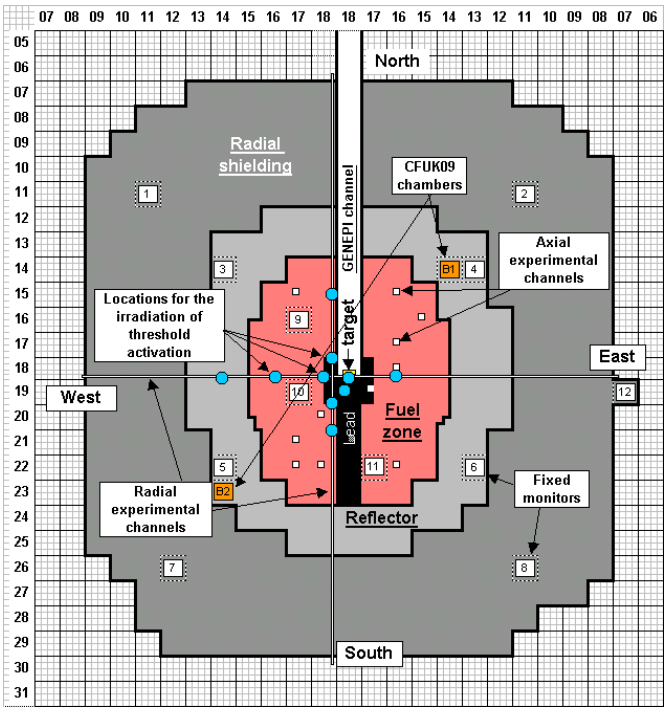


*FIG. 4.155 .Radial cut of the MUSE critical configuration.*

An intense variable external neutron source was used to simulate the spallation source supposed to be used in an ADS. A specific pulsed deuteron accelerator, GENEPI (GEnérateur de NEutrons Pulsés Intense), was specifically designed and realized by CNRS [4.201]. GENEPI produces neutrons by the $D(d,n)^3He$ (deuteron–deuterium) or $T(d,n)^4He$ (deuteron–tritium) nuclear fusion reactions on different targets. The simulation of the spallation source is approached by the lead buffer surrounding the targets, where (n,2n) reactions can occur.

A schematic description is given Fig. 4.156 presenting the GENEPI implantation in the MASURCA facility. In the 250 kV High Voltage Head, the deuterium atoms are ionised by an arc discharge using a hot filament and form a plasma into the 'duoplasmatron' source. The discharge is triggered by an auxiliary electrode at a rate ranging from 10 Hz up to 4,7 kHz and its duration is determined by an LC delay line. The ions are then extracted and focused creating a deuterons ($D^+$) beam. This beam is accelerated up to 250 kV maximum (3) and deviated by a 45° magnet (5) in order to select the $D^+$ ions (and remove the molecular $D^{++}$). This deviation is also necessary for first allowing GENEPI to enter in the MASURCA accelerator room and second for the withdrawal of the thimble of GENEPI introduced into the core. Indeed, the thimble is movable and is inserted into a channel dug along the North–South direction inside MASURCA core tubes.

The deuteron beam is transported over the 5 m beam line and focused by magnetic and electrostatic quadrupoles all along its trajectory. Magnetic and electrostatic Steerers associated to diagnostics finely adjust the beam position down to the copper target (49 mm diameter) supporting a TiT or TiD deposit (30 mm diameter). The mass of tritium or deuterium deposit is about 1.2 mg/cm$^2$, which corresponds to about a 12 Curies tritium activity.

A FARADAY cage surrounds the GENEPI design in order to avoid the electromagnetic interferences in case of sparking. Local and remote control of the accelerator is provided through a dedicated software, 'LABWINDOWS', and specific embedded PC cards.

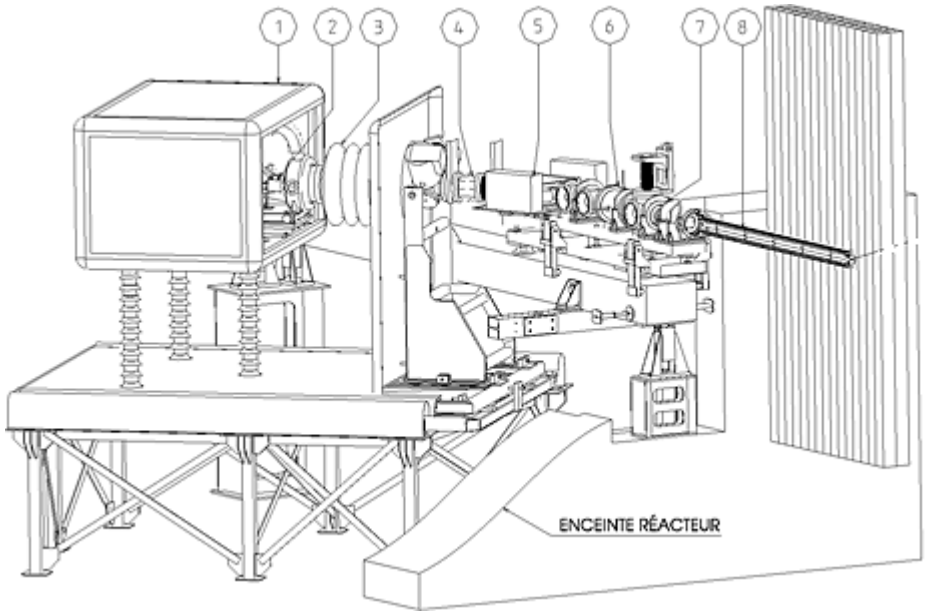


1) High Voltge Head
2) duoplasmatron
3) accelerator tube
4) quad Q1
5) magnet
6) quad Q2
7) quad Q3
8) quad Q4 +

*FIG. 4.156. GENEPI implantation in the MASURCA facility.*

The GENEPI performances are summarized in the Table 4.41.

TABLE 4.41. GENEPI BEAM CHARACTERISTICS

| | |
|---|---|
| Beam energy (keV) | 140–240 |
| Peak current (mA) | 50–60 |
| Repetition rate (Hz) | 10–4700 |
| Minimum pulse duration (10–9 s) (at mid height signal) for the target current signal | 500–00 |
| Minimum pulse duration (10–9 s) (at mid height signal) for the neutrons pulse signal ( detector) | 400–500 |
| Mean beam current (μA) ) (to be divided by 1.6 for an effective value) | 150 (for a duty cycle of 4700 Hz) |
| Spot size diameter (mm) | ≈ 25 mm |
| Pulses reproducibility | Fluctuations at 1% level |

The first coupling between MASURCA core and the GENEPI neutron generator happened on November 2001. A series of preliminary measurements in slight sub-critical configurations ( $k_{eff}$=0.995) was performed at the beginning of the year 2002 to get not only first results but, to have also a feedback on experimental conditions necessary to improve and optimize measurements in the following phases.

Then, the full characterization of the reference critical configuration was achieved from April to June 2002 it exists a well established reference measurement point. This programme included importance traverses using a $^{252}$Cf source, foil irradiations, spectral indices and numerous axial and radial traverses of fission rates. Rod-drop experiments and measurements of kinetic parameters have been also achieved in view to determine reference reactivity levels.

The study of sub-critical states restarted at the beginning of October 2002 with the investigation of the SC0 clean core configuration using neutron external sources provided by D(d,n)$^3$He and T(d,n)$^4$He on both TiD and TiT targets. This measurement phase ended on March 2003, configurations with reactivity levels more representative of an industrial ADS were studied later on: SC2 configuration

($k_{eff}$ around 0.97) from April to July 2003, SC3 configuration with a $k_{eff}$ around 0.956 representative of the sub-criticality level at the end oflife. A last configuration for simulating a core partially cooled by lead was studied during the year 2004.

Static measurements have been performed with and without external neutron sources to study the physics of such cores and notably to characterize the neutron spectrum variations and the fission rate relative distribution changes in zones of interest. PNS (Pulsed Neutron Source) and SJ (Source Jerk) techniques, the transfer function method as well as noise methods like Rossi-α and Feynman-α have been greatly applied in order to determinate the prompt decay constant, kinetic parameters and finally the reactivity of such configurations.

Concerning the subcriticality techniques, among the major conclusions of the MUSE-4 experiments [4.194][4.202], the common agreement is the following:

— Demonstration is done that it is possible to determine the reactivity of a subcritical system without the need of a critical reference.

— In a multiple regions system, there is a complicated distribution of flux in space and energy and the time evolution of a pulse is difficult to predict.

— Because of the characteristics of the GENEPI accelerator, MUSE couldn't provide results concerning the on-line monitoring.

— The consistency between MSM method and other subcriticality techniques should be verified one more time. This will be done during the GUINEVERE programme.

The detailed analysis of the MUSE experimental results [4.203] is summarized in the Table 4.42 (Reactivity in dollars and standard error in percent):

TABLE 4.42. MUSE EXPERIMENTAL RESULTS

| Configration | MSA | PNS-F | | | Kp | PNS-A | SJ-Cf | MOD | Rossi-α |
|---|---|---|---|---|---|---|---|---|---|
| | | 1 | 2 | 3 | | | | | |
| SC0 | -1.9 | -1.93 | -1.9 | --- | -2.2 | -2.0 | -1.92 | -1.96 | -2.04 |
| | (4.7) | (1.6) | (0.3) | --- | (15.0) | (1.0) | (5.2) | (0.2) | (6.9) |
| SC2 | -9.1 | --- | --- | -8.7 | --- | -8.9 | --- | --- | -8.8 |
| (1006 cells) | (5.5) | --- | --- | (8.0) | --- | (3.4) | --- | --- | (2.2) |
| SC2 | -9.7 | --- | --- | --- | -9.6 | --- | --- | -9.23 | --- |
| (1004 cells) | (5.2) | --- | --- | --- | (3.1) | --- | --- | (1.3) | --- |
| SC3 | -14.1 | --- | 15.6 | -11.7 | -14.2 | -13.7 | -14.6 | --- | -13.4 |
| | (5.7) | --- | (3.8) | (7.7) | (2.1) | (3.6) | (6.2) | --- | (3.7) |

In the table, the reactivities are given in dollar units ($\beta_{eff}$ for MUSE is approximately 335 pcm; 1 pcm is $10^{-5}$ Δk/k), while the standard errors are in percent. The MSM column gives the results of source multiplication with a rod-drop giving conventionally the reference reactivity. The columns of PNS-F give the PNS exponential fitting results using 1, 2, or 3 exponentials reflecting the non-point kinetic behaviour of the MUSE system.

The Kp method makes use of the fact that the time behaviour of the pulse decay in the reflected MUSE configuration can be explained by assuming a spread in the effective generation time. SJ-Cf is the standard source jerk using a Cf source, and MOD is a method developed to estimate the reactivity based on running the neutron generator at different frequencies.

The Rossi-α method uses the correlation of detector events to deduce the fission chain decay curve, which is related to the reactivity, generation time and β analogous to a PNS decay curve. In these

Rossi-α results the areas under the deduced decay curves were analyzed in a manner similar to the PNS area method (PNS-A). The effort for the next programme GUINEVERE will consist in looking after a better consistency for the MSA-MSM method during the overall programme. It will be looked at the effect on the prompt neutron decay curve coming from the lead reflector. The analysis of the uncertainties concerning bias and discrepancies of the different techniques will be under way. During this programme (fast uranium core, lead cooled type), the importance of the lead will be increased in comparison with MUSE (fast MOX core, sodium cooled type) that was in the last phase only partially loaded with lead. And the major new prospect of the GUINEVERE experiments will be the use of a continuous beam to monitor the power and the reactivity measurements.

#### *4.9.3.3. The RACE experiments at low power*

The RACE experiments at Low Power were operated until 2006 in two different facilities: the TRIGA reactor of the ENEA-CASACCIA (Fig. 4.157) named 'RACE-T' and the RACE subcritical assembly of the Idaho Accelerator Center (Fig. 4.158) named 'RACE-LP/IAC'.

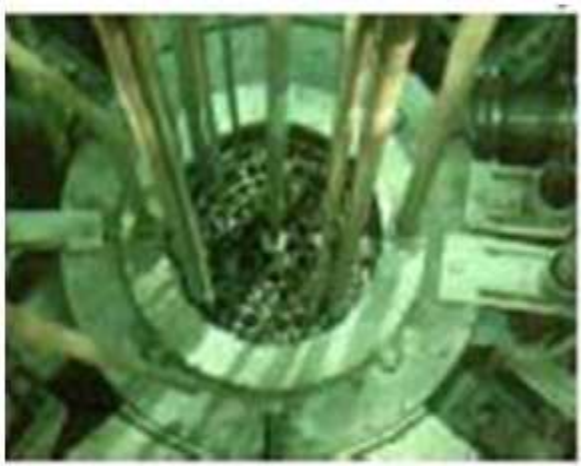

*FIG. 4.157. View of the TRIGA CASACCIA.*

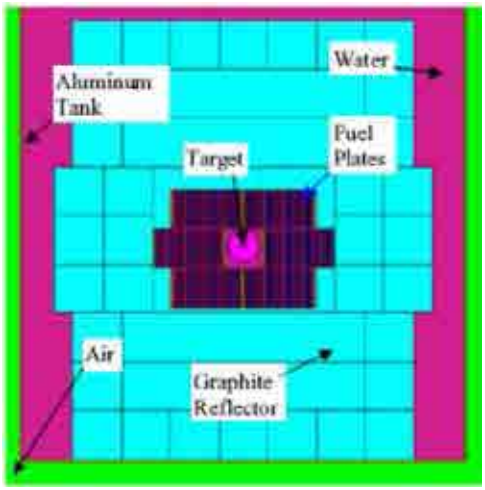


*FIG. 4.158. Cross-section of the ISU/RACE subassembly.*

In RACE-T [4.204], a wide range of subcriticality levels could be explored to validate experimental techniques and provide significant results on the subcritical monitoring, thanks to the ~$10^8$n/s (D,T) neutron generator. The validation of these techniques are also made by comparing systematically the results obtained with the reference method used in critical core which is the Multiplication of Source Method (MSM). This method can provide a precise and reliable measurement of the subcriticality for all the configurations of the system. Preliminary tests of instrumentation and techniques are also performed during this programme: Piccolo-Micromegas detector; X-mode advanced acquisition system for ADS.
This experimental campaign took an end at the beginning of 2006 and resulting to a reduction of the uncertainties and coherence among the methods: Source Multiplication, Rod-Drop, Source-Jerk techniques, Pulsed Neutron Source.

The first experiment of the RACE project has been performed at the Idaho Accelerator Centre of the Idaho State University (ISU-IAC). The core of the ISU RACE subcritical assembly is constructed of 6 modular aluminum trays each containing 25 flat plates of 20% enriched uranium–aluminum alloy with aluminium-clad. Each fuel plate is 0.2032 cm thick 7.62 cm wide and 66.0 cm long. These are total 7615 grams of uranium in the full core configuration: with 1510 grams being U-235. The subcritical assembly is surrounded by a graphite reflector and water inside an aluminum tank that is ~1 m (see cross-section above). The $k_{eff}$ of a such subassembly is typically in the range of 0.90.

The current ISU RACE target is a 2.75 inch diameter, 3.5 inch long cylinder made from 75% of W and 25% Cu. A series of calculations show that the neutron yield of the bare target is not really

sensitive to the target geometry as long as it is big than certain size that practical designs normally do. This can be explained by the flux profile of electrons, photons and neutrons in the target. As it can be calculated, most of the electrons are distributed very close to where the electron beam impinged, while the bremsstrahlung photons can travel further into the target and photo-neutrons can apparently penetrate even deeper into the target. However, the high flux regions are mostly populated in the adjacent area of the target end connecting to the accelerator beam port since majority of the photo-nuclear reactions are taking place there. Also, most of the energy deposited are from photon interactions, thus the energy deposition profile is very similar to photon flux profile. For the incident electron at 25 MeV, each source electron will deposit about 11.40 MeV energy in the target through bremsstrahlung photon and neutron scattering interactions, hence, about 45.6% of beam power is dissipated by the target.

In the first phase of the RACE-LP/IAC experiment [4.205], it was paid attention to the characterization of the electron beam and of the neutrons produced by different targets: W-Cu, lead and uranium. The order of magnitude of the neutrons source is here ~ $10^9$n/s. The power of the subcritical system was checked and a first test of reactivity measurements at beam trip was performed.

### 4.9.4. India

#### *4.9.4.1. Reactor physics and core design issues*

(a) Reactor R&D and technology

In ADS, since reactor control system is not required to maintain criticality, it is possible to increase burnup i.e. to extract more energy from a given mass of fuel till such time that the $k_{eff}$ of the system falls to a value below which it is no more economical to maintain the fission power merely by increasing accelerator current. An interesting argument in support of ADS-based thorium utilization emanates from possibility of starting such reactor without a seed fissile species. On the basis to these possibilities, development of calculation codes and some investigative simulations of ADS operation with them were carried out, which are presented in the following section.

#### *4.9.4.2. R&D activities in reactor physics of ADS at BARC*

(a) Computer codes for ADS analysis

New approach to reactor physics analysis of ADS core is dictated by many of its functional differences over the conventional reactor. The absolute fission power and its distribution in ADS are sensitive to the value of multiplication factor ($k$). This imposes restrictions on the error in estimation of $k_{eff}$ that may be tolerated throughout the burnup cycle. Since, ADS is meant for higher fuel burnup, lumping of fission product (FP) may not be a correct process and explicit calculation for concentrations of a large number of fission products becomes necessary. Moreover, treatment of interaction of the high energy proton beam with target (spallation) to estimate number and distribution of neutrons, spallation products and heat distribution in the target requires special calculation tools and methods.

For analysis of high energy proton interactions in spallation region of the target, we use particle transport codes FLUKA and CASCADE. For the low energy neutrons in blanket (reactor core) region, we have developed simulation codes McBurn and BURNTRAN [4.206] [4.207] for carrying out fuel burnup simulations based on the Monte Carlo method and the multi group transport theory method respectively. Interfacing of the high energy code CASCADE with McBurn has already been carried out. So, these programmes can be run together. The codes are functional for fixed fuel (one batch fueling), and are being used for evaluating some interesting ADS concepts as discussed later. Further development of McBurn is being carried out to include fueling operations (insertion, removal, or shuffling of fuel assemblies).

(b) McBurn: A continuous energy Monte Carlo burnup code

In this computer code, the region of interest (or the entire reactor core) is divided into a suitable number of burnup zones. McBurn works in tandem with a MC code, where the MC code calculates the reaction rates in each burnup zone at any instant of time while McBurn solves the burnup equations using the reaction rates thus computed. About 300 actinide and fission products can be considered for the following nuclear reactions: neutron capture, fission, n2n, alpha–beta decay. Burnup with energy (thermal, fast and high) dependent fission yields are taken from a recent table of T. R. England numerical integration of the burnup equations over a time step is carried out using Gears method, which is suitable for a system of stiff equations. Within a burnup zone and during a burnup step, the reaction rates, per atom of any species, are assumed to be, constant.

Validation of the code has been carried out by (i) study of the IAEA ADS benchmark (fast system) and (ii) cell level burnup of 19 rod U and Th cluster used in Indian 220 MW PHWRs previously studied by other codes.

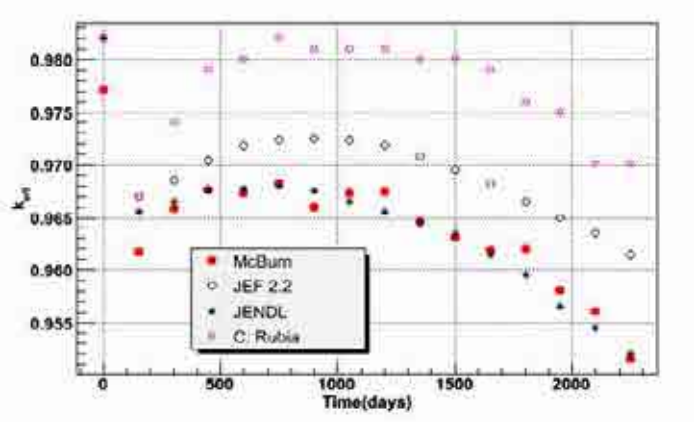


*FIG. 4.159. McBurn calculation.*

Fig. 4.159 shows how the results compare with those obtained by other participants of the benchmark exercise using different codes and nuclear data. Our results fall within the same band. However, the overall spread in the results is fairly large and it is not possible at this stage to resolve the differences and ascertain the causes.

The $k_\infty$ for the PHWR lattice cell with 19 rod Th fuel cluster is shown in adjacent Fig. 4.160 and compares well with CLUB, the maximum difference being about 0.004.

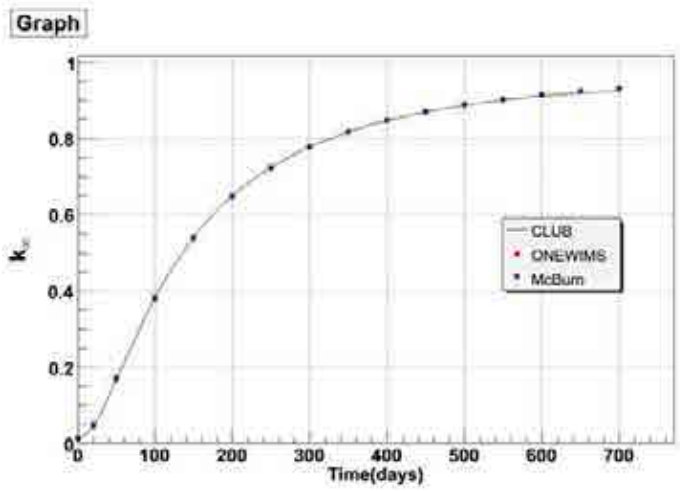


*FIG. 4.160. k∞ for the PHWR lattice cell with 19 rod Th fuel cluster.*

(c) BURNTRAN: A Transport theory burnup code

The code package BURNTRAN consists of a burnup module BURN, developed by us, and the one and two dimensional multi group discrete ordinates codes DTF [4.208] and ATRAN [4.209], and a 172-group WIMS neutron data library. A number of modifications were carried out in the transport theory modules. As discussed in the case of McBurn, the region of interest is divided into several burnup zones and the transport theory codes provide the necessary reaction rates. The burnup module is based on Gear's method for integrating a system of stiff differential equations. The code package BURNTRAN will be quite useful for quick investigative studies of various ADS configurations. Highly detailed and (time consuming) Monte Carlo burnup computations need to be undertaken only at the final design stage.

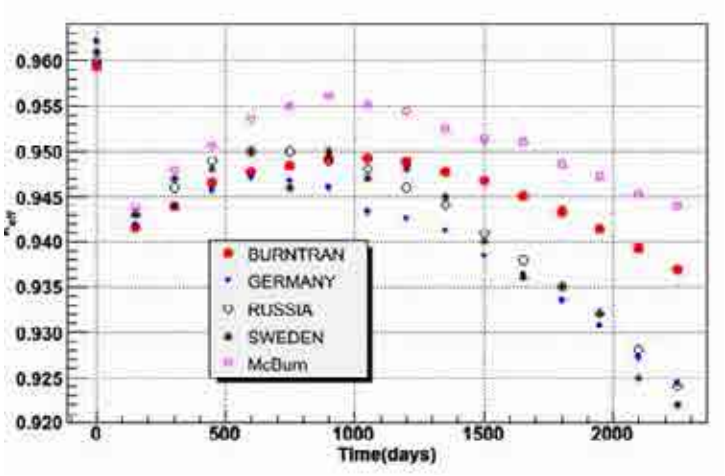


*FIG. 4.161. Burtran results.*

Validation of this code has been done by studying ADS benchmarks and 19 rod and 37 rod PHWR clusters and comparing the results with other codes. Some of the results of this exercise are shown in Table 4.43 and Fig. 4.161 We again observe that while PHWR lattices involving 19 rod Th and 37 rod U are predicted well, due to the large spread in the results of the ADS benchmark exercise; it is difficult to draw any definite conclusions.

TABLE 4.43. INTER COMPARISON OF IMPORTANT PARAMETERS OBTAINED BY BURNTRAN AND BY VARIOUS OTHER PARTICIPANTS FOR THE IAEA PHWR BENCHMARK [258]

| Burnup (MWd/t) | Code /participant | $k_{iff}$ | $U^{235}$ (%) | $Pu^{239}$ | Reactivity (mk) | |
|---|---|---|---|---|---|---|
| | | | | | Void | Doppler |
| 0 | CLUB | 1.1150 | 0.7114 | --- | 15.97 | 5.58 |
| | WIMS (Arg.) | 1.1155 | 0.7110 | --- | 16.82 | 5.78 |
| | BURNTRAN | 1.1154 | 0.7113 | --- | 15.17 | 5.27 |
| 4000 | CLUB | 1.0413 | 0.3796 | 1.931 | 13.51 | 2.81 |
| | WIMS (Arg.) | 1.0456 | 0.3837 | 1.979 | 13.76 | 2.03 |
| | BURNTRAN | 1.0411 | 0.3813 | 1.932 | 12.96 | 1.29 |
| 8000 | CLUB | 0.9749 | 0.2020 | 2.490 | 13.66 | 1.88 |

| | | | | | |
|---|---|---|---|---|---|
| WIMS (Arg.) | 0.9777 | 0.2073 | 2.539 | 13.72 | 0.37 |
| BURNTRAN | 0.9762 | 0.2059 | 2.496 | 13.27 | 0.67 |

(d) Theoretical studies on reactor noise in ADS

Reactor Noise methods have long been used for measuring reactor kinetics parameters in low power critical and sub-critical reactors. The interest in accelerator driven sub-critical systems (ADS) and the necessity of measuring-monitoring their degree of sub-criticality has created a renewed interest in these methods. At a theoretical level, we believe, that the principal difference between ADS and critical reactor noise is due to the accelerator characteristics. Some of the accelerators used for experimental purposes could actually be pulsed accelerators operating at pulse rates ranging from a few Hz to kilo-Hz. Even the so called continuous (CW) accelerators produce protons in sharp bursts at a frequency related with the RF frequency driving the system. Apart from pulsing, the noise characteristics of the ADS source will be non-Poisson. As such, a fundamentally different theoretical approach for deriving mathematical expressions for the noise descriptors, than that used in various noise-based experimental measurement techniques, is necessary.

We have developed such a theoretical approach and have derived formulas for interpreting some of the classical noise methods such as Rossi alpha, the variance to mean, auto (and cross) correlation functions and (auto & cross) power spectral density, as well as some recently proposed methods such as the cross power spectral density between the proton current and the neutron detector signals for systems driven by periodically pulsed non-Poisson sources having a large multiplicity. It was shown that the rather high contribution due to the large multiplicity of the accelerator driven source to the variance (or any other measure of the noise) is significantly different for a periodically pulsed source as compared to that for Poisson source events.

In particular, it was shown that the periodic source cannot, generally speaking, be considered as a random source with a periodically modulated intensity. We have further elucidated the noise character of the ADS neutron source[4.210] by describing it as a doubly stochastic Poisson point process, in which the proton beam current is described as an exponentially correlated Gaussian process. This description has the added advantage that it permits treatment of pulses of finite width as against the delta function pulses in our earlier formulation. Experimental evidence from measurements of accelerator beam current statistics in published literature seems to support such a description. Using such a description we have re-derived expressions for various noise descriptors. One consequence of our studies on noise would be that it might be necessary to interpret ADS noise experiments using the newly derived formulas.

### 4.9.5. The TRADE core neutronics in Italy

The TRADE (TRiga Accelerator Driven Experiment) programme [4.211], which was foreseen in RC-1 TRIGA reactor located at ENEA-Casaccia research centre near Rome, was planned to investigate the static and dynamic behaviour of ADS at power in thermal neutron spectrum. Because problems in financial backing, the programme has been interrupted at the end of 2004.

The experiment, consisting in the coupling of an external proton accelerator to a target to be installed in the central channel of the reactor core loaded in subcritical configurations, aimed to explore experimentally the transition from an external source dominated regime to a core thermal feedback dominated regime. This transition is relevant, in particular to understand the dynamic behaviour of ADS, which, in the future full scale demonstrations of transmutation, could have both a very low βeff and very low Doppler reactivity effect.

The spallation target consisted of solid tungsten. The target had to be hosted in the central thimble, usually used for high neutron flux irradiation. The target performances were limited by the geometry

of the irradiation channel: notwithstanding an adequate power (few tens kW up to 50÷80 kW) was possible to be achieved in the target.

A core power of several hundreds kW was needed in order to explore the dynamics, reactivity control and power monitoring in an ADS, in the subcriticality range ranging from source dominated to reactor feedback dominated regime, e.g. from $k$=0.9 to $k$=0.99 or more. The use of protons of about 100 MeV was suggested by considerations on maximum power (which can be evacuated in the solid tungsten target), accelerator cost and minimum size of the bending magnets needed to introduce the beam inside the core. With these parameters (i.e. about 500 kW in the core, 50 ÷80 kW in the target, subcriticality as low as $k$ = 0.9 and proton energy Ep = 100 MeV), one has the requirement for a maximum proton current value of about 500 μA.

The present section gives some results about the neutronics of some selected configurations. Monte Carlo simulation codes were used [4.212] [4.213] at CERN, and MCNP-4C [4.214] at ENEA for static and burnup-evolution analyses. A simple tool, obtained by coupling a core channel time dependent thermalhydraulics code with a neutron point kinetics code, was used to perform some preliminary dynamic analyses [4.215].

### *4.9.5.1. General characteristics of the NOMINAL TRIGA core*

The TRIGA core consists of an annular structure immersed in water, which serves as primary coolant. The core is arranged in a honeycomb like array forming an annulus with six coaxial cylindrical rings of fuel elements (Fig. 4.162).

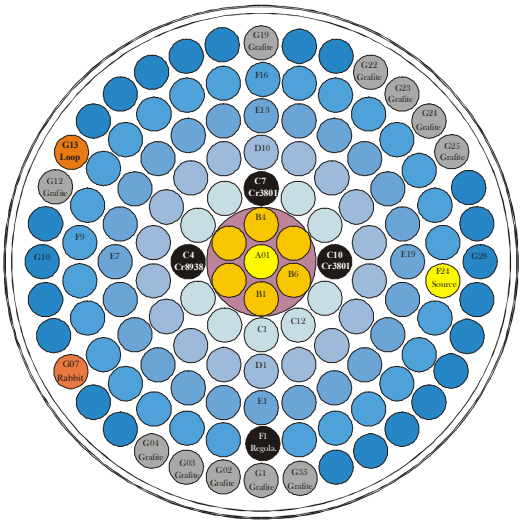


*FIG. 4.162. Schematic view of the TRIGA core.*

The core, which is surrounded by the graphite reflector, consists of a lattice of fuel elements, graphite dummy elements, control and regulation rods. There are 127 channels divided in seven concentric rings (from 1 to 36 channels per ring). The channels are loaded with fuel rods (blue elements in Fig. 4.166), regulation and control rods (black elements in the figure) depending on the power level required, graphite dummies (grey elements) and a central thimble for high flux irradiations (element A01), plus supplementary experimental channels. The diameter of the core is about 56.5 cm while the height is 72 cm. Neutron reflection is provided by graphite contained in an aluminium container, which is surrounded by 5 cm of lead acting as a thermal shield. The reactor core is cooled by natural convention of the water in the reactor pool.The fuel element has an external diameter of 3.73 cm (clad included) and a total height of 72 cm (Fig. 4.163).

*FIG. 4.163. Fuel rod section (scale 1:5).*

The fuel is a cylinder (38.1 cm high, 3.63 cm in diameter) of uranium–zirconium–hydrogen ternary alloy (1.7:1 H/Zr atom ratio and 8.5 wt% of Uranium 20 wt% enriched in 235U) with a metallic zirconium rod inside. There are two graphite cylinders at the top and bottom of the fuel rod. The regulation rod has the same morphological aspect as the fuel rod, with the exception that the fuel is replaced by the absorber (graphite with powdered boron carbide). The control rods are fuel followed with geometry similar to that of the regulation rod.

### *4.9.5.2. Fuel rods and control rods reactivity worth*

The analyses aimed to draw a first picture about the modularity of the TRIGA reactor concerning different fuel rod (FR) subcritical configurations and control rod (CR) arrangements. The nominal (reference) configuration for the analyses (Fig. 4.162) was characterized by the central thimble (that should host the target), 108 FR and 3 CR. Table 4.44 shows the results concerning different hypothesis about the fuel loading and the CR insertion level and positions. In particular, the following situations were taken into account with respect to the nominal configuration: concerning FR, no ring B in the core (shadowed central zone in Fig. 4.162), with water replacing fuel, and no rings B and G in the core, with fuel in ring G replaced by graphite elements; concerning CR, elements were positioned in ring C, as in the nominal configuration, or positioned in ring D, with different insertion levels (critical relative to the nominal loading, completely withdrawn or fully inserted).

TABLE 4.44. FR AND CR REACTIVITY WORTH

(↔ = CR at critical insertion for the nominal fuel loading,
↑ = CR completely withdrawn, ↓= CR fully inserted)

| Fuel rods loading | Control rods insertion level and position | 20 W | | 200 kW | | 500 kW | |
|---|---|---|---|---|---|---|---|
| | | Δk/k (pcm) | | Δk/k (pcm) | | Δk/k (pcm) | |
| | | To criticality | CR worth | To criticality | CR worth | To criticality | CR worth |
| Nominal | ↑ in ring C | + 4390 | -8280 | + 3800 | -8280 | + 2950 | -8280 |
| | ↓ in ring C | -4250 | | -4790 | | -5570 | |
| Without ring B | ↔ in ring C | -4630 | | -4860 | | -5030 | |
| | ↑ in ring C | -1360 | -6440 | -2070 | -6440 | -2740 | -6440 |
| | ↓ in ring C | -7710 | | -8380 | | -9000 | |
| | ↑ in ring D | -1360 | -6660 | -2070 | -6660 | -2740 | -6660 |
| | ↓ in ring D | -7930 | | -8590 | | -9220 | |
| Without rings B and G | ↔ in ring C | -9040 | | -9070 | | -9120 | |
| | ↑ in ring C | -4180 | -8060 | -5800 | -8060 | -6580 | -8060 |
| | ↓ in ring C | -11900 | | -13390 | | -14110 | |
| | ↑ in ring D | -4180 | -7590 | -5800 | -7590 | -6580 | -7590 |
| | ↓ in ring D | -11450 | | -12950 | | -13670 | |

Three power levels (each one with different CR insertion levels into the core at criticality) were taken into account: 20 W, 200 kW and 500 kW (respectively, Tfuel =27°C, 114°C and 174°C in calculations). In Table 4.44, FR (negative) worth in ring B were calculated with respect to water (water minus fuel), whereas FR ring G worth were calculated with respect to graphite (graphite minus fuel). CR worth were calculated with respect to the fuel follower. As already mentioned, the critical insertion level for CR in Table 4.44 (indicated as ↔) is relative to the nominal fuel loading.

Concerning the different fuel loadings of the core, results showed:

— The FR worth in ring B depends on the CR level insertion (for example, at 20 W, FR ring B worth is + 4390-(-360) = +5750 pcm with CR ↑ positioned in ring C against -4250 - (-7710) = +3460 pcm with CR ↓). In particular, it is maximum with CR withdrawn from the core (FR in ring B are well coupled with the core) and minimum with CR fully inserted into the core (FR in ring B are less coupled with the core).

— The FR ring G worth, without FR in ring B, depends on the CR level insertion (for example, at 20 W, FR ring G worth is -1360 - (-4180) = + 2820 pcm with CR ↑ positioned in ring C against -7710- (-11900) = + 4190 pcm with CR↓). In particular, it is minimum with CR withdrawn from the core (less importance of the core peripheral zones) and maximum with CR fully inserted into the core (more importance of the core peripheral zones).

— The FR ring G worth, without FR in ring B, is smaller with CR fully inserted in ring D with respect to the situation with CR fully inserted in ring C (for example, at 20 W, FR ring G worth is -7710-(-11900) = +4190 pcm with CR ↓ positioned in ring C against -7930-(-11450) = + 3520 pcm with CR ↓ positioned in ring D).

Concerning control rods, results showed:

— CR worth are practically independent on the power level: for this reason, mean values among different power levels are quoted in Table 4.44;

— CR worth are smaller without FR in ring B (CR positioned at the internal boundary of the core), and increase without FR in rings B and G (core more compact).

As a general point of view, TRADE seemed to offer a variety of suitable subcritical loadings. At a first glance, one loading could be with FR ring B removed from the core and with CR positioned in ring D. In such a case, the target value $k_{eff}$ 0.97–0.98 could be attained with CR in ring D completely withdrawn from the core (safe condition), and tuning the $k_{eff}$ value by progressive loading (or unloading) of the FR in ring G. It should be noted that, though removing FR ring B from the core decreases CR worths, at cold condition (20 W) the subcriticality level with CR inserted (about-7700 - (-7900) pcm depending on the CR positioning) is almost twice the reference value (-4250 pcm, second row in Table 4.44) calculated for the current TRIGA layout.

FIG. 4.164 shows the behaviour of $k_{eff}$ as a function of the number of fuel elements loaded (CR completely withdrawn from the core).

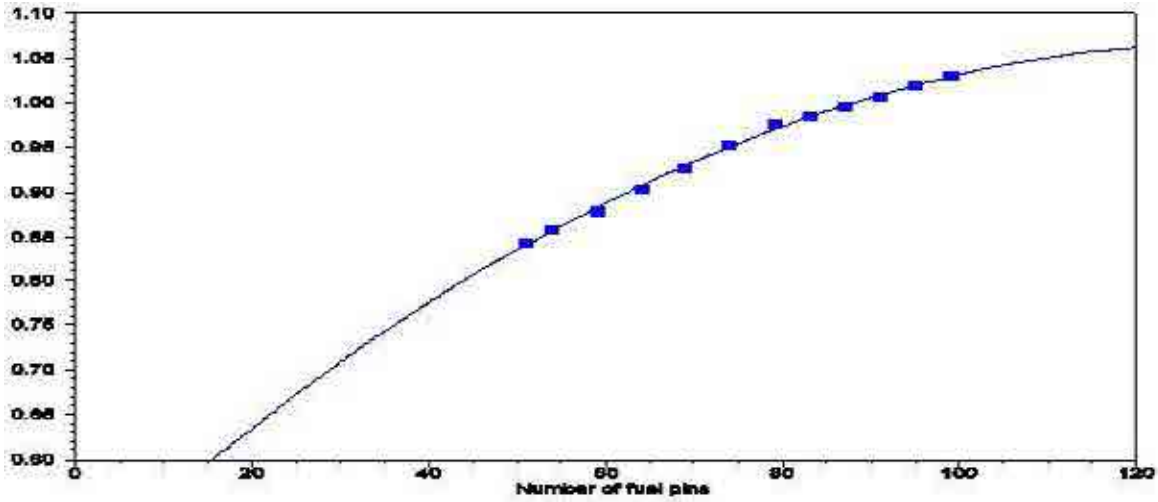


*FIG. 4.164. $k_{eff}$ behaviour as a function of the fuel loading.*

### *4.9.5.3. Power and temperature coefficients*

Concerning power and temperature coefficients, from the first row of Table 4.44 (nominal fuel loading with CR withdrawn in ring C), the following values can be derived: about -3.0 pcm/kW (-6.8 pcm/°C in terms of medium temperature rise in the core) going from 20 W – 200 kW, and about -2.8 pcm/kW (-14.2 pcm/°C) going from 200 kW – 500 kW. Reactivity insertion measurements made during the first Casaccia TRIGA tests have been analysed by the TIESTE-MINOSSE code [4.215].

The TIESTE-MINOSSE code is a simple tool developed at ENEA by coupling a core channel time dependent thermalhydraulics code with a neutron point kinetics code. The resulting fuel feedback features have been compared with statically measured temperature and power coefficients, obtained by measuring both the fuel temperature and the reactivity of a calibrated control rod at different power levels. The comparison shows a significant agreement between the above mentioned analysis of TRIGA dynamics and the more recent power coefficient static measurements.

Fig. 4.165 shows a first temperature coefficient linear fit function used in the dynamic code to analyze the available experimental results. The same plot shows the results obtained by Monte Carlo calculations (first row of Table 4.44).

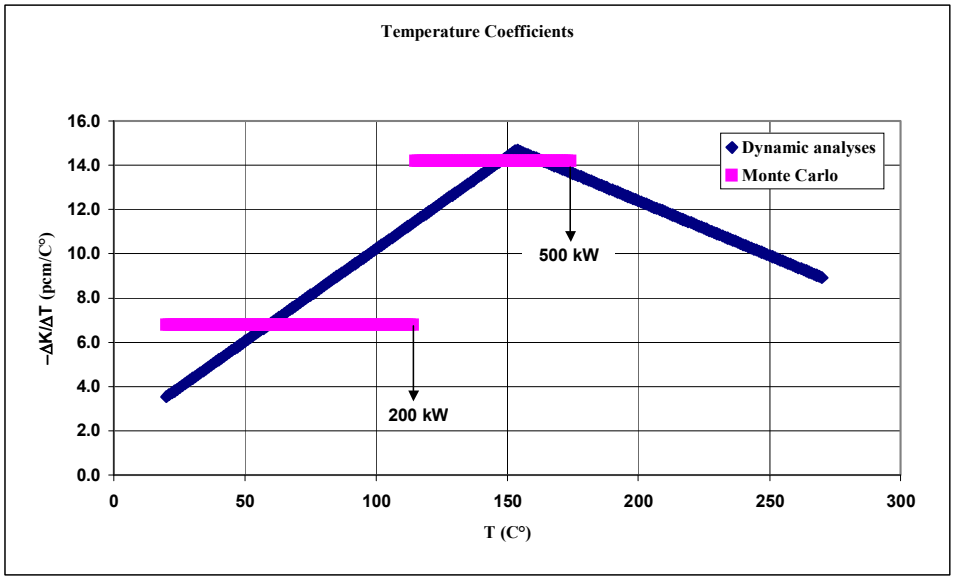


*FIG. 4.165. TRIGA temperature coefficients analysis.*

*4.9.5.4. Core spatial distribution of the neutron flux*

A refined modelling of the TRADE experiment was implemented. Fig. 4.166 shows the calculation model for the TRADE analysis by FLUKA and EA-MC.

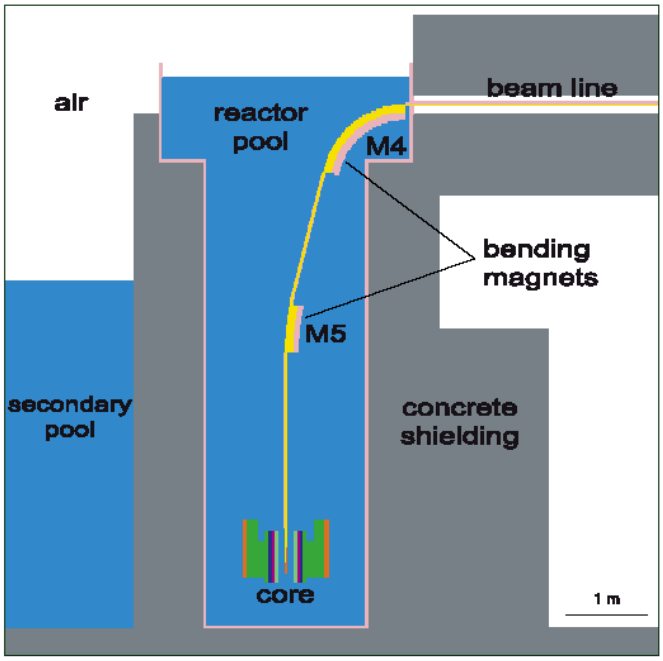


*FIG. 4.166. Schematic view of the implemented model.*

Fig. 4.167 and Fig. 4.168 show the radial flux distribution averaged over the channels of a given cylindrical ring and the axial flux distribution for the hottest fuel pin respectively, for different subcriticality levels. Neutron flux is normalized at 1 MWth thermal power. Different rings positions are also indicated in Fig. 4.167.

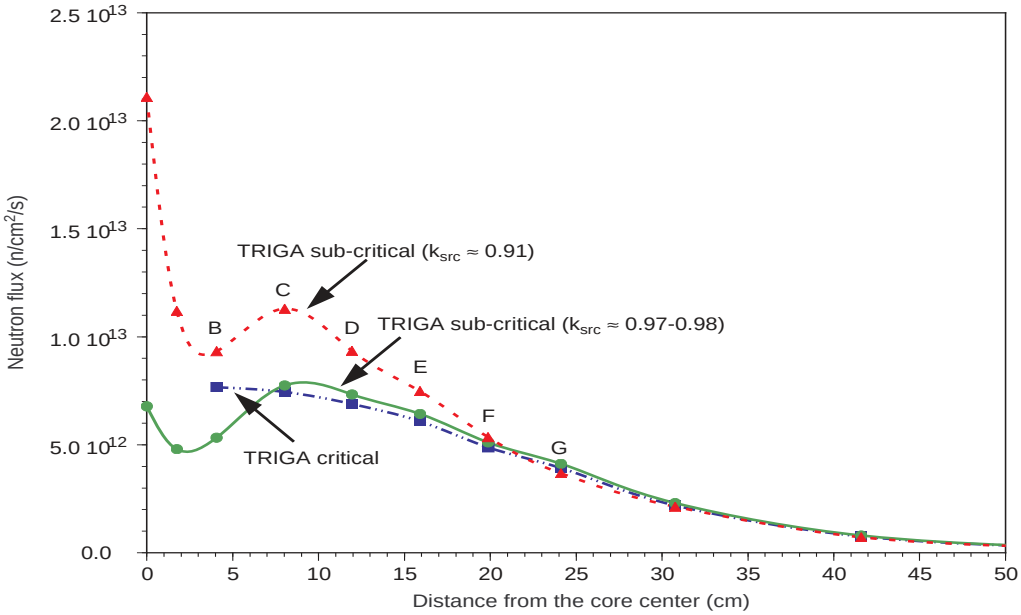


*FIG. 4.167. Radial distribution of the neutron flux in the TRIGA core.*

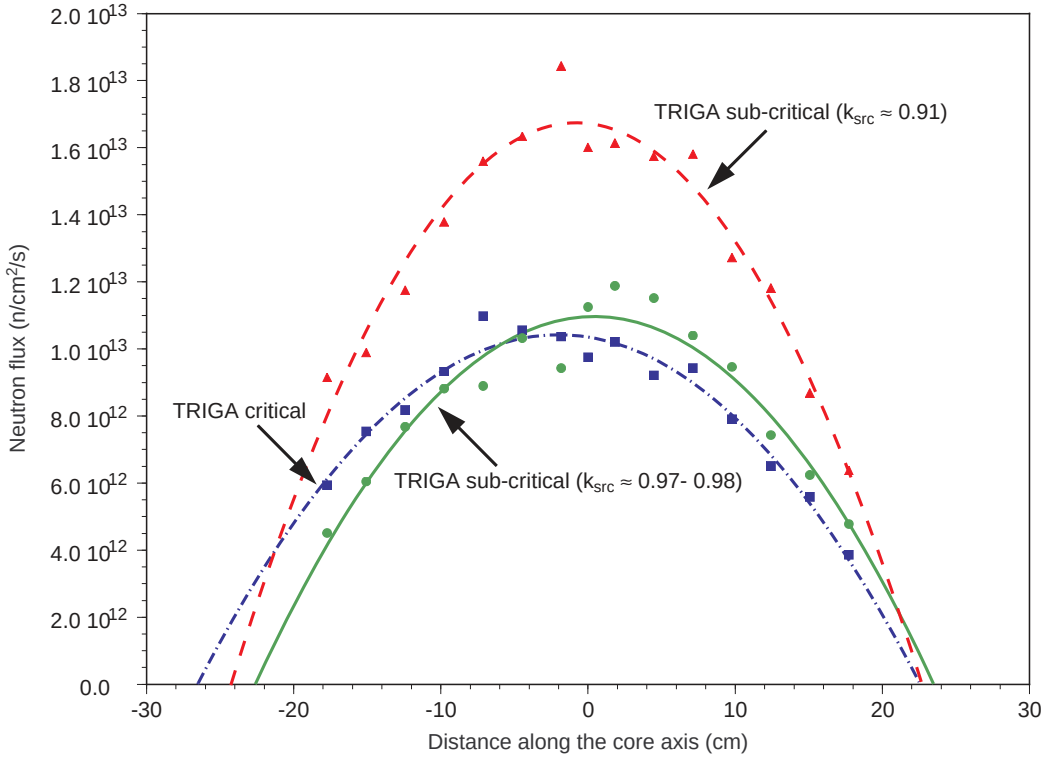


*FIG. 4.168. Axial distribution of the neutron flux in the hottest fuel pin.*

It is worth noting that despite the large subcriticality margin, the radial and axial power profiles have a moderate peaking factor. This implies that, in a first approximation, the thermalhydraulic properties of the core were compatible with a presence of an intense spallation neutron source in the central channel.

### *4.9.5.5. Global neutronic parameters*

Three subcritical core configurations, operated at 200 kWth, have been chosen for the initial feasibility study phase:

— A reference configuration consisting of 102 fuel rods (nominal configuration as in Section 3 without fuel rods in ring B and with the 3 control rods withdrawn, i.e. fuel follower inserted) resulting in a $k_s \approx 0.97–0.98$ (see below for the definition of $k_s$);

— A second configuration consisting of 107 fuel rods (same as (i) with 5 additional fuel rods in ring G) resulting in a slightly subcritical core, i.e. $k_s \approx 0.99$;

— A third configuration consisting of 79 fuel rods (nominal configuration as in Section 3 without fuel rods in rings B and G, and with the 3 control rods at critical level, resulting in a deep subcritical core, i.e. $k_s \approx 0.90$;

For the sake of comparison, the nominal configuration has been included. The main global results of the three TRIGA subcritical configurations, in addition to the critical case, are summarised in Table 4.45.

TABLE 4.45. MAIN PARAMETERS OF THE TRIGA SUBCRITICAL CONFIGURATIONS

| Global parameters | Symbol | Reference case | Critical | High ks | Low ks |
|---|---|---|---|---|---|
| Thermal power output | $P_{th}$ (kW) | 200 | 200 | 200 | 200 |
| Proton beam energy | $E_p$ (MeV) | 110 | — | 110 | 110 |
| Spallation neutron yield | $N_{(n/p)}$ (n/p) | 0.451 | — | 0.451 | 0.451 |
| Neutron multiplication | $M_s$ | 44.1 | — | 84.1 | 10.4 |
| Multiplication coefficient | $k_s=(M_s-1)/M_s$ | 0.977 | 1.000 | 0.988 | 0.903 |
| Energetic gain | G | 15.1 | — | 28.1 | 4.0 |
| Gain coefficient | $G_0$ | 0.34 | — | 0.33 | 0.39 |
| Accelerator current | $I_p$ (mA) | 0.13 | — | 0.07 | 0.61 |
| Beam power | $P_{beam}$ (kW) | 14.2 | — | 7.4 | 66.9 |
| | Core power distributions | | | | |
| Av. fuel power density | $P_{th}/V_{fuel}$ (W/cm$^3$) | 4.9 | 4.8 | 4.7 | 6.5 |
| Max. linear power | $P_l$ (W/cm) | 75.6 | 70.2 | 70.5 | 118.2 |
| Radial peaking factor | $P_{max}/P_{ave}$ | 1.48 | 1.45 | 1.46 | 1.76 |
| Linear peaking factor | $P_{max}/P_{ave}$ | 1.51 | 1.45 | 1.48 | 1.78 |

$M_s$ indicates the net multiplication factor in the presence of an external source. Table 4.46 reports a source multiplication coefficient $k_s$, formally defined as $k_s$ = 1-1/$M_s$, of 0.977 for the reference configuration, which is different in general from the effective neutron multiplication factor, $k_{eff}$. This value has been chosen in such a way that criticality conditions are prevented, with adequate margins, under all normal conditions as well as following transient and accident conditions. The main neutronic parameters for the different source configurations are shown in Table 4.46.

TABLE 4.46. MAIN NEUTRONIC PARAMETERS FOR THE DIFFERENT SOURCE CONFIGURATIONS

| Parameter | Reference | High $k_s$ | Low $k_s$ |
|---|---|---|---|
| $k_s$ | 0.977 | 0.988 | 0.903 |
| $k_{eff}$ | 0.974 | 0.988 | 0.894 |
| $\varphi^*$ | 1.142 | 1.035 | 1.110 |

Where $\varphi^*$ is the importance of source neutrons, defined as:

$$\varphi^* = \frac{v}{v'}\frac{\frac{1-K_{eff}}{K_{eff}}}{\frac{1-K_s}{K_s}}$$

Fig. 4.169 shows some spectra, which allows further insight into the neutronic characteristics of the device.

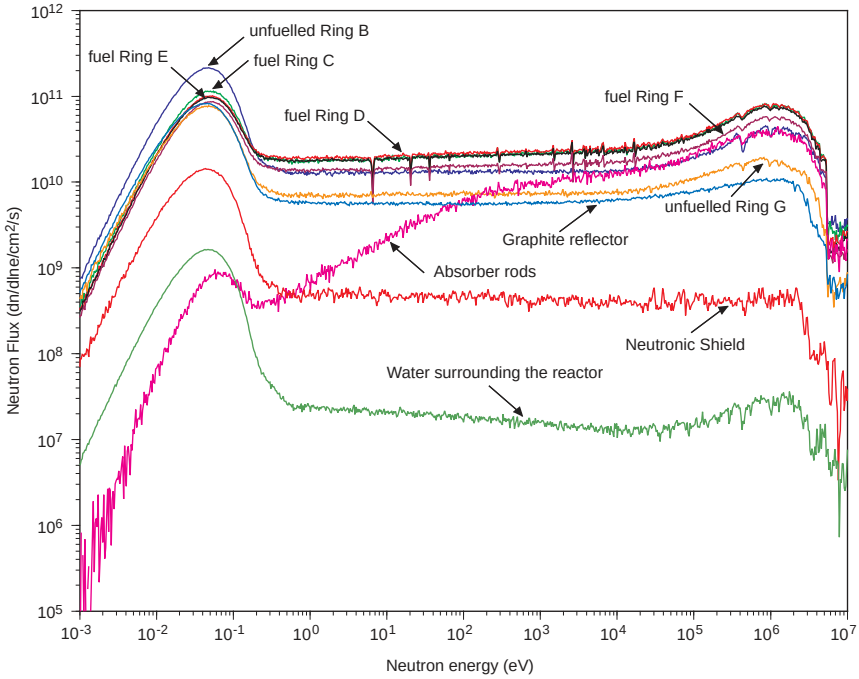


*FIG. 4.169. Neutron flux spectra at selected locations of TRADE reference configuration.*

### *4.9.5.6. Representativity of the experiment*

Some reactivity insertion transients have been simulated by the TIESTE-MINOSSE code [4.215]. Three different subcriticality levels (-3.81$, -1.74$ and -0.72$, with 1$ ~ 700 pcm for TRIGA) were assumed for the analysis. The power level was 200 kW at the transient beginning. The fuel temperature feedback effects were taken into account.Fig. 4.170 shows the power transients induced by a reactivity linear ramp of 50 cents in 2 s for the three subcritical levels considered. For sake of comparison, the response of a Pb-Bi cooled experimental 100 MWth XADS [4.216] to the same reactivity insertion is shown in the Fig. 4.170. The influence of different thermal feedback impacts on power allow to evaluate in what extent feedback effects on the experimental power transients will decrease by decreasing the multiplying system effective multiplication factor, $k_{eff}$.

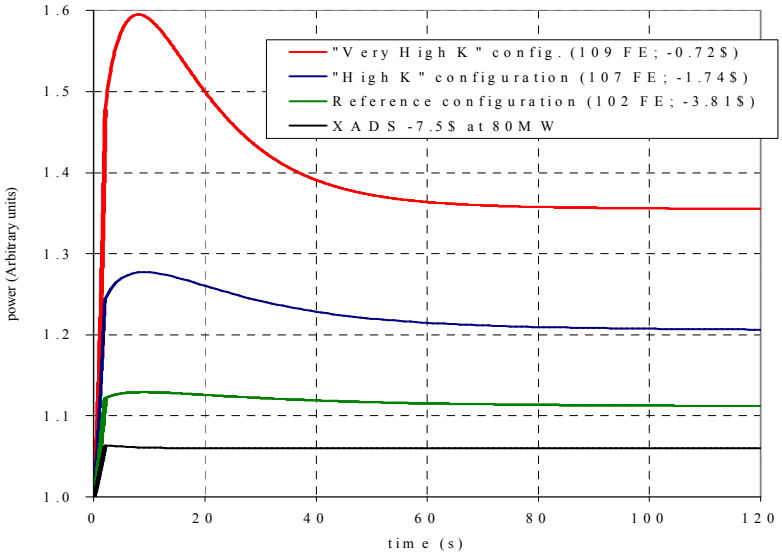


*FIG. 4.170. Normalized power transients induced by reactivity insertion (50 cents in 2s) for different TRADE configurations.*

Results indicate that TRADE experiments performed by configurations closer to the criticality conditions should be representative of the ADS dynamics relevant to higher power systems.

As far as the spectrum, TRADE will bring essential demonstration elements, valid for any type of ADS, e.g. with fast spectrum. In fact, although the kinetics parameters of a TRIGA ($\beta e_{ff} \sim 0.007$, $\Lambda e_{ff} \sim 10^{-4}$ s) and a fast spectrum ADS like XADS ($\beta_{eff} \sim 0.003$, $\Lambda eff \sim 0.5 \cdot 10^{-6}$ s) are very different, the dynamic response to perturbations are very similar.

#### *4.9.5.7. Conclusions*

A number of neutronic features of the proposed TRADE experiment, interrupted at the end of 2004, have been presented. Simplified dynamic codes were used to evaluate the dynamic behaviour of the TRADE subcritical core to some reactivity insertion transients.

The results show that the desired subcriticality levels and power distributions could be achieved. In particular, TRADE allowed to investigate a significant range of subcriticality levels, going from 0.90 (source dominated) to near critical. Assuming 200 kW as core power, the corresponding accelerator current, of the order of ~ 0.5 mA for $k$=0.90 and 0.07 mA for $k$=0.99, produced a power in the target that could be easily evacuated.

The dynamic neutronic conditions that could be experimentally realized in TRADE were well representative of dynamic ADS behaviour at higher powers [4.217]. In particular, the results shown in this Section indicate that TRADE would validate the transition between the source and the feedback dominated dynamic behaviour of ADS. Finally, further studies [4.218] performed at Argonne National Laboratories indicated that the dynamic response of a fast spectrum reference ADS of several hundreds MW to, e.g., reactivity insertions, is matched, as general behaviour, by the responses obtained in a thermal spectrum subcritical system, to similar reactivity insertions.

All these considerations allowed considering TRADE as a full scale demonstration of the ADS concept, in particular for what concerns the dynamic behaviour of the system.

### 4.9.6. Japan

#### *4.9.6.1. Neutronics of LBE target-cooled ADS for MA transmutation*

(a) Purpose and goal

JAEA's reference design of ADS is a tank type 800 $MW_{th}$ subcritical reactor to transmute about 250 kg of minor actinides annually [4.219] [4.220]. A lead-bismuth eutectic (LBE) is used as both the primary coolant and the spallation target. A superconducting linear accelerator (SC-LINAC), whose proton energy and maximum current are 1.5 GeV and 20 mA (30 MW), is connected to produce spallation neutrons. The (MA, Pu) N fuel diluted by ZrN is used in the subcritical core. Because the relatively high power peaking factor will be observed at the burnup stage of low $k_{eff}$ value, where the influence of the spallation neutrons is strong, Pu is added at the beginning of the first burnup cycle to mitigate the rapid increase of the burnup reactivity.

(b) Most important results

Table 4.47 summarizes the specific parameters for the subcritical core of LBE Target-Cooled ADS. The large power peaking near the spallation target is one of the difficult issues in the design of the subcritical core. Fig. 4.171 shows a radial power distributions of two radial fuel zone core at the beginning of cycle (BOC) of the initial cycle ( $k_{eff}$ = 0.97) and at the end of cycle (EOC) of the second cycle ( $k_{eff}$ = 0.94). As shown in the figure, the power peaking is significant in lower $k_{eff}$ case. This high power density dominates the maximum temperature of the fuel cladding which should be restricted below about 550–600 degree centigrade to control the material corrosion by LBE. Optimized design is, therefore, being investigated from viewpoints of the power peaking and the

burnup reactivity swing by adjusting the Pu and inert matrix (ZrN) contents of each zone, the pin diameter, the height of the active core, position of the spallation target, etc.

TABLE 4.47. CORE PARAMETERS OF 800 MWTH, LBE- COOLED, TWO-ZONE ADS

| Parameters | Values |
|---|---|
| Thermal power | 800 MW |
| Cycle length | 600 EFPD |
| Active core diameter | 236.6 cm |
| Active core tallness | 100.0 cm |
| Inert matrix (ZrN) | 49.9 w% |
| Initial Pu (inner / outer) | 30.0 % / 48.5 % |
| Total heavy metal inventory | 4,115 kg |
| Initial MA inventory | 2,500 kg |
| Effective multiplication factor ( $k_{eff}$) | Initial : 0.970<br>Max. : 0.970<br>Min. : 0.940 |
| Burnup reactivity swing | 3.01 %Δk/k |
| Peaking factor (whole core) | Max. : 2.52<br>Min. : 1.70 |
| Average power density | 191 W/cm$^3$ |
| Proton beam energy | 1.5 GeV |
| Proton beam current | Max. : 17.9 mA<br>Min. : 8.1 mA |

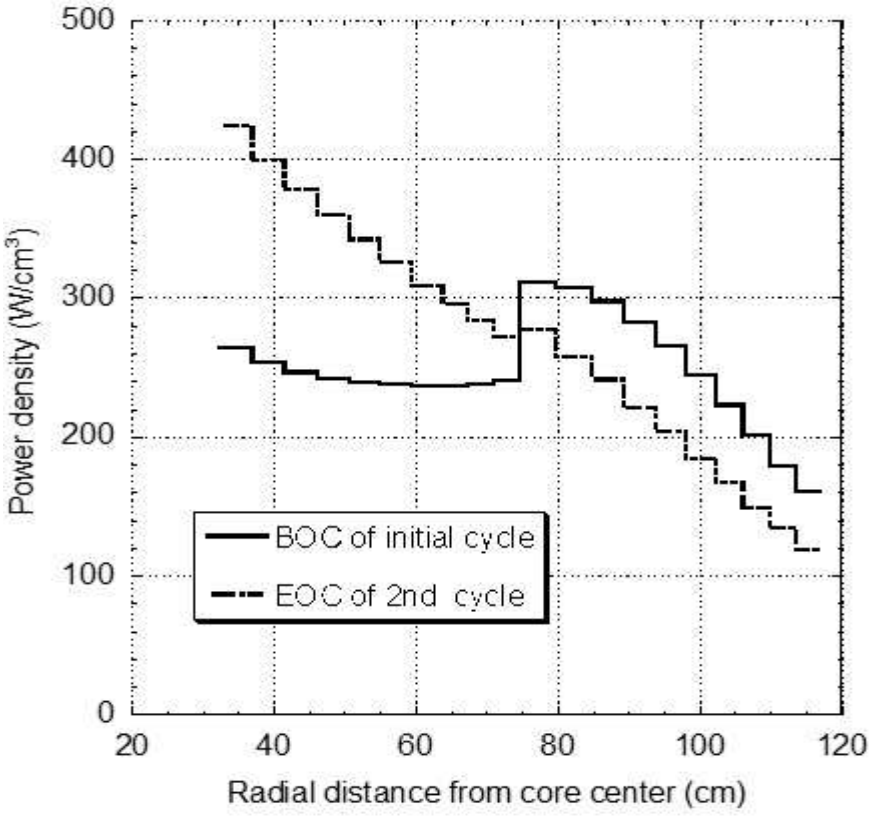


*FIG. 4.171. Power density of two-zone core (Axial position: center).*

*4.9.6.2. ADS neutronic research at KURRI*

(a) Purpose and goal

The main objectives of the present experiments are to examine experimentally the neutronic characteristics of the reaction rate distribution and the neutron spectrum of the Accelerator Driven Subcritical Reactor (ADSR) at Kyoto University Critical Assembly (KUCA), to establish measurement techniques of neutronic parameters in the subcritical system and to investigate the accuracy of the neutronic design of the ADSR in its present state.

(b) Theoretical explanation

At KUCA, by combining a critical assembly of a solid moderated and -reflected type core with a Cockcroft-Walton type accelerator, 14MeV pulsed neutrons generated by D-T (Deuteron–Tritium) reactions were injected through a polyethylene reflector into the subcritical system, where uranium fuel was loaded together with the moderated polyethylene reflector. In these preliminary experiments, subcriticality is varied systematically by inserting control or safety rods, or both, into critical system. Presently, the collimator and the beam duct are installed in the reflector region for directing the high energy neutrons generated in a tritium target to the fuel region, since the tritium target used by D-T reactions is located outside the core.

(c) Instruments description

KUCA comprises solid moderated and reflected type-A and -B cores, and water moderated and -reflected type-C core. In the present series of experiments, the solid moderated and reflected type-A core was combined with a Cockcroft-Walton type pulsed neutron generator installed at KUCA. The pulsed neutron generator was combined with the A-core, where 14MeV pulsed neutrons were injected into the subcritical system through the polyethylene reflector. In the experiments, the deuteron beam (accelerated up to 160 keV in beam energy, 4.5 mA in beam current, 10μs in pulse width and 500 Hz in pulse repetition rate) was led to the tritium target located outside the polyethylene reflector. At the pulsed neutron generator, the beam peak intensity is about 0.5mA for a pulse width of up to 100 μs, and the repetition rate varies from a few Hz to 30 kHz, providing up to $1\times10^{8}$ n/s.

(d) Most important results

— Excess reactivity and Subcriticality: The critical state was adjusted by maintaining the control rods in certain positions, and the subcritical state was acquired by inserting the control or safety rods, or both, up to the lower limit in the critical state. The subcriticality was obtained from the combination of both the reactivity worth of each control rod evaluated by the rod drop method and the excess reactivity on the basis of its integral calibration curve obtained by the positive period method. Refer to Refs [4.221]–[4.225] in detail.

— Indium (In) reaction rate distribution: Indium (In) wire 1.5mm in diameter and 60cm long was set in the axial center position, for measuring the reaction rate distribution.

— Reaction rates of activation foils: Activation foils were set in an objective position for measuring the neutron spectrum. The size of the activation foils was 45mm × 45mm with thickness varying between 3 and 5mm. They were selected for covering as wide a range as possible of threshold energy values within 14MeV neutrons. The experimental results of the reaction rates of all the irradiated, including the In wire and the activation foils, were obtained by measuring total counts of the peak energy of γ ray emittance and normalized by the counts of another irradiated In foil ($20\times20\times1$ mm$^3$) emitted from $^{115}$In (n, n') $^{115m}$In reactions set in the location of the tritium target. Refer to References in detail.

### 4.9.7. Russia

#### *4.9.7.1. SAD: Neutronics researches*

(a) SAD design neutronics calculations

Neutronics of the subcritical assembly was calculated at two stages. At the first stage, proton beam interaction with target was calculated and space energy distribution of neutrons generated in the target

was formed. At the second stage, space energy distribution of neutron flux densities of reactor energies (below 20 MeV) and neutron and gamma ray field functionals were calculated for a subcritical task with external source (results of the first stage were used). At the second stage, $k_{eff}$ is also calculated in conditionally critical approximation to determine the subcriticality level and reactivity effects.

An important parameter of the SAD is value and energy distribution (spectrum) of neutron flux density in experimental channels. These values are calculated for all channels. Fig. 4.172 and Fig. 4.173 show the neutron spectra in core (1–3) and reflector (4–6) vertical experimental channels (VECs) for operation with lead target. Graphs show neutron flux densities averaged over 50 mm height cells in the central part of the core. Integral values for neutron flux density in channels 1–6 are $2.43\times10^{12}$ 1/(cm$^2$·c), $2.21\times10^{12}$ 1/(cm$^2$·c), $1.85\times10^{12}$ 1/(cm$^2$·c), $1.47\times10^{12}$ 1/(cm$^2$·c), $1.15\times10^{12}$ 1/(cm$^2$·c), $8.96\times10^{11}$ 1/(cm$^2$·c) correspondingly. In case of operation with tungsten target the corresponding values are 9% lower due to lower thermal power of the facility.

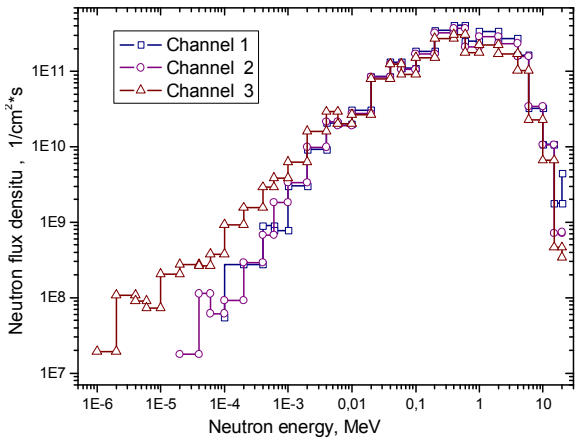


*FIG. 4.172. Neutron flux density in core VECs.*

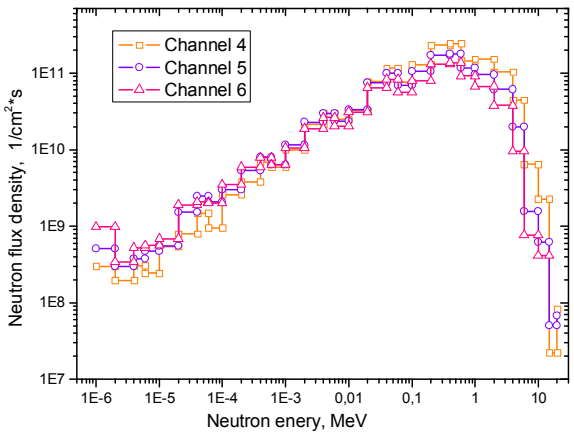


*FIG. 4.173. Neutron flux density in side reflector VECs.*

(b) Planned programme of neutronics researches at the SAD facility

Research programme for SAD facility is forming in collaboration between scientific teams and design organizations. Main points of the SAD experimental programme are:

— Qualification of subcriticality monitoring, experiments with Pulsed Neutron Generator (PNG), precise on-line monitoring of $k_{eff}$;

— Validation of the core power-beam current ratio, precise measurements;

— Measurements of the spallation neutrons spectral and angular distributions with actual targets;

— Measurements of the high energy neutrons spectral and angular distributions behind thick concrete shielding;

— Post-irradiation and on-line spallation products yields investigation;

— Measurements of spectral dependencies of neutron flux density and power density in different places of the installation, neutron lifetime and effective fraction of delayed neutrons;

— Transmutation reactions rates, integral cross-sections and spectral indices measurements;

— Interpretation and validation of experimental data, codes validation, benchmarking.

One of the main points of experimental research programme is development of experimental techniques for deep subcriticality measurements and monitoring. This question is vitally important for

safety assessment of the subcritical systems of high power driven by external sources. Such investigations were performed at subcritical assemblies of zero power with fast [4.226] and thermal [4.227] neutron spectra. At the SAD facility these researches will be continued making important step towards construction of industrial scale ADS, where reactivity trips caused by beam and coolant fluctuations will determine the safety margins.

Within SAD research programme it is planned to pay special attention to the experiments on $k_{eff}$ measurements and monitoring by inverse multiplication, asymptotic period and other methods. The time structure of the proton beam will give ample opportunities for application the pulsed techniques for subcriticality measurements, when one measures the time constant of the neutron flux density decreasing after the proton pulse at different levels of subcriticality. During the stage of detailed design the experiments at BFS facility in IPPE (Obninsk) will be performed and SAD facility will be simulated with high precision and approaching the critical mode. Experimental results, technique and apparatus will be used during SAD physical startup.

#### *4.9.7.2. Conceptual study of ADS driven by electron accelerator*

In SSC RF-IPPE, a conceptual study of ADS with a lead-bismuth cooled fast reactor and driven by electron accelerator has been carried out [4.228]. The purpose of this research was the evaluation of parameters that can be really achieved within the framework of such ADS concept and formulation of scientific and technical decisions necessary for implementation of these parameters.

The following postulates were accepted as the basic conceptual provisions of this ADS and initial data for its development:

- Electron beam parameters are accepted in accordance with the characteristics declared now for perspective linear accelerators (electron energy E = 50 MeV, current I = 80 mA, electron beam power W = 4 MW);
- Windowless option of a target is accepted;
- Two zoned cascade subcritical blanket developed on the basis of the SVBR-75-100 modular fast reactor design is chosen;
- Rod type fuel pin with screw fins used in the SVBR-75-100 design is accepted for subcritical blanket zones;
- Design value of effective multiplicity coefficient $k_{eff}$ of the system is equal to 0.980.

This concept provides generation of neutrons by interacting high energy electrons with a target material (liquid Pb-Bi), that then are multiplied in two zoned cascade subcritical blanket.

A pipe of 18 cm external diameter with lead-bismuth alloy flowing inside is located at the center of the system and applied as windowless target. The height of the alloy in the central channel is 40 cm, the level of the alloy is lower than top end of the facility by 12 cm. The electron beam enters the central channel from the top end. The neutron output in such target is equal to 0.063 neutrons per one electron of 50 MeV energy.

Two zoned subcritical blanket (Fig. 4.174) consists of an internal zone with a fast neutron spectrum and an external zone with thermal neutron spectrum. A high enriched uranium dioxide $UO_2$ is applied as fuel in the fast zone, and the fuel composition based on zirconium hydride and uranium–zirconium alloy is used in the thermal zone. A special valve screen from $B_4C$-$ZrH_2$ is located between external and internal zones, that reduces influence of neutrons of the thermal zone on the fast zone. The two zoned blanket is surrounded with a reflector from Pb-Bi which has thickness of 20 cm.

The presence of valve screen consisting from a boron carbide layer with 50% enrichment of isotope 10B and from zirconium hydride layer provides reflection of about 30% of neutrons from the side of the fast zone (93% of them with energy more than 0.1 MeV) and passing of about 42% of neutrons to the thermal zone with an essential softening their spectrum (15% of passed neutrons have energy less

than 4.6 eV). The share of neutrons passed in the opposite direction from the thermal zone to the internal zone is equal to ~17%, ~0.3% of them with energy less than 4.6 eV.

The power of the facility is equal to ~50 MW at the electron beam power of 4 MW 27.6% of this power is released in the fast zone of the blanket, 72.4% is released in the thermal zone. The average neutron flux is 3.8·1014 n/cm2s in the fast zone and 6.0·1013 n/cm$^2$s in the thermal one.

Thus, the system provides total energy amplification in ~12 times, including amplification in ~3 times by application of cascade configuration of the blanket.

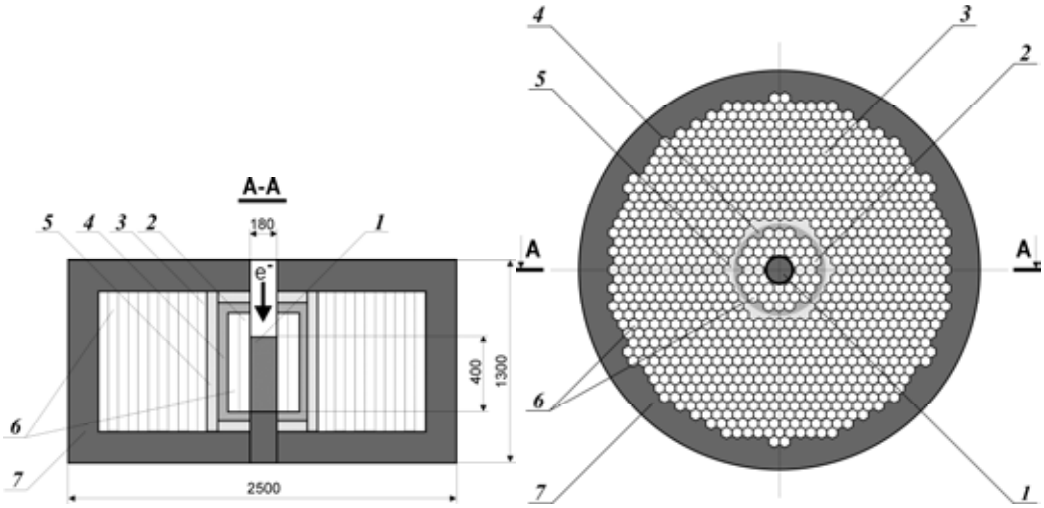


1 - target; 2 - fast zone; 3 - external thermal zone; 4 - layer of B4C; 5 - layer of ZrH2;
6 - fuel subassemblies; 7 - external neutron reflector.

*FIG. 4.174. A general design of two-zoned blanket of the ADS with electron accelerator.*

Use of wrapped fuel subassemblies in both blanket zones allows facility operation in a mode of partial refuellings. The blanket of the ADS examined has the following thermalhydraulic characteristics:

- Inlet coolant temperature ~310°C;
- Outlet coolant temperature ~475°C;
- Maximum fuel pin cladding temperature ~600°C;
- Average coolant velocity in the fast zone ~1.5 m/s;
- Average coolant velocity in the thermal zone ~0.19 m/s.

The results of the conceptual analysis of ADS driven by an electron accelerator demonstrate a feasibility of similar ADS option for the research purpose.

## 4.10. COMPONENTS DEVELOPMENT

The section provides an overview on the international efforts devoted to component development.

### 4.10.1. Components development in the EU

In the Euratom Sixth Framework Programme (FP6) an integrated project IP-EUROTRANS (transmutation) is ongoing. One of this project's objectives is to develop and assess structural materials and heavy liquid metal (HLM) lead–lead-bismuth technologies for transmutation systems, where the HLM is both the spallation material and the core coolant. This involves specification and fabrication of reference materials, their characterisation in HLM and in representative conditions (with and without irradiation environment) in order to provide the data base needed for design

purposes (e.g. fuel cladding, in-vessel components, primary vessel, instrumentation, target container, beam window), thermalhydraulics, measurement techniques, large scale integral tests and PTA studies for the MEGAPIE spallation target of FP5. In particular the ongoing R&D for the subcritical reactors XT-ADS, cooled by LBE, and EFIT, cooled by pure lead are:

— To provide necessary information for designers, as concerns both T91 and 316L steels in contact with LBE and lead. This R&D is aimed to:
  - Determine the creep, low cycle fatigue, relaxation (fatigue and creep) fatigue behaviour of T91 and 316L in contact with lead and LBE, both qualitatively and quantitatively;
  - Characterize their fracture resistance, once again both qualitatively and quantitatively,
  - Constitute reliable data base over a wide temperature range, attaining 550°C;
  - Determine the fracture mechanisms of both ferritic–martensitic and austenitic materials in contact with HLMs.
— This means that information on the materials selected for specific applications like T91 preselected as cladding tube material will be provided. The mechanical properties of both homogeneous and heterogeneous welds, assuming optimized and standardized process of fabrication will be determined as well as the susceptibility to LME of both T91 and 316L in contact with LBE or lead will be determined to the purpose of quantifying the LME effects.
— To provide the mechanical behaviour of the reference structural materials (including high temperature corrosion barrier) under proton–neutron mixed spectrum and under neutron spectrum exploring the temperature and dpa ranges on the basis of the ADS design. The ongoing LBE-irradiation experiments are aimed at characterising the combined effect on the mechanical and corrosion behaviours of the reference material as well as on the study of the Po production, release and deposition. In particular the ongoing R&D focuses on: neutron irradiation experiment on materials with and without corrosion protection barrier in Phénix and He effects; on irradiation tests under proton–neutron mixed spectrum at SINQ facility and PIE; on modelling of irradiation damage; and on corrosion mechanisms and mechanical properties under irradiation in presence of lead alloy and mechanism of Po, Hg and I release and deposition.
— To develop the heavy liquid metal chemistry control and monitoring that is one of the critical issues for nuclear systems using lead alloys either as a spallation target or as a coolant. Indeed, the chemistry interacts with at least 3 operating specifications of any nuclear system:
  - The contamination control, to ensure stable hydrodynamics and heat transfer during service life time that means to avoid lead oxide clogging or even corrosion products plugging due to mass transfer in a non-isothermal system, to avoid deposits that eventually reduce the heat transfer capacity, etc.;
  - The corrosion control, to ensure sufficient resistance of the structural materials during the expected service lifetime, which includes the self-healing oxide protection layers for iron-based alloys that requires oxygen control, etc.;
  - The radioactivation control, to ensure a safe management of the operations and maintenance phases. These three requirements refer all to the chemistry control in lead alloys systems as regards the oxygen and others relevant impurities such as the corrosion products, spallation and activation products.
— The principal scopes of development or validation concern at first the following issues:
  - The development of on-line monitoring systems for dissolved oxygen, as well as of the processes required to adjust the oxygen activity to a specified value;
  - The characterization of impurities and definition of purification process and monitoring method by liquid metal sampler and analytical techniques.
— To study the interaction between LBE and water coming from large leaks as a consequence of a

cooling tube rupture inside the steam generator of the reference reactors (XT-ADS and EFIT). The aim of the experimental campaign is both to assess the physical effects and the possible consequences related with this kind of interaction and to provide data for the validation of the mathematical modeling.

— Large scale tests to characterize crucial components of an ADS are ongoing: the focus is on single pin and fuel bundle validation and the main component chain acting on the primary coolant loop in the reactor pool. The activities cover thermalhydraulic and thermo-mechanic studies, materials issues and technical aspects such as instrumentations for ISI&R. Different facilities and test settings are involved with this approach. Three main large thermalhydraulic facilities are involved into this work conceived and constructed yet by the different partners in Europe with the primary purpose of supporting the European Transmutation Demonstration XT-ADS using LBE cooled Accelerator Driven Systems (ADS). All the main facilities considered have lead-bismuth eutectic as HLM coolant, used to represent the reactor core primary coolant and, for these specific tasks, all admit internal heat sources represented at a most intensity scale level as into an ADS reactor core but with a different degrees of overlooking extension zone. A single fuel rod simulator made by a rod electrically fed with an internal electrical resistance on a one to one geometrical scale and approaching the full power density scale, is a common basic module adopted for all experimental facilities by which the heat source is produced for the different experiments, assembling into bundles a number of them up to reaching the appropriate overall heating scale power allowed by the facility. On the ground of the ISI&R strategy applied for SPX1, experiments are ongoing to find ultrasonic velocity in LBE in various operating conditions for non-destructive control, telemetry and visualisation.

— Post-Test Analysis (PTA) in MEGAPIE are ongoing aimed at the interpretation of the data collected during the irradiation experiment and to compare them with the predicted performance. In Service Inspection and Repair (ISI&R) is important, as it allows to fulfil one of the most difficult points in the former liquid metal cooled nuclear reactor life (as Safety Authority requirements increase and plant availability has to remain as high as possible). The goal of low need for MEGAPIE operating and maintenance operations underlines the importance of a right ISI&R approach. Here MEGAPIE is an illustration selected for ISI&R strategy description, even if MEGAPIE design was mostly fixed by the targets already developed for the SINQ facility in PSI. This R&D deals with the definition of ISI&R criteria which are proposed for design phase of liquid metal systems such as MEGAPIE target. On the basis of requirements and of existing feedback experience, it gives also the existing or promising ISI techniques which could be adopted as regards the ADS systems and more particularly the spallation target.

Most of the above R&D is also used for the ELSY project (another project funded in the Euratom Sixth Framework Programme aims to demonstrate that it is possible to design a competitive and safe fast critical reactor using simple engineered technical features) that use pure lead as primary coolant and almost the same operating conditions (fast neutron flux and high coolant temperature). Most of the experimental results obtained with LBE are easy applicable also to pure lead. Hence the ELSY will profit from the large technological experience acquired in Europe because of the national activities in the field of the heavy liquid metals carried out in the frame of ADS studies and also, particularly, in the FP5 EURATOM projects and the FP6 EURATOM IP EUROTRANS and I3 VELLA. However, as far as the technological development is concerned a limited amount of R&D is ongoing for ELSY to acquire new information fort three basic topics, which are considered of fundamental importance, such as:

— Lead–Water interaction. It is mandatory to acquire reliable information, concerning the evolution of the SG tube break accident with supercritical steam cycle (the existing information from Fusion Programme regards Pb-17Li, whereas in IP EUROTRANS the steam is superheated, owing to the fact that plant efficiency is not such an important item as in ELSY). High pressure tests for the validation of computer codes intended for the study of the lead–water interaction in case of the SG tube break accident are ongoing: small scale tests, which foresee the injection of several kg of water in a lead filled vessel, recording pressure and temperature transients.

— Fuel cladding development. The corrosion–erosion protection by coatings-surface treatments of the fuel cladding is a key issue. The protection by means of a natural oxide barrier could not be effective for the high temperature of the fuel pin. Taking advantage of what has been done in the past and of what is in progress in EUROTRANS specific work is ongoing for Pb. FeCrAlY coated, GESA treated and composite samples for cladding are tested in lead.

— Material for pump impeller. The high lead velocity inside the pumps and the relative high operating temperature (480°C) requires the investigation of new materials to be successively validated at larger scale in the frame of the European or national programmes. A limited test programme, including corrosion tests, is ongoing for select a suitable pump impeller material to withstand at high lead velocity.

### 4.10.2. Components development in Japan

#### *4.10.2.1. Purpose and goal*

To examine the feasibility and applicability of the lead-bismuth eutectic to accelerator driven transmutation systems, JAEA has static corrosion experimental apparatus and three experimental lead-bismuth loops. The electromagnetic pumps and flowmeters, mechanical pump, oxygen sensors and ultrasonic flow velocity meter are now under development [4.229] [4.230] [4.231].

#### *4.10.2.2. Description of instruments*

(a) Electromagnetic pump and flowmeter

The electromagnetic pump (EMP) and electromagnetic flowmeter (EMFM) have been used in JLBL-1. During the 1st run at 450°C for 3000h, decrease in flowmeter indications was observed under the same output of the EMP together with remarkable corrosion at high temperature parts. According to inspection of the EMP and EMFM, it was found that main reason for the flow rate reduction was the clogging with precipitation of Fe-Cr crystals in the flow channel of the EMP. A wide channel gap in the EMP and metallic wool filters were adopted in JLBL-1 after the 2nd run. Concerning the EMFM, it was found that surface oxides with high electric resistance might influence induced current flux and potential of the EMFM.

(b) Oxygen control system

The oxygen control system investigated at JAEA is composed of oxygen sensors and a gas supply system for oxygen control in LBE. Several types of oxygen sensors were fabricated and tested in LBE. Yttria stabilized zirconia (YSZ) was used in all sensors as a solid electrolyte. Pt/air, Mo-Bi-$Bi_2O_3$ and Fe-$Fe_2O_3$ were tested as reference electrodes of YSZ sensors. Pt/air, Mo-Bi-$Bi_2O_3$ and Fe-$Fe_2O_3$ were gas, liquid metal and solid reference electrode systems, respectively. Ar-$H_2$-$H_2O$ mixture gas was used to control oxygen concentration in LBE.

While some types of oxygen sensors are under development, the YSZ oxygen sensor with Pt/air reference system has been used in static corrosion tests as a reliable sensor for long time.

FIG. 4.175 shows a schematic diagram of the YSZ oxygen sensor with Pt/air reference system which has been used at JAEA. It was also pointed out that calibration tests of oxygen sensors were often required for long time use. Although use of cover gas of Ar-$H_2$-$H_2O$ mixture is effective to adjust oxygen concentration in LBE, it seems to take time to control oxygen concentration in LBE at the required level. Some improvement in a gas control system is tried.

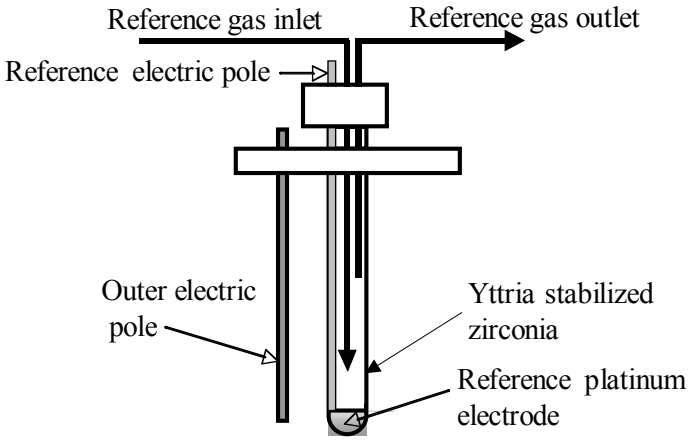


*FIG. 4.175. Schematic diagram of the YSZ oxygen sensor with Pt/air reference system used at JAEA.*

(c) Ultrasonic velocity profiler system

Ultrasonic Velocity Profiler (UVP) has been established in experimental applications in fluid dynamics and engineering applications involving flow measurements. It is a novel measurement method involving of line measurements and, while measuring a one dimensional velocity component, it enables obtaining the instantaneous velocity distribution as a function of time, and the quantitative spatio-temporal information of the flow field. The use of ultrasonic sound is advantageous in that it makes the method applicable to opaque liquids such as liquid metals and it can be applied non-intrusively behind opaque container walls. In JAEA, this system applied to the velocity measurement in a Pb-Bi loop and it was successfully realized to get the velocity information. The following shows the examples of measurement result.

The measurement target was a closed loop driven by an electromagnetic pump. Flow rate of the working fluid driven by this pump was constant and it was observed by an electromagnetic flowmeter. This model loop had coaxially arranged annular and tube channels. Fig. 4.176 shows the experimental configuration. The temperature of the loop and the liquid Pb-Bi were monitored by a plural thermocouple, and kept uniformly at 150° C. The Pb-Bi flow passed the gap between the two cylinders, turned over and then formed the reverse direction flow in the inner cylinder. UVP system was used for the velocity measurement. An ultrasonic transducer of the high temperature type undertakes the emission and the reception of the ultrasonic burst signals. Argon gas bubbles rolled up at the free surface in the Pb-Bi tank was used as reflectors for the ultrasonic burst signal to be able to trace the Pb-Bi flow. The velocity measurement was performed at the edge of the loop end of the window sphere where a proton beam was incident to the target. This window sphere had a spherical shape and is 3.5 mm thick. As shown in the figure, the measurement position was located at the center of the window sphere, and eight points on an arc had this point as their center. The radius of this arc was 14 mm, and measurement positions were located at every 45 degrees. As well, the ultrasonic transducer was installed perpendicular to the surface of the window sphere as a countermeasure to prevent the refraction phenomenon of an ultrasonic pulse beam that was caused at the wall surface of the window sphere.

Experimental results are shown in Fig. 4.177, which presents the velocity profiles of each flow rate at the centerline of the inner cylinder of the loop. In this figure, the horizontal axis represents the measured position and corresponds to the distance on the centerline assuming the edge of the loop as the origin. The vertical axis represents averaged velocity data; that is, the number of averaged velocity profiles is 512. In this experiment, the averaged velocity (U) in the annular region of the loop was changed, and then measured with an electromagnetic flowmeter installed in the upstream side of the loop. The velocity conditions were set to four phases (U= 0.25, 0.50, 0.75, and 1.00 m/s). Under all velocity conditions, in the averaged velocity profiles provided by this experiment the velocity data shows zero data from the starting position of the measurement to a neighborhood distance of 15 mm. At the inner wall surface of the target window sphere, the LBE flows coming from annular channels collide with each other. Therefore, a local dead region is formed for the LBE flow near the center of

the edge of the loop. It is thought that this result represents a dead region of the LBE flow that extends to the neighborhood a distance of 15 mm from the inner wall surface at the center of the loop. Even if the LBE flow rate of in JLBL-2 increases, the formation of this dead region cannot be avoided. Fig. 4.178 shows the experimental results of the averaged velocity profiles. Each velocity profile (A) to (H) shows a result measured counterclockwise from positions at intervals of 45 degrees. A velocity condition is U1. This figure represents that the LBE flow is approximately symmetric. In the position near the window sphere, it was observed that the flow of the upper side was fast and the lower side was slow. Furthermore, the velocity profiles of the lower side (A, B, H) changes from negative velocity to positive velocity continually. This shows the possibility that a vortex flow caused by the characteristic of the equipments is formed in the lower side. The size of this vortex flow depends on the configuration of flow passage.

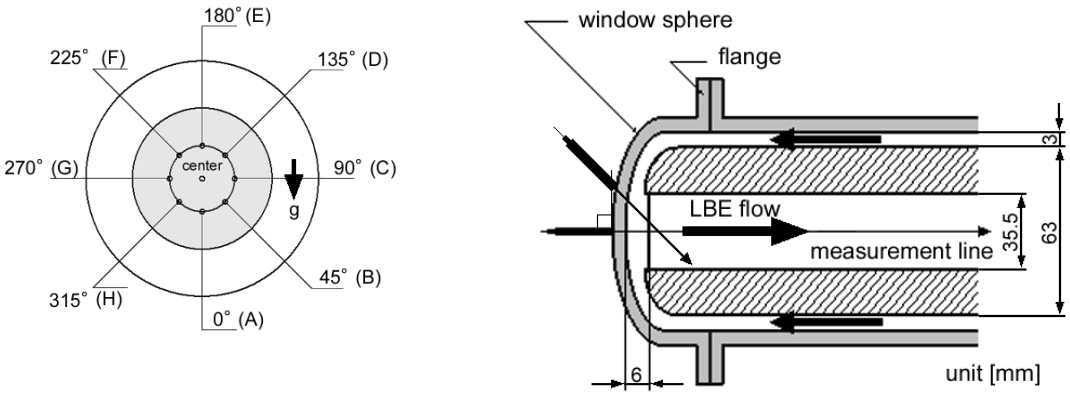


*FIG. 4.176. Experimental configuration of the measurement line on the window sphere.*

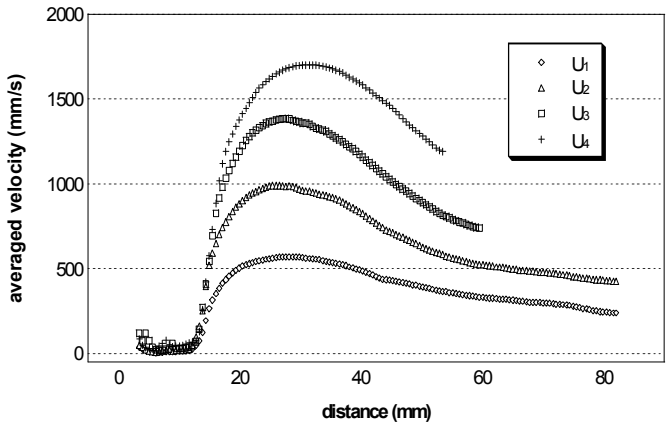


*FIG. 4.177. Averaged velocity profile at the centerline of JLBL-2.*

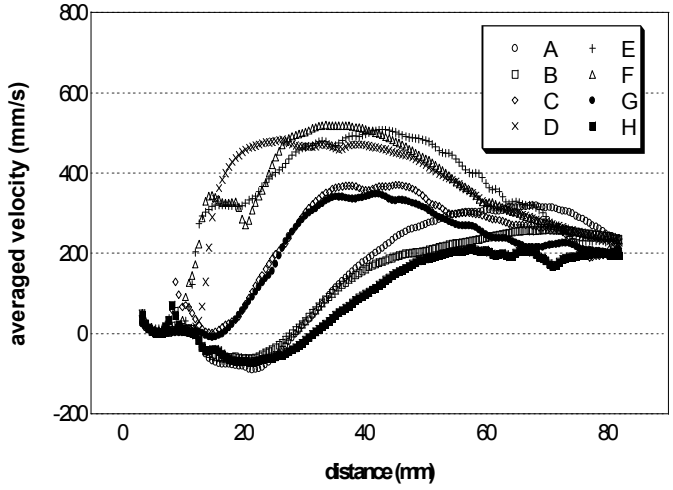


*FIG. 4.178. Averaged velocity profiles measured around the centerline of the measurement window at even intervals of angle.*

## 4.11. SYSTEM & SAFETY ANALYSIS

The section presents an overview on the international activities devoted to system and safety analysis.

### 4.11.1. System & safety analysis in the EU

The section presents an overview on the international activities devoted to system and safety analysis [4.232]–[4.304].

#### *4.11.1.1. Introduction*

Accelerator driven systems (ADS), as transmuters, introduce several major innovations, compared e.g. to critical sodium cooled fast spectrum burner reactors. Especially to name are the subcritical reactor driven by an external neutron source, the heavy liquid metal coolant and the new dedicated fuels. All these innovations introduce new interrelated safety issues. Besides the dynamics of the subcritical system and the chosen Pb or Pb-Bi coolant, especially the innovative fuels will be a key focus in the safety investigations.

Source driven systems have a special dynamic behaviour. As long as deep subcriticality level is maintained, a reactivity addition or reactivity reduction does not have a significant impact on the power level. This is of advantage in case of any reactivity addition but is a disadvantage in the way that the reactor is not shutdown e.g. by thermal structural axial and-or radial expansion or fuel removal under a severe transient. The power only drops slightly and finally the beam has to be shut off to stabilize the reactor after a transient. Thus the effect of absorber rods is also limited and therefore usually absorber rods are neglected in the ADS.

The success of the transmutation idea strongly depends on the fuel issue and the successful development of these fuels represents a corner stone of the ADS programme. These so called dedicated fuels should allow a maximization of the incineration–transmutation rates. The fuels are characterized by a high Minor Actinide (MA) content and by the lack of classical fertile materials as U-238. European R&D for ADS fuels within the 5th and 6th Framework Programme, namely FUTURE and EUROTRANS has concentrated on CERCER and CERMET oxide fuel forms. As matrix materials MgO and Mo are currently favored. The safety behaviour of these fuels is rather complex and significant R&D efforts are required. Strong interest focuses on the performance of these

fuels under transient conditions and under accident scenarios, also with the goal to identify any 'show stoppers'. New phenomena and safety issues have been identified and will need closer investigation. The performance of these fuels can be viewed firstly under the aspect of the fuel behaviour itself and secondly on their impact on the overall reactor safety parameters. Generally, the high MA load leads to a deterioration of safety parameters which has to be balanced by the subcriticality and other safety measures.

Besides the fuel the clad material plays a significant role. Clad behaviour is determined strongly by oxidation and corrosion under heavy liquid metal conditions, the irradiation and the internal pressure loading by the fission gas and the strong helium production of the transmutation process.

The heavy liquid metal cooling defines structural limits on the operational temperatures, with a lower limit of ~ 620 K to prevent embrittlement of the structures and an upper limit of ~ 820 K for corrosion reasons. Temperatures above the upper limit are naturally a concern under transient conditions. In addition the formation of oxide layers, their possible spalling and corrosion products have an impact on the risk for blockage formation in bundles with grids.

Several analysis tools are under development for adequately simulating the transient behaviour of ADS and to address the whole spectrum from normal operation to the behaviour under low probability events which could lead to core melting and destruction. The code development comprises neutronic and thermalhydraulic models up to new equations of states for the various materials. Based on these safety analyses the design and the performance of ADS can be optimized and cliff edge effect phenomena can be identified and eliminated.

#### *4.11.1.2. General safety issues and generic safety behaviour*

(a) ADS general transient behaviour

A solid fuel critical fast reactor, in which neutron production (due to fission) and neutron losses (due to absorption and leakage) are in balance, may contain quite a limited amount (few per cents only) of TRU mixture components, like Np, Am or Cm isotopes, due to safety constraints. The reason is that important reactor reactivity coefficients and kinetics parameters deteriorate when these isotopes are added in appreciable amount to the reactor fuel. In ADSs, the neutron production (due to fission) is smaller than the neutron losses (so the system is subcritical), the balance being maintained by neutrons emitted via a spallation process from a suitable target, a region in the central part of the reactor.

The response of an ADS to a perturbation differs appreciably from that one of a similar critical system: similar variations in the reactor configuration result in significantly smaller power shifts in the ADS. On the other hand, two (instead of one) perturbation types should be considered:

— Perturbation of the core reactivity due to variation of material and temperature distributions in the reactor; and

— Perturbation of the beam intensity (e.g. switching off-on the beam, beam over power)

To avoid a very fast increase of the reactor power (excursion), the reactivity in any critical reactor (where reactivity is very close to zero at nominal conditions) should stay well below the effective delayed neutron fraction. This fraction (β-eff or 1$) is usually a value between 200 and 350 pcm depending upon the reactor type, the higher value corresponding to fast sodium cooled reactor with MOX fuel, the lower one corresponding to fast reactor systems fuelled with TRUs. It is possible to keep the reactivity in operating reactors within the 1$ margin since a small reactivity increment leads to a small power increment that heats up the fuel thus initiating a reduction of reactivity, due to increasing of neutron absorption in the fuel when the fuel temperature rises (Doppler effect). In a reactor with solid inert TRU fuel the Doppler effect is almost negligible. A coolant density reduction during a transient may instead lead to a sharp reactivity increase. A similar or higher reactivity increment may result from a gas injection into coolant (through clad failures). A critical reactor may thus be difficult to operate and may hardly be safe. In an ADS fuelled with TRUs, the reactivity at

nominal conditions is therefore assumed to be in the range from 10$ to 30$. At nominal conditions, minor reactivity variations do not affect significantly the reactor power. Variations of the beam intensity are restricted due to technical constraints and should not initiate a dramatic increase of the system power. However, maximum positive reactivity variations (coming from core voiding processes or clad–fuel rearrangement might exceed 10$, which would make the system close to critical. That is why transient analyses are important to prove the ADS safety case.

Based on the dynamic intrinsic behaviour of an ADS some key safety criteria were developed for the design of an ADS:

— the ADS shall remain subcritical under any foreseeable occurrence pertaining either to Design Base Conditions (DBC) or Design Extension Conditions (DEC). A proposed subcritical approach for special ADS, the PDS-XADS (PDS-XADS 2001; Bianchi 2005, Mansani, 2002) is summarized in Fig. 4.179. Based on analyses of many DBC and DEC events for a core fuelled with MOX the proposed margin to criticality amounts to 3000 pcm for DBC and DEC and 5000 pcm during refuelling, which implies that for refuelling neutron absorbing devices are foreseen to remove this excess reactivity;

— The reactor power following any DBC can be reduced to decay heat level by means of accelerator beam shutoff (without resorting to a reactivity control system);

— For the PDS-XADS global reactivity coefficients are not allowed to be positive.

For a transmuter with a high minor actinide load this last criterion must be relaxed as one is usually confronted with a strong positive coolant reactivity feedback. Therefore one might look for another criterion for limiting the impact of the positive reactivity feedback.

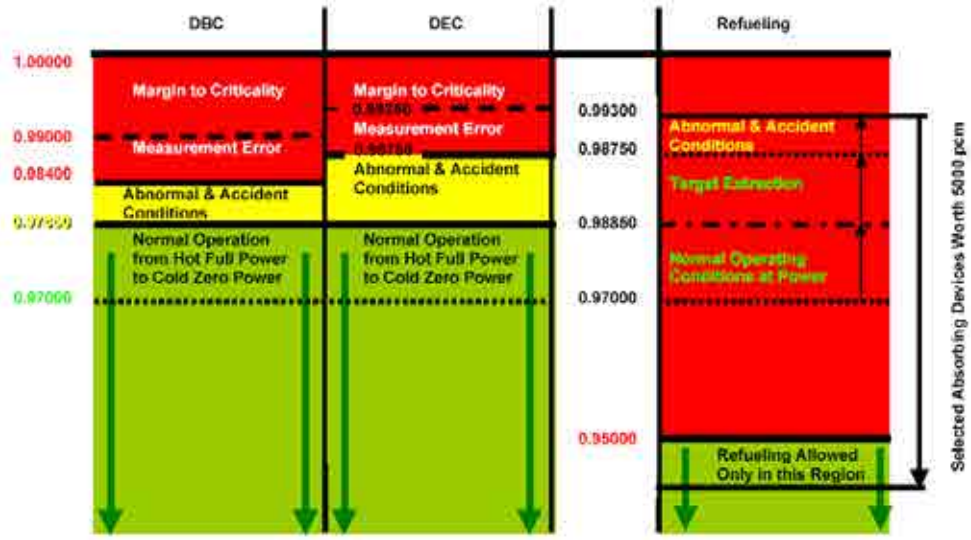


*FIG. 4.179. Subcritical level approach for the PDS-XADS (Mansani, 2002).*

In Table 4.48 some nuclear parameters of interest for the PDS-XADS are given.

TABLE 4.48. NUCLEAR PARAMETERS OF THE PDS-XADS (MANSANI, 2002)

| | | | |
|---|---|---|---|
| $k_{eff}$ at full power | 0.96802 | Reactivity worth (pcm): | |
| $k_{eff}$ at cold state (20°C) | 0.98099 | Cold state full power | -1322 |
| $k_{eff}$ at refueling | 0.93238 | Cold state cold shutdown | -250 |
| M | 29.92 ± 0.31 | Cold to hot shutdown | -156 |
| $k_s$ | 0.96765 ± 0.33E-3 | Hot shutdown full power | - 920 |

Compared to a critical reactor, the reactivity monitoring in an ADS is a more challenging issue since ADS steady state operation is possible at different reactivity levels. Most of the reactivity measurement techniques are based on analyzing the system response (count rates of neutron detectors placed at different locations) to a very short beam amplitude variation performed during reactor operation.

(b) Fuel safety issues for transmuters

The major goal for a transmuter is to load large quantities of MA into the core and achieve a high burning rate. A very high support ratio for the LWR and possible FR fleet is desirable in a second strata strategy some advantages are seen with fertile free fuels, as a Uranium containing fuel would again lead to Pu production. Therefore, the ADS is loaded with so-called 'dedicated' fertile free fuels. The potential fuels for transmutation and their safety impact in an ADT. The 5th FPs on coolant, corrosion and neutronics issues supported both the PDS-XADS and FUTURE programmes related investigations. In the 6th FP of the EU all activities centred around the ADS are concentrated in EUROTRANS, with its domains for design, experiments, fuel, structural materials, coolants and nuclear data. Two ADS design routes are followed, the XT-ADS and the EFIT. The XT-ADS is designed to provide the experimental demonstration of transmutation in an Accelerator Driven System. The longer term EFIT (European Facility for Industrial Transmutation) development aims at a generic conceptual design of a full transmuter.

The EFIT is the final goal of development as a transmutation device. Therefore the safety issues discussed in this chapter concentrate on transmuter issues. Naturally the fuels play the essential role for a transmuter and also within its safety concept. Within EUROTRANS-AFTRA the work on fuels mainly concentrates on MgO and Mo-92 as matrices for the Pu-Am-Cm fuels. Many other matrices have been investigated but discarded because of fabrication, reprocessing, operational and safety reasons. Stable matrices with high thermal conductivities are essential for theses MA fuels. The EFIT proposed with a MgO matrix based fuel has a power level of 400 MWth. ADS safety experience has been gained with the PDS-XADS, but this device did not contain any MA fuels. Therefore already within the 5th FP FUTURE an 800 MWth ADT has been developed with the main goal to investigate the feasibility of utilization of these advanced fuels. Details can be found in. One of the important issues was the demonstration of an adequate safety level for cores with these advanced fuels. Experience on other ADT power sizes and designs has also been generated with a very large ADT of 1200 MWth and a mid-size type of 500 MWth, a benchmark study within a Coordinated Research Programme of the IAEA on different transmuter systems.

The utilization of such fertile free fuels together with the ADS dynamics and the heavy metal coolant requires the investigation of new safety issues. These new fuels significantly differ both in their thermal-physical mechanical data and their behaviour from conventional fast reactor fuels. The omission of uranium has a significant impact on the fuel properties and on the overall core safety. The differences to fast reactor MOX can be briefly described as follows:

— A dedicated fuel consisting of Am and Cm will have a lower melting point and lower thermal conductivity than (U, Pu)$O_2$ fuel, which will however be improved by the use of composites like CERCER or CERMET fuels. Phenomena as eutectic formation, actinide redistribution during irradiation (e.g. $AmO_2$), radiation impact on the matrix, cladding corrosion, higher fission gas release and pressure buildup due to helium formation (resulting from alpha decay) have to be taken into account. Helium production could have a decisive influence on pin failure mechanisms and is a potential source for initiating a core voiding transient. The fuels are still under testing and only a limited data base is available both for steady state irradiation conditions and also transient conditions.

— The high Minor Actinide (MA) content will lead to a deterioration of the safety parameters of the core. Besides the strongly reduced negative Doppler feedback and the reduction of β-effective, the reactivity potentials of the coolant, the steel (clad) and of the fuel are significant in these cores. Operation of such reactors is only feasible in the subcritical mode. In this respect the subcriticality is not an additional safety feature for an ADS but a necessity for the safe operation of the reactor. Similar as in a critical fast reactor, the ADS core is not in

its neutronically most reactive configuration and the assessment of severe accidents will therefore play a role in the safety assessment.

The safety investigations in an early stage for these fuels are performed to identify any 'show stoppers'. Fuel development is a costly and long term endeavor and the risk choosing the wrong fuel should therefore be kept at a minimum. The safety assessment therefore also includes unprotected accidents with potential core damage and core disruption. This class of accidents is judged as hypothetical, because of the very low probability of occurrence. They will nevertheless be investigated because of their damage potential. In addition, these investigations provide information on the very intrinsic behaviour of a reactor under fault accident conditions, they help to identify and exclude cliff edge effects and they provide information for containment design. The new dedicated fuels show some new features and phenomena especially under design extension conditions (DEC), which have not been encountered in the classical $(U,Pu)O_2$ fast reactor fuels. The safety conditions for these fuels have to be re-assessed including the complete defence in depth strategy range. An extensive experimental programme ranging from irradiation to safety related experiments will be necessary for a final judgement on these innovative fuels.

#### *4.11.1.3. Impact of dedicated fuels on adt safety behaviour*

As mentioned before, the impact of the utilization of dedicated fuels can be discussed both on the fuel issues itself and the influence on the core safety parameters.

Because of the vast European experience in oxide fuels, the main emphasis of the ADT fuel development concentrates on the oxide route. The FUTURE and the EUROTRANS-AFTRA project assessed various fuel forms such as solid solution, CERCER and CERMET composites. The composite CERMET fuel $(Pu0.5,Am0.5)O_2$-x - Mo (with the isotope Mo-92 comprising 93% of the molybdenum) has been recommended by AFTRA as the primary candidate for the EFIT. This CERMET fuel fulfils adopted criteria for fabrication and reprocessing, and provides excellent safety margins. Disadvantages include the cost for enrichment of 92Mo and a lower specific transmutation rate of minor actinides, because of the higher neutron absorption cross-section of the matrix. The composite CERCER fuel $(Pu0.4,Am0.6)O_2$-x - MgO has therefore been recommended as a backup solution as it might offer a higher consumption rate of minor actinides, and can be manufactured for a lower unit cost.

To test and assess the behaviour of the chosen CERCER (MgO) and CERMET (Mo-92) fuels under normal operation and transient conditions, the AFTRA domain performed some preliminary core design studies on an EFIT. Already in the FURURE project an accelerator driven transmuter of the 800 MWth power class (ADT-800) had been developed. This ADT-800 core is characterized by a relatively high fuel power density in the range of 700–800 $MW/m^3$. Safety analyses revealed high coolant and clad temperatures for various transients in these high power density cores. As the T91 clad was chosen for the preliminary design of EFIT, problems showed up with a low creep failure temperature under transient conditions given the internal pin pressure. A first set of failure limits for the T91 clad have been provided by EUROTRANS DESIGN domain. In a first step for the EFIT, one safety issue was therefore the reduction of the power density, besides achieving a flat power profile. These include single zone and 3-zone cores with high and low power densities. The EFIT CERCER and CERMET fuelled cores belong to the 400 MWth class with fuel volumetric powers ranging between 250–550 MW/m3. As the fuels still need a long time development also other clad options have been considered within AFTRA which were supposed to give a higher resistance to transients. For a safety classification, AFTRA has provided fuel limits related to the different safety categories of the defence in depth concept. To test the safety classification and safety performance, these fuels have been subjected to various transients under EFIT core conditions. Because of the unique high temperature behaviour of these fuels, the investigation of design extension conditions is of special interest. The SIMMER-III code has been used as a main tool for this work and has been adapted for the conditions of innovative fuels in a heavy liquid metal cooling environment.

Recently the reference design of EFIT with MgO based CERCER fuels from the DESIGN group in EUROTRANS has been released and the safety calculations will be started. The overall safety concept for the EFIT has also be provided for the EFIT plant.

(a) Fuel development

The CERCER and CERMET fuels, whose in-pile behaviour have to be studied in the frame of the EUROTRANS Project, consist of composite materials of microdispersed fissile oxide inclusions in a molybdenum or magnesia matrix. The fabrication of composite pellets is considerably more difficult than solid solution oxide pellets. This is a result of the specific requirements of size and homogeneous distribution of the dispersed actinide phase. The fuel development for AFTRA is performed at CEA and at the Institute for Transuranium Elements (ITU). In the framework of the EFIT design the fissile phase volumetric content of these fuels is around 50%. The samples made for in-pile tests hold less than 30–40% of fissile particles because of nuclear facility constraints. Moreover, the fabrication feasibility of these tailored ceramics with a higher content of fissile compounds has not yet been proven. The fabrication route used at the laboratory scale for these highly radioactive materials minimizes contamination in the gloveboxes by manufacturing fissile particles with dust free methods. Two processes are used: an oxalic co-precipitation route for CEA and a combination of external gelation and infiltration methods for ITU. The composite materials are then made with conventional powder metallurgy methods: mixing and grinding the non-radioactive powders with the fissile powders. The blends are sieved and pressed. The green pellets are then sintered. Within the AFTRA framework, CERMET and CERCER pellets dedicated to irradiation tests have been fabricated using both procedures. Irradiation tests are performed FUTURIX-FTA in the Phenix fast reactor. The FUTURIX tests are of central importance for the development of these dedicated fuels.

(b) Fuel data and their impact on safety

The safety objectives common to all approaches for nuclear plants, including accelerator driven transmuters, are that all reasonably practicable measures are taken to prevent accidents in nuclear installations, and to mitigate their consequences. This is achieved through the application of the defence in depth concept. The demonstration of the adequacy of design with the safety objectives is structured along three kinds of basic conditions: The Design Basis Conditions (DBC, structured into 4 categories), Design Extension Conditions (DEC, limiting events, complex sequences and severe accidents) and Residual Risk Situations. Both the CERCER MgO and CERMET Mo based fuels have much lower ‘melting’ points than MOX fuel. ‘Melting’ could be real melting, disintegration–evaporation of one individual component and-or eutectic formation. The high temperature region is therefore of special importance and new safety issues come into play compared to more standard fast reactor fuels. Experimental data are scarce and no transient experiments have been performed up to now. The matrix generally represents the ‘continuous phase’ and is thus the mechanically stabilizing structure. The disintegration point of the matrix is therefore a key safety criterion. For MgO CERCER Table 4.49 gives the melting and eutectic points of the current data base. The ‘melting’ temperatures are a strong function of the oxidation level (burnup dependent). A concern of MgO is the identified potential for vaporization and-or destabilization in the temperature range around T ~ 2200 K. This could lead to a disintegration of the fuel pin after pin failure under a severe transient, to an in-pin rearrangement of the TRUs with a subsequent compaction. In the MgO case the matrix material tends to disintegrate before the TRU ‘fuel phase’. The matrix ‘vaporization’ temperature is thus the leading safety relevant temperature.

For the Mo CERMET based fuel the melting temperature of Mo is given as 2896 K in. With AmO2 having a melting point of 2448 K, the matrix would be stable beyond the fuel phase ‘melting’ point. The ‘leading’ phase for melting–disruption is thus the TRU in the composite. For Mo the boiling point is at 4885 K, nearly 2000 K above its melting point.

Due to the limited amount of data available, and as transient tests have not yet been performed, detailed fuel failure criteria cannot yet be given. Under these circumstances a conservative approach has been taken, and fuel and clad temperatures have been utilized to start the safety classification. Category IV events (see Table 4.50) thus should not lead to fuel ‘melting’. In addition, and in common practice with international procedures, peak temperatures are used as a reference for

classification purposes. This procedure is in accordance with the specific characteristics of the composite fuels; that the individual component has to be respected for categorization. Besides the fuel limits, clad limits of EFIT are of major interest. Clad creep induced fuel pin failures for non-irradiated T91 were given by at expected EFIT plena pressures in the short time range with around 1100 K.

TABLE 4.49. MELTING AND EUTECTIC TEMPERATURES RELEVANT TO CERCER MgO FUELS

| Material | Melting or eutectic temperature (lower limits) |
|---|---|
| $PuO_2$ | 2663 K |
| $Pu_2O_3$ | 2358 K |
| $AmO_2$ | 2448 K |
| MgO-$PuO_2$-x system | 2341 K |
| MgO-$AmO_2$-x ($1.62 \leq 2\text{-}x \leq 2$) | 2319 K |
| MgO-$AmO_2$ | 2291 K |
| MgO-$AmO_2$-x ($1.5 \leq 2\text{-}x \leq 1.62$) | 1930 K |

TABLE 4.50. CATEGORIZATION OF FUEL LIMITING TEMPERATURES (BOL FUEL) FOR EFIT

| | | | MgO-CERCER | Mo92-CERMET |
|---|---|---|---|---|
| Melting temperature | | Matrix | 2130 K* | 2896 K |
| | | Fuel | 2450 K | 2450 K |
| DBC | Category I | No melting-disintegration | 1750 K | 2300 K |
| | Category II | No melting-disintegration | 1850 K | 2350 K |
| | Category III | No melting-disintegration | 1950 K | 2400 K |
| | Category IV | No ‘melting’ for CERCER & CERMET fuels | 1950 K | 2400 K |
| DEC | | Limited up to extended ‘melting’ | 2130 K | 2450 K |

* Matrix evaporation limit

The values given in Table 4.48 should be regarded as working hypothesis. To substantiate the limits, fuel performance and transient calculations have to be performed. The fuel performance codes could provide the fuel temperature, gas pressure, clad strain development dimensional changes and loadings on fuel and cladding, given the design and irradiation history and indicating the influence of the ongoing operation (including beam trips). Power to melt, stored energy, gas pressures etc. must be evaluated providing also the initial conditions of the transient calculations. Safety analyses for the CERCER and the CERMET core show that especially for unprotected transients as the ULOF or UBA the clad limits are the dominating issue.

Pressure buildup due to helium formation in the fuel (resulting from alpha decay), in addition to fission gases, is of importance, as the large gas production is a potential source for initiating core voiding transients. Note that helium is further produced after a shutdown of the ADS. This has to be taken into account for both outage times and restart operations. The in-pile experiments planned within AFTRA, FUTURIX (Phenix), will provide information on the irradiation behaviour of CERCER and CERMET fuels. Information on He release will be provided by the HELIOS and BODEX experiments in the HFR. As this information will become available only towards the end of the AFTRA project, the above conservative procedures are recommended for EUROTRANS.

(c) Fuel Safety Issues under Transients

— CERMET or CERCER behaviour at high temperatures and under melting conditions

Both the MgO and Mo based fuels are composites with either individual 'melting' points of the matrix and fuel phase or eutectic 'melting' behaviour. A key question is the potential of the separation of components under high temperature conditions. In the case of individual 'melting', besides the disintegration of the fuel pin a separation of the individual constituents can be assumed. In the case of the separation of the fissile and the underlying matrix, subsequent layering and fuel compaction, a recriticality concern might exist. This is a certain concern for MgO fuel in the case of 'vaporization' of the matrix starting in the temperature range about 2100 K. Further questions are related to the matrix behaviour after severe clad failures or clad removal. Does the matrix and-or fuel column stay in place or disrupt into particles and do these particles agglomerate or disperse? The consistency and viscosity of these mixtures defines the velocity of any fuel motion, fuel relocation (sweep out)–and the blockage potential. Due to the coupling of neutronics and thermalphysical-mechanical thermalhydraulic fuel behaviour, any change of the fuel-matrix ratio opens up specific accident scenarios.

— Dispersiveness of fuel configurations

In a general sense the dispersiveness of core material mixtures is important for the achievement of non-compact fuel configurations, implying neutronically a low reactivity and the absence of recriticality phenomena. Different mechanisms such as boiling and intrinsic pressure buildup could prevent compacted fuel configurations. For ordinary $(Pu,U)O_2$ oxide fast reactor fuel under sodium coolant conditions a key safety issue and dispersal mechanism is the close proximity of the fuel melting point (Tf melt) with the steel boiling point (Tss boil). It could even be claimed that in a general sense the safety philosophy for FRs in the late accident phases was built on this principle. For the new ADT fuels with a much lower melting point, or 'multiple' melting point, this condition does not hold any longer. The heat generating constituents $AmO_2$ or $(Pu,Am)O_2$ have melting points way below the steel boiling point. The impact of this new situation has to be investigated. The potential contribution of the HLM coolant serving as a 'dispersive substitute' for steel must be further analyzed.

— Fission gas and He behaviour

The MA fuels will contain He as an additional pressure source. The amount, location, and kinetics of the combined fission gas and He release has to be investigated. The presence of pressure sources could lead to both dispersive (fuel dispersal) and compaction effects (in-pin fuel compaction, pin-stub motion by plenum gas). The impact of the gas production on the composite fuels and influence of the large pressure potential of the helium must be extensively investigated. Current analyses e.g. show that local pin failures could lead to gas release and voiding and via the positive power feedback to further propagation and gas release. In addition the presence of pressure sources could lead to both dispersive (fuel dispersal) and compaction effects (pin fuel compaction or pin-stub motion by plenum gas).

— Fuel pin failure modes

The fuel pin behaviour and potential failure modes under various transient conditions and accident scenarios is an essential issue to be investigated in the future. Most results from former experiments as TREAT and CABRI cannot be directly transferred to the transients in a HLM cooled reactor with CERCER or CERMET fuels as most of these experiments where related to sodium and sodium boiling conditions under unprotected loss of flow conditions with MOX fuels. Even for single phase coolant conditions results are not directly applicable due to the differences to composite fuels and the heavy liquid metal. In sodium cooled reactors under loss of flow conditions coolant boiling usually precedes clad failure, in a HLM cooled reactor the scenario would be reverse with clad melting before coolant boiling. In the HLM reactor a fission gas and He blowndown is connected with the clad failure. The impact of the burnup (transmutation) and He production and redistribution and release from the matrix on failure has to be understood. As shown in simulations, the processes of fuel sweep out under Pb-Bi flowing conditions, blockage potentials etc. are of paramount importance for

understanding the course of local blockage and overpower transients. As cladding for ADTs, the T91 steel is currently favored. Its behaviour under transients must also be further assessed.

— Core disruption processes

Due to the neutronic 'features', as a reduced Doppler feedback and the smaller neutron generation time, one has to investigate a possible increase in the severity of a power excursion when the subcriticality is consumed by the existing reactivity potentials. The fuel and core disruption process is strongly determined by the vapour pressure, the gas (He) content of the fuel and the confinement of the fuel masses. The He gas could serve as an additional dispersive force whereas the heavy coolant could be a hampering buffer with its large inertia and could favor an additional energy accumulation before core dispersal. In case of a severe transient with acceleration of the coolant by a core internal pressure source or a Pb water coolant–coolant interaction the impact of a lead hammer on the surrounding structures is different than sodium because of the higher density of lead and its low compressibility.

— Post-Accident Heat Removal (PAHR)

The PAHR problem is closely related to the fuel and is an example how severe accident safety issues have an impact on the design of the plant. The potential of fuel solubility and the close density ratio of fuel and coolant have to be taken into account in the overall decay heat removal strategy. A partial solubility of fuel in the coolant and-or a separation of the matrix from the fuel would have a major impact on decay heat removal, as redistribution of heat sources may have an impact on planned natural convection cooling strategies. Depending on the fuel and burnup the decay heat will also be significantly higher than ordinary MOX fuel. Decay heat production were evaluated in several systems with a fast spectrum. At nominal conditions, the decay heat in fuels with MAs may be lower by ca 10% than that one in UOX, but higher by ca. 10% than that one in MOX. For cooling times exceeding 1 min, the decay heat in fuels with MAs may be several times higher than in MA free fuels. The major decay heat contributions relevant for safety analyses come from FPs, U239 and Np239 (if U238 is present) and Cm242 (if MAs are present in the fuel). FPs contribution plays the major role at nominal conditions and for short cooling times (until 1 minute) in all cases. For longer cooling times, MA contribution may be more important for fuels with MAs. The FPs decay heat (relative to the total reactor power) is largest in the UOX case, intermediate in the MOX case, and lowest for fuels with MAs. For all fuels, the FPs value decreases similarly with cooling time.

#### *4.11.1.4. Dedicated fuels and their impact on core safety behaviour*

The omission of uranium from the fuel has a significant impact on the core safety properties in various aspects: In the early accident phases two reactivity potentials may be decisive for reactivity changes: the coolant density void worth and the clad stucture worth potentials. In later accident phases, in case of fuel mobilization, the fuel worth will dominate due to its magnitude. Reactivity potentials and feedback effects will play a role in case the subcriticality can be marginalized and criticality is approached. The major differences to an ordinary MOX fuelled core can be listed as follows:

(a) Coolant void worth potential

The large void worth potentials were already reported in (Maschek, 2003) and also became obvious after the analyses made for the ADTs with 500 MWth of the IAEA (Maschek 2007), the 800 MWth for the FUTURE project and the 400MWth EFIT. In Table 4.51 typical void values and additionally other important safety parameters (discussed in the following) for typical AFTRA 400 MWth cores with MgO and Mo-92 matrix are given. The three zone cores have 'enrichment' zones with a transuranics (TRU) share of 30, 40 and 50 percent in the CERCER. The Pu: Am: Cm ratio is 40:50:10 with a Pu-vector from a once through LWR irradiation cycle of 50 GWd/tHM. It should be kept in mind that the subcriticality limit chosen for these cores is 3000 pcm at BOL ( $k_{eff}$ = 0.97).

The strong positive feedback caused by coolant heat-up and density reduction during a DBC transient must be taken into account. In this respect an adequate equation of state for the coolant is essential for

a sound calculation of the reactivity effects. Voiding in the core could happen via pin failures and the release of fission gas and helium from the plena of the fuel pins. Coolant boiling is not expected before massive fuel melting due to the high Pb-Bi boiling point of 1934 K. Another source for a voiding transient could be a failure of the steam generator and the introduction of steam into the core after the Pb-water reaction. Recent analyses have shown that this scenario has not to be expected for the EFIT. The clad worth in this core (removal of clad) is in the range of 2000 pcm. Note that the maximum positive void will even be larger by another 2000 pcm.

TABLE 4.51. MAIN CORE DESIGN DATA OF AFTRA-EFIT DESIGNS

| Core Parameter | Units | High power density 1 zone core | | Low power density 3 zone core | |
|---|---|---|---|---|---|
| | | AFTRA-MgO | AFTRA-Mo92 | AFTRA-MgO | AFTRA-Mo92 |
| Nom. thermal power | MWth | 400 | 400 | 400 | 400 |
| Average linear power | W/cm | 131 | 226 | 65 | 112 |
| Fuel volumetric power | $MW/m^3$ | 571 | 568 | 285 | 286 |
| Coolant inlet/outlet | K | 673/753 | 673/753 | 673/753 | 673/753 |
| $k_{eff}$ | --- | 0.98246 | 0.97890 | 0.97370 | 0.97156 |
| Void worth | pcm | 5869 | 4393 | 6237 | 6565 |
| Doppler constant | pcm | -6 | -50 | +4 | -24 |

The investigations performed on ADTs of the 1200 MWth class showed some safety problems where the initial pin failure and voiding led to a failure propagation and severe core damage. To exclude such a design a safety indicator SI has been devised, which should stay below a certain limit during the core burnup. SI basically compares the core void with the subcriticality and should stay less than three. The criterion is mainly intended to check for severe accident potentials. During the studies that were conducted on the ADT cores, sensitive points were identified, which have an influence on the void calculations. The utilized nuclear data basis may be a cause for large deviations in the void worth. Differences range up to 2000 pcm. The correspondence between the deterministic and Monte Carlo methods utilized was usually good, ranging only around 100 pcm. The influence of the heterogeneity treatment seems not to be decisive with deviations less than 100 pcm for these cores. As stated before, a strong influence can be caused by the equation of state used for LBE. Due to the very high absolute value of the void worth small differences in the equation of state can lead to significant effects.

(b) Clad-steel worth potential

The clad-steel worth potential could be activated during undercooling transients. While in sodium cooled reactors coolant boiling precedes any clad motion, with Pb cooling and a boiling point at 1943 K, any significant heat up of the coolant will first lead to steel melting. The steel will be dragged away and buoyed by the approximately 30% heavier Pb. The molten core steel could freeze out on the colder surfaces of the structures of the downstream regions having implications on the later accident phases and post-accident heat removal (e.g. natural convection paths).

(c) Fuel worth potential

Fuel has the highest reactivity potential, if activated, it dominates over all the other processes, both in case of a reactivity increase (e.g. fuel compaction), or decrease (e.g. fuel dispersion or expansion). Likewise, the fuel reactivity potential plays a decisive role for the eventual occurrence of recriticalities, in the event of core disruptive accidents. ADTs contain multiple critical masses; any fuel agglomeration, either upstream, or downstream (depending on the actual fuel and coolant densities and temperatures), could as a result overcome the designed subcriticality of the core.

(d) Doppler and axial expansion feedbacks

The Doppler feedback and the axial expansion of the fuel are regulative measures to stabilize the power of the core. The reactivity swing from cold zero power (CZP) to hot full power (HFP) will be rather small in the ADT. In addition, in a source driven system, feedback effects will be damped as long as a significant subcriticality margin exists. However, a stabilizing negative feedback against the strong coolant density effect is advantageous under perturbation and transient conditions. Since the Doppler is rather small, the axial fuel expansion and radial structural expansion effects will become important. The core structural feedback (e.g. grid expansion) depends on the detailed core-plant layout for the transmuter. Especially the core-plant structural feedbacks act on a long time scale. For severe transients leading to core damage, the small magnitude of the Doppler effect is an issue to be aware of, since, without this prompt negative feedback, only a core disassembly would stop a power excursion.

(e) Kinetic quantities

The β-effective is small for all MA loaded cores. Under the condition of transients and-or accidents, the β-effective could play a role when the criticality limit is approached and eventually exceeded, e.g. by fuel compaction and a recriticality scenario. Another important parameter for the transient behaviour is the prompt neutron generation time. Under normal operating conditions it depends on the fuel-matrix and on the p/d ratio of the reactor. In case of a core disruption, a separation of the fuel from the matrix, or a redistribution of the fuel and of the clad steel, may actually lead to a drastic reduction of the neutron generation time.

#### *4.11.1.5. Some typical results of safety calculations for EFIT type reactors*

The dynamic behaviour of an EFIT type ADT is characterized by the lack of a prompt fuel feedback effect (Doppler), and significant positive (delayed) reactivity feedback potentials. The coolant void worth of the MgO and Mo-92 fuel type core is approximately 6000 pcm. The clad worth potentials are about 2000 pcm. These reactivity values are close to or larger than the assumed subcriticality margin of 3000 pcm and their safety impact has to be assessed. Analyses have been performed for various protected and unprotected transients as P-UTOP protected-unprotected transient over power, UTOC (unprotected over current), beam trip (BT) and ULOF (unprotected loss of flow). For the safety assessment of final EFIT MgO matrix fuel design a long list of transients will be analyzed from normal operation up to unprotected transients. The results will be available near the end of the EUROTRANS project. Therefore the consistent transient analyses performed in the AFTRA domain for preliminary EFIT designs will be presented here to give an impression of accident specifics, power development and temperatures of the different core constituents. Due to a short flow reversal caused by the different coolant levels in the vessel after pump coast down a slight overshooting of temperatures can be observed during the transient. But again, as also revealed from the AFTRA analyses both fuel and clad limits are not jeopardized by the ULOF transient.

(a) ULOF Analyses

The ULOF is of special interest as former analyses have revealed high clad and coolant temperatures under power-flow mismatch conditions. Clad failure could trigger a gas release from the plena with massive voiding and pin failure propagation. The current calculations have been performed with the SIMMER-III accident code. A complete and rapid loss of forced coolant circulation caused by a pump coast down has been assumed for the ULOF calculations. The coolant flow decreases with a flow-halving time of 5 sec and approaches a stable natural convection value of about 30–35% (defined by the axial position of the steam generators and the p/d ratio (p/d = 1.5)). For the cores with the high power density, fuel ‘melting’ is prevented and fuel failure limits are not reached. The clad temperatures are however close to the failure limits at 1100 K and coolant temperatures are in the same temperature range. The ULOF simulations in the low power density MgO core (Fig. 4.180 and Fig. 4.181 show that fuel temperatures are well below the Category IV (1950 K) and DEC limits. The maximum clad temperatures increase up to 950 K, thus possible failure limits for T91 are also not reached. In Fig. 4.182and Fig. 4.183 the results of the analyses for the Mo-92 CERMET core are

displayed. Again all fuel and clad limits are respected under ULOF condition00s. In addition the higher safety margins of the CERMET fuels are demonstrated. For the CERMET core peak fuel temperatures of ~1100 K are reached, about 900 K below Category IV and 1300 K below DEC limit values. Clad temperatures are still below ~ 1000 K. Coolant temperatures are in the range of 900 K and significantly lower than in the high power cores (ca. 1100 K). As a result of these calculations it can be deduced that the low power density cores behave favorably under ULOF accident conditions and safety margins both for fuel and clad are fully respected. No pin failure has to be expected with the blowdown of fission gas and helium and the potential for voiding and failure propagation. In addition the recently available ULOF safety results for the DOMAIN-I CERCER EFIT will be provided in Fig. 4.184 and Fig. 4.185 completing the overall picture. In general, limitations on the cladding seem to be mostly responsible for reducing the flexibility in the ADS design e.g. concerning the core power density. As the maximum dose target for EFIT is no more than 130 dpa, a stabilized austenite clad might give better high temperature stability during transients, in conjunction with an acceptable swelling rate. Further, Forschungszentrum Karlsruhe has recently developed aluminum surface alloying techniques for austenitic steels. These techniques may provide sufficient protection of the austenitic steel claddings against corrosion, in lead so allowing a long term operation of the cores with low power density. An austenitic clad backup option for the design of EFIT should be seriously considered.

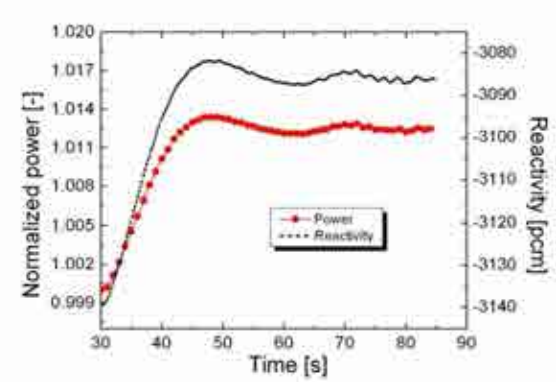


*FIG. 4.180. Power and reactivity transients (MgO).*

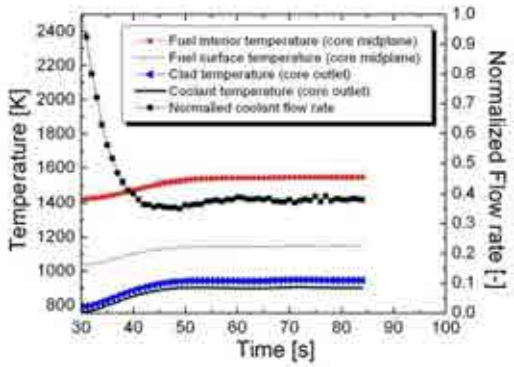


*FIG. 4.181. Temperature and Pb flow rate transients (MgO).*

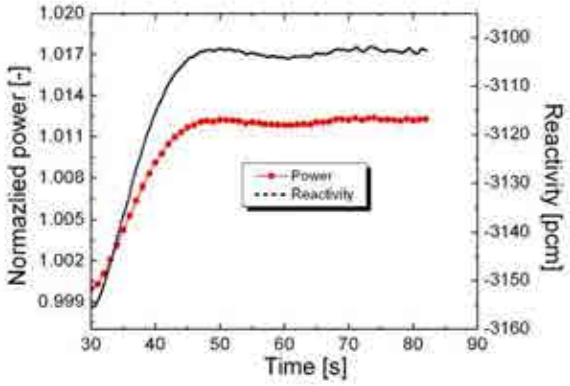


*FIG. 4.182. Power and reactivity transients (Mo92).*

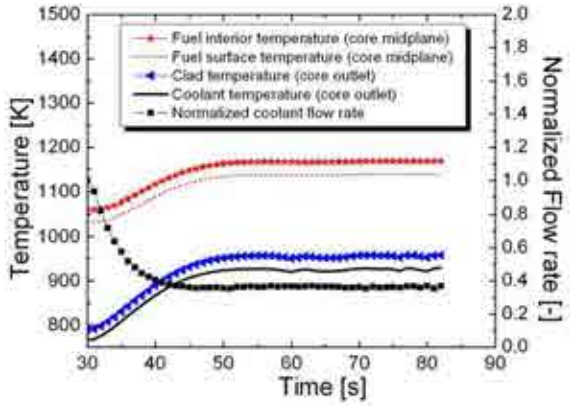


*FIG. 4.183. Temperature and Pb flow rate transients (Mo92).*

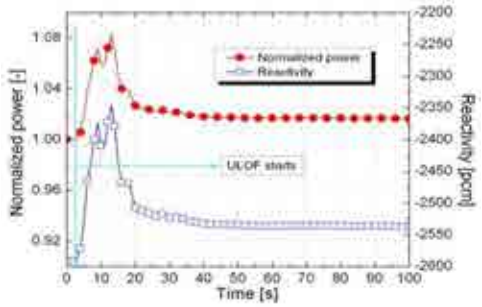


*FIG. 4.184. Power and reactivity transients (CERCER EFIT).*

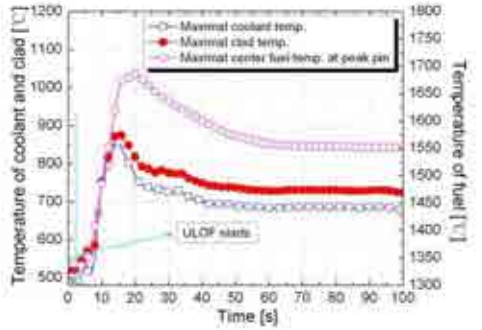


*FIG. 4.185. Temperature levels for fuel, clad and coolant in a ULOF (CERCER EFIT).*

(b) UBA Analyses

For the blockage accidents, in case of pin failures, the local release of helium, which may cause voiding and a reactivity increase and swing, could be a concern in an ADT, as no limiting Doppler effect is available during a transient. Analyses have however shown the mitigating potential of a fuel sweep out effect.

In SIMMER-III code simulations, the following assumptions are defined. The blockage location in both MgO-CERCER and Mo92-CERMET cores are chosen at the core inlet of the first fuel ring and the coolant mass flow rate reduce to 6.5% in the blocked channel. The clad will first fail at around 1100 K which causes a gas blowout but the fuel is still covered by the clad and clad removal is assumed to occur at around 1700 K, the clad melting temperature. The fuel then is assumed to break up into fuel chunks. Can-wall temperatures are also in the range close to melting in the current simulation. With the current assumptions, both cores show a similar behaviour during UBA. Fig. 4.186 shows the power and reactivity transients during an UBA in the MgO-CERCER core; in Fig. 4.187 the material redistribution is displayed.

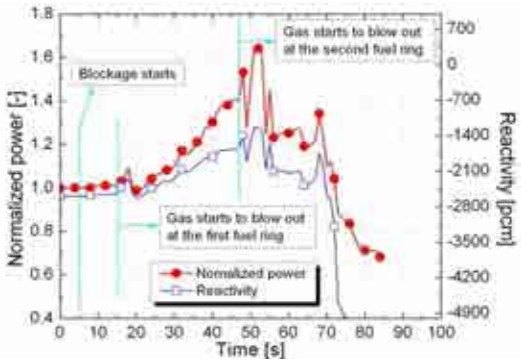


*FIG. 4.186. Power and reactivity transient in an UBA (CERCER EFIT).*

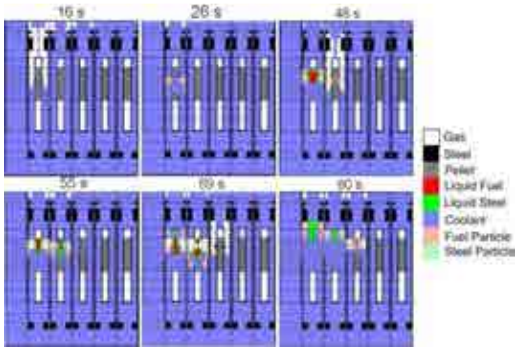


*FIG. 4.187. Material distribution and released fuel particle distribution in the first three fuel rings (CERCER EFIT).*

The scenario is as follows. When the clad temperature arrives at 1120 K, the clad fails and a fission gas He blown down takes place which causes a positive void effect and, in turn, a power and reactivity increase. Fortunately, the positive void does not induce a very significant reactivity—power increase. And hereafter with the fuel pin failure, broken fuel particles are first blocked but after damage propagation into the neighboring subassemblies (hexcan failure) can be swept out, as shown in Fig. 4.187, which finally decrease the power and reactivity. The decrease of power is limited in a source driven system but helps to allow for a longer grace time to shut down the beam before significant damage propagation might take place. The analyses identified the influence of the failure temperatures of the cladding (failure temperature for gas blowndown and temperature for release of fuel pellets or chunks from pellet stack), the behaviour of the pellets and the influence of the upper pin and bundle structures. The new born fuel particle size and the clad removal temperature have significant influence on the inherent fuel sweep out mechanism. Therefore, the clad and fuel behaviour at the high temperature range should be experimentally understood.

*4.11.1.6. Possible safety measures and improvements*

To cope with the fuel safety issues of an ADS one might respect or might optimize some design measures, which however have to take into account several boundary conditions to be respected e.g. for transmutation efficiency (given in parenthesis below). Generally a highly reliable detection and beam shutdown system is required.

- Adequate subcriticality (the limits of accelerator power and the core power form factors);
- Linear power limitation (power to melt ratio-melt ratio);
- Choice of Pu:MA ratio, TRU content in matrix and matrix material for improving reactivity worth potential and generate a moderate prompt temperature feedback effect (transmutation strategy, transmutation capability, CERMETs for void reduction with core optimization);
- Void reduction measures by introducing B4C layers above–below the core or add empty space above core (design and neutronics, local power peaking);
- Limitation of subassembly size for limiting fuel worth and impact of local perturbations (core steel volume fraction);
- Helium release impedance by installing in-pin orifices to limit gas blowndown in case of local pin failure (pin construction);
- Guarantee natural convection paths under fuel relocation conditions (plant design).

The analyses performed for the CERCER and the CERMET cores demonstrate the general high safety potential of an ADS like the EFIT. The safety analyses reveal that the most limiting conditions in design and safety are mostly related to the T91 clad and not to the innovative fuels.

*4.11.1.7. Analysis tools*

For an adequate simulation of the rather complex questions related to the ADS safety, elaborate code systems are needed. The SIMMER code family developed by an international team (JAEA, FZK, CEA, IRSN and ENEA) seems to be the adequate platform in this respect. SIMMER-III is a two dimensional (2-D), SIMMER-IV a three dimensional (3-D), multi velocity field, multi phase, multi component, Eulerian fluid dynamics code coupled with a structure model including fuel-pins, hexcans etc., and a space, time and energy dependent neutron transport theory dynamics model. The advantage of the SIMMER system is its unique potential to simulate a transient from its initiation up to possible pin failure, core material redistribution and finally up to in-vessel phenomena. Thus the whole range of the defense in depth categories can be followed and the phenomena mentioned before can be simulated mechanistically and consistently. Therefore SIMMER is described in some detail in this paragraph. The overall SIMMER fluid dynamics solution algorithm is based on a time factorization approach, in which intra-cell interfacial area source terms, heat and mass transfers, and the momentum exchange functions are determined separately from inter-cell fluid convection. In addition, an analytical equation of state (EOS) model is introduced to close and complete the fluid dynamics conservation equations. The structure model represents the configuration and the time dependent disintegration of fuel pins and subassembly can walls. A simple fuel-pin (SPIN) model, in which the fuel pellet is represented with surface and interior temperature nodes, is available, where the breakup of structure components is based on thermal conditions and no mechanical failure is modeled. An advanced pin model for MOX fuels (detailed fuel-pin model: DPIN) including mechanical failure modes has been successfully developed. In neutronics, the transient neutron flux distribution is calculated with the improved quasi-static method. For the space dependent part, a TWODANT or THREEDANT based flux shape calculation scheme (transport theory) has been implemented. Three geometrical mesh grids (fluid dynamics, pin structure, neutronics) and three time step hierarchies (neutron flux shape, reactivity-heat transfer and fluiddynamics / nuclear power) are applied.

For simulating the ADSs, quite a number of model improvements had to be made. Starting with neutronics, a space energy time dependent external neutron source has been implemented into SIMMER. Various weighting functions can be applied in the quasi-static scheme (mainly $\lambda$ and $\alpha$ weighting is applied.). The quasi-static option is especially important for more severe transients e.g.

including partial voiding of the core or reactivity changes, because of the related changes in the power and flux profiles. The source importance is calculated transiently too, as the influence of the source might change during a severe accident with material (fuel) relocation. A new cross-section processing system C4P, based on a 545 group master library has been recently developed for the ADS simulations. A new fuel pin model reflecting the conditions of CERCER and CERMET heterogeneous fuels is under development. For these new fuels also new equations of state extending into the high temperature range have to be generated. These fuels show a rather complicated behaviour in the high temperature range, including issues as dissociation and eutectic formation. Due to the lack of high temperature data the extrapolation into this high T regime is based on MOX fuel. In addition new equations of state are available for Pb-Bi and Pb. Other new models describe the melting of clad under heavy liquid metal (HLM) flow and the blowdown of fission gases and helium after pin failure and general two phase flow in heavy metal liquids. The blowndown model describes the gas flow from the upper and lower plena to the pin-failure location and the gas injection into the coolant. Based on experiments discussed in, the multi phase model in SIMMER has been extended to simulate capsize bubbles characteristic for gas in heavy liquid metal flow. For achieving a high accuracy in the relative motion of the various constituents under accidental conditions and HLM flow, the number of independent velocity fields has been increased to eight. With the new developments, both critical and subcritical systems for transmutation can be well described, also helping to define necessary experiments, especially in the domain of new fuels.

Other codes and code system are in use to assess the safety behaviour of ADSs. An elaborate code system is e.g. the SAS code. Other codes are mainly used to describe the system and plant behaviour, also long time behaviour but excluding failure conditions. Codes of this type are e.g. SIM-ADS, RELAP or SITHER.

The SIM-ADS code is a PC based; multi node point kinetic model that describes the nuclear and thermalhydraulic characteristics of critical and subcritical reactor cores. Two separate neutronic core models are run simultaneously, namely a single node PK model that acts as driver for a multi node (16 axial nodes) thermohydraulic model, and a multi node neutronic model (16 axial neutronically coupled nodes) which allows the axial power profile to change during the transient according to nodal temperature and nodal reactivity variations. In the single node PK neutronic model, the axial power profile is assumed to remain unchanged during the transient. Under normal, simple transient conditions that are not dependent on a transient axial power profile, both neutronic models (single node and 16 axial nodes) should yield identical results in core averaged parameters, thereby serving as a constant calculational cross check. The neutron kinetics of each nuclear model is described by 6 delayed neutron precursor groups on the nodal level, and a complete set of nodal dependant reactivity feedback coefficients such as Doppler, coolant, fuel expansion, diagrid expansion, void, control rod, Xenon (for thermal reactors), etc. The nodal time characteristics of the decay heat after shutdown is described by 6 decay heat groups. The 16 axial node, full scope thermalhydraulic model assumes an initial axial radial power distribution (provided as input to the kinetics models by the detailed neutronic analysis performed during the design phase of the core), and then calculates the radial heat transfer through a typical fuel pin consisting of the detailed description of the heat transfer mechanisms between cladding and coolant, the heat transfer through the clad material, the heat transfer in the gap between clad and fuel, and the fuel matrix itself assuming appropriate material property data and applicable coolant type dependant heat transfer correlations (correlation for Nusselt numbers, friction factors, etc.). This heat transfer analysis is performed for the peak pin and the average pin of the core where the radial core power distribution is assumed to be represented by radial power form factors. The primary loop is nodalized into several appropriate hydraulic nodes with corresponding volumes, internal masses and surface areas (lower vessel plenum, the 16 axial core nodes, upper vessel plenum, the piping to and from the HX, (HX and DHRS itself are modeled by appropriate internal nodalization)) to account for all relevant thermalhydraulic effects including radiation (from vessel wall) to the ambient and all relevant pressure loss calculations inside the core region (i.e. due to grid or wire wrap spacers) and the primary system (heat exchangers, pumps, loops, etc). Particular attention is placed on the correct formulation of all relevant heat transfer mechanisms between cladding surface and coolant (such as for example roughened surface areas) in the core region and in the HX and DHRS systems, in particular accounting for the physical phenomena

encountered in various flow regimes (i.e turbulent and laminar flow under forced flow and natural convection conditions) for heavy metals (Na, or Pb, or LBE), water or gas coolants (He, Air or $CO_2$).The codes system SIM-ADS has been used to perform the transient analysis of both the LBE cooled and He cooled PDS-XADS designs during the PDS-XADS Project and during the MOST molten salt project to analyze the AMSTER molten salt reactor design. SIM-ADS has been tested and validated extensively against actual LWR plant data (plant transient data) for both PWRs and BWRs, Superphenix (SPX1) plant data, and by code to code comparisons of results obtained using RELAP, SAS4A, TRAC and other large transient code systems.

The thermalhydraulic code RELAP5, originally developed, under NRC contract, by INEEL for LWRs LOCA analysis, has been extensively validated and is actually used worldwide as a best estimate code for LWRs transient analysis. This code was chosen in the frame of the Italian research programme on ADS (TRASCO) as the reference code for the thermalhydraulics analysis of Pb and Pb-Bi cooled ADS. Several original RELAP routines have been updated in order to implement suitable correlations generating the reference physical and thermodynamic properties for Pb and Pb-Bi. Similarly, some specific heat transfer correlations for liquid metals have been added. New correlations for the evaluation of thermal conductivity, surface tension and fluid viscosity have been introduced. The correlations for the liquid phase have been assumed also for the vapour phase because two phase conditions for liquid metals are not expected in ADS like systems. Convective heat transfer coefficient is evaluated according the so-called Seban-Shimazaki correlation in pipe configuration or the Subbotin Ushakov correlation in tube bundle configuration. The introduced modifications give also the possibility to consider steam as a non-condensable gas when the evaluation of its physical properties, for instance density, is performed. A number of routines have also been entirely developed to calculate thermodynamics properties as a function of temperature and pressure and, in particular, in order to provide temperature and pressure points for calculating the physical properties of Pb and Pb-Bi according to the soft sphere model.

The RELAP5 thermalhydraulic code was coupled to the neutronic code PARCS to evaluate the dynamic behaviour of ADS. The neutronic code PARCS, originally developed, under NRC contract, by Purdue University School of Nuclear Engineering, solves the time dependent, two group, neutron diffusion equation in tridimensional Cartesian geometry by using an hybrid scheme based on analytical nodal method (ANM) and nodal expansion method (NEM). The code can provide $k_{eff}$ calculation and simulation of a large number of transients, originated both by control rod movements and by thermalhydraulic or neutronic events. The possibility of using the coupled code RELAP5-PARCS for the analysis of fast spectra subcritical systems required, first of all, the external neutron source terms being introduced in neutron diffusion equations and, secondly, an estensive modification of the same neutron diffusion equations in order to deal with fast spectra. Several PARCS routines were modified for taking into account the neutron external source. All the routines controlling the time integration algorithm, setting the initial values of the time dependent constants and evaluating the total source of neutrons as a function of time in the transient fixed source problem scheme were modified. The possibility of dealing with fast spectra systems has required a large modification of the original code concerning the initialization, input, output and, especially, operating subroutines. As for RELAP5 modifications also PARCS modifications were made according the logic and the format of the original version. These let the modified coupled code RELAP5-PARCS deal with Pb and Pb-Bi cooled, fast spectra, subcritical systems such as ADS.

Activities concerning the qualification of the RELAP5 T/H code modified for ADS analysis started in 2004. The modifications, that mainly concern Pb and Pb-Bi physical properties and thermal exchange correlations, have been validated against experimental data. The qualification was mainly based on experimental programme carried out at ENEA Research Centre of Brasimone (Italy) on support of XADS design and MEGAPIE experiment.

An experimental campaign was conducted on CIRCE (CIRCuito Eutettico), the largest facility for heavy liquid metal technology development (Fig. 4.187), to provide experience on thermalhydraulic and material behaviour in a pool configuration. Two series of tests were carried out in CIRCE to verify the performance of the LBE circulation enhanced by argon gas injection that was one of the main peculiarity of the XADS design. The experimental loop characterization, in term of argon mass

flowrate injected LBE mass flowrate entrained, was previously supported by a test for calibrating the device chosen for the LBE mass flowrate measurements (Venturi nozzle). The RELAP5 simulation of the calibrating tests, besides confirming the code capability to simulate LBE flow in presence of free level, allowed assessing the Venturi nozzle nodalization implemented in the overall model of the gas lifting test.

Post-test calculations for the CIRCE gas lifting test were performed. The characteristic curve predicted by RELAP5 was compared with the experimental curve. Due to the lack of information on the real pressure drops in the loop, it was impossible to evaluate the origin of the quasi-constant discrepancy between the LBE mass flowrate calculated by RELAP5 and the experimental data. A subsequent experimental campaign showed to be more reliable. In fact the discrepancies ranged between 1% and 19% (see Fig. 4.189), which appeared to be quite acceptable owing to the occurrence of instability phenomena declared by the experimental researchers for lowest values of argon mass flow rate. Another step of the RELAP qualification concerned the experimental campaign performed on CHEOPE (CHEmical OPErational transient) facility in order to measure the thermal exchange characteristics between the lead-bismuth eutectic alloy and the heat removing fluid (diathermic oil) in a single element of the 12 exchanger elements foreseen for the experimental installation MEGAPIE (PSI-CH). The tests carried out on the plant aimed at simulating the behaviour of a single element of the 12 exchanger elements foreseen for the experimental installation MEGAPIE. In this case the comparison between experimental results and post-test calculations allowed the validation of the heat exchange correlations for liquid metal introduced in the modified version of RELAP5. The correlation used for the convective heat transfer on LBE side appeared sufficiently adequate, whereas a dedicated correlation was implemented in the code for the heat transfer on oil side.

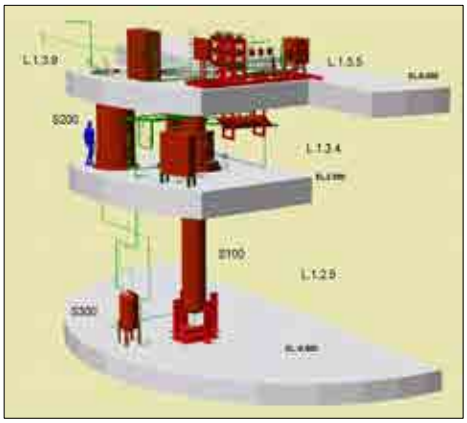

*FIG. 4.188. Isometric view of the CIRCE facility.*

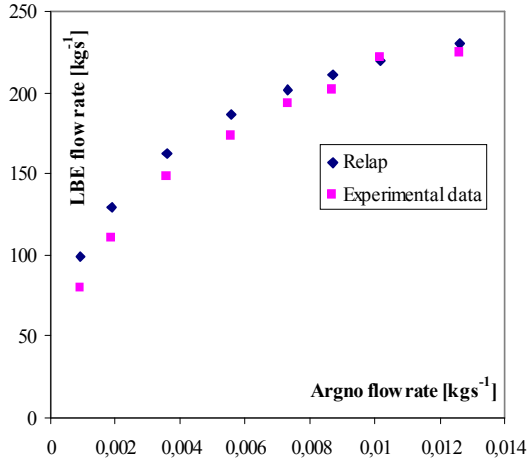


*FIG. 4.189. Comparison between calculated and experimental LBE versus argon flowrate at T = 200 °C.*

The post-test analysis calculations of the MEGAPIE experiment conducted in SINQ spallation neutron source (PSI, Ch) have confirmed the adequacy of the heat exchange correlations to predict the LBE-Oil Heat Exchanger (THX) performances in a larger range of mass flowrates and temperatures. Moreover, the RELAP5 capability in simulating the thermalhydraulic performance of the cooling system has been demonstrated both in steady state and in transient conditions, as showed by the loop temperature evolutions in Fig. 4.190.

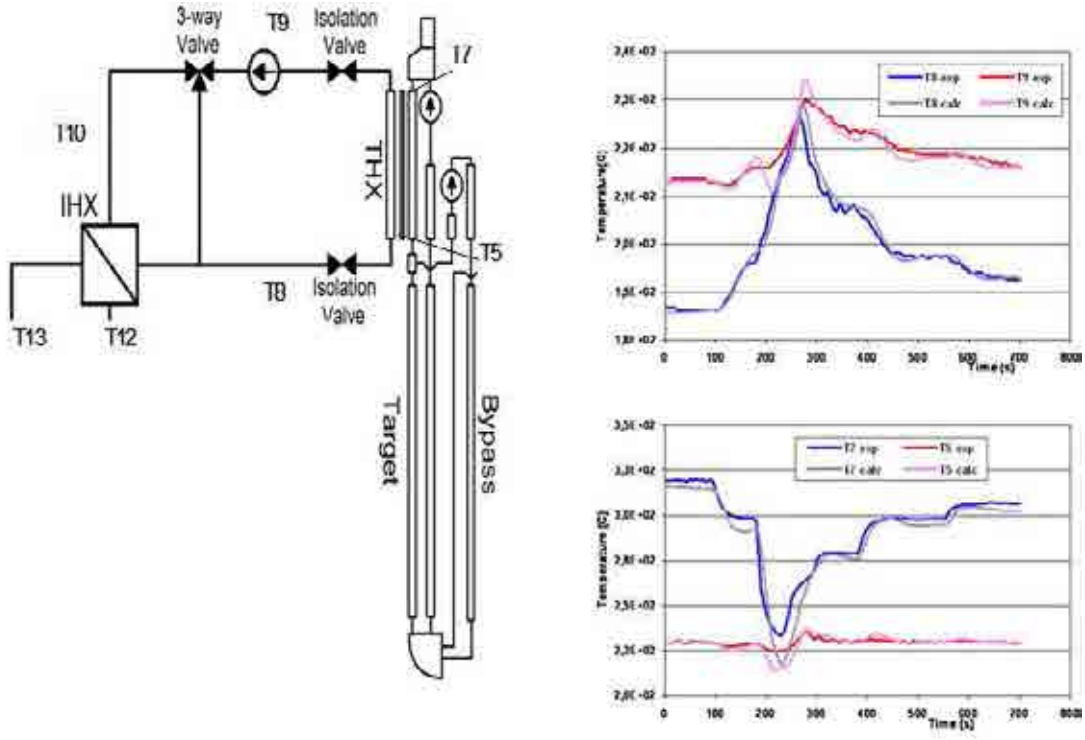


*FIG. 4.190. a) SINQ loop layout b) THX LBE and oil temperatures.*

Further validation activities are planned in the near future on the basis of a new experimental programme foreseen on the CIRCE facility, namely the Integral Circulation Experiment (ICE), regarding the investigation of Pb natural circulation in a pool type ADS loop and heat exchange in steam generators. Moreover, the large scale Pb-Bi coolant loop test facility HELIOS (Heavy Eutectic liquid metal Loop for Integral test of Operability and Safety of PEACER ) of the Seoul National University in the Republic of Korea will be used as the reference of the benchmark study of the WPFC Expert Group on LBE Technology: Benchmarking of Thermalhydraulic Loop Models for lead Alloy Cooled Advanced Nuclear Energy Systems (LACANES). This benchmark study will characterize the thermalhydraulic behaviour of the LACANES under the various operational conditions, which is critical for the development of such nuclear systems. The HELIOS experiment comprises the isothermal steadystate forced convection and non-isothermal natural circulation cases.

The modified versions of RELAP5 stand alone and RELAP5-PARCS coupled codes have been widely used for accidental transient analysis of Accelerator Driven Systems (ADS), such as XADS and EFIT, within the participation in European research programmes. Their use is also planned for the safety studies of the European lead cooled System (ELSY) within the IV EU Framework Programmes. The XADS reactor design has been developed within the PDS-XADS Project of V Framework European Programmes on Partitioning & and Transmutation. The XADS reactor is a pool type reactor cooled by LBE (lead bismuth eutectic). The natural circulation of LBE in the primary circuit is enhanced by gas injection. The core power, 80 MWth, is removed by two secondary loops filled by organic diathermic oil in forced circulation through four heat exchanger immersed in the primary pool, and, finally released to the atmosphere by air coolers in forced circulation. A wide set of enveloping plant specific transients were selected to assess the intrinsic safety characteristics of the reactor. These transients were categorized into Protected Transients and Unprotected Transients, depending on the proton beam shut off takes place or not upon request by the protection system. The XADS response to protected transients has been analyzed with the stand alone RELAP5 code, as the mutual interaction between neutronics and thermalhydraulics can be neglected being the temperature excursion limited by the protection system. Differently, due to large temperature excursion, the

unprotected transients have been analyzed with the coupled RELAP5-PARCS code, in order to take into account significant core reactivity feedbacks.

The following protected transients have been analyzed with RELAP5:

— Loss of enhanced and forced circulation in primary and secondary systems with six to one air coolers working in natural circulation (PLOF);

— Loss of enhanced and forced circulation in primary and secondary systems without air coolers (PLOF+PLOH). In this accident, due to the loss of heat sink, the core decay power is removed only by the RVACS (Reactor Vessel Air Cooling System). Fig. 4.191 illustrates the time evolution of temperatures calculated by RELAP5 code;

— Spurious accelerator beam trips of different length (0.5–10 s) followed by power restart, which simulate a malfunction of the accelerator control.

The following unprotected transients have been analyzed with RELAP5-PARCS:

— Loss of enhanced and forced circulation in primary and secondary systems with air coolers in forced circulation (ULOF);

— Loss of enhanced and forced circulation in primary and secondary systems without air coolers (ULOF+ULOH). Fig. 4.192 illustrates the time evolution of temperatures calculated by RELAP5-PARCS code;

— Partial LBE flow blockage in the hottest fuel assembly of the core without heat exchange with surrounding fuel assemblies;

— Accelerator current jump to 200% from HFP (Hot Full Power) and to 100% from HZP (hot zero power) conditions.

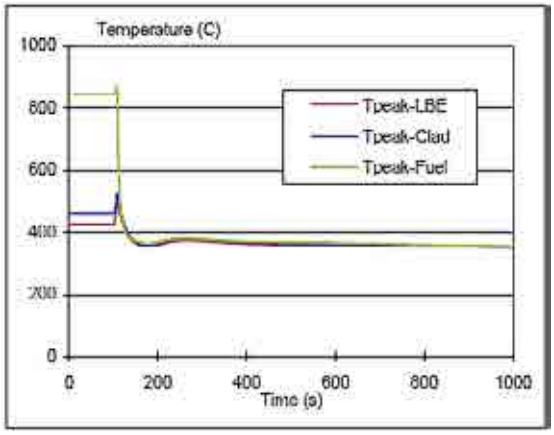


*FIG. 4.191. PLOF+PLOH transient results for XADS: time evolution of peak fuel, clad and coolant temperatures.*

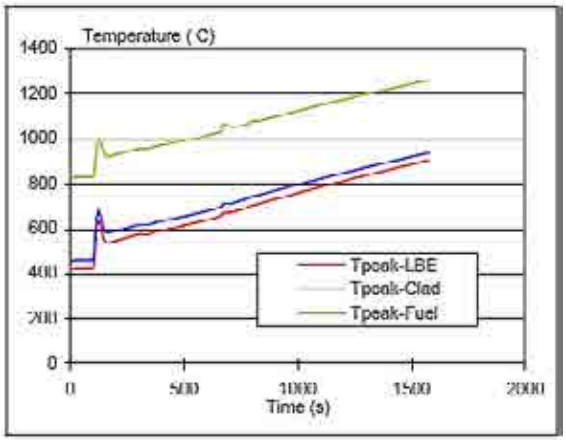


*FIG. 4.192. ULOF+ULOH transient results for XADS: time evolution of peak fuel, clad and coolant temperatures.*

The results of the accidents analyzed showed that the LBE cooled XADS is a very robust design. This conclusion was confirmed by all results of the protected transient analyses that showed temperatures well below the safety limits. Instead, some unprotected scenarios showed very high temperature values and clad melting could occur in the peak channel, but however the calculations estimate a large grace time period for these transients, thanks to the high thermal inertia of the primary system. Similar analyses are under way for the EFIT reactor. Protected and unprotected transients are being analyzed with RELAP5 stand alone and RELAP5-PARCS coupled codes respectively.

The results of protected transient analyses have shown good EFIT performances in withstanding core and vessel temperatures below safety limits even in the worst cases of total loss of heat sink or total loss of forced circulation in the primary system. In particular, the DHR system is able to face up PLOH accidents with limited increase in core and vessel structure temperatures. In case of unprotected transients, such as the ULOF, the grace time period is large enough to bring the plant in safe conditions without significant core damage.

#### *4.11.1.8. Conclusion*

The transmutation technology with accelerator driven systems introduces a formidable chance to reduce the amount and toxicity of radioactive waste. Various innovations are realized and require significant research and development efforts. The innovations also require a new look from the safety point of view. The safety objectives common to all approaches for future nuclear plants, including accelerator driven systems and transmuters (ADT), are the protection of individuals, the society and the environment from harm of radiological hazards, the assurance of that radiation exposure of all operational states is kept below prescribed limits and as low as reasonably achievable (ALARA principle) and that all reasonably practicable measures are taken to prevent accidents in nuclear installations and to mitigate their consequences, are achieved through the application of the defence in depth strategy.

The general safety approaches for future nuclear reactors have been proposed for application in the conceptual design phases of the PDS-XADS (5th FP of the EU) and also for the XT-ADS and EFIT (6th FP of the EU) taking into account the specifics of accelerator driven systems. In Europe, these enhanced safety approaches have been defined for:

— For Light Water Reactors (LWRs). The safety approach is defined in the European Utilities Requirements and has been applied during the design phase of the European Pressurized Reactor (EPR), which project has been presented to the French and German safety authorities.

— For Liquid Metal Fast Reactors (LMFRs). The safety approach has been defined for the European Fast Reactor. It has been examined by a European group consisting of national licensing experts.

The respective safety approaches are not completely similar but for these two reactor system types (EPR, EFR), the basic safety principles and objectives are consistent with the existing IAEA recommendations.

One of the key safety issues is the safety of the new fuels under the boundary conditions of the system dynamics of an ADS and the heavy metal cooling. Analyses are performed to identify open issues and provide adequate solutions. For the new ADT fuels the knowledge base has to be significantly expanded compared to the ordinary oxide fast reactor fuel under sodium cooling conditions. Important safety relevant points in this respect are e.g. the high temperature behaviour, the helium release problem, the large reactivity worth potentials, especially the coolant void worth and the lacking Doppler effect. For the fuels itself a broad technological programmes has to be launched. This must include investigation of (1) the fundamental material properties up into the high temperature range, (2) the irradiation behaviour, (3) the interaction–reaction between fuel, clad and coolant, (4) the fuel and fuel pin behaviour under transient conditions. A sound fuel characterization for steady state and transient conditions has to be developed and failure criteria have to be derived for accident scenarios. A sufficient experimental capability, both out of pile and in-pile, has to be provided to tackle these issues. In addition the analytical capability (integrated accident code development) has to be significantly extended, including the modeling of the new fuels, covering new phenomena and scenarios.

### 4.11.2. Safety Analyses of JAEA-ADS in Japan

#### *4.11.2.1. Introduction*

It is considered that the ADS is safer than conventional critical nuclear reactors because the operation of the ADS is able to be stopped by the shutdown of the accelerator. Meanwhile, it is important to comprehend transients at the failure of the proton beam shutdown for the discussion of the ADS inherent safety. To investigate transients at such unprotected accidents, safety analyses for the JAEA ADS [4.305] were performed.

#### *4.11.2.2. Calculation condition*

(a) Calculation model

In this analysis, the reference model of lead-bismuth (LBE) target-cooled ADS proposed by JAEA was employed (Fig. 4.193). Main parameters are shown in Table 4.52. Fig. 4.194 shows the calculation model for the safety analysis.

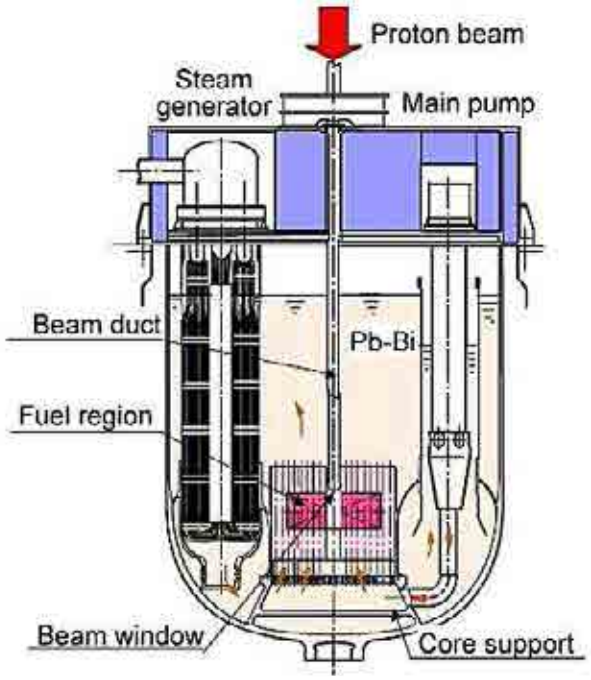


*FIG. 4.193. Conceptual view of JAEA-ADS.*

TABLE 4.52. MAIN PARAMETERS FOR THE REFERENCE DESIGN

| | | |
|---|---|---|
| Plant | Thermal power | 800 MWt |
| | Coolant | LBE |
| | Inlet temperature | 300°C |
| | Coolant velocity | 2.0 m/sec |
| | Upper limitation of $k_{eff}$ | 0.97 |
| | Operation period | 600 EFPDs* |
| Fuel assembly | Type | Hexagonal ductless |
| | Number of fuel assemblies | 84 |
| | Pitch | 233.9 mm |

| | | |
|---|---|---|
| Fuel | Width | 232.9 mm |
| | Number of fuel pins per assembly | 391 |
| | Number of tie rods per assembly | 6 |
| | Composition | (MA+Pu)N+ZrN |
| | Pu enrichment (inner–outer) | 15.1–21.3 wt% |
| | ZrN ratio (inner–outer) | 49.7–49.7 wt% |
| | Theoretical density | 90% |
| | Smear density | 85% |
| | Pin outer diameter | 7.65 mm |
| | Thickness of cladding tube | 0.5 mm |
| | Pin pitch | 11.48 mm |
| | Active height | 1000 mm |

(b) Calculation code

SIMMER-III was employed for the safety analysis. SIMMER-III is an advanced safety analysis code, which has been developed to investigate postulated core disruptive accidents in fast reactors (FRs) [4.306]. SIMMER-III is a two dimensional three velocity field, multi phase, multi component, Eulerian fluid dynamics codes coupled with a structure model and a space, time and energy dependent neutron kinetics model. The latest version of SIMMER-III is available to analyze the LBE cooled ADS by adding features to treat the external source, the subcritical state and properties for the LBE [4.307]. For properties of (MA+Pu) nitride fuel, properties for nitride uranium and plutonium (UN and PuN) investigated in the feasibility study on commercialized fast reactor systems [4.308] were used as alternative data.

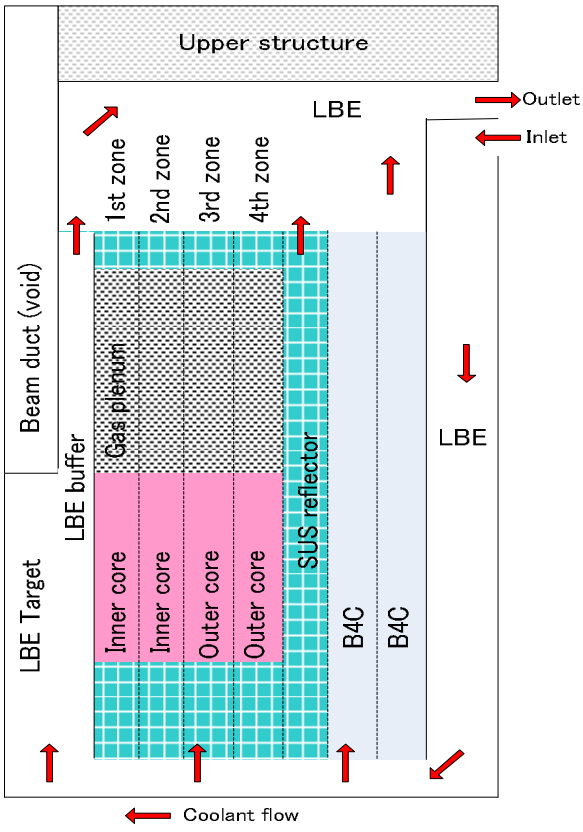


*FIG. 4.194. Calculation model for safety analysis.*

(c) Calculation case

As typical accident scenarios, following two cases were analyzed by SIMMER-III code; unprotected beam overpower (UBOP) and unprotected loss of flow (ULOF) [4.309]. In this study, the word 'unprotected' means no shutdown of the proton beam during severe sequences.

*4.11.2.3. Result and discussion*

(a) Unprotected Beam Overpower (UBOP)

The beam overpower is considered as an inherent accident for the ADS. The proton beam current required for the reference ADS changed from 10.2 to 20.3 mA during the burnup cycle [4.310]. Based on this specification, a transient with doubled intensity of the external neutron source was analyzed.

The change of the core power for UBOP is presented in Fig. 4.195 the power was increased up to about 205% within at 1sec by the doubled intensity of the external neutron source. Fig. 4.196 and Fig. 4.197 show the fuel and fuel pin temperature changes, respectively, for the assembly in the nearest position from the target region. The maximum temperatures of the fuel and the fuel cladding were 2500°C and 900°C, respectively, though they were 1450°C and 609°C in normal operation. From these results, it was found that there was no possibility to occur a pin failure with the doubled intensity of the external neutron source since the melting points of the nitride fuel and the fuel pin (SS316) are 2780°C and 1400°C, respectively.

In Fig. 4.197 the maximum temperature at the surface of the fuel pin was 456°C at 0 sec, meanwhile, that was 500°C at the beginning of the first cycle in the neutronics design. The reason of this difference was a difference of a method to calculate the temperature at the surface of the fuel pin. In the neutronics design, the fuel pin temperature was calculated based on an analytical calculation of a single pin and uniform flow. In the safety calculation, on the other hand, the fuel pin temperature was calculated based on the fluid dynamics calculation with detailed models and material properties. In this calculation, the cross flow in the duct less assemblies was also considered.

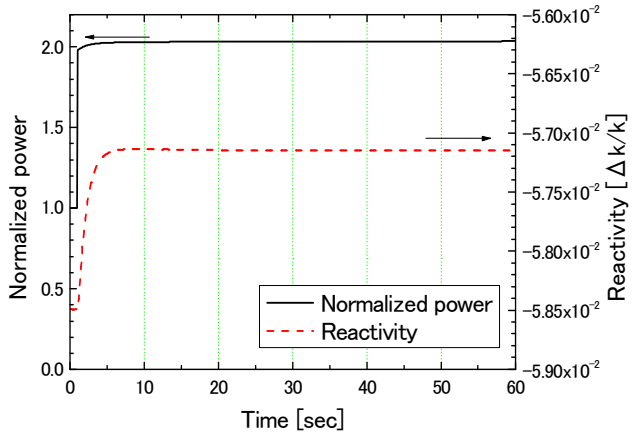


*FIG. 4.195. Power change (UBOP).*

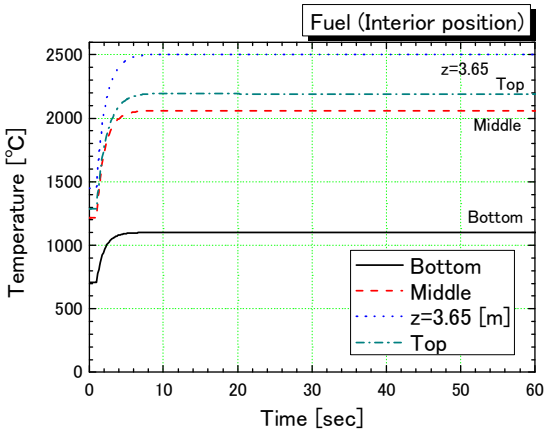


*FIG. 4.196. Fuel temperature changes (UBOP).*

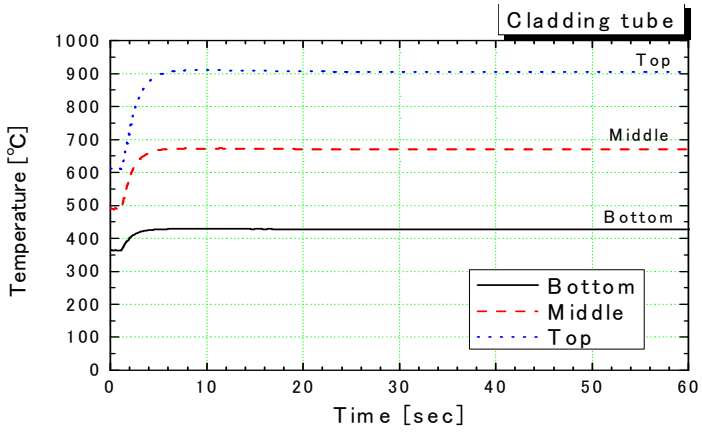


*FIG. 4.197. Fuel pin temperature changes (UBOP).*

(b) Unprotected Loss of Flow (ULOF)

It is expected that a transient of loss of flow with the unprotected state is one of the severest sequences for the ADS. In this study, the ULOF analysis was performed to confirm whether the pin failure would occur in the ADS. In the analysis, the coast down of a pump was assumed from 0 sec to 20 sec.

The change of the power for ULOF is shown in

FIG. 4.198. The power was increased by about 3.8% at 20 sec and slightly decreased due to a coolant natural convection.

FIG. 4.199 and Fig. 4.200 show the fuel and fuel pin temperature changes. The maximum temperature of the fuel reached 1140°C and that of the fuel pin reached 910°C. These analysis results indicated that there was very little possibility of core disruptive accidents in the ADS at the ULOF accident since both the fuel and the fuel pin temperatures were lower than their melting points.

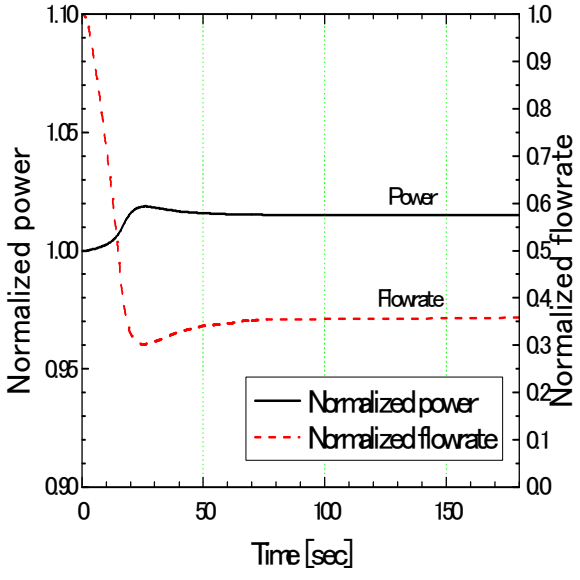


*FIG. 4.198. Power and flow rate changes.*

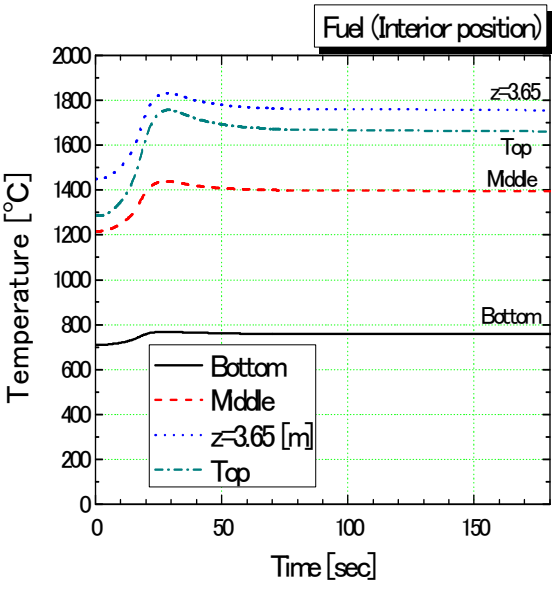


*FIG. 4.199. Fuel temperature changes (ULOF).*

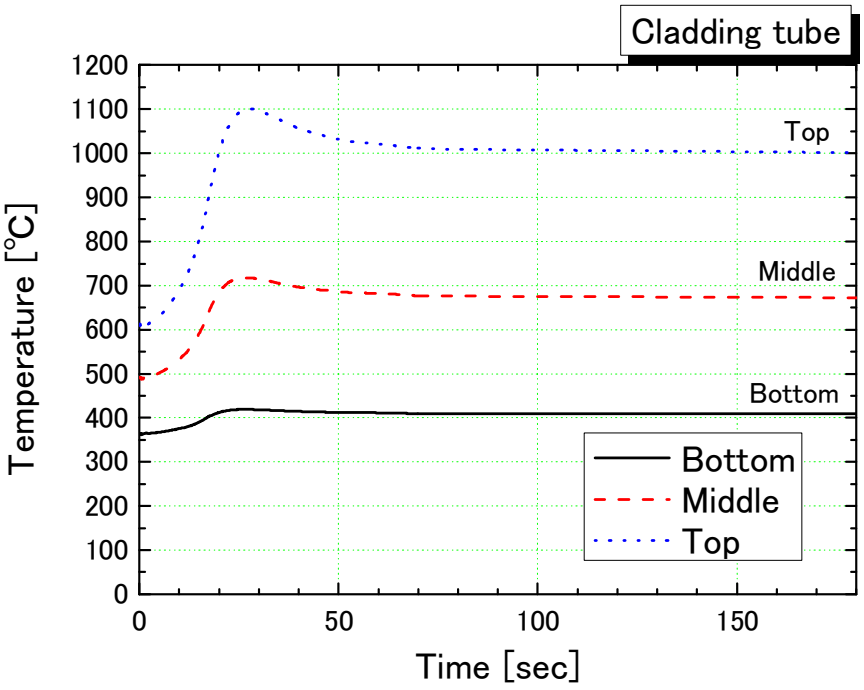


*FIG. 4.200. Fuel pin temperature changes (ULOF).*

## 4.12. REFERENCES TO CHAPTER 4


[4.1] VOROZHTSOV, S.B., SHAKUN, N.G., Orbit Parameters in the central Region of the JINR Phasotron. Microbunch Acceleration, Technical Report JINR-R-9-83-658, Joint Inst. for Nuclear Research, Dubna (September 1983).

[4.2] MOSES, D.L., et al., Plutonium disposition in the BN-600 fast neutron reactor at the Beloyarsk nuclear power plant, Nucl. Instr. & Meth. Phys. Res., A 414 (1998) pp 28–35.

[4.3] OIGAWA, H., et al., Concept of transmutation experimental facility, Proc. of the 4th Int. Workshop on the Utilization and Reliability of High Power Proton Accelerator, Daejeon, Republic of Korea, 16–19 May 2004, Korea Atomic Energy Research Institute (2005), pp. 507-517.

[4.4] SASA, T., et al., Design study of the J-PARC transmutation experimental facility, Proc. GLOBAL 2005, Tsukuba, Japan, 9–13 October 2005 (Ed.: Hajimu Yamana), Atomic Energy Society of Japan, ISBN: 4-89047-133-2.

[4.5] DI GABRIELE, F., DOUBKOVÁ, A., Sensitivity to environmental assisted cracking of steels in contact with lead alloys, paper presented in the 1st Int. Conf. Corrosion and Material Protectionm Prague, Czech Republic, 1–4 October 2007.

[4.6] DI GABRIELE, F., DOUBKOVÁ, A., HOJNÁ, A., Investigation of the sensitivity to EAC of Steel T91 in contact with liquid LBE, J. Nucl. Mat., 376, Issue 3 (2008) pp. 307–311.

[4.7] DOUBKOVÁ, A., DIGABRIELE, F., BRABEC, P., KEILOVÁ, E., Corrosion behaviour of steels in flowing lead-bismuth under abnormal conditions, J. Nucl. Mat., 376, Issue 3 (2008) pp. 260–264.

[4.8] ILINČEV, G., Research results on the corrosion effects of liquid heavy metals, Pb, Bi and Pb-Bi on structural materials with and without corrosion inhibitors, Nucl. Engin. Des, 217 (2002) p. 167.

[4.9] ILINČEV, G., KÁRNÍK, D., PAULOVIČ, M., DOUBKOVÁ, A., The impact of the composition of structural steels on their corrosion stability in liquid Pb-Bi at 500 and 400°C with different oxygen concentrations, J. Nucl. Mat, 335 (2004) p. 210.

[4.10] ILINČEV, G., KÁRNÍK, D., PAULOVIČ, M., DOUBKOVÁ, A., The effect of temperature and oxygen content on the flowing liquid metal corrosion of structural steels in the Pb-Bi eutectic, Nucl. Engin. Des, 236 (2006) p. 1909.

[4.11] KOBZOVÁ, A., UJV DITI 302/457 Corrosion tests Hot spot simulations summary for deliverables D4.20, Internal report (September 2007).

[4.12] KOBZOVÁ, A., DI GABRIELE, F., KEILOVÁ, E., BRABEC, P., Corrosion and mechanical properties of ferritic martensitic steel T91 in LBE, Corrosion and material protection, 3 (2007) p. 51.

[4.13] KNEBEL, J., et al., Design and corrosion study of a closed spallation target module of an accelerator driven system (ADS), Nuc. Eng. Des., 202, 2–3 (2001) p. 279.

[4.14] VELLA (Virtual European Lead Laboratory), EU-Contract no. VELLA-FP6-036469 (2006).

[4.15] AIELLO, A., AZZATI, M., BENAMATI, G., GESSI, A., LONG, B., SCADDOZZO, G., Corrosion behaviour of stainless steels in flowing LBE at low and high oxygen concentration, Journal of Nuclear Materials, 335, Issue 2 (2004) pp. 169–173.

[4.16] CIAMPICHETTI, A., AGOSTINI, P., BENAMATI, G., BANDINI, G., PELLINI, D., FORGIONE, N., ORIOLO, F., AMBROSINI, W., LBE water interaction in subcritical reactors: first experimental and modelling results, paper presented in IV Workshop on materials for HLM cooled reactors and related technologies, Rome, Italy, 21–23 May 2007.

[4.17] CINOTTI, L., The Pb-Bi Cooled XADS Status of Development, paper presented in II Int. Workshop on Materials for Hybrid Reactors and Related Technologies, Bologna, Italy, 18–20 April 2001.

[4.18] AMBROSINI, W., AZZATI, M., BENAMATI, G., BERTACCI, G., CINOTTI, L., FORGIONE, N., ORIOLO, F., SCADDOZZO, G., TARANTINO, M., Testing and qualification of CIRCE instrumentation based on bubble tubes, Journal of Nuclear Materials, 335 (2004) pp. 293–298.

[4.19] AGOSTINI, P., ALEMBERTI, A., AMBROSINI, W., BENAMATI, G., BERTACCI, G., CINOTTI, L., ELMI, N., FORGIONE, N., ORIOLO, F., SCADDOZZO, G., TARANTINO,

M., Testing and qualification of CIRCE venture nozzle flowmeter for large scale experiments, paper presented in 13th Int. Conf. on Nuclear Engineering, Beijing, China, 16-20 May 2005.
[4.20] RICHARD, P., DELPECH, M., RIMPAULT, G., PDS-XADS: Technical Specifications, Missions of XADS, Recommendations for the Main Characteristics, Deliverable of the PDS-XADS WP1, DEL02/001 rev1 (2002).
[4.21] THE EUROPEAN TECHNICAL WORKING GROUP ON ADS, A European Roadmap for Developing ADS for Nuclear Waste Incineration, ENEA, Italy (April 2001).
[4.22] KNEBEL, J., AÏT ABDERRAHIM, H., CINOTTI, L., MANSANI, L., DELAGE, F., FAZIO, C., GIOT, M., GIRAUD, B., GONZALEZ, E., GRANGET, G., MONTI, S., MUELLER, A., EUROTRANS: European Research Programme for the Transmutation of High level Nuclear Waste in an Accelerator driven System, paper presented in Ninth Information Exchange Meeting, Nimes, France, 25–29 September 2006.
[4.23] OECD-NEA NUCLEAR SCIENCE COMMITTEE, Handbook on lead-bismuth Eutectic Alloy and lead Properties, Materials Compatibility, Thermalhydraulics and Technologies, NEA No.6195, ISBN 978-92-64-99002-9 (2007).
[4.24] PARK, W.S., et al., Development of Nuclear Transmutation Technology, Technical Report No. KAERI/RR-1702/96, Korea Atomic Energy Research Institute (1996).
[4.25] SONG, T.Y., et al., The lead and LBE corrosion research at KAERI, paper presented in the OECD/NEA Workshop on Structural Materials for Innovative Nuclear Systems, Karlsruhe, Germany (2007).
[4.26] LEONOV, V.N., et al., Pre and in-pile tests of fuel element mock-ups for the BREST OD 300 in the independent lead-cooled channel of the BOR-60 reactor, paper presented in 11th Int. Conf. on Nuclear Engineering, Tokyo, Japan, 20–23 April 2003.
[4.27] OECD NUCLEAR ENERGY AGENCY, paper presemted in the Int. Workshops on Utilization and Reliability of High Power Proton Accelerators (HPPA).
[4.28] OUCHI, N., et al., Development of superconducting proton linac, Technical Report No. KAERI/RR-1702/96, Korea Atomic Energy Research Institute (1996).
[4.29] TAKEI, H., et al., Comparison of beam trip frequencies between estimation from current experimental data of accelerators and requirement from ADS transient analyses, paper presented in 5th Int. Workshops on Utilization and Reliability of High Power Proton Accelerators (HPPA), Mol, Belgium, 7–9 May 2007.
[4.30] OGAWA, Y., et al., Operation status and statistics of the KEK Electron-Positron LINAC, paper presented in the Tenth European Particle Accelerator Conference, Edinburgh, Great Britain, 26–30 June 2006.
[4.31] ERIKSSON M., Reliability Assessment of the LANSCE Accelerator System, M.Sc. thesis, Stockholm, Sweden (1998).
[4.32] The principal institutions in the accelerator work package WP1.3 of EUROTRANS are CNRS (F), CEA (F), IBA (B); IAP Frankfurt University (D) and INFN (I). Additional contributions, especially in issues dealing with the interface accelerator-reactor, are provided from ANSALDO (I), AREVA NP (D), ITN (P) and UPM (S). The programme has the financial support of the European Commission through the contract FI6W-CT-2004-516520.
[4.33] EUROPEAN TECHNICAL WORKING GROUP, The European Roadmap for Developing ADS for Nuclear Waste Incineration, ISBN 88-8286-008-6, ENEA (2001).
[4.34] MUELLER, A.C., The PDS-XADS reference accelerator, paper presented in the Int. Workshop on P&T and ADS Development, SCK•CEN, Belgium, October 2003.
[4.35] BIARROTTE, J-L., et al., A reference accelerator scheme for ADS applications, Nuclear Instruments and Methods, 562 (2006) pp. 565–661.
[4.36] BIARROTTE, J-L., et al., Beam dynamics studies for the fault tolerance assessment of the PDS-XADS linac design, paper presented in 4th Int. Workshop on Utilization and Reliability of High Power Proton Accelerators (HPPA), 16–19 May 2004, Daejon, Republic of Korea.
[4.37] PIERINI, P., ADS Reliability Activities in Europe, paper presented in 4th Int. Workshop on Utilization and Reliability of High Power Proton Accelerators (HPPA), 16–19 May, 2004, Daejon, Republic of Korea.
[4.38] BEAUVAIS, P.Y., Recent evolutions in the design of the French high intensity proton injector (IPHI), paper presented in EPAC 2004, Luzern, Switzerland, 5–9 July 2004.

[4.39] PODLECH, et al, Development of room temperature and superconducting CH Structures for high power applications, paper presented in 5th Int. Workshops on Utilization and Reliability of High Power Proton Accelerators (HPPA), Mol, Belgium, 7–9 May 2007.
[4.40] PONTON, A., et al., Development of superconducting spoke cavities for an ADS Linac, paper presented in 5th Int. Workshop on Utilization and Reliability of High Power Proton Accelerators (HPPA), Mol, Belgium, 7–9 May 2007.
[4.41] PANZERI, N., et al., Status of the preparation of the elliptical cavity system for the EUROTRANS cryomodule, paper presented in 5th Int. Workshop on Utilization and Reliability of High Power Proton Accelerators (HPPA), Mol, Belgium, 7–9 May 2007.
[4.42] BARBANOTTI, S., et al., Design of a Test Cryomodule for the High energy Section of the EUROTRANS Linac, paper presented in 5th Int. Workshop on Utilization and Reliability of High Power Proton Accelerators (HPPA), Mol, Belgium, 7–9 May 2007.
[4.43] BARBANOTTI, S., et al., The prototype cryomodule for the EUROTRANS programme, paper presented in 13th Int. Workshop on RF Superconductivity (SRF 2007), Beijing, China, 14–19 October 2007.
[4.44] BIARROTTE, J-L., URIOT, D., Beam dynamics calculations for fault tolerance, Phys. Rev. ST Accel. Beams, 11 (2008) 072803.
[4.45] PIERINI, P., BURGAZZI, L., Reliability studies for a superconducting driver for an ADS Linac, paper presented in 5th Int. Workshops on Utilization and Reliability of High Power Proton Accelerators (HPPA), Mol, Belgium, 7–9 May 2007.
[4.46] GALAMBOS, J., et al, Operational experience of a superconducting cavity fault recovery system at the spallation neutron source, paper presented in 5th Int. Workshops on Utilization and Reliability of High Power Proton Accelerators (HPPA), Mol, Belgium, 7–9 May 2007.
[4.47] BAUER, G., SALVATORES, M., HEUSENER, G., MEGAPIE, A 1 MW Pilot Experiment for a Liquid Metal Spallation Target, Journ. Nucl. Mater. 296 (2001) p. 17.
[4.48] WAGNER, W., The MEGAPIE operation synthesis, Paper ADS/ET-09, paper presented in Int. Topical Meeting on Nuclear Research Applications and Utilization of Accelerators (AccApp09), Vienna, May 2009.
[4.49] TSCHALÄR, C., Spallation Neutron Source at SIN, Proc. ICANS IV, KENS report II, Tsukuba (1981) pp. 56–76.
[4.50] PLATNIEKS, I., BAUER, G.S., LIELAUSIS, O., TAKEDA, Y., Measurement of Heat Transfer at the Beam Window in a Mockup Targez for SINQ Using Mercury, Proc. ICANS XIV, ANL-98/33 (1998) pp. 382–395.
[4.51] PATORSKI, J.A., TAKEDA, Y., Liquid Metal Target; Experimental Study (Phase 1) of the Cooling of a SINQ type Mercury Target Window, ESS Report, ISSN 1433-559X, ESS 00-101-T, Forschungszentrum Jülich GmbH (March 2000).
[4.52] ATCHISON, F., Nuclide Production in the SINQ Target, report SINQ/816/AFN-702 (1997).
[4.53] FAZIO, C., et al., The MEGAPIE-TEST project: Supporting research and lessons learned in first of a kind spallation target technology, Nucl. Engineering and Design, 238 (2008) pp. 1471–1495.
[4.54] CORSINI, G., DUBS, M., SIGG, B., WAGNER, W., Heat Removal System: Final Update of Concept and Detail Design, Dimensional and Functional Issues, Proc. 4th MEGAPIE Technical Review Meeting, FZKA 6876 (2003) p. 34.
[4.55] WAGNER, W., GROESCHEL, F., CORSINI, G., Cover Gas System: Updated Boundary Conditions and Current Concept, Proc. 4th MEGAPIE Technical Review Meeting, FZKA 6876 (2003) p. 40.
[4.56] WAGNER, W., WELTE, J., JORAY, S., SIGG, B., Insulation Gas System of MEGAPIE: A Concept Update, Proc. 4th MEGAPIE Technical Review Meeting, FZKA 6876 (2003) p. 52.
[4.57] TURRONI, P., MEGAPIE Project Fill and Drain System Functional description, ENEA Report FIS-P817-001 (2005).
[4.58] WAGNER, W., TURRONI, P., AGOSTINI, P., THOMSEN, K., WAGNER, E., WELTE, J., Fill and Drain and Freezing: System Modifications for Merely non-active Draining, Proc. 4th MEGAPIE Technical Review Meeting, FZKA 6876 (2003) p. 46.
[4.59] THOMSEN, K., VIMOS, near target Beam Diagnostics for MEGAPIE, Nuclear Instruments & Methods A 575 (2007) p. 347.

[4.60] SASA, T., et al., Code Development for the Design Study of the OMEGA Programme Accelerator Driven Transmutation Systems, Nuclear Instruments and Methods in Physics Research A 463 (2001) pp. 495–504.
[4.61] SASA, T., et al., Design Study of the J–PARC Transmutation Experimental Facility, Proc. GLOBAL 2005, Tsukuba, Japan, 9–13 October 2005, (Ed.: Hajimu Yamana), Atomic Energy Society of Japan, ISBN: 4-89047-133-2.
[4.62] BORONIN, A.A., IVANOV, E.F., LEVCHENKO, Yu.D., ORLOV, Yu.I., SOROKIN, A.P., FEDOTOVSKY, V.S., YEFANOV, A.D., Study of Thermal and Hydrodynamic Process in Experimental Target Model of NC-1 Liquid Metal Target System, paper presented in Topical Meeting of the American Nuclear Society Winter Meeting on Nuclear Applications in the New Millenium (AccApp 01-ADTTA 01), Reno, Nevada, USA, 11–15 November 2001.
[4.63] EFANOV, A.D., ORLOV, Yu.I., SOROKIN, A.P., E.F., BOGOSLOVSKAIA, G.P., Thermal Experiments on the Target Model for Accelerator Driven System / Atomic Energy, Vol. 93, No 5 (2002) p. 384.
[4.64] TAKATA, T., YAMAGUCHI, A., HACHIMOTO, A., Benchmark Calculation of the Thermal Experiments in the ADS Target Model, paper presented in Int. Working Group on Thermohydraulics of Advanced Nuclear Reactors, Obninsk, Russian Federation, 17–19 July 2001.
[4.65] PENA, A., CASTRO, A., ESTEBAN, G.A., et.al. Benchmark Activities of UPV/EHU and LAESA Concerning the TS-1 Target System Experiments, paper presented in Int. Working Group on Thermohydraulics of Advanced Nuclear Reactors, Obninsk, Russia, 17–19 July 2001.
[4.66] CHEN, H.Y., Calculation Results of the benchmark problem, paper presented in Int. Working Group on Thermohydraulics of Advanced Nuclear Reactors, Obninsk, Russia, 17–19 July 2001.
[4.67] MIKHIN, V.I., VECCHI, M., Results of testing the ANSYS (part FLOTRAN) code in the ADS Target Model Thermohydraulic Calculations. ENEA, Bologna, Italy (December 2001).
[4.68] KNEBEL, J.U., AÏT ABDERRAHIM, H., CARON-CHARLES, M., DE BRUYN, D., DELAGE, F., FAZIO, C., GIOT, M., GONZALEZ, E., GRANGET, G., MANSANI, L., MONTI, S., MUELLER, A.C., EUROTRANS: European Research Programme for the Transmutation of High Level Nuclear Waste in an Accelerator Driven System: Towards a Demonstration Device of Industrial Interest, paper presented in EU Research and Training in Reactor Systems 2009, (FISA 2009), Prague, Czech Republic, 22–24 June 2009.
[4.69] SCHUURMANS, P., VAN TICHELEN, K., Report on the selection of the reference target design and specifications. Deliverable D1.19 of the IP_EUROTRANS project (2008).
[4.70] MALAMBU, E., AOUST, TH., Compared design parameters of a 50 MWth MYRRHA core: 350 MeV versus 600 MeV proton beam, SCK•CEN Report, RF&M/EM/em.34.B043200/85/MYRRHA-Design/05-39, Mol, Belgium (2005).
[4.71] DIERCKX, E., HEYSE, J., XT–ADS LIDAR Specifications, SCK•CEN Report R-4561, Mol, Belgium (2007).
[4.72] PILLON, S., PLANCK, D., VASILE, A., MIGNANELLI, M., THETFORD, R., Preliminary assessment of targets and fuels dedicated to the minor actinide transmutation in the frame of CADRA programme, paper presented in GLOBAL'09, 29August–3September 2009, Jackson Hole, Wyoming, USA.
[4.73] KONINGS, R.J.M., et al., EURATOM report, EUR 19928 EN: Advanced fuel cycles for accelerator driven systems: fuel fabrication and reprocessing (2001).
[4.74] RUBBIA, C., et al., A European Roadmap for developing Accelerator Driven Systems (ADS) for Nuclear Waste incineration, ENEA report, ISBN 88-8286-008-6 (April 2001).
[4.75] KIM, Y.S., HOFMAN, G.L., report ANL-AAA-068: AAA Fuel Handbook (2003).
[4.76] WALTERS, L.C., Thirty years of fuels and materials information from EBR-II, Jour. Nuc. Mat., 70 (1999) pp. 39–48.
[4.77] US DEPARTMENT OF ENERGY, Office of Nuclear Energy, Science and Technology, Report to congress: Advanced Fuel Cycle initiative the future path of advanced spent fuel treatment and transmutation research (January 2003).

[4.78] MEYER, M.K., HAYES, S.L., CRAWFORD, D.C., PAHL, R.G., TSAI, H., Fuel design for the US accelerator driven system 2001, paper presented in Topical Meeting of the American Nuclear Society Winter Meeting on Nuclear Applications in the New Millenium (AccApp 01-ADTTA 01), Reno, Nevada, USA, 11–15 November 2001.
[4.79] HILTON, B.A., HAYES, S.L., MEYER, M.K., CRAWFORD, D.C., The AFC-1AE and AFC-1F irradiation tests of metallic and nitride fuels for nitride fuels for actinide transmutation, Proc. GLOBAL 2003, New Orleans, 16–20 November 2003, ANS, ISBN: 0-89448-677-2, CD-ROM.
[4.80] KENNEDY, J.R., KEISER, D.D. LAMBREGTS, M.J., FRANK, S.M., Phase, microstructure and thermo-physical properties of U-Pu-Np-Am-Zr bearing alloys as nuclear transmutation fuels, paper presented in ATALANTE'04 conference, Nîmes, France, 21–24 June 2004.
[4.81] MATZKE, H.J., Science of LMFBR fuels, Elsevier Science Publishers B.V., (1986).
[4.82] WALLENIUS, J., PILLON, S., N-15 requirement and 2nd stratum ADS nitride fuels, paper presented in Topical Meeting of the American Nuclear Society Winter Meeting on Nuclear Applications in the New Millenium (AccApp 01-ADTTA 01), Reno, Nevada, USA, 11–15 November 2001.
[4.83] TAKANO, M., R&D on fuel for transmutation in JAEA Recent activities of research group for actinide science. Proc. GLOBAL 2005, Tsukuba, Japan, 9–13 October 2005 (Ed.: Hajimu Yamana), Atomic Energy Society of Japan, ISBN: 4-89047-133-2.
[4.84] WALLENIUS, J., TUCEK, K., GUDOWSKI, W., Safety analysis of nitride fuels in cores dedicated to waste transmutation, paper presented in 6-IEMPT, Madrid, Spain, 11–13 December 2007.
[4.85] SASA T., OIGAWA, H., TSUJIMOTO, K., NISHIHARA, K., KIKUCHI, K., KURATA, Y., SAITO, S., FUTAKAWA, M., UMENO, M., OUCHI, N., ARAI, Y., MINATO, K., TAKANO, H., Research and development on accelerator driven transmutation system at JAERI.Nuclear Engineering and Design, Vol. 230, No. 1–3 (2004) pp. 209–222.
[4.86] BAILLY, H., MÉNESSIER, D., PRUNIER, C., The nuclear fuel of pressurized water reactors and fast neutron reactors Design and behaviour (Ed.: Lavoisier), IBSN CEA-2727201982 (1999).
[4.87] LEGGETT, R.D., WALTERS, L.C., Status of LMR Fuel Development in the United States of America, Journal of Nuclear Materials, 204 (1993) pp. 23–32.
[4.88] RICHTER, K, Fabrication of fuel units consisting of a dispersion of $PuO_2$ in a matrix of MgO and $Al_2O_3$, report EURAEC-908 (1963).
[4.89] KNEBEL, J., AÏT-ABDERRAHIM, H., CINOTTI, L., DELAGE, F., FAZIO, C., GIOT, M., GIRAUD, B., GONZALEZ, E., GRANGET, G., MUELLER, A.C., MONTI, S., European research programme for the transmutation of high level nuclear waste in an accelerator driven system paper presented in FISA 2006, Luxembourg, 13–16 March 2006.
[4.90] KONINGS, R.J.M., CONRAD, R., DASSEL, G., PIJLGROMS, B., SOMERS, J., TOSCANO, E., The EFFTRA-T4 experiment on americium transmutation, Jour. of Nuc. Mat., 282 (2000) pp. 159–170.
[4.91] INTERNATIONAL ATOMIC ENERGY AGENCY, IAEA-TECDOC 970, Vienna (1996).
[4.92] BONNEROT, M., WARIN, D., FERROUD-PLATTET, M-P., GOSMAIN, L., LAMONTAGNE, J., Progress on inert matrix fuels for minor actinide transmutation in fast reactor, Proc. GLOBAL 2007, Boise, Idaho, 9–13 September 2007, ANS, ISBN: 0-89448-055-3, CD-ROM.
[4.93] KLAASSEN, F.C., BAKKER, K., SCHRAM, R.P.C., KLEIN MEULEKAMP, R., CONRAD, R., SOMERS, J., KONINGS, R.J.M., Post-irradiation examination of irradiated americium oxide and uranium dioxide in magnesium aluminate spinel, Jour. Nuc. Mat., 319 (2003) pp. 108–117.
[4.94] NICOLAOU, G., RICHTER, K., KOCH, L., PRUNIER, C., Experience with fast reactor fuels containing minor actinides: Transmutation rates and radiation doses, paper presented in Technical Committee Meeting, 29 November–2 December 1993, pp. 203–208.
[4.95] HAIRE, R.G., The high temperature vaporization-decomposition of actinides materials: fundamental and technological aspects, Jour. Nuc. Mat., 247 (1997) pp.1–6.

[4.96] TAKANO, M., ITOH, A., AKABORI, M., MINATO, K., NUMATA, M., Study on the stability of AmN and (Am,Zr)N., Proc. GLOBAL 2003, New Orleans, 16–20 November 2003, ANS, ISBN: 0-89448-677-2, CD-ROM.
[4.97] GRANDJEAN, S., ARAB-CHAPELET B., ROBISSON A.C., PICART, S. DANCAUSSE J.P., BARON, P., BROSSARD, P., WARIN, D., Synthesis of mixed actinide compounds by hydrometallurgical Coconversion methods, Proc. GLOBAL 2007, Boise, Idaho, 9–13 September 2007, ANS, ISBN: 0-89448-055-3, CD-ROM.
[4.98] FERNÁNDEZ, A., RICHTER, K, SOMERS, J, Preparation of spinel ($MgAl_2O_4$) spheres by hybrid solgel technique, Advances in Science and Technology, 15 (1999) pp. 167–174.
[4.99] FERNANDEZ, A., SOMERS, J, Design and fabrication of specific ceramic metallic fuels and targets J. Nucl. Mater., 319, 4 (2003) pp.44–50.
[4.100] HOBBS, J.W., PARKES, P., CHILTON, G.R., Alternative forms of nuclear fuel, paper presented in EUROMAT'96: Materials and nuclear power, Bournemouth, Great Britain, 21-23 October 1996.
[4.101] AKABORI, M., MINATO, K., ARAI, Y., Nitride Fuel and Pyrochemical Process Developments for Transmutation of Minor Actinides in JAERI, paper presented in 8th OECD-NEA Information Exchange Meeting on Actinide and Fission Product Partitioning and Transmutation, 9–11 November 2004, Las Vegas, USA.
[4.102] ARAI, Y., AKABORI, M., MINATO, K., 2006, JAEA's Activities on Nitride Fuel Research for MA Transmutation, paper presented in 9th OECD-NEA Information Exchange Meeting on Actinide and Fission Product Partitioning and Transmutation, Nîmes, France, 26–28 September 2006.
[4.103] ARAI, Y., MINATO, K., Fabrication and Electrochemical Behaviour of Nitride Fuel for Future Applications, J. Nucl. Mater., 344 (2005) pp. 180–185.
[4.104] OIGAWA, H., et al., Present Status and Future Perspectives of Research and Development on Partitioning and Transmutation Technology at JAERI, Proc. GLOBAL 2005, Tsukuba, Japan, 9–13 October 2005, (Ed.: Hajimu Yamana), Atomic Energy Society of Japan, ISBN: 4-89047-133-2.
[4.105] ARAI, Y., AKABORI, M., MINATO, K., Progress of Nitride Fuel Cycle Research for Transmutation of Minor Actinides, Proc. GLOBAL 2007, Boise, Idaho, 9–13 September 2007, ANS, ISBN: 0-89448-055-3, CD-ROM.
[4.106] GROMOV, B.F., et al., Liquid metal systems, Plenum, New York (1995) p 339.
[4.107] MÜLLER, G., et al., Control of oxygen concentration in liquid lead and lead bismuth, Journal of Nuclear Materials, 321 (2003) pp. 256–262.
[4.108] SCHROER, C., et al., Oxygen Sensor Reliability Improvement for Nuclear Use: Activities performed at FZK, Report for the Eurotrans Project D24 (2007).
[4.109] ASKHADULLIN, R.S.; MARTYNOV, P.N., et al, Development of oxygen sensors, systems of control of oxygen content in lead coolants for test loops and facilities, International Science and Technology Centre contract n°3020 (2005),
[4.110] ASKHADULLIN, R.S.; MARTYNOV, P.N., SIMAKOV, A.A., EMEPIANTSEVA, Z.I., SISOEV, O.M., LANSKIKH, V.S., GULEVSKIY, V.A, CHERNOV, M.E., Regulation of the thermodynamic activity of oxygen in lead and lead-bismuth by the dissolution of the oxides in heat transfer systems, paper presented in Fast Neutrons Reactors Conference, 8–12 December 2003, Obninsk, Russian Federation (in Russian).
[4.111] AZZATI, M., GESSI, A., BENAMATI, G., Experimental results on oxygen control systems-TECLA D28, ENEA FIS ENG Technical Note (5 December 2003).
[4.112] CHERNOV, M.E., MARTYNOV, P.N., GULEVSKIY, V.A., Development of electrochemical capsule oxygen sensor for control and monitoring of heavy metal coolant condition, paper presented in Fast Neutrons Reactors Conference, Obninsk, Russian Federation, 8–12 December 2003 (in Russian).
[4.113] COLOMINAS, S. ABELLA, J., VICTORI, L., Characterisation of an oxygen sensor based on In/In2O3 reference electrode, Journal of Nuclear Materials, Vol. 335 (2004) pp. 260–263.
[4.114] COUROUAU, J-L., Oxygen control systems, comparison between oxygen probes, paper presented in 1st MEGAPIE Technical Review Meeting, Cadarache, France, 14–15 June 2000.

[4.115] COUROUAU, J-L., P., DELOFFRE, R, ADRIANO, Oxygen control in lead-bismuth eutectic: first validation of electrochemical oxygen sensor in static conditions, Journal de Physique IV, France 12, Pr8, (2002) pp. 141–153.
[4.116] COUROUAU, J-L., Impurities and purification processes in lead-bismuth systems. TECLA deliverable n25, CEA Technical note DER/STR/LCEP 03/001 (2003).
[4.117] COUROUAU, J-L., PIGNOLY, L., DELISLE, C., DELOFFRE, P., BALBAUD, F., Report on the long term validation of electrochemical sensor: TECLA Deliverable n°32, CEA technical note DER/STR/LCEP 03/031 (2003).
[4.118] COUROUAU, J-L., Electrochemical oxygen sensors for online monitoring in lead-bismuth alloys: status of development, Journal of Nuclear Materials, Vol. 335 (2004a) pp 254–259.
[4.119] COUROUAU, J-L., SELLIER, S., CHABERT, C., PIGNOLY L., Electrochemical oxygen sensor for online measurement in liquid lead alloys systems at relatively low temperature, to be issued in AFINIDAD, Journal of theoretical and applied chemistry, chemistry institute de Sarria (IQS), Barcelonna, Spain, 2005.
[4.120] BUONGIORNO, J., et al. Nuclear Technology, 147 (2004) pp. 406–417.
[4.121] MIURA, T., OBARA, T., SEKIMOTO, H., Nuclear Technology, 15, (2006) pp. 78–89.
[4.122] OBARA, T., MIURA, T., SEKIMOTO, H., Journal of Nuclear Materials, 343 (2005) pp. 297-301.
[4.123] OHNO, S., et al., Journal of Nuclear Science and Technology, 42, No.7 (2005) pp.593–599.
[4.124] OHNO, S., et al., Journal of Nuclear Science and Technology, 43, No.11 (2006) pp. 1359-1369.
[4.125] OHNO, S., et al., ICONE14-89187, Proc. ICONE 14, Miami, Florida, 17–20 July 2006 (5 Vols), ASME.
[4.126] ZRODNIKOV, A.V., EFANOV, A.D., ORLOV, YU.I., MARTYNOV, P.N., TROYANOV, B.M., Technology of heavy liquid metal coolants: lead-bismuth and lead, Atomic Energy, , Vol. 87, No. 2 (2004) p. 98.
[4.127] MARTYNOV, P.N., GULEVICH, A.V., ORLOV, YU., GULEVSKY, V.A., Water and Hydrogen in Heavy 2. Liquid Metal Coolant Technology // Innovative Nuclear Energy Systems for Sustainable Development of the World. Paper presented in First COE-INES International Symposium (INES-1), Tokyo, Japan, 31 October - 4 November 2004.
[4.128] PAPOVYANTS, A.K., ORLOV, Y.I., MARTYNOV, P.N., BOLTOEV, Y.D., Hydrodynamics of heavy liquid metal coolant processes and filtering apparatus, Eleventh international topical meeting on nuclear reactor thermalhydraulics (NURETH 11), Avignon, France, 2–6 October 2005, Book of abstracts, p. 223, CD-ROM.
[4.129] DAI, Y., HENRY, J., AUGER, T., VOGT, J., AL MAZOUZI, A., GLASBRENNER, H., ET AL., Assessment of the lifetime of the beam window of MEGAPIE target liquid metal container, Journal of nuclear materials, 356:1–3, ISSN 0022-3115 (2006) pp. 308–320.
[4.130] SAPUNDJIEV, D., AL MAZOUZI, A., VAN DYCK, S., A study of the neutron irradiation effects on the susceptibility to embrittlement of A316L and T91 steels in lead-bismuth eutectic, Journal of nuclear materials, 356:1–3, ISSN 0022-3115 (2006) pp. 229–236.
[4.131] VAN DEN BOSCH, J., SAPUNDJIEV, D., AL MAZOUZI, A., Effects of temperature and strain rate on the mechanical properties of T91 material tested in liquid lead bismuth eutectic, Journal of nuclear materials, 356:1–3, ISSN 0022-3115 (2006) p.p. 237–246.
[4.132] WENGER, H., AL MAZOUZI, A., ATCHISON, F., BURGHARTZ, M., CHAWLA, R., GUENTHER-LEOPOLD, I., ET AL., Isobaric production cross-sections from 0.6 GeV proton irradiation of neptunium and thorium using mass spectrometry, Nuclear Physics, 764, ISSN 0375-9474 (2006) pp. 1–14.
[4.133] AL MAZOUZI, A., LUCON, E., Mechanical Behaviour of Neutron Inrradiated High Cr Ferritic-Martensitic Steels, TMS letters, 2:3 (2005) pp. 73–74.
[4.134] SAPUNDJIEV, D., AL MAZOUZI, A., VAN DYCK, S., Materials for Accelerator Driven System, TMS Letters, 2:3 (2005) pp. 69–70.
[4.135] VAN DEN BOSCH, J., AL MAZOUZI, A., BENOIT, PH., BOSCH, R.W., Claes, W., SMOLDERS, B., SCHUURMANS, P., AÏT ABDERRAHIM, H., TWIN ASTIR, An Irradiation Experiment In Liquid Pb-Bi Eutectic Environment, accepted for publication in J. Nuc. Mat. (2007).

[4.136] XU, Y-L., LONG, B., XU, Y.C., LI, H.Q., Investigation of the Compatibility of Tungsten and High Temperature Sodium, Journal of Nuclear Materials, 343 (2005) pp. 360–365.
[4.137] ZHAO, F., WAN, K., WAN, F., LONG, Y., XU, Y., HUANG, Q., The Structure and Properties of Low Activation Ferritic–Matensitic steel, paper presented in 5th Pacific Rim Int. Conference on advanced Materials, Beijing, China 2–5 November 2004.
[4.138] XU, Y., ZHANG, J., LI, H., Investigation of the HIP Process for Tungsten Target Samples, paper presented in 8th Int. Workshop on Spallation Materials Technology, 16–21 October 2006, USA.
[4.139] SHENGYUN, Z., YONGJUN, X., ZHIQIANG, W., et al., Positron annihilation lifetime spectroscopy on heavy ion irradiated stainless steels and tungsten, Journal of nuclear materials, Vol. 343 (2005) pp. 330–332.
[4.140] POLAT, A., ZHIGUO, F., LUO, Q., et al., Nuclear Science and Techniques 11 (2000) p. 52.
[4.141] POLAT, A., ZHIGUO, F., LUO, Q., et al., Atomic Energy Science and Technology, 37 (2003) pp. 18–21 (in Chinese).
[4.142] PUSKA, M.J., NIEMINEN, R.M., J. Phys. F13 (1983) p. 333.
[4.143] RUBBIA, C., RUBIO, J.A., BUONO, S,. Conceptual design of a fast neutron operated high power enegry system, CERN/AT/95-44(ET) (1995).
[4.144] DING, D., A new option for exploitage of future nuclear energy accelerator driven radioactive clean nuclear power system, Selected Works of Concept Research of accelerator driven radioactive clean nuclear power system (Ed.: Zhao Zhixiang) Atomoc Energy Press, Beijing (2000) pp. 3–16 (in Chinese).
[4.145] EXEL, K., et al., in Nuclear Physics methods in Materials Research (Eds: K. Bethge, H. Baumann, et al.,) (1980) p. 478.
[4.146] ZHU, S., et al., Chin. Phys. Lett., Characterization of High-Energy-Heavy-Ion-Induced Defects in GaAs by Positron Annihilation, vol 14 (1997) p. 535.
[4.147] HAUTOJARVI, P., Positrons in solids, Springer Verlag Berlin Heidelberg New York, (1979).
[4.148] KRAUSE-REHBERG, R., LEIPNER, H.S., Positron annihilation in semiconductors, Springer-Verlag Berlin Heidelberg New York (1999).
[4.149] KANSY, J, Microcomputer program for analysis of positron annihilation lifetime spectra, Nuclear Instmments and Methods in Physics Research A 374 (1996) 235-244.
[4.150] ZHU, S., et al., Chin. Phys. Lett., Characterization of High-Energy-Heavy-Ion-Induced Defects in GaAs by Positron Annihilation
[4.151] ZHU, S., IWATA, T., XU, Y., et al., Experimental Verification of Heavy Ion Irradiation Simulation, Mordern Physics Letters B18 (2004) p. 88.
[4.152] ZHU, S., ZHENG, Y., POLAT, A., et al., Temperature and dose dependences of radiation damage in modified stainless steel Journal of nuclear materials Vol. 343 (2005) pp. 325–329.
[4.153] ZHENG, Y., ZUO, Y., ZHOU, D., et al., Dose dependence of radiation damage In W investigated by heavy ion irradiation simulation, Nuclear Physics Review 23 (2006) p. 207 (in Chinese).
[4.154] ASHER, R.C., DAVIES, D., BEETHAM, S.A., Corrosion Sci., Vol. 17 (1977) pp. 545–557, Pergamon Press.
[4.155] ENGELKO, V., YATSENKO, B., MÜLLER, G., BLUHM, H., Vacuum, Vol. 62 (2001) pp. 211–216.
[4.156] FAZIO, C., BENAMATI, G., MARTINI, C., PALOMBARINI, G., J. Nucl. Mater. 296 (2001) p. 243.
[4.157] GROMOV, B.F. (Editor in chief), Proc. Of Heavy Liquid Metal Coolants in Nucl. Tech. (HLMC-98), Vol. 1, SSC RF-IPPE, Obninsk, Russia (1999) p. 87.
[4.158] LAI, G.Y., High Temperature Corrosion of Engineering Alloys, ASM Int., Materials Park, OH 44073 (1990).
[4.159] STRUWE, D., PFRANG, W., private communication Forschungszentrum Karlsruhe, IRS-2007.
[4.160] WEISENBURGER, A., MÜLLER, G., HEINZEL, A., ENGELKO, V., ROUSANOV, A., Proc. Eurocorr 2005, Lisbon, Portugal, 4–8 September 2005, ISBN 972-95921-2-8.
[4.161] WEISENBURGER, A., HEINZEL, A., MÜLLER, G., ROUSANOV, A., MUSCHER, H. J., Nucl. Mater. (to be published in 2007)

[4.162] WEISENBURGER, A., HEINZEL, A., FAZIO, C., MÜLLER, G., MARKOW, V.G., KASTANOV, A.D., J. Nucl. Mater. (accepted for publication 2007).
[4.163] AIELLO, A., et al, Mechanical properties of Eurofer 97 in Pb-16Li and irradiation effect, paper presented in the IV Workshop on materials for HLM cooled reactors and related technologies, 2007, submitted to Journal of Nuclear Materials, special issue.
[4.164] AIELLO, A., et al., Corrosion behaviour of stainless steels in flowing LBE at low and high oxygen concentration, Journal of Nuclear Materials, 335, 2, (2004) pp. 169–173.
[4.165] AIELLO, A., et al., Mechanical properties of martensitic steels after exposure to flowing liquid metals Journal of Nuclear Materials, 335, 2 (2004) pp. 217–221.
[4.166] BARBIER, F., et al, Compatibility tests of steels in flowing liquid lead bismuth, Journal of Nuclear Materials, 295, 2–3 (2001) pp. 149–156.
[4.167] BENAMATI, G., et al., Corrosion experiments in flowing LBE at 450 °C Journal of Nuclear Materials, 356, 1–3 (2006) pp. 198–202.
[4.168] BENAMATI, G., GESSI, A., Corrosion behaviour of steels and refractory metals in flowing lead-bismuth eutectic at low oxygen activity, Journal of Materials Science, 40, 9 (2005) pp. 2465–2470.
[4.169] BENAMATI, G., et al., Temperature effect on the corrosion mechanism of austenitic and martensitic steels in lead bismuth, Journal of Nuclear Materials, 301, 1 (2002) pp. 23–27.
[4.170] BENAMATI, G., et al, Mechanical and corrosion behaviour of Eurofer 97 steel exposed to Pb-Li, Journal of Nuclear Materials (2002) pp. 307–311, 1391–1395.
[4.171] BENAMATI, G., et al., Behaviour of materials for accelerator driven systems in stagnant molten lead, Journal of Nuclear Materials, 279, 2–3 (2000) pp. 308–316.
[4.172] FAZIO, C., et al., Corrosion behaviour of steels and refractory metals and tensile features of steels exposed to flowing PbBi in the LECOR loop, Journal of Nuclear Materials, 318 (2003) pp. 325–332.
[4.173] FURUKAWA, T., et al., Journal of Nuclear Science and Technology, Vol.41, No. 3 (2004a), pp. 265–270.
[4.174] FURUKAWA, T., et al., Journal of Nuclear Materials, 335 (2004) pp. 189–193.
[4.175] KURATA, Y., FUTAKAWA, M., Journal of Nuclear Materials, 325 (2004) pp. 217–222.
[4.176] KURATA, Y., FUTAKAWA, M., SAITO, S., Journal of Nuclear Materials, 343 (2005) pp. 333–340.
[4.177] KURATA, Y., FUTAKAWA, M., SAITO, S., Journal of Nuclear Materials, 373 (2008) pp. 164–178.
[4.178] KUMAWAT, H., et al., Nucl. Instr. and Meth. B, doi:10.1016/j.nimb.2007.11.064. (2007).
[4.179] KUMAWAT, H., BARASHENKOV, V.S., The Euro. Phys. J. A 26 (2005) p. 61.
[4.180] GOHAR, Y., J. of Nucl. Mat. 318 (2003) p. 185.
[4.181] ICHIHARA, A., et al., Programme POD; A Computer Code to Calculate Cross-sections for Neutron Induced Nuclear Reactions, JAEA Data/Code 2007-012 (2007).
[4.182] NIITA, K., et al., High Energy Particle Transport Code NMTC/JAM, Jaeri-Data/Code 2001-007 (2001).
[4.183] IWASE, H., et al., J. Nuc. Sci. Technol. 39, (2002) p. 1142.
[4.184] SHIBATA, K., et al., J. Nucl. Sci. Technol. 39, (2002) p. 1125.
[4.185] FUKAHORI, T., et al., J. Nucl. Sci. Technol. Suppl. 2, (2002) p. 25.
[4.186] KISHIDA, N., et al., J. Nucl. Sci. Technol. Suppl. 2, (2002) p. 56.
[4.187] MATVEENKO, I.P., TSIBOULIA, A.M., IPPE Critical Facilities and Their Research Programmes, paper presented in the IAEA Technical Meeting to Coordinate the Agency's Fast Reactor Knowledge Preservation International Project in Russia, Obninsk, Russia, 17–18 February 2005.
[4.188] D'HONDT, P., et al., The REBUS experimental programme for burnup credit, paper presented in 12th Int. Conf. on Nuclear Engineering, Arlington, Virginia, USA, 25–29 April 2004.
[4.189] CNRS, L'accélérateur GENEPI: Conception, technologie, caractéristiques, Technical report CNRS/IN2P3/ISN-GENEPI-NT-4031 index 0, 13/10/1999.
[4.190] DESTOUCHES, C., The GENEPI accelerator operation feedback at the MASURCA reactor facility, Nuclear Instruments and Methods in Physics Research, 562 (2006) pp. 601–609.

[4.191] BILLEBAUD, A., Cahier des charges de la source de neutrons GENEPI-3C en mode continu, Technical report IN2P3_LPSC_GPR, GUI-SPE-1.1-0001-LPSC, Rev. 1, 23/07/2007.
[4.192] VERSTREPEN, L., Ontmanteling van de VENUS reactor in het kader van de opbouw van het Guinevere project, Technical report SCK•CEN, ANS/RRO-LV/3920.B045002. 516/07-04, 09/09/2007.
[4.193] MELLIER, F., et al., Design of the GUINEVERE core Status and Progress, paper presented in PHYSOR conference 2007.
[4.194] CARTA, M., Reactivity assessment and spatial time effects from the MUSE kinetics experiments, paper presented in PHYSOR conference 2004.
[4.195] SHI, Y., DING, D., LUO, Z., et al, A Conceptual study of Hybrid System for Nuclear Energy Generation and Transmutation at CIAE, paper presented in IAEA Technical Committee Mtg., Madrid, Spain, 17–19 September 1997.
[4.196] ZHAO, Z., DING, D., et al, Conceptual Research on Reactor Core Physics for Accelerator Driven Subcritical Reactor, Conceptual Research Reports for Accelerator Driven Radioactivity Clean Nuclear Power system[R], Atomic Press (2000) p. 17.
[4.197] LI, Z., HUANG, J., Neutron spectrum and mean energy of the Venus-1 subcritical assembly, Atomic Energy Science and Technology 40(2) (2006) pp. 168–171.
[4.198] SHI, Y., ZHU, Q., XIA, P., et al, Neutron source multiplication method research in reactor physics experiment, Chinese J. Nuclear Science and Engineering. 25,1,14, (2005).
[4.199] ENEA, A European roadmap for developing accelerator driven systems (ADS) for nuclear waste incineration, ISBN 88 8286 008 6 (2001).
[4.200] EURATOM, The MUSE experiments for sub-critical neutronics validation. Contract N° FIKW-CT-2000-00063. Deliverable N° 8 Final report (2004).
[4.201] CNRS,. L'accélérateur GENEPI: Conception, technologie, caractéristiques. Technical report CNRS/IN2P3/ISN-GENEPI -NT-4031 index 0, 13/10/99.
[4.202] CARTA, M., Reactivity assessment and spatial time effects from the MUSE kinetics experiments, paper presented in PHYSOR conference 2004.
[4.203] IMEL, G., MELLIER, F., et al., ADS Reactivity Measurement from MUSE to TRADE (and Where Do We Go From Here ?) paper presented in PHYSOR conference 2006.
[4.204] ROSA, R., Report on the RACE-T results, EURATOM contract N° FI6W-CT2005-516520 (2006).
[4.205] JAMMES, CH., Results of the experimental programme RACE-ISU. EURATOM contract N° FI6W-CT2005-516520 (2007).
[4.206] GHOSH, B., DEGWEKER, S.B., Report BARC/ThPD/594 (2004).
[4.207] GHOSH, B., BAJPAI, A., PARANJAPE, S.D., DEGWEKER. S.B., Report BARC/ThPD/604 (2005).
[4.208] LATHROP, K.D, DTF-IV, A Fortran-IV Program for Solving the Multigroup Transport Equation'With Ansotropic Scattering- LA-3373, LASL, Los Alamos, New Mexico.
[4.209] KUMAR, V., MENON, S.V.G., PARANJAPE, S.D., Report BARC/ThPD/566 (2003).
[4.210] DEGWEKER, S.B., RANA, Y.S., Annals of Nuclear Energy (Submitted 2006).
[4.211] RUBBIA, C., CARTA, M., et al., Preliminary Neutronic Analyses of The TRIGA-ADS Demonstration Facility, Nucl. Sci. and Eng. 148, (2004), pp. 103–123.
[4.212] RUBBIA, C., et al., Conceptual design of a fast neutron operated high power Energy Amplifier, CERN report CERN/AT/95-44 (EET), Geneva, Switzerland, 29 September 1995.
[4.213] KADI, Y., et al., The EA-MC Monte Carlo Code Package, paper presented in Fifth Int. Meeting on Simulating Accelerator Radiation Environment —SARE-5: Models and Codes for Spallation Neutron Sources, Paris, France, 17–18 July 2000.
[4.214] BRIESMEISTER F.J., (Ed.), MCNP TM -A General Monte Carlo N-Particle Transport Code, Version 4C, Los Alamos National Laboratory report LA-13709-M, March 2000.
[4.215] D'ANGELO, A., BIANCHINI, G., CARTA, M., BOSIO, P., RAVETTO, P., ROSTAGNO, M.M., A simple model to evaluate the natural convection impact on the core transients in Liquid Metal Cooled ADS, paper presented in 6th OECD-NEA Information Exchange Meeting on Actinide and Fission Product Partitioning and Transmutation, Madrid, Spain, 11-13 December 2000.

[4.216] The European Technical Working Group on ADS, A European Roadmap for Developing Accelerator Driven System (ADS) for Nuclear Waste Incineration, April 2001, Published by ENEA, www.enea.it.
[4.217] SALVATORES, M., D'ANGELO, A., NABEREJNEV, D.G., The demonstration of the ADS concept, paper presented in Third Int. Workshop on the Utilisation and Reliability of High Power Proton Accelerators, Santa Fe, New Mexico, 12–16 May 2002.
[4.218] NABEREJNEV, D.G., SALVATORES, M., PALMIOTTI, G., KONDEV, F.G., IMEL, G., BAUER, T., HARMON, F., Possible experiment for study of the ADS dynamics, Proc. PHYSOR 2002, Seoul, Korea, 7–10 October 2002, ANS, ISBN: 0-89448-672-1, CD-ROM.
[4.219] OIGAWA, H., et al., R&D Activities on Accelerator Driven Transmutation System in JAERI, paper presented in OECD-NEA 8th Information Exchange Meeting on Actinide and Fission Product Partitioning & Transmutation, Las Vegas, USA, 9–11 November 2004.
[4.220] TSUJIMOTO, K., et al., Research and Development Programme on Accelerator Driven Subcritical System in JAERI, Proc. GLOBAL 2005, Tsukuba, Japan, 9–13 October 2005, (Ed.: Hajimu Yamana), Atomic Energy Society of Japan, ISBN: 4-89047-133-2.
[4.221] HERVAULT, M., et al., Monte Carlo Analysis of Subcriticality for Accelerator Driven Subcritical Reactor Mock Up in Kyoto University Critical Assembly, paper presented in Int. Topl. Mtg. on Mathematics and Computation, Supercomputing, Reactor Physics and Nucl. Biological Applications (M&C2005), Avignon, France, 12–15 September 2005.
[4.222] PYEON, C.H., et al., 2003, Preliminary Study on ADSR by using FFAG Accelerator in KUCA, Proc. GLOBAL 2003, New Orleans, 16–20 November 2003, ANS, ISBN: 0-89448-677-2, CD-ROM.
[4.223] PYEON, C.H., et al., 2005, Experimental Analyses for Accelerator Driven Subcritical Reactor in Kyoto University Critical Assembly by using Foil Activation Method, paper presented in Int. Topl. Mtg. on Mathematics and Computation, Supercomputing, Reactor Physics and Nucl. Biological Applications (M&C2005), Avignon, France, 12–15 September 2005.
[4.224] PYEON, C.H., et al., Present Status of Accelerator Driven Subcritical Reactor in Kyoto University Critical Assembly, Proc. PHYSOR 2006, Vancouver, Canada, 10–14 September 2006, ANS, ISBN: 0-89448-697-7, CD-ROM.
[4.225] TAGEI, H., et al., 2004, Activation Experiment at KUCA for Establishing an Experimental Facility of Accelerator Driven Subcritical Reactor, paper presented in Int. Conf. on Nucl. Data for Sci. & Technol. ND2004, Santa Fe, New Mexico, 26 September -1 October 2004.
[4.226] SOULE, R., et al., Neutronic studies in support of accelerator driven systems: the MUSE experiments in the MASURCA facility, Nuclear Science and Engineering 148 (2004), pp. 124–152.
[4.227] PERSSON, C.-M., Reactivity Determination and Monte Carlo Simulation of the Subcritical Reactor Experiment Yalina Master of Science Thesis Department of Nuclear and Reactor Physics Royal Institute of Technology, Stockholm, Sweden, 2005.
[4.228] ZEMSKOV, E.A., Conceptual Development Works of the Accelerator Driven Systems with lead-bismuth coolant, Yadernaya Energetika, No. 1 (2007) pp. 69–78.
[4.229] OBAYASHI, H., KIKUCHI, K., TAKEDA, Y., Flow Measurement of lead bismuth eutectic in Spallation Target Model Loop, Proc. 5th Int. Symposium on Ultrasonic Doppler Methods for Fluid Mechanics and Fluid Engineering (ISUD5), ETH Zurich, Switzerland, September 12–14, 2006 (2006) pp.81–84.
[4.230] Atomic Energy Society of Japan, Handbook on Application Technologies for lead-bismuth Eutectic (2007) CD-ROM.
[4.231] OECD-NEA Nuclear Science Committee, Handbook on lead-bismuth Eutectic Alloy and lead Properties, Materials Compatibility, Thermalhydraulics and Technologies, NEA, No.6195, ISBN 978-92-64-99002-9 (2007).
[4.232] ARIEN, B., DANIËLS, J., SITHER: a module for steady and unsteady thermohydraulic calculations in single rod channels, int. report 63-151/80-88, Mol, SCK•CEN (1980).
[4.233] ARTIOLI, C., A_BAQUS; A Mukti-entry Graph Assisting the Neutronic Design of an ADS, Case Study : EFIT, HPPPA5, Mol, Belgium (2007)

[4.234] BRUNON, E., DONNET, LThe FUTURIX FTA experiment in Phénix, paper presented in 8th IEMPT conference, 9–11 November 2004, Las Vegas, Nevada, USA.
[4.235] CAHALAN, J.E., TENTNER, A.M., MORRIS, E.E., Advanced LMR Safety Analysis Capabilitties in the SASSYS-1 and SAS4A Computer Codes, paper presented in Int. Topical Mtg. on Advanced Reactors Safety, 17–21 April 1994, Pittsburgh, PE, USA.
[4.236] CAPRA Rapport de Faisabilite CAPRA, SIS/CAPRA 95/10059 JR/CL (1994).
[4.237] CASAMIRRA, M., et al., RELAP5 Simulations for CIRCE Experiments, paper presented in XXV National Heat Transfer Conference UIT, Trieste, Italy, 15–20 June 2007.
[4.238] CASAMIRRA, M., et al., RELAP5 Modification for CHEOPE Simulations, paper presented in Int. Conf. Nuclear Energy for New Europe 2005, Bled, Slovenia, 5–8 September 2005.
[4.239] CHEN, X-N., SUZUKI, T., RINEISKI, A., MATZERATH BOCCACCINI, C., MASCHEK, W., SMITH, P., Source and Reactivity Perturbations in ADS with Conventional. MOX and Advanced Fertile Free Fuels, PHYSOR'2004, April 25–29, Chicago, IL, USA.
[4.240] CHEN, X-N., SUZUKI, T., RINEISKI, A., MORI ,M., MATHERATH BOCCACCINI, C., MASCHEK, W., MORITA, K., Analysis of Transients and Severe Accidents in Accelerator Driven Transmuters (ADTs) of the 800 MWth Class with Fertile Free Fuels, Proc. GLOBAL 2005, Tsukuba, Japan, 9–13 October 2005 (Ed.: Hajimu Yamana), Atomic Energy Society of Japan, ISBN: 4-89047-133-2.
[4.241] CROIXMARIE, Y., ABONNEAU, E., FERNANDEZ, A., KONINGS, R.J.M., DESMOULIERE, F., DONNET, L., Fabrication of transmutation fuels and targets: the ECRIX and CAMIX-COCHIX experience, submitted to Journal of Nuclear Materials in 2006.
[4.242] DONNET, L., JORION, F., DRIN, N., HAYES, S., KENNEDY, J.R., PASAMEHMETOGLU, K., VOIT, S.L., HAAS, D., FERNANDEZ, A., The FUTURIX-Transmutation Experiment in PHENIX: Status of Fuel Fabrication, GLOBAL 2005, Tsukuba, Japan, 9–13 October 2005 (Ed.: Hajimu Yamana), Atomic Energy Society of Japan, ISBN: 4-89047-133-2.
[4.243] EHSTER-VIGNAUD, S., EFIT safety requirements, EUROTRANS internal report (EUROTRANS (2006), EUROpean Research Programme for the TRANSmutation of High Level Nuclear Waste in an Accelerator Driven system, FI6W-CT-2004-516520) (2007).
[4.244] EUROTRANS, EUROpean Research Programme for the TRANSmutation of High Level Nuclear Waste in an Accelerator Driven system, FI6W-CT-2004-516520 (2006).
[4.245] FERNANDEZ, A., RICHTER K., SOMERS, J., Preparation of spinel ($MgAl_2O_4$) spheres by hybrid solgel technique, Advances in Science and Technology, 15 (1999) pp. 167–174.
[4.246] FERNANDEZ, A., KONINGS, R.J.M., SOMERS, J., Design and fabrication of specific ceramic metallic fuels and targets, submitted to Journal of Nuclear Materials in 2003.
[4.247] FERNANDEZ, A., HAAS, D., HIERNAUT, J.P., KONINGS, R., NÄSTREN, C., OTTMAR, H., SOMERS, J., STAICU, D., Overview of ITU work on inert matrix fuels, paper presented in 9th-IEMPT, Nîmes, France, 25–29 September 2006.
[4.248] FUTURE FUels for Transmutation of TransURanium Elements, Contract FIKI-CT-2001-00148, 5th Framework Programme EU (2001).
[4.249] HAAS, D., FERNANDEZ, A., STAICU, D., SOMERS, J., MASCHEK, W., LIU, P., CHEN, X., Cermet Behaviour and Properties in ADS Reactors, paper presented in 13th Int. Conf. on Emerging Nuclear Energy Systems (ICENES'2007) 3–8 June 2007, Istanbul, Turkey.
[4.250] KLAASSEN, F., The BODEX experiment, personal communication (2006).
[4.251] KONDO, S., MORITA, K., TOBITA, Y., SHIRAKAWA, N., SIMMER-III: An Advanced Computer Programme for LMFBR Severe Accident Analysis, paper presented in ANP'92, Tokyo, Japan.
[4.252] KONDO, S., YAMANO, H., SUZUKI, T., TOBITA, Y., FUJITA, S., CAO, ,X., KAMAYAMA, K., MORITA, K., FISCHER, E.A., BREAR, D.J., SHIRAKAWA, N., MIZUNO, M., HOSONO, S., KONDO, T., MASCHEK, W., KIEFHABER, E., BUCKEL, G., RINEISKI, A., FLAD, M., COSTE, P., PIGNY, S., LOUVE, J., CADIOU, T., SIMMER-III: A Computer Programme for LMFR Core Disruptive Accident Analysis, Japan Nuclear Cycle Development Institute (JNC) TN9400 2001-002, (2000).
[4.253] LIU, P., CHEN, X.-N., RINEISKI A., MATZERATH BOCCACCINI, C., GABRIELLI, F., MASCHEK, W., MORITA, K., BIANCHI, E., (2007), First Safety Analyses for an EFIT

Type Accelerator Driven Transmuter, Proc. AccApp'07, Pocatello, Idaho, 29 July-2 August 2007, ANS, ISBN: 0-89448-054-5, CD-ROM.
[4.254] MANSANI, L., LBE and gas cooled XADS core configurations, paper presented in ENC 2002, Lille, France, 2002.
[4.255] MANSANI, L., EFIT Design, EUROTRANS internal report, EUROTRANS (2006), EUROpean Research Programme for the TRANSmutation of High Level Nuclear Waste in an Accelerator Driven system, FI6W-CT-2004-516520 (2007).
[4.256] BIANCHI, E.C., ARTIOLI, C., BURN, W., GHERARDI, G., MONTI, S., MANSANI, I., CINOTTI, L., STRUWE D., SCHIKORR, M., MASCHEK, W., AÏT ABDERRAHIM, H., DE BRUYN, D., RIMPAULT, G., Status and Trend of Core Design Activities for Heavy Metal Cooled Accelerator Driven System, paper presented in ICENES 2005, Brussels, Belgium, 2005.
[4.257] MASCHEK, W., RINEISKI, A., MORITA, K., FLAD, M., Inherent and Passive Safety Measures in Accelerator Driven Systems: A Safety Strategy for ADS, paper presented in GLOBAL 2001, Paris, France, 2001.
[4.258] MASCHEK, W., RINEISKI, A., FLAD, M., MORITA, K., COSTE, P., Analysis of Severe Accident Scenarios and Proposals for Safety Improvements for ADS Transmuters with Dedicated Fuel, Nuclear Technology, Vol 141, 2 (2003) p. 186.
[4.259] MASCHEK, W., MORI, M., RINEISKI, A., Safety Issues and Safety Indicators for ADTs with Dedicated Oxide Fuels, paper presented in NEA 8th Information Exchange Meeting, 9-11 November 2004, Las Vegas, USA.
[4.260] MASCHEK, W., RINEISKI, A., SUZUKI, T., WANG, S., MORI, MG., WIEGNER, E., WILHELM, D., KRETZSCHMAR, F., TOBITA, Y., YAMANO, Y., FUJITA, S., COSTE, P., PIGNY, S., HENRIQUES, A., CADIOU, T., MORITA, K., BANDINI, G., (2005)., SIMMER-III and SIMMER-IV Safety Code Development for Reactors with Transmutation Capability, paper presented in M&C 2005, Avignon, France, 12–15 September 2005.
[4.261] MASCHEK, W., STANCULESCU, A., IAEA CRP on 'Studies of Advanced Reactor Technology Options for Effective Incineration of Radioactive Waste', Proc. GLOBAL 2005, Tsukuba, Japan, 9–13 October 2005 (Ed.: Hajimu Yamana), Atomic Energy Society of Japan, ISBN: 4-89047-133-2.
[4.262] MASCHEK, W., STANCULESCU, A., ARIEN, B., BAI, Y., CHABERT, CH., CHEBESKOV, A.A., CHEN, X., DA CRUZ, D.F., DEKOUSSAR, V., DEVAN, K., DULLA, S., GOPALAKRISHNAN, V., FEYNBERG, O., HARISH R., IGNATIEV, V., KOPHAZI, J., LI, J., MALAMBU, E., MOHANAKRISHNAN, P., MORITA, K., PANDIKUMAR, PENELIAU, G.,Y., RAVETTO, P., RINEISKI, A., SCHIKORR, M., SRIVENKATESAN, R., SUBBOTIN, V., SURENKOV, A., SZIEBERTH, M., TACZANOWSKI., S., TUCEK, K., VERTES, P., VOROTYNTSEV, M., UHLIR, J., WIDER, H., WU, Y., ZAKIROV, R., ZHENG, S., Intermediate Results of the IAEA CRP on Studies of Advanced Reactor Technology Options for Effective Incineration of Radioactive Waste, paper presented in 13th Int. Conf. on Emerging Nuclear Energy Systems (ICENES'2007) 3–8 June 2007, Istanbul, Turkey.
[4.263] MASCHEK W., CHEN, X., MATZERATH BOCCACCINI, C., RINEISKI A., WALLENIUS, J., SOBOLEV, V., SMITH, P., THETFORD, T., P. OTTAVIANI, J.P., PILLON, S., HAAS, D., First Results of Safety Analyses for ADTs with CERCER and CERMET Fuels within the EUROTRANS-AFTRA Programme, paper presented in NEA OECD 9th Information Exchange Meeting, Actinide and Fission Product Partitioning & Transmutation, Nimes, France, 25–29 September 2006.
[4.264] MASCHEK, W., SUZUKI, T., CHEN, X., RINEISKI,A., MATZERATH BOCCACCINI, MORI, M., MORITA, K., Analyses of transients for an 800 MW-class ADT with fertile-free fuels, Nuclear Instruments and Methods in Physics Research A 562 (2006) p. 863.
[4.265] MASCHEK, W., CHEN, X.-N., DELAGE, F., FERNANDEZ-CARRETERO, A., HAAS, D., MATZERATH BOCCACCINI, C., RINEISKI, A., SMITH, P., SOBOLEV, V., THETFORD, R., WALLENIUS, J., , Accelerator Driven Systems for Transmutation: Fuel Development, Design and Safety, paper presented in 2nd COE-INES Int. Symposium on Innovative Nuclear Energy Systems (INES-2), Yokohama, Japan, 2006.

[4.266] MELONI, P. et al., Implementation and Preliminary Verification of the RELAP5/PARCS Code for Pb-Bi Cooled Subcritical System, paper presented in Topical Meeting of the American Nuclear Society Winter Meeting on Nuclear Applications in the New Millenium (AccApp 01-ADTTA 01), Reno, Nevada, USA, 11–15 November 2001.
[4.267] MELONI, P., et al., Verification of the RELAP5 Code against the MEGAPIE Irradiation Experiment, paper presented in 10th Int. Exchange Meeting on Transmutation and Partitioning, 6–10 October 2008, Mito, Japan.
[4.268] MELONI, P., BIANCHI, F., MATTIODA, F., Accident Analysis of an Experimental Accelerator Driven System, paper presented in 13th Int. Conf. on Nuclear Engineering (ICONE-13), Chinese Nuclear Society, Bejing, China, 2005.
[4.269] MELONI, P., et al., Preliminary T/H and Transient Analyses for EFIT Reactor design, Proc. ICAPP'07, Nice, France, 13–18 May 2007 (5 Vols), Curran Associates, Inc. (February 2008)
[4.270] MELONI, P., BANDINI, G., POLIDORI, M., T/H and Transient Analyses to Confirm EFIT Preliminary Design, ELSEVIER, Journal of Nuclear Materials 376 (2008) pp. 405–408.
[4.271] MELONI, P., BANDINI, G., POLIDORI, M., T/H and Transient Analyses to Confirm EFIT Preliminary Design, IV Workshop on Materials for HLM cooled Reactors and Related Technologies, Journal of Nuclear Materials 376, (2008) pp. 405–408.
[4.272] MIGNANELLI, M.A., THETFORD, R., Thermophysical and Chemical Properties of Minor Actinide Fuels, paper presented in Advanced Reactors with Innovative Fuels, Chester, Great Britain, 2001.
[4.273] MORITA, K., MASCHEK, W., FLAD, M., Thermodynamic Properties of lead-bismuth Eutectic for Use in Reactor Safety Analysis, paper presented in ICONE-13, Beijing, China, 2005.
[4.274] MORITA, K., Equation of States for CERCER and CERMET fuels. Internal FZK report (2004).
[4.275] MORITA, K., MASCHEK, W., FLAD, M., YAMANO, H.,. TOBITA, Y., Thermophysical Properties of lead-bismuth Eutectic Alloy in Reactor Safety Analyses, J. Nuclear Science and Technology, Vol. 43, No. 5 (2006) pp. 526–536.
[4.276] MORITA, K. SOBOLEV, V., FLAD, M., Equation of State for Heavy Liquid Metal Targets, paper presented in ERMS-2006, Nice, France, 2006.
[4.277] MÜLLER, G., HEINZEL, A., KONYS, J., SCHUMACHER, G., WEISENBURGER, A., ZIMMERMANN, F., ENGELKO, V., RUSANOV, A., MARKOV, V., Behaviour of steels in flowing liquid PbBi eutectic alloy at 420–600°C after 4000–7200 h, Journal of Nuclear Materials 335 (2004) p. 163.
[4.278] PDS-XADS Preliminary Design Studies of an Experimental Accelerator Driven System, EU Contract No. FIKW-CT-2001-00179, 5th Framework Programme EU (2001).
[4.279] RICHTER, K., FERNÁNDEZ, A., SOMERS, J., Infiltration of highly radioactive materials: a novel approach to the fabrication of targets for the transmutation and incineration of actinides, Journal of Nuclear Materials, 249, (1997) p. 121.
[4.280] RINEISKI, A., MASCHEK, W., MERK, B., FLAD, M., Neutron Kinetics Developments of the SIMMER-III Safety Code for ADS Application, paper presented in 2nd OECD/NEA Workshop on Utilization and Reliability of High Proton Accelerators, Cadarache, France (1999).
[4.281] RINEISKI, A., MASCHEK, W., RIMPAULT, G., Performance of Neutron Kinetics Models for ADS Transient Ananlyses, paper presented in Topical Meeting of the American Nuclear Society Winter Meeting on Nuclear Applications in the New Millenium (AccApp 01-ADTTA 01), Reno, Nevada, USA, 11–15 November 2001.
[4.282] RINEISKI, A., MASCHEK, W., Kinetic Models for Safety Studies of Accelerator Driven Systems, Annals of Nuclear Energy 32, (2005) 1348–1365.
[4.283] RINEISKI, A., SINITSA, V., MASCHEK, W., C4P, a Multigroup Nuclear CCCC Data Processing System for Reactor Safety and Scenario Studies, paper presented in Annual Meeting of Nuclear Technology (JK2005), Nürnberg, Germany (2005).
[4.284] RINEISKI, A., Decay Heat Production in a TRU Burner, paper presented in 2nd COE-INES Int. Symposium on Innovative Nuclear Energy Systems, paper presented in INES-2, Yokohama, Japan, 2006.

[4.285] SALVATORES, M., SCHNEIDER, E., GROUILLER, J.P., SCHWENK-FERRERO, A., WIESE, H.-W., DELPECH, M., KNEBEL, J., P/T Potential for Waste Minimisation in a Regional Context, paper presented in 8th Inf. Exchange Mtg on Actinide and Fission Product P&T Meeting 2004, Las Vegas, Nevada, USA, 2004.
[4.286] SAROTTO, M., ARTIOLI, C., PELUSO, V., Prliminary Neutronic Analyses of the Three Zones EFIT MgO/Pb Core, ENEA Report FPN-P815-004, Italy (2007).
[4.287] SCAFFIDI-ARGENTINA F., HAAS, D., SOMERS, J., KLAASEN, F., SCHRAM, R., WARIN D., BONNEROT, J.M., GARZENNE, C., (2006), HELIOS: Irradiation of U-Free Fuels and Targets for Americium Transmutation, Proc. ICAPP'06, Reno, Nevada, 4–8 June 2006, ANS, ISBN: 0-89448-698-5 (CD-ROM).
[4.288] SCHIKORR, M., Assessment of the kinetic and dynamic transient behaviour of subcritical systems (ADS) in comparison to critical reactor systems, Nuclear Engineering and Design, 210 (2001) pp. 95–123.
[4.289] SCHIKORR, M., EUROTRANS internal report, EUROpean Research Programme for the TRANSmutation of High Level Nuclear Waste in an Accelerator Driven system, FI6W-CT-2004-516520 (2006).
[4.290] SCHWENK-FERRERO, A., RINEISKI, A., WIESE, H.-W., MASCHEK, W., Validation of KORIGEN decay heat assessment for EFIT cores, paper presented in Annual Meeting of Nuclear Technology (JK2007), Karlsruhe, Germany, (2007).
[4.291] SMITH, P., Design Studies on the AFTRA EFIT Core, paper presented in EUROTRANS DM1-DM3 Meeting, Cadarache, France, 12–14 June 2006.
[4.292] SOBOLEV, V., First Approach to EFIT Specifications, paper presented inEUROTRANS DM1-DM3 Meeting, 10 June 2005, Winfrith, Great Britain.
[4.293] STRUWE, D., PFRANG, W., Conceptual approach for determination of limit conditions to relevant clad creep induced fuel pin failures (unpublished FZK report) (2006).
[4.294] SUZUKI, T., CHEN, X.N., RINEISKI, A., MASCHEK, W., Transient analyses for accelerator driven system PDS-XADS using the extended SIMMER-III code, J. Nuclear Engineering and Design, No. 235 (2005) pp. 2549–261.
[4.295] SUZUKI, T., TOBITA, T., KONDO, Sa., SAITO, Y., MISHIMA, K., Analysis of Gas-Liqid Metal Two phase Flows Using a Reactor Safety Analysis Code SIMMER-III, Nuclear Engineering and Design 220, (2003), pp. 207–223.
[4.296] SUZUKI, T., CHEN, X.N., RINEISKI, A., MASCHEK, W., TOBITA, Y., FUJITA, S., YAMANO, H., KONDO, S., Multiphase Flows and Fuel Relocations in Disrupted Core of Accelerator Driven System PDS-XADS , paper presented in 6th Int. Conf. on Nuclear Thermalhydraulics, Operations and Safety (NUTHOS-6) Nara, Japan, 2004.
[4.297] SUZUKI, T., TOBITA Y., KONDO S., SAITO Y., MSIHIMA K., Analyses of Gas-Liquid Metal Two phase Flows Using a Reactor Safety Analysis code SIMMER-III, Journal of Nuclear Engineering and Design, No. 220 (2003) pp. 207–223.
[4.298] THETFORD, R., SOBOLEV, V., Recommended properties of fuel, cladding and coolant for EFIT pre-design, AFTRA Del. 3.4, (EUROTRANS N°: FI6W-CT-2004-516520) (2005).
[4.299] THORIUM CYCLE Development Steps for PWR and ADS Applications, EU Contract No. FIKI-CT-2000-00042, 5th Framework Programme EU (2001).
[4.300] TOBITA, Y., KONDO, S., YAMANO, H., MORITA, K., MASCHEK, W., COSTE, P., CADIOU, T., The development of SIMMER-III, an advanced computer programme for LMFR safety analysis, and its application to sodium experiments, Nuclear Technology 153 (2006) pp. 245–255.
[4.301] VAN TUYLE, G.J, SLOVIK, G.C., KENNETT, R.J., CHAN, B.C., ARONSON, A.L., Analyses of Un-scrammed Events Postulated for the PRISM Design, Nuclear Technology, Vol. 91, 2 (1990) p. 165.
[4.302] WANG, S., FLAD, M., MASCHEK, W., AGOSTINI, P., PELLINI, D., BANDINI, G., SUZUKI, T., MORITA, K., Evaluation of a Steam Generator Tube Rupture Accident in an Accelerator Driven System with lead Cooling, paper presented in COE-INES Int. Symposium on Innovative Nuclear Energy Systems (INES-2), Yokohama, Japan, 2006.
[4.303] WALLENIUS, J., CONFIRM: Collaboration on Nitride Fuel Irradiation and Modeling, paper presented in paper presented in Topical Meeting of the American Nuclear Society Winter

Meeting on Nuclear Applications in the New Millenium (AccApp 01-ADTTA 01), Reno, Nevada, USA, 11–15 November 2001.
[4.304] YOUNG, D.A., A Soft-Sphere Model for Liquid Metals, Laurence Livermore Laboratory University of California UCLR-52352 (1977).
[4.305] TSUJIMOTO, K., SASA, T., NISHIHARA, K., et al., Neutronics Design for lead-bismuth Cooled Accelerator-Driven System for Transmutation of Minor Actinide, J. Nucl. Sci. and Technol., 41, Issue 1 (2004) p. 21.
[4.306] KONDO, S., TOBITA, Y., MORITA, Y., et al., SIMMER-III: an advanced computer programme for LMFBR severe accident analysis, Proc. of the Int. Conf. on Design and Safety of Advanced Nuclear Power Plant (ANP'92), Tokyo, Japan, 25-29 October 1992, Vol. IV (1992) pp. 40.5.1-40.5.11.
[4.307] MASCHEK, W., et al., SIMMER-III, a code for analyzing transients and accidents in ADS, paper presented in Topical Meeting on AccApp'00, Washington DC, USA 2000.
[4.308] JAPAN ATOMIC ENERGY AGENCY, Feasibility Study on Commercialized Fast Reactor Cycle Systems: Technical Study Report of Phase II Fast Reactor Plant System, JAEA Research 2006-042, Japan Atomic Energy Agency (2006) (in Japanese).
[4.309] SUZUKI, T., CHEN, X., RINEISKI, A., MASCHEK W., Transient analyses for accelerator driven system PDS-XADS using the extended SIMMER-III code, Nuclear Engineering and Design, 235 (2005) pp. 2594–2611.
[4.310] SUGAWARA, T., et al., Feasibility Study of Accelerator Driven System Proposed by JAEA, Proc. GLOBAL 2007, Boise, Idaho, 9–13 September 2007, ANS, ISBN: 0-89448-055-3, CD-ROM.

# CHAPTER 5
# ADS NATIONAL PROGRAMMES

## 5.1. BELARUS

The Belarus activities in the field of Accelerator Driven Systems (ADS) are mainly related to the investigations performed at the subcritical facility YALINA. Yalina is a zero power subcritical facility to study neutronics of ADS and the transmutation reaction rates.

The first assembly YALINA-T was put into operation in 2000. YALINA-T is a multiplying system ($kmax$<0.98), located inside a graphite reflector of parallelepiped configuration that is arranged of high purity reactor graphite blocks. The core of the assembly is of parallelepiped configuration too and consists of bare polyethylene subassemblies where fuel rods of EK-10 type (UO2 of 10% enrichment by U235) are located. At the core center a neutron producing Pb target is located that reminds fuel subassembly by shape and size. Graphite reflector is covered from outside by Cd. At the distances R=50 mm, 100 mm, 150 mm from the core center three experimental channels (D=25 mm) are situated for location of samples of radioactive targets and various detectors for measurement of neutron flux density functionals. For the same purpose two axial channels (D=25 mm) are located in graphite reflector at the distances 250 mm and 358 mm; by Z=H/2 one more radial channel (D=25 mm) is located.

YALINA-B core is arranged of rectangular parallelepipeds too. The fast (booster) zone consists of lead subassemblies, the thermal one of polyethylene subassemblies. Central part of the booster zone, containing highly enriched (90%) metallic uranium fuel and Pb target is encased into a separate stainless steel frame. The absorber zone is located at the outer boundary of the booster zone. It consists of inner layer of rods with metallic natural uranium fixed in lead blocks, as in the previous cases, and of an outer layer of rods filled by boron carbide powder, B4C. Boron carbide rods are located in the same lattice as the uranium fuel pins in the booster zone with pin pitch 16.00 mm. This absorber zone enables fast neutrons to penetrate into the thermal zone, outside the absorber and fast zones, and prevents thermal neutrons from entering the booster zone from the thermal zone. The result is a fast neutron coupling of the fast and the thermal zones. The absorbing rods with B4C are fastened rigidly and may not be taken out accidentally, to prevent undesired reactivity insertions.

The thermal zone surrounds the booster zone and the absorber zone. There are three experimental channels in the thermal zone. Finally, the thermal zone is surrounded radially by a graphite reflector. In the reflector there are three experimental channels. Axially, the core is limited by borated polyethylene.

The theoretical and experimental investigations of ADS neutronics have been performed in the framework of national scientific programmes and international cooperation: IAEA CRPs, ISTC projects and the Integrated Project EUROTRANS of the European Commission. The following R&D activities on the YALINA facility were carried under these initiatives:

— Validation of methods of subcriticality level monitoring;

— Experimental study of subcritical systems kinetics;

— Measurements of spatial distribution of neutron flux density;

— Time behaviour of neutron flux depending upon neutron pulse parameters;

— Measurements of long lived fission products and minor actinides transmutation rates.

## 5.2. BELGIUM

The Belgian activities in the field of Accelerator Driven Systems (ADS) are mainly related to the MYRRHA project development. MYRRHA is an accelerator driven, multi purpose fast neutron spectrum facility for R&D, cooled by a lead-bismuth eutectic.

SCK•CEN has started the MYRRHA project as a national programme with several national & international bilateral collaboration agreements; the project has now evolved as an European integrated project in the frame of the IP_EUROTRANS (European Commission, Sixth Framework Programme). The MYRRHA 'Draft-2' predesign file (completed in the early 2005) has been proposed to the partners as a basis for the XT-ADS machine. After a detailed investigation of potential alternatives, the MYRRHA concept (for the subcritical core, the primary coolant system, the accommodation of experimental rigs, the reactor vessel and the spallation target) has been kept with some modifications to achieve the XT-ADS objectives. The most recent version of the XT-ADS design has been presented in the 2007 TWG meeting.

The R&D programme is also partly included in IP_EUROTRANS. The most recent results have been obtained in the domain of the WebExpIr experiment, where we study the interaction between the lead-bismuth free surface and a high power DC electron beam (mainly the free flow distortion and the lead-bismuth evaporation due to surface heating).

Beyond 2008 (at the end of IP_EUROTRANS) perspectives are under consideration with several EU partners and the EC, for structuring the implementation and the deployment of the XT-ADS. SCK•CEN is considering Joint Undertaking for setting up this frame and has already declared its readiness to welcome a fast spectrum irradiation facility at its technical site in Mol. In this purpose, several bilateral agreements have been signed or existing agreements are currently being refreshed, the most recent agreements being with CEA (October 4th, 2006), with JAEA (November 23rd, 2006) and with CIEMAT (April 17th, 2007).

SCK•CEN in association with 18 Europeans partners from industry, research centra and academia, responded to the second FP7 call from the European Commission to establish a Central Design Team for the design of a FAst Spectrum Transmutation Experimental Facility (FASTEF) able to demonstrate efficient transmutation and associated technology through a system working in subcritical and-or critical mode. The proposal prepared by the consortium coordinated by SCK•CEN has been accepted for funding and the project has started on April 01st, 2009 for a period of three years.

A business plan, including the project costs (both investment and operational) as well as the proposed project structure for building the different components, assembling them and finally operate the facility, has been submitted to several Belgian political levels to ensure a strong support from the Belgian government to the project.

## 5.3. CHINA

In China the conceptual study of an ADS concept which lasted for about five years ended in 1999. As one project of the National Basic Research Programme of China (973 Programme) in energy domain, which is sponsored by the China Ministry of Science and Technology (MOST), a five year programme of fundamental research of ADS physics and related technology was launched in 2000 and passed national review at the end of 2005. From 2007, another five year 973 Programme Key Technology Research of Accelerator Driven Subcritical System for Nuclear waste Transmutation started. The research activities were focused on HPPA physics and technology, reactor physics of external source driven subcritical assembly, nuclear data base and material study. For HPPA, a high current injector consisting of an ECR ion source, LEBT and an RFQ accelerating structure of 3.5 MeV has been built and were being improved. In reactor physics study, a series of neutron multiplication experimental study has been carrying out. The VENUS I facility has been constructed as the basic experimental platform for neutronics study in ADS blanket. VENUS I a zero power subcritical neutron multiplying assembly driven by external neutron produced by a pulsed neutron

generator or 252Cf neutron source. The theoretical, experimental and simulation studies on nuclear data, material properties and nuclear fuel circulation related to ADS are carried out in order to provide the database for ADS system analysis. China Institute of Atomic Energy (CIAE), Institute of High Energy Physics (IHEP) and other Chinese institutes carried out the MOST project together.

Besides CIAE, China Academy of Science (CAS) pays more and more attention to Advanced Nuclear Fuel Cycles (ANFC). A large programme of ANFC, including ADS and Th based nuclear fuel cycle, has been launched by CAS. A roadmap of ADS has been proposed by CAS. Around 201X, small experimental ADS will be build. The reactor power is ~4MW, and the proton LINAC is 40MeV, 10mA. Around 2022, a medium size experimental ADS will be built. The reactor power is 80~100MW, and LINAC is~600MeV, 10mA. Around 2032, ADS Demo Facility will be built. The reactor power is~1000MW and the LINAC is ~1.5GeV, 10mA.

## 5.4. FRANCE

### 5.4.1. CNRS

Studies related to nuclear reactors and radioactive waste started at the French National Centre for Scientific research, CNRS, as a result of the French law on radioactive waste that was published in 1991.

They were initially organized around the programme PACE (Physique pour l'Aval du Cycle Electronucléaire = physics of the back end of the nuclear fuel cycle), which became PACEN (Physique pour l'Aval du Cycle et production d'Energie Nucléaire = Physics of the back end of the nuclear fuel cycle and production of nuclear energy) in 2006. Research on accelerator driven systems was from the beginning part of this programme. This research is mainly funded by the National Institute for Nuclear end Particle Physics (IN2P3) of CNRS and within the EURATOM European programmes (FP5, 6 and 7).

The programme took place in several stages, and covered various scientific fields, benefitting from expertise of CNRS in the field. More specifically, it aimed and still aims to:

— Test and verify the feasibility and design of the ADS concept, in terms of neutronics, physics of materials, design of the accelerator and tests of its prototypical components that have been built (or are at present under construction);

— Measure and-or improve nuclear data related to radioactive waste transmutation.

First, CNRS participated in the international collaborations FEAT and TARC. These studies were continued through the MUSE programme, of which the goal was to develop techniques for measuring on-line the absolute reactivity of a subcritical core. In this frame, the accelerator based neutron source GENEPI neutron source was developed at CNRS/IN2P3/LPSC at Grenoble. The success of this programme has led CNRS teams to invest, at the end of 2006, alongside SCK•CEN in Belgium, in the construction and cofinancing of an experimental zero power mockup reactor driven by an upgraded GENEPI (mark 3C). This experiment is dedicated to the study of fast subcritical system and relies on the reconfigured VENUS reactor of SCK•CEN. The project, called GUINEVERE (Generator of Uninterrupted Intense NEutron at the lead VEnus REactor), aims at the full validation of a procedure for reactivity monitoring of an ADS. It was actually started as a principal working package (domain) of the FP6 Integrated Project (IP) EUROTRANS. The coupling has successfully taken place, and GUINEVERE is today fully exploited within the FP7 project FREYA (Fast Reactor Experiment for Hybrid Applications). The experiments extend, for the subcritical configurations, to design, safety studies and licensing aspects for the reactor MYRRHA (Multi purpose hYbrid Research Reactor for High tech Applications). The front end engineering Design of MYRRHA is at present pursued by the FP7 CDT (central design team) in which CNRS is fully engaged.

In parallel, R&D on the spallation target was also carried out (FP5 and 6): on the one hand, CNRS (IN2P3-SUBATECH, Nantes) was responsible for the spallation target design of the MEGAPIE experiment (MEGAwatt PIlot Experiment) at PSI, Switzerland, and, on the other hand, it participated to the SPIRE programme (FP5-ADOPT) in evaluating the different contributions to irradiation damage induced in structural materials in a spallation target environment. In the framework of EUROTRANS (FP6. 2005–2010), CNRS participated also to the domains DESIGN, and DEMETRA, in particular by the study of the size of the target, the behaviour of materials (T91) under irradiation, and the evaluation of proton flux vertical, coaxial to the flow of the (spallation target but also reactor coolant material) Pb-Bi.

Regarding accelerator physics, ADS researches have benefited from the know-how acquired and developed for other programmes in nuclear physics (for instance, EURISOL, SPIRAL2, ESS, XFEL) and for which the technological platform SUPRATECH has been specifically developed at CNRS/IN2P3/IPN at Orsay. First studies of the architecture of the superconducting linac dedicated for ADS were performed in the framework of FP5 PDS-XADS. Test of prototype cavities were performed, as well as first reliability studies. This work continued through EUROTRANS (FP6), to achieve more precise studies and to construct a prototype cryo-module. Fault tolerance was also addressed in this programme as well as studies for the coupling of the accelerator and the spallation target. In the FP7, CNRS coordinates today the MAX project (MYRRHA Accelerator eXperiment), of which the objective is to provide a detailed design (ready for construction) for the accelerator of MYRRHA.

In this general context, CNRS teams performed also simulations of ADS cores (and different target configurations) that were related to deployment scenarios in order to optimize the performance of transmutation.

Relying on their expertise in nuclear physics as well as in the development of state of the art detectors, CNRS research teams have carried out nuclear data measurements since the 90's (through different European programmes, such as HINDAS (FP5), NUDATRA (FP6) or ANDES (FP7) for instance. These studies concern both spallation cross-sections measurements (these studies were performed in the FP5 and FP6, and are now finished) and nuclear data for Gen 4 systems (cross-sections measurements of fission and capture on actinides). These last are conducted with facilities such as the n-TOF line at CERN, and GELINA in Geel. They are also complemented by more fundamental studies of fission (for instance at n-TOF-CERN, GANIL at Caen and Tandem-ALTO at Orsay) which allow to improve the models needed for data evaluations.

Main results related to CNRS contribution are:

— The concept of the super conducting cavities for the accelerator has been validated and the overall structure of the LINAC is designed and its beam dynamics fully simulated and understood. It remains to further refine methods for improving the so-called reliability (i.e. the countermeasures for avoiding trips, that are non-voluntary interruptions of the beam). The obtained results allow us to assess with reasonable confidence that the specifications for the accelerator of an ADS will be fulfilled.

— While it is clear that further testing must be continued and that the results of GUINEVERE will play also a key role for an overall validation, CNRS already confirms the reliability of the methods developed within the MUSE programme and their extrapolation to a continuous beam.

— The concept of target with window has been validated by the MEGAPIE results for the part of neutrons production. The holding of materials (dpa in the structures) seems also robust.

Today, most of the activities in support to ADS development carried out by CNRS focus on accelerator developments, GUINEVERE experiment, ADS core studies, deployment scenarios and nuclear data measurements.

Achievements of all these studies (combined to the studies made by all the other actors) reasonably allow foreseeing the feasibility and interest of a ADS demonstrator. The MYRRHA project is thus the

logical continuation of the R&D performed by CNRS, and its possible success in line to deployed efforts of the research teams.

### 5.4.2. CEA

The CEA R&D programmes on ADS are mainly focused on the European project EUROTRANS of the 6th Framework programme (2005–2010) and continued in the FREYA project of the 7th Framework Programme.

Within the EUROTRANS Project, the domain 1_DESIGN has included the task to provide the pre-conceptual design of an European Transmutation Demonstrator (ETD) able to demonstrate the feasibility aspects of the radioactive waste transmutation burning in Accelerator Driven System (ADS) at industrial scale. The reference proposal was based on the lead cooled EFIT (European Facility for Industrial Transmutation). The He-EFIT (helium cooled EFIT) concept was the option considered as the back up solution.

The pre-conceptual design of the He-EFIT plant has been developed by CEA during the EUROTRANS Project. The plant has a power of approximately 400 MWth. Likewise all the ADS plants, it consists of three main components: the accelerator, the spallation target module and the subcritical core.

A plant pre-conceptual design has been proposed and studies have been performed to support this design. These studies essentially dealt with the spallation performances, transmutation capabilities and the plant safety analysis.

Regarding nuclear physics, the main CEA activities can be summarized as follows:

— The lead of the field 2/ECATS (Experimental Coupling in EUROTRANS);

— The loan of the fuel to be used in the VENUS facility (SCK•CEN, Mol), about 1.2 tons of uranium metal enriched to 30% uranium 235, and 3 tons of lead from MASURCA;

— The development of GENEPI-3C, and actively participating in the dismantling of the neutron generator (GENEPI-1) installed on MASURCA, and its return to CNRS/IN2P3/LPSC/Grenoble then installed in the new version of the neutron generator now installed in VENUS F;

— The contribution to the specifications and design of the GUINEVERE core configuration;

— The definition of the necessary instrumentation for the experiments;

— The provision of sensors and equipment for measurements;

— The definition of the experimental programme;

— The provision of information related to the preparation and feedback programme MUSE-4 (specific studies, startup procedure in coupled configuration, REX on tritium releases).

— The lead of the Work Package n° 1 task 1.1 (SC2 and SC3 experiments) of FREYA; and

— A major contribution in defining and implementing the GUINEVERE measures.

For fuel developments, CEA has lead and significantly contributed to the domain AFTRA (Advanced Fuels for Transmutation) within EUROTRANS as well as Domain 3 dealing with Post-irradiation Examinations and Modelling within FAIRFUELS (2009–2013). Regarding technical progress, a wide range of results has been provided on primary candidates that are MgO-CERCER and 92Mo-CERMET fuels:

— CEA successfully prepared and implemented the irradiation FUTURIX-FTA in PHENIX reactor;

— MgO-CERCER fuels and pins for that irradiation were manufactured in ATALANTE labs;

— Regarding HELIOS irradiation scheduled (and completed in HFR) within EUROTRANS, the MgO-CERCER fuels were fabricated in ATALANTE labs;

— Thermal properties of several fuel compositions and first mechanical properties of TRU-oxide compounds were measured at the LEFCA facility;

— First compatibility tests were performed between: actinide phases, inert matrix candidates, T91 cladding and Pb coolant;

— Finally, significant progress was made in Pu-Am-O phase diagram investigation.

The Post-irradiation examinations of the 2 MgO-CERCER pins irradiated within FUTURIX FTA test are expected in a near future in the hot cells of PHENIX (for non-destructive examinations) and at the LECA facility (for destructive examinations).

For corrosion developments, CEA contributed since 1999 in several European projects in the frame of the Vth and VIth PCRD within TECLA and MEAGAPIE (Vth PCRD) and then EUROTRANS-DEMETRA (VIth PCRD).

In this framework, corrosion facilities as COLIMESTA (experimental device to perform corrosion tests in static lead bismuth) and CICLAD (corrosion loop to perform tests in flowing lead bismuth) were built providing many results and understanding about corrosion processes of the ADS structural steels: mainly T91 (ferritic martensitic Fe-9Cr steel) but also 316L (austenitic Fe-17Cr-10Ni steel).

T91 corrosion modelling has been performed as a function of temperature and dissolved oxygen concentration in the liquid alloy melt leading to two models: one corresponding to the oxidation mechanism of T91 in liquid Pb-Bi (for the high dissolved oxygen concentration domain) and one for the dissolution mechanism, depending on the Pb-Bi fluid velocity (for the low oxygen concentration domain).

Experiments were also performed on other steels and on protective coatings developed by the various international partners of the research programmes.

Some investigations were also performed on chemical data in Pb-Bi concerning the measurement of the nickel solubility limit and the iron diffusion coefficient in Pb-Bi at various temperatures.

In addition, a Gas Cooled ADT (Accelerator Driven Transmuter) core neutronic benchmark has been proposed by CEA for an IAEA Coordinated Research Project (CRP) on Studies of Advanced Reactor Technology Options for Effective Incineration of Radioactive Waste.

A comparison has been carried out at BOL and EOL for the following parameters: $k_{eff}$, reactivity coefficients, kinetic parameters and transmutation rate. Four institutions have contributed to this benchmark using various computational tools: Monte Carlo codes (MCNP(X), TRIPOLI4) and deterministic codes (ERANOS, DANTSYS) and nuclear data libraries (JEF2.2, JEFF3, JENDL3.3, ENDF/B-VI).

## 5.5. GERMANY

The German R&D programme for ADS development is related to the partitioning and transmutation of spent fuel. This programme is implemented mainly by the three national research centres belonging to the Helmholtz Association, i.e. Karlsruhe Institute of Technology (KIT), Forschungszentrum Jülich (FZJ) in cooperation with the Technical University of Aachen (RWTH Aachen) and the Helmholtz Zentrum Dresden Rossendorf (HZDR). The main purpose of this R&D programme is the prospect to manage the high level radioactive waste such as to reduce the burden on a final repository. P&T does not eliminate the need for a final repository whatever the strategy, but it allows the reduction of the radiotoxicity associated with radioactive waste, the increase of the repository capacity as a consequence of the reduction of masses to be stored and their associated residual heat load.

Different fuel cycle scenarios to implement P&T can be envisaged. These scenarios have been evaluated to identify the impact of P&T on the characteristics, number and deployment pace of the

installations of the fuel cycle (reprocessing, fuel fabrication, storage etc). Almost all activities conducted in the R&D programme are embedded in European and international projects and initiatives. In the following more details on the relevant components of the R&D programme are summarised.

### 5.5.1. Scenario studies

The scenario studies are aimed at evaluating possible strategies and implementations of ADS in order to reduce the TRU legacy inventory as discharged from LWR. These studies are performed within a single country context and in a regional context. The preliminary results of these studies have been helpful a) to assess partitioning and transmutation strategies and options in order to implement the different objectives; b) to define and quantify possible regional facilities which can be shared by different countries even if with diverging objectives and c) to understand potential benefits in reducing the burden on geological disposal. Further activities are focussed on:

— Investigation of different scenarios for transmutation including analysis on economic impact and proliferation risk,

— Global and regional scenario studies for waste minimisation and sustainable development of nuclear energy.

Moreover, in the frame of the scenario studies advanced software tools are developed as well as methods to evaluate and collect data necessary to perform studies for various P&T strategies at national and international level. These methods include investigations on economic impact of the various scenarios and the assessment of their proliferation risk.

### 5.5.2. Partitioning

Hydrometallurgical processes are being developed for separating the trivalent actinides by means of liquid–liquid extraction from the spent fuel. The R&D work is performed with highly radioactive liquid waste from reprocessing according to the PUREX process. However, partitioning of the trivalent An(III) (Am, Cm) actinides is not possible with the present reprocessing technique. Therefore the R&D focus is on:

— The development of improved extracting agents for the separation of americium and curium from lanthanides. Moreover, the investigations on the driving forces for such extracting agents' selectivity and the investigation on the stability of selective extracting agent are as well part of the activity.

— Development of an efficient separation process by application of hollow fiber technology and by centrifugal contactors-mixer settler. In this context the implementation of cold, spiked and hot laboratory tests for the demonstration of the technical feasibility of partitioning processes is performed.

— Coconversion routes such as co-precipitation and solgel routes.

The research goals addressed within the topic of efficient separation of americium and curium from radioactive waste by solvent extraction are related to the fundamental understanding of the extraction mechanism. For this purpose, advanced spectroscopic methods as EXAFS, laser and NMR spectroscopy as well as theoretical methods (quantum chemistry) are applied. The combination of the experimental and the theoretical methods allows the elucidation of the structures of the complexes formed by actinide species and extracting agents thus enabling a realistic description of the selectivity mechanism of the extractants. Based on this knowledge, the extracting agents are modified in order to improve radiolytic and hydrolytic stability without compromising the extraction performance.

The mechanistic understanding of the extraction reaction, the quantification of underlying kinetics and thermodynamics are relevant parameter used for the Optimization and the implementation of a robust

partitioning process. Cold, spiked and hot laboratory tests for the demonstration of the technical feasibility of partitioning processes are finally implemented.

### 5.5.3. Transmutation

The considered transmutation system is an Accelerator Driven Subcritical system cooled with HLM as Pb or lead-bismuth Eutectic (LBE) and all activities performed are embedded in international initiatives (e.g. Projects supported by the European Commission, OECD and IAEA Working Groups, etc.).

The past and on going R&D activities performed in Germany have contributed to the assessment of the main components of ADS as e.g. the neutron spallation target and the subcritical blanket. As an example, R&D activities have been conducted, in an international context, to contribute to the demonstration of the feasibility, the licensing and safe operation of the 1 MW liquid lead-bismuth neutron spallation target MEGAPIE (MEGawatt Pilot Experiment). MEGAPIE has been successfully operated for four months at the target location SINQ at PSI. Currently the PIE programme of the irradiated target is being set up and executed.

As far as the design studies of subcritical blanket is concerned, major activities have been conducted within past European Programmes in the areas of development of designs of ADS facilities, the development of Heavy Liquid Metal technologies, thermalhydraulics tools and materials. The completion of these experimental programmes has allowed defining relevant follow-up projects. In particular the following research areas are addressed:

#### *5.5.3.1. Safety and design oriented safety studies*

The studies are performed within international cooperation with the objective to develop and evaluate optimum design solutions of subcritical systems which allow an efficient-optimum reduction of the actinide inventory.

— Detailed design and more realistic safety analyses are conducted by considering inert matrix fuels and others matrix material.

— Methods and Code Development: Improvement and extension of the safety code systems (e.g. SIMMER-III, SIMMER-IV, SAS4A, TRACE, RELAP, SIM-ADS, CFD) in terms of thermalhydraulics, neutronics and component simulation. In parallel an extensive models development for the analysis of the behaviour of the innovative fuels and their interaction with the specific coolants over the whole range of transients from design basis to design extension conditions is performed.

— Database generation: Extension and further buildup of the thermal-physical and thermal-mechanical data base and equation of state for the constituents for innovative fuels including the effects of irradiation and helium production. This activity has taken advantage of irradiation programmes on innovative fuels.

#### *5.5.3.2. Physics of transmutation*

The focus is on improvement of nuclear data base for waste incineration and impact of nuclear data uncertainties; to reach these goals following activities are performed:

— Development of new cross-section processing techniques.

— Investigation of spatial kinetics models for possible future implementation in the KIN3D model of the ERANOS.

— Improvement of approximations of neutron transport problem solutions with application in Monte Carlo and deterministic multi group codes.

— Support to the demonstration of the safe operability of subcritical systems by appropriate dynamics and kinetics experiments, within international initiatives (e.g. GUINEVERE, YALINA).

— Improvement of methods and data bases to quantify sensitivities and uncertainties of nuclear data needed to assess the transmutation capabilities.

— Enhancement of deterministic and Monte Carlo Methods for the prediction of the radiation damage and energy deposition in the neutron spallation target and vessel components.

— Shielding and activation optimization for the whole ADS system (accelerator, beam line, and subcritical core).

— Basic studies on relevant long lived fission products and actinides under various irradiation conditions.

#### *5.5.3.3. Thermalhydraulics studies*

The goal is to provide best practice guidelines for the application of computational fluid dynamics in nuclear reactor design assuring reliable results. To achieve this goal combined experimental and numerical efforts are performed:

— Models, experimental campaigns and validation: The limits of the parameter field in simple geometrical configurations (e.g. heated rod experiment in horizontal and vertical directions and backward facing step experiment) are detailed and the numerical models describing the single effects in the individual parameter regime are developed and validated through experimental campaigns. Experimental data and numerical simulations are compared and best practice guidelines for mixed convective flows are given.

— Instrumentation: several sensor as e.g. flowmeters, free surface sensors, etc are developed and or improved taking into account their application for scientific purposes and for nuclear installations.

— Engineering and component development: (1) an induction pump for high temperature application is under development and going to be qualified in a prototypical experiment. (2) nuclear positioning elements, produced with laser melting techniques are qualified. (3) design guidelines for heat exchangers to be used in HLM systems have been prepared.

#### *5.5.3.4. Materials studies*

The goal is to assess and if possible to enhance the compatibility of structural materials in terms of corrosion and mechanical resistance in HLM. The assessment the GESA surface alloying process to be applied on claddings to improve their corrosion resistance is as well foreseen. Prerequisite of these studies is the understanding of the effect of chemical species dissolved in the liquid metal on the compatibility. The activities are:

— ODS materials to enhance clad irradiation resistance and therefore improve fuel burnup capabilities are developed and tested. The preferred fabrication route is the powder metallurgy.

— HLM quality control: The focus is put on the measurement and adjustment of the oxygen activity in the liquid metal. The oxygen solubility is experimentally evaluated to confirm the thermochemical calculations. Oxygen exchange rate is experimentally evaluated and a model approach adapted for the development of an optimised technology to control the oxygen activity in larger pool type. Electrochemical probes used to measure the oxygen activity are tested for their long term behaviour and an optimised calibration method has been defined.

— Materials assessment in HLM: Selected structural materials (ODS, austenitic and ferritic martensitic steels) and their welds identified for the subcritical transmutation systems are

analysed in a representative range of parameters (temperature, oxygen activity, flow velocity) for their long term corrosion and mechanical resistance. The assessment of the corrosion and mechanical resistance improvement, with the surface alloying technique (GESA), of highly loaded components (e.g. cladding) is completed with the aim to scaleup of this technique to real cladding tubes and to develop an appropriate qualification methodology.

— Irradiation effects: PIE has been established within the MEGAPIE initiative to analyze the samples extracted from the neutron spallation Target. The PIE foresees both microstructural and mechanical investigations. The performance of the GESA alloyed structural materials are tested in a neutron irradiation field and in a combined neutron-HLM environment.

— Materials modeling: the activities are focused on the development of simulation of radiation damage effects and of mass transfer models for the prediction of corrosion rate. The models will be validated with available experimental results.

— Conversion of actinides for fuel fabrication: the objective is to develop methods for the coconversion of separated actinides for fuel preparation. The focus is on the solgel routes to fabricate mixed actinide oxides, with an appropriate matrix.

## 5.6. INDIA

### 5.6.1. Development of ADS concepts and chalking out the roadmap plans

Initial preliminary studies in India on ADS concepts were aimed toward applications such as, one way coupled booster reactor concept, thorium burner concept, enhancement of breeding rate of thorium–fueled fast reactors, and to incinerate Pu and minor actinides discharged from heavy water and fast reactors. These studies led to a roadmap on development of ADS subsystems in India, which was chalked out initially in June 2001. It was realized in these studies that the most challenging subsystem in terms of technology development and capital investment for ADS in India would be the high intensity proton accelerator, and that it must be accomplished in phased manner. Of the two alternative accelerator types, viz. the cyclotron and linear accelerator (linac), it is concluded that only linac would provide the necessary intense beam current for ADS applications.

The energy amplifier (EA) scheme, with lead (45.5%) bismuth (55.5%) eutectic (LBE) as target & coolant, which was proposed in the early nineties would be one of the desired configurations of ADS for Indian applications. Additionally, subcritical reactor core of Indian Advanced Heavy Water Reactor (AHWR), with advantages of its low fission power density, and neutron economy is also a candidate among various ADS reactor configurations. These options of ADS configurations for thorium utilization are based on the neutronic properties of $^{233}U$ isotope as fissile fuel, which are more or less similar in thermal and in moderately fast neutron spectra.

### 5.6.2. Plans for R&D on ADS

The Indian efforts of ADS development are now coordinated by a Steering Committee on ADS Programme (SC-ADSP) under the Indian Department of Atomic Energy (DAE). Under its framework, two pronged strategy has been devised:

Firstly, specific facilities would be constructed for key technology demonstration of ADS segments or part thereof, e.g. proton accelerator, target and materials testing loops and subcritical core assemblies etc.

Secondly and in parallel, intensive R & D in specific pertinent technology areas would be launched by involving specialists available in various R&D centers of the department. Many a material and fuel related development which is non-exclusive to the ADS applications, comes under this category.

A complementary addition to the above efforts would come with the possibility of conducting scientific studies and R&D through specific technological task forces that would derive strength from scientific excellence available with the academic and non-profit research institutions across the country.

The presently adopted roadmap on ADS envisages following developmental deliverables over next 10–15 years of R&D:

— An ongoing 20 MeV high current proton linac project in BARC, Mumbai is due for completion by end of year 2013. In next phase, its beam would be led though an underground beam line to reactor pile block in a nearby building of AHWR critical facility. The injected protons on a beryllium target would emit neutrons, which get coupled with the subcritical core for conducting reactor physics experiments.

— Programme to develop ~ 1000 MeV proton linac would be initiated in the next five year plan (2012–2017) in RR CAT, Indore as a $H^-/H^+$ injector of 1 MWt beam power. That would also inject its beam into a proton synchrotron to be constructed there in future for applications as spallation neutron source (SNS).

— Successful completion of above linac projects should lead to requisite technological developments for taking up construction of a moderate to high energy (e.g. 600 MeV), high current accelerator in new BARC campus at Visakhapattanam on the east coast of the country.

— Construction of ADS subcritical demonstration reactor of about 20–40 MWt fission power would be planned in Visakhapattanam campus. This will be utilized to demonstrate proton beam coupling to drive fissions in a reactor of sizable thermal power and operating at low temperature. The 600 MeV proton linac would be utilized as driver accelerator for this ADS.

— The above mentioned planned accelerator for a demonstration ADS in Visakhapattanam could be further extendable in size and proton energy up to 1 GeV at the same site, so that construction of a full-scale ADS power plant there might be undertaken in future.

— Concurrent to developments envisaged in (i) and (ii) above, VECC, Kolkata would continue development of high current proton cyclotron technology in suitably planned project modules for applications such as Radioactive Ion Beam (RIB) research programme.

### 5.6.3. Ongoing activities for R&D on ADS

A beginning of the above scheme is made with (a) the design and construction of a low energy high intensity proton linear accelerator (LEHIPA) facility at BARC and (b) high current proton injector system for a compact cyclotron at VECC.

Experimental facilities for development of technological details of lead-bismuth eutectic based spallation target subsystems and materials tests are in progress at BARC.

Initial design studies on and work to set up technological facility for fabrication and characterization of superconducting RF cavities from bulk niobium have also been taken up in BARC, which will be expanded to include the expertise available in other institutions notably in RRCAT, Indore and IUAC, New Delhi.

## 5.7. ITALY

Following a preliminary design developed in 1998, based on the Energy Amplifier concept proposed by CERN, a first configuration of a lead-bismuth Eutectic cooled Experimental ADS (LBE-XADS) was worked out in the period 1999–2001, under the aegis of MURST, by a group of Italian

organizations led by Ansado Nucleare, with the aim of assessing the feasibility of a small sized (80 MWth) ADS.

At the end of 1997 a joint effort of ENEA (National Agency for New Technology, Energy and the Environment) and INFN (National Institute for Nuclear Physics) led to the approval of a national programme by MURST (Minister for University and Scientific and Technological Research) named TRASCO (TRAsmutazione SCOrie) aiming at the study of physics and technologies needed to design an ADS for radioactive waste transmutation.

The programme consisted of research subprogrammes on accelerator, neutronics, thermalhydraulics analysis, beam window technology, and material technology and compatibility with Pb and Pb-Bi.

At now, most of the activities in support to the ADS development carried out at national level are part of EU-funded Projects. These activities are complemented by the programme agreement (*AdP -Accordo di programma*), signed between ENEA and the Ministry of Economic Development, which provides in general a range of activities aimed at the development of sustainable nuclear fission systems.

Several universities and the national industry are involved, besides ENEA, in the activities.

Specifically, the programme aims to:

— Retrain the national manufacturing industry to allow the participation in the abroad achievements (design and implementation of the AP1000 and EPR critical components, development of modern and-or innovative building processes, development of new methods of calculation).

— Concentrate resources on an international programme such as the IRIS Project where it becomes possible to play a significant industrial role (integral test of the system, qualification of components and systems, seismic analysis of the plant, etc…).

— Exploit the skills still existing to participate fully in the development of a Generation IV reactor as the lead Fast Reactor and-or the Very High Temperature Reactor within Euratom and GIF (integral test of the system, development of methods and core design, seismic and security analysis, etc…) as well as the ADS.

In order to achieve the proposed objectives, the programme is divided into four areas:

— LP1. Studies of scenario of new nuclear systems, innovative fuel cycles and of techniques for minimizing radioactive waste; technical support to relevant institutions in the field of nuclear energy is envisaged (*advisor* function);

— LP2. Evolutionary reactors INTD *International Near Term Deployment;*

— LP3. Generation IV reactors;

— LP4. Reactors near to market.

The third area is specifically dedicated to the generation IV nuclear systems and foresees the implementation of support activities to the technological development of lead fast reactors, Accelerator Driven Systems and very high temperature reactors.

More specifically, the LP3 includes those activities related to the technology development and to the optimization of the lead and lead-bismuth cooled system components, neutronic activation and the core thermo-hydraulics and the development of methods for the design of innovative cores of the LFR and ADS. Attention is paid to the aspects of seismic vulnerability, always in reference to the lead cooled reactors.

In detail, the activities concern:

### 5.7.1. Thermalhydraulic

— HLM thermalhydraulic laboratory implementation;

— Primary Pump definition, conceptual design, testing and qualification on large scale system;
— Fuel bundle investigation, under forced and free convection;
— Decay heat removal system definition, design and testing on large scale system;
— Lead Loop multipurpose facility implementation (HELENA);
— Conceptual design of a large scale pool system (ATHENA) for the ADS licensing.

### 5.7.2. Structural material develpment

— Coating Development (FeAl, FeCrAl, TiN, Ta)
— Stainless Steel and Ferritic–Martensitic steel coated qualification (corrosion, LME, fretting, mechanical behaviour, irradiation damage, creep,..)
— Refractory material development as structural material
— Mechanical testing laboratory implementation and qualification

### 5.7.3. ADS safety assesment

— Fuel–cladding coolant interaction;
— Release and capture of radioisotopes;
— Hot cells implementation;
— Coolant chemistry control implementation;
— Flow induced vibration assessment on fuel assembly;
— Steam generator tube rupture analysies and steam trapping scenario evaluation;
— Flow blockage scenario evaluation and analysis;
— FA manipulations and coolability assessment (free level transition);
— Core degradation analysis and fuel-FP migration.

### 5.7.4. Core design

— Fuel assembly transport calculations;
— Stand alone neutronic calculations: criticality (steady state), power deposition, reactivity worth and coefficients;
— 3-D NK-TH coupled calculations;
— Burnup calculations;
— Spallation target: neutronic coupling with a subcritical core;
— ADS fuel for transmutation.

## 5.8. JAPAN

In Japan, the research and development (R&D) activities on partitioning and transmutation (P&T) technology had been promoted under the OMEGA programme since 1988. The main institutes

involved in these activities were the Japan Atomic Energy Research Institute (JAERI), the Japan Nuclear Cycle Development Institute (JNC), and the Central Research Institute of Electric Power Industry (CRIEPI). Among these institutes, JAERI had mainly conducted the R&D on ADS.

In 1999 and 2000, the Atomic Energy Commission (AEC) of Japan implemented the check and review (C&R) on the P&T technology, and the ADS was considered as one of candidates for transmutation systems together with fast reactors. In 2005, JAERI and JNC were merged and the Japan Atomic Energy Agency (JAEA) was established. In JAEA, the R&D activities on both ADS and fast reactors have been continued.

In August, 2008, the AEC of Japan launched the Technical Subcommittee on P&T Technology under the Advisory Committee on R&D, and conducted the discussion about the current state of the art concerning P&T technology in Japan and the future R&D programme. The Subcommittee issued the final report in April, 2009. The final report covered the impact of the P&T technology, the state of the art of the technology, evaluation on the progress of the R&D, and the recommendations of the future R&D.

As the basic policy on the P&T technology, the report stated that the R&D should not aim at only the improvement of the P&T performance, but at the achievement of the requirements for whole performance of nuclear power generation. This means that the performance of the Double strata fuel cycle concept should be evaluated from viewpoints of safety, economy, environmental friendliness, saving resource, and non-proliferation of the first stratum as well as those of the second stratum. The Double strata concept, therefore, should be studied as a part of the whole nuclear system both in the transient phase of LWR to FBR and the equilibrium state of FBR. R&D of FBR and ADS should be coordinated strongly and their periodic evaluation was required.

Regarding the ADS, the report appreciated the significant progress in the design study, accelerator development, LBE technology including a spallation target, etc. It was, however, pointed out that the ADS was still in the fundamental stage as a whole and that further accumulation of basic data was necessary to step up to the next stage to verify the engineering feasibility. The report pointed out the required R&D issues on ADS as follows:

— Accelerator with sufficient economy and reliability;

— Feasibility of the beam window;

— Reactor physics of subcritical core including its control;

— Design and safety of LBE cooled core; and

— Feasibility of MA nitride fuel and its dry reprocessing.

The report also pointed out that the lack of basic data of MA seemed serious for the transmutation systems, both FBR and ADS, and emphasis was put on the necessity of the reactor physics experiments using a certain amount of MA to verify the safety and performance of the systems. The report recommended to consider the possibility to utilize the Transmutation Physics Experimental Facility (TEF-P) being proposed as the Phase-II of J-PARC project for this purpose. As for the coupling experiment of a fast neutron subcritical core with a spallation target, the report expressed the hope that the TEF-P would play an important role, and suggested to refer to the results of FFAG-KUCA experiment which was about to start.

Based on these descriptions in the report of the Subcommittee, various R&D activities on ADS and the preparation for the Transmutation Experimental Facility are under way.

## 5.9. REPUBLIC OF KOREA

ADS research of Korea was carried out at KAERI (Korea Atomic Energy Research Institute) for the transmutation of long lived nuclides in spent fuels. The KAERI ADS system was called HYPER (HYbrid Power Extraction Reactor). The HYPER research was carried out as a 10 year nuclear

research programme funded by the government. The ADS research of KAERI consisted of 3 phases. A basic concept of HYPER was established in the first phase (1997– 2000) of the development. The key technologies related to HYPER was studied in the second phase (2001–2003) while upgrading the design. The conceptual design of HYPER core was completed in the third phase (2004–2006). The research of key technologies was continued in the third phase. The research results can be summarized in three categories.

### 5.9.1. Design and analysis

HYPER was designed to transmute TRU and some fission products such as I-129 and Tc-99. HYPER was a 1000 $MW_{th}$ system and its $k_{eff}$ was 0.98. The metal alloy TRU-Zr fuel was adopted. I-129 and Tc-99 were put together in the same fission product rod. The required current was 10.6 mA at BOC and 16.4 mA at EOC. The inventory of TRU was 6,510 kg at BOC, and 282 kg of TRU can be transmuted per year. In the case of fission products, I-129 and Tc-99 can be transmuted with the rates of 7 and 27 kg/yr respectively. Pb-Bi was used as the coolant and spallation target material. The coolant was not separated from the target. The inlet temperature of coolant was 340°C, and the average outlet temperature was 490°C. The target window material was 9Cr steel such as T91 and 9Cr-2WVTa. The window had a hemispherical shape. Some transient characteristics of HYPER were also studied.

### 5.9.2. Fuel experiment

KAERI used U to make surrogate metal alloy fuel, U-Zr. Thermal properties of those U metal fuel was measured and used for studying characteristics of TRU metal fuel. We adopted Pb bonding, and reaction characteristics were studied among Pb bonding, cladding material (HT-9) and U surrogate fuel. HYPER adopted FP target system including Tc-99 and I-129 together in one target rod. HT-9 or $ZrH_2$ moderator was located at the center of the target depending on the position of the target inside the core. Then $CaI_2$ surrounded the moderator, and Tc metal was located between $CaI_2$ and the cladding. The FP target with the height of 5 mm was fabricated using surrogate materials. I-127 was used instead of I-129, and Tc-99 was replaced by Ru. After the fabrication, the compatibility study was performed at 600°C.

### 5.9.3. Pb-Bi experiment

KAERI joined MEGAPIE project in 2001 for the experimental study of Pb-Bi. MEGAPIE was one megawatt proton beam irradiation test of Pb-Bi target. The most significant problem in handling Pb-Bi is corrosion. Therefore, KAERI built a static Pb-Bi corrosion test facility and performed experiments using it in 2003. The construction of Pb-Bi corrosion loop was completed in 2005. The temperature range of the loop was between 450°C and 550°C. The oxygen control method was considered to test the protection of steel structure materials against Pb-Bi corrosion. Materials such as 316L, HT-9 and T91 were tested.

## 5.10. NETHERLANDS

The ADS related activities within the Netherlands are concentrated at NRG. From 2000 to 2006, NRG supported SCK•CEN in their development of MYRRHA. The support was mainly devoted to Computational Fluid Dynamics (CFD) simulations for the windowless target option. This collaboration was prolonged within the framework of the EU FP6 EUROTRANS project. Eventually this lead to a solution strategy for the hydraulic (without heat transfer) evaluation of a windowless target with one free surface using an Eulerian-Eulerian modeling approach. As a second free surface was added to the target design later, this approach would need to be revisited. The developed

approach was applied to an assess the feasibility of a three feeder windowless target design. This preliminary assessment confirmed that there were no serious show stoppers for a three feeder design. Another study undertaken using related to the windowless target was a preliminary assessment of the risk of lead-bismuth splashing in case of a sudden heat deposition by the beam, e.g. at beam startup or beam interuptions. Within the framework of the EU FP7 CDT project, a window target is currently being assessed thermalhydraulicly in collaboration with SCK•CEN.

The other important topic within the bilateral cooperation with SCK•CEN from 2000 to 2006 was the preliminary assessment of the flow structure in the lower plenum of the reactor with emphasis on the mixing. In 2010, this work was revisited in a more detailed assessment within the framework of the EU FP7 THINS project in support of the ESCAPE experimental scaled pool facility to be erected at SCK•CEN.

Within the EU FP5 ASCHLIM project, the state of the art with regard to turbulence modelling for CFD approaches was determined. It was concluded that accurate simulation of heat transport in HLM was not feasible, especially in natural or mixed convection regimes. Within the EU FP7 THINS project this issue is currently being treated. NRG assists the commercial CFD code vendor CD adapco in implementing and testing a promising, academically tested, algebraic heat flux model.

Validation of state of the art models for detailed fuel assembly sub-channel simulations was performed within a Dutch national long term nuclear research programme and partly within the EU FP6 EUROTRANS project where experimental data was available. The validated models were applied in the EU FP6 ELSY project to select heat transfer correlations for bare rod bundles. In addition, a heat transfer correlation was developed for the interfuel assembly heat transfer in an open lattice design. Another development in the framework of this project was to develop a low resolution geometry resolving CFD approach to evaluate the flow in one or more fuel assemblies. Such an approach allows to evaluate effects of possible flow blockages. Within the EU FP7 LEADER project, application of different spacer design is compared using CFD. Whereas within the EU FP7 THINS project, validation is ongoing for a numerical approach of wire wrapped fuel assemblies. The approach which is still to be validated is foreseen to be applied in the framework of the EU FP7 SEARCH project where the aim is to evaluate the thermalhydraulic behaviour of MYRRHA subassemblies. For that purpose, next to the detailed CFD analyses also the low resolution CFD approach needs to be adapted for application of wire wraps. This work will be complemented by a bilateral cooperation with SCK•CEN from 2012 to 2015. Within this cooperation, also the effect of inter wrapper flow is foreseen to be analysed.

Pool thermalhydraulics of the upper (hot) plenum is another major subject within this bilateral cooperation with SCK•CEN. The issue to be analysed here is a detailed assessment of thermal fluctuations occurring in the core outlet region on the above core structure. Apart from that, in the framework of the EU FP7 CDT project, the cooling of the in vessel spent storage fuel under operational forced convection and natural convection conditions was analysed with the aim of improving the design.

The in house developed system code SPECTRA for LWRs and HTRs was extended for liquid metal reactor applications within the framework of the EU FP6 ELSY project and later further improved within the framework of the EU FP7 LEADER project. The results were benchmarked against RELAP5-Pb results from ENEA.

## 5.11. RUSSIAN FEDERATION

Studies on accelerator driven systems (ADS), which be used as burners of long lived radioactive waste accrued due to operation of thermal reactors, first of all, minor actinides (MA), are carried out in some Russian research institutes (ITEP, SSC RF - IPPE, VNIIEF, JINR, RSC KI, IYaI RAN, OKB 'GIDROPRESS', VNIITF etc.). These researches are mainly connected with studying physical processes existing in ADS and their parameters and with design studies and substantiation of experimental ADS facilities.

One of the most important directions of researches is the acquirement of quite precise and reliable nuclear data on MA with reference to conditions existing in ADS. Now a coordinated programme of researches on measurement and estimation of nuclear data for 22 isotopes of U, Pu, Np, Am, Cm, Bk and Cf in neutron energy range from 0.05 eV up to 30 MeV has been prepared:

- BOR-60 and SM-3 reactors located in RIAR (Dimitrovgrad) are supposed to be used for integral inpile experiments;
- Differential measurements of neutron cross-sections of MA are planned being carried out at the linac LU-50 (VNIIEF, Sarov) and pulse electrostatic accelerators EG-1 and EG-15 (IPPE, Obninsk);
- Measurements of fission cross-sections of $^{241}$Am, $^{242m}$Am, $^{243}$Am, $^{243}$Cm, $^{244}$Cm, $^{245}$Cm, $^{246}$Cm, $^{247}$Cm, $^{248}$Cm, $^{236}$U in resonance neutron energy range (0.05–30 keV) where dispersion of nuclear data is especially large, are carried out with using lead slowdown spectrometer (lead mass, 100 t) at the base of linear proton accelerator of 'Moscow meson factory' (IYaI RAN, Troitsk; IPPE, Obninsk);
- Benchmark experiments are scheduled to be implemented at the critical facilities BFS-1 and BFS-2 (IPPE, Obninsk);
- Total and relative outputs of delayed neutrons for a number of nuclides including $^{241}$Am, $^{243}$Am will be measured at the accelerator EG-2.5; a database systematizing time and energy spectra of delayed neutrons in reactor neutron energy range will be created for all set of U, Np, Pu, Am isotopes.

Conceptual studies of various variants of ADS were carried out with the purpose of investigation of their characteristics:

- Development and substantiation of two cascade concept of blanket that allows essentially decreasing required capacity of an ADS accelerator;
- Theoretical and experimental substantiation of the concept of Cascade Subcritical Molten Salt Reactor (CSMSR) (RSC KI) that confirms an opportunity of providing reactor power level equal to 800 MW for the proton accelerator power 10 MW;
- Study of proposal on demonstration ADS on the base of a fast reactor with lead-bismuth coolant, so called Nuclear Waste Burner (NWB) (SSC RF-IPPE) with blanket power of 100 MW;
- Study of proposal on experimental facility with ~5–10 MW power on the base of the linac of 'Moscow meson factory' (IYaI RAN) modeling ADS with lead-bismuth coolant;
- Development of a concept of ADS based on modular fast reactor with lead-bismuth coolant driven by electron accelerator (SSC RF-IPPE);
- Development of a design of experimental ADS with power of 100 kW based on decommissioned experimental heavy water reactor and pulse proton linear accelerator ISTRA-36 - Electro-Nuclear Neutron Generator (ENNG) (ITEP);
- Development of a design of Subcritical Assembly at Dubna (SAD) with power of 28 kW driven by linear accelerator with proton energy 660 MeV and maximum beam current equal to 3.2 μA which is located in JINR.

Last two from the above mentioned ADS designs reached certain completeness. The main part of R&D has been completed and basic design has been issued in the frame of the ENNG Project. Now a basic design of the SAD facility has been completed and it is passing through the licensing procedure.

Development of different variants of ADS has put a task of comparison of their efficiency as burners of MA.

Now the comparative analysis of the following ADS concepts is carrying out:

— Concept of blanket with fast neutron spectrum on the base of design of SVBR-75-100 reactor being developed in the IPPE;

— Concept of blanket with intermediate neutron spectrum on the base of molten salt reactor concept developed in the RSC KI;

— Concept of blanket with thermal neutron spectrum on the base of heavy water reactor proposed by ITEP.

This programme of comparative researches assumes:

— Creation of specialized database for ADS calculation;

— Study of various characteristics and properties of ADS and their optimization for the purpose of decreasing accelerator capacity;

— Development of techniques of comparison of various ADS;

— Comparative analysis of various ADS designs;

— Implementation of comparative analysis of different ADS options.

Now methodology of comparison and uniform criteria for evaluation of efficiency of MA incineration are being developed.

# CHAPTER 6
# INTERNATIONAL PROGRAMMES ON ADS

## 6.1. EUROPEAN COMMISSION

Euratom research projects related to the design and the use of ADS facilities started in the 4th Framework Programme (FP4) (1996–2001) with the project 'Impact of Accelerator Based Technologies on Nuclear Fission Safety—IABAT'. The overall objective of the IABAT project was a preliminary assessment of the potential of Accelerator Driven Systems for transmutation of radioactive waste and, additionally, for nuclear energy production with minimum waste generation. This first project was followed by a much larger ADS oriented programmes in the FP5 (2002–2005), FP6 (2005–2010) and FP7 (2008–2013).

In the frame of the FP6, special attention was devoted to the EUROTRANS integrated Project (2005–2010), dedicated to study the transmutation of high level radioactive waste in an ADS.

Based on the three FP5 Clusters FUETRA, BASTRA and TESTRA together with the PDS-XADS Project, the EUROTRANS Project was aimed to carry out a first advanced design of an approximately 50 to 100 MWth eXperimental facility (realization in a short term, say about 10 years) demonstrating the technical feasibility of Transmutation in an ADS (XT ADS), as well as to accomplish a generic conceptual design (several 100 MWth) of a modular European Facility for Industrial Transmutation (EFIT) (realisation in the long term). Those two facilities have been described in chapter 4.

Instead of the FP5 separated projects, which were well linked into clusters and where the ADOPT network was dedicated to coordination, EUROTRANS contained the different topics within one sole project structure, namely

— Design of ADS facilities;

— Coupling experiments;

— Development of adequate fuel;

— Experiments and modeling related to structural materials;

— Relevant neutronic data.

The activities carried out in EUROTRANS were complemented by three FP6 Projects:

— PATEROS (P&T European Roadmap for Sustainable Nuclear Energy, 2006-2008), a Coordination Action aimed at establishing a global P&T roadmap leading up to the industrial scale deployment of necessary facilities.

— RED-IMPACT, a 3-year project studying the impact of P&T, conditioning and waste reduction technologies on reducing the burden associated with radioactive waste management and disposal.

— VELLA, a 3-year Integrated Infrastructure Initiative project with the goal to create a virtual European laboratory for lead Technologies'. Its final goal has been the creation of a network of the EU laboratories that operate devices using heavy liquid metals technologies, especially lead alloys.

In FP7 the EUROTRANS project is currently being continued by CDT (Central Design Team for a Fast Spectrum Transmutation Experimental Facility). The materials testing reactor Belgian Reactor 2 (BR2), located in Mol, Belgium, is used for nuclear research and production of medical isotopes. The BR2 reactor will eventually be replaced by the multipurpose hybrid research reactor for high tech applications (MYRRHA, which will represent a new kind of research reactor, also capable of demonstrating the technical feasibility of efficient transmutation, which can significantly reduce the toxicity and quantity of the long lived components of radioactive waste.

The Central Design Team (CDT) for such a Fast Spectrum Transmutation Experimental Facility (FASTEF) is a multidisciplinary European team representing experts from both industry and research organizations.

Crosscutting FP7 Projects have then been launched to complement the design based CDT Initiative:

— GETMAT, a 5-year project on materials that started on 1 March 2008, devoted to characterize materials for nuclear applications in the area of Transmutation and Generation IV systems. The focus of GETMAT is on ferritic martensitic and oxide dispersion strengthened steels, as cross-cutting structural material choice for core and primary components. Moreover, the project aims to streamline the efforts on (i) availability, fabricability and fundamental properties, (ii) compatibility with coolants, (iii) response to irradiation and (iv) efforts to understand physical reasons for their behaviour under these conditions. Other priorities include joining and welding procedures qualification, development and definition of corrosion protection barriers and improved modelling and experimental validation.

— FAIRFUELS (Fabrication, Irradiation and Reprocessing of Fuels and targets for transmutation), aimed at providing a way towards a more efficient use of fissile material in nuclear reactors and at reducing the volume and hazard of high level long lived radioactive waste. In fabrication technology and assessment of transmutation performance, FAIRFUELS focuses on minor actinides. Dedicated fuels are fabricated and a comprehensive irradiation programme is carried out to address transmutation performance. Certain Post-Irradiation Examinations (PIE) of earlier irradiated fuels and targets is conducted. In support of the PIE, modelling aspects of these fuels are developed.

— THINS (Thermalhydraulics of Innovative Nuclear Systems) a cross-cutting Project on thermalhydraulic issues encountered in various innovative nuclear systems.

— FREYA ( Fast Reactor Experiments for hYbrid Applications), built up on the former activities accomplished in the previous FPs, namely MUSE in FP5 and EUROTRANS in FP6, aimed to extend the investigations of the subcritical configurations for validation of the methodology for on-line reactivity monitoring of ADS systems.

— MAX (MYRRHA Accelerator eXperiment), an R&D programme devoted at investigating sustainable ways of managing high level, long lived radioactive wastes, using the MYRRHA facility to transmute radioactive isotopes into less toxic elements with shorter lifespans.

— HeLiMnet (Heavy Liquid Metal network), a coordination action aimed at integrating the R&D efforts going on within and outside Europe, in different areas of investigation, to create a large and strong network for the diffusion of information on the HLM technologies

— ADRIANA (ADvanced Reactor Initiative And Network Arrangement), a coordination action dedicated to the mapping and gap analysis of research infrastructures in support of the European Sustainable Nuclear Industrial Initiative: ‘ESNII’ established under the umbrella of the Sustainable Nuclear Energy Technology Platform (SNETP).

— SEARCH (Safe Exploitation Related Chemistry for HLM reactors and lead cooled Advanced Fast Reactor), investigating safe chemical behaviour of fuel and coolant in lead cooled reactor and support of MYRRHA technology.

— SILER (Seismic-Initiated events risk mitigation in lead cooled Reactors), aimed to study risks associated to seismic initiated events in Gen-IV Heavy Liquid Metal reactors and develop adequate mitigation strategies.

## 6.2. IAEA

The IAEA recognizes that there are four major challenges facing the long term development of nuclear energy as a part of the world’s energy mix: improvement of the economic competitiveness, meeting increasingly stringent safety requirements, adhering to the criteria of sustainable

development, and public acceptance. Meeting the sustainability criteria is the driving force behind IAEA's activity in the area of innovative transmutation reactor technology development and, in particular, Accelerator Driven Systems.

The framework for all the IAEA activities in the ADS area is the Technical Working Group on Fast Reactors (TWG-FR). In response to strong common R&D needs in the Member States, the TWG-FR acts as a catalyst for international information exchange and collaborative R&D. It provides a forum for exchange of non-commercial scientific and technical information, and a forum for international cooperation on generic research and development programmes on advances in fast reactors and fast spectrum accelerator driven systems. Its present members are the following 15 IAEA Member States: Belarus, Brazil, China, France, Germany, India, Italy, Japan, Kazakhstan, Republic of Korea, Russian Federation, Sweden, Switzerland, United Kingdom, and United States of America, as well as 3 international organizations: ISTC, OECD-NEA, and EU (EC). As observers, the TWG-FR has welcomed Argentina and Belgium.

The TWG-FR advises the Deputy Director General Nuclear Energy on status of and recent results achieved in the national technology development programmes relevant to the TWG-FR's scope, and recommends activities to the Agency that are beneficial for these national programmes. It furthermore assists in the implementation of corresponding Agency activities, and ensures that through continuous consultations with officially nominated representatives of Member States all the project's technical activities performed within the framework of the Nuclear Power Technology Development subprogramme are in line with expressed needs from Member States. The scope of the TWG-FR is broad; it includes, in particular: design, technologies, performance and safety characteristics, economics, etc. for current and advanced fast reactors and transmutation systems like critical fast 'burner' reactors and ADS. Many related specific technologies, e.g. in the field of associated fuel cycles, are addressed in detail by other projects within the IAEA and in other international organizations. The TWG-FR keeps abreast of such work, avoiding unproductive overlap, and engages in cooperative activities with other projects where appropriate. The TWG-FR thus coordinates its activities in interfacing areas with other Agency projects, especially those of the International Working Group on Nuclear Fuel Cycle Options, INPRO and the Department of Nuclear Safety, as well as with related activities of other international organizations (ISTC, OECD-NEA, and EC).

At large, the IAEA activities in the field of ADS concern:

— Topical meetings on the different aspects of the ADS technology and related issues;

— Coorganization of the biannual International Topical Meeting on Nuclear Applications and Utilization of Accelerators (AccApp);

— Preparation of Technical Reports, e.g. [6.1]–[6.6];

— Education & Training. In collaboration with the International Centre for Theoretical Physics (ICTP), the IAEA regularly organizes in Trieste the School on Physics, Technology and Applications of Accelerator Driven Systems (ADS) and the Workshop on Technology and Applications of Accelerator Driven Systems. The School familiarizes the students with the status of the R&D activities in the area of ADS for energy production and transmutation.

— Coordinated Research Projects (CRPs)

As far as this last point, the IAEA has recently completed to CRPs in the field of ADS and radioactive waste transmutation:

— Studies of Advanced Reactor Technology Options for Effective Incineration of Radioactive Waste (2002–2007). This CRP was joined by participants from 17 institutions in 13 Member States, and the EC (JRC). Its objective was to produce a comparative assessment of the transient behaviour of advanced transmutation systems, both critical and subcritical. The CRP performs benchmarks on critical liquid metal, and gas cooled fast reactor, heavy liquid metal, and gas cooled ADS, critical and subcritical molten salt concepts, and fusion–fission hybrid subcritical systems.

— Analytical and Experimental Benchmark Analyses of Accelerator Driven Systems (2005–2010). 27 institutions in 18 Member States and two international organizations were actively participating in this CRP. The objective was to improve the understanding of the physics of the coupling of external neutron sources with subcritical cores. Experimental backing of analytical benchmarks was the major thrust of this CRP. The participants applied integrated calculation schemes to perform computational and experimental benchmark analyses concerning: (i) YALINA Booster; (ii) Kyoto University Critical Assembly (KUCA) subcritical experiments: (iii) Pre-TRADE experimental benchmark; (iv) FEAT, TARC, SAD Shielding experimental benchmarks; (v) Kharkov Institute for Theoretical Physics (KIPT) electron based ADS design; (vi) ADS kinetics analytical benchmark; (vii) Actinides cross-sections; (viii) Spallation targets; and (ix) ADS performance, burnup codes, and transmutation experimental data.

Last but not least, the IAEA is providing the ADS Research and Development Database. It contains information about ADS related R&D programmes, existing and planned experimental facilities as well as programmes, methods and data development efforts, design studies, and so forth. While operational on the WWW and open to all users (http://www-adsdb.iaea.org/index.cfm), the database has to rely on content contributed by the interested community. Data and information can be provided on-line, and contributions are solicited and always welcome.

### 6.3. ISTC

The International Science and Technology Center (ISTC) is an intergovernmental organization, created to serve the goal of improving global safety and security. The European Union, Japan, the Russian Federation and the United States of America, on the basis of a multinational agreement, established ISTC in 1992.

The ISTC focused its efforts on funding research projects related to key safety and security technologies including advanced nuclear technology. Since the first ISTC funded project in 1994, Accelerator Driven Systems, Transmutation research and a holistic approach to the nuclear fuel cycle were the areas where ISTC made a real impact on international development in these fields.

Given the international dimension of the problem, the research communities of the ISTC member states quickly realized that ISTC projects offered a very flexible and fruitful cooperation platform to address many difficult issues of the nuclear fuel cycle. Highly competent expert communities of ISTC member states benefited from a well defined and transparent mode of operation of ISTC and objective oriented project funding strategy.

ISTC support for the radioactive waste transmutation with ADS started early with #0017 project: '*Feasibility study of technologies for accelerator based conversion of military plutonium and long lived radioactive waste'*. This project identified and unified a strong international research community deeply interested in transmutation of radioactive waste, at the time when this activity emerged internationally in post-cold war cooperative spirit.

The ISTC projects related to transmutation of radioactive waste and ADS can be classified in the following thematic areas:

— ADS concepts;

— Accelerator development;

— Spallation target studies;

— Nuclear data and spallation process studies;

— Minor actinides studies related to ADS;

— Partitioning and extraction

The ISTC project results have been presented in hundreds of scientific papers on many the international conferences starting as early as in 1995 at the Accelerator driven transmutation

technology (ADTT) Conference, Las Vegas, (USA), at the second ADTT Conference in Kalmar (Sweden) 1996, at conferences in Dubna (Russia), and follow up ADTT-ADS conferences in Czech Republic, Spain, France, Japan, Korea, USA etc.

A detailed information about each ISTC project related to ADS and transmutation including summary of the results can be found at:

http://www.istc.ru/istc/db/projects.nsf/fa_WebForSearch?openform&count=20&lang=Eng

It is also worth mentioning that in 1997 an International Contact Expert Group (CEG) on ISTC ADS&Fuel Cycle Projects was established in order to coordinate and stimulate international research efforts and in particular to harmonize cooperation between ISTC funded projects and other national and international programmes. IAEA has been an active member of this group from the very beginning and created a lot of synergetic activities.

This Group has played an important role in harmonizing some important international efforts in ADS research. For example construction of 1 MW spallation Pb-Bi target in the frame of ISTC Project #559 and #2083-P initiated European interest in this technology resulted in construction of advanced 1 MW Pb-Bi spallation target at PSI in Switzerland in the frame of the European Project MEGAPIE (see paragraph 7.1). Similarly, Pb-Bi laboratory KALLA at FZK in Germany has its origin in cooperation with the ISTC project #559. Yalina subcritical experiment driven by a neutron generator in 'Sosny' Joint Institute for Power and Nuclear Research Institute in Minsk was a predecessor of similar experiments at CEA_Cadarache ('Muse' European Project) and on going Guinevere project at SCK•CEN in Mol. Finally, the ISTC projects Subcritical Assembly in Dubna, so called SAD design (Project #2267) stimulated further development of the European facility MYRRHA being under construction at SCK•CEN in Mol.

## 6.4. OECD-NEA

The long term hazard of radioactive wastes arising from nuclear energy production is a matter of continued discussion and public concern in many countries. By the use of partitioning and transmutation (P&T) of the actinides and some of the long lived fission products, the radiotoxicity of the high level waste (HLW) and, possibly, the safety requirements for its geological disposal can be reduced compared with the current once through fuel cycle. To make the technologically complex enterprise worthwhile, a reduction in the HLW radiotoxicity by a factor of at least one hundred is desirable. This requires very effective reactor and fuel cycle strategies, including fast reactors (FRs) and-or accelerator driven, subcritical systems. The accelerator driven system (ADS) has recently been receiving increased attention due to its potential to improve the flexibility and safety characteristics of transmutation systems.

The present study compares FR and ADS based actinide transmutation systems with respect to reactor properties, fuel cycle requirements, economic aspects, and R&D needs. The essential differences between the various systems are evaluated with the help of a number of representative fuel cycle schemes. The strategies investigated include an evolutionary transmutation strategy in which the ADS provides additional flexibility by enabling plutonium utilisation in conventional reactors and confining the minor actinides to a small part of the fuel cycle, and two innovative transuranics (TRU) burning strategies, with an FR or an ADS, in which plutonium and minor actinides are managed together to minimize the proliferation risk. A novelty in the present study is that the analyses are carried out in a consistent manner using reactor and fuel cycle parameters which have been agreed upon by international experts.

## 6.5. THE ASIAN ADS NETWORK

As the management of radioactive wastes is a common issue for all the countries utilizing nuclear energy and also for those intending to start it, international multilateral collaboration must be of great importance for effective research and development of transmutation technology for long lived

nuclides. Collaboration in Asian region, however, had been less active in comparison to European countries, though nuclear power generation would increase significantly in Asia. Considering this context, the former Japan Atomic Energy Research Institute (JAERI) convened the 'International Symposium on Accelerator driven Transmutation Systems and Asia ADS Network Initiative' on March 24 and 25, 2003 at Tokyo, Japan in cooperation with Kyoto University, Osaka University, High Energy Accelerator Research Organization and Tokyo Institute of Technology [6.1]. Through the discussion in the symposium, common understanding was developed in Japanese, Korean and Chinese scientists concerning the importance of establishing an international network among Asian countries to facilitate information exchange for R&D of ADS.

Based on this understanding, five workshops were held so far (until 2008) at Daejeon, Korea (2004), Beijing, China (2005), Kumatori, Japan (2006), Seoul, Korea (2007), and Xi'an, China (2008). The next workshop will be held in Tokai, Japan in 2009.

The workshop covers the national R&D programmes on ADS including subcritical reactor physics, cross-section measurements, high energy particle physics, accelerator technology, material technology and MA fuel technology. From the fifth workshop, information exchange for R&D on innovative fast reactors for nuclear transmutation was also included.

## 6.6. REFERENCES TO CHAPTER 6


[6.1] INTERNATIONAL ATOMIC ENERGY AGENCY, Accelerator driven systems: Energy generation and transmutation of nuclear waste. Status report, IAEA-TECDOC-985 (1997).

[6.2] INTERNATIONAL ATOMIC ENERGY AGENCY, Power Reactor and Subcritical Blanket Systems with lead and lead-bismuth as coolant and/or Target Material, IAEA-TECDOC-1348 (2000).

[6.3] INTERNATIONAL ATOMIC ENERGY AGENCY, Emerging nuclear energy and transmutation systems: Core physics and engineering aspects, TECDOC-1356(2000).

[6.4] INTERNATIONAL ATOMIC ENERGY AGENCY, Review of national accelerator driven system programmes for partitioning and transmutation, TECDOC-1365 (1999).

[6.5] INTERNATIONAL ATOMIC ENERGY AGENCY, Theoretical and Experimental Studies of Heavy Liquid Metal Thermal Hydraulics, IAEA-TECDOC-1520 (2006).

[6.6] INTERNATIONAL ATOMIC ENERGY AGENCY, Advanced Reactor Technology Options for Utilization and Transmutation of Actinides in Spent Nuclear Fuel, IAEA-TECDOC-1626 (2009).

[6.7] OIGAWA, H., (Ed.), Proceedings of the International Symposium on Accelerator-driven Transmutation Systems and Asia ADS Network Initiative, JAERI-Conf 2003-012 (2003).

# CHAPTER 7
# CONCLUSIONS

Partitioning and transmutation could address the high-level radioactive waste issue and prepare the ground for a more resource efficient nuclear energy system in the future and may become an attractive and appropriate intermediate strategy on the way to the ultimate goal of the sustainable nuclear energy system. In this context, the ADS could play an interesting role as a minor actinide or transuranics (TRU) burner. The amount of results obtained in those 15 years is really impressive, both in the R&D efforts described in chapter 5 and in the engineering design, even still at conceptual level (chapter 4). Many experimental facilities have been designed and constructed in the world; they are now operated on a regular basis, producing essential information for the designers.Chapter 3 presents the ADS system that are conceived worldwide as demonstration plants, like EAP80-Italian XADS, PDS-XADS, JAEA Experimental ADS and HYPER while on industrial scale EFIT, ADS-800 MW(th) shows significant progress.

Several countries are now committed to go to the real deployment of small to mid scale ADS facilities:

— The GUINEVERE facility, described in chapter 5, has been in the meantime officially inaugurated in March 2010 and the coupling accelerator target has been accomplished in October 2011.

— In Belarus ADS activities are mainly related to study of neutronics at zero power.

— On March 3rd, 2010, the Council of Ministers of the Belgian Federal Government has taken the decision to support the realisation of the MYRRHA project (see chapter 4) and, consequently to allocate a specific endowment to SCK•CEN of 60 million Euros over the period 2010–2014 as to go from the existing conceptual design towards the so-called Front End Engineering Design (in other words the basic design allowing to go to tendering of components).

— In 2007, China started a 973 Programme Key Technology Research of Accelerator Driven Subcritical System for Nuclear waste Transmutation. The research activities were focused on high power proton accelerators physics, technology, reactor physics of external source driven subcritical assembly, nuclear data base and material study

Another comment to conclude this report is the growing importance of international collaboration and the role of international bodies:

— More and more, R&D efforts are performed at international level, through either bilateral research agreements or collaborative projects, like those organized by the European Commission in its framework programmes.

— International bodies, like the IAEA ,ISTC and NEA, have also their role to play, by bringing together different players around the world that are involved in the same topic; sharing information when possible is essential, and can be a first step towards real, formalizes, collaborations; knowledge preservation is also compulsory.

— Nuclear power generation are being on incresae in Asia. The Asian ADS Network Initiative could play a substantial role on development of ADS technology.

# ABBREVIATIONS

| | |
|---|---|
| AAA | Advanced Accelerator Applications |
| AFCI | Advanced Fuel Cycle Initiative |
| ADS | Accelerator Driven System |
| ALINA | Anlage für LIthium und NAtrium |
| ATW | Accelerator Driven Transmutation of Waste |
| BARC | Bhabha Atomic Research Centre |
| BOL | Beginning Of Life |
| CANDU | CANada Deuterium Uranium (Atomic Energy of Canada Limited) |
| CCD | Charge-Coupled Device |
| CERN | French Conseil Européen pour la Recherche Nucléaire (European Organization for Nuclear Research) |
| CHEOPE | CHEmical and OPErational |
| CIAE | China Institute of Atomic Energy |
| CIRCE | CIRCuito Eutettico |
| CLAM | China Low Activation Martensitic |
| COLONRI | COnvection LOops in the NRI |
| CORRIDA | CORRosion In Dynamic lead Alloys |
| CW | Continuous Wave |
| CZP | Cold Zero Power |
| DBTT | Ductile to Brittle Transition Temperature |
| DBC | Design Basis Conditions |
| DEC | Design Extended Conditions |
| DESINUR | Design Evaluation and SImulation of NUclear Reactor |
| DHR | Decay Heat Removal |
| DPMS | Differential Pressure Measurement System |
| DRC | Direct Reactor Cooling |
| DTL | Drift Tube Linac |
| EA | Energy Amplifier |
| ECR | Electron Cyclotron Resonance |
| EFPD | Effective Full Power Days |
| EFIT | European Facility for Industrial Transmutation |
| EFP | European Framework Programme |
| ELSY | European lead cooled System |
| EMF | ElectroMotive Force |

| | |
|---|---|
| ENEA | Ente per le Nuove Tecnologie, l'Energia e l'Ambiente (Agency for New Technologies, Energy and Environment) |
| ENNG | Electro Nuclear Neutron Generator |
| ETD | European Transmutation Demonstration |
| ETWG | European Technical Working Group |
| EOL | End Of Life |
| EUROTRANS | EUROpean Research Programme for the TRANSmutation of High Level Nuclear Waste in an Accelerator Driven System |
| FA | Fuel Assembly |
| FEAT | First Energy Amplifier Test |
| FE | Fuel Element |
| FR | Fast Reactor |
| GIF | Generation IV International Forum |
| HEX | Heat EXchanger |
| HFP | Hot Full Power |
| HIP | Hot Isostatic Press |
| HLW | High Level Waste |
| HLM | Heavy Liquid Metal |
| HPPA | High Power Proton Accelerators |
| HTR | High Temperature Reactor |
| HTM | Hydraulic Target Model |
| HM | Heavy Metal |
| HYPER | HYbrid Power Extraction Reactor |
| IAHR | International Association for Hydraulic Engineering and Research |
| IGS | Insulating Gas System |
| IHX | Intermediate Heat eXchanger |
| ILC | Independent lead cooled channel |
| IMF | Inert Matrix Fuel |
| INPRO | International Project on Innovative Nuclear Reactors and Fuel Cycles |
| ITEP | Institute of Theoretical and Experimental Physics, Moscow |
| JAEA | Japan Atomic Energy Agency |
| KAERI | Korea Atomic Energy Research Institute |
| KALLA | KArlsruhe Liquid Metal Laboratory, Germany |
| LBE | Lead-bismuth Eutectic |
| LCF | low cycle fatigue |
| LEBT | Low Energy Beam Transport |
| LECOR | LEad CORrosion |

| | |
|---|---|
| LFR | Lead cooled Fast Reactor |
| LHGR | Liner Heat Generation Rate |
| LINAC | linear accelerator |
| LIDAR | LIght Detection And Ranging |
| LLFP | Long Lived Fission Product |
| LMFBR | Light Metal Fast Breeder Reactor |
| LMS | Level Measurement System |
| LME | Liquid Metal Embrittlement |
| LWR | Light Water Reactor |
| MA | Minor Actinides |
| MEBT | Medium Energy Beam Transport |
| MEGAPIE | MEGAwatt Pilot Experiment |
| MSS | Modified Stainless Steel |
| MOX | Mixed Oxide Fuel |
| MUSE | MUltiplication of External Source |
| MYRRHA | Multipurpose hYbrid Research Reactor for High tech Applications |
| NEA | Nuclear Energy Agency |
| NUCEF | Nuclear Fuel Cycle Safety Engineering Facility |
| OCS | Oxygen Control System |
| ODS | Oxide Dispersion Strengthened Steel |
| OECD | Organisation for Economic Cooperation and Development |
| OFM | Oxygen Fine Measure |
| ORS | Oxygen Reactivity Sensors |
| PATEROS | Partitioning and Transmutation European Roadmap for Sustainable Nuclear Energy |
| PCS | Power Conversion System |
| PP | Primary Pump |
| P&T | Partitioning and Transmutation |
| RCS | Cycling Proton Synchrotron |
| RFQ | Radio Frequency Quadrupole |
| RVACS | Reactor Vessel Air Cooling System |
| SAD | Subcritical Assembly at Dubna |
| SCS | Shutdown Cooling System |
| SCC | Separated Sector Cyclotron |
| SCK • CEN | Studie Centrum voor Kernenergie; Centre d'Étude de l'énergie Nucléaire (Belgian nuclear research centre located in Mol, Belgium) |
| SG | Steam Generators |
| SNS | Spallation Neutron Source |

| | |
|---|---|
| TARC | Test of Adiabatic Resonance Crossing |
| TEF | Transmutation Experimental Facility |
| TELEMAT | TEchnology Loop for LEad MATerial Qualification |
| THESYS | Technologies for HEavy metal SYStems |
| THEADES | THErmalhydraulics and Ads DESign |
| TRU | Transuranic |
| TTM | Thermal Target Model |
| TWG-FR | Technical Working Group of Fast Reactor |
| ULOF | Unprotected Loss of Flow |
| USA | United State of America |
| UVP | Ultrasonic Velocity Profiler |
| VEC | Vertical Experimental Channels |
| VECC | Variable Energy Cyclotron Centre |
| XADS | eXperimental Accelerator Driven System |
| XADT | eXperimental Accelerator Driven Transmuter |

## CONTRIBUTORS TO DRAFTING AND REVIEW

| | |
|---|---|
| Abderrahim, H. A. | SCK•CEN, Belgium |
| Arai, Y. | JAEA, Japan |
| Arien, B. | SCK•CEN, Belgium |
| Artioli, C. | ENEA, Italy |
| Ashurko, Y. | IPPE, Russian Federation |
| Benoit, P. (†) | SCK•CEN, Belgium |
| Baeten, P. | SCK•CEN, Belgium |
| Baoqun, C. | CIAE, China |
| Benamati, G. | ENEA, Italy |
| Biarrotte, J. L. | CNRS, France |
| Carluec, B. | AREVA, France |
| Carta, M. | ENEA, Italy |
| Cao, J. | CIAE, China |
| Crespo, L. S. | CIEMAT, Spain |
| De Bruyn, D. | SCK•CEN, Belgium |
| De Grandis, S. | SINTEC S.r.l., Italy |
| Delage, F. | CEA, France |
| Dierckx, M. | SCK•CEN, Belgium |
| Ding, D. | CIAE, China |
| Du, E. | CIAE, China |
| Fazio, C. | KIT, Germany |
| Giraud, B. | ITER |
| Gómez-Briceño, D. | CIEMAT, Spain |
| Granget, G. | CEA, France |
| Gudowski, W. | KTH, Sweden |
| Hojná, A. | Nuclear Research Institute Řež plc., Czech Republic |
| Jilani, G | IAEA |
| Kikuchi, K. | JAEA, Japan |
| Knebel, J. U. | KIT, Germany |
| Kikuchi, K. | JAEA, Japan |
| Kobzová, A. | Nuclear Research Institute Řež plc., Czech Republic |
| Konys, J. | KIT, Germany |
| Kurata, Y. | JAEA, Japan |
| Larmignat, S. | Alstom Power, Switzerland |

| | |
|---|---|
| Li, H. | CIAE, China |
| Li, J. | CIAE, China |
| Li, Y. | CIAE, China |
| Long, B. | CIAE, China |
| Luo, H. | CIAE, China |
| Luo, Z. | CIAE, China |
| Maes, D. | SCK•CEN, Belgium |
| Malambu, E. | SCK•CEN, Belgium |
| Mansani, L. | Ansaldo Nucleare, Italy |
| Martín-Muñoz, F. J. | CIEMAT, Spain |
| Maschek, W. | KIT, Germany |
| Mellier F. | CEA, France |
| Minato, K. | JAEA, Japan |
| Monti, S. | IAEA |
| Mueller, A. | CNRS, France |
| Müller, G. | KIT, Germany |
| Nema, P.K. | Bhabha Atomic Research Centre, India |
| Obayashi, H. | JAEA, Japan |
| Oigawa, H. | JAEA, Japan |
| Polat, A. | CIAE, China |
| Pyeon, C. H. | Kyoto University, Japan |
| Quan, Y. | CIAE, China |
| Reale, M. | Ansaldo Nucleare, Italy |
| Richard, P. | CEA, France |
| Rimpault, G. | CEA, France |
| Rineiski, A. | KIT, Germany |
| Roelofs, F. | RNG, Netherlands |
| Sasa, T. | JAEA, Japan |
| Schroer, C. | KIT, Germany |
| Schulenberg, T. | KIT, Germany |
| Schuurmans, P. | SCK•CEN, Belgium |
| Seliverstov, V. V. | ITEP, Russian Federation |
| Shi, Y. | CIAE, China |
| Shinian, F. | Institute of High Energy Physics, China |
| Shvetsov, V. N. | JINR, Russian Federation |
| Sobolev, V. | SCK•CEN, Belgium |
| Song, T. Y. | KAERI, Republic of Korea |

| | |
|---|---|
| Stanculescu, A. | INL, USA |
| Stieglitz, R. | KIT, Germany |
| Takei, H. | JAEA, Japan |
| Van den Eynde, G. | SCK•CEN, Belgium |
| Vasile A. | CEA, France |
| Wan, F. | University of Science and Technology, China |
| Wan, K. | University of Science and Technology, China |
| Weisenburger, A. | KIT, Germany |
| Woaye-Hune, A. | Alstom Power, Switzerland |
| Wu, X. | CIAE, China |
| Xia, H. | CIAE, China |
| Xia, P. | CIAE, China |
| Xu, Y. | CIAE, China |
| Yuan, D. | CIAE, China |
| Zhang, J. | CIAE, China |
| Zhang, W. | CIAE, China |
| Zhao, F. | University of Science and Technology, China |
| Zhao, Z. | CIAE, China |
| Zheng, Y. | CIAE, China |
| Zhou, D. | CIAE, China |
| Zhu, J. | CIAE, China |
| Zhu, S. | CIAE, China |
| Zhu, Q. | CIAE, China |
| Zuo, Y. | CIAE, China |

IAEA
International Atomic Energy Agency

No. 23

# ORDERING LOCALLY

In the following countries, IAEA priced publications may be purchased from the sources listed below or from major local booksellers.

Orders for unpriced publications should be made directly to the IAEA. The contact details are given at the end of this list.

**AUSTRALIA**
***DA Information Services***
648 Whitehorse Road, Mitcham, VIC 3132, AUSTRALIA
Telephone: +61 3 9210 7777 • Fax: +61 3 9210 7788
Email: books@dadirect.com.au • Web site: http://www.dadirect.com.au

**BELGIUM**
***Jean de Lannoy***
Avenue du Roi 202, 1190 Brussels, BELGIUM
Telephone: +32 2 5384 308 • Fax: +32 2 5380 841
Email: jean.de.lannoy@euronet.be • Web site: http://www.jean-de-lannoy.be

**CANADA**
***Renouf Publishing Co. Ltd.***
5369 Canotek Road, Ottawa, ON K1J 9J3, CANADA
Telephone: +1 613 745 2665 • Fax: +1 643 745 7660
Email: order@renoufbooks.com • Web site: http://www.renoufbooks.com

***Bernan Associates***
4501 Forbes Blvd., Suite 200, Lanham, MD 20706-4391, USA
Telephone: +1 800 865 3457 • Fax: +1 800 865 3450
Email: orders@bernan.com • Web site: http://www.bernan.com

**CZECH REPUBLIC**
***Suweco CZ, spol. S.r.o.***
Klecakova 347, 180 21 Prague 9, CZECH REPUBLIC
Telephone: +420 242 459 202 • Fax: +420 242 459 203
Email: nakup@suweco.cz • Web site: http://www.suweco.cz

**FINLAND**
***Akateeminen Kirjakauppa***
PO Box 128 (Keskuskatu 1), 00101 Helsinki, FINLAND
Telephone: +358 9 121 41 • Fax: +358 9 121 4450
Email: akatilaus@akateeminen.com • Web site: http://www.akateeminen.com

**FRANCE**
***Form-Edit***
5 rue Janssen, PO Box 25, 75921 Paris CEDEX, FRANCE
Telephone: +33 1 42 01 49 49 • Fax: +33 1 42 01 90 90
Email: fabien.boucard@formedit.fr • Web site: http://www.formedit.fr

***Lavoisier SAS***
14 rue de Provigny, 94236 Cachan CEDEX, FRANCE
Telephone: +33 1 47 40 67 00 • Fax: +33 1 47 40 67 02
Email: livres@lavoisier.fr • Web site: http://www.lavoisier.fr

***L'Appel du livre***
99 rue de Charonne, 75011 Paris, FRANCE
Telephone: +33 1 43 07 50 80 • Fax: +33 1 43 07 50 80
Email: livres@appeldulivre.fr • Web site: http://www.appeldulivre.fr

**GERMANY**
***Goethe Buchhandlung Teubig GmbH***
Schweitzer Fachinformationen
Willstätterstrasse 15, 40549 Düsseldorf, GERMANY
Telephone: +49 (0) 211 49 8740 • Fax: +49 (0) 211 49 87428
Email: s.dehaan@schweitzer-online.de • Web site: http://www.goethebuch.de

**HUNGARY**
***Librotade Ltd., Book Import***
PF 126, 1656 Budapest, HUNGARY
Telephone: +36 1 257 7777 • Fax: +36 1 257 7472
Email: books@librotade.hu • Web site: http://www.librotade.hu

**INDIA**
***Allied Publishers***
1st Floor, Dubash House, 15, J.N. Heredi Marg, Ballard Estate, Mumbai 400001, INDIA
Telephone: +91 22 2261 7926/27 • Fax: +91 22 2261 7928
Email: alliedpl@vsnl.com • Web site: http://www.alliedpublishers.com

***Bookwell***
3/79 Nirankari, Delhi 110009, INDIA
Telephone: +91 11 2760 1283/4536
Email: bkwell@nde.vsnl.net.in • Web site: http://www.bookwellindia.com

**ITALY**
***Libreria Scientifica "AEIOU"***
Via Vincenzo Maria Coronelli 6, 20146 Milan, ITALY
Telephone: +39 02 48 95 45 52 • Fax: +39 02 48 95 45 48
Email: info@libreriaaeiou.eu • Web site: http://www.libreriaaeiou.eu

**JAPAN**
***Maruzen Co., Ltd.***
1-9-18 Kaigan, Minato-ku, Tokyo 105-0022, JAPAN
Telephone: +81 3 6367 6047 • Fax: +81 3 6367 6160
Email: journal@maruzen.co.jp • Web site: http://maruzen.co.jp

**NETHERLANDS**
***Martinus Nijhoff International***
Koraalrood 50, Postbus 1853, 2700 CZ Zoetermeer, NETHERLANDS
Telephone: +31 793 684 400 • Fax: +31 793 615 698
Email: info@nijhoff.nl • Web site: http://www.nijhoff.nl

***Swets Information Services Ltd.***
PO Box 26, 2300 AA Leiden
Dellaertweg 9b, 2316 WZ Leiden, NETHERLANDS
Telephone: +31 88 4679 387 • Fax: +31 88 4679 388
Email: tbeysens@nl.swets.com • Web site: http://www.swets.com

**SLOVENIA**
***Cankarjeva Zalozba dd***
Kopitarjeva 2, 1515 Ljubljana, SLOVENIA
Telephone: +386 1 432 31 44 • Fax: +386 1 230 14 35
Email: import.books@cankarjeva-z.si • Web site: http://www.mladinska.com/cankarjeva_zalozba

**SPAIN**
***Diaz de Santos, S.A.***
Librerias Bookshop • Departamento de pedidos
Calle Albasanz 2, esquina Hermanos Garcia Noblejas 21, 28037 Madrid, SPAIN
Telephone: +34 917 43 48 90 • Fax: +34 917 43 4023
Email: compras@diazdesantos.es • Web site: http://www.diazdesantos.es

**UNITED KINGDOM**
***The Stationery Office Ltd. (TSO)***
PO Box 29, Norwich, Norfolk, NR3 1PD, UNITED KINGDOM
Telephone: +44 870 600 5552
Email (orders): books.orders@tso.co.uk • (enquiries): book.enquiries@tso.co.uk • Web site: http://www.tso.co.uk

**UNITED STATES OF AMERICA**
***Bernan Associates***
4501 Forbes Blvd., Suite 200, Lanham, MD 20706-4391, USA
Telephone: +1 800 865 3457 • Fax: +1 800 865 3450
Email: orders@bernan.com • Web site: http://www.bernan.com

***Renouf Publishing Co. Ltd.***
812 Proctor Avenue, Ogdensburg, NY 13669, USA
Telephone: +1 888 551 7470 • Fax: +1 888 551 7471
Email: orders@renoufbooks.com • Web site: http://www.renoufbooks.com

**United Nations**
300 East 42nd Street, IN-919J, New York, NY 1001, USA
Telephone: +1 212 963 8302 • Fax: 1 212 963 3489
Email: publications@un.org • Web site: http://www.unp.un.org

## Orders for both priced and unpriced publications may be addressed directly to:

IAEA Publishing Section, Marketing and Sales Unit, International Atomic Energy Agency
Vienna International Centre, PO Box 100, 1400 Vienna, Austria
Telephone: +43 1 2600 22529 or 22488 • Fax: +43 1 2600 29302
Email: sales.publications@iaea.org • Web site: http://www.iaea.org/books

International Atomic Energy Agency
Vienna
ISBN 978–92–0–105315–2
ISSN 1011–4289